GEOLOGICAL SURVEY OF CANADA
DEPARTMENT OF ENERGY, MINES AND RESOURCES, OTTAWA

PAPER 75-1 PART C

REPORT OF ACTIVITIES
PART C

1975

Technical editing and compilation
R.G. Blackadar
P.J. Griffin
Helen Dumych

Production editing and layout
Leona R. Mahoney

Printed from text typed by:
Janet Gilliland
Sharon Parnham
Debbie Busby

Energy, Mines and Resources Canada
Énergie, Mines et Ressources Canada

GEOLOGICAL SURVEY
PAPER 75-1C

REPORT OF ACTIVITIES
PART C

Release
date Nov 7th

1975

Available by mail from *Information Canada*, Ottawa, K1A 0S9

from the Geological Survey of Canada
601 Booth St., Ottawa, K1A 0E8

and

Information Canada bookshops in

HALIFAX — 1683 Barrington Street
MONTREAL — 640 St. Catherine Street W.
OTTAWA — 171 Slater Street
TORONTO — 221 Yonge Street
WINNIPEG — 393 Portage Avenue
VANCOUVER — 800 Granville Street

or through your bookseller

A deposit copy of this publication is also available
for reference in public libraries across Canada

Price - Canada: $5.00
Other Countries: $6.00

Catalogue No. M44-75-1C

Price subject to change without notice

Information Canada
Ottawa
1975

Table of Contents

Page

PRECAMBRIAN GEOLOGY

QUATERNARY GEOLOGY: ENVIRONMENTAL AND ENGINEERING GEOLOGY STUDIES

QUATERNARY GEOLOGY: INVENTORY MAPPING AND STRATIGRAPHIC STUDIES

QUATERNARY GEOLOGY: PALEOECOLOGY GEOCHRONOLOGY

QUATERNARY SEDIMENTOLOGY AND GEOMORPHOLOGY

STRATIGRAPHY

REPRINTS

A limited number of reprints of the papers that appear in this volume are available by direct request to the individual authors.

INTRODUCTION

The Geological Survey of Canada is charged with providing a comprehensive inventory and understanding of the geology of Canada as a basis of national planning and policy making. Its main objectives follow seven major thrusts directed to: ascertaining Canada's energy and mineral resources; facilitating exploration and development; encouraging regional development; promoting effective use of the Canadian terrain; identifying and assessing natural hazards; identifying geological features affecting environmental equilibrium; and disseminating information on Canada's landmass and the resources it contains.

Publication of the results of its scientific activities has, since 1845, been an essential part of the Survey's program. The many thousands of geological maps and the nearly 5000 reports published during the past 130 years testify to this. Changing needs for information require changing methods of publication; today the demand for rapid release of new data to assist in government planning and policy making or in decision making in industry, is growing yearly with the result that the classical, almost archival, definitive publications of the past are becoming less common and new approaches for information release are being used.

The Report of Activities is one way in which the need for rapid information release is met. Begun in 1958 as a brief, informal, internal report concerned with the results of the previous summer's field work, the series has expanded greatly and during 1975 about 200 papers totalling more than 1200 pages of text will have been published in this form. In addition of course the Survey has continued its more formal publications and in 1974-75 published 5 memoirs, 13 bulletins, 2 economic geology reports, 4 miscellaneous reports 22 multicoloured geological maps, 9 preliminary maps and 51 paper series reports. In addition 69 items were placed on Open File and 341 new aeromagnetic maps were released.

In order to expedite the production of this report, it was necessary to change the format slightly from that used in recent issues. The Table of Contents groups the papers by subject and although in the text they follow an apparently random order it is the order in which they were submitted. This change resulted in accelerating the production time by almost one week because as each individual paper was received, it was possible to proceed with its preparation in final form suitable for printers copy. Material for this issue was received and edited between September 1 and September 15; production editing and typing, proofreading and preparation of camera-ready copy were carried out between September 10 and September 29 and printing of the text was scheduled for the month of October in anticipation of an early November release of the printed text.

The subject categories into which the papers are grouped in the Table of Contents include only some of the Survey's programs. Programs may cut across discipline lines (for example the Uranium Reconnaissance Program depends on studies in Geochemistry and Geophysics) and to show how each project reported in this publication fits into the different programs would result in a far too lengthy introduction. However, it may be of some interest to the users of this publication to learn of the general objectives of the Surveys programs.

The Uranium Reconnaissance Program has been designed to provide high-quality systematic reconnaissance data relating to the distribution of uranium in Canada to serve as a guide and incentive in exploration for new

deposits and to provide a basis for national uranium resource appraisal. The Geological Survey is undertaking preliminary reconnaissance and feasibility studies as required but the principal operations are being done under contract and entail airborne radioactivity and ground geochemical surveys. The Survey plans to maintain on-going Research and Development activities relating to methods of uranium exploration. The program is being cost-shared with the provinces and extended discussions with technical representatives of all the provinces have been carried out. Reports 40, 45, 48, 49, 50 and 57 present results of projects carried out as part of the Uranium Reconnaissance Program.

The various geophysical programs are designed to encourage research and development into geophysical methods for application to mineral resource evaluation and exploration, terrain investigations and the better definition of bedrock geology. Reports 30 to 33, a group of papers describing the Cavendish Test Range, illustrate how various techniques used in gravity, seismic, and magnetic surveys are evaluated.

Report 34 describes work carried out as part of the Magnetic Survey Program, a program designed to develop new magnetic survey instrumentation and techniques, to conduct experimental aeromagnetic surveys over land and sea, and to devise new techniques for the digital treatment, presentation and interpretation of the resultant data.

Studies in economic geology are designed to relate the genesis of economic concentrations of minerals to the evolution of the geological framework of Canada and thereby determine regional and local geological features that favour the occurrence of mineral deposits and are guides to their discovery thus permitting an evaluation of the distribution, character and amount of Canada's mineral resources. Reports 22 to 29 describe progress in one aspect of Project Appalachia, a study that seeks to combine regional geology, metallogeny and geomathematics in the development and application of computer-based methods of regional resource appraisal. These papers report developments in the geomathematics program in which models are being developed whose assumptions and restrictions are geologically acceptable but yet are models that can accommodate the unavoidably imprecise nature of many geological data.

Regional studies of Quaternary deposits such as those presented in reports 17, 18 and 55 are designed to provide a Canada-wide inventory of the unconsolidated deposits and landforms and to establish their stratigraphic and environmental history. The information obtained is of value to forestry, agriculture, engineering, construction and the mineral industry and is used in land use and environmental impact studies.

Studies such as those reported in Papers 19, 16 and 53 are designed to define and illustrate geomorphological processes, especially in areas of permafrost and physical and chemical aspects of fresh and weathered glacial sediments.

Nearly one quarter of the reports in this publication are concerned with the stratigraphy of the consolidated deposits of Western and Arctic Canada. Such studies are fundamental to programs such as ascertaining and evaluating Canada's energy minerals (specifically petroleum, gas, coal and other minerals) and facilitating exploration and development by providing geological information related to the occurrence of hydrocarbons, coal and other minerals. Report 12 is of particular interest in that it suggests a possible, new approach in the search for hydrocarbons.

R. G. Blackadar,
Chief Scientific Editor.

DISTRIBUTION OF FORAMINIFERA IN CHALEUR BAY

Project 730092

C. T. Schafer
Atlantic Geoscience Centre, Dartmouth

Seasonal sampling of dominant foraminiferal species in western Chaleur Bay was completed in December, 1974. This phase of the project was designed to identify variations in the Foraminiferal Number (the total number of specimens per cc) as a function of time and/or environment. Data analyzed to date demonstrate the practical limits beyond which the interpretation of quantitative foraminiferal faunal information derived from nearshore environments becomes relatively speculative. Environmentally dependent limits appear to be valid regardless of the number of specimens that have been counted in any given set of examples. A guiding philosophy can now be developed which considers the application for which purely quantitative data are being utilized. For example, the inclusion of rarely occurring species might be justified in quantitative environmental mapping applications but would be of questionable benefit for interpreting paleoecological variations in older sediments. Older (i.e., Pleistocene-Holocene) sediments contain fossil populations that have survived several destructive processes which can be both biological (e.g., ingestion) or physical (e.g., dissolution). The surviving specimens are usually associated with the dominant members of living populations which often are among the more morphologically robust forms.

Studies of temporal variations of species abundance in an estuarine environment were carried out at two locations (lines A and C) at the western end of Chaleur Bay (Fig. 1.1). A determination of total species diversity (D) in this area shows that the environment near line C is less stable than that found near line A. This stability difference is due primarily to the commonly shallower water depths near line C, and to the proximity of this area to discharges of relatively less saline and polluted water from the Restigouche River to the west.

There are about twelve species of foraminifera which are abundant throughout the entire study area. At line A *Eggerella advena* represents one of the two most abundant forms (Fig. 1.2). Its relative abundance increases on the south side of the bay in response to the modal direction of flow of Restigouche River water. In the deeper offshore areas near line A *E. advena* is replaced, in part, by *Spiroplectammina biformis* and *Reophax arctica*. At line C *Ammobaculities salsus*, *Reophax arctica* and *Spiroplectammina biformis* are replaced by *Ammotium cassis*. *A. cassis* and *E. advena* represent more than 90 per cent of the total population at line C and thus reflect the environmental influence of freshwater and sewage discharge into the western end of the bay.

Specimens in A- and C-line samples were compared using the coefficient of variation (V). V is proportional to the standard deviation (S) of a set of species abundance counts divided by the mean value ($\bar{X}$) of the

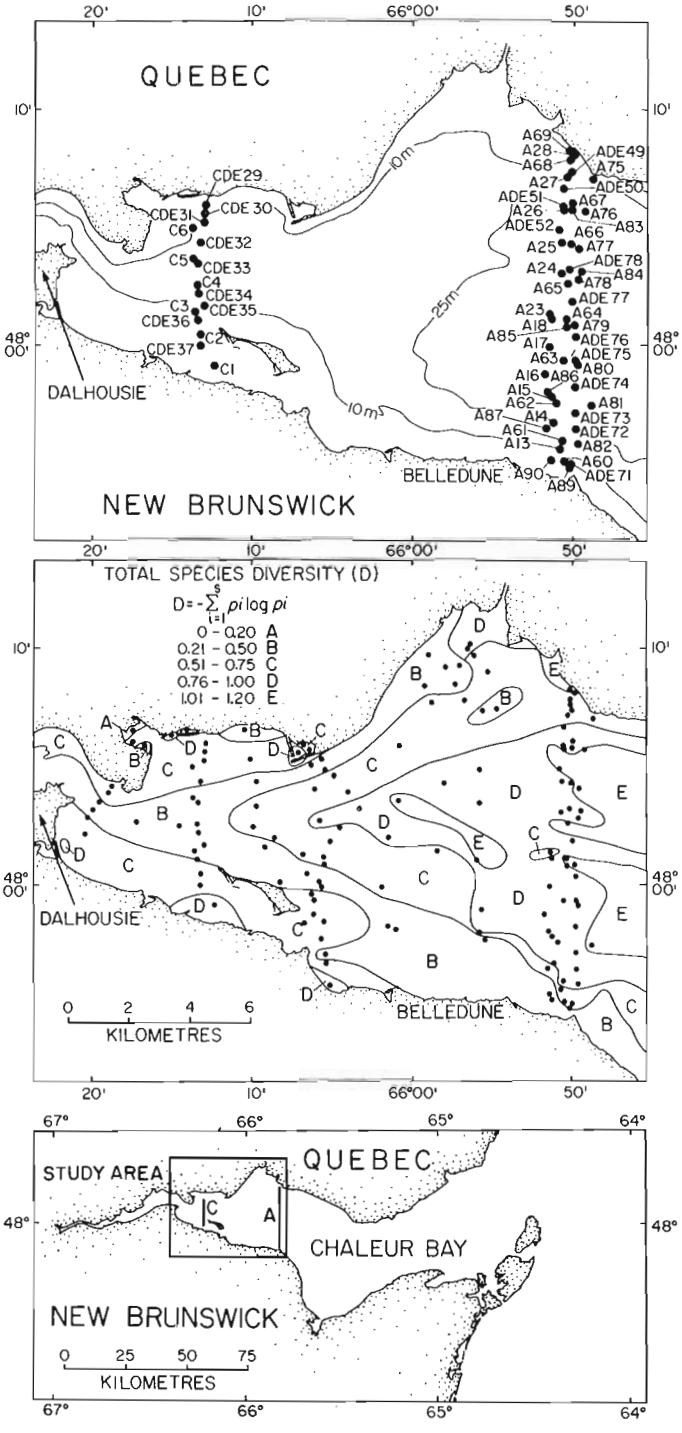

Figure 1.1. Index map, station locations and compound diversity (D) of total foraminifera populations in western Chaleur Bay.

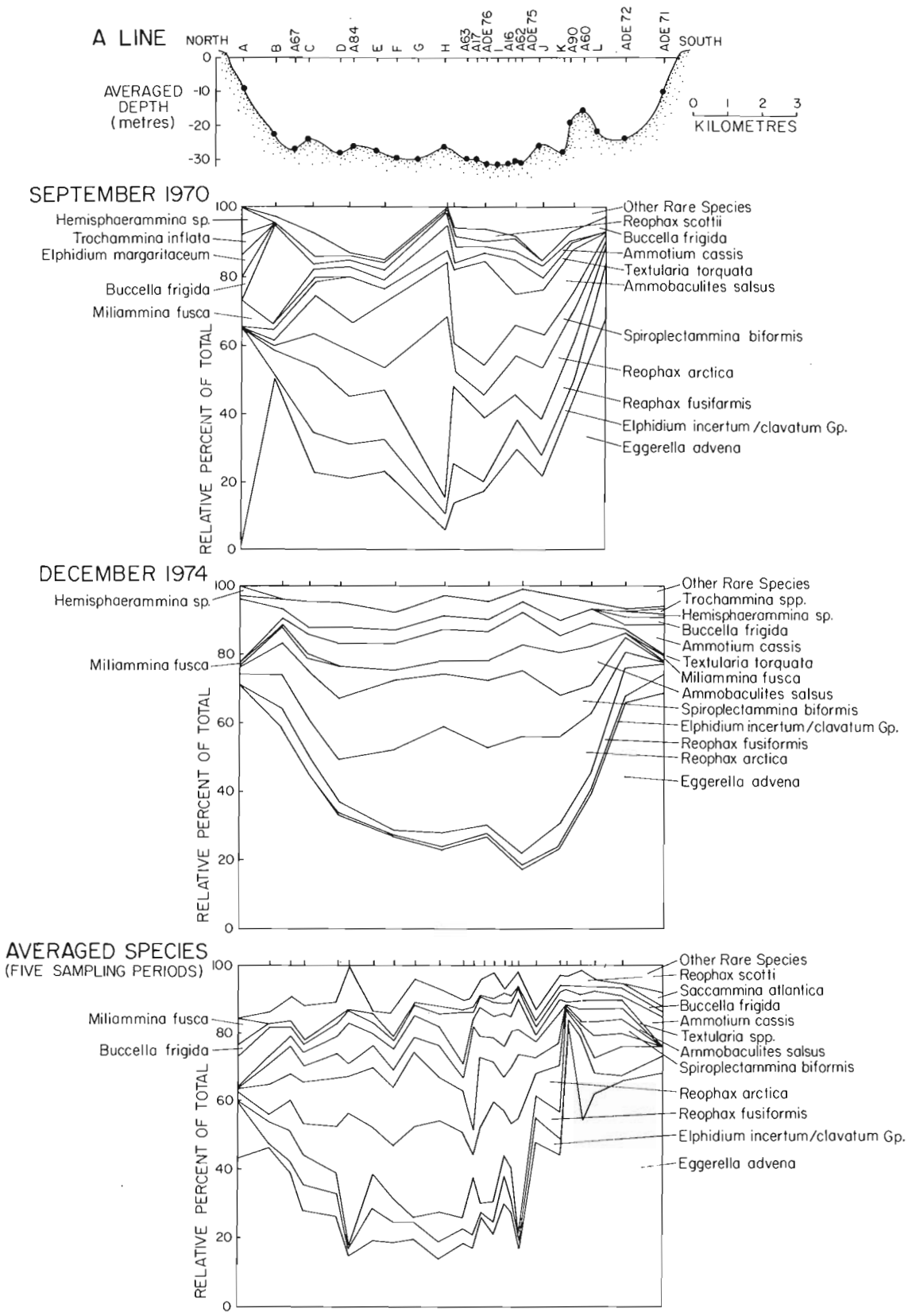

Figure 1. 2. Temporal change in the total number of dominant foraminifera at line A between September, 1970 and December, 1974. Lowermost profile shows dominant species total counts averaged over five sampling periods between 1970 and 1974.

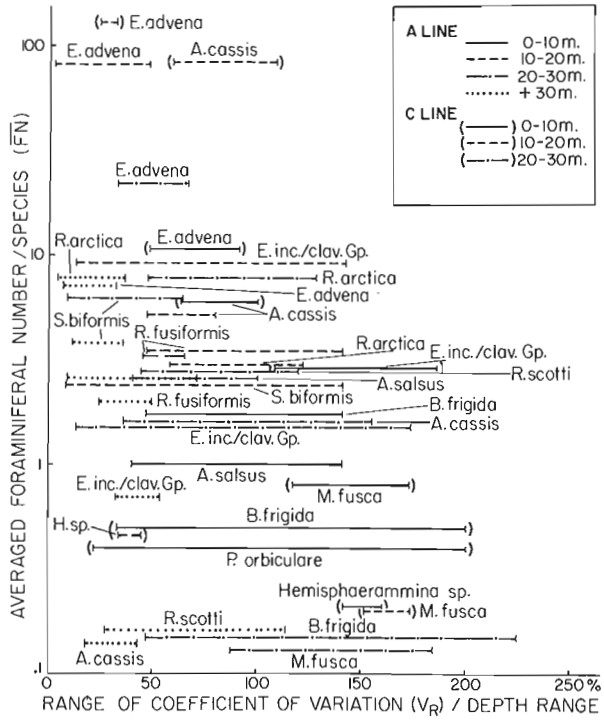

Figure 1.3. Spatial variability of dominant foraminifera species as a function of absolute abundance and mean water depth (environmental stability). Spatial variability of a species is expressed as the range of V (V_R) for several samples collected at the same locality and at various depth ranges.

counts. The quotient of this relationship is multiplied by 100 and expressed as a per cent value. A detailed analysis of temporal and spatial variations in species counts is now in preparation and will include an interpretation of the relationship between absolute abundance of specimens, distribution uniformity (V) and environmental stability (water depth). An example of this relationship among the more dominant species is summarized in Figure 1.3 which shows the decrease in maximum values of V/species ($\bar{\bar{<}}$ 110%) which occurs when the Foraminiferal Number (FN) exceeds 10. At lower values of FN, maximum values of V/species are less than 110 per cent in about half of all instances at water depths greater than 30 m, and in about 23 per cent of all instances at water depths between 20-30 m. Thus 77 per cent of all occurrences of V $\bar{\bar{<}}$ 110 per cent are related to relatively deep water (stable) conditions including those species characterized by relatively low FN values. If individual species are considered, there are repeated examples of the range of V ($V_{max_i} - V_{min_i}$) decreasing in size and shifting to the left of Figure 1.3 as water depth increases. These data show the importance of water depth (stability) in determining the degree of distribution uniformity at very low abundance levels and suggest a measure of caution when quantitatively monitoring rare forms in waters less than 20 m deep.

The regional sampling grid covering the eastern end of Chaleur Bay was completed during May and September, 1974. A map of foraminiferal biotopes and grain size distribution for the entire bay is near completion at this time.

2. FORAMINIFERA AND ORGANIC GEOCHEMISTRY OF TWO SEDIMENT CORES FROM A POCKMARKED BASIN OF THE SCOTIAN SHELF

Project 750038

G. Vilks and M. A. Rashid
Atlantic Geoscience Centre, Dartmouth

Introduction

The muddy seafloor of La Have, Emerald and Roseway basins contains crater-like depressions known as pockmarks. King and MacLean (1970) described these submarine features from echograms, side scanning sonograms and by direct observations via a submersible. The diameter of the pockmarks range from 30-400 m with a corresponding range of depths from 6-30 m.

With very few exceptions pockmarks occur in La Have clay and in those parts of the basins that are underlain by Cretaceous strata. These are the main factors that led King and MacLean (1970), to conclude that the cone-shaped features were created in the seafloor as a result of gas escaping from the Cretaceous strata. To gather more possible evidence for these theories, sediment cores were collected in the area. This report describes some aspects of organic geochemistry and foraminifera from two sediment cores, one of which was taken inside a pockmark.

Field Methods

The coring of sediment was carried out during April 1975 in conjunction with a detailed side-scan and continuous seismic survey of Emerald Basin (*see* Fig. 2.1 and McKeown, 1975). The seismic and side-scan records were used for the selection of coring sites.

Cores were taken with a Benthos piston corer fitted with a 900-kg core head and a 6.7-cm ID core barrel containing a plastic liner. Shortly after the recovery of the cores, subsamples for the determination of gases were sealed in metal cans and kept at temperatures close to 0°C.

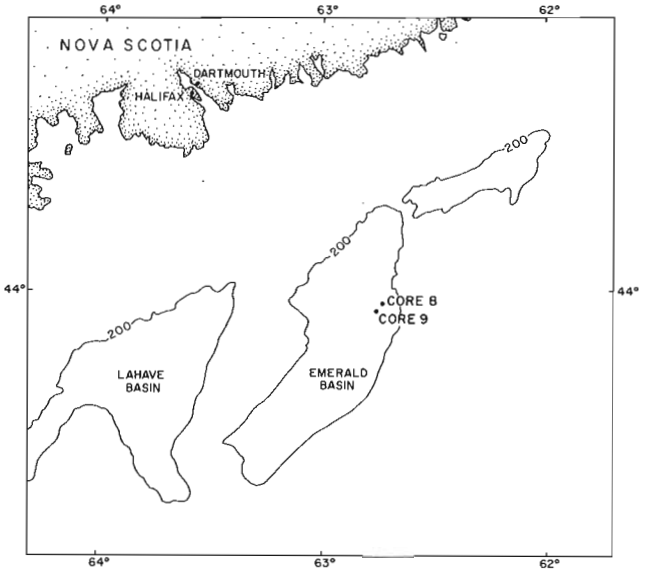

Figure 2.1. Index map showing core locations and a 200-metre isobath bordering three basins.

Analytical Methods

The geochemical parameters measured in this study are organic carbon, gaseous hydrocarbons (C_1-C_4), chlorophyll, and phaeophytin.

Organic carbon was determined on a Leco WR 12 carbon analyzer after acidification of the sediments to remove carbonates. Hydrocarbon gases were measured by degasification of the canned samples and gas chromatographic analysis as described by Rashid *et al.* (1975). Chlorophyll and phaeophytin were measured using the fluorometric method described by Yentsch and Menzel (1963).

Foraminifera were counted in sediments coarser than 125 microns and relationships of sediment texture in the various core intervals were determined by estimating the fraction of sediments coarser than 63 microns in diameter.

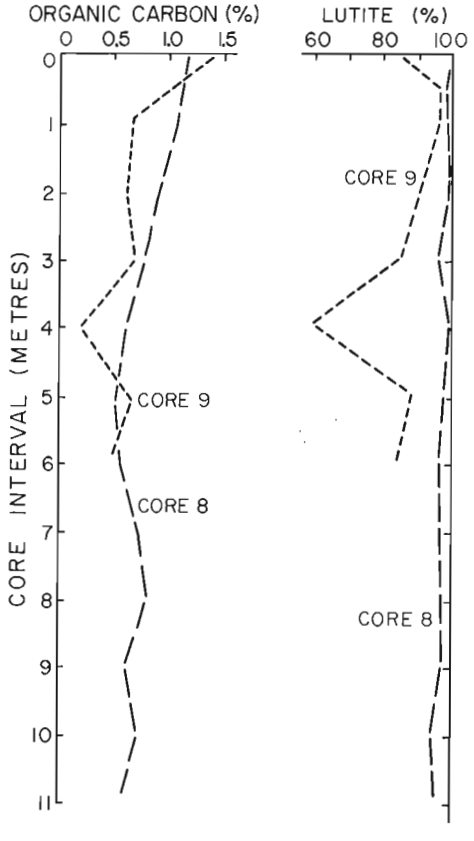

Figure 2.2. Per cent organic carbon and lutite in sediment cores.

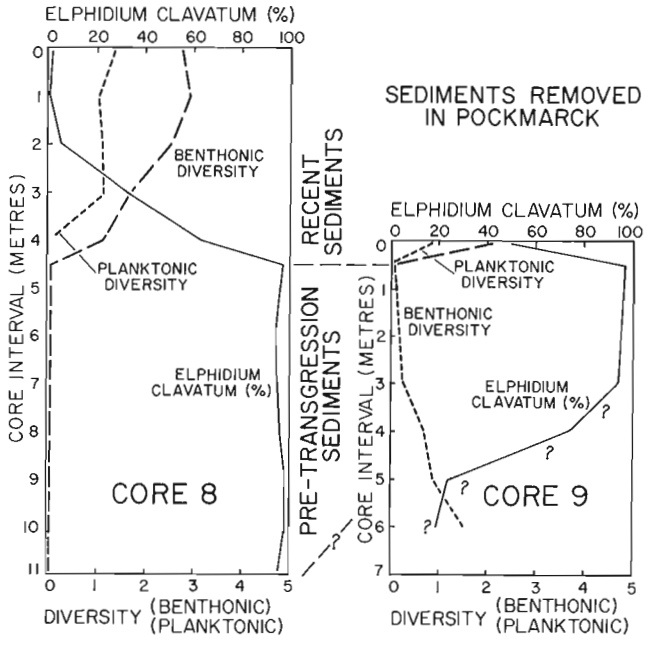

Figure 2.3. Relative per cent of *Elphidium clavatum* and the diversities of benthonic and planktonic foraminifera. (Diversity = $\sum_{i=1}^{N}$ Pi ln Pi where p is the proportion of the i th species in the sample and N is the total number of species.)

Results

With the assistance of acoustic positioning it was possible to place the corer within a few metres of a known feature on the seafloor. Core 9 was taken from inside a pockmark and core 8 from a flat bottom at a distance of 280 m from the site of core 9.

The sediments in both cores consist of dark brown lutite that decreases slightly in relative amounts with the depth of sediment. Core 9 contains coarser sediments throughout its length than core 8 and is also shorter (*see* Fig. 2.2). It seems that the sediments on the bottom of a pockmark are slightly coarser and more compact than those outside and nearby.

The foraminiferal assemblages show distinct faunal changes with depth of sediment in both cores (Fig. 2.3). In the surface layer a highly diversified benthonic foraminiferal population is present and is associated with planktonic species that are found in warm-temperate waters. The diverse continental shelf fauna is replaced by an essentially monospecific population of foraminifera dominated by the estuarine-nearshore species *Elphidium clavatum* Cushman. The faunal change occurs between 200 cm and 400 cm in core 8 and between surface and 50 cm in core 9. In core 9 the shelf fauna reappears at the bottom, and it is possible that surface sediments were resampled during core retrieval.

The sediments contain methane in amounts less than 20 ppm, which is a background value. Other geochemical results are summarized in Figure 2.2 and Table 2.1. The per cent of organic carbon is low in both cores in comparison to other basins in the Gulf of St. Lawrence (Rashid *et al.*, 1975) and Labrador Shelf (Vilks *et al.*, 1974). The amounts of preserved chlorophyll and phaeophytin are also low (*see* Table 2.1) in comparison to Chaleur Trough, where excessive methane was found in the sediment.

Conclusions

The low amounts of methane, plant pigments and organic carbon indicate that efficient oxidation of organic matter takes place at the sediment-water interface. The present day open shelf conditions are also indicated by the high diversity of foraminifera in the surface layers. The lower stand of sea level during early Holocene is reflected by the dominance of *Elphidium clavatum* in lower levels of the cores. The break between the sediments representing present day conditions and the near-shore-estuarine conditions during the early Holocene is rather sharp and may indicate a period of non-deposition or erosion.

The low amount of dissolved gaseous hydrocarbons (C_1-C_4) in the sediments of the pockmark was unexpected in view of the postulated origin of the pockmarks. However, it is possible that the movement of escaping gas takes place along a restricted funnel from a point source in the bedrock, without any lateral migration in the sediments. Therefore, dissolved seepage gas may only be detected by sampling sediments from one of these funnels.

References

King, L.H. and MacLean, B.
1970: Pockmarks on the Scotian Shelf; Geol. Soc. Am. Bull., v. 81, p. 3141-3148.

McKeown, D.L.
1975: Report of Cruise No. 75-007, AOL, Bedford Institute of Oceanography, Dartmouth, N.S.

Rashid, M.A., Vilks, G., and Leonard, J.D.
1975: Geophysical environment of a methane-rich Recent sedimentary basin in the Gulf of St. Lawrence; Chem. Geol., v. 15, p. 83-96.

Vilks, G., Rashid, M.A., and van der Linden, W.J.M.
1974: Methane in Recent sediments of the Labrador Shelf; Can. J. Earth Sci., v. 11, no. 10, p. 1427-1434.

3. PROGRESS IN THE ESTABLISHMENT OF A CURATION FACILITY FOR GEOLOGICAL SAMPLES

A. G. Sherin
Atlantic Geoscience Centre, Dartmouth

The decision to establish a curation facility at the Atlantic Geoscience Centre was made in late 1973. A curator was hired in August 1974 and he and management established the following objectives for the facilities.

1. The facilities should provide orderly and appropriate storage for all geological samples acquired.
2. They should provide a system for easy retrieval of any and all samples.
3. They should provide a useful resource of geological sample material for geoscientists.
4. They should provide a data base of basic location and field information on samples acquired by the Centre and those taken in conjunction with Atlantic Geoscience Centre projects.
5. They should provide the basis for the extension of the primary data base to include information on analyses of sample material.
6. They should provide a basis for information exchange with other institutions.

In the summer of 1974 the new curator found that construction of the repository was nearing completion and that the inventory of sample material was stored haphazardly in a large number of separate locations. After consolidating the inventory under one roof in the repository it was found that the inventory occupied almost 90 per cent of the available space. A considerable amount of material was found to be unidentifiable. Basic location information was unknown for an even larger amount of material.

The curator initiated a "macro" inventory and researched annual reports, cruise reports, and personal records of various scientists and almost eliminated the unidentifiable material and found a large amount of location information. Finding location information was and still is hampered by the fact that many scientists who worked at the Bedford Institute of Oceanography in the 1960's, have left to work elsewhere.

In the last year several steps have been taken to meet the objectives listed above:

1. A prototype field data acquisition system was designed and is being used by all Atlantic Geoscience Centre scientists and several hydrographers of the Canadian Hydrographic Service during the 1975 field season. It is currently being evaluated (Autumn, 1975) and will be modified if necessary.
2. A data file containing all basic location and field information on samples as obtained from the field data acquisition system and other sources is in the final stages of development and will use on an experimental basis the MARS vi file management package available at the departmental Computer Science Centre in Ottawa.
3. A sample distribution policy was proposed by the Curation Committee and accepted by management. The curator's office has processed ten requests from scientists from outside the Centre within the last year under the conditions of this policy. Also under the conditions of this policy the curator has accepted samples from four non-government agencies for inclusion in the curation system.
4. A detailed inventory of all recently acquired samples has been undertaken and this will be extended to include all samples as manpower resources allow. The issuing of a contract to accomplish this inventory is being considered.

The curator wishes to expand the services offered by providing the results of routine procedures such as core descriptions and core photography.

The new systems will also be linked to and compatible with the systems established at the Atlantic Geoscience Centre for the storage and retrieval of geophysical data and documents (Shih (Feb. 1972), Shih (April, 1972), Sparkes *et al.* (1972), Ross *et al.* (1973), Shih (1973), Shih (1974)), the curation system developed jointly by the Eastern Petroleum Geology Subdivision and the Resource Management and Conservation Branch for eastern Canada offshore and onshore well and outcrop samples, and the well data system under development at AGC Shih *et al.* (1974).

In the future, the establishment of analytical data files directly linked to the primary field data file will result in a geological data base which will be an invaluable resource to any scientist undertaking research in the geoscience in eastern Canada.

References

Ross, D.I., Shih, K.G., Johnston, B.L., and Porteous, D.
Computor Note/B1-C-73-3/ Sept. 1973
GEOFILE A Revised Manual on the Storage and Retrieval of Geophysical Data.

Shih, K.G.
Computor Note/B1-C-72-1/Feb. 1972
Marine Geophysical Data Presentation Part 1

Computor Note/B1-C-72-2/April 1972
Marine Geophysical Data Presentation Part II

Report Series/B1-R-73-13/Sept. 1973
Shipboard Computor Systems for the Processing and Display of Bathymetric, and Magnetic Data at Sea.

Shih, K. G. (cont.)
AGC Marine Geoscience Data Storage and retrieval system *in* Computer Use in Projects of the Geological Survey of Canada, Terry Gordon and W. W. Hutchison (editors); Geol. Surv. Can., Paper 74-60, p. 85-89.

Shih, K. G., Hardy, I. A., and Sherin, A. G.
Subsurface data system at the AGC *in* Computer Use in Projects of the Geological Survey of Canada, Terry Gordon and W. W. Hutchison (editors); Geol. Surv. Can., Paper 74-60, p. 91-94.

Sparkes, R.
Haworth and Cousins Report Series/B1-R-72-5/ July 1972 Document Storage and Retrieval.

4. AGE AND DEPOSITIONAL ENVIRONMENT OF THE LOWER PART OF ESCALANTE FORMATION, WESTERN VANCOUVER ISLAND, BRITISH COLUMBIA (92E)

Project 490001

J. A. Jeletzky
Institute of Sedimentary and Petroleum Geology, Ottawa

Introduction and Acknowledgments

The upper part of Division A (present Escalante Formation) of Nootka Island was dated definitively (Jeletzky, 1954, 1973, p. 338, 339, 341, 342, Fig. 1) as of the general Lincoln (i.e., late Refugian or early to middle Oligocene) age. However, the exact age of the, in general, rarely fossiliferous lower part of this formation and of the correlative lower part of the Escalante Formation (Bancroft, 1937) of Hesquiat Peninsula was left in doubt (Jeletzky, 1973). Although strongly suggestive of the Lincoln age of these beds,

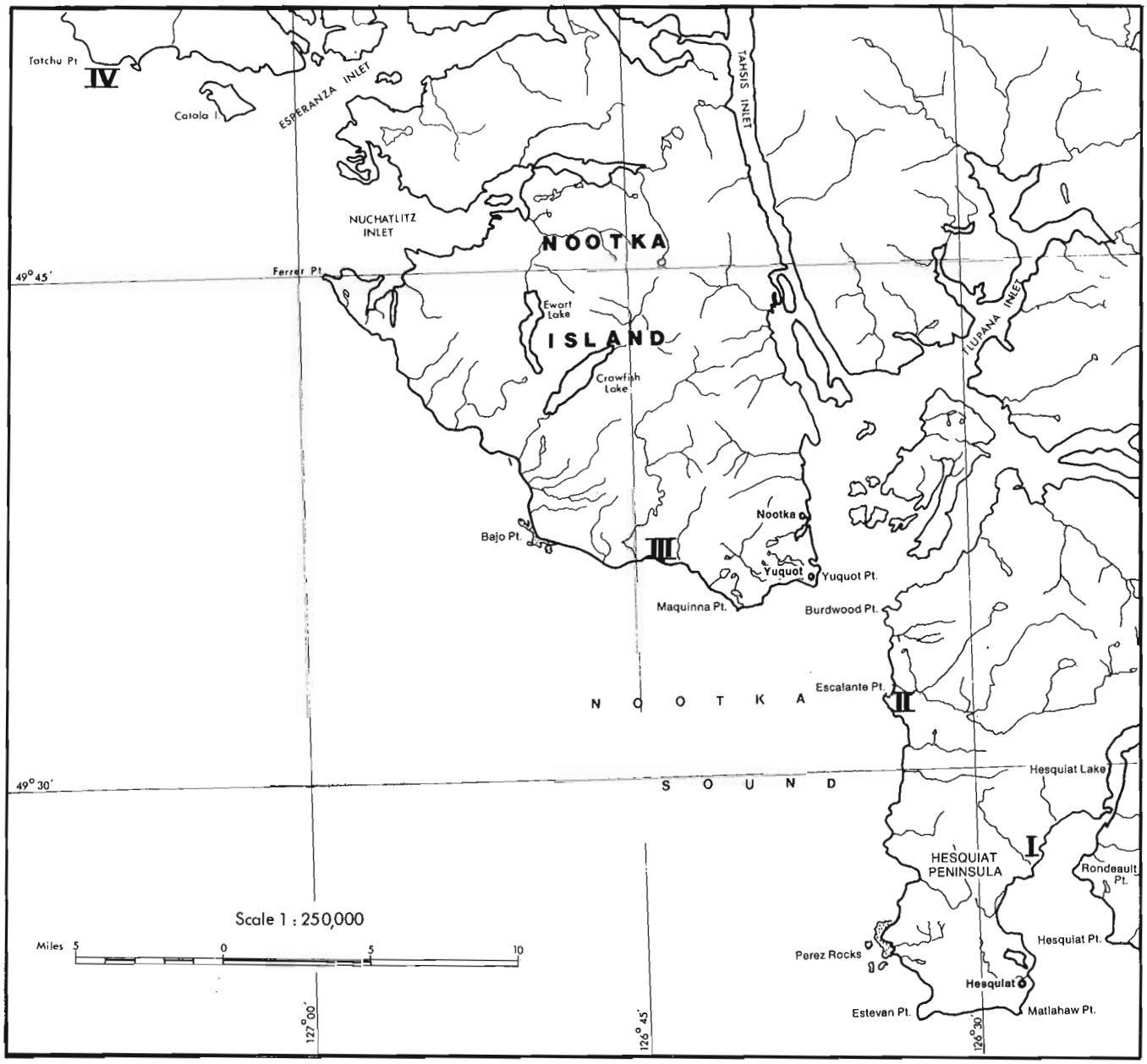

Figure 4.1. Index map of the Esperanza Inlet-Hesquiat Peninsula, western Vancouver Island, B.C. Described sections of Escalante Formation are marked by Roman numbers.

the macrofossil evidence then available was judged insufficient to deny categorically the validity of their latest Eocene dating based on an undocumented identification of the *Bulimina schencki* fauna (Cameron, 1971, 1972).

A subsequent study of some diagnostic molluscs found in the basal beds of the Escalante Formation provides conclusive evidence of their early Lincoln (= late Refugian) age. This paper presents this evidence, together with additional evidence indicating an exclusively shallow-water origin of the Escalante Formation.

Dr. Joseph H. Peck and Dr. Wyatt Durham, University of California, Berkeley, kindly loaned original specimens of several diagnostic Lincoln gastropods from the State of Washington, U.S.A., which were figured in Durham's (1944) paper. The present writer was permitted to refigure some of these specimens. Dr. Ellen J. Moore, U.S. Geological Survey, San Diego, California, generously provided original specimens and photographs of several diagnostic gastropods from the Pittsburg Bluff Formation of Oregon. Dr. Warren O. Addicott, U.S. Geological Survey, Menlo Park, California, kindly advised the writer about the nomenclature and geological occurrences of some gastropods discussed in this paper, identified two particularly difficult gastropod specimens, critically read the manuscript, and gave other valuable paleontological and biochronological advice. The writer gratefully acknowledges this help and advice but assumes full responsibility for conclusions made on the basis of this information.

Stratigraphy and Depositional Environment

The writer (Jeletzky, 1954, p. 23) did not adopt the name "Escalante Formation" for the basal division of Tertiary rocks outcropping in the Hesquiat-Nootka area and elsewhere on the west coast of Vancouver Island because of the inadequacy of the type locality proposed by Bancroft (1937, p. 8). Because the name was more recently used by Cameron (1971, p. 92; 1972, p. 201; 1973), the name Escalante Formation will now be used in this paper instead of Division A as used by Jeletzky (1954).

Approximate locations of principal sections of the Escalante Formation discussed in this paper are indicated by Roman numbers in Figure 4.1. These sections are similarly numbered and discussed in the same order in the following text for the convenience of the reader.

I. EAST SIDE OF HESQUIAT PENINSULA

Diagnostic gastropods have been obtained from the section of the Escalante Formation measured across the Tertiary fault block that has been mapped and briefly described by Jeletzky (1954, p. 24, geol. map 2). This section is situated about 2112 m (1.3 miles) north of Leclaire Point. The downward succession of beds is as follows:

Division C (basal part)

4. Shale, brownish grey when weathered, dark grey when fresh, fissile, soft; no concretions noted; top concealed and evidently faulted some 144 m (480 ft.) north of the mouth of a small creek; contact with unit 3 poorly exposed but appears to be gradational; visible on the tidal flat up to 105 m (350 ft.) (est.).

Escalante Formation
(= Division A)

3. Sandstone, brownish grey, very thickly bedded, calcareous, mostly coarse grained, surface locally honeycombed; calcareous concretions are very rare or absent; includes two or three beds of fine pebble-conglomerate, grey, rich in sandy matrix; pebbles composed of volcanic and intrusive rocks, including granitic pebbles probably derived from the Coast Intrusions; no fossils seen; thickness 60 m (200 ft.) (est.).

2. Interbedding of lenticular beds 15 cm (6 in.) to 1.5 m (5 ft.) thick of sandstone and conglomerate; sandstone green-grey, coarse grained, gritty, resistant, poorly sorted and rounded (greywacke type); conglomerate, pebble, medium to coarse, dull grey; pebbles consist exclusively of the intrusive and volcanic rocks of the Vancouver Group and the Coast Intrusions; abundant arenaceous and gritty matrix between the pebbles; a bed of a coarse pebble to boulder conglomerate 1.8 to 3 m (6 to 10 ft.) thick at the base; contact with unit 3 apparently conformable, that with unit 1 is a marked angular discordance.

Macroinvertebrate fauna (GSC loc. 21739) collected from pebbly sandstone and sandy matrix of pebble- conglomerate immediately above the basal conglomerate bed includes (writer's identifications, except where otherwise indicated): a crab claw possibly of *Eumorphocorystes naselensis* Rathbun; *Siphonalia* cf. *wheatlandensis* (Clark and Anderson) (identified by Dr. Warren O. Addicott); *Molopophorus stephensoni* Dickerson; *Molopophorus effingeri* Weaver; *Polinices* (*Polinices*) cf. *P. washingtonensis* Weaver; indeterminate gastropods; cf. *Pachydesma gastonensis* (Clark) (mass occurrence), *Acila* (*?Truncacila*) sp. indet., indeterminate pelecypods (common), *Dentalium* (sensu lato) sp. indet.; thickness 90 m (300 ft.) (est.).

Karmutsen Group (metamorphic facies)

1. Volcanic rocks (apparently metamorphosed volcanic tuffs and ?felsitic lavas), green-grey, schistose, thinly bedded, mildly metamorphosed, sheared, faulted and cut by quartz veinlets; visible to the sea level; 45 m (150 ft.) (est.).

Depositional Environment of Unit 2

The apparently lower littoral to inner neritic (abundance of deeply burrowing pelecypods, absence of *Mytilus*) fauna of GSC locality 21739 is characterized by

the prevalence of well- to excellently preserved, complete shells with little or no sign of abrasion. The thick-shelled pelecypods are invariably single valves with well-preserved beaks, while most gastropods retain the delicate initial coils. This mode of preservation is unusual for fauna occurring in "pockets" of finer grained sediment wedged in between large pebbles and boulders of an evidently marginal marine conglomerate (a pebble beach deposit). It suggests that the predominantly dead animals (as indicated by a total absence of articulated shells) were washed out of their normal lower energy habitat during unusually strong storms, and deposited in the supratidal zone of the Escalante sea and, equally rapidly, permanently buried there. The fauna could hardly have been buried in an intertidal environment since shells deposited within the intertidal zone of an unprotected pebble to boulder beach are invariably moved around, buried and reburied repeatedly before being covered permanently. Such shells should have been much more fragmented and abraded than are the shells of GSC locality 21739 (compare with the oysters of Tatchu Creek fauna described below). The hypothesis of Cameron (1971, p. 92), suggesting a redeposition of macrofossils of the Escalante Formation in bathyal depth by turbidity currents (or for that matter by any kind of plastic flow in the sense of Dott, 1963) is considered to be most unlikely in view of their state of preservation. Such redeposition (*see* Jeletzky, 1973, p. 345) should result in fragmentation, scattering, and abrasion of shells, all of which is absent in the fauna concerned. The coarse clastics of unit 2 of the section described are, therefore, inferred to be supratidal deposits of early Escalante time marking the eastern shoreline of that sea.

II. TYPE LOCALITY OF ESCALANTE FORMATION

As pointed out by Jeletzky (1954, p. 22, 23), the type locality of the Escalante Formation is not a well-exposed succession and is poorly fossiliferous. No diagnostic fossils have been found in the lower part of the formation exposed on the northwestern side of Escalante Point (Jeletzky, 1954, p. 23). However, these poorly fossiliferous beds are considered to be correlative with the reliably dated basal beds of the Escalante Formation on the eastern side of Hesquiat Peninsula and on the southeastern coast of Nootka Island because of similar stratigraphic position and an identical lithology.

Thick-shelled, littoral to inner neritic pelecypods (deeply burrowing) and other shallow-water molluscs (gastropods, scaphopods) occur locally in the lower part of the type section of the Escalante Formation (e.g., GSC loc. 20527; *see* Jeletzky, 1954, p. 23). The actual mode of preservation of the fossils, characterized by prevalence of shell-covered, complete specimens, is similar to that of the previously discussed fauna of GSC locality 21739. However, it was not possible to extract any shell-covered, complete, definitively identifiable specimens from the extremely indurated rocks at this locality. Thus, this fauna is "poorly preserved" in that sense. The above preservation suggests a similar supratidal mode of burial for the marine fauna of the lower part of the type Escalante Formation. The fauna evidently was buried near its original habitat and was not redeposited in a bathyal environment.

An apparently complete absence of oysters and any other brackish water molluscs in the lower part of the type Escalante Formation (and elsewhere on Hesquiat Peninsula) indicates a normal salinity of the Escalante sea in this area in contrast to the Tatchu Point area (*see* below).

III. SOUTHEASTERN COAST OF NOOTKA ISLAND

The diagnostic Lincoln age pectinid — *Chlamis (Vertipecten) porterensis* — was obtained from the following section of the Escalante Formation (formerly Division A; *see* Jeletzky, 1954, 1973) measured in the coastal bluff at the point 180 to 210 m (600 to 700 ft.) northwest of Marble Creek. The downward sequence comprises:

Escalante Formation (lower part)

6. Sandstone, greenish grey, fine to medium grained, calcareous and with a pronouncedly honeycombed surface; no concretions seen; top cut off by a fault; visible up to 6 m (20 ft.) (est.).
5. Pebble-conglomerate, grey, fine; minor lenticular beds and thin layers of calcareous, coarse grit with honeycomb-like weathered surface occur most commonly near the top of the unit; grades upward into unit 6; thickness 6-7.5 m (20-25 ft.) (est.).
4. Grit, dark green to green-grey, coarse to medium; numerous interbeds of pebble-conglomerate as in bed 5; specimen of *Chlamis (Vertipecten) porterensis* (Weaver) was collected *in situ* in the middle part of the unit (GSC loc. 20732); grades downward into unit 3; thickness 30 m (100 ft.) (est.).
3. Pebble-conglomerate, grey, fine (much as in bed 5); interbedded with lenses and pods of coarse grit (as in bed 4) and sandstone; locally some lenses and pods of coarse-pebble conglomerate; all rock varieties poorly rounded and sorted as to the clast size; contact with bed 2 abrupt and uneven; thickness varies from 5.4 to 7.5 m (18-25 ft.).
2. Conglomerate, very coarse, consists largely of big boulders and blocks of volcanic rocks, up to 4.5 m (15 ft.) in diameter, locally derived from unit 1; boulders of granitoid rocks occur locally; groundmass consists of pebble-conglomerate and sandstone; rests discordantly on deeply eroded surface of unit 1; thickness varies from 0.6 to 2.4 m (2-8 ft.).

Karmutsen Subgroup (uppermost part)

1. Volcanic tuff, dark grey to greenish grey, ?basic, fine grained and very thinly bedded; interbeds of coarse-grained volcanic tuff; base concealed at base of bluff; visible up to 15 m (50 ft.).

PLATE 4. 1

Figure 1. *Ostrea* (sensu lato) *lincolnensis* Weaver, 1916. GSC loc. 18490; GSC No. 43076. Lincoln molluscan Stage (lower to middle Oligocene). Escalante Formation (Sandstone-conglomerate member), Vancouver Island, west coast. At the tip of nameless rocky point situated about 0. 5 km (0. 3 mile) east-southeast of Tatchu Point. Fig. 1a. View of the right valve; Fig. 1b. View of left valve. 1c. Posterior view of both valves; 1d. View of the beak and hinge from above. All photographs are natural size.

Figure 2. *Chlamis* (*Vertipecten*) *porterensis* (Weaver, 1912). GSC loc. 20732; GSC No. 43077. Lincoln molluscan Stage (lower to middle Oligocene). Escalante Formation (basal beds). Nootka Island. Shore bluff situated 182 to 213 m (600-700 ft.) northwest of Marble Creek; middle part of unit 4 (*see* text for details). Photograph of a rubber mould made from an imprint in the rock, xl.

Figure 3. *Molopophorus stephensoni* Dickerson, 1917. Hypotype. GSC loc. 21739; GSC No. 43078. Basal part of Lincoln molluscan Stage (*Molopophorus stephensoni* Zone). Escalante Formation (basal conglomerate); near the base of unit 2 (*see* text for details). Eastern side of Hesquiate Peninsula; on tidal flat about 2 km (1. 3 mile) northwest of Leclaire Point. Fig. 3a. Apertural view, xl; Fig. 3b. Nonapertural view, xl. An exceptionally large representative closely matching that figured by Durham (1944, Pl. 18, fig. 1; *see* this report, fig. 5).

Figure 4. ?*Siphonalia* cf. *wheatlandensis* (Clark and Anderson, 1938). Hypotype. GSC loc. 21739; GSC Cat. No. 43079. *See* description of Figure 3 for further details. Fig. 4a. Apertural view, xl; 4b. Nonapertural view, xl. Figs. 4c and 4d. Same views as in 4a and 4b but x2, to show structural detail. A juvenile shell apparently belonging to this species. Identified by Dr. Warren O. Addicott, U. S. G. S. , Menlo Park, Calif. , U. S. A.

Figure 5. *Molopophorus stephensoni* Dickerson, 1917. Hypotype. University of California Cat. No. 33599; Loc. 3607. Reproduction of the presumably adult representative figured by Durham (1944, Pl. 18, fig. 1). Introduced for comparison with the Canadian representative of the species. Fig. 5a. Apertural view; Fig. 5b. Nonapertural view; Fig. 5c. Apical view. All photographs are natural size.

Figure 6. *Siphonalia* cf. *wheatlandensis* (Clark and Anderson, 1938). Hypotype. GSC loc. 21739; GSC No. 43080. *See* description of Figure 3 for further details. Fig. 6a. Apertural view, xl; Fig. 6b. Nonapertural view; xl. A somewhat deformed and mostly weathered representative of the species. Identified by Dr. Warren O. Addicott, U. S. G. S. , Menlo Park, Calif. , U. S. A.

Figure 7. *Molopophorus effingeri* Weaver, 1942. Hypotype. GSC loc. 21739; GSC No. 43343. *See* description of Figure 3 for further details. Fig. 7a. Apertural view, xl; 7b. Nonapertural view, xl; 7c. Same view as in 7a, x3; 7d. Same view as in 7b, x3. An internal cast of a large, originally complete specimen (early whorls destroyed during extraction from the rock) closely resembling the holotype (*see* Weaver, 1942, Pl. 90, Figs. 2, 3) in general proportions but preserving some of the diagnostic radial ornament (cf. Fig. 9).

Figure 8. *Molopophorus effingeri* Weaver, 1942. Hypotype. GSC loc. 21739, GSC No. 43081. *See* description of Figure 3 for further details. Fig. 8a. Apertural view, xl; Fig. 8b. Same view as last, x3; Fig. 8c. Nonapertural view, x3; Fig. 8d. Apical view, x3. An internal cast of an originally complete specimen (early whorls destroyed during extraction from the rock) closely resembling the holotype (*see* Weaver, 1942, Pl. 90, figs. 2, 3) in general proportions and an almost complete secondary obliteration of the diagnostic radial ornament (cf. Fig. 9).

Figure 9. *Molopophorus effingeri* Weaver, 1942. Hypotype. University of California Cat. No. 35361; Loc. A1802. Reproduction of an exceptionally well preserved representative figured by Durham (1944, Pl. 18, Fig. 11). Introduced for comparison with the Canadian representatives of the species. Fig. 9a. Apertural view, xl; Fig. 9b. Nonapertural view, xl; Fig. 9c. Apical view, xl; Figs. 9d-9f. The same views as in Figs. 9a-9c respectively but x3 to show structural detail.

Figure 10. *Molopophorus effingeri* Weaver, 1942. Hypotype. GSC loc. 21739; GSC No. 43082. *See* description of Figure 3 for further details. Fig. 10a. Apertural view, xl; Fig. 10b. Nonapertural view, xl; Fig. 10c. Apical view, x3; Fig. 10d. Apertural view, x3; Fig. 10e. Nonapertural view, x3. An originally complete specimen (early whorls destroyed during extraction from the rock) with considerable patches of typically sculptured shell (note characteristic radial ornament) preserved.

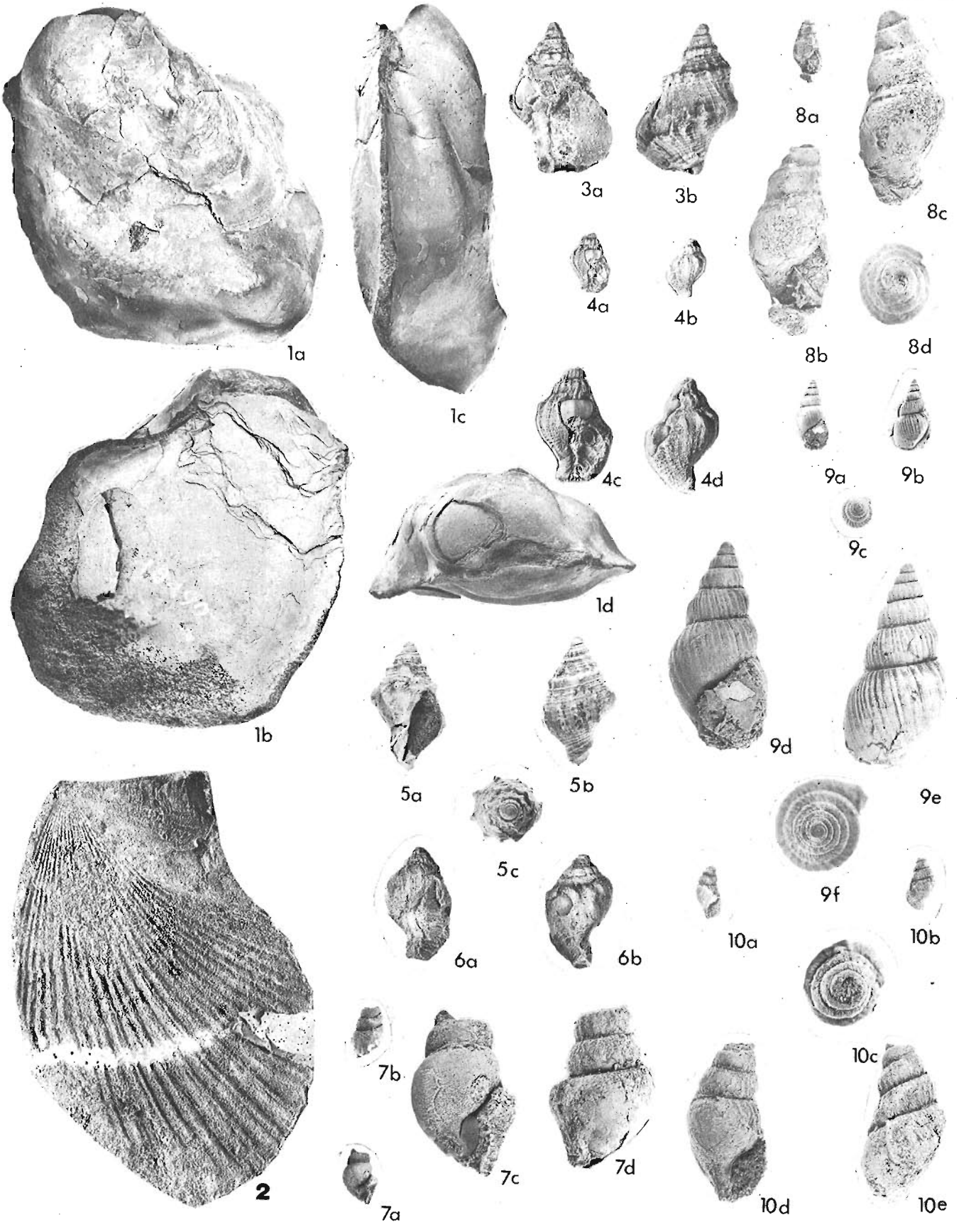
1a
1c
3a
3b
8a
8c
4a
4b
8b
8d
1b
4c
4d
9a
9b
9c
1d
9d
5a
5b
9e
5c
9f
10a
10b
6a
6b
10c
2
7b
7c
7d
10d
10e
7a

Depositional Environment of Unit 6

The good preservation of ribbing pattern and anterior ear of the solitary specimen of *Chlamis* (*Vertipecten*) *porterensis* found at GSC locality 20732 (Pl. 4. 1, fig. 2) contradicts the assumption (Cameron, 1973, p. 20) that neritic molluscs of the Escalante Formation had been redeposited into the bathyal environment either by turbidity currents or by any kind of plastic flow. That part of the shell (an imprint) now missing obviously was lost because of recent weathering rather than through a pre-burial fragmentation of the shell. As shown by Jeletzky (1973, p. 344), the lithology of units 6 to 2 inclusive also indicates the shallow-water origin of the lower part of the Escalante Formation in the above-described and other sections measured on Nootka Island.

IV. TATCHU POINT

The lower part of the Escalante Formation (formerly Division A; *see* Jeletzky, 1954, p. 17) outcropping on both sides of Tatchu Point at the mouth of Esperanza Inlet (Jeletzky, 1950, p. 44-46, geol. map) yielded only invertebrates suggestive of the Lincoln age (Jeletzky, 1973, p. 338, 342). However, its fauna is extremely important from a paleoecological and paleobathymetrical standpoint.

Most of the macroinvertebrate faunas collected in the local Sandstone-conglomerate member of the formation (Jeletzky, 1950, p. 44-46) include a moderate to large proportion of *Ostrea* (sensu lato) shells (e. g., GSC locs. 18378, 18388, 18389, 18391, 18490). All identifiable specimens belong to *Ostrea* (sensu lato) *lincolnensis* Weaver (*see* Pl. 4. 1, figs. 1a-1d). The shells are generally more or less worn, single, commonly fragmentary valves. A few shells, however, are preserved in a life-like position with valves closed or only slightly displaced in relation to one another (*see* Pl. 4. 1, figs. 1a-1d). The oysters, therefore, were buried either exactly, or close to, where they lived. The oyster-bearing sediments of the Sandstone-conglomerate member of the Escalante Formation of the Tatchu Point outcrop-area must have been deposited in a high energy, intertidal (i. e., littoral) environment which facilitated disarticulation, abrasion or even fragmentation of most, locally derived oyster shells. An almost complete absence of deeply burrowing pelecypods and the common occurrence of shallow-water, ornate gastropods (*Epitonium, Priscofusus, Bruclarkia*) agree well with this conclusion. No supratidal environment comparable with that of the eastern side of Hesquiat Peninsula (*see* above) is apparent in any of the studied sections of the Sandstone-conglomerate member within the Tatchu Point outlier.

The lithology of the Sandstone-conglomerate member is similar to that of the equivalent beds of Escalante Formation outcropping on Nootka Island (*see* Jeletzky, 1973, p. 344) and Hesquiat Peninsula (*see* preceding sections of this report). It agrees well with the predominantly intertidal origin of the member inferred from its paleoecology.

An unusual abundance of variously shaped, well-preserved burrows and, locally, strong bioturbation appear to be peculiar features of the Tatchu Point sections of the Sandstone-conglomerate member, especially of its finer grained, calcareous interbeds. These intensely burrowed and bioturbated sandstones were probably deposited in a relatively low energy, lowermost littoral or even innermost neritic environment.

The common to abundant occurrence of oyster shells in the lower part of the Escalante Formation of the Tatchu Point outlier and their apparent absence in correlative beds elsewhere in the report-area indicate an appreciably lowered salinity of sea water in the Tatchu Point area. It is a well known fact that oysters survive best in considerable to large numbers in brackish water conditions which prevent a large-scale invasion of their strictly stenohaline, carnivorous enemies such as starfishes, octopi, and others.

From the above, it is inferred that a relatively large or ?major, westward- or ?southwestward-flowing river draining the tectonic land of Vancouver Island, debouched into the early Escalante sea just east of Tatchu Point. Because of the well-documented, gradual regional subsidence of the west coast of Vancouver Island in Escalante (i. e., early to mid-Oligocene) time after the initial transgression of the early Oligocene sea (*see* Jeletzky, 1973, p. 344), the writer assumes that the local Sandstone-conglomerate member of the Tatchu Point outlier, as defined by Jeletzky (1950, p. 44-46), was deposited on intertidal flats at the mouth of an estuary, rather than in an outer deltaic or lagoonal environment. The western shoreline of early to mid-Oligocene Vancouver Island must have been situated no more than a couple of miles east of Tatchu Point.

The data presented are incompatible with Cameron's (1973, p. 20) conclusions that the basal Tertiary beds in the Kyuquot Sound-Esperanza Inlet area contain bathyal-water foraminifera, insofar as these conclusions are based on study of this principal Tertiary outlier of the area. As pointed out by the writer, the lower part of the Escalante Formation of Tatchu Point outlier is of a shallow-water origin and consists, either exclusively or predominantly, of intertidal deposits which formed in a brackish water environment. A redeposition of these sediments by turbidity currents or plastic flow of any kind is improbable because of the above-mentioned sedimentological and paleoecological evidence. Cameron's (1973, p. 20) conclusions on the subject are considered therefore to be erroneous.

BIOCHRONOLOGY

Among the fossils of GSC locality 21739 so far identified (*see* previous section of this report), the gastropods *Molopophorus stephensoni* Dickerson, 1917, and *Molopophorus effingeri* Weaver, 1942 are reliable index fossils of the early to middle Oligocene Lincoln Stage of the macrofossil standard (*see* Jeletzky, 1973, Fig. 1). Neither of these two gastropods has been found in older or younger units of the western North American faunal province since the original recognition of their time-ranges in northwestern part of the State of Washington,

U. S. A. (Durham, 1944, p. 111, 112, Fig. 7, faunal checklists 3-6). To document the exact nature of these gastropods, some of their best-preserved representatives are reproduced (Pl. 4. 1, figs. 3, 7, 8, 10) alongside well-preserved representatives of the same species from classical localities in the State of Washington (Pl. 4. 1, figs. 5, 9).

Dr. Warren O. Addicott kindly identified two additional gastropod specimens from GSC locality 21739 (Pl. 4. 1, figs. 4, 6). He states (written comm., April 29, 1975): "GSC Catalogue No. 43080 is a somewhat deformed specimen but sufficiently well preserved, in my opinion, to permit identification. The specimen appears to be a *Siphonalia* on the basis of overall proportions, sculpture, and shape of the body whorl. It is close to *S. wheatlandensis* Clark and Anderson (1938); I would identify it as *S.* cf. *wheatlandensis* Clark and Anderson. This is a Refugian ("Lincoln" Stage) species from the Great Valley of Central California. It fits in perfectly well with your determination for this part of the Escalante Formation".

"GSC Catalogue No. 43079. This small specimen appears, to me, to be conspecific with the above (GSC No. 43080). The high position of the noded angulation of the body whorl rules out the possibility of it being a *Molopophorus*, as does the relatively high spire including strongly angulated whorls. The sculpture and shape of the whorls are, to my eye, extremely close to GSC No. 43080. Admittedly, it is very difficult to identify minute specimens such as this one with complete confidence".

In northwestern Washington, U. S. A. *Molopophorus effingeri* is restricted to the lower part of the Lincoln Stage comprising the zones of *Molopophorus stephensoni* and *Molopophorus gabbi* of Durham (1944, p. 112, 116, 118, 119, 170, Fig. 7). It was not known anywhere outside of that area prior to its discovery in the report-area.

Molopophorus stephensoni has an even more limited time range than *M. effingeri*, being restricted to the basal beds of the Lincoln Stage in the northwestern part of the State of Washington which constitute the *Molopophorus stephensoni* zone (Durham, 1944, p. 112, 116, 118, 171, Fig. 7). Unlike *M. effingeri*, this species also occurs in the Oligocene Pittsburg Bluff Formation of the western part of Oregon (Dickerson, 1917, p. 177, Pl. 30, figs. 10a, b).

The combined evidence of *M. stephensoni*, *M. effingeri*, and *Siphonalia* cf. *wheatlandensis* Clark and Anderson amply demonstrates the early Lincoln (i. e., zone of *Molopophorus stephensoni* of Durham, 1944) age of the basal beds of the Escalante Formation on the eastern side of Hesquiat Peninsula in contrast to Cameron's (1971, p. 92; 1972, p. 201) claim of late Eocene age for these beds based on undocumented identification of the *Bulimina schencki* fauna. The presence of these gastropods at the top of the thin, basal conglomerate of the Escalante Formation (*see* previous section) leaves little room for older macro- or microfaunas in the formation. A detailed discussion of the conflicting correlations of the basal beds is deferred until full publication of the micropaleontological evidence. However, it seems most likely that the *Bulimina schencki* fauna is a long-ranging and facies-bound assemblage which does not have the biochronological significance ascribed to it by Cameron (1971, 1972, 1973) and other micropaleontologists (*see* Jeletzky, 1973, p. 345, 346 for further details).

Chlamis (*Vertipecten*) *porterensis* found in the basal beds of Escalante Formation on Nootka Island (*see* Pl. 4. 1, fig. 2) is a reliable indicator of a general Lincoln age for these beds because:

1. The species has been found, only in the Lincoln Stage (= *Acila shumardi* zone) of the northwestern and southwestern parts of the State of Washington (Weaver, 1912, p. 57; 1942, p. 87; Durham, 1944, p. 138; Addicott, 1974, p. 182); and
2. Giant pectinids of the size of *C.* (*V.*) *porterensis* make their first appearance in the Oligocene (i. e., Lincoln) rocks throughout western North America (Addicott, 1974, p. 182, fig. 2).

Since *Chlamis* (*Vertipecten*) *porterensis* was found so close to [about 24 m (80 ft.) stratigraphically above] the basal conglomerate of the Escalante Formation, and because the lithology is suggestive of very rapid deposition, it seems likely that no pre-Lincoln rocks occur in the underlying basal beds of the formation on Nootka Island.

In conjunction with less definitive but, nevertheless strongly suggestive, previously published (Jeletzky, 1973, p. 338, 339, 341, 342, fig. 1) data, the evidence presented in this report clearly indicates that the basal beds of Escalante Formation do not include any pre-Lincoln (i. e., pre-Oligocene) rocks anywhere on the west coast of Vancouver Island.

Cameron's (1973, p. 19) conclusion that: "The basal Tertiary, Escalante Formation (Division A, of Jeletzky, 1954) .....is older on Hesquiat Peninsula than on Nootka Island (Upper Eocene)" is invalidated by the occurrence, described in this paper, of the lower Lincoln gastropod fauna in the basal conglomerate of the formation.

References

Addicott, W. O.
1974: Giant pectinids of the eastern North Pacific margin, significance in Neogene zoogeography and chronostratigraphy; J. Paleontol., v. 48, no. 1, p. 180-194.

Bancroft, M. F.
1937: Gold-bearing deposits on the west coast of Vancouver Island between Esperanza Inlet and Alberni Canal; Geol. Surv. Can., Mem. 204.

Cameron, B. E. B.
1971: Tertiary stratigraphy and microfaunas from the Hesquiat-Nootka area, west coast, Vancouver Island (92-E); *in* Report of Activities, Pt. B, Geol. Surv. Can., Paper 71-1, Pt. B, p. 91-94.

Cameron, B. E. B.
1972: Tertiary foraminiferal succession of the western Cordillera and Pacific Margin; *in* Report of Activities, Pt. A, Geol. Surv. Can., Paper 72-1, Pt. A, p. 198-201.

1973: Tertiary stratigraphy and microfaunas from the Pacific Margin, west coast, Vancouver Island; *in* Report of Activities, Pt. A, Geol. Surv. Can., Paper 73-1, Pt. A, p. 19, 20.

Dickerson, R. E.
1917: Climate and its influence upon the Oligocene faunas of the Pacific Coast with description of some new species from the *Molopophorus lincolnensis* zone; Proc. Calif. Acad. Sci., Ser. 4, v. 7, no. 6, p. 157-192.

Dott, R. H., Jr.
1963: Dynamics of subaqueous gravity depositional processes; Am. Assoc. Pet. Geol., Bull., v. 47, no. 1, p. 104-128.

Durham, J. W.
1944: Megafaunal zones of the Oligocene of northwestern Washington; Calif. Univ., Dept. Geol. Sci., Bull. 27, no. 5, p. 101-211.

Jeletzky, J. A.
1950: Stratigraphy of the west coast of Vancouver Island, between Kyuquot Sound and Esperanza Inlet, British Columbia; Geol. Surv. Can., Paper 50-37.

1954: Tertiary rocks of the Hesquiat-Nootka area, west coast of Vancouver Island, British Columbia; Geol. Surv. Can., Paper 53-17.

1973: Age and depositional environments of Tertiary rocks of Nootka Island, British Columbia (92-E): Mollusks versus Foraminifers; Can. J. Earth Sci., v. 10, no. 3, p. 331-365.

Weaver, C. E.
1912: A preliminary report on the Tertiary paleontology of western Washington; Wash. Geol. Surv., Bull. 15.

1942: Paleontology of the marine Tertiary formations of Oregon and Washington; Univ. Wash. Publ. Geol., v. 5.

5. LATE QUATERNARY SEA LEVEL FLUCTUATIONS, PACIFIC COAST OF CANADA AND ADJACENT AREAS

J.J. Clague
Terrain Sciences Division, Vancouver

Introduction

Changes in land-sea positions on the Pacific Coast of Canada during Quaternary time have resulted from a combination of eustatic, isostatic, and tectonic adjustments. Because these adjustments may occur independently or semi-independently of one another, it is difficult to assess the contribution of each to dated sea level stands different from the present. However, it is possible to date former shorelines and sediments deposited during former sea level stands, and thus to construct curves showing the net effect on sea level of eustatic, isostatic, and tectonic adjustments through time.

This report is a summary of published accounts of former land-sea relationships in British Columbia and adjacent parts of the State of Washington. Sea level changes in southeastern Alaska are also briefly discussed. Published information pertains almost entirely to relative sea level positions which postdate the late Wisconsin glaciation in the Pacific Northwest (referred to as the Fraser Glaciation).

Southwestern British Columbia and adjacent Washington State

Numerous writers have commented on late Quaternary sea levels different from the present in the Georgia Depression and Puget Sound. Marine sediments occurring above present sea level within lowland areas bordering the Strait of Georgia and Puget Sound were noted by Arnold (1906), Bretz (1913), Clapp (1913, 1914), McConnell (1914), Johnston (1921), and MacKenzie (1923). Subsequent studies of late Quaternary terrestrial and marine deposits and landforms, coupled with the radiocarbon dating of shells, wood, peat, and charcoal, have resulted in a better understanding of the chronology and environmental significance of relative sea level highs (submergent phases) and lows (emergent phases). Such studies include those of Armstrong and Brown (1953, 1954), Armstrong (1960), Fyles (1963), and Easterbrook (1963).

Much of the current knowledge of late Quaternary land-sea positions in southwestern British Columbia and northwestern Washington is summarized by Mathews (1970)[1]. Sea level curves for the last 13 000 years were constructed for four areas (eastern Vancouver Island, Victoria area, Fraser Lowland, and Whatcom County, Washington). The curves are based on radiocarbon-dated terrestrial and marine deposits which formed when sea level was different from the present[2].

The curves (Fig. 5.1) indicate submergent conditions at the end of the Fraser Glaciation. The present altitude of the upper marine limit decreases in the elevation across the Georgia Depression from 175 m near Vancouver and 180 m near Bellingham, Washington to 75 m near Victoria. The upper marine limit was attained immediately after ice retreat.

This submergence was followed by rapid emergence such that by 12 000 B.P. sea level on eastern and southern Vancouver Island was near the present; in the Fraser Lowland sea level was about +50 m; and in Whatcom County, about +12 m.

This emergence terminated in the Fraser Lowland, Whatcom County, and, to a lesser extent, on eastern Vancouver Island with a submergence which peaked about 11 500 B.P. Sea levels at this time in the Vancouver area were up to 175 m higher than at present. This brief submergence apparently did not affect the Victoria area near the southwest corner of the Georgia Depression.

A second rapid emergence occurred after 11 500 B.P.; between 9000 and 6000 B.P. sea level was up to 11 m below the present in some parts of the area. Dated terrestrial sediments occur below present sea level in the Vancouver area near New Westminster (-11 m, 7600 B.P.), Pitt Meadows (-11 m, 8290 B.P.), and Sumas (-11 m, 8360 B.P.). Sea level was at least 6 m below the present at Comox on eastern Vancouver Island between 8680 B.P. and 6820 B.P., but was at about its present position by 5680 B.P. At Victoria sea levels were lower than at present from 9250 B.P. to 5470 B.P.

During the past 5500 years sea levels have not fluctuated significantly, but have been perhaps a few metres below the present. Peat beds associated with Fraser Delta sediments occur to about 2 m below sea level. Rooted stumps in one such bed, about 1.8 m below an elevation where tree growth could occur, yielded a radiocarbon date of 4350 B.P. An archeological site on Galiano Island, now partially inundated at high tide, contains material 3160 years old. North of Victoria tree stumps 1.5 m below high tide have been dated at 2040 B.P.

In summary, sea levels were high between 13 000 and 9000 B.P. In some areas a brief submergence occurred within this period. Sea levels were about 10 m lower than at present in some parts of the area between 9000 and 6000 B.P. During the last 5500 years sea levels have not fluctuated significantly from the present.

---

[1] Research in the Fraser Lowland by J.E. Armstrong of the Geological Survey of Canada will provide additional information on postglacial sea level position in southwestern British Columbia.

[2] A tabulation of radiocarbon dates for southwestern British Columbia and adjacent Washington State compiled in connection with this study is present in the Depository of Unpublished Data of the National Research Council of Canada.

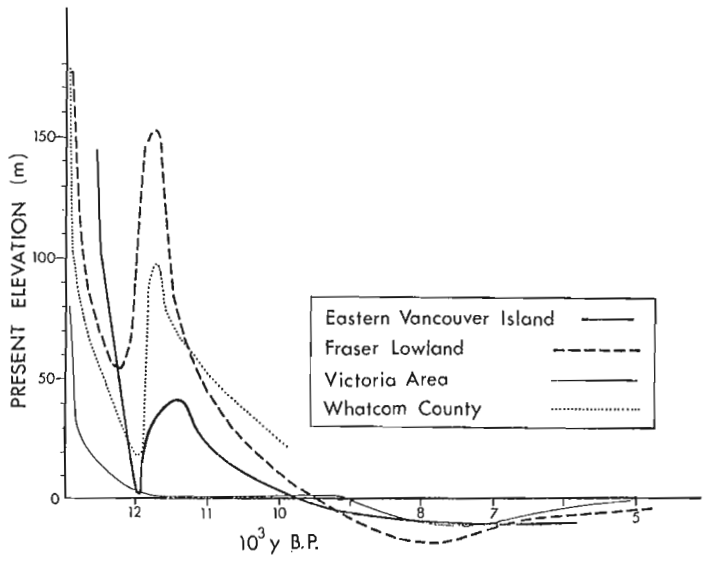

Figure 5.1. Sea-level curves, southwestern British Columbia and adjacent Washington State (after Mathews *et al.*, 1970, Fig. 4).

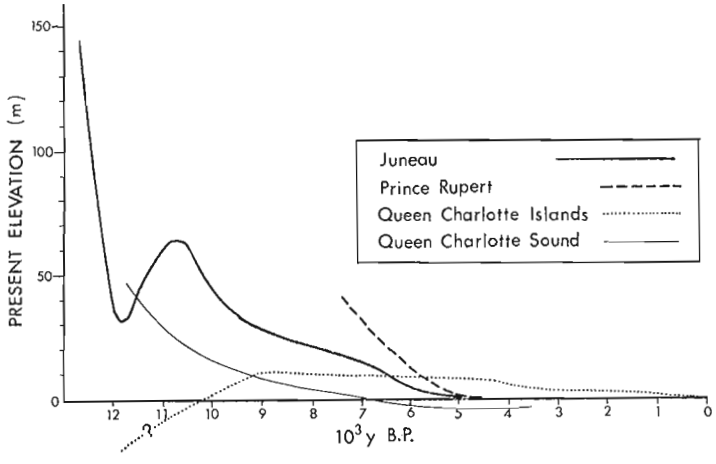

Figure 5.2. Sea-level curves, north coast of British Columbia and adjacent Alaska (after Fladmark, 1974, Figs. 5 and 6).

Northern Coast of British Columbia

An understanding of postglacial sea level changes for coastal areas north of Vancouver Island is incomplete because relatively few sequences have been dated (Fig. 5.2).

Heusser (1960, p. 194) undertook palynological studies on Hope Island near the northeastern end of Vancouver Island and concluded that the shore stood about 5 m higher 3500 years ago.

On the basis of archeological studies on the central mainland coast near Queen Charlotte Sound, Fladmark (1974, p. 150-151) concluded that sea level was +20 to +35 m, 10 200 B.P., and +10 m, about 9000 B.P. Emergence continued between 9000 and 3500 B.P.; by 3400 B.P. sea level was -2 to -3 m.

Farther north between Kitimat and Terrace, marine sediments occur up to an elevation of 120 m (Armstrong, 1966). Shells from these sediments have yielded dates of 10 790, 10 420, and 9880 B.P. A till overlies the marine sediments dated at 10 790 B.P., and deltaic gravel and sand occurring up to an elevation of 230 m were deposited between about 10 420 and 9880 B.P. The latter sediments are thought to be marine deltaic deposits. Armstrong concluded that the Kitimat-Terrace valley was depressed at least 300 m below its present elevation during the last glaciation.

Nearby, at Prince Rupert, sea level may have been 41 m higher than at present about 7500 years ago. Also at Prince Rupert, 12 radiocarbon dates obtained from archeological sites at the present shoreline indicate only minor sea level fluctuations over the last 5000 years (MacDonald, 1969).

The pattern of late Quaternary sea level changes on the Queen Charlotte Islands is different from that of the southern coast of British Columbia and from the Prince Rupert-Terrace-Kitimat area. Sutherland Brown (1968, p. 35), Nasmith (1970, p. 7), and Fladmark (1974, p. 153-156) have presented evidence that sea level was as much as 33 m lower during the terminal phase of the Fraser Glaciation. The evidence includes drowned and outwash-filled channels graded to levels below the present sea level on Graham Island and submerged, wave-cut scarps at -20 and -33 m east of Graham Island. Lower sea levels here during the Fraser Glaciation contrast with high sea levels on the south and central mainland coast at the close of the Fraser Glaciation.

Sea levels on the Queen Charlotte Islands apparently rose rapidly at the end of the Pleistocene, because littoral deposits with shells dating at 8620 and 8060 B.P. occur, respectively, on Graham Island (at +3 m) and on Moresby Island (at +6 m). On Prince of Wales Island north of the Queen Charlotte Islands, shells from beach deposits at an elevation of about 10 m yielded a date of 9510 B.P. (Swanston, 1969, p. 30-31). In contrast to the south coast, no marine deposits higher than about +10 m have been recognized on the Queen Charlotte Islands.

Dated archeological materials associated with raised beach deposits (Fladmark, 1971) indicate that higher sea levels apparently existed on the Queen Charlotte Islands until at least 4000 B.P. There is no evidence for major sea level fluctuations within this interval.

Gradual emergence began about 4000 B.P. and was probably interrupted by stand-stills or slight resubmergences. Sutherland Brown (1968, p. 35-36) recognized three separate complexes of raised shoreline deposits and landforms. The highest is thought to date from about 9500 to 4000 B.P.; the middle is dated archeologically between 3000 and 2000 B.P.; the lowest consists of a wave-cut bench at present high tide and has not been dated (Fladmark, 1974, p. 158). However, Haida village sites located on the shoreline at the time

of European contact (1774 A.D.) are now separated from the high-tide limit by as much as 300 m (Fladmark, 1971).

Southeastern Alaska

Sea level changes in southeastern Alaska are only briefly considered in this report. Continuing research by scientists of the United States Geological Survey will result in a better understanding of late Quaternary land-sea relationships in this area.

Published information is summarized by Twenhofel (1952), Heusser (1960), and Fladmark (1974). Tectonism has been a major factor affecting land-sea positions, thus there are considerable variations between local sea level curves.

Heusser (1960, p. 192) constructed postglacial sea level curves at four places in southeastern Alaska on the basis of 11 radiocarbon dates. Heusser's Juneau curve can be extended back to 13 000 B.P. (Retherford, 1972, p. 69-71) to produce a curve similar to those characterizing the Georgia Depression (Fig. 5.2). It indicates a maximum sea level of about 150 m at about 13 000 B.P., a drop to +30 m at 12 000 B.P., a resubmergence to over 60 m about 11 000 B.P., and a gradual emergence until 6000 B.P. when sea level was stabilized near its present position.

In Cook Inlet, marine sediments dated at about 14 000 B.P. are found up to an elevation of 36 m. Between 6000 and 5000 B.P. and at 1500 B.P., sea level in Cook Inlet was only a few metres higher than at present (Karlstrom, 1964, p. 47-62).

In the Icy Straits area opposite the northern end of the Alexander Archipelago, archeological research has indicated human occupation of sites about 8 m above present sea level from 9000 to 2000 B.P. (Ackerman, 1968, p. 55-78). Thus, in this area, sea level has been at or below +8 m since 9000 B.P.

Many other southeastern Alaska sites exhibit postglacial stands of the sea higher than present. Unlike Juneau, however, they show sea levels much higher than present during the last 6000 years (e.g., southeast Lituya Bay: +45 m at 3250 B.P., +30 m at 2790 B.P.). At these sites tectonic uplift has been superimposed on isostatic and eustatic effects. The dominance of tectonic effects in some areas of southeastern Alaska is shown by the occurrence of wave-cut terraces up to 523 m at Lituya Bay (Heusser, 1960, p. 21) and up to 770 m at Icy Bay (Twenhofel, 1952, p. 536). Early Pliocene and older glaciomarine sediments occur up to 1520 m in the vicinity of Yakutat Bay (Heusser, 1960, p. 20), and Miocene and possibly early Pliocene glaciomarine sediments are elevated to at least 2560 m in the Robinson Mountains near Yakataga (Heusser, 1960, p. 20). In contrast, at a few sites there has been tectonic subsidence (Prince William Sound and Copper River delta, for example).

Discussion

Postglacial sea level curves for the west coast of Canada may be summarized as follows. Curves constructed from areas along the southern inner coast (that is, areas within or marginal to the southern Coast Mountains) show higher sea levels relative to the present for the first few thousand years following deglaciation and lower positions from about 9000 to 5000 B.P. The northern inner-coast curves (Juneau and Prince Rupert), although fragmentary, are similar to southern curves, except that sea level apparently was not lower than present during postglacial time. Contrasting strongly with the inner-coast curves is the Queen Charlotte curve, perhaps representative of the outer coast. It shows low sea levels before 10 000 B.P. and high sea levels after 10 000 B.P. (Fladmark, 1974, p. 167).

The difference between inner and outer coastal curves may be explained by one or both of the following:

(1) Eustatic control of the early postglacial portion of the Queen Charlotte curve and isostatic control of the early postglacial portions of inner-coast curves. Isostatic effects would dominate over eustatic factors near the zone of maximum ice build-up, but would become less important away from this area. Mathews *et al.* (1970) showed that the magnitude of early postglacial emergence along the southern coast is appropriate for isostatic rebound. The observed decrease in uplift to the southwest, away from the Coast Mountains, is compatible with decreasing ice thickness in this direction.

(2) Vertical crustal movement along the periphery of the ice sheet which is opposite that at the site of maximum isostatic depression (McGinnis, 1968; Walcott, 1970). During glaciation the zone of isostatic depression would be bordered by a forebulge zone of uplift. With removal of ice load, the peripheral forebulge zone would drop as the isostatically depressed area rose. This phenomenum may in part explain the rise in the Queen Charlotte curve at a time when inner-coast curves fell.

Superposed on the general trends of emergence of the south coast and Juneau curves is a resubmergence climaxing about 11 000 B.P. Mathews *et al.* (1970, p. 700) offer three hypotheses to explain the resubmergence in southwestern British Columbia: (1) an increase in the rate of the eustatic sea level rise about 12 000 B.P. resulting in the eustatic rise temporarily exceeding isostatic rebound; (2) isostatic depression due to a build-up of ice in the Coast and Cascade mountains; (3) localized tectonic movements. Whatever the explanation for this transgression, it was followed by rapid emergence; by about 8000 B.P. sea level shifts along the southern coast appear to be dominantly eustatic because the curves are parallel to the eustatic sea level curves of Fairbridge (1960), Kenney (1964), Curray (1965), and Hopkins (1967).

Historic Sea Level Changes

Except in areas of active tectonism, sea level changes on the west coast of Canada during the last 5000 years have been relatively minor. Mathews *et al.* (1970) present tide gauge records and geodetic measurements

relating to historic sea level changes on the south coast. The tide gauge records all show a long-term rise in sea level attributable to the worldwide shrinkage of glaciers. Differential movements of land and sea were detected by comparing the tide records for pairs of stations. For example, the recorded water level at Seattle and Caulfield near Vancouver has risen more rapidly than at Victoria, and it is suggested that the first two stations are sinking relative to the last.

Geodetic measurements were made in the Vancouver area by the Geodetic Survey of Canada between 1914 and 1924 and again between 1958 and 1967. Comparison of the computed elevations of resurveyed benchmarks indicates downward movement of almost all stations in the Fraser Lowland with an increase in the rate of displacement southward across the International Boundary. Maximum subsidence rates are about 0.15 m/century. Apparently, the sinking is not related to loading of the crust by deltaic sediments of the Fraser River because it is not concentric about the mouth of the river. Rather, subsidence in this area is perhaps due to tectonic movements associated with the pre-Cretaceous bedrock surface (Mathews *et al.*, 1970, p. 701). Whatever its cause, modern subsidence appears to be substantially greater than the long-term average inferred from submergence of terrestrial features 4000 to 8000 years old in the Vancouver area.

References

Ackerman, R.E.
1968: The archeology of the Glacier Bay region, southeastern Alaska; Wash. State Univ., Lab. Anthropology, Rept. Invest. 44.

Armstrong, J.E.
1960: Surficial geology of Sumas map-area, British Columbia; Geol. Surv. Can., Paper 59-9.

1966: Glacial studies, Kitimat-Terrace area; Geol. Surv. Can., Paper 66-1, p. 50.

Armstrong, J.E. and Brown, W.L.
1953: Ground-water resources of Surrey Municipality, British Columbia; Geol. Surv. Can., Water Supply Paper 322.

1954: Late Wisconsin marine drift and associated sediments of the lower Fraser valley, British Columbia, Canada; Geol. Soc. Am., Bull., v. 65, p. 349-364.

Arnold, R.
1906: Geological reconnaissance of the coast of the Olympic Peninsula, Washington; Geol. Soc. Am., Bull., v. 17, p. 451-468.

Bretz, J.H.
1913: Glaciation of the Puget Sound region; Wash. Geol. Surv., Bull. 8.

Clapp, C.H.
1913: Geology of the Victoria and Saanich map-areas, Vancouver Island, B.C.; Geol. Surv. Can., Mem. 36.

1914: Geology of the Nanaimo map-area; Geol. Surv. Can., Mem. 51.

Curray, J.E.
1965: Late Quaternary history, continental shelves of the United States; *in* the Quaternary of the United States; Wright, H.E., Jr., and Frey, D.G. (eds.), Princeton Univ. Press, p. 723-735.

Easterbrook, D.J.
1963: Late Pleistocene glacial events and relative sea-level changes in the northern Puget Lowland, Washington; Geol. Soc. Am., Bull., v. 74, p. 1465-1483.

Fairbridge, R.W.
1960: The changing level of the sea; Sci. Am., v. 202, p. 70-79.

Fladmark, K.R.
1971: Radiocarbon dates from the Queen Charlotte Islands; The Midden, v. 3, p. 11-15.

1974: A paleoecological model for Northwest Coast prehistory; unpubl. Ph.D. thesis, Univ. Calgary.

Fyles, J.G.
1963: Surficial geology of Horne Lake and Parksville map-areas, Vancouver Island, British Columbia; Geol. Surv. Can., Mem. 318.

Heusser, C.J.
1960: Late-Pleistocene environments of North Pacific North America – an elaboration of late-glacial and postglacial climatic, physiographic, and biotic changes; Am. Geog. Soc., Spec. Publ. 35.

Hopkins, D.M.
1967: The Cenozoic history of Beringia, a synthesis; *in* The Bering land bridge; Hopkins, D.M. (ed.), Stanford Univ. Press, p. 451-484.

Johnston, W.A.
1921: Pleistocene oscillations of sea level in the Vancouver region, British Columbia; Trans. Roy. Soc. Can., ser. 3, v. 15, sec. 4, p. 9-19.

Karlstrom, T.N.V.
1964: Quaternary geology of the Kenai Lowland and glacial history of the Cook Inlet region, Alaska; U.S. Geol. Surv., Prof. Paper 443.

Kenney, T.C.
1964: Sea-level movements and the geological histories of the postglacial marine soils at Boston, Nicolet, Ottawa, and Oslo; Geotechnique, v. 14, p. 203-230.

MacDonald, G. F.
1969: Preliminary cultural sequence from the Coast Tsimshian area, British Columbia; Northwest Anthropological Res. Notes, v. 3, p. 240-254.

MacKenzie, J. D.
1923: Alberni area, Vancouver Island, B. C.; Geol. Surv. Can., Sum. Rept. 1922, p. 51A-67A.

Mathews, W. H., Fyles, J. G., and Nasmith, H. W.
1970: Postglacial crustal movements in southwestern British Columbia and adjacent Washington State; Can. J. Earth Sci., v. 7, p. 690-702.

McConnell, R. G.
1914: Texada Island, B. C.; Geol. Surv. Can., Mem. 58.

McGinnis, L. D.
1968: Glacial crustal bending; Geol. Soc. Am., Bull., v. 79, p. 769-776.

Nasmith, H. W.
1970: Pleistocene geology of the Queen Charlotte Islands and southern British Columbia; *in* Early man and environments in northwest North America; Smith, R. A., and Smith, J. W. (eds.), Calgary Univ. Archeol. Assoc., Proc. 2nd Ann. Paleoenvironmental Workshop, p. 5-8.

Retherford, R. M.
1972: Late Quaternary geologic environments and their relation to archeological studies in the Bella Bella-Bella Coola region of the British Columbia coast; unpubl. M. Sc. thesis, Univ. Colorado.

Sutherland Brown, A.
1968: Geology of the Queen Charlotte Islands, British Columbia; B. C. Dept. Mines Pet. Resourc., Bull. 54.

Swanston, D. N.
1969: A late-Pleistocene glacial sequence from Prince of Wales Island, Alaska; Arctic, v. 22, p. 25-33.

Twenhofel, W. S.
1952: Recent shore-line changes along the Pacific coast of Alaska; Am. J. Sci., v. 250, p. 523-548.

Walcott, R. I.
1970: Isostatic response to loading of the crust in Canada; Can. J. Earth Sci., v. 7, p. 716-727.

6. HOODOO L-41: DIAPIRIC HALITE FACIES OF THE OTTO FIORD FORMATION IN THE SVERDRUP BASIN, ARCTIC ARCHIPELAGO

Project 750054

Graham R. Davies
Institute of Sedimentary and
Petroleum Geology, Calgary

Introduction

Diapiric masses of anhydrite and gypsum intrude Mesozoic sediments of the Sverdrup depositional basin exposed on northwestern islands of the Canadian Arctic Archipelago (Fig. 6.1). The source of the intrusive evaporites has been established from stratigraphical, lithological and paleontological studies to be the Upper Mississippian to Middle Pennsylvanian Otto Fiord Formation which is exposed as anhydrite with interbedded limestone and sandstone on northwestern Ellesmere Island (Thorsteinsson, 1970, 1974; Davies and Nassichuk, 1975).

Although the diapirs have been described in various geological and geophysical publications since the early 1950's, the presence or absence of an active halite core below the bedded sulphate cap has been a matter of conjecture (*see* Thorsteinsson, 1974, p. 74-81, for an historical review and references). Indirect evidence from gravity data (negative anomalies over diapirs; Thorsteinsson, *ibid.*) and from water chemistry of saline springs on Axel Heiberg Island (Hoen, 1964, appendix; R.O. van Everdingen, Water Resource Branch, unpublished report, 1973) indicate the presence of halite below some diapirs and elsewhere in the subsurface of the Sverdrup Basin, yet there is no direct evidence from in-place outcrops or surface exposures in diapirs of the existence of a halite lithofacies of the Otto Fiord Formation.

Not until the Hoodoo L-41 well was drilled southeast of the exposed part of Hoodoo Diapir on Ellef Ringnes Island (Fig. 6.1) by Imperial Oil Limited and other companies in 1972, was direct proof finally provided of a halite core below a large diapir in the Sverdrup Basin and, thus, also of a halite lithofacies (subsurface) of the Otto Fiord Formation. This report is a summary of the lithological and limited paleontological (GSC source) data from the Hoodoo L-41 well; the well was released from confidential status on July 24th, 1974.

THE HOODOO L-41 WELL

The Imperial Panarctic Dome *et al.* Hoodoo L-41 wildcat well was drilled by Imperial Oil Ltd. as operator with Panarctic Oils Ltd. as permitee on southeastern Ellef Ringnes Island at co-ordinates 78°10'37"N, 99°54'13"W. It was spudded on May 6, 1972 and completed drilling at a total depth of 14 045 feet (log) on July 18, 1972. The well was abandoned and the rig released on July 24, 1972.

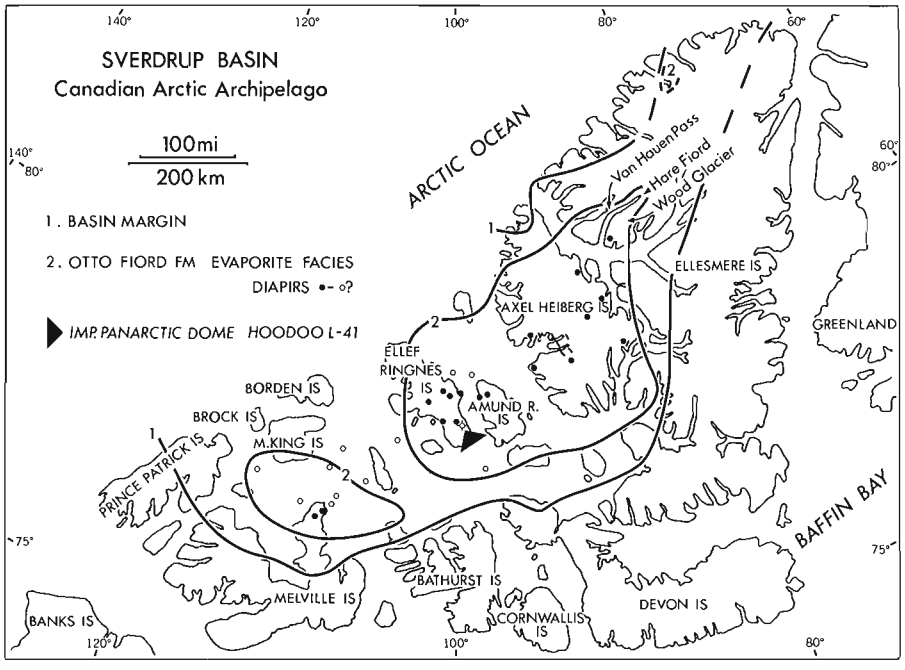

Figure 6.1.

Localities, boundaries of the Sverdrup Basin, distribution of evaporites of the Otto Fiord Formation, and location of the Hoodoo L-41 well, Canadian Arctic Archipelago. Subdivision of evaporite basin modified from Meneley *et al.* (in press).

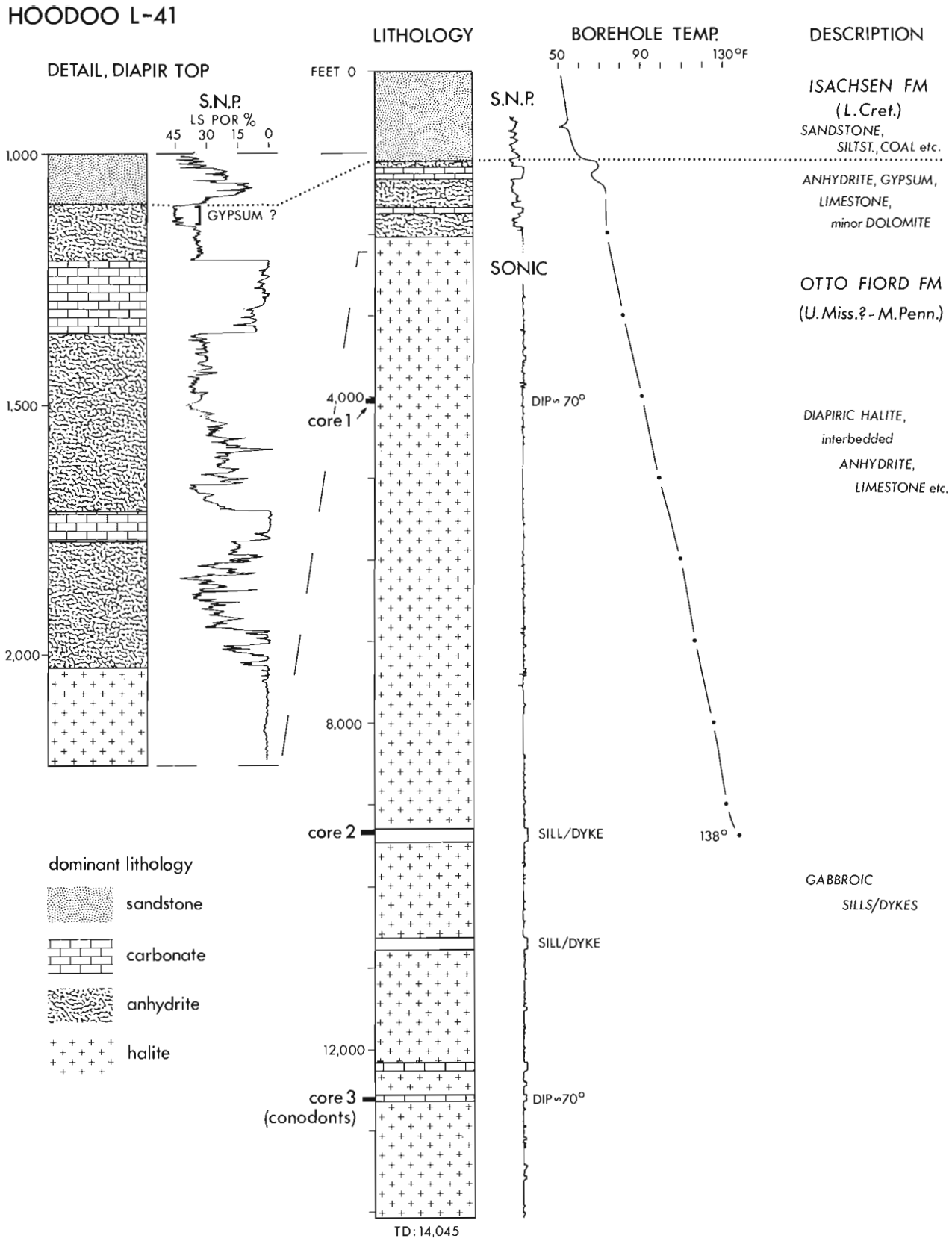

Figure 6. 2. Summary of well data, Imperial Panarctic Dome *et al.* Hoodoo L-41.

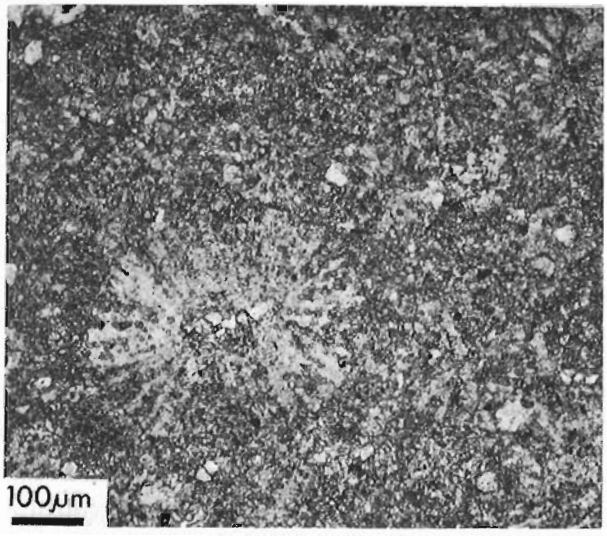

Figure 6. 3. Photomicrograph of authigenic rosettes, preserved now as calcite, in cuttings of limestone interbedded with diapiric halite at a depth of 4220 feet, Hoodoo L-41 well.

Gamma-ray, sonic, sidewall neutron porosity, formation density, dual laterolog and temperature logs were run for various intervals in the well. Cores were taken at three intervals: Core 1, 4004 to 4033 feet (rec. 29 ft; halite); Core 2, 9307 to 9317 feet (rec. 9. 5 ft; igneous sill/dyke); Core 3, 12 594 to 12 628 feet (rec. 34 ft; carbonate, anhydrite). Twenty-one sidewall cores were taken in the interval between 1222 and 2022 feet. There were not drillstem tests.

Stratigraphic Summary

The Hoodoo L-41 well (Fig. 6. 2) was spudded in the Lower Cretaceous Isachsen Formation and penetrated about 1100 feet of Isachsen strata comprising sandstone with interbedded siltstone, shale and coal.

At 1105 feet, from SNP and BCS logs, the well entered gypsum/anhydrite at the top of the subsurface extension of the Hoodoo Diapir. This contact corresponds with a marked increase in the borehole temperature (Fig. 6. 2). The upper 40 feet of the sulphate "cap" probably are gypsum (SNP log), grading downward into mixed gypsum and anhydrite to a depth of 1213 feet.

From 1213 to 1360 feet, about 150 feet of limestone were penetrated; thin sections of selected cuttings from this limestone unit show that it has a recrystallized microspar texture, often stylolitic, but with no visible preserved bioclasts or other primary fabrics. This limestone unit is underlain by about 670 feet of anhydrite with interbedded limestone and dolomite and minor calcite-cemented sandstone and siltstone; some of the sand grains include pleochroic (dark green to olive-brown) minerals. Some cuttings are composed of coarsely crystalline, rhombic calcite suggestive of calcitized dolomite ("dedolomite" fabrics).

Figure 6. 4. Slabbed core of steeply dipping, coarsely recrystallized halite containing angular lithoclasts of pale olive-grey mudstone or clay. Core 1, 4027 to 4028 feet, Hoodoo L-41.

At 2032 feet, the well entered halite (logs), and remained in halite-dominant lithologies to a total depth of 14 045 feet (log). Within the steeply inclined halite mass are numerous interbedded, thin anhydrite, limestone, dolomite and, in places, sandstone-shale beds.

Thin sections of selected cuttings from some interbeds show that the limestones normally are recrystallized microspars, often with some detrital and authigenic quartz, and scattered authigenic pyrite.

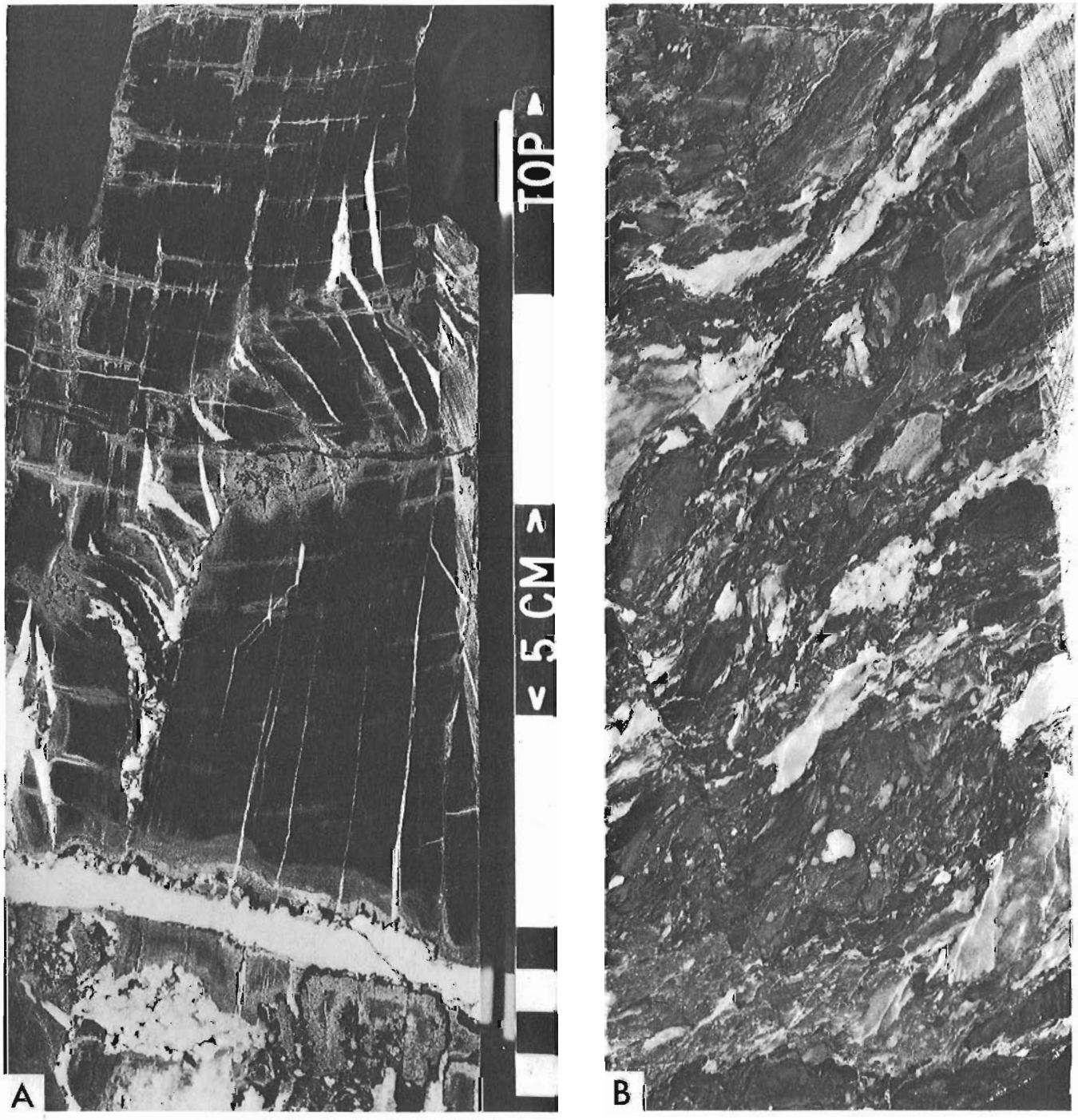

Figure 6. 5A. Deformed laminated argillaceous micritic limestone with kink-bands. Fractures filled by white calcite, minor halite and elemental sulphur. Stylolites common. Core 3, 12 598 feet, Hoodoo L-41.

6. 5B. Intensely sheared, steeply dipping anhydrite and non-calcareous shale (?). Core 3, 12 617 to 12 618 feet, Hoodoo L-41.

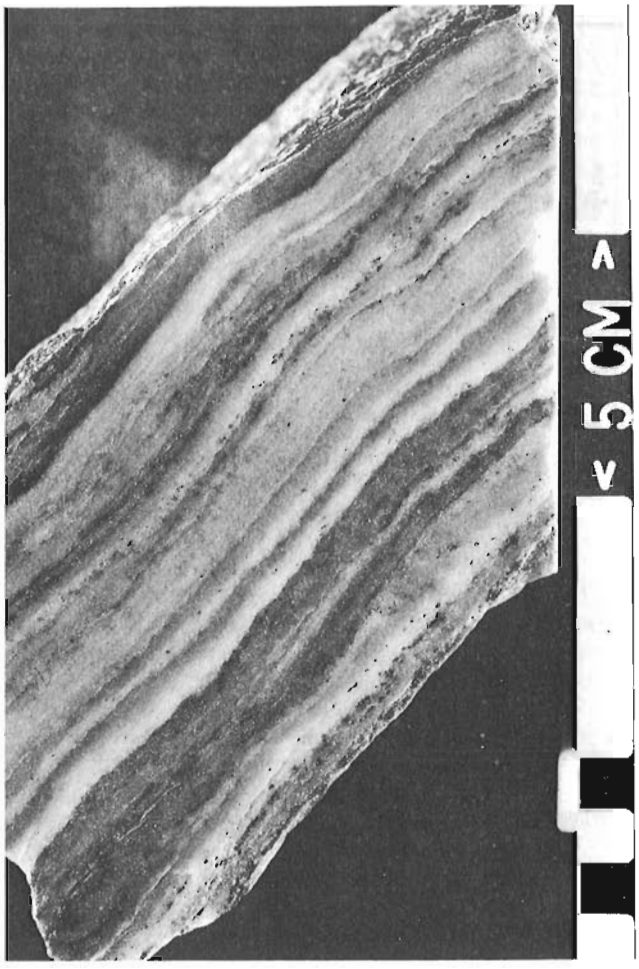

Figure 6. 6. Laminated anhydrite; dark "grains" in laminae are crystals of authigenic pyrite, possibly also other sulphides. Core 3, 12 619 feet, Hoodoo L-41.

In a few less altered limestone samples, an original wackestone to lime mudstone texture is preserved. Some have a pelletoidal (clotted) fabric, with a few calcite-filled molds of thin-walled bivalved molluscs, ostracodes, and also calcispheres (spar-filled, no skeletal wall) about 120μ m in diameter. Rosettes of radiating authigenic crystals about 400μ m in diameter, preserved now as calcite, are common in some cutting samples (Fig. 6. 3). Other limestone samples show extensive replacement by euhedral, authigenic anhydrite along former fractures.

Salt cored at about 4000 feet (Core 1) is a coarsely recrystallized halite containing many angular and sheared mudstone-like or clay lithoclasts (Fig. 6. 4). Some anhydrite stringers and beds also are present. Dips in the halite core range from 70^{o} to 80^{o}.

At a depth of close to 9300 feet, and again near 10 700 feet, thick (160 ft and 110 ft, respectively) gabbroic igneous intrusions, either sills or dykes, were intersected in the salt section; a short core (Core 2) was obtained from the higher of these two intrusives.

Figure 6. 7. Photomicrograph of bioclastic grainstone with small gastropods, brachiopods and bivalved molluscs (?) in a grainstone matrix. Core 3, 12 595 feet, Hoodoo L-41.

From Core 3, at a depth of 12 600 feet, steeply dipping and deformed carbonate and anhydrite (Fig. 6. 5) with minor halite stringers and beds were recovered. Some of the anhydrite preserves a primary laminated fabric (Fig. 6. 6). Thin sections of limestone types from the cored interval reveal that some are diagenetically altered, bioclastic, rounded grainstones which contain gastropods (several spire types), bivalved molluscs and brachiopods, and small ostracodes (Fig. 6. 7). Many of the larger bioclasts have been crushed, and replaced by solution-moldic diagenetic processes. Many rounded grains preserve a radial and concentric pseudo-spherulitic to pseudo-oolitic texture, but are of indeterminate origin. The present fabric comprises large, interlocking, anhedral calcite crystals that transect primary grain boundaries. Indistinct remnants of "cloudy" rhombic cores to many of these calcite crystals (Fig. 6. 8 A, B) suggest strongly that these limestones represent calcitization of coarsely crystalline dolomite which had replaced the original primary sediment or rock. These limestones also yielded the only microfossils (conodonts) found in the Paleozoic rocks in this well.

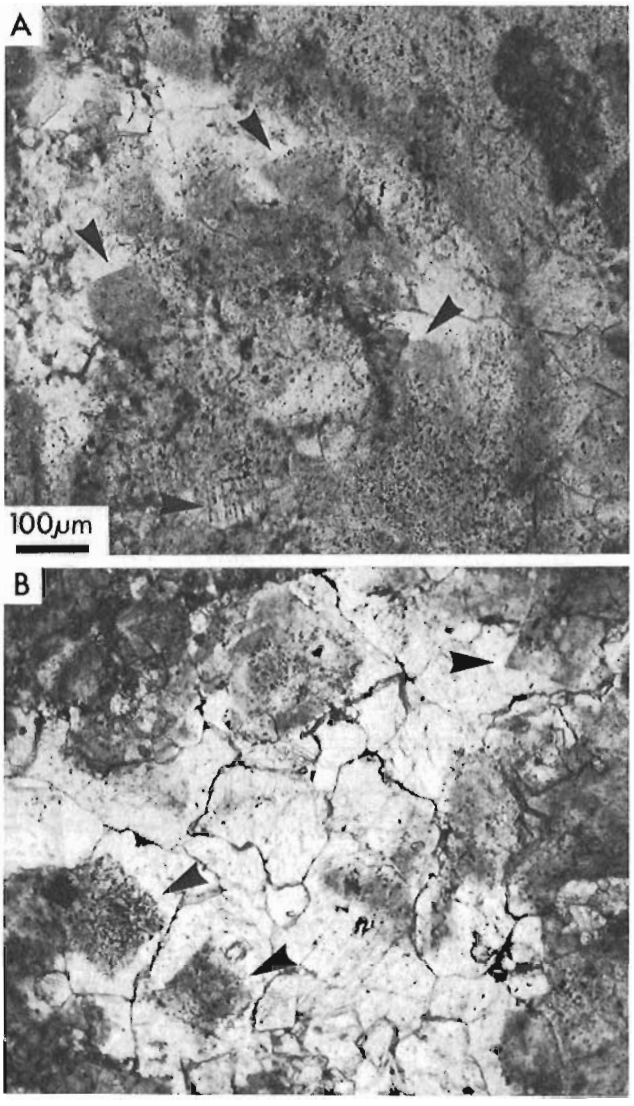

Figure 6. 8. Photomicrographs of inclusion-rich, rhombic-shaped cores (arrows) in large anhedral calcite crystals of bioclastic grainstone (Fig. 6. 7) suggestive of a calcitized dolomite ("dedolomite") fabric. Core 3, 12 595 feet, Hoodoo L-41.

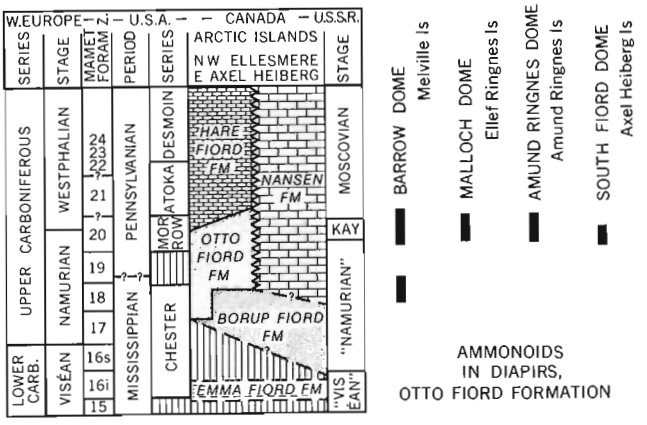

Figure 6. 9. Age distribution of ammonoids identified from limestone blocks in anhydrite/gypsum diapirs from the southern and central Sverdrup Basin, correlated with age data for the Otto Fiord Formation exposed on northwestern Ellesmere Island (ammonoid data and correlation table from Nassichuk, 1975). In conjunction with the conodont data reported in this paper, the ammonoids confirm the correlation between the Otto Fiord anhydrite where exposed in normal stratigraphic sequence and the halite-anhydrite lithofacies found in the Hoodoo L-41 well.

Paleontology and Stratigraphic Correlation

In an attempt to obtain paleontological age data from the Hoodoo L-41 evaporite section, samples of carbonate from Core 3 were processed for palynomorphs and conodonts, resulting only in a poor yield of conodonts. Subsequently, large samples of halite from Core 1 were dissolved and the residues processed for palynomorphs; these yielded only highly carbonized, non-specific plant detritus.

Only three conodonts were recovered from Core 3. Two of the three are *Cavusgnathus lautus* Gunnell, while the third is a broken piece of an unidentified bar-like conodont (P. Bender, pers. com., December, 1973). Unfortunately, *Cavusgnathus lautus* ranges in age from Early Pennsylvanian to Early Permian and, thus, is not of great stratigraphic value. Bender has found this conodont in one other sample from the Otto Fiord Formation where it is exposed in normal stratigraphic succession near easternmost Hare Fiord on northwestern Ellesmere Island (Fig. 6. 1); this outcrop sample is dated on foraminiferal evidence as of latest Mississippian or Early Pennsylvanian age. *Cavusgnathus lautus* also has been found by Bender at different horizons in the Nansen Formation, the Pennsylvanian to Lower Permian carbonate shelf lithofacies exposed in the northern Sverdrup Basin.

The conodont evidence is inconclusive for a precise correlation with the Otto Fiord Formation exposed on Ellesmere Island, but with the evidence from the paleontological data (ammonoids, brachiopods) obtained from surface samples from other diapirs on Melville, Ellef Ringnes, Amund Ringnes and Axel Heiberg Islands (Fig. 6. 9; Nassichuk, 1975); there is no doubt that the diapirs represent an intrusive halite lithofacies of the Otto Fiord Formation.

Discussion

The Hoodoo L-41 well establishes: a) that at least one, and thus, logically, many other large diapirs in the Sverdrup Basin are underlain and cored by halite; and b) the existence of a halite lithofacies of the Otto Fiord Formation that otherwise is exposed only in the calcium sulphate evaporite mineral phase.

The anhydrite exposed at the surface of the Arctic diapirs, although usually contorted, brecciated or sheared, often preserves remnants of primary laminations and bedding similar to those found in *in situ* exposures of the Otto Fiord Formation (Davies and Nassichuk, 1975, Fig. 6). Carbonate inclusions in diapirs, usually limestone, also are brecciated but are recognizably the remnants of carbonate units interbedded in the anhydrite, and similar to limestone interbeds in the type section of the Otto Fiord (*ibid.*, Fig. 3). The 930-foot unit of gypsum, anhydrite and limestone above the halite section in the Hoodoo L-41 well probably represents a similar distorted, yet essentially stratigraphically intact, "plug" displaced upward from its original depositional position overlying a thick, bedded salt unit. Some of this plug, particularly in the lower part, may comprise compacted residues after solution of some of the halite core.

Stratigraphic sections based on structural (Balkwill, 1974) and geophysical (Meneley *et al.*, in press) data for Ellef Ringnes and Amund Ringnes Islands suggest that the source of Otto Fiord halite lies at a present depth of about 25 000 feet. A generalized cross-section showing the possible relationship between the Hoodoo diapir, the Hoodoo L-41 well, and depth to halite source has been published elsewhere (Davies, 1975, Fig. 5).

The borehole temperature log (Fig. 3), recorded about 24 hours after cessation of drilling and circulation when the well was at 9400 feet, demonstrates the high heat conductivity and capacity of the intrusive halite. In the Mesozoic section, a general borehole temperature gradient of about 0.5°F/100 feet (100- to 800-ft depth) increases to a mean of 2.5°F/100 feet over the diapir contact interval between 800 and 1500 feet, with local gradients at the contact equivalent to 14°F/100 feet. Within the halite mass, a borehole thermal gradient of 0.85 to 0.9°F/100 feet was measured. These temperatures and gradients are not, of course, in equilibrium with true geothermal gradients.

References

Balkwill, H.R.
1974: Structure and tectonics of Cornwall Arch, Amund Ringnes and Cornwall Islands, Arctic Archipelago *in* Geology of the Canadian Arctic; Aitken, J.D. and Glass, D.J., eds., Geol. Assoc. Can. and Can. Soc. Pet. Geol. Proc., p. 39-62.

Davies, G.R.
1975: Upper Paleozoic carbonates and evaporites in the Sverdrup Basin, Canadian Arctic Archipelago; Geol. Surv. Can., Report of Activities, Part B, Paper 75-1B, p. 209-214.

Davies, G.R. and Nassichuk, W.W.
1975: Subaqueous evaporites of the Carboniferous Otto Fiord Formation, Canadian Arctic Archipelago: as summary; Geology, v. 3, no. 5, p. 273-278.

Hoen, E.W.
1964: The anhydrite diapirs of central western Axel Heiberg Island; Axel Heiberg Res. Reports, McGill Univ., Montreal, Geology, no. 2.

Meneley, R.A., Henao, D., and Merritt, R.K.
The northwest margin of the Sverdrup Basin *in* Yorath, C.J. *et al.*, eds., Canada's continental margin and offshore exploration; Can. Soc. Pet. Geol., Mem. 4. (in press)

Nassichuk, W.W.
1975: Carboniferous ammonoids and stratigraphy in the Canadian Arctic Archipelago; Geol. Surv. Can., Bull. 237, 240 p.

Thorsteinsson, R.
1970: Geology of the Arctic Archipelago *in* Douglas, R.J.W., ed., Geology and economic minerals of Canada; Geol. Surv. Can., Econ. Geol. Rept. No. 1, 5th ed., p. 548-590.

1974: Carboniferous and Permian stratigraphy of Axel Heiberg Island and western Ellesmere Island, Canadian Arctic Archipelago; Geol. Surv. Can., Bull. 224, 115 p.

7. "ARNICA PLATFORM DOLOMITE" (NTS 85, 95, 96, 105, 106), DISTRICT OF MACKENZIE

Project 710033

G. K. Williams
Institute of Sedimentary and
Petroleum Geology, Calgary

As a result of Operation Mackenzie (Lat. 61°N to 64°N, Long. 122°W to 126°W), several new formation names were introduced for Middle Devonian and older rocks (Douglas and Norris, 1960). Below the Nahanni Formation (the highest Middle Devonian carbonate), these new names include: Headless, Landry, Manetoe, Funeral, Arnica, Sombre, Camsell, Delorme and Whittaker formations. Some of these names are facies terms for equivalent strata. For example, the Funeral shale, in places, is equivalent to all or parts of the Landry limestone, the Manetoe dolomite and the Arnica dolomite. No such intertonguing has been recognized between the older formations; the Sombre dolomite, Camsell carbonate breccia and the Delorme clastic-rich carbonate have all been mapped as distinct blanket deposits. The upper formations – Headless, Landry, Manetoe, Funeral and the top of the Arnica – are identified easily in the subsurface; there is no great problem in correlating from well to well or from well to outcrop. But the lower formations (Sombre, Camsell and Delorme) do present a problem; correlation of these formations is, at present, quite uncertain. Furthermore, apart from the upper marker, there never have been any firm criteria for relating the 10 000 feet of section represented by the Arnica to Delorme formations of the mountains to the 1000 to 2000 feet of the Bear Rock Formation of the plains.

Table 7.1

Wells and field sections used as control points

Well name	Location	Abbreviation
Texaco Teck Iverson Lake M-69	62°28'57", 124°27'59"	M-69
Pacific et al. Carlson Lake A-50	62°29'08", 123°52'40"	A-50
Horn R Candel et al. Willowlake G-47	62°36'23", 122°53'12"	G-47
FPC Tenneco Root River I-60	62°39'32", 123°24'29"	I-60
Shell West Wrigley G-70	63°09'17", 124°11'50"	G-70
Decalta et al. Wrigley I-54	63°13'33", 123°54'32"	I-54
IOE et al. Dahadinni I-70	63°19'41", 124°56'35"	I-70
Union Japex Blackwater E-11	63°40'20", 123°03'30"	E-11
Candel et al. Dahadinni M-43A	63°52'59", 124°39'15"	M-43A
Shell Cloverleaf I-46	63°55'44", 124°52'39"	I-46
Amoco et al. Red Dog K-29	64°08'43", 125°34'55"	K-29
Candel et al. Stewart B-30	64°19'12", 125°19'20"	B-30

Field section name	Location	Field number
Tundra Creek	61°51'30", 124°52'00"	407 NB
Whittaker Range	62°30'00", 124°45'00"	114 PI
Pastel Creek	62°47'00", 125°15'00"	408 NB
Smith Ridge	62°35'00", 123°15'00"	86 BI

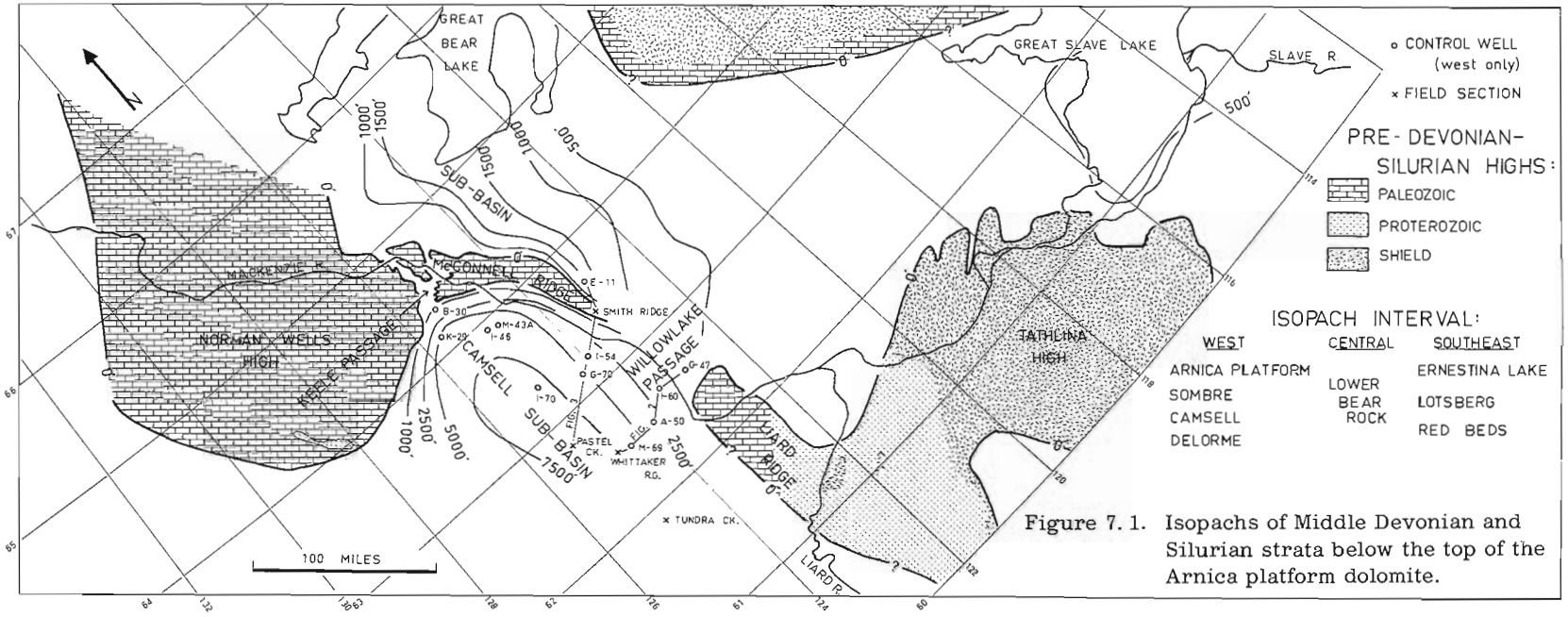

Figure 7.1. Isopachs of Middle Devonian and Silurian strata below the top of the Arnica platform dolomite.

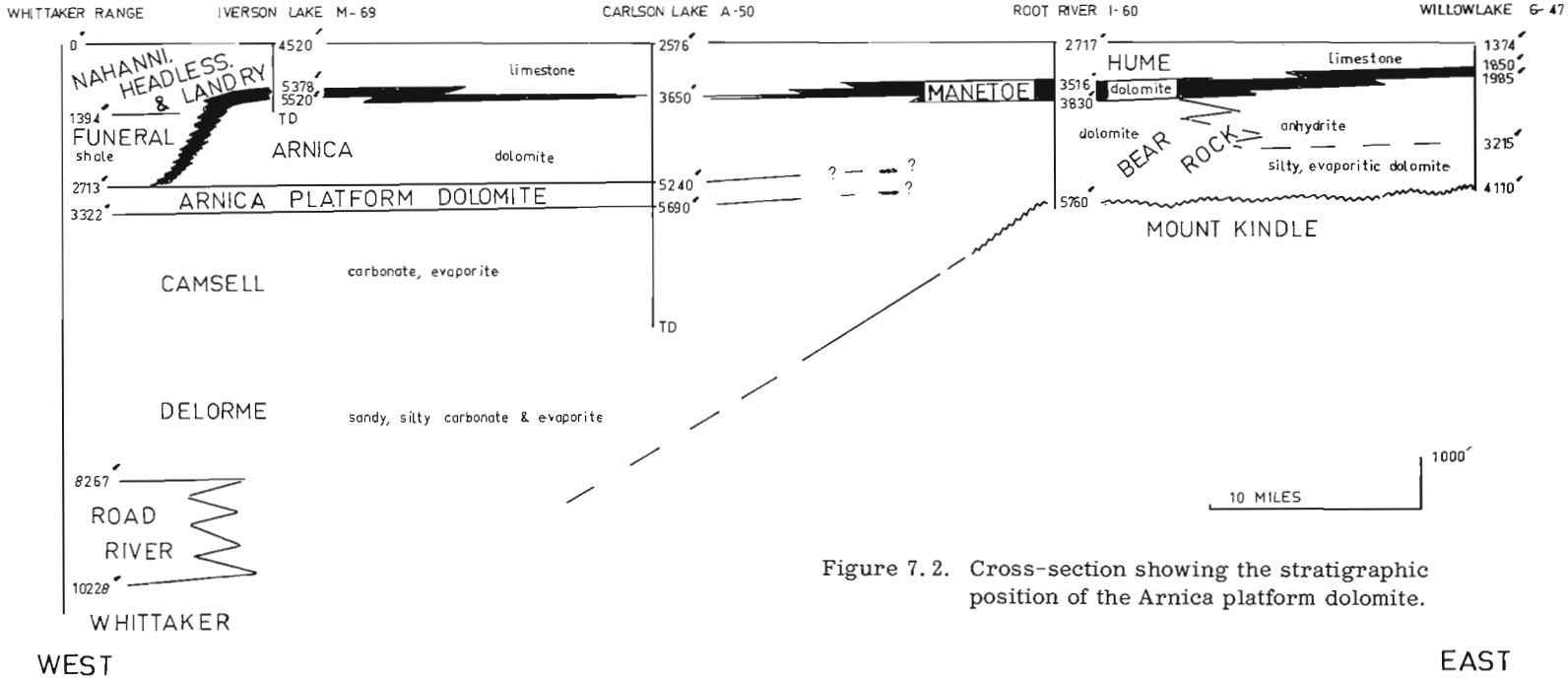

Figure 7.2. Cross-section showing the stratigraphic position of the Arnica platform dolomite.

Table 7.2

Control points, "Arnica platform dolomite". Measurements are in feet.

Well	Location	Top	Base	Thickness	Criteria[1]
A-50	62°29'08", 123°52'40"	5,240	5,690	450	1, 2, 5, 6
G-70	63°09'17", 124°11'50"	5,690	6,270	580	1, 2, 4, 6
I-54	63°13'33", 123°54'32"	4,190	4,670	480	1, 2, 3, 4, 6
I-70	63°19'41", 124°56'35"	4,520	5,250	730	1, 2, 4, 5
M-43A	63°52'59", 124°39'15"	9,750	TD	527+	1, 2, 3, 4
I-46	63°55'44", 124°52'39"	10,780	TD	538+	1, 2, 3, 4
K-29	64°08'43", 125°34'55"	2,245	2,790	545	2, 4
B-30	64°19'12", 125°19'20"	8,240	8,625	385	4
Field section	**Location**	**Top**	**Base**	**Thickness**	**Criteria**
Tundra Creek	61°51'30", 124°52'00"	10,149[2]	9,714?	435	4, 5
Pastel Creek	62°47'00", 125°15'00"	12,150	11,400	750	1, 2, 4, 6
Whittaker Range	62°30'00", 124°45'00"	2,713	3,322	609	1, 2, 4, 5, 6
Smith Ridge	62°35'00", 123°15'00"	Not present?			

[1] Criteria for recognition
1. Dark colour, contrasting noticeably with rocks above (except Funeral) and below.
2. Crinoids
3. "Two-hole" crinoids
4. Other fossils or fossil fragments
5. Black chert
6. Similar thickness of interval from top of Nahanni compared to closest section

[2] Footages from field notebooks

Table 7.3

Control points from Table 7.2 arranged to show the nature of overlying and underlying strata.

	Funeral shale	Arnica dolomite	Bear Rock anhydrite and dolomite
Overlying rocks	Whittaker Range	Pastel Creek	I-54, I-70, M-43A
	Tundra Creek	A-50	I-46, K-29, B-30
		G-70	

"Arnica platform dolomite"

	Sombre dolomite	Camsell breccia (surface) or anhydrite and dolomite (subsurface
Underlying rocks	Tundra Creek	A-50, G-70, I-54, I-70, K-29, B-30,
	Pastel Creek	Whittaker Range

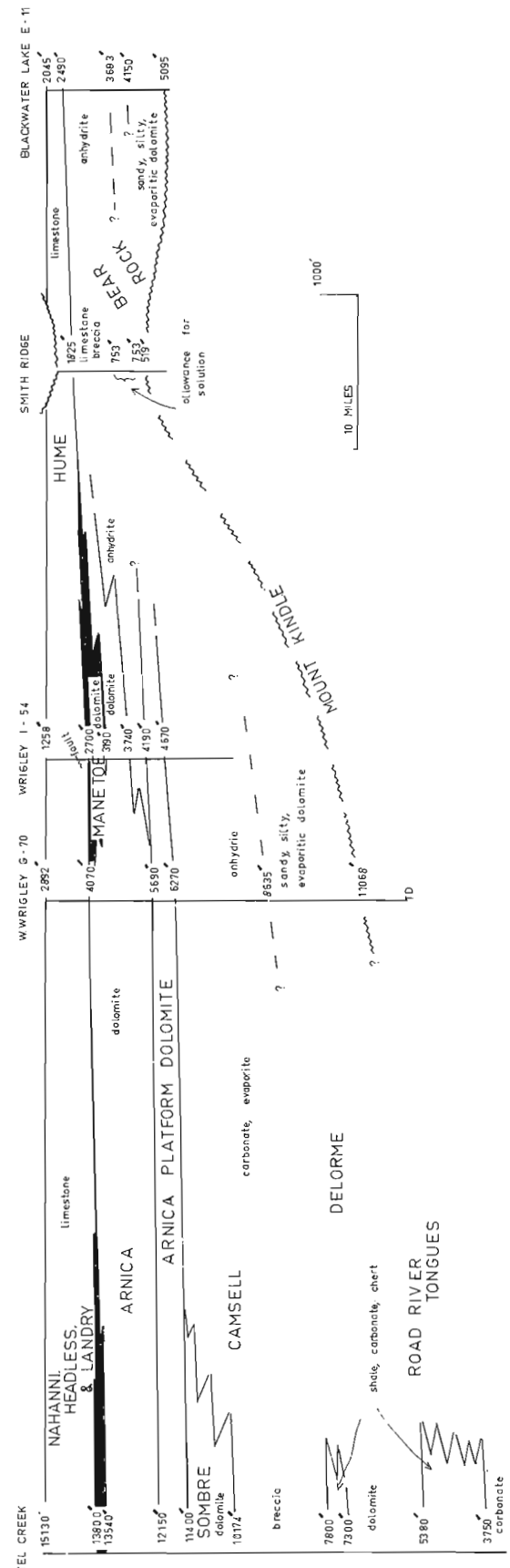

Figure 7.3. Cross-section showing the stratigraphic position of the Arnica platform dolomite.

A marker unit, herein temporarily called the "Arnica platform dolomite", appears to be recognizable in many of the Mackenzie Plains wells (west of the Mackenzie River) and also in a few of the Operation Mackenzie field sections. This marker, if it survives critical appraisal, will add one more correlation point – the base of the Arnica Formation – between wells within the Mackenzie Plains and between these wells and the surface sections. Also, it may provide a correlation link from the Mackenzie Mountains to the Elk Point Basin of Alberta.

Table 7.1 lists the wells in the Mackenzie Plains and field sections in the mountains that have been used in this report with well name abbreviations, that have been used in the illustrations.

Wells and field sections, in which the "Arnica platform dolomite" is recognized tentatively, are listed in Table 7.2, with criteria for its recognition. Although mechanical well logs are a help, recognition of the unit in the subsurface requires sample examination. Summaries of the field section have been published (Douglas and Norris, 1960, 1961, 1963); however, in most cases, the detail is not adequate and the original field notes must be consulted. This detailed material has not been published.

In Table 7.3, the control points from Table 7.2 are arranged to show the nature of overlying and underlying strata; the cross-sections in Figures 7.2 and 7.3 show the interpretation of the data.

Assuming that the correlations of Table 7.2 are correct, the "Arnica platform dolomite" can be interpreted as a blanket carbonate deposited during a major transgressive pulse, somewhat analogous to the Keg River platform of Alberta. It overlies a sub-basin previously filled with evaporites (Camsell Formation) or partly equivalent carbonates (Sombre Formation) and laps onto topographic highs. It was succeeded by thick carbonate bank (Arnica Formation), or evaporites behind the carbonate bank (Bear Rock Formation as that term is used in the Norman Wells area), or by shales in front of the bank (Funeral Formation). Like the Keg River platform its vertical limits are hazy where it overlies, or is overlain by normal marine carbonate. As is so common with Devonian carbonates in western Canada, it can be expected to become evaporitic eastward.

In certain parts of the Mackenzie Mountains and Mackenzie Plains, the "Arnica platform dolomite" is a normal marine tongue separating evaporites; this is the case in the Decolta *et al.* Wrigley I-54 well (Fig. 7.3). It is this phenomenon, plus a rough coincidence of the intervals below the Nahanni Formation, which leads to a leap in correlation, across a knowledge-gap, to the plains.

In northern Alberta, the Lower Elk Point Group is divided neatly into upper and lower salts (Cold Lake and Lotsberg) by a near-normal marine carbonate, the Ernestina Lake Formation. This threefold division can be followed into the Great Slave Lake region with little change in character. Northwest from Great Slave Lake, correlation becomes difficult. It is possible, however, using well logs and lithology, to carry the

top of the Ernestina Lake equivalent into the Willowlake area north of the Tathlina High and, with less confidence, into the Great Bear Lake area. The Bear Rock Formation (in the sense meaning the pre-Hume Devonian) is divisible, therefore, into upper and lower anhydritic units by a vaguely defined interval of more normal marine dolomite with interbedded anhydrite. By correlating the degree of salinity, one is led to equating the "Arnica platform dolomite" with the Ernestina Lake Formation and its northern equivalent. This is the basis for the isopach map (Fig. 7.1). Control points used in the plains area of Figure 1 are not shown, nor is the basis of the correlation documented here. In the cross-sections (Figs. 7.2 and 7.3), the markers that are correlated tentatively with the top of the Ernestina Lake Formation occur at 3215 feet (Fig. 7.2) in Horn R. Candel *et al.* Willowdale G-47 and at 3683 feet (Fig. 7.3) in Union Japex Blackwater E-11.

Figure 7.1 is presented only as a working hypothesis; it should be regarded very critically indeed. In the "Camsell sub-basin"[1], there is no satisfactory base for the isopached interval and there are few control points. The location of the western edge of the Liard Ridge is a guess, but as far as can be determined from the available measured sections, the "Arnica platform dolomite" is not present along the Nahanni Range. The presence of the Tathlina High is well documented but the existence of a high north of Great Slave Lake is assumed. The "McConnell Ridge" is mainly speculation but, from the scant control available, the Bear Rock Formation appears to be thin, even if allowance is made for solution of anhydrite. The "Willowlake Passage" is defensible but the "Keele Passage" is mostly geofantasy. There is some evidence, however, in this area suggesting sub-Devonian erosion channels with some hundreds of feet of relief.

[1]The terms "Camsell sub-basin", McConnell Ridge", "Keele Passage" and "Willowlake Passage" are used only for convenience; until their reality is established, a formal naming would be premature. The terms "Liard Ridge" and "Norman Wells High" (or variations of these terms) have been in use for several years, although they may not have been formally described.

Assuming, for the moment, that the interpretation of Figure 7.1 has some validity, it leads to some interesting implications:

(1) Most of the tectonic sagging, tilting or rifting occurred during the Silurian or earliest part of the Devonian Period. During the after deposition of the "Arnica platform dolomite", movements were chiefly epeirogenic.

(2) The outline of the Camsell sub-basin suggests a fault-bounded graben, with a mile or more of relative movement. How did its steep northwestern boundary escape being reflected in the structural style of the Mackenzie Mountains?

(3) A structurally created topographic barrier trended north-south, roughly coincident with the Franklin Mountains, possibly linking the Tathlina and Norman Wells Highs. (Note the similarity to the West Alberta Ridge.)

(4) There is a theoretical potential for evaporite-encased reefs (Keg River type) on the top of the "Arnica platform dolomite", especially within or near the passages.

It must be repeated that this is presented only as a hypothesis. It is evident that much work remains to be done. More field work will be required, especially in the McConnell Range. In the meantime, the field sections measured during Operation Mackenzie, with their lithologic samples and fossil collections, should be restudied and published.

References

Douglas, R.J.W. and Norris, D.K.

1960: Virginia Falls and Sibbeston Lake map-areas, Northwest Territories; Geol. Surv. Can., Paper 60-19, 8 p.

1961: Camsell Bend and Root River map-areas, District of Mackenzie, Northwest Territories; Geol. Surv. Can., Paper 61-13, 36 p.

1963: Dahadinni and Wrigley map-areas, District of Mackenzie, Northwest Territories; Geol. Surv. Can., Paper 62-33, 34 p.

8. SOME COAL-BEARING EOCENE SEDIMENTS AND COMMENTS ON THEIR COMBINED MICROFLORA, CLIFF CREEK, YUKON TERRITORY

Project 750066

W. S. Hopkins, Jr., O.L. Hughes, and M. Milner[1]
Institute of Sedimentary and Petroleum Geology, Calgary

Two exposures of coal-bearing beds of Tertiary age along Cliff Creek were examined on 8 July 1975. These sediments, located approximately at 64°33'N, 139°28'W have been referred to briefly in a number of papers (*see* references in Milner and Craig, 1963). Despite the fact that this locality, around the turn of the century, supplied several thousand tons of coal for use in Dawson City and aboard river steamers, little detailed geological work has been done. Because these coals have a potential value as a future energy source they were sampled for both coal and palynological analysis. The former analyses have not yet been completed but the following is a brief report on the results of a palynological study.

The first exposure (*see* Loc. 1 on Fig. 8.1) is on the right bank of Cliff Creek where Milner (Milner and Craig, 1973, p. 16) had uncovered remains of a portal in 1973. The exposure was sampled by Hopkins (samples C-44510 to C-44515 inclusive) but because slump and underbrush had almost obscured the outcrop a section was not measured. However, a considerable thickness of coal is indicated.

At the second exposure (Loc. 2 on Fig. 8.1), coal-bearing beds are exposed on the left bank of a southeast flowing branch of Cliff Creek immediately upstream from the remains of a building. The locality is the "upper workings" of Milner and Craig and is approximately the point shown by Green (1972) as locality 27 on Map 1284A. The beds strike approximately 332° and dip about 80° southwest. Unfortunately, no evidence was found by which tops could be determined and additional coal is possible on either side of the measured section. The sequence from Location 2 (Table 8.1) was measured after trenching across the exposed face. Channel samples for coal studies were collected over three selected intervals and two samples for palynological analysis were collected also. The locations of these five samples are indicated on the accompanying stratigraphic section (Table 8.1).

Five samples from Location 1 and two from Location 2 were examined palynologically. All but one of the samples yielded a good and well-preserved microflora which are essentially the same for all samples. These microflora are listed in Table 8.2.

Green (1972, p. 102, 103) cites several reports on plant megafossils from this coal-bearing unit, but from localities other than Cliff Creek, in which ages varying from latest Cretaceous to mid-Miocene are suggested. The fossil material was fragmentary, and evidently not specifically age diagnostic. Another sample from Coal Creek (64°27.5'N; 140°07'W) was thought, on palynological grounds, to be Tertiary, probably Eocene. Although Coal Creek samples have not yet been examined correlation of the Cliff Creek localities with those of Coal Creek is indicated as is the Eocene designation.

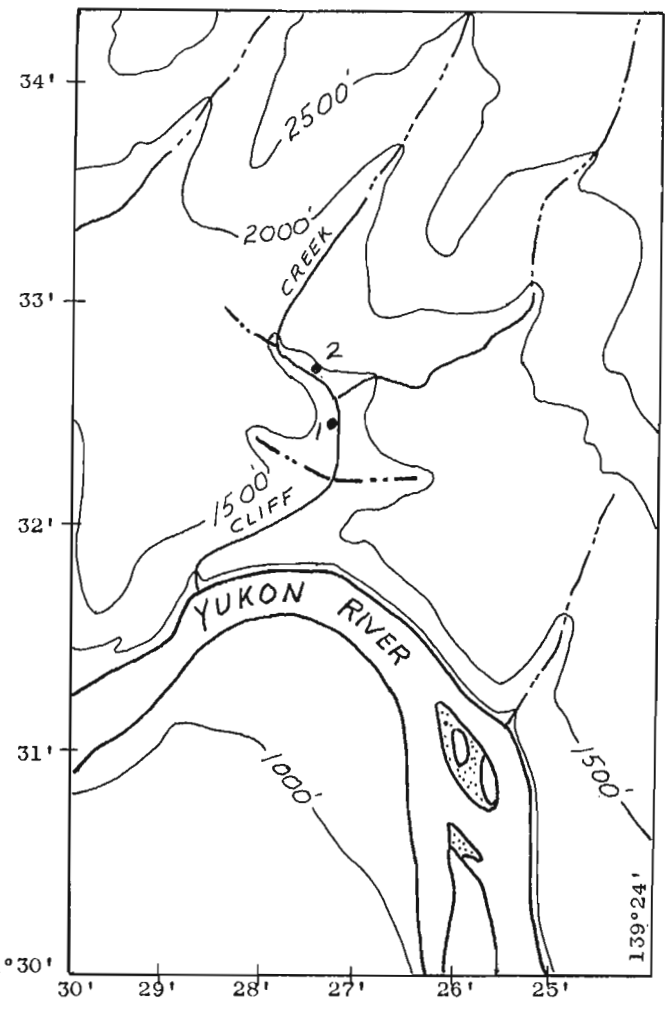

Figure 8.1. Sketch map of Cliff Creek area showing collecting localities.

The arguments advanced by Hopkins and Norris (1974) for the age of sediments in the Old Crow structural depression would apply largely here, and indeed the recovered microfloras are remarkably similar. Also present, in the Cliff Creek rocks is a specimen of

[1]Department of Indian and Northern Affairs.

Table 8. 1

Measured stratigraphic section from Location 2 (Fig. 8. 1) showing the locations of the samples taken for coal studies and palynological analysis.

Thickness	Cum. Thickness	Description
3. 00 m	3. 00 m	Coal Coal sample No. 1
0. 12	3. 12	Shale, dark brown
0. 07	3. 19	Bentonite
0. 10	3. 29	Coal
0. 10	3. 39	Bentonite
0. 70	4. 09	Coal
0. 80	4. 89	Shale, black, carbonaceous Palynology Sample C-044516
0. 10	4. 99	Bentonite
0. 48	5. 47	Coal
0. 06	5. 53	Bentonite
0. 45	5. 98	Coal
0. 22	6. 20	Shale, coaly, with coal bands
0. 08	6. 28	Bentonite
0. 20	6. 48	Shale, black, coaly
0. 50	6. 98	Shale, grey, clayey
0. 25	7. 23	Bentonite, yellow-brown
0. 33	7. 56	Coal
0. 10	7. 66	Bentonite
1. 70	9. 36	Coal, several resinous bands Coal Sample No. 2
. 04	9. 40	Bentonite
. 22	9. 62	Coal, shaly
. 05	9. 67	Bentonite
. 25	9. 92	Coal Palynology Sample C-044515
. 30	10. 22	Shale
1. 10	11. 32	Coal with thin partings, resinous bands
1. 60	12. 92	Coal Coal Sample No. 3
0. 30	13. 22	Shale
1. 00	14. 22	Coal
0. 95	15. 17	Covered by large tree roots — coal or coaly shale
0. 90	16. 07	Coal
Total Coal = 11. 83 m:		COAL = 73. 6% OF TOTAL SECTION

Gothanipollis, a pollen grain of unknown affiliation, which would appear critical, because apparently it is restricted to Eocene rocks in North America, although it may occur in the earliest Oligocene. Therefore, all factors considered, a late Eocene age for the Cliff Creek assemblage is most probable.

Again, to quote Hopkins and Norris, "It would seem that during the Paleogene the climate of the northern Yukon was not significantly different from that of interior British Columbia. Therefore, this assemblage would suggest a temperate to warm temperate climate, a conclusion consistent with a late Eocene age interpretation. "

Table 8. 2

Microflora present in the 5 samples from Location 1 (Fig. 8. 1) and 2 samples from Location 2 (Fig. 8. 1)

Division EUMYCOTA
- Class FUNGI IMPERFECTI
  - *Pleuricellaesporites* sp.

Division BRYOPHYTA
- Class MUSCI
  - *Sphagnum* sp.

Division LYCOPODOPHYTA
- Family LYCOPODIACEAE
  - *Lycopodium* sp.

Division PTEROPHYTA
- Family OSMUNDACEAE
  - *Osmunda* spp.
  - *Baculatisporites* sp.
- Family POLYPODIACEAE
  - *Laevigatosporites* sp.

Division CONIFEROPHYTA
- Family PINACEAE
  - *Pinus* sp.
  - *Picea* sp.
  - *Tsuga* sp.
  - cf. *Abies* sp.
  - cf. *Cedrus* sp.
- Family TAXODIACEAE
  - *Taxodium* sp.
  - *Glyptostrobus* sp.
  - *Metasequoia*-type

Division ANTHOPHYTA
- Family cf. SALICACEAE
  - cf. *Salix* sp.
- Family BETULACEAE
  - *Alnus* sp.
  - *Betula* sp.
- Family cf. CARPINACEAE
  - cf. *Carpinus* sp.
- Family cf. CORYLACEAE
  - cf. *Corylus* sp.
- Family FAGACEAE
  - *Castanea* sp.
- Family JUGLANDACEAE
  - *Juglans* sp.
  - *Pterocarya* sp.
- Family TILIACEAE
  - *Tilia* spp.
- Family ERICACEAE
  - ?*Rhododendron* sp.

Dicotyledonae *incertae sedis*
- *Pistillipollenites macgregori* Rouse
- *Tricolpites* sp.
- *Tricolporopollenites* spp.
- *Triporopollenites* spp.
- *Gothanipollis* sp.
- Stephanocolporate grain

References

Green, L. H.
1972: Geology of the Nash Creek, Larsen Creek and Dawson map-areas, Yukon Territory; Geol. Surv. Can., Mem. 364, 157 p.

Hopkins, W. S., Jr. and Norris, D. K.
1974: An occurrence of Paleogene sediments in the Old Crow Structural Depression, Northern Yukon Territory; *in* Report of Activities, Part A, Geol. Surv. Can., Paper 74-1A, p. 315-316.

Milner, M. and Craig, D. B.
1973: Coal in the Yukon; unpubl. Ms., 27 p.

9. GEOCHEMISTRY OF OILS AND CONDENSATES FROM THE MACKENZIE DELTA BASIN, N.W.T.

Project 740038

T. G. Powell and L. R. Snowdon
Institute of Sedimentary and Petroleum Geology, Calgary

Preliminary geochemical analyses have been carried out on 46 oils and condensates from twelve petroleum exploration wells in the Mackenzie Delta Basin. For reasons of confidentiality the wells are only distinguished by the letters A to L. The hydrocarbons in this region occur in fluviatile and deltaic sandstones of Tertiary and Cretaceous ages (Lerand, 1974). The oils were distilled to 210°C and the residues, after precipitation of the asphaltenes, were fractionated into saturated hydrocarbons, aromatic hydrocarbons and resins by liquid chromatography. Quantitative assessments of n-alkanes and acyclic isoprenoid alkanes (^{15}C to ^{20}C) were carried out by gas chromatographic analysis of the saturate fractions.

The oils and condensates show a wide range of gravities (20-48°API) and their sulphur contents are generally below 0.4 per cent. Analyses of the residues remaining after distillation has shown that they all have a low content of resins and asphaltenes, but with varying amounts of aromatic hydrocarbons (Fig. 9.1). The oils and condensates from the Mackenzie Delta Basin are depleted in resins, asphaltenes and aromatics compared with both the conventional and heavy oils from the Alberta part of the Western Canadian Sedimentary Basin (Deroo *et al.*, in press). In terms of gross composition, the majority are more like Australian oils, many of which are nonmarine in origin (Powell and McKirdy, 1975).

The compositions of the saturate fractions are variable (Fig. 9.2). Many of the oils contain no n-alkanes or acyclic isoprenoids (^{15}C-^{20}C) and such oils often have a low content (below 25 per cent) of gasoline-range hydrocarbons. Moreover, within a given well in which there are a number of producing zones, a whole spectrum of saturated hydrocarbon compositions can be observed (Fig. 9.2). In these cases, the shallowest samples contain no n-alkanes or isoprenoid alkanes but, with increasing depth, the oils contain first isoprenoid alkanes and the isoprenoid and n-alkanes together (Fig. 9.2, Well J). In some wells, n-alkanes are

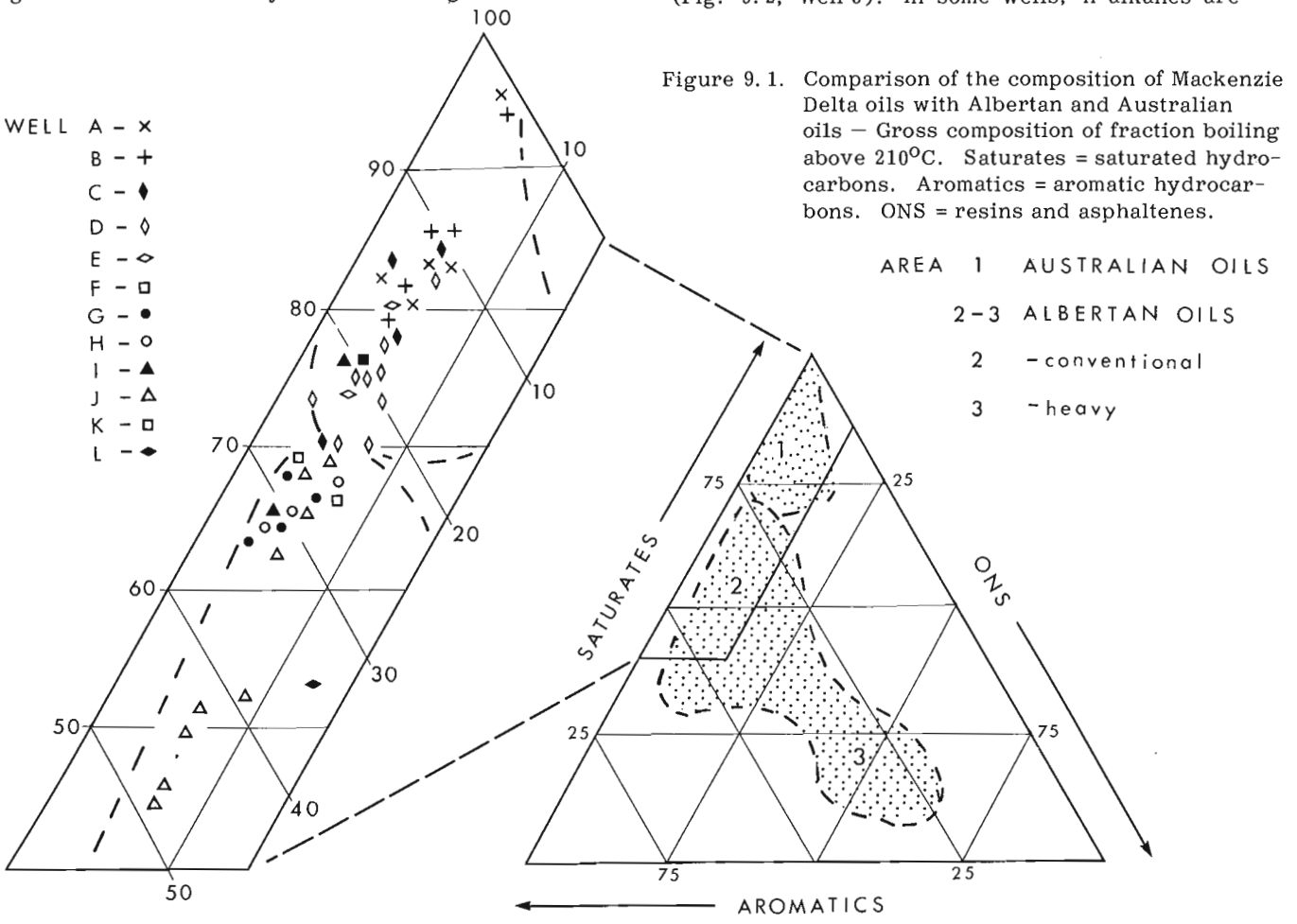

Figure 9.1. Comparison of the composition of Mackenzie Delta oils with Albertan and Australian oils — Gross composition of fraction boiling above 210°C. Saturates = saturated hydrocarbons. Aromatics = aromatic hydrocarbons. ONS = resins and asphaltenes.

always present in the oils but their concentration may increase with greater burial depth (Well B). These changes have been observed in both oils and condensates. The actual depth interval over which the variations occur may not be large and in some cases the trend is irregular (Well D).

The question arises as to the nature of the process which has caused these changes. The two possibilities are maturation or biodegradation. The maturation hypothesis requires that a heavy oil (rich in asphaltenes) gives rise to lighter more paraffinic crudes by thermal cracking which results in the formation of n-alkanes and simple branched alkanes. The biodegradation hypothesis requires that bacteria selectively metabolize first n-alkanes and then isoprenoids. Under the maturation hypothesis, immature oil containing no n-alkanes or isoprenoids and with a low gasoline content gives rise to mature gasoline-rich oils containing n-alkanes or isoprenoids and with increasing burial. Under the biodegradation hypothesis mature oils become biodegraded at relatively shallow depths resulting in the removal of n-alkanes and isoprenoids and a depletion of the gasoline content.

The maturation hypothesis cannot be considered for the Mackenzie Delta oils for the following reasons. There is no difference in asphalt content between oils with and without n-alkanes and isoprenoids. The sequence in which isoprenoids appear first followed by n-alkanes, cannot be explained by the maturation hypothesis (Deroo *et al.*, 1974). Drastic changes occur in the composition of the saturated hydrocarbons over very short depth intervals where the temperature differences are extremely small. Regular variations in saturate composition were observed also in condensates which are thermally mature products.

The similarity in gross composition of oils within a particular well suggests that the changes in the composition of the saturate fractions must be due to biodegradation. The sequential disappearance of n-alkanes and isoprenoids with decreasing depth is consistent with the experimental results obtained on biodegradation of crude oil (Bailey *et al.*, 1973). Similar results, also attributed to biodegradation, have been obtained for oils in the Western Canadian Sedimentary Basin (Bailey *et al.*, 1974; Deroo *et al.*, 1974). In this case the oils become heavier as biodegradation proceeds due to concentration of asphaltenes. In the Mackenzie Delta oils this process is not observed since their asphaltene content is extremely low. The loss of gasoline-range hydrocarbons can be explained also by biodegradation since the n-alkane content of this fraction is substantial and water washing which often accompanies biodegradation (Bailey *et al.*, 1973) adds to the loss of low boiling components.

There are, however, several conceptual problems associated with the biodegradation hypothesis. Firstly, it appears from experimental results, that biodegradation is caused only by aerobic bacteria, i.e., oxygenated waters are required for biodegradation to occur. In other cases, such as the Athabasca Tar Sands, biodegradation occurs at shallow depth (above 2000 ft.) and is caused by invasion of the petroleum reservoir

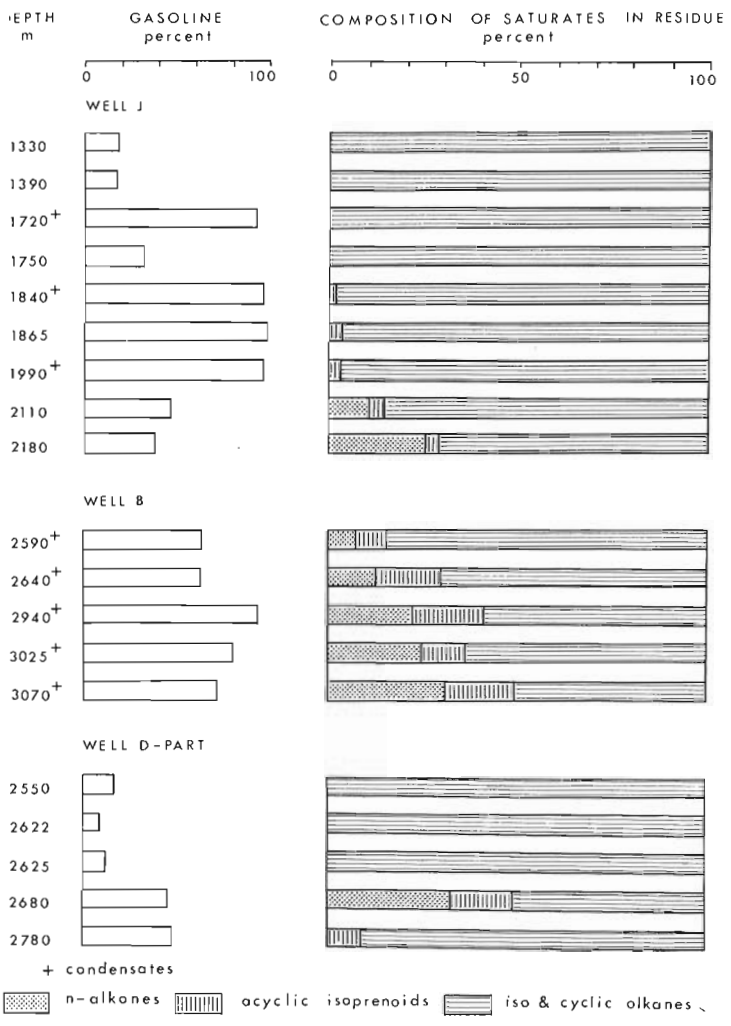

Figure 9.2. Variations in compositions of the saturated hydrocarbons in oils and condensates from three exploration wells in the Mackenzie Delta.

by meteoric waters bearing oxygen and bacteria. In the Mackenzie Delta, biodegradation appears to have occurred at least to a depth of 2600 m. Thus, within the limits of our knowledge it is necessary to admit the presence of meteoric waters at this depth, but at the moment we have no means of determining how this might have occurred. The second problem concerns the process of biodegradation. In experimental studies it has been shown that oil can be biodegraded in a matter of weeks under ideal conditions, that is where the culture is agitated, bacterial growth factors are added and the oil becomes emulsified (Bailey *et al.*, 1973). In the geological context biodegradation appears to occur in discrete and often massive oil bodies and may, as in the Athabasca Tar Sands, go essentially to completion. Presumably bacterial activity occurs at the oil/water interface. Another conceptual difficulty is, how can a complete oil pool become biodegraded when only the margins of the pool are exposed to bacterial activity.

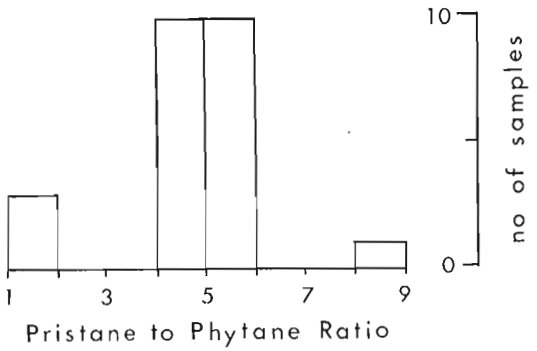

Figure 9.3. Frequency distribution of pristane to phytane ratios from those oils and condensates containing acyclic isoprenoid alkanes in the Mackenzie Delta. Total number of samples = 24.

Oils and condensates from the Mackenzie Delta are paraffinic-naphthenic to naphthenic in composition. The naphthenic oils are probably derived from the more paraffinic types of biodegradation. Powell and McKirdy (1975) have subdivided Australian paraffinic-naphthenic oils into two groups on the basis of their overall composition, wax content, ^{19}C to ^{20}C isoprenoid ratios (pristane to phytane ratios) and the depositional environment of their presumed source beds. This classification appears to be relevant to the Mackenzie Delta oils. High wax and predominantly paraffinic oils with generally high pristane to phytane ratios (above 4.5) occur in lacustrine, fluviatile and deltaic sequences with little or no marine influence and are of nonmarine origin. Paraffinic-naphthenic oils with intermediate pristane to phytane ratios (3.0 to 4.5) occasionally with a high wax content occur in marginal marine clastic sequences or in deltaic sediments with some marine influence and are probably derived from organic matter of mixed origins (marine and terrestrial). The non-biodegraded oils from the Mackenzie Basin appear to fall in the second category. The wax content (n-alkanes above $n_{22}C$) of these oils is low (below 5 per cent); the pristane to phytane ratios are higher than most marine oils (1-3) but are lower than many nonmarine oils (above 4.5) (Fig. 9.3); the depositional environments of the sedimentary sequence in the Mackenzie Delta Basin ranges from deltaic to marginal marine.

There is considerable variation in the aromatic content of the distillation residues, but the pristane to phytane ratios are very similar. At the moment it is unclear whether there is more than one type of oil in this region or whether the variations in composition merely represent slight changes in the character of the source organic matter.

References

Bailey, N.J.L., Evans, C.R., Krouse, H.R., and Rogers, M.A.
1973a: Alteration of crude oils by waters and bacteria: Evidence from geochemical and isotopic studies; Am. Assoc. Petrol. Geologists Bull., v. 57, p. 1276-1290.

Bailey, N.J.L., Jobson, A.M., and Rogers, M.A.
1973b: Bacterial degradation of crude oil; comparison of field and experimental data; Chem. Geol., v. 11, p. 203-221.

Deroo, G., Powell, T.G., Tissot, B., McCrossan, R.G., and Hacquebard, P.A.
The origin and migration of petroleum in the Western Canadian Sedimentary Basin, Alberta: A geochemical and thermal maturation study; Geol. Surv. Can., Bull. (in press).

Deroo, G., Tissot, B., McCrossan, R.G., and Der, F.
1974: Geochemistry of the heavy oils of Alberta; *in* Oil Sands, Fuel of the Future, L.V. Hills ed., Can. Soc. Pet. Geol., Mem. 3, p. 148-167.

Lerand, M.
1973: Beaufort Sea; *in* Future Petroleum Provinces of Canada, R.G. McCrossan ed., Can. Soc. Pet. Geol., Mem. 1, p. 315-386.

Powell, T.G. and McKirdy, D.M.
1975: Geological factors controlling crude oil composition in Australia and Papua, New Guinea; Am. Assoc. Pet. Geol., Bull., v. 59, p. 1176-1197.

10. DIFFERENTIATION AND QUANTITIZATION OF SULPHUR-BEARING MINERALS IN SEDIMENTARY ROCKS AND SOILS BY DIFFERENTIAL HEAT TREATMENT

Project 680090

R. R. Barefoot, A. E. Foscolos and R. A. Juska
Institute of Sedimentary and Petroleum Geology, Calgary

Introduction

The quantitization of sulphur-bearing minerals in rocks and soils is becoming increasingly important in geological and engineering sciences. The presence of small amounts of pyrite (FeS_2) has a large effect on the formation density log leading to inaccurate estimates of lithology and porosity from well logs (Knutson and Ellis, 1972). Sulphates in soils can affect the resistance of concretes (Swanson, 1968); since pyrite may be readily converted to gypsum, it is important for the civil engineer to know the amount of pyrite present.

A common method for total sulphur determination is to decompose the sample in an oxidizing environment, thereby converting sulphur to sulphate. Upon addition of barium chloride, barium sulphate precipitates out. Sulphate can be analyzed directly by measuring the weight of barium sulphate precipitate (Assoc. Offic. Agric. Chemists, 1955; Goldrich *et al.*, 1959; Shapiro and Brannock, 1962; Wilson *et al.*, 1963). This technique is applicable to samples that have an appreciable amount of sulphur. Another method of measuring the $BaSO_4$ precipitate is by turbidimetry as discussed by Shapiro (1973).

Determination of small amounts of sulphur in samples can be accomplished by igniting such samples in a current of oxygen, thus producing sulphur dioxide which is absorbed in an excess of potassium iodate-iodide solution; the excess is then back-titrated with thiosulphute solution (Sen Gupta, 1963). A similar method is described by Finch and Ives (1973), while a different approach in determining very small amounts of sulphide minerals is presented by Van Loon *et al.* (1968).

The aim of this paper is to show that several sulphur-bearing minerals can be successfully removed by differential heat treatment and then quantitized by sulphur analysis. The method used for total sulphur determination is the one described by Foscolos and Barefoot (1970). This procedure uses a Leco induction furnace with an automatic sulphur titrator.

Procedure

Material

The following sulphur-bearing reagents and sulphur-bearing minerals were used:

Calcium sulphate $CaSO_4$
analytical reagent from Mallinckrodt
Calcium sulphate hydrate $CaSO_4 \cdot 2H_2O$
analytical reagent from Mallinckrodt
Supric sulphate $CuSO_4$
analytical reagent from Mallinckrodt

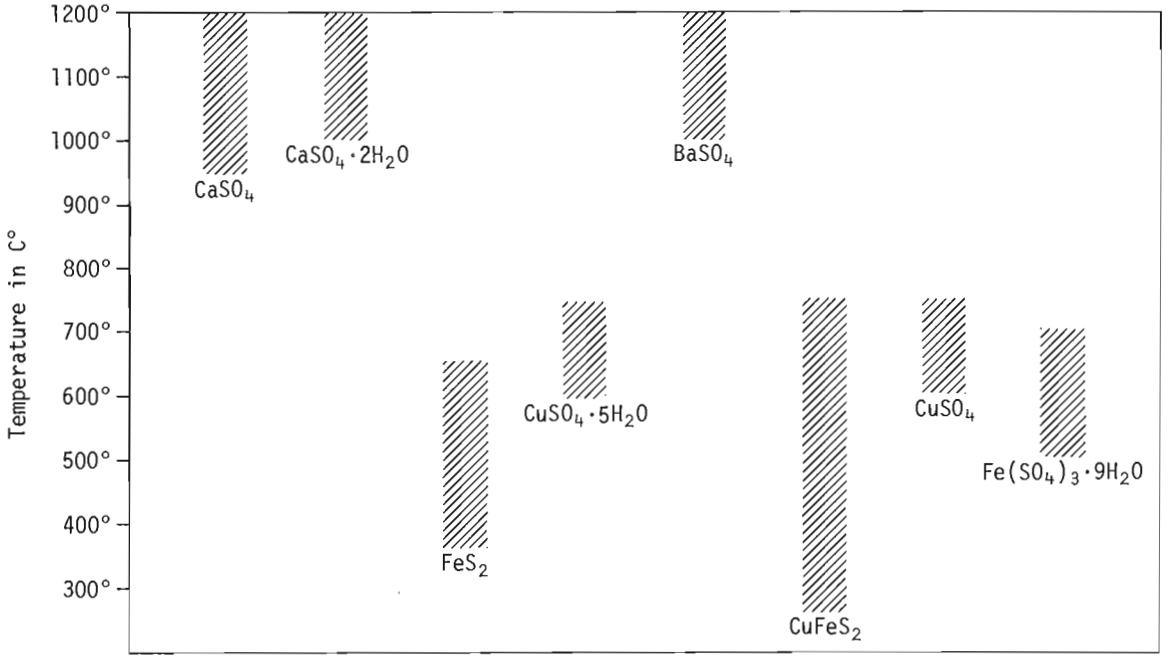

Figure 10.1. Ranges of decomposition temperatures in C° for 15-minute heating, <140 mesh size, 125 mg sample of sulphur-bearing minerals and reagents.

Table 10.1

Comparison of Empirical per cent Sulphur with analyzed per cent Sulphur

Sample	% Sulphur (Analysed Average)	% Sulphur (Empirical)
$CaSO_4$	2.2	2.35
$CaSO_4 \cdot 2H_2O$	1.7	1.86
FeS_2	1.8	2.67
$CuSO_4 \cdot 5H_2O$	2.3	2.56
$BaSO_4$	2.6	2.76
$CuFeS_2$	2.0	3.49
$CuSO_4$	1.8	2.01
$Fe(SO_4)_3 \cdot 9H_2O$	1.8	1.71

Copper sulphate hydrate $CuSO_4 \cdot 5H_2O$
analytical reagent from Mallinckrodt
Ferric sulphate hydrate $Fe_2(SO_4)_3 \cdot 9H_2O$
analytical reagent from Fisher Sci. Co.
Pyrite from Colorado FeS_2
from Wards Natural Science Establishment
Barite from North Carolina $BaSO_4$
from Wards Natural Science Establishment
Chalcopyrite from Kansas $CuFeS_2$
from Wards Natural Science Establishment

Apparatus

A Leco induction furnace, with a purifying train to remove water and sulphur compounds from the oxygen flow, was used for the analyses, coupled with a Leco automatic sulphur titrator in which titration proceeds continuously by means of an electronic circuit and the end point is arrived at automatically.

The differential heat treatments were carried out in a Lindberg muffle furnace, capable of producing temperatures in the range of from 200°C to 1200°C in 50°C increments.

Reagents

A potassium iodate (KIO_3) solution (1 ml KIO_3 = 0.2 mg S) was prepared by dissolving 0.444 gm of KIO_3 in double-distilled water in a one-litre volumetric flask and diluting to volume. The buret range for this solution is 0.00 to 4.00 per cent sulphur. Multiples of this range can be obtained by preparing potassium iodate solutions with corresponding multiples of 0.444 gm KIO_3.

The starch solution was prepared by adding 2 gm of Arrowroot starch to 50 ml of double-distilled water and stirring. This mixture was then added to 150 ml of boiling double-distilled water while stirring. After 2 minutes of boiling, it was cooled to room temperature and 6 gm of potassium iodide were added.

The hydrochloric acid solution was prepared by diluting 15 ml of concentrated hydrochloric acid to 1000 ml with double-distilled water.

Method

Ground samples of <140 mesh in size were diluted with Al_2O_3 in order to bring the sulphur concentration within the range of the automatic sulphur titrator (1-3 per cent). The mixture was transformed into sulphur-free, porous combustion crucibles, and 1 gm of iron chips and 1 gm of tin flux were added. Each sample was placed in the Leco induction furnace, while the acid and starch solutions were added to the automatic titrator. The per cent sulphur readings were obtained from the buret at 5-second intervals for the first 4 minutes and a final reading was taken after another 2 minutes, for a total of 6 minutes.

For the differential heat treatment, seven 125 mg samples were weighed into combustion crucibles, and heated for 15 minutes. Each crucible containing one sample was heated to a specific temperature. Temperatures ranged from 200°C to 1200°C, in 200°C increments. The samples were cooled and the rate of sulphur evolution was recorded at the same time intervals as before. The approximate decomposition points were graphically determined, and the procedure was repeated using 50°C increments to determine more precisely the

Table 10.2

Reproducibility of sulphur determinations in sulphur-bearing minerals and reagents of six identical runs

Sulphur-bearing minerals and reagents	Number of Runs 1	2	3	4	5	6
$CaSO_4$	2.16	2.14	2.19	2.18	2.22	2.20
$CaSO_4 \cdot 2H_2O$	1.66	1.72	1.62	1.70	1.64	1.72
FeS_2	1.83	1.82	1.70	1.76	1.70	1.73
$CuFeS_2$	1.83	2.04	1.78	2.01	1.91	1.94
$Fe(SO_4)_3 \cdot 9H_2O$	1.74	1.85	1.85	1.83	1.72	1.70
$CuSO_4$	1.81	1.80	1.82	1.74	1.80	1.77
$CuSO_4 \cdot 5H_2O$	2.42	2.49	2.39	2.33	2.34	2.36
$BaSO_4$	2.55	2.46	2.64	2.54	2.49	2.56

Table 10.3

Efficiency of separation of mineral mixtures by varying heating time and/or temperatures to remove the lower decomposed component (125 mg samples)

Mixtures (1:1 by Weight of Dilute Samples)		Per cent end member which decomposes at lower temperature	
Anhydrite:Pyrite	(800°C)	97%	(½ hour)
	(800°C)	95%	(1 hour)
Gypsum:Pyrite	(800°C)	94%	(½ hour)
	(800°C)	101%	(1 hour)
Gypsum:Copper Sulphate	(800°C)	100%	(½ hour)
	(800°C)	97%	(1 hour)
Gypsum:Chalcopyrite	(900°C)	99%	(½ hour)
	(900°C)	101%	(1 hour)
Gypsum:Ferric Sulphate	(900°C)	94%	(½ hour)
	(900°C)	100%	(1 hour)
Pyrite:Chalcopyrite	(525°C)	*157%	(16 hours)
Pyrite:Ferric Sulphate	(430°C)	8%	(½ hour)
	(500°C)	58%	(1 hour)
	(500°C)	56%	(2 hours)
	(500°C)	78%	(3 hours)
	(500°C)	*164%	(19 hours)
	(525°C)	58%	(½ hour)
	(525°C)	96%	(1 hour)
	(525°C)	*169%	(16 hours)

*Some of the higher temperature decomposed mineral was also destroyed.

decomposition temperature of each compound. Afterwards, 1:1 mixtures of sample pairs with appreciably differing decomposition temperatures were prepared. One hundred and twenty-five mg samples of these mixtures were transferred into crucibles and heated for one-half hour at temperatures higher than the lower point of decomposition of the one component, and lower than the higher point of decomposition of the other component. Total sulphur analyses, prior to and after the heat treatment, were used to determine the concentration of both components by the differential heat treatment technique.

In addition, the effect of varying amounts of accelerator (iron) and flux (tin) on the rate of sulphur evolution was studied. This was done by either keeping the amount of iron constant and varying the amount of tin or by keeping the amount of tin constant and varying the amount of iron, or by keeping the ratio of tin and iron constant but varying their weight.

Results and Discussion

Comparisons between per cent sulphur obtained from the theoretical formula of the sulphur-bearing minerals and reagents and that obtained from the analyses (Table 10.1) reveal discrepancies due to impurities and to hydration. Ferric sulphate showed a negative discrepancy; that is, the empirical formula indicates less sulphur than was actually measured due to the fact that ferric sulphate is not fully hydrated as indicated by the formula. The large difference in per cent sulphur between theoretical and actual values with pyrite (FeS_2) and chalcopyrite ($CuFeS_2$) is due to impurities. As a result, the empirical formulas do not reflect their precise mineral composition.

Repeated measurements of the unheated samples did not give identical second decimals (Table 10.2). Thus, experimental and instrumental parameters dictate values with two significant figures.

The temperatures of decomposition as well as the ranges of decomposition for the sulphur-bearing minerals and reagents studied using 125 mg samples and 15-minute heating are presented in Figure 10.1. The decomposition temperature is the most important value since, with time, a sample could be completely destroyed at this temperature. However, the temperature ranges as such are of little value because the rate of sulphur evolutions depends upon time, amount of sample, particle

Table 10.4

Percentage of total sulphur evolved as a function of heating time in the Leco Induction Furnace

Sample	Time (Min.) 1.0	1.2	1.4	1.6	1.8	2.0	2.2	2.4	2.6	3.0	4.0	5.0	6.0
$CaSO_4$	0	0	0	0	5	29	53	76	95	100	100	100	100
$CaSO_4 \cdot 2H_2O$	0	0	0	0	19	42	67	90	99	100	100	100	100
FeS_2	0	0	0	0	2	13	40	68	96	100	100	100	100
$CuSO_4 \cdot 5H_2O$	0	0	0	0	8	25	55	71	87	100	100	100	100
$BaSO_4$	0	0	4	22	53	82	97	100	100	100	100	100	100
$CuFeS_2$	0	0	0	2	22	54	83	96	100	100	100	100	100
$CuSO_4$	0	0	4	25	59	87	100	100	100	100	100	100	100
$Fe_3(SO_4)_3 \cdot 9H_2O$	0	0	14	49	84	100	100	100	100	100	100	100	100

Table 10.5

Effects of varying amounts of iron chips and/or tin flux on rate of SO_2 evolution (samples were 125 mg of anhydrous copper sulphate)

Ratios (Fe Const.)	Time For SO_2 Evolution	Ratios (Sn Const.)	Time For SO_2 Evolution	Ratios (1:1)	Time For SO_2 Evolution
1.0g:0.0g	1.2 min.	0.0g:1.0g	*	0.0g:0.0g	*
1.0g:0.2g	1.3 min.	0.2g:1.0g	*	0.2g:0.2g	*
1.0g:0.4g	1.1 min.	0.4g:1.0g	1.0 min.	0.4g:0.4g	0.8 min.
1.0g:0.6g	1.2 min.	0.6g:1.0g	1.0 min.	0.6g:0.6g	1.0 min.
1.0g:0.8g	1.2 min.	0.8g:1.0g	1.0 min.	0.8g:0.8g	1.0 min.
1.0g:1.0g	1.2 min.	1.0g:1.0g	1.2 min.	1.0g:1.0g	1.3 min.
1.0g:1.2g	1.1 min.	1.2g:1.0g	1.2 min.	1.2g:1.2g	1.2 min.
1.0g:1.4g	1.3 min.	1.4g:1.0g	1.2 min.	1.4g:1.4g	1.7 min.

*No SO_2 evolved.

size, distribution in the crucible, crucible mass, and the atmosphere within the muffle furnace. Figure 10.1, therefore, is a good indicator of pairs which are potentially separable. Preparation of sulphur-bearing mixtures heated to appropriate temperatures with varying time and/or temperature gave good separation for the samples with widely differing decomposition temperatures, and poor separation for those with close decomposition points (Table 10.3). Separation may be improved by increasing time and/or temperature. The latter can be done as long as the decomposition temperature of the sulphur-bearing mineral which is destroyed at the highest temperature is not reached. Table 10.4 indicates that all samples gave relatively rapid sulphur evolution. However, from Figure 10.1 it is deduced that heating to the initial point of decomposition is not sufficient for the complete destruction of the sulphur-bearing mineral due to the extent of the range of decomposition temperatures for some minerals, e.g., chalcopyrite ($CuFeS_2$).

Table 10.5 shows that varying ratios of iron chips and tin flux have little or no effect on the starting time of SO_2 evolution. The results also indicate that, regardless of the variation in the amounts of iron or tin fluxes, SO_2 evolution from the minerals tested required 1 minute or more to begin. Once evolution began, the rate was relatively constant, with some variation due to mineral character, as well as to extent of mixing of iron and tin with the sample. It may be concluded that any appreciable sulphur evolution occurring within one minute could indicate the presence of a different sulphur source, possibly organic in nature, and that any change in the rate of evolution would have to be due to the nature of the sample. Finally, the total amount of fluxes affects the starting time of SO_2 evolution. The larger the amount of flux, the more time is required. This probably is due to heat absorption by the flux rather than by the sulphur-bearing minerals and reagents.

From Figure 10.1 and Table 10.3 it can be deduced that calcium and barium sulphates in sedimentary rocks and soils can be quantitized, in the presence of pyrite, chalcopyrite and copper and iron sulphates, by differential heat treatment and subsequent sulphur determination. The best procedure is to heat 125 mg samples of <140 mesh at 800°C for 30 minutes and determine the sulphur content before and after the heat treatment. Differentiation between copper and iron sulphites and sulphates on one hand and calcium and barium sulphates on the other cannot be achieved by differential heat treatments.

Thus the method as described is rapid and accurate for quantitizing some sulphur-bearing minerals. Though it is restricted to the minerals tested here, it is obvious that, once the decomposition point of other minerals is known, then the quantitization of many more sulphur-bearing minerals can be achieved.

References

Association of Official Agricultural Chemists
1955: Official methods of analysis; Ed. 8, Assoc. Offic. Agric. Chemists, Washington, D.C.

Finch, J. and Ives, M.
1973: Rapid and simple determination by combustion of wide ranges of sulphur minerals and mineral products; N.Z. J. Sci., v. 16, p. 171-183.

Foscolos, A.W. and Barefoot, R.R.
1970: A rapid determination of total sulphur in rocks and minerals; Geol. Surv. Can., Paper 70-11, 14 p.

Goldrich, S.S., Ingamells, C.O., and Thaemlitz, D.
1959: The composition of Minnesota lake-marl-comparison of rapid and conventional methods; Econ. Geol., v. 54, p. 285-300.

Knutson, G.C. and Ellis, J.A.
1972: Effects of pyrite on well log interpretation of complex lithology; Trans. Can. Well Logging Soc., Fourth Form. Evol. Symposium, p. M1-M3.

Sen Gupta, J.G.
1963: Determination of microgram amounts of total sulphur in rocks; Anal. Chim. Acta, v. 35, p. 1971-1973.

Shapiro, L.
1973: Rapid determination of sulphur in rocks; U.S. Geol. Surv., J. Res., v. 1, no. 1, p. 81-82.

Shapiro, L. and Brannock, W.W.
1962: Rapid analysis of silicate, carbonate and phosphate rocks; U.S. Geol. Surv., Bull. 1144-A, p. A53.

Swanson, C.G.
1968: Performance of concrete; *in* Resistance of concrete to sulphate and other environmental conditions; Univ. Toronto Press, p. 243.

Van Loon, J.C., Parissis, C.M., and Kingston, P.W.
1968: Analysis of very small samples of sulphide minerals; Anal. Chim. Acta, v. 40, no. 2, p. 334-338.

Wilson, A.D., Sergeant, G.A., and Lionnel, L.J.
1963: The determination of total sulfur in silicate rocks by wet oxidation; Analyst, v. 88, p. 138-140.

11. THE LITTLE DOCTOR SANDSTONE (NEW SUB-UNIT) AND ITS RELATIONSHIP TO THE FRANKLIN MOUNTAIN AND MOUNT KINDLE FORMATIONS IN THE NAHANNI RANGE AND NEARBY SUBSURFACE, DISTRICT OF MACKENZIE

Project 710011

N.C. Meijer-Drees
Institute of Sedimentary and Petroleum Geology, Calgary, Alberta

Introduction

About 103 km (64 miles) west of Fort Simpson and 19 km (12 miles) south of Little Doctor Lake, lower Paleozoic rocks form a prominent, east-facing scarp in the Nahanni Mountain range (Fig. 11.1). There, dark grey beds of the Mount Kindle Formation (map-unit 4 of Douglas and Norris, 1960) overlie pale brown and yellowish brown dolomite assumed to belong to the Franklin Mountain Formation (map-unit 2 of Douglas and Norris, 1960). The top of the yellowish brown dolomite of the Franklin Mountain Formation can be traced northward and southward along the escarpment until it disappears below the surface in both directions. A dark grey recessive unit, about 24 m (80 ft) thick, occupies the interval between the yellowish brown dolomite cliffs of the Franklin Mountain Formation below and the dark grey cliffs of the Mount Kindle dolomite above (Fig. 11.2). Brady (*in* Brady and Wissner, 1961) noted the presence of sandstone in this recessive unit and included this distinctive facies in the Franklin Mountain Formation. In the subsurface of the Fort Simpson area (Meijer-Drees, in press), a sandstone unit, similar to the one described by Brady, conformably underlies the dolomite of the Mount Kindle Formation and unconformably overlies Cambrian and (?)Helikian formations.

Because of the similarity in stratigraphic position of this subsurface sandstone unit with that described by Brady *(ibid.)*, the writer visited the location south of Little Doctor Lake (Fig. 11-1) during the summer of 1974. Evidence indicating an unconformity at the base of the sandstone beds was found at this time.

A significant regional unconformity at the base of the Mount Kindle Formation was recognized during the field studies of Operation Norman (Macqueen, 1970). In 1965, B.S. Norford visited the type section at Mount Kindle in the McConnell Range and recognized the unconformity at the base of a dark grey, recessive unit consisting of dolomite and shale, which overlies the Franklin Mountain Formation. This argillaceous unit at Mount Kindle is 21 m (70 ft) thick and is referred to informally as the "basal member" of the Mount Kindle Formation (Norford and Macqueen, in press).

In the Nahanni Range, the following two facts suggest that the sandstone beds mentioned by Brady (*in* Brady and Wissner, 1961) should, more properly, comprise part of the Mount Kindle rather than part of the Franklin Mountain Formation.

1. The sandstone beds overlie unconformably the main part of the Franklin Mountain Formation.
2. The sandstone beds contain brachiopods of the same genus as those found in the "basal member" of the Mount Kindle Formation at Mount Kindle.

Additional work established the similarity between surface and subsurface geology and it became clear that the sandstone unit in the Nahanni Range is equivalent to the sandstone unit that underlies the Mount Kindle dolomite in the subsurface of the Fort Simpson area.

This sandstone unit is distinct, widespread and probably equivalent in age to all or part of the "basal member" of the Mount Kindle Formation at Mount Kindle. Therefore, the writer proposes that this sandy facies be known as the Little Doctor sandstone.

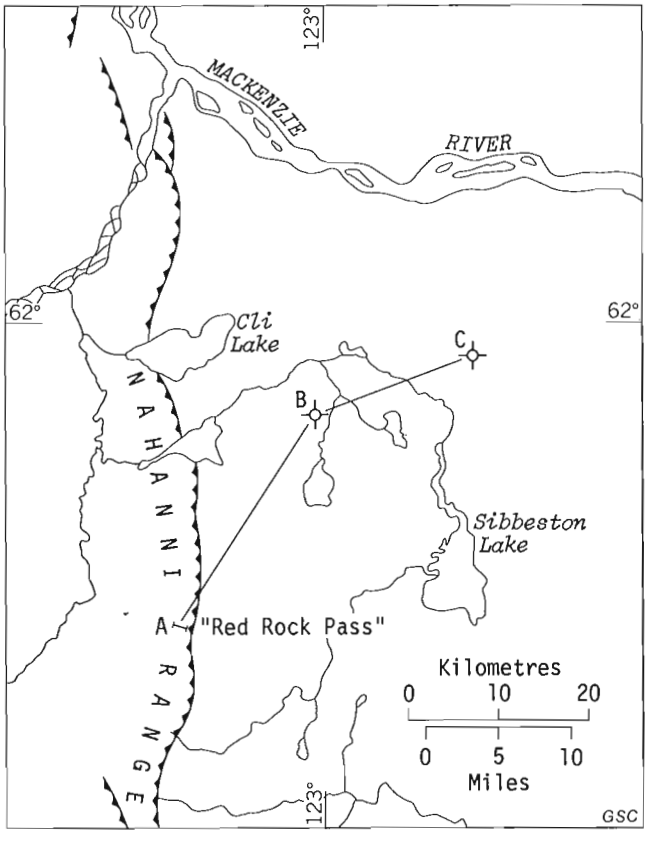

Figure 11.1: Location of the "Red Rock Pass" composite section and of the cross-section on Figure 11.3.

Stratigraphic Succession

Franklin Mountain Formation

Strata underlying the Little Doctor sandstone include those of the Franklin Mountain Formation (Williams, 1923). In the Nahanni Range, the Franklin Mountain Formation consists of arenaceous dolomite, dolomite, and dolomitic sandstone. The succession is well bedded, in places laminated, and weathers pale grey, pale yellowish brown and pale reddish brown. At "Red Rock Pass" (Brady and Wissner, 1961; Lat. 61°42'20"N, Long. 123°18'20"W), the section is incomplete and the lower contact is not exposed. The rocks are extremely fractured. The presence of scattered black, silicified oolites and the absence of chert and shale beds in the dolomite (*see* Appendix) suggest that the entire succession at that locality belongs to the rhythmic unit of the Franklin Mountain Formation (Macqueen, 1970). The top of the Franklin Mountain Formation, as shown on Figure 11.2, gives the impression of being an unconformity that cuts downsection in both northerly and southerly directions.

In the nearby subsurface, east of the Nahanni Range, the Franklin Mountain Formation is present in the Horn R. Am. Hess Gulf Cli Lake M-05 well (Lat. 61°54'58"N, Long. 123°01'47"W) between depths of 6240 and 6322 feet (1872 and 1895 m), and overlies the Saline River Formation. However, in the area east of

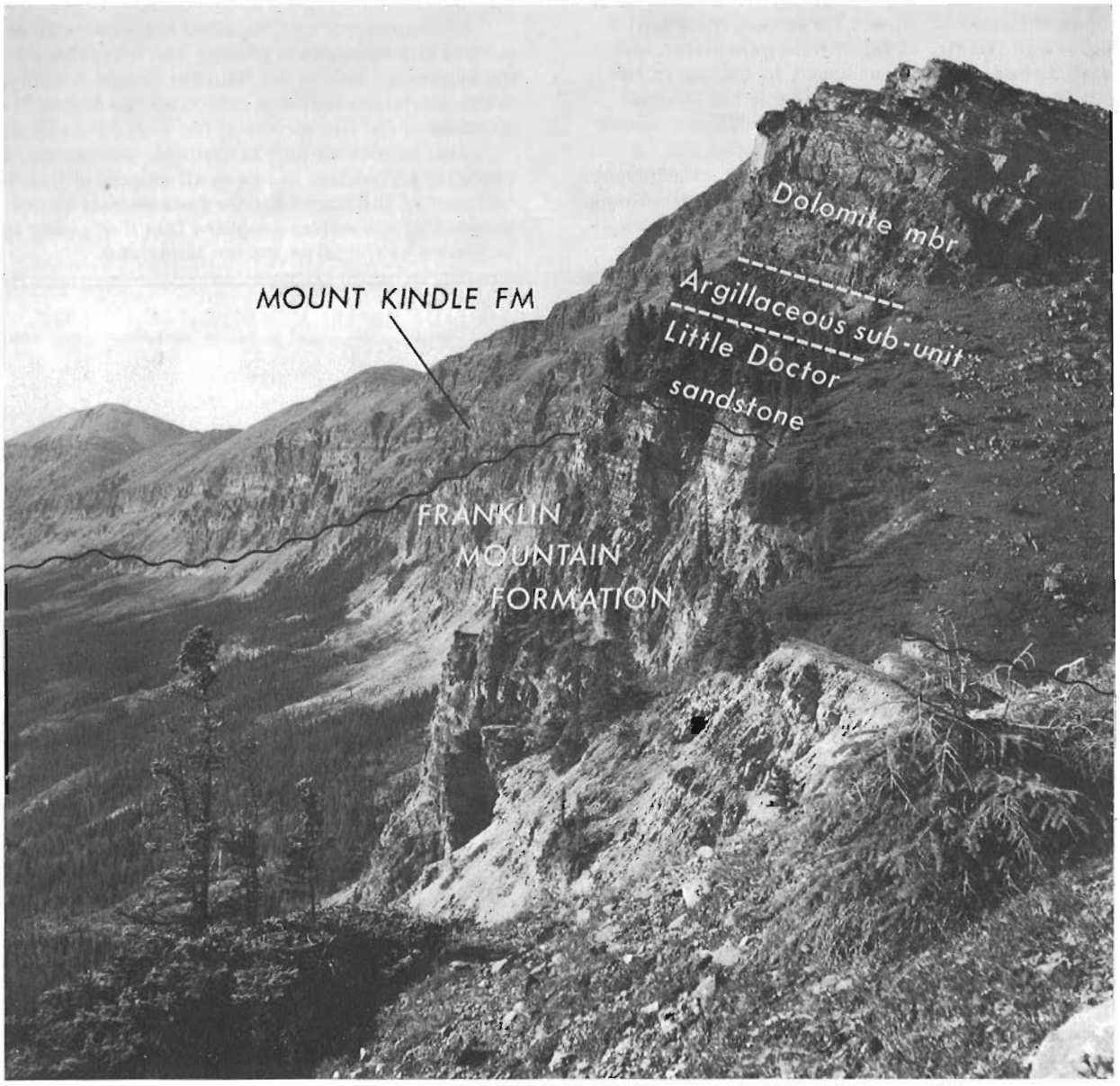

Figure 11.2: View from "Red Rock Pass" southward along the east-facing scarp of the Nahanni Range showing assumed unconformity between Franklin Mountain and Mount Kindle Formations.

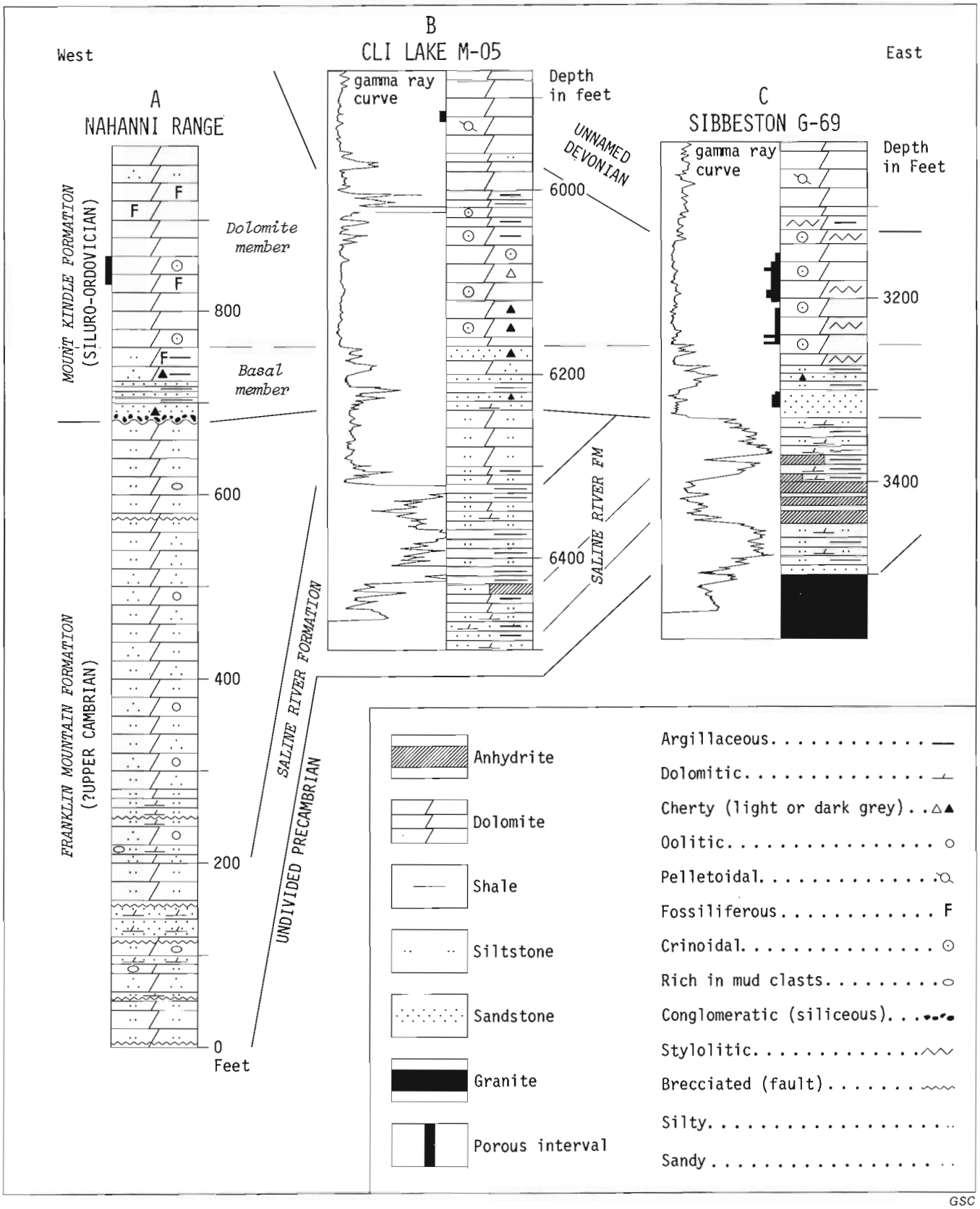

Figure 11.3: Correlation along section ABC (Fig. 11.1) of the lower Paleozoic formations southwest of Little Doctor Lake.

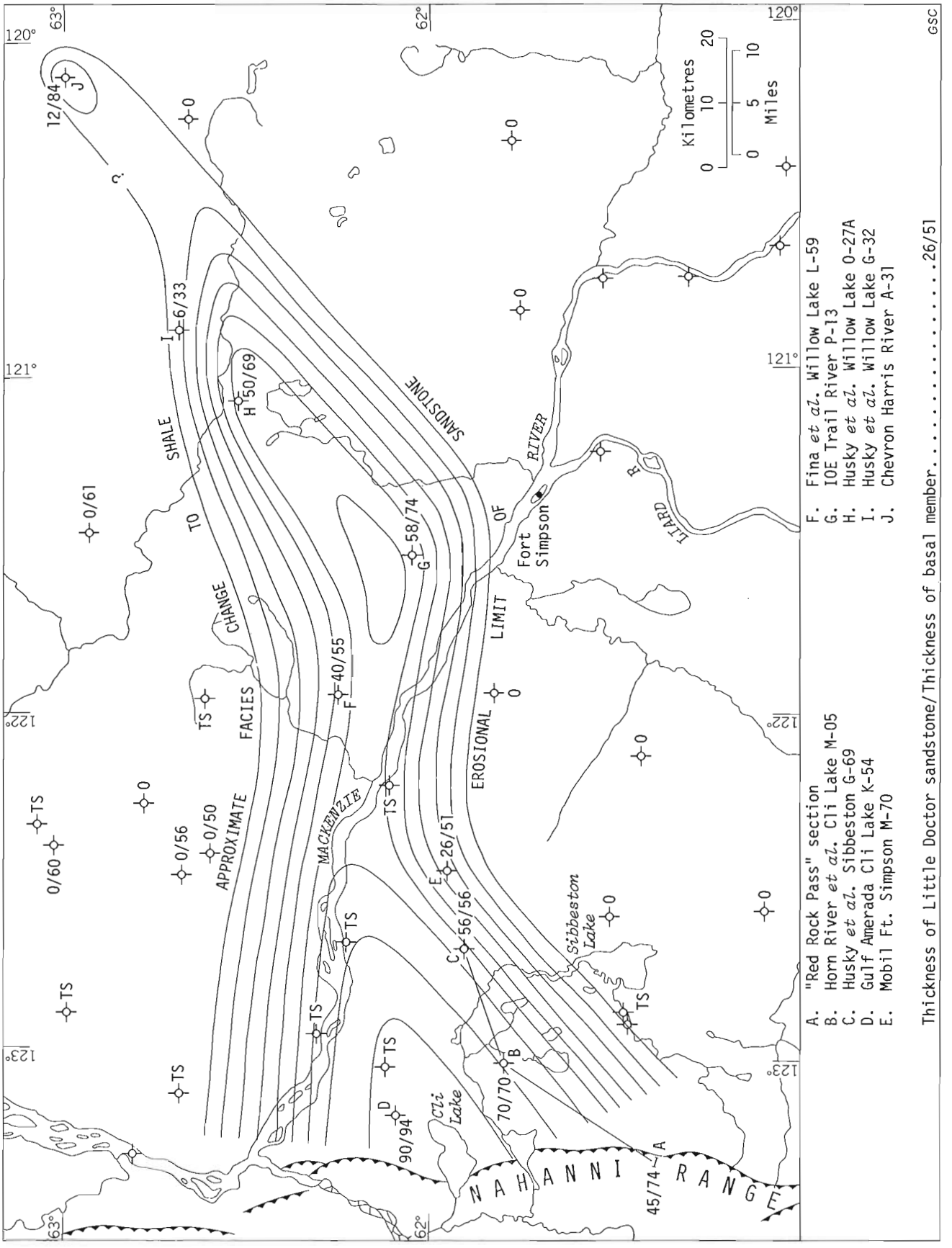

Figure 11.4: Isopach map of Little Doctor sandstone in basal member of the Mount Kindle Formation.

Stratigraphic unit		Lithology	Approximate percentages of minerals present					
			Dolomite	Gypsum	Quartz	Feldspar	Illite	Pyrite
MOUNT KINDLE FORMATION	*Dolomite mbr*	Dolomite, dark grey, fossiliferous	98			2		
	Basal member	Dolomite, dark grey, silty, fossiliferous	72		25	2	1	
		Quartz sandstone, dark grey			95	2	3	
		Quartzitic sandstone, grey			100*			
		Quartzitic sandstone, dark grey			93*	5		2?
		Conglomeratic sandstone, greyish brown			83*	7	7	3
		Shale, dark grey, pyritic					85	15
		?Crinoidal dolomite crystals in dark grey pyritic matrix	62	2	4	11**	5	16
FRANKLIN MOUNTAIN FORMATION	*Rhythmic member*	Dolomite, brown weathered with gypsum needles	72	24	2	1	1	
		Dolomite, light reddish brown, silty	95		3	2		
		Dolomite, dark grey, silty, oolitic, in part silicified	25		74	1		
		Dolomite, grey, oolitic, in part silicified	52		45	2	1	
		Dolomite breccia, greyish brown, silty	79		16	5		

GSC

*These samples give an anomalous peak at 3.74 Å **Two types of feldspars are present in this sample

Figure 11.5: Results of semi-quantitative X-ray diffraction analyses of selected samples from composite measured section. (Analyses by A.G. Heinrich, Institute of Sedimentary and Petroleum Geology, Calgary.)

the Cli Lake M-05 well, the erosion associated with the sub-Mount Kindle unconformity has removed the Franklin Mountain Formation. The Franklin Mountain is absent also in the BAOH Cli Lake K-54 well (Lat. 62°03'41.7"N, Long. 123°10'24"W), and there the Mount Kindle Formation directly overlies sedimentary rocks of Precambrian age.

Mount Kindle Formation

Basal member

In the subsurface east of the Nahanni Range, the basal member of the Mount Kindle Formation (Williams, 1922) overlies progressively older rock units in an eastward direction (Fig. 11.3) and, north of Fort Simpson, it rests directly on Proterozoic quartzite and argillite. The basal member in the Horn R. Am. Hess Gulf Cli Lake M-05 well (Lat. 61°54'58"N, Long. 123°01'47"W) and in the BAOH Cli Lake K-54 well (Lat. 62°03'41.7"N, Long. 123°10'24"W) consists of pale to dark grey, very fine to medium-grained, in places quartzitic sandstone, interbedded with dark grey shale and arenaceous, dark grey dolomite. In all other wells in the Fort Simpson area and in the Nahanni Range south of Little Doctor Lake, the basal member comprises two facies: a basal sandstone facies (herein referred to as Little Doctor sandstone) and an upper argillaceous facies.

Little Doctor sandstone

The Little Doctor sandstone is 13.7 m (45 ft) thick in "Red Rock Pass" (*see* Appendix) and starts at the base with a 30 cm (1 ft) thick, sandy, chert-pebble conglomerate. The conglomerate forms the base of an interbedded succession of pale and dark grey sandstone and lesser amounts of dark grey shale. The sandstone beds are fine- to coarse-grained quartz arenites with less than 10 per cent feldspar (Fig. 11.5) and, in general, are poorly sorted. Some sandstone samples have a biomodal texture; well-rounded, medium to coarse or fine to medium quartz grains are imbedded in a matrix of very fine subangular grains. In the thicker beds, a transition occurs from light grey, medium- to coarse-grained, in places planar crossbedded sandstone to dark grey, bioturbated, argillaceous, fine- to medium-grained sandstone at the top. The sandstone beds grade upward into dark grey sandy shale, but have sharp basal contacts. Shale comprises only 10 to 20 per cent of the Little Doctor sandstone, consists mainly of illite (Fig. 11.5), and commonly is interbedded with bioturbated and poorly sorted, argillaceous sandstone. Two brachiopods found in the shale were identified as *Plaesiomys?* sp. by B.S. Norford, of the Institute of Sedimentary and Petroleum Geology, Calgary. These brachiopods suggest a Middle to Late Ordovician age for the Little Doctor sandstone and are indicative of a marine environment. Crinoidal debris found in a dolomitic sandstone near the top of the Little Doctor sandstone in "Red Rock Pass" (Sec. 3), and a thick (120 cm, 4 ft) bed of sandy, medium to coarsely crystalline, crinoidal dolomite (encrinite) in "Red Rock Pass" (Sec. 2) also indicate that the Little Doctor sandstone is a marine deposit.

In the subsurface, the Little Doctor sandstone varies in thickness from 1.8 to 17.6 m (6-58 ft) and the isopach

map (Fig. 11.4) suggests that the sandstone forms a continuous elongate body, 161 km (100 miles) long, 32 km (20 miles) wide and 15.2 m (50 ft) thick. The sandstone grades laterally to shale in a northwesterly direction. It probably had, originally, a much larger distribution to the southeast but pre-Devonian erosion, associated with the unconformity at the top of the Mount Kindle Formation, has removed the sandstone entirely in the area south of Sibbeston Lake and Fort Simpson (Fig. 11.4).

Other sandstone lenses in the basal member of the Mount Kindle Formation are present in the subsurface east and north of the continuous sandstone beds shown on Figure 11.4. Present data suggest that these lenses are discontinuous and limited in distribution and are not considered to be part of the Little Doctor sandstone. Outside the area shown on Figure 11.4, two wells contain sandstone: the Imperial Willow Lake B-28 (Lat. 62°17'05"N, Long. 119°04'25"W) and Imperial Cartridge B-72 (Lat. 63°11'19"N, Long. 120°29'40"W). In the Willow Lake B-28 well, 7.9 m (26 ft) of very dolomitic, very fine to fine-grained sandstone overlie Precambrian granite. In the Imperial Cartridge B-72 well, 2.1 m (7 ft) of medium- to very coarse grained, dolomitic sandstone overlies the sandy dolomite of the Franklin Mountain Formation.

Argillaceous-dolomitic facies

The upper facies of the basal member consists of a recessive, dark grey, argillaceous and variably silty and sandy dolomite interbedded with minor, thin, nodular beds of dolomitic sandstone. Black chert lenses are scattered throughout the interval and some beds contain Middle or Late Ordovician corals in growth position. The upper facies is 9.4 m (31 ft) thick in "Red Rock Pass" (Sec. 3; *see* Appendix). One sample was analyzed semi-quantitatively by X-ray diffraction and contains approximately 72 per cent dolomite, 25 per cent quartz, 2 per cent feldspar and 1 per cent illite (Fig. 11.5).

In the subsurface in the area north of the postulated position of the facies change from sandstone to shale on Figure 11.4, the basal member of the Mount Kindle Formation consists of interbedded, dark grey, argillaceous dolomite, argillaceous siltstone and shale (Meijer-Drees, in press). This lithology is similar to that of the basal member of the Mount Kindle Formation at the type section in the McConnell Range.

Dolomite member

The dolomite member of the Mount Kindle Formation overlies the basal member with a gradation contact. It is resistant and forms the cliffs at the top of the picture in Figure 11.2. According to Brady (*in* Brady and Wissner, 1961), the Mount Kindle dolomite member is about 417.5 m (1370 ft) thick in the Nahanni Range south of Little Doctor Lake. Only the lower 61 m (200 ft) of the section were examined by the writer during the summer of 1974 (*see* Appendix). The lower 61 m (200 ft) of the dolomite member consist of dark grey, very finely to finely crystalline, poorly bedded, fossiliferous dolomite (*see* Appendix). Some beds are biostromal and contain an abundance of corals in near growth position, other beds contain abundant crinoid and brachiopod debris. Porosity is present in the form of scattered vugs which are commonly associated with the fossils, and as poorly developed intercrystalline porosity A recessive, rusty brown weathering, slightly silty and sandy dolomite unit overlain by a coarse-grained dolomitic sandstone bed is present between 54.25 and 58.8 m (178-193 ft) above the base of the dolomite member in the "Red Rock Pass" area (*see* Appendix).

Fossils collected from the lower part of the dolomite at "Red Rock Pass" include Late Ordovician to Silurian corals and Early Silurian pentamerid brachiopods. According to B.S. Norford (pers. comm.) only the basal part of the Mount Kindle dolomite is of Late Ordovician age and the first occurrence of pentamerid brachiopods marks the base of the Silurian. In the subsurface of the Fort Simpson area, only the basal part of the dolomite member of the Mount Kindle Formation is present (Fig. 11.3). It consists of a dark or light greyish brown, very finely to finely crystalline crinoidal dolomite containing scattered corals. The dolomite has, in places, vulgar porosity and contains chert nodules.

References

Brady, W.B. and Wissner, U.F.G.
1961: A stratigraphic reconnaissance of the western part of the District of Mackenzie, N.W.T., and biostratigraphic correlation of Middle Devonian strata in the N.W.T.; Tech. Rept. 28-1-5-5, submitted by Union Oil Co. of California to the Department of Indian Affairs and Northern Development, Canada.

Douglas, R.J.W. and Norris, D.K.
1960: Virginia Falls and Sibbeston Lake map-areas, Northwest Territories; Geol. Surv. Can., Paper 60-19.

Macqueen, R.W.
1970: Lower Paleozoic stratigraphy and sedimentology, eastern Mackenzie Mountains, northern Franklin Mountains; *in* Report of Activities Part A, Geol. Surv. Can., Paper 70-1, Pt. A, p. 225-230.

Meijer-Drees, N. C.
Geology of the lower Paleozoic formations in the subsurface of Fort Simpson area, District of Mackenzie, N. W. T.; Geol. Surv. Can., Paper 74-40. (in press)

Norford, B. S. and Macqueen, R. W.
Lower Paleozoic Franklin Mountain and Mount Kindle Formations, District of Mackenzie: their type sections and regional development; Geol. Surv. Can., Paper 74-34. (in press)

Williams, M. Y.
1922: Exploration east of Mackenzie River between Simpson and Wrigley; Geol. Surv. Can., Sum. Rept. 1921, Pt. B, p. 56-66.

1923: Reconnaissance across northeastern British Columbia and the geology of the northern extension of Franklin Mountains, N. W. T.; Geol. Surv. Can., Sum. Rept. 1922, Pt. B, p. 97-104.

Appendix

Composite section, "Red Rock Pass", Nahanni Range
Mount Kindle and Franklin Mountain Formations

This composite section is compiled from three sections measured on the east-facing scarp of the Nahanni Range about 32 km (12 miles) south of Little Doctor Lake, near a small pass known as "Red Rock Pass" (Brady and Wissner, 1961) located at Latitude 61°42'20"N and Longitude 123°18'20"W (Fig. 1). The sections were measured with a five-foot staff by W. S. MacKenzie and N. C. Meijer-Drees in August, 1974. The fossils were identified by B. S. Norford of the Institute of Sedimentary and Petroleum Geology, Calgary.

Section 1 was measured north of the pass (Lat. 61°42'30"N, Long. 123°18'00"W) in the Franklin Mountain Formation. Section 2, located near the pass (Lat. 61°42'22"N, Long. 123°18'15"W), comprises the top of the Franklin Mountain Formation and the lower part of the Mount Kindle Formation. Section 3 is located south of the pass (Lat. 61°42'15"N, Long. 123°18'20"W) and describes the basal member of the Mount Kindle Formation.

Unit	Lithology	Thickness metres (ft)	Height Above Base metres (ft)
	MOUNT KINDLE FORMATION		
	Dolomite member		
	Measured in Section 2 (Lat. 61°42'22"N, Long. 123°18'15"W)		
9	Sandstone, dolomitic, grey mottled with yellowish brown, fine to very coarse grained; clear and rarely pink, poorly sorted, subrounded quartz grains in a silty dolomite matrix; interbedded with sandy dolomite 59.1-59.7 m (194-196 ft) above base. Unit grades upward to dark grey dolomite	0.9 (3)	59.7 (196)
8	Dolomite, silty and quartzose, dark grey mottled with rusty brown, weathering brown. Interval lacks bedding and is recessive	4.6 (15)	58.8 (193)
7	Dolomite, dark grey, weathering dark grey, very finely to medium crystalline; very fossiliferous with 50 per cent recrystallized fossil fragments (mostly crinoidal); contains thin, white, dolomite veins; abundant corals in near growth position. The fossils collected include the following corals: *Favosites* sp., *Palaeofavosites* sp. and *Bighornia?* sp. (GSC loc. C-39008). *Bighornia* is thought to be indicative of a Late Ordovician age	0.91 (3)	54.25 (178)
6	Dolomite, somewhat argillaceous and silty, dark grey, weathering dark grey, poorly bedded; very finely to finely crystalline with light grey, medium to coarsely recrystallized fossil fragments (mostly crinoidal debris). Some beds sucrosic with poor intercrystalline porosity; some scattered, large vugs lined or filled with white dolomite. At 45.4 m (149 ft) above the base of the dolomite member of the Kindle Fm. is a bed with poorly preserved pentamerid brachiopods (GSC loc. C-39006). These indicate an Early Silurian age. Corals from 30.7 and 52.7 m (101 and 173 ft) above base include *Palaeophyllum?* sp. (GSC loc. C-39002) and *Favosites* sp. (GSC loc. C-39007)	31.6 (104)	53.3 (175)

Unit	Lithology	Thickness metres (ft)	Height Above Base metres (ft)
5	Dolomite, slightly silty, grey to dark grey, weathering dark grey, poorly bedded (massive), very finely to finely crystalline, pyritic; contains patches and veinlets of white, secondary dolomite and small vugs lined with white dolomite	10 (33)	31.6 (71)
4	Dolomite, massive, cliff-forming, slightly argillaceous and silty, dark grey, dark grey weathering, pyritic, micro- to finely crystalline, scattered recrystallized coarse, fossil fragments (mostly crinoidal debris). Contains patches and veinlets of secondary, white dolomite. Poor intercrystalline porosity and small vugs lined with white dolomite. At Section 3 (Lat. 61°42'15"N, Long. 123°18'20"W) numerous corals are present in growth position in the basal part of this unit. The following corals were collected from this location near the base of the unit: *Catenipora* 2 spp. and *Palaeofavosites* sp. (GSC loc. C-33917). According to B.S. Norford, these indicate probably a Late Ordovician age.	11.6 (38)	11.6 (38)
	Basal member (Argillaceous-dolomitic facies)		
	Measured in Section 3 (Lat. 61°42'15"N, Long. 123°18'20"W)		
3	Dolomite, argillaceous, slightly silty and sandy, dark grey, weathers dark greyish brown. A few thin (up to 4 cm or 1.5 in. thick), dark grey, sandy, finely crystalline dolomite beds in lower half of interval. Unit is recessive; upper contact sharp, lower contact gradational	0.6 (2)	22.6 (74)
2	Dolomite, argillaceous, variably silty and sandy, dark grey, weathers dark greyish brown; beds 5-28 cm (2-12 in.) thick; interbedded with dark grey, argillaceous and silty fossiliferous dolomite; black chert lenses and nodules are present throughout interval. Near the top of the unit is a bed of fine-grained, argillaceous, bioturbated, dolomitic sandstone. The lower contact of the interval is sharp. Fossils collected at 21.3 and 10.1 m (70 and 66 ft) include the corals *Palaeophyllum* sp. (GSC loc. C-33918) and *Catenipora* cf. *C. rubra* Sinclair and Bolton (GSC loc. C-33916). Age indicated is late Middle or Late Ordovician	8.2 (27)	21.9 (72)
	(Little Doctor sandstone)		
1	Interbedded sandstone, quartzitic sandstone and minor shale; beds 1 to 4 ft thick. The thick beds are light grey, rusty brown weathering, quartz arenites. Sandstones are poorly sorted and contain medium to coarse, well-rounded grains of milky or pink quartz and black chert in a very fine grained quartz matrix. In the thicker beds there is a gradation		

Unit	Lithology	Thickness metres (ft)	Height Above Base metres (ft)
	from light grey, medium- to coarse-grained, laminated sandstone at the base to dark grey nodular, argillaceous and/or dolomitic sandstone at the top. The dark grey, nodular sandstone grades upward to shale. Basal contacts of sandstone beds are sharply defined. The shale is commonly interbedded with nodular, poorly sorted, bioturbated, and friable sandstone beds. A 30 cm (1 ft) thick, sandy, chert-pebble conglomerate forms the base of the unit. This is light greyish brown to dark grey, rusty brown weathering, and consists of rounded pebbles (up to 4 cm or 1.5 in.) of light and dark coloured chert in a matrix consisting of fine to coarse quartz grains. Two brachiopods were collected from shale scree 6.4 m (21 ft) above base of unit and were identified as *Plaesiomys?* (GSC loc. C-33916). A Middle to Late Ordovician age is indicated	13.7 (45)	13.7 (45)
	The lower contact of the chert-pebble conglomerate is not exposed in Section 3, but is exposed in Section 2. Here a grey to dark grey, conglomeratic, fine- to coarse-grained, pyritic sandstone bed, 10 cm (4 in.) thick, overlies grey, micro- to very finely crystalline, silty dolomite with a sharp irregular contact. In Section 2, the basal member is poorly exposed and repeated due to faulting.		
	FRANKLIN MOUNTAIN FORMATION (210.3 m; 190 ft; incomplete)		
	Measured in Section 1 (Lat. 61°42'30"N, Long. 123°18'00"W)		
5	Dolomite, silty to fine sandy, micro- to very finely crystalline, pale yellowish brown, weathers light grey, interbedded with dolomite, grey to dark grey, finely to medium crystalline. Thin beds and laminae rich in fine to coarse, subrounded quartz grains are present throughout unit. Some beds contain dolomite mud pebbles or are pelletoidal or ?oolitic. Contact with unit 4 is gradational	47.2 (155)	210.3 (690)
4	Dolomite, light grey, light yellow-brown and light reddish brown, weathering pale reddish and yellowish brown, micro- to finely crystalline and variably silty; a well-bedded succession with some laminae containing abundant quartz sand and some beds medium to coarse pelletoidal and ?oolitic. The above is interbedded with sandstone, dolomitic, pale reddish brown, fine to coarse grained, quartzose; mottled red-brown in places (hematite?); beds from 1-60 cm (0.5 to 24 in.) thick	44.2 (145)	163 (535)
3	Dolomite, siltstone and sandstone interbedded. Dolomite, laminated, grey and dark grey, pale yellow-brown weathering, silty to fine sandy, pyritic, micro- to finely crystalline, pelletoidal and ?oolitic in places, some dark grey contorted laminae ("soft sediment disturbance"). Siltstone, dark grey, very dolomitic,		

Unit	Lithology	Thickness metres (ft)	Height Above Base metres (ft)
	somewhat argillaceous. Sandstone, light grey, fine to coarse grained, dolomitic, quartzose, reddish brown oolites or dolomitic mud clasts in places. Beds in unit range between 5-60 cm (2-24 in.) thick	30.5 (100)	118.8 (390)
2	Dolomite, siltstone and sandstone interbedded. Dolomite, mottled pale reddish brown and grey, variably silty, micro- to very finely crystalline, laminated, coarse, indistinct pelletoids and oolites in places. Siltstone, dolomitic, grey and dark grey laminated. Sandstone, pale reddish brown or light grey, dolomitic, quartzose, abundant dolomitic mud clasts	25.9 (85)	88.4 (290)
1	Dolomite, siltstone, claystone and sandstone interbedded. Unit considerably fractured and contains brecciated zones. Unit weathers yellowish to reddish brown. Dolomite, silty to fine sandy, mottled grey and light grey, some laminae contain abundant quartz sand. Siltstone, dolomitic, laminated grey and dark grey, in places pyritic. Claystone, very dolomitic, silty, dolomitic mud clasts, in part laminated with pyrite crystals. Sandstone, pale reddish brown or light grey, fine to coarse grained, quartzose, some rounded, dolomitic mud pebbles. The brecciated zones consist of subangular pieces of dolomite (0.2 mm to 2 cm) in pale yellowish grey matrix of silty and sandy dolomite. The dolomite pieces usually are fractured and most fracture planes abut against the matrix	62.5 (205)	62.5 (205)

12. POSSIBLE LARGE DOMAL STRUCTURES ALONG A REGIONAL ARCH IN THE NORTHERN INTERIOR PLAINS

Project 720066

N. E. Haimila
Institute of Sedimentary and Petroleum Geology, Calgary

In the District of Mackenzie, N. W. T., large domal structures may occur on a broad regional, structural high which extends southward from the Anderson Plain toward the confluence of the Great Bear and Mackenzie Rivers. From the vicinity of Latitude 67°N and Longitude 125°30'W southward to Latitude 65°N and Longitude 125°30'W rocks consisting mainly of Ordovician to Silurian Franklin Mountain Formation are exposed along the crest of this arch (Fig. 12.1 compiled from published and unpublished GSC maps). The Ordovician to Silurian Mount Kindle Formation and the Middle Devonian Bear Rock Formation outcrop on the western flank of the arch which exposes Franklin Mountain Formation in the north. In the south the Middle Devonian Bear Rock Formation outcrops along the flanks of the arch and is overlain to the west by remnants of Cretaceous rocks. Cretaceous units flank and overlap the Bear Rock Formation to the east of the arch. This regional arch is described in more detail on the basis of structural and stratigraphic data by D. G. Cook (pers. comm.).

To date, the dominant structural features that have been recognized on this undulating structural high are a number of narrow, elongate, structurally complex anticlinal features which subparallel and sometimes transgress the axis of the arch. These narrow anticlines are usually less than two miles wide and may extend for tens of miles as sinuous traces. The anticlines probably were formed relatively late (Lower Cretaceous or later) but may have been initiated earlier. They appear to be associated with basement faults and may be enhanced by evaporite flowage in the Cambrian Saline River Formation.

The large domal features that may be aligned in a north-south direction along the crest of the arch were first observed by the writer on satellite imagery of the area. They are outlined on Figure 12.1. The domal features are tentatively named, from north to south, the "Tweed Lake Dome", the "Tunago Lake Dome", the "Mahony Lake Dome" and the "Brackett Lake Dome". Additional smaller domes may exist. It should be noted that the existence of these domes has not been proven completely by delineation on the ground but the possibility of their existence has been strengthened by investigations of stratigraphic sections, outcrop patterns and gravity anomalies.

Transverse cross-sections of the "Mahony Lake Dome" and the "Tunago Lake Dome" were constructed from stratigraphic sections (Macqueen, R. W., pers. comm., 1975) and geological mapping (Cook and Aitken, 1970; and Yorath and Cook, pers. comm., 1975). These traverse sections were tied into a north-south longitudinal section which reconciles scanty geological information with the satellite image interpretations along the crest of the arch. Schematic representations of these cross-sections accompany Figure 12.1 and illustrate the possibility of multiple closures along the crest of the arch.

Although the presence of unconformities in the area indicates that the units have been truncated by erosion at various times, the outcrop pattern indicates that, at present, the southern end of the arch is structurally higher than the northern end. The present cycle of erosion has revealed outcrops of the Cambrian Saline River Formation in the "Brackett Lake Dome" (Cook, D. G., pers. comm., 1975) while the culmination of the "Tweed Lake Dome" is still capped for the most part by the Middle Devonian Bear Rock Formation. Between these extremes the "Tunago Lake Dome" appears to have remnants of the Mount Kindle Formation well up on its flanks (Macqueen, R. W., pers. comm., 1975) and the "Mahony Lake Dome" mainly exposes rocks of the Franklin Mountain Formation (Cook, D. G., pers. comm., 1975).

Additional evidence for the presence of the domes was found on residual gravity maps constructed from the published Bouguer Anomaly Map of Arctic Red River – Norman Wells (Hornal *et al.*, 1970). This map has a contour interval of 50 gravity units (5.0 milligals) and the resulting anomalies on the residual gravity map lack definition and control. The Gravity Section of the Earth Physics Branch of Energy, Mines and Resources provided a plot of the gravity values for the individual gravity stations in the vicinity of the arch. These values had been converted to the Internal Gravity Standardization Net 1971, since the publication of the Arctic Red River – Norman Wells map (*ibid.*, 1970). Because of the conversion of the data to the new base, the values were recontoured by the writer. Any errors in the recontoured Bouguer map or the resulting residual map are the responsibility of the writer. The residual gravity map (Fig. 12.2) was produced by subtracting a contour-smoothed regional (Fig. 12.2b) approximating a fourth or fifth order surface from the new Bouguer map (Fig. 12.2a), in the manner reviewed by Nettleton (1954).

A series of profiles across the anomalies from three of the domes are presented in Figure 12.3. Locations of the profiles are shown on the residual gravity map (Fig. 12.2). The "Mahony Lake Dome" coincides with an isolated high surrounded by a series of gravity lows (Fig. 12.2 and Fig. 12.3A-A', B-B', C-C', and D-D'). The "Tunago Lake Dome" coincides with a positive shoulder associated with a larger regional gravity high to the west (Fig. 12.2 and Fig. 12.3E-E' and F-F'). The "Tweed Lake Dome" coincides with a terracing of the gravity gradient associated with the same regional gravity to the west (Fig. 12.2 and Fig. 12.3G-G', H-H',

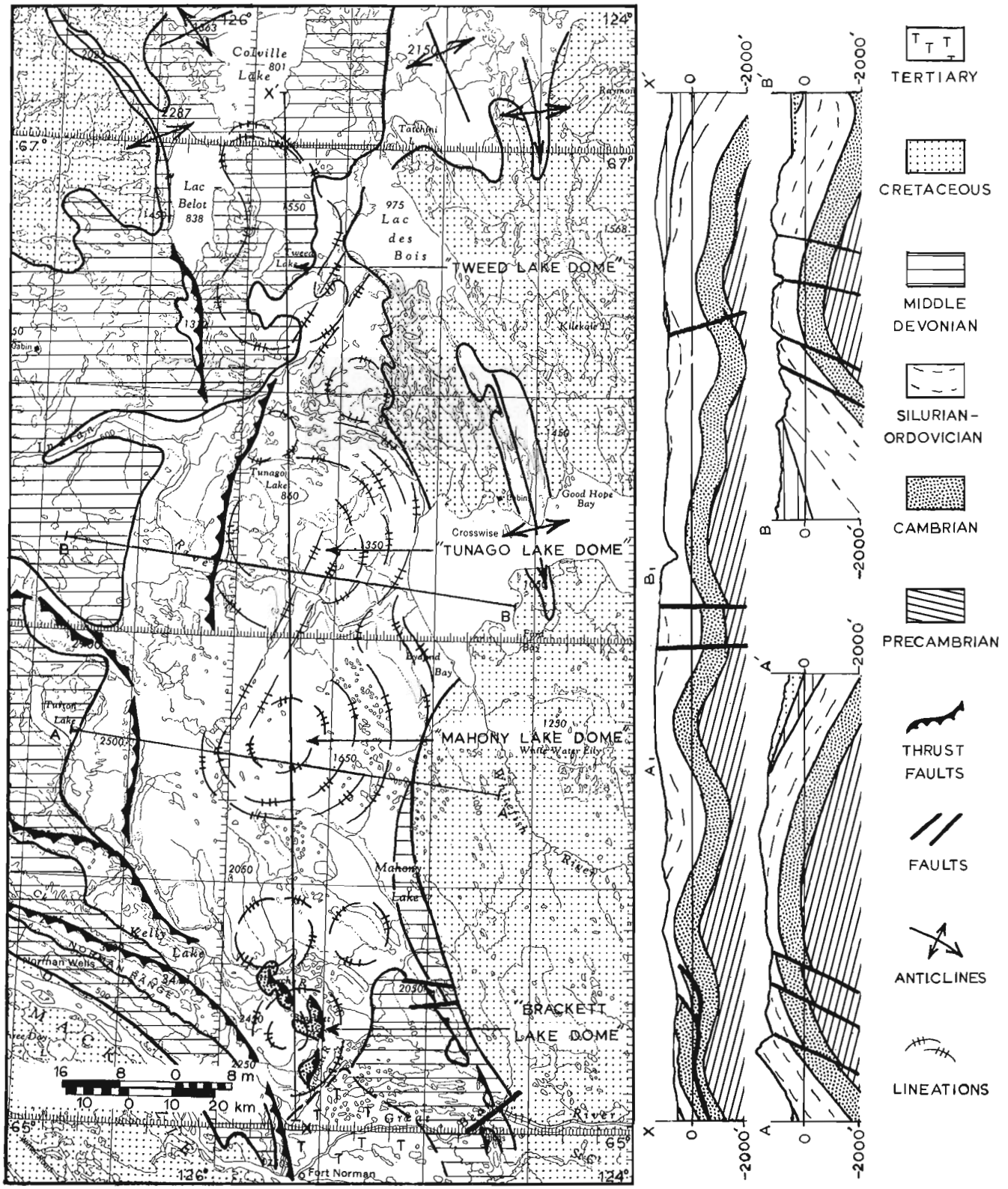

Figure 12.1. Generalized geological sketch map (compiled from published and unpublished GSC maps).

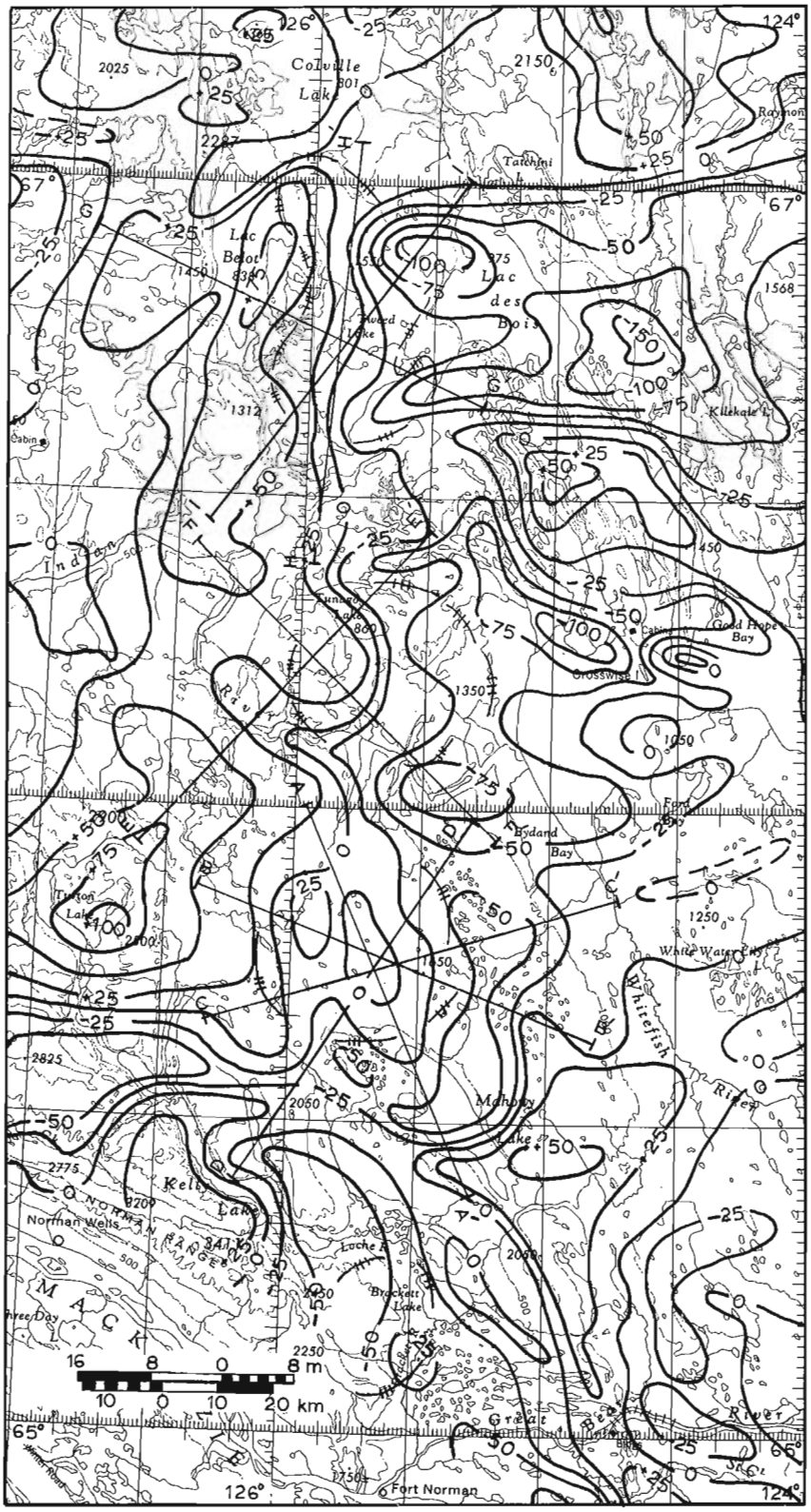

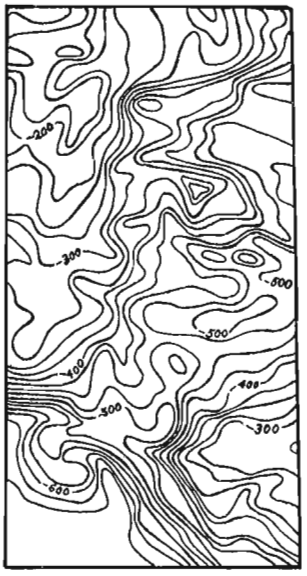

(a) BOUGUER MAP

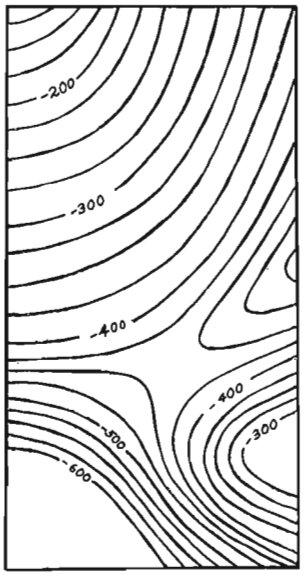

(b) REGIONAL MAP
(Contour-Smoothed)

Figure 12.2. Contour-smoothed residual gravity map.

and I-I'). In all instances, there are reductions in the gravity anomalies at distances of 8 to 16 miles from the proposed culminations. The size of these reductions in the gravity values usually varies from 25 to 70 gravity units (2.5 to 7.0 milligals) although they may be less.

The reductions in the gravity values around the culminations are not readily explained by the configurations of the domes or by the stratigraphy of the area. Spatially, the minimums do not coincide with the structural depressions bordering the domes since the domes may be over 50 miles across. In addition, the halite in

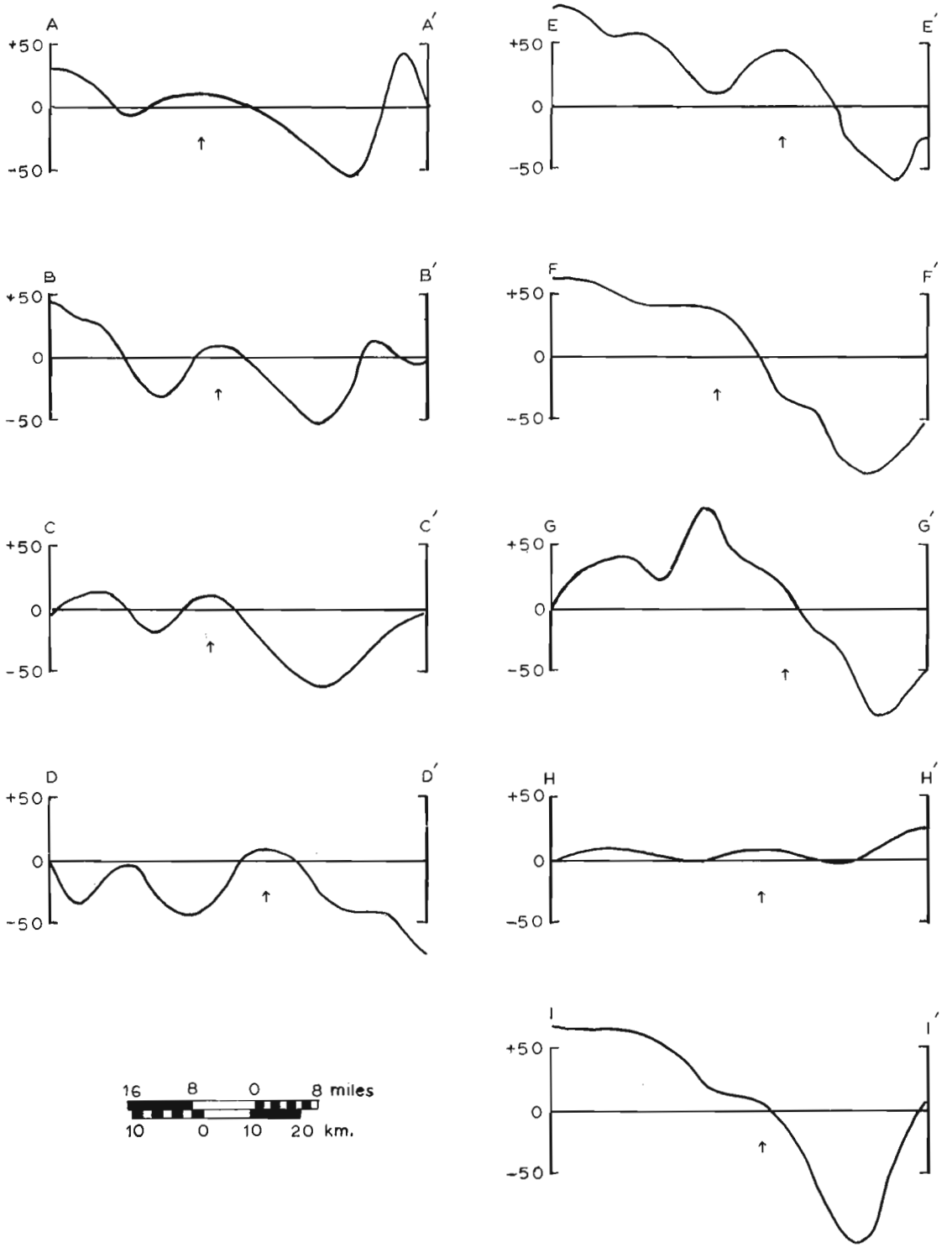

Figure 12.3. Profiles from residual gravity map.

the Saline River Formation does not account for the anomalies unless unusual facies relationships exist within the domes. The presence of variable porosity and pore-fillings in the Cambrian Mount Clark Formation may have some effect on the gravity values and this will be discussed later.

The possible existence of domal structures along the regional arch also raises the possibility of hydrocarbon accumulations within these structures. Since the Franklin Mountain Formation is exposed along most of the arch and the Saline River Formation is exposed at isolated localities, the most likely hydrocarbon reservoir is the basal Paleozoic sandstone. The hydrocarbon potential of this basal Paleozoic sandstone has already been indicated by the gas found in the Ashland Oil, Tedji Lake F-24 well (Latitude 67°43'25"N, Longitude 125°49'46"W) which tested 3.5 to 4.4 MM cf/d from a thin pay zone (Petersen, 1974). This well is approximately 50 miles north-northwest of the "Tweed Lake Dome". The basal sandstone in the vicinity of the arch may be the Cambrian Mount Clark Formation or its equivalent the Old Fort Island Formation. The Mount Clark Formation is a sandstone at the base of the Paleozoic sequence in the Franklin Mountains and surrounding areas. Information obtained from wells drilled in the Great Bear Basin, Colville Hills, and proximal Mackenzie Valley indicate that the Mount Clark Formation usually has a thickness of 50 to 200 feet. The Old Fort Island Formation in outcrop overlies and pinches-out on Precambrian highs. In these instances the thickness varies from 0 to 200 feet (Cook and Aitken, 1970). If the basal Paleozoic sandstone has the same configuration as the Old Fort Island Formation and if the arch is formed over an older Precambrian structure, the basal sand may not cover all of the domal structures. In these instances the location of a Mount Clark Formation trap becomes a stratigraphic-structural problem with the pinch-out location of the sandstone being the important parameter.

A seal for any reservoir in the Mount Clark Formation could be provided by both the Cambrian Mount Cap and Saline River Formations. The Mount Cap Formation, composed mainly of grey, green and red shale with some sandstone and siltstone overlays the Mount Clark Formation. The Mount Cap Formation, in turn, is overlain by the Saline River Formation composed of fine-grained clastics and evaporites. The three Cambrian formations mentioned above usually total more than 700 feet in thickness.

Porosity estimates for the sandstone in the Mount Clark Formation were made through the use of sonic logs from released wells; porosities range from 2 to 25 per cent. With these porosities, the size of the structures, and the proper hydrocarbon generating conditions, domes along the regional arch could be capable of trapping many trillions of cubic feet of gas or equivalent volumes of oil.

A situation in which an onlap sandstone had its pore-filling fluids displaced by gaseous material could help explain a part of the gravity deficiencies associated with the domal features but could not explain the total negative anomalies (McCulloh, 1967). In this situation the density contrast and gravity deficiencies would be proportional to the porosity of the reservoir.

To prove the existence of the domes and the attendant possibility of hydrocarbon accumulations would require that seismic lines in the order of 80 miles long be placed over the outlined culminations. Actual proof of hydrocarbon accumulations would require the drilling of wells to depths of approximately 2000 feet to intersect the Mount Clark Formation at favourable locations.

Summary and Conclusions

1. It is likely that a regional arch in the Northern Interior plains has domal culminations superimposed along its crest. These domal features are orders of magnitude larger than the narrow anticlinal structures which have been recognized and tested to date.

2. The domal structures along the regional arch are indicated on satellite imagery, on gravity residual maps prepared from data provided by the Gravity Section of the Earth Physics Branch of the Department of Energy, Mines and Resources and by geological field work.

3. The basal Paleozoic sandstone, the Mount Clark Formation, where tested has porosities ranging from 2 to 25 per cent and thicknesses ranging from 0 to 200 feet. In the Tedji Lake F-24 well the basal Paleozoic has tested 3.5 to 4.4 MM cf/d of gas on drillstem tests and other wells in the area have had oil and gas shows.

4. Any of the interpreted domal structures could have the capacity to hold several trillion cubic feet of gas or equivalent quantities of oil.

5. To date, none of the domal structures has been drilled and it appears that no seismic line completely traverses one of the domal structures. Properly placed lines in the order of 80 miles in length would be needed to test the hypothesis presented and drilling would be required to test for the presence of hydrocarbons.

References

Cook, D.G.
1975: The Keele Arch, a pre-Devonian and pre-Late Cretaceous paleoupland in the northern Franklin Mountains and Colville Hills; *in* Report of Activities, Part C, Geol. Surv. Can., Paper 75-1C.

Cook, D.G. and Aitken, J.D.
1970: Geology, Colville Lake map-area and part of Coppermine map-area, Northwest Territories; Geol. Surv. Can., Paper 70-12, 42 p.

Hornal, R.W., Sobczak, L.W., Burke, W.E.F., and Stephens, L.E.
1970: Preliminary results of gravity surveys over the Mackenzie Basin and Beaufort Sea. Map No. 118, Arctic Red River – Norman Wells; Gravity Map Ser., Earth Physics Branch.

McCulloh, T. G.
1967: Mass properties of sedimentary rocks and gravimetric effects of petroleum and natural gas reservoirs; U. S. Geol. Surv. Prof. Paper 528-A.

Nettleton, L. L.
1954: Regionals, residuals and structures; Geophysics, v. XIX, no. 1, p. 1-22.

Petersen, E. V.
1974: Promising new play gaining momentum in the Great Bear Lake area of N. W. T.; Oilweek, v. 25, No. 41, November 25, 1974, p. 14-15.

13. PATTERN OF POSTGLACIAL EMERGENCE, CAPE STORM AND SOUTH CAPE FIORD, SOUTHERN ELLESMERE ISLAND, N.W.T.

Project 670031

W. Blake, Jr.
Terrain Sciences Division

Introduction

This note presents, in summary fashion, the results of a study of postglacial emergence along the southern coast of Ellesmere Island, adjacent to Jones Sound (Fig. 13.1). Glacial geological investigations were carried out in this area in 1967, 1968, and 1970, and some of the geomorphological features in the environs of Cape Storm are displayed in Figure 13.2.

Field and Laboratory Data

Because of the abundance of driftwood and whale bones, which are imbedded in the well preserved raised beaches, considerable time was devoted to collecting samples for radiocarbon dating. For Andersrag Beach near Cape Storm 53 age determinations have been made on 38 samples (26 dates on 25 driftwood samples, 18 dates on six whale bone samples, eight dates on six samples of marine molluscs, and one date on a single sample of organic detritus), and for the southwestern side of South Cape Fiord nine age determinations have been made on the same number of samples (eight driftwood, one whale bone). It is this rich material which has provided details of the pattern of postglacial emergence.

All field data pertaining to the collections, together with details of laboratory treatment and counting procedure, are presented in tabular form in the original article (Blake, 1975a), which was published in Sweden as part of a dissertation defended recently at the University of Stockholm (Blake, 1975b). Figures 13.3 to 13.5 refer to the Cape Storm area at the mouth of Muskox Fiord. They show, respectively, the general nature of the landscape, the location of samples used for age determinations, and the resulting emergence curve. Figures 13.6 to 13.8 comprise the same sequence for a locality on the southwestern side of South Cape Fiord, some 70 km to the east of Cape Storm.

Discussion

One comment regarding ^{14}C age determinations, especially in relation to the apparent ages of marine shells, is appropriate here. In the original article in 'Geografiska Annaler' it was concluded that the marine molluscs were no more than 350 years older than the ages of contemporaneous terrestrial plants. This conclusion was based on age determinations carried out on marine pelecypods, *Astarte borealis* (Schumacker), collected alive in the same area by the Second Norwegian Expedition in the "Fram", 1898-1902. The age calculations for these shells, and for all other shells on which $^{13}C/^{12}C$ ratios have been determined, were normalized to $\delta\,^{13}C = 0^{o}/oo$ PDB, which has been standard practice at the Geological Survey's Radiocarbon Dating Laboratory since 1968 when the first measurements of isotopic ratios became available (e.g., *see* Lowdon and Blake, 1973). However, if the ages of marine molluscs are corrected by normalizing to $\delta\,^{13}C = -25^{o}/oo$ PDB, which is the average value for terrestrial plants, approximately 400 years must be added to the apparent age. This is the procedure that has been followed by Mangerud and Gulliksen (1975) for age determinations on three samples of *Astarte borealis* from Ellesmere Island. Their determinations were made independently by the Radiological Dating Laboratory at the Norwegian Institute of Technology, Trondheim; the collections used were made at the turn of the century by the same "Fram" expedition. For Ellesmere Island Mangerud and Gulliksen (1975) propose an average apparent age of 750 years, a difference of 400 years from the value determined in Ottawa. There is considerable merit in the idea of normalizing all ages to the same value, i.e., $\delta\,^{13}C = -25^{o}/oo$, although the Trondheim laboratory itself, in its published date lists, normalizes to $\delta\,^{13}C = {}^{o}/oo$ (Nydal *et al.*, 1972), and although other values could also be used (cf. Olsson and Osadebe, 1974). This was one of the main points which Mangerud took up for discussion and criticism in his capacity of "faculty's opponent" at the public defence of the writer's dissertation in May 1975.

Fortunately, the difference in the method of calculating the apparent ages of molluscs collected alive (prior to the nuclear bomb testing which began in the 1950's) does not affect the age values obtained for postglacial molluscs after the correction for apparent age has been applied. The original GSC determinations (on pelecypod shells of *Mya truncata* L.) gave values of 9330 ± 110 years (GSC-1415), 9350 ± 80 years (GSC-1488, outer fraction) and 9370 ± 100 years (GSC-1488, inner fraction) after normalization to $\delta\,^{13}C = 0^{o}/oo$; i.e., the average of these three determinations is 9350 years, and this value should be corrected for an apparent age of 350 years. The same result, if it had been calculated by Mangerud and Gulliksen (1975) would have been 9750 years (normalized to $\delta\,^{13}C = -25^{o}/oo$), and this value should be corrected for an apparent age of 750 years. The corrected age of the early postglacial shells at Cape Storm is close to 9000 years whichever method of calculation is used, as is indicated by the position of the dashed line in Figure 13.5.

Conclusions

The major conclusions derived from this study can be summarized as follows:

1. Radiocarbon age determinations on marine molluscs and whale bones indicate that during postglacial

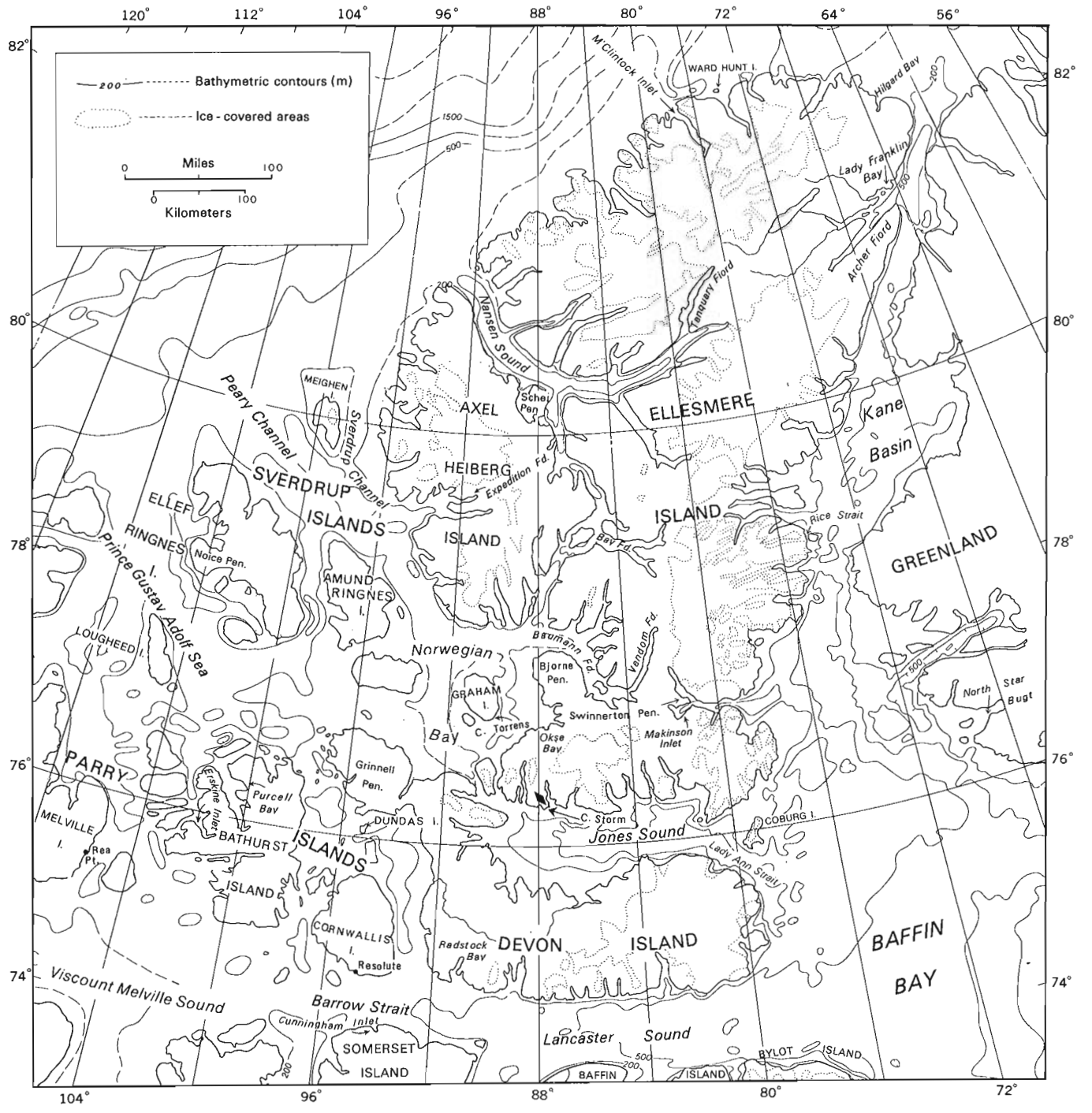

Figure 13. 1. Location map, Queen Elizabeth Islands. Position of Cape Storm, Ellesmere Island, is indicated by the black diamond.

Figure 13. 2. (opposite) Location map, topography, and selected glacial features, Muskox Fiord and Baad Fiord, Ellesmere Island. Base map is sheet 49 B, Baad Fiord (1: 250 000), Surveys and Mapping Branch, Dept. of Energy, Mines and Resources, 1967. Note that elevations of dated samples north of the head of Muskox Fiord do not correspond to position of the 400-foot (120+ m) contour; measurements with altimeters in the field, later checked by plotting instruments, indicate that the base map is in error in that valley.

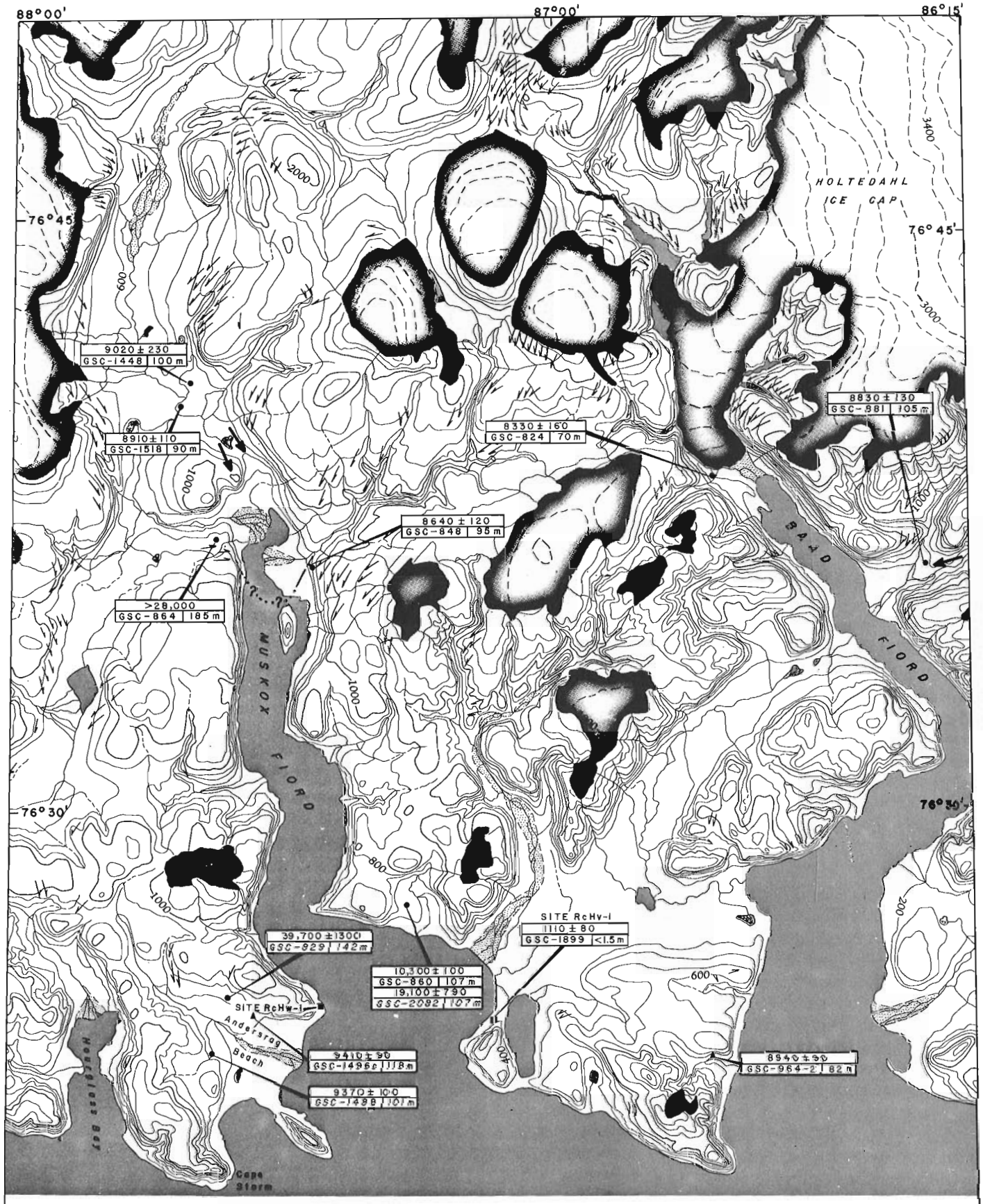
88°00'
87°00'
86°15'
76°45'
76°30'
HOLTEDAHL ICE CAP
3400
3000
2000
1000
800
600
400
200
9020 ± 230
GSC-1448 | 100 m
8910 ± 110
GSC-1518 | 90 m
8330 ± 160
GSC-824 | 70 m
8830 ± 130
GSC-981 | 105 m
8640 ± 120
GSC-848 | 95 m
>28,000
GSC-864 | 185 m
MUSKOX FIORD
BAAD FIORD
39,700 ± 1300
GSC-829 | 142 m
10,300 ± 100
GSC-860 | 107 m
19,100 ± 790
GSC-2092 | 107 m
SITE RcHv-1
1110 ± 80
GSC-1899 | <1.5 m
SITE RcHw-1
Andersag Beach
9410 ± 90
GSC-1496c | 118 m
9370 ± 100
GSC-1488 | 101 m
8940 ± 90
GSC-964-2 | 82 m
Hoseason Bay
Cape Storm
Marine mollusks
Whale bones
Archeological sites
9370 ± 100
GSC-1488 | 101 m
Radiocarbon age, with laboratory number and elevation (m)
Features indicating direction of ice flow
Marginal drainage channels (barb on downslope side)
Moraine (dots mark inferred position)
Ice Caps
2 0 2 4 6 8
KILOMETERS
2 0 2 4 6
MILES
Contour interval 200 feet (~60 m)

Figure 13. 3. Emerged strandlines at Andersrag Beach, north of Cape Storm. Position of the main pumice horizon (22. 0 to 22. 5 m a. s. l.) is indicated by the line of black dots. Other symbols: circles = whale bones; white squares = driftwood; diamonds = dated "old" molluscs; black arrow = highest postglacial molluscs along "Nuculana Creek"; plus sign in circle = organic debris at site along river; white arrow = former Eskimo campsite (RcHw-1) north of Andersrag Beach; white and black arrows = 3 sites where limit of postglacial marine submergence was determined. Enlargement from air photograph A16756-149, taken from an altitude of approximately 9100 m, July 24, 1959; courtesy National Air Photo Library, Ottawa.

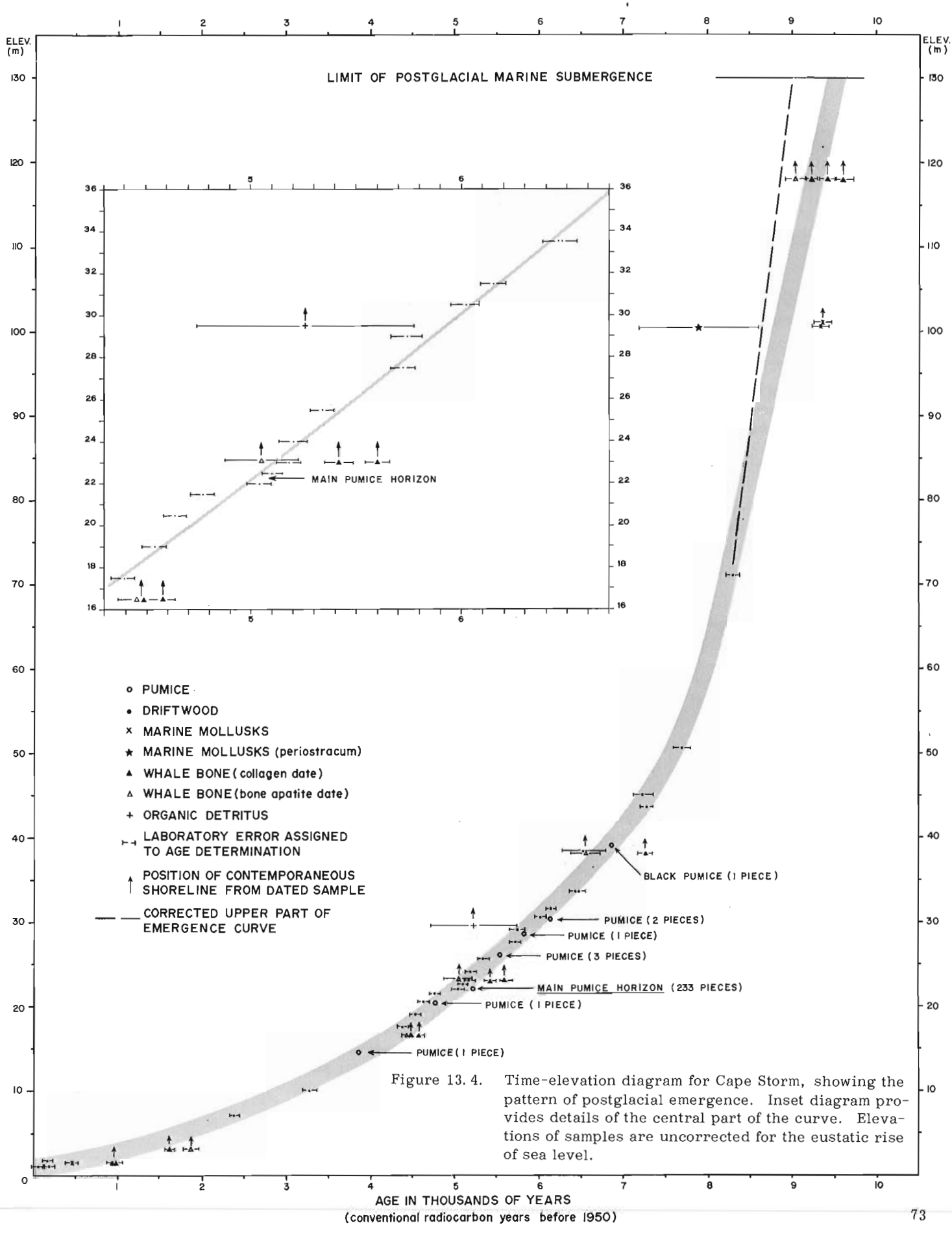

Figure 13.4. Time-elevation diagram for Cape Storm, showing the pattern of postglacial emergence. Inset diagram provides details of the central part of the curve. Elevations of samples are uncorrected for the eustatic rise of sea level.

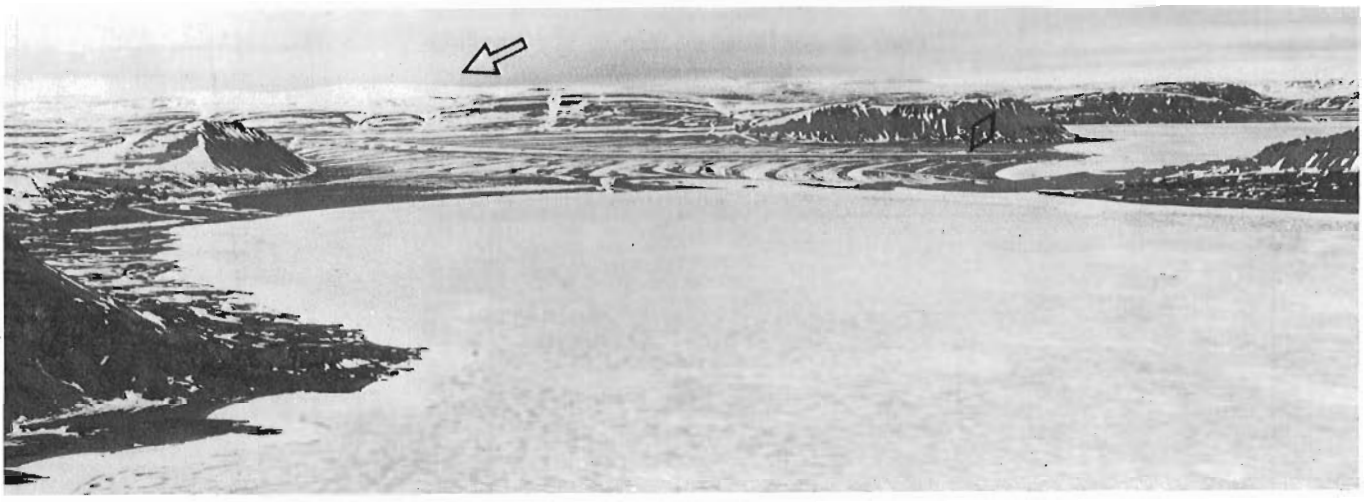

Figure 13. 5. Aerial view north from Cape Storm toward raised beaches at Andersrag Beach. Muskox Fiord in right distance. Note small ice cap (arrow) above 300 m level on plateau to north. Position of base camp is at the base of the diamond. June 29, 1970 (GSC-202911).

Figure 13. 6. Aerial view northward along the west side of South Cape Fiord. 'South Cape Ice Cap' is in left foreground, with an outlet glacier from it cutting across the raised beaches. At the head of the fiord is 'Boxn Glacier' leading from 'Holtedahl Ice Cap', which covers the plateau in the distance. Note prominent shoreline defined by longitudinal snow patches (arrows); pumice is concentrated at the foot of the steep rise. July 2, 1970. (GSC-202912).

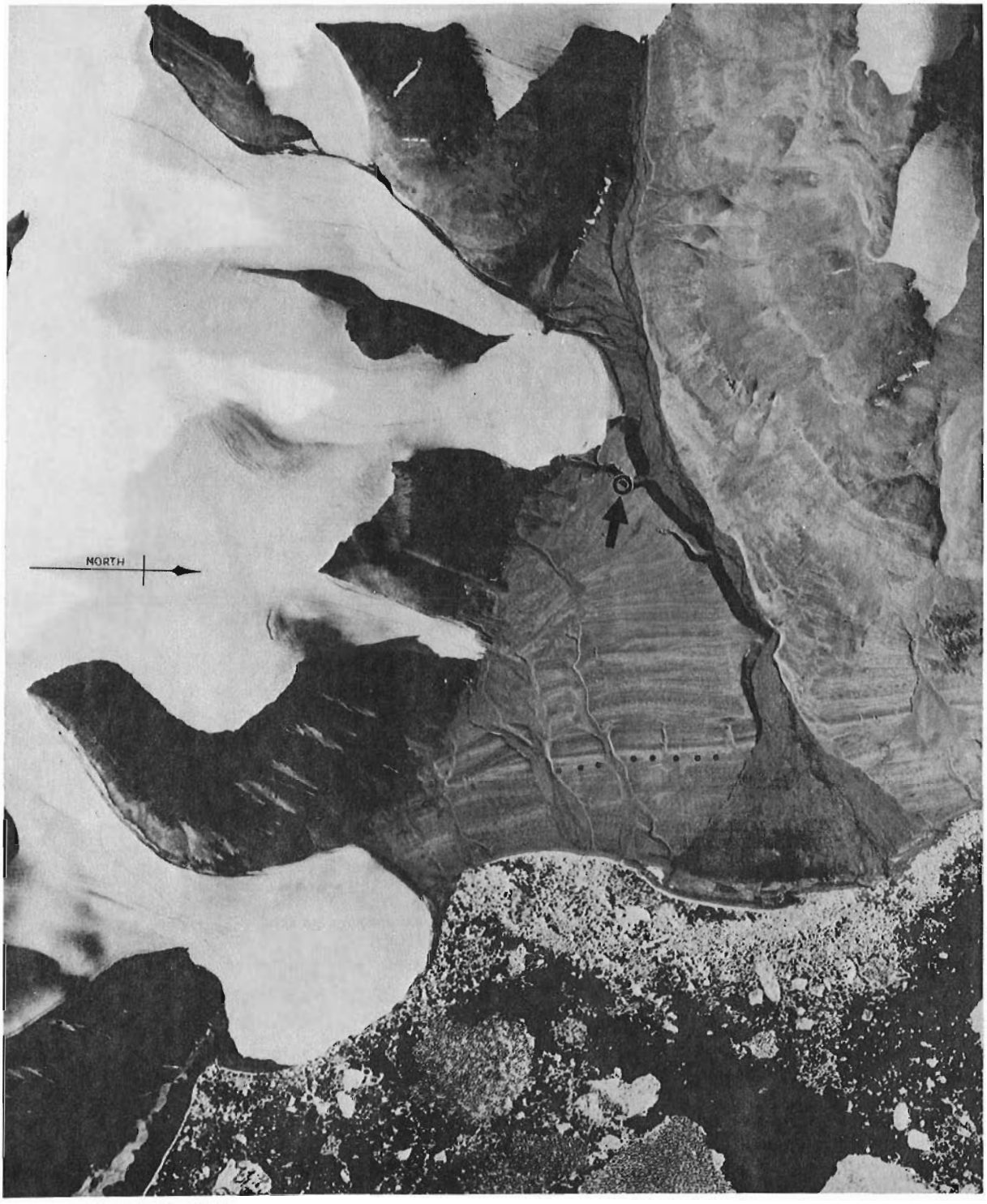

Figure 13. 7. Raised beaches and outlet glaciers from 'South Cape Ice Cap' on the southwest side of South Cape Fiord. Position of pumice (17. 5 m a. s. l.) is indicated by the line of black dots, and a high level whale skeleton (9070 ± 90 years old, GSC-1748, elev. 80. 5 m; cf. Fig. 8) is indicated by a black arrow and circle at the edge of a gully in front of an outlet glacier. Enlargement from air photograph A16722-7, taken from an altitude of approximately 9100 m, August 13, 1959; courtesy National Air Photo Library, Ottawa.

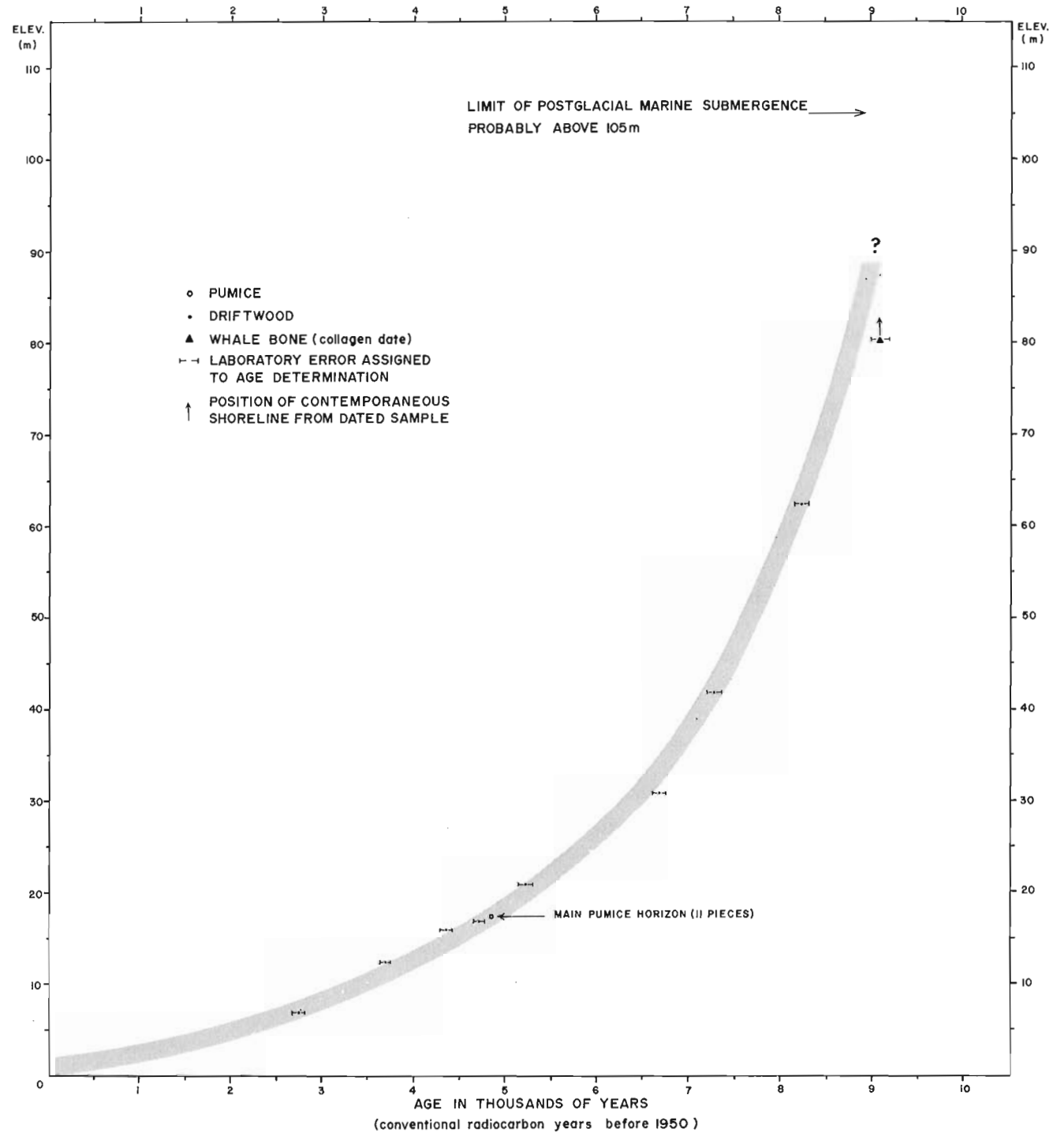

Figure 13.8. Time-elevation diagram for the southwestern part of South Cape Fiord, showing the pattern of postglacial emergence. Elevations of samples are uncorrected for the eustatic rise of sea level.

time the northwestern coast of Jones Sound, Arctic Canada, first became open to the sea between 9500 and 9000 years ago (conventional radiocarbon years).

2. The presence of raised beaches and other features of marine origin at elevations of up to 130 m near Cape Storm, southern Ellesmere Island, provides indirect evidence that a significant cover of glacier ice existed in this area. The differential uplift of pumice, driftwood, and other materials associated with raised beaches indicates that the ice was thicker toward the west and toward the north; i.e., isobases of equal emergence trend roughly northeast-southwest across

southern Ellesmere Island and Devon Island to Somerset Island. The tilt up to the northwest is approximately 16 cm/km for the 6500 year old strandline and 12 cm/km for the beach, with pumice, which formed 5000 years ago.

3. Dating of logs on the modern beach ridges near Cape Storm and on Melville and Axel Heiberg islands, as well as wood on multi-year sea ice in Nansen Sound (between Axel Heiberg and Ellesmere Islands) shows that this wood is indeed "modern" (all <250 years old). Also, some of the driftwood (*Larix* sp. at the modern shore and on raised beaches) can be shown to derive from Eurasia on the basis of the resins it contains. At Cape Storm all the modern driftwood is within 2 m of the present shoreline, and no evidence was found that the imbedded wood on the raised beaches was thrown any greater distance above the contemporaneous sea level. Thus the driftwood provides an excellent means of documenting the changing position of the shoreline through time, a period of more than 8000 years in the case of southern Ellesmere Island.

4. Numerous cross-check age determinations between driftwood and whale bones have shown that in this type of arctic environment, utilizing the organic (collagen) fraction of whale bones for radiocarbon dating gives reliable results, whereas in most cases determinations on the bone apatite fraction give ages that are too young.

5. Holocene marine molluscs yield reliable ^{14}C age determinations, even in areas where carbonate rocks are widespread, such as southern Ellesmere Island and northern Bathurst Island.

6. Dating of the abundant driftwood on the raised beaches near Cape Storm and in South Cape Fiord, supplemented by ^{14}C determinations on whale bones and molluscs, has allowed construction of curves which show in detail the changing pattern of emergence through time. Emergence between 9000 and 8000 years ago at Cape Storm proceeded at a rate of 7 m per century, and over one-half of the total emergence, since the initial incursion of the sea, took place during this interval. By 6500 to 4500 years ago emergence had slowed to 0.8 m per century, and for the last 2400 years it has averaged less than 0.3 m per century.

7. The emergence curves, particularly the one from Cape Storm, are sufficiently well controlled that one can concur with Walcott (1972, p. 855): "... that there have been no oscillations of sea level with periods greater than 500 years or amplitudes exceeding 2 metres, although oscillations of shorter period or smaller amplitude are still possible". Walcott's conclusion was drawn for the period 8000 to 3500 years B.P., and new data obtained since his paper was written confirm the validity of his statement, especially for the period from 6500 to 4400 years B.P.

8. The way in which the pumice is concentrated on the beaches, and the nature of the features with which it is associated, suggests that its deposition may be related to:

a) a eustatic rise of sea level, within the limits quoted above, close to 5000 years ago;
b) a period of more open water, when wave action and storm surges would be more effective; or
c) a combination of these two factors.

The formation of the strandline where the pumice occurs is not believed to be related to a slowing down or cessation of uplift due to a thickening of ice caps and glaciers. Many of the glaciers presently are impinging on undisturbed marine deposits; these glaciers are thus at, or are close to, the maximum extent attained since general deglaciation some 9000 years ago.

Acknowledgments

Dr. J. Mangerud, University of Bergen, Norway, and J.A. Lowdon have read this manuscript; their advice on a number of points is greatly appreciated.

References

Blake, W., Jr.
1975a: Radiocarbon age determinations and postglacial emergence at Cape Storm, southern Ellesmere Island, Arctic Canada; Geogr. Ann., Ser. A, v. 57, p. 1-71.

1975b: Studies of glacial history in the Queen Elizabeth Islands, Canadian Arctic Archipelago; Naturgeogr. Inst., Stockholms Universitet; Forskningsrapport 21, 14 p.

Lowdon, J.A. and Blake, W., Jr.
1973: Geological Survey of Canada radiocarbon dates XIII; Geol. Surv. Can., Paper 73-7, 61 p.

Mangerud, J. and Gulliksen, S.
1975: Apparent radiocarbon ages of recent marine shells from Norway, Spitsbergen, and Arctic Canada; Quat. Res., v. 5, p. 263-273.

Nydal, R., Gulliksen, S., and Lövseth, K.
1972: Trondheim natural radiocarbon measurements VI; Radiocarbon, v. 14, p. 418-451.

Olsson, I.U. and Osadebe, F.A.N.
1974: Carbon isotope variations and fractionation corrections in ^{14}C dating; Boreas, v. 3, p. 139-146.

Walcott, R.I.
1972: Late Quaternary vertical movements in eastern North America: quantitative evidence of glacio-isostatic rebound; Rev. Geophys. Space Phys., v. 10, p. 849-884.

Project 750073

B.D. Bornhold, C.F.M. Lewis and N.E. Fenerty[1]
Terrain Sciences Division

Introduction

From May 3 to May 14, 1975 the writers carried out a program of sediment sampling and sea floor photography at the Arctic Ice Dynamics Joint Experiment (AIDJEX) site in the Arctic Ocean at approximately 76°25'N, 145°00'W (Fig. 14.1). The objectives of the project were: (1) to develop a portable system and techniques for obtaining gravity cores, grab samples, and bottom photographs from the ice surface, where water depths exceed 3000 metres; and (2) to obtain short cores and sea floor photographs from the Canada Abyssal Plain.

Equipment

A gasoline-driven hydraulic winch (Fig. 14.2) was designed and built such that it could be manoeuvred on the ice by two men, broken down into smaller components for shipment, and could hold 5000 metres of 5/32-inch wire rope. The winch was housed in a tent mounted on the ice surface and was situated adjacent to an insulated hut. The gasoline motor-hydraulic pump assembly was placed outside the tent.

A deep-sea camera system (Fig. 14.3) was so designed and built that it could be deployed through a hole in the ice as small as one foot in diameter. The camera system (camera, strobe, and 12 kHz pinger), launched vertically through the hydrohole, assumed a horizontal attitude beneath the ice. A tripline returned the unit to the vertical before retrieval through the hydrohole. A bottom-contact switch activated the camera and strobe and simultaneously stopped the pinger. Bottom contact was monitored by noting the cessation of the pinger signal using earphones and an oscilloscope.

Benthos and Alpine gravity corers were used to sample the sea floor. Recovery, however, was generally poor; after much experimentation, it was found that the best configuration and technique was to lower a heavily weighted Benthos corer with only a plastic core liner (no steel barrel, cutter, or retainer) slowly into the sediment. The longest core thus obtained was 62 cm. In addition to the cores, samples of surface sediments were obtained by the camera trigger weight and by the camera frame itself. A wire depth of approximately 3700 m consistently was recorded at the sample stations.

An Edo 120 kHz echo sounder was operated continuously for two days with the transducer suspended just

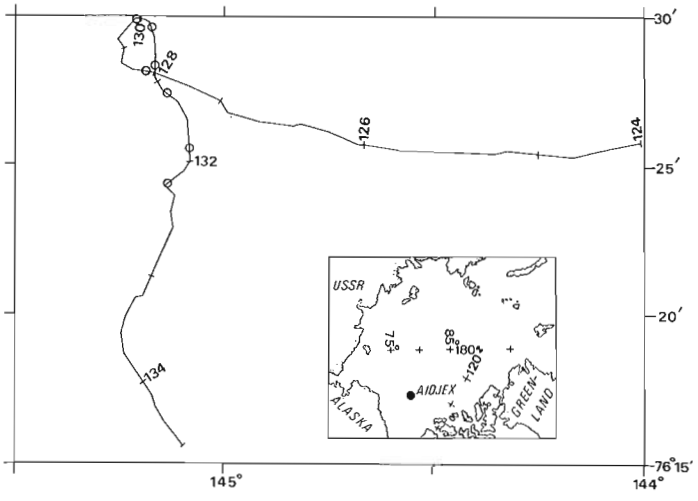

Figure 14.1. Drift of the AIDJEX camp from May 4 to May 14, 1975. Julian days (GMT) are indicated along the drift track. Open circles are bottom sample and camera stations.

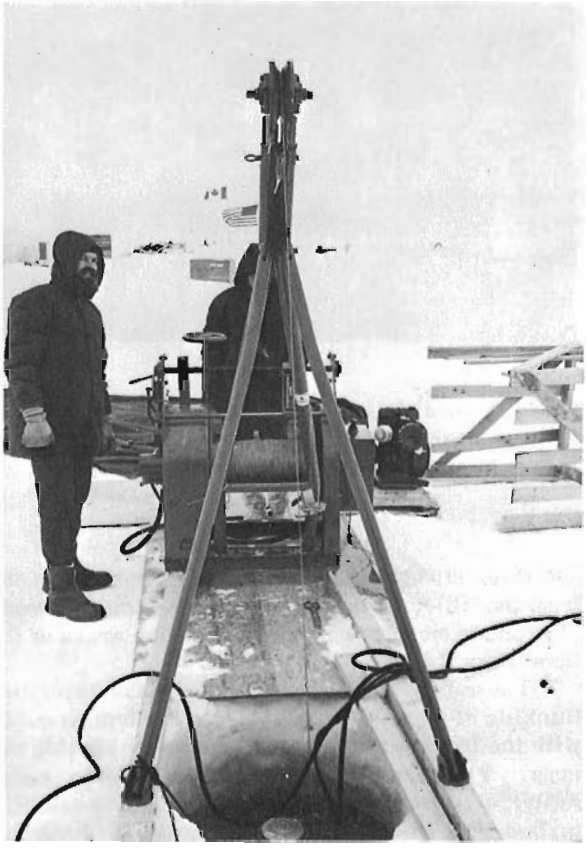

Figure 14.2. Winch set-up, with gasoline motor-hydraulic pump assembly in background and hydrohole in foreground.

[1]Atlantic Oceanographic Laboratory, Bedford Institute of Oceanography, Dartmouth, Nova Scotia.

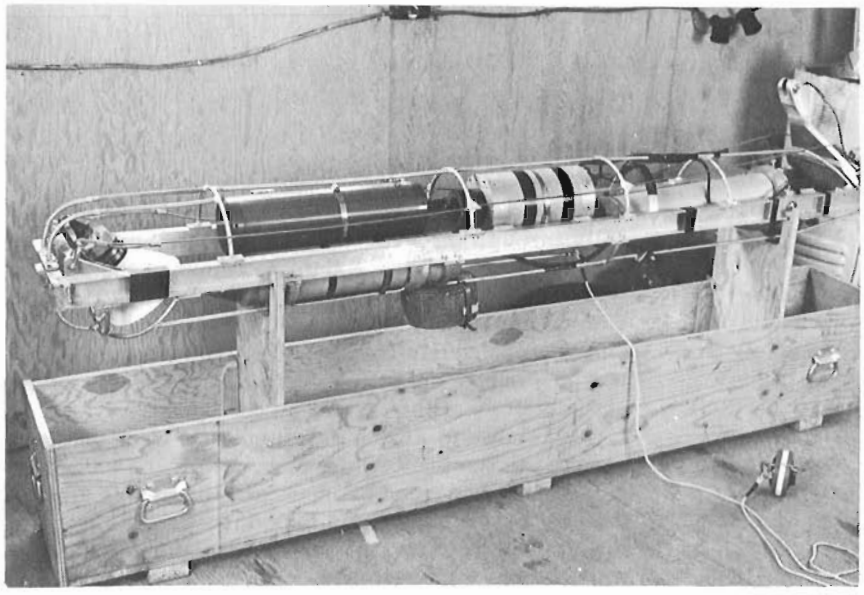

Figure 14. 3.

Deep-sea camera system designed for use from an ice platform. The trigger weight and line are on the floor by the camera.

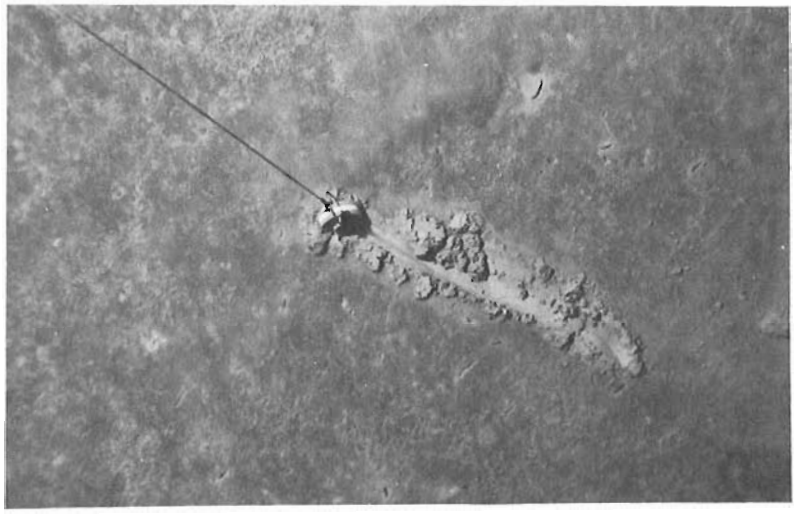

Figure 14. 4.

Depression in the sea floor, produced by camera trigger weight, showing the thin, darker surficial layer of fine sediment and the stiffer, light-coloured underlying material. Trigger weight is approximately 15 cm in diameter.

below the sea surface in the hydrohole. Good bottom returns were received and revealed an extremely flat bottom at approximately 3550 metres (uncorrected).

Bottom Photographs

Over 110 usable sea floor photographs were obtained from the AIDJEX site. Many of these could be combined to produce mosaics covering extensive areas of the sea floor (Fig. 14. 5).

These photographs, similar to those described by Hunkins *et al.* (1970), revealed a flat bottom covered with the tracks, trails, and burrows of benthic organisms. The surficial sediment was a dark, very soft lutite, at most one centimetre thick, and readily disturbed into suspended clouds by the trigger weight. This thin surface layer was underlain by a stiffer, lighter coloured sediment, exposed in the burrows and trails and in the depressions created by the trigger weight (Fig. 14. 4).

Several distinct types of biogenic structure were apparent:

(1) short (less than 10 cm), deeply incised trails, generally arcuate or winding;
(2) long (greater than 0. 5 m), meandering, shallow trails, some branching;
(3) oval to circular rings (10 to 20 cm diameter);
(4) long (greater than 2 m), very straight, non-branching, shallow trails (Fig. 14. 6);
(5) single mounds with central depressions (2 to 3 cm diameter); and
(6) shallow, circular features (20 cm in diameter) (Fig. 14. 7).

In spite of the obvious abundance of life, none of the organisms responsible for these features was photographed.

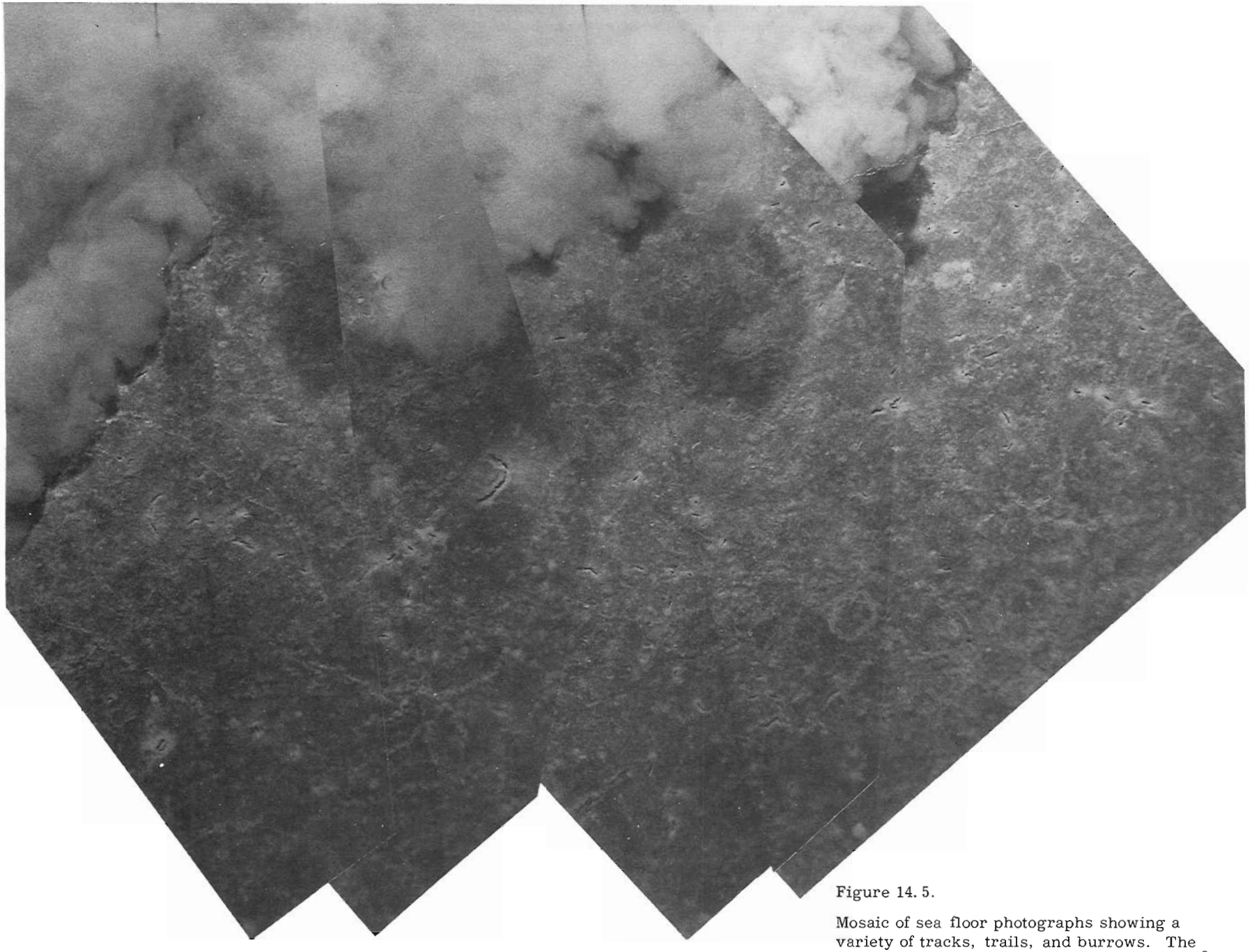

Figure 14.5.

Mosaic of sea floor photographs showing a variety of tracks, trails, and burrows. The area of visible sea floor is approximately 8 m^2.

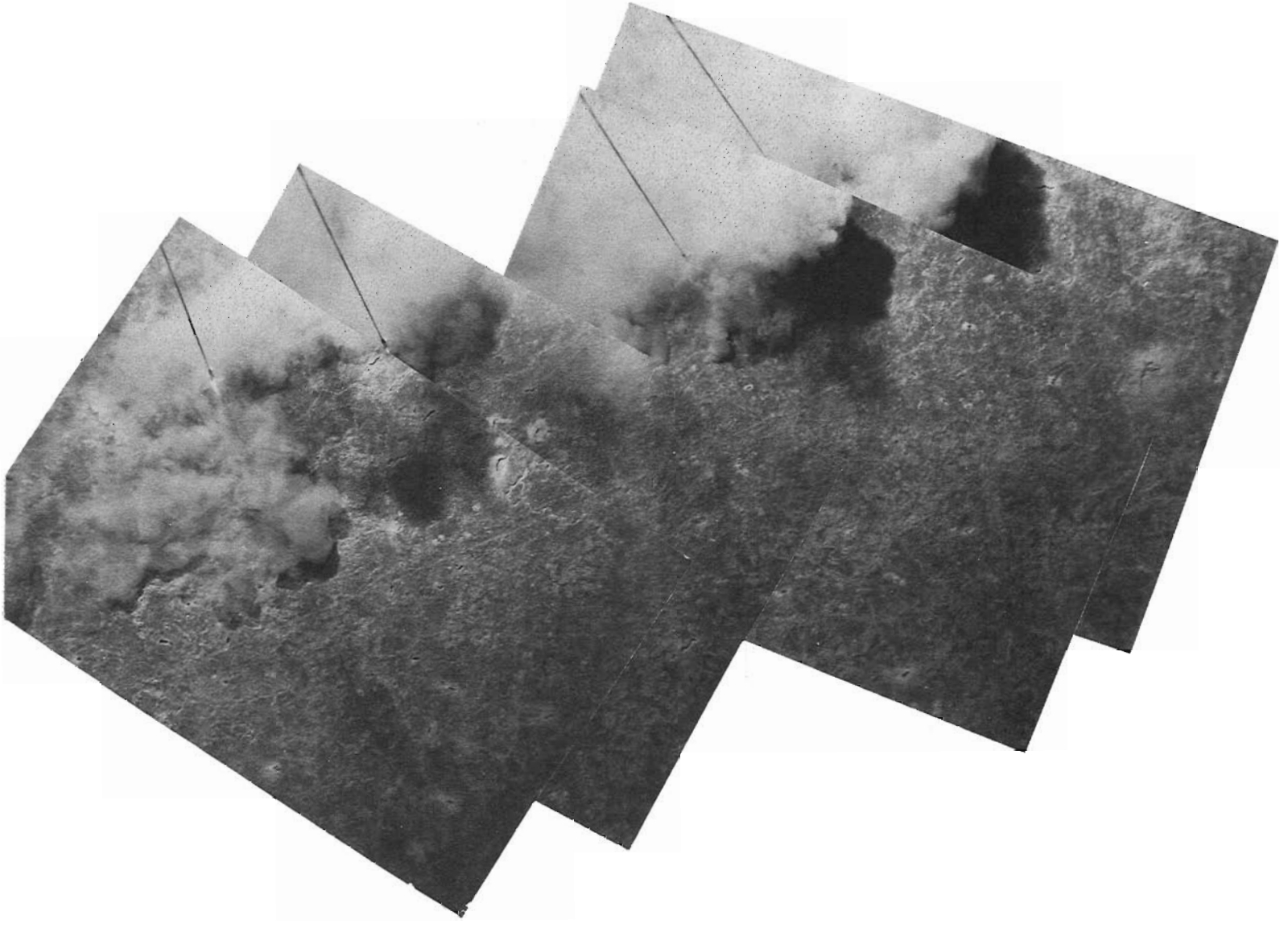

Figure 14.6. Mosaic of sea floor photographs showing long, straight, non-branching trails. Area of visible sea floor is approximately 10 m^2.

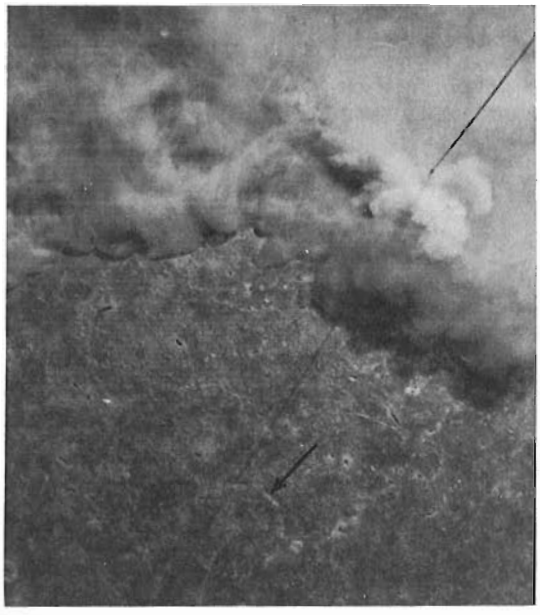

Figure 14. 7. Photograph of unusual circular biogenic structure (arrow). Area of visible sea floor is approximately 3 m^2.

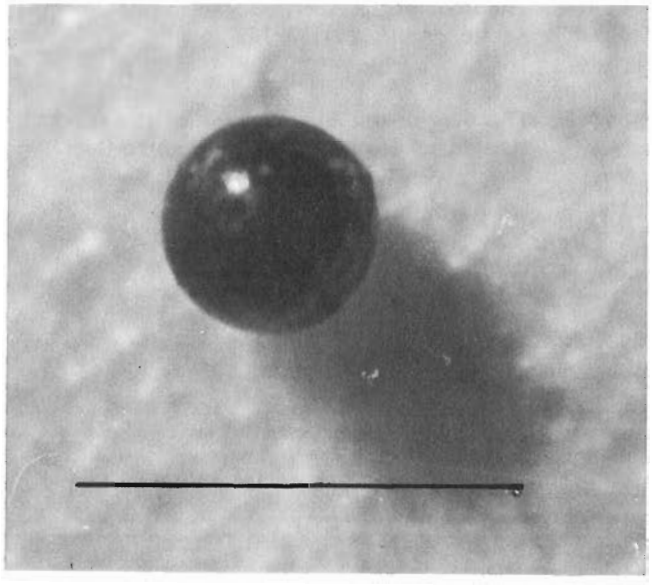

Figure 14. 8. Photomicrograph of shiny, black, cosmic spherule. Scale is 0. 5 mm.

Figure 14. 9. (right) X-radiograph of gravity core showing several turbidites (dark) and intervening pelagic lutites. The Bouma sequence of internal structures is indicated for the longest turbidite unit. A worm burrow (b) is visible in the upper part of this turbidite. Core length is in cm.

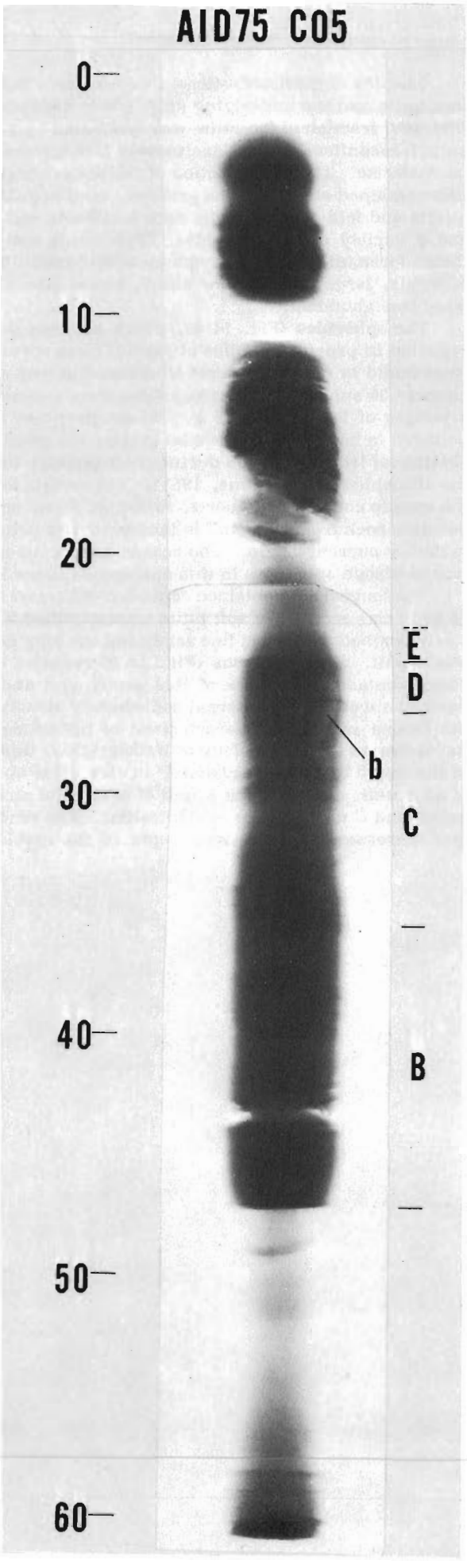

Bottom Samples

Samples of surficial sediment were of both the surface lutite and the underlying stiff, sandy sediment. The sand fraction of the lutite was dominated by planktonic foraminifera, almost exclusively *Globigerina pachyderma*. The sand fraction of the underlying sandy unit contained abundant fine grained, very angular quartz and feldspar, volcanic rock fragments and glass, and a variety of types of mica. Planktonic and benthonic foraminifera, sponge spicules, fish teeth, heavy minerals, large diatoms, and shiny, black spherules were less abundant.

The spherules (Fig. 14.8), which have not been reported in previous studies of Arctic Ocean cores, were found in relatively great abundance in only one sample; 35 spherules of various sizes were counted in a sample of less than 0.25 g. These particles are believed to be of extraterrestrial origin, the result of ablation of iron meteorites during their passage through the atmosphere (Arrhenius, 1963). The remainder of the sample consisted of quartz, feldspar, mica, and volcanic rock fragments and is interpreted as being of turbidity current origin. The reason for the concentration of cosmic spherules in this one sample is not known.

The longest core obtained consisted of several short (5 to 10 cm) sections of soft lutite interstratified with finely laminated silts and fine sands and one long (21 cm) sandy unit. X-radiographs (Fig. 14.9) revealed the sharp contact at the base of this sandy unit and the vertical succession of internal sedimentary structures, the Bouma sequence, characteristic of turbidites. According to the terminology of Walker (1965) this turbidite would be classed as "distal" in view of the absence of an A unit, and the thick B unit of horizontal stratification and C unit of cross-stratification. The sand content increases markedly with depth in the turbidite, from less than 5 per cent at the top to more than 50 per cent at the base. Compositionally the turbidite remains relatively homogeneous throughout except for the uppermost part of the unit which possesses a great abundance of sponge spicules and a much greater proportion of rock fragments and glass than samples from the base of the unit.

Acknowledgments

Co-ordination and logistical support for this program were kindly provided by the Polar Continental Shelf Project, Department of Energy, Mines and Resources, and by the Naval Arctic Research Laboratory, Point Barrow, Alaska.

We would like to express our thanks to Rolf Bjørnert, Manager of Field Operations at the AIDJEX site, and his staff for their excellent assistance and co-operation. Mr. Andy Heiberg, at the Naval Arctic Research Laboratory was extremely helpful in making travel arrangements and expediting the shipment of our equipment.

References

Arrhenius, G.
1963: Pelagic sediments; *in* The Sea, v. 3, ed. M.N. Hill; Interscience, p. 655-727.

Hunkins, K., Mathieu, G., Teeter, S., and Gill, A.
1970: The floor of the Arctic Ocean in photographs; Arctic, v. 23, p. 175-189.

Walker, R.G.
1965: The origin and significance of the internal structures of turbidites; Yorkshire Geol. Soc. Proc., v. 35, p. 1-32.

15. PLANT MEGAFOSSILS FROM MID-WISCONSIN SEDIMENTS IN WEST-CENTRAL ALBERTA

Project 690064

Sigrid Lichti-Federovich
Terrain Sciences Division

Introduction

The Pleistocene environments of west-central Alberta are of great interest, primarily because of the possible significance for both biotic and hominid migrations of a suggested ice-free corridor between Laurentide and Cordilleran Ice Sheets (cf. Reeves, 1973). A section of fossiliferous sediments, dated as mid-Wisconsin by ^{14}C, has been discovered near Watino, Alberta (55°43'N, 117°38'W), and preliminary analyses of geochronological and certain paleoecological data are reported by Westgate *et al.* (1971, 1972). They suggest that the data on sediment type, ^{18}O analysis, and faunal records imply an alluvial depositional environment, changing from "a moderately flowing stream to a quiet, shallow oxbow-type lake".

Samples from this section were submitted to the author for analysis of the moderately abundant seeds and other plant megafossils. The results are of sufficient interest and relevance to the general reconstruction of the environment that they are presented here as separate contribution.

Megafossil Analysis

Methods

Variable volumes of sample lithology were available for megafossil analysis from the different levels of the section, as shown in Table 15.1. Each sample was soaked in water, with the addition of 10% nitric acid where necessary to facilitate disaggregation of the matrix. Megafossils were recovered as flotsam and subsequently by sieving the remainder of the sample. The megafossils were stored in vials with glycerine-alcohol.

Megafossils were identified by reference to the descriptions, illustrations, and keys in various works, particularly Berggren (1969), Katz *et al.* (1965), Martin and Barkley (1961), Ogden (1953), and by direct comparison with reference material from herbaria and in reference collections.

Results

Although a reasonably rich assemblage of megafossils was recovered from the section, a selection of which is illustrated on Plates I and II, it should be noted that many seeds were in degraded condition making identification difficult or impossible.

The results of the analysis are shown in Table 15.1 and are summarized in a relative frequency diagram (Fig. 15.1). The latter was prepared by computing the percentages of the seed total for each type at each level, except for levels where the seed total was less than 35.

Between levels 215 and 203 inches (546 and 516 cm), at the base of the fossiliferous units, the following assemblage was recorded: abundant *Hippuris vulgaris*, *Potamogeton filiformis*, *Carex aquatilis*, *C. rostrata* and *Ranunculus gmelinii* var. *hookeri*, associated with occasional *Myriophyllum verticellatum*, *Sparganium chlorocarpum*, *Eleocharis palustris*, *Carex* cf. *pseudocyperus*, and *C. chordorrhiza*.

A similar assemblage occurs between levels 144 and 102 inches (366 and 259 cm). In addition to abundant *Hippuris vulgaris*, *Myriophyllum verticellatum*, *Potamogeton filiformis*, *Carex aquatilis*, *C. rostrata*, and *Ranunculus gmelinii* v. *hookeri* there are some occurrences of *Selaginella selaginoides*, *Myriophyllum exalbescens*, *Sparganium chlorocarpum*, *Potamogeton vaginatus*, *P. richardsonii*, *Carex* cf. *physocarpa*, *C. lacustris*, *C.* cf. *flava*, *C.* cf. *disperma*, *Ranunculus circinatus*, *Juniperus horizontalis*, *Fragaria vesca*, *Sonchus arvensis*, *Chenopodium glaucum*, and *Arctostaphylos Uva-ursi*.

The uppermost unit of the section (Unit K), between sample levels 32 and 6 inches (81 and 15 cm), yielded an assemblage of megafossils as follows: numerous needles of *Picea glauca*, seeds of *Hippuris vulgaris* (rare), *Myriophyllum exalbescens* (infrequent), *M. verticellatum* (rare), *Eleocharis palustris* (abundant), *Potamogeton filiformis*, *P. vaginatus* and *P. richardsonii* (all common); *Carex aquatilis* (rare), *C. lacustris* (frequent), and *C. atherodes* (rare); *Ranunculus circinatus* v. *subrigidus* was recorded at three levels.

Interpretation

The assemblage recorded from this site provides some useful information about the broad floristic affinity of the plants. There is a notable absence of arctic-subarctic forms, with the single exception of *Selaginella selaginoides*, and of grassland elements. The assemblage is temperate-boreal, similar in many respects to the modern flora of central, forested Alberta (Moss, 1959). Indeed, there is a remarkable similarity between the species list presented here and the species recorded by van der Valk and Bliss (1971) in their recent study of the aquatic vegetation of oxbow lakes in central Alberta.

There is substantial agreement between the regional vegetation as reconstructed by Aario (unpubl. rept.; pers. comm.) on the basis of his pollen diagram from the Watino site and the broad floristic-vegetational affinities of the megafossil assemblage reported in Table 15.1. There are notable absences from both the pollen diagram (e.g., *Pinus*, *Betula*, *Quercus*) and the megafossil record (*Typha*, *Ceratophyllum*, *Lemna*, *Najas*, *Nuphar*, and *Acorus*), but the similarity in general floristic features between the Watino assemblage,

Table 15. 1

A list of seeds and spores showing the actual numbers recovered at each sample level.

C14 - ACE	SAMPLE DEPTH inches	cm	VOL. cc.	CHARA	HIPPURIS vulgaris	POTAMOGETON filiformis	POTAMOGETON vaginatus	POTAMOGETON richardsonii	HYRIOPHYLLUM exalbescens	MYRIOPHYLLUM verticillatum	MYRIOPHYLLUM app. (poor pres.)	SPARGANIUM chlorocarpum	RANUNCULUS circinatus v. subrig.	RANUNCULUS gmelinii v. hookeri	Alismataceae (poor pres.)	ELEOCHARIS palustris	CAREX aquatilis	CAREX rostrata	CAREX cf. pseudocyperus	CAREX vulpinoidea	CAREX lacustris
	0-6	0-15.2	1.5																		
	4-8	10.2-20.3	conc																		
	6-8	15.2-20.3	1.4	++																	
	8-12	20.3-30.5	conc	+++	7	6	42	76	8	2			27		2	23				15	
	8-14	20.3-35.5	42.0	+++	1	4	5	35	1		1		5			4	2			6	
	12-18	30.5-45.7	conc			20	12	7	9				1			35					
	14-20	35.5-50.8	17.0		1	12	3	8	1		1					5				5	
27,400 + 850 (I-4878)	20-26	50.8-66.0	13.0		1	14	3	3	4		4										
	26-32	66.0-81.3	10.0			9								1						3	
	32-44	81.3-111.7	23.0		2	51								3			2			4	
	44-50	111.7-127.0	2.2																		
	50-56	127.0-142.2	2.0																		
K	60-66	152.4-167.6	6.0																		
	56-62	142.2-157.5	2.4																		
	66-72	167.6-182.9	6.6																		
	62-68	157.5-172.7	2.9																		
	72-78	182.9-198.1	6.1																		
	76-82	193.0-208.3	6.4																		
$35,000^{+3300}_{-2300}$ (I-2615)	78-88	198.1-223.5	15.0																		
	90-96	228.6-243.8	5.5																		
	96-102	243.8-259.1	62.0			2								6	1			4	1		
	102-108$_1$	259.1-274.3$_1$	42.0		2	1		1	1					35			4	12			
	102-108$_2$	259.1-274.3$_2$	44.0		8	18		7	2	2	2	2		129			3	65			1
	108-114	274.3-289.6	52.4		77	72	9	8		19	10	6		124			2	357	6	8	
	114-120	289.6-304.8	44.0		34	14		2		2		1		263	1		7	82			
local unconformity	120-130	304.8-330.2	conc		164	258	6	2		13		8	2	341			14	201	6		
	120-126$_1$	304.8-320.0$_1$	53.0		51	66					3	1		129	1		5	211			
	120-126$_2$	304.8-320.0$_2$	50.0		48	49	3			5	4	1		4	2		27	256	2		
J	126-132	320.0-335.3	71.0		79	150				3				71			34	236	1		
	132-138	335.3-350.5	69.0		28	38				3				72			158	99	1		
	138-144	350.5-365.8	49.0		4	3								10	1		43	13			
$35,000^{+2300}_{-1800}$ (I-2516)	144-150	365.8-381.0	21.0														28				
	154-164	391.2-416.6	2.2																		
	164-174	416.6-442.0	4.6			1								1			1				
	174-184	442.0-467.4	13.0																		
43 500 + 620 (GSC-1020)	184-190	467.4-482.6	5.8																		
	191-197	485.1-500.4	11.0			1															
	197-203	500.4-515.6	46.0		64	17				1	1	1		175		2	72	62	8		
	203-209	515.6-530.9	54.0		145	91				2	2	4		237		1	8	196	1		
38,000 (GX-1207)	209-215	530.9-546.1	61.0		22	32				1		3		156			11	137	3		

+present, ++frequent, +++abundant

poor pres. — poor preservation

conc. — liquid concentrate of unknown volume of sediment sample

I = Isotopes Ltd.

GX = Geochron

GSC = Geol. Surv. Can.

Unit J — consists of fine-grained alluvium with a woody layer at 158 inches (400 cm) and 195 inches (495 cm)

Unit K — consists of fine-grained alluvium with a peaty layer at 78 inches (198 cm) and separated by a local unconformity at 120 inches (305 cm).

covering the interval from approximately 44 000 to 27 000 years ago, and the modern southern Boreal forest of Alberta is remarkable.

Referring specifically to the assemblage of aquatic and semi-aquatic plants recorded from the site, certain ecological inferences can be drawn as follows: without exception, the types preserved in these sediments are plants which occur today in shallow, alkaline waters. A scrutiny of the more important published accounts of the vegetation and ecology of aquatic communities in the

Table 15.1 (cont'd.)

C^{14} - AGE	SAMPLE DEPTH inches	cm	VOL. cc.	CAREX cf. diasperma	CAREX chordorrhiza	CAREX cf. physocarpa	CAREX cf. flava	CAREX atherodes	CAREX spp.	Perigynia	SELAGINELLA selaginoides	FRAGARIA vesca	SONCHUS arvensis	CHENOPODIUM glaucum v. salinum	RANUNCULUS spp.	POTENTILLA spp.	Rosaceae	ARCTOSTAPHYLOS uva-ursi	JUNIPERUS horizontalis	PICEA glauca (seed)	PICEA glauca (needles)	TOTAL No. of SEEDS
	0-6	0-15.2	1.5																		+	
	4-8	10.2-20.3	conc																		++	
	6-8	15.2-20.3	1.4						1												+++	1
	8-12	20.3-30.5	conc					10	16												+++	234
	8-14	20.3-35.5	42.0						6													70
	12-18	30.5-45.7	conc																			84
	14-20	35.5-50.8	17.0					3	5													44
27,400 + 850 (I-4878)	20-26	50.8-66.0	13.0						5	2												36
	26-32	66.0-81.3	10.0						3						2							18
	32-44	81.3-111.7	23.0																			64
	44-50	111.7-127.0	2.2						1													
	50-56	127.0-142.2	2.0																			
K	60-66	152.4-167.6	6.0																			
	56-62	142.2-157.5	2.4																			
	66-72	167.6-182.9	6.6																			
	62-68	157.5-172.7	2.9																			
	72-78	182.9-198.1	6.1																			
	76-82	193.0-208.3	6.4																		+	
$35,000^{+3300}_{-2300}$ (I-2615)	78-88	198.1-223.5	15.0																			
	90-96	228.6-243.8	5.5						1													1
	96-102	243.8-259.1	62.0						3												+	17
	$102-108_1$	$259.1-274.3_1$	42.0						7		3			1							+	67
	$102-108_2$	$259.1-274.3_2$	44.0	1			3		7											1		251
	108-114	274.3-289.6	52.4				2		119	1			1			1		2	5			831
	114-120	289.6-304.8	44.0				3		15						2						+	426
local unconformity	120-130	304.8-330.2	conc						37	7		1										1,060
	$120-126_1$	$304.8-320.0_1$	53.0						24	1												492
	$120-126_2$	$304.8-320.0_2$	50.0			1			37						2							441
J	126-132	320.0-335.3	71.0						27													601
	132-138	335.3-350.5	69.0						54								1					454
	138-144	350.5-365.8	49.0						19													93
$35,000^{+2300}_{-1800}$ (I-2516)	144-150	365.8-381.0	21.0						4							1	1				+	34
	154-164	391.2-416.6	2.2																			
	164-174	416.6-442.0	4.6																			3
	174-184	442.0-467.4	13.0																			
43 500 + 620 (GSC-1020)	184-190	467.4-482.6	5.8																			
	191-197	485.1-500.4	11.0			1			2												+	4
	197-203	500.4-515.6	46.0						17	2												422
	203-209	515.6-530.9	54.0		2				36	2							1					728
38,000 (GX-1207)	209-215	530.9-546.1	61.0						30													395

Western Interior of Canada (Moyle, 1945; Lewis *et al.*, 1928; Walker and Coupland, 1968; van der Valk and Bliss, 1971) suggests that the lower two assemblages (levels 546 to 516 cm, 366 to 259 cm) represent a pioneer aquatic community in a shallow lake with alkaline, probably somewhat calcareous conditions subject to periodic flooding; the upper assemblage represents a similar environment except that the lake was probably very shallow, perhaps seasonally almost dry.

The recent paper by van der Valk and Bliss (1971) is particularly helpful in reconstructing the local vegetation and environment of the site. They have described the plant communities, water chemistry, and productivity of 15 oxbow lakes from the Pembina River in central Alberta. Also, they have described a successional pattern for these lakes which provides a useful framework for interpretation of the results presented here.

The three separate assemblages (Fig. 15.1) all fall into the early or pioneer hydrarch stages, and it is interesting that no megafossil assemblage was recorded which suggests a late, mature stage in the succession. This accords with the suggestion of Westgate *et al.* (1971, 1972) that the sediment stratigraphy can be accounted for most satisfactorily in terms of an alluvial environment, probably an oxbow lake system, subject to periodic inundation.

The subfossil seed of *Sonchus arvensis* is interesting since *Sonchus* (*S. uliginosus*) occurs in the succession described by van der Valk and Bliss (1971); however, perhaps it can be accounted for as a contaminant during field sampling, as *Sonchus* is regarded as a postsettlement introduction from Europe (cf. Moss, 1959).

References

Berggren, G.

1969: Atlas of Seeds, Part 2, Cyperaceae; Swed. Nat. Sci. Res. Coun., Berlingska Boktryckeriet, Lund., 68 p.

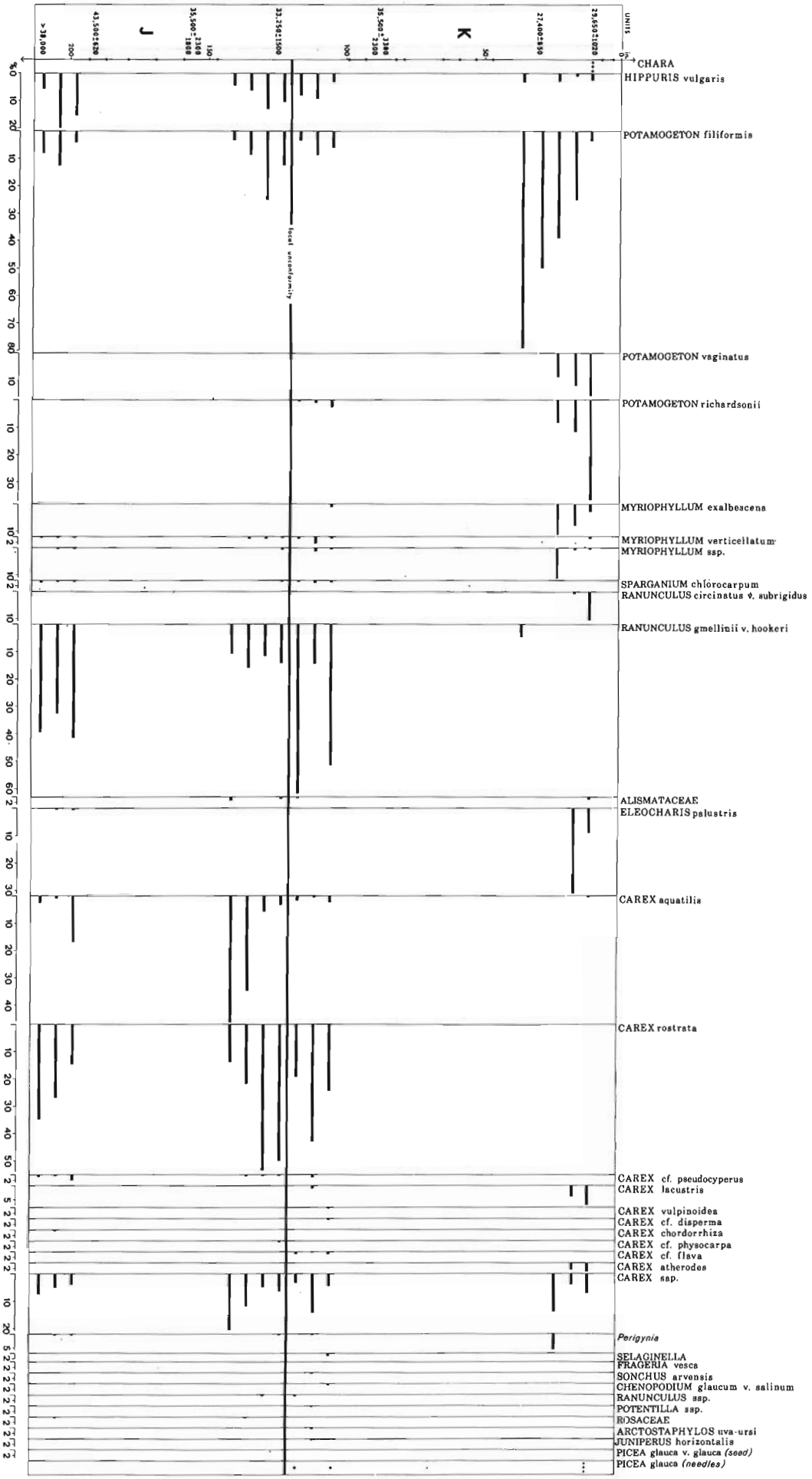

Figure 15. 1. Diagram of seed percentages from the Watino Section, Alberta. • indicates samples with a seed total of less than 35.

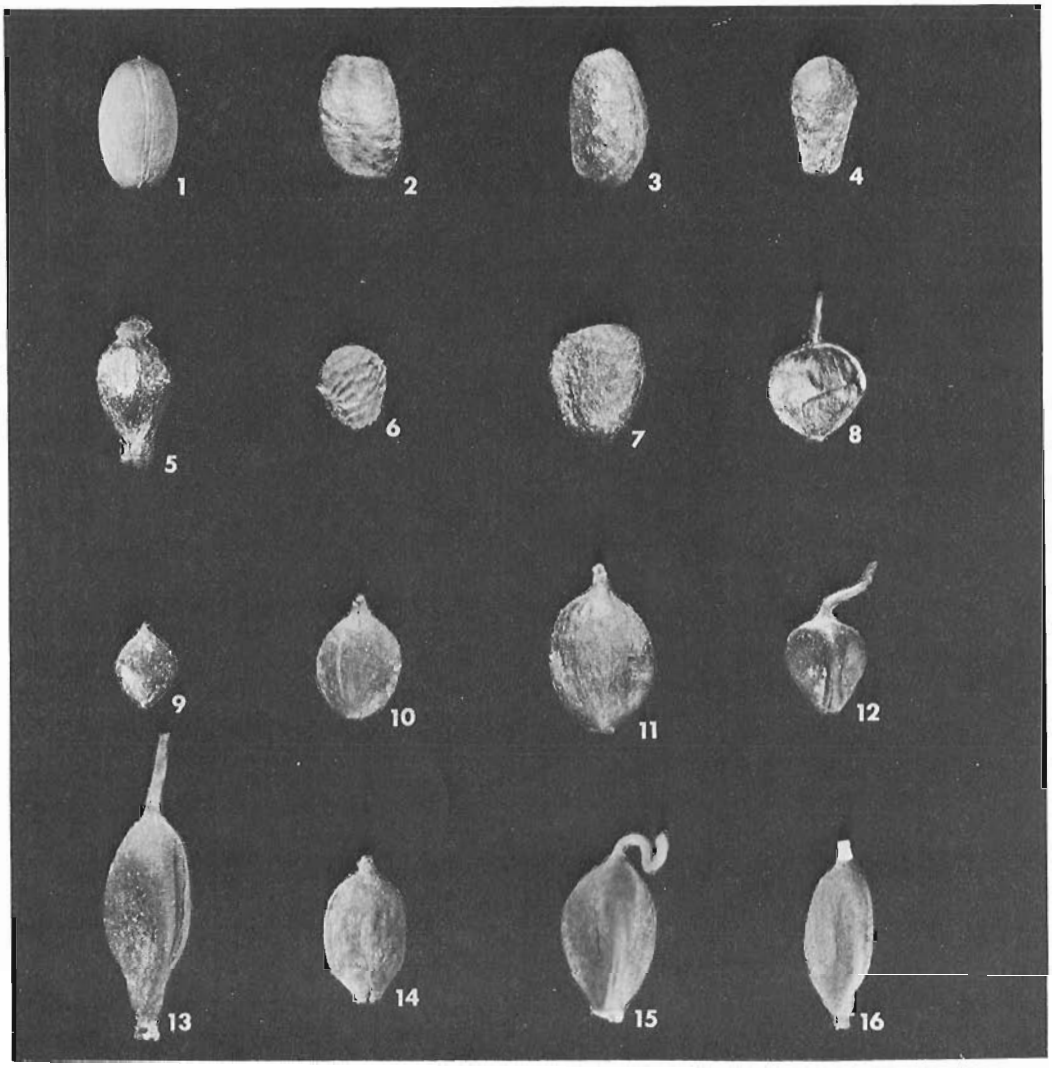

Plate 15. 1: Figs. 1-16. (All figures magnified x 10.)

1. *Hippuris vulgaris*
2. *Myriophyllum verticellatum*
3. *Myriophyllum exalbescens*
4. *Sparganium chlorocarpum*
5. *Eleocharis palustris*
6. *Ranunculus circinatus* v. *subrigidus*
7. *Ranunculus gmelinii* v. *hookeri*
8. *Carex aquatilis*
9. *Carex vulpinoidea*
10. *Carex* cf. *disperma*
11. *Carex* cf. *physocarpa*
12. *Carex* cf. *flava*
13. *Carex atherodes*
14. *Carex chordorrhiza*
15. *Carex rostrata*
16. *Carex lacustris*

Katz, N. J., Katz, S. V., and Kipiani, M. G.
1965: Atlas and keys of fruits and seeds occurring in the Quaternary Deposits of the USSR; Moscow, 364 p. (Private transl. by J. C. Ritchie.)

Lewis, F. J., Dowding, E. S., and Moss, E. H.
1928: The vegetation of Alberta II. The swamp, moor, and bog forest vegetation; Ecology, v. 14, p. 317-341.

Martin, A. C. and Barkley, W. D.
1961: Seed identification manual; Univ. of California Press, Berkeley and Los Angeles, 221 p.

Moss, E. H.
1959: Flora of Alberta; Univ. of Toronto Press, 546 p.

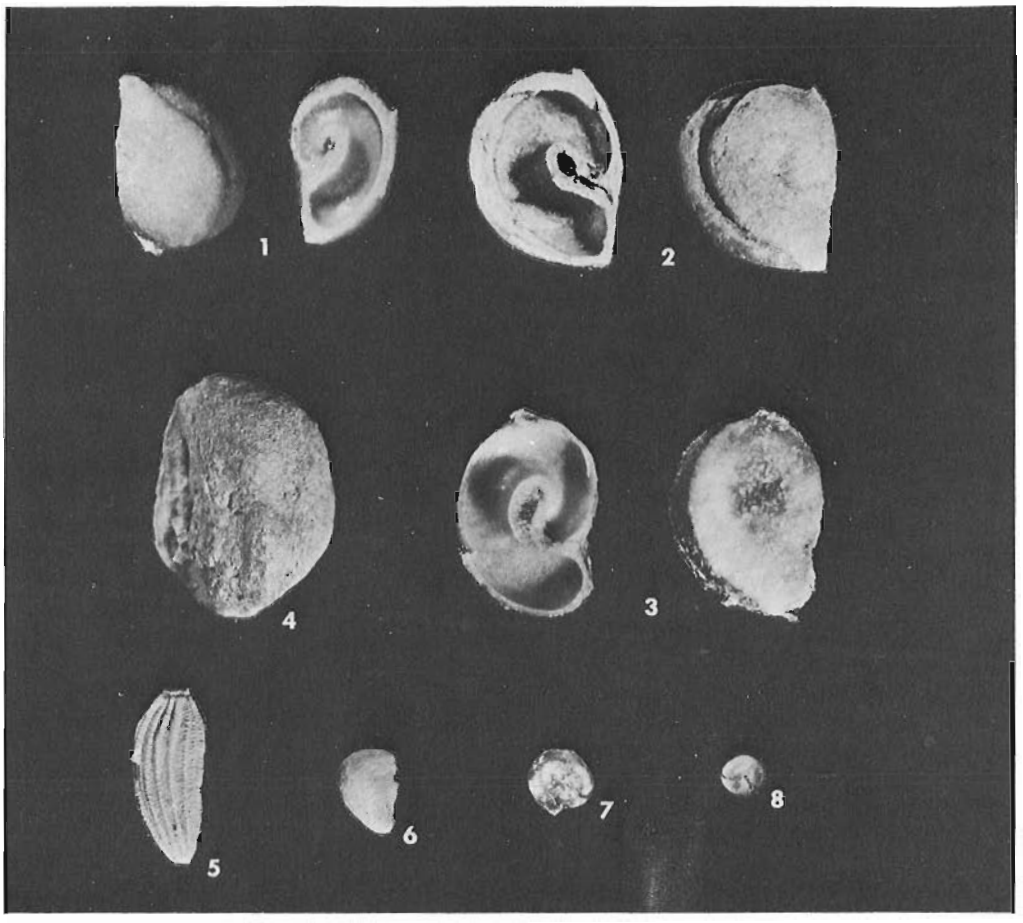

Plate 15. 2. Figs. 1-8. (All figures magnified x 10.)

1. *Potamogeton filiformis*
2. *Potamogeton vaginatus*
3. *Potamogeton richardsonii*
4. *Juniperus horizontalis*
5. *Sonchus arvensis*
6. *Fragaria vesca*
7. *Chenopodium glaucum* v. *salinum*
8. *Selaginella selaginoides*

Moyle, J. B.
1945: Some chemical factors influencing the distribution of aquatic plants in Minnesota; Am. Midl. Nat., v. 34, p. 402-420.

Ogden, E. C.
1953: Key to the North American species of Potamogeton; N. Y. State Mus. Sci. Serv., Circ. 31, 11 p.

Reeves, B. O. K.
1973: The nature and age of the contact between the Laurentide and Cordilleran Ice Sheets in the western interior of North America; Arct. Alp. Res., v. 5, no. 1, p. 1-16.

van der Valk, A. G. and Bliss, L. C.
1971: Hydrarch succession and net primary production of oxbow lakes in central Alberta; Can. J. Bot., v. 49, p. 1177-1199.

Walker, B. H. and Coupland, R. T.
1968: An analysis of vegetation environment relationships in Saskatchewan sloughs; Can. J. Bot., v. 46, p. 509-522.

Westgate, J. A., Fritz, P., Matthews, J. V., Jr., Kalas, L., and Green, R.
1971: Sediments of mid-Wisconsin age in west-central Alberta: Geochronology, insects, ostracodes, mollusca and the oxygen isotopic composition of molluscan shells; Geol. Soc. Am., Abstracts with Programs, v. 3, no. 6, p. 419.

Westgate, J. A., Fritz, P., Matthews, J. V., Jr., Kalas, L., Delorme, L. D., Green, R., and Aario, R.
1972: Geochronology and palaeoecology of mid-Wisconsin sediments in west-central Alberta, Canada; 24th Int. Geol. Cong., Montreal 1972, Abstracts, p. 380.

Project 750076

R. J. Fulton
Terrain Sciences Division

During mapping of Quaternary deposits in south-central British Columbia (Fulton, 1975) altered rock was noted in a number of places. At that time all occurrences were interpreted as either weathering horizons of Tertiary age or zones of hydrothermal alteration. Evidence brought to light subsequent to these regional studies suggests that this alteration may be the product of subaerial weathering of Quaternary age.

To date the weathered deposits have been subjected to only brief field studies. It is hoped however that this note will draw attention to them and possibly will encourage research into the nature of rock alterations, the time and climatic factors involved, and the significance of this period of weathering in terms of engineering and mineral exploration considerations.

Mission Flats Locality (Kamloops)

Proof that deep alterations of bedrock took place during the Quaternary can best be seen at Mission Flats, 6 km (3.5 miles) west of the Overlander bridge in Kamloops (A of Fig. 16.1). Here excavation for a trunk sewer line and for a garbage disposal site has exposed a sequence of Quaternary sediments overlying altered and fresh bedrock (Fulton and Halstead, 1972, stop 5-7). Cockfield (1948) includes this area within the volcanic rocks of his Tertiary Kamloops Group. At this locality the bedrock consists of a fine grained, dark grey basalt with acicular pyribole phenocrysts, containing scattered small vesicles and drusy vesicles and in some places amygdaloidal with calcite and chalcedony as vesicle fillings. The volcanics are largely massive but appear to lie in thick beds that possibly dip to the southwest at about 20 degrees. In many places the rock is highly fractured so that it is difficult to see fresh surfaces, but locally it occurs as solid glacially abraided knobs.

Approximately 5 m of the alteration product is exposed in one section. At the base the basalt has been bleached from a dark grey colour to an olive grey (5Y4/2) and breaks out of the exposure in angular peds[1] up to 2 cm in size that can be easily crushed with the fingers. When pressed between the fingers, the crushed weathering product can be moulded into slick-surfaced flakes. Upward in the section the colour lightens and becomes more brown, and a contrast between the colour adjacent to the fractures and that of the interior of the peds becomes marked. In general the peds are smaller, higher in the section; near the top of the exposure the altered material looks like a coarse grained sand. Despite its appearance, however, it becomes a fine

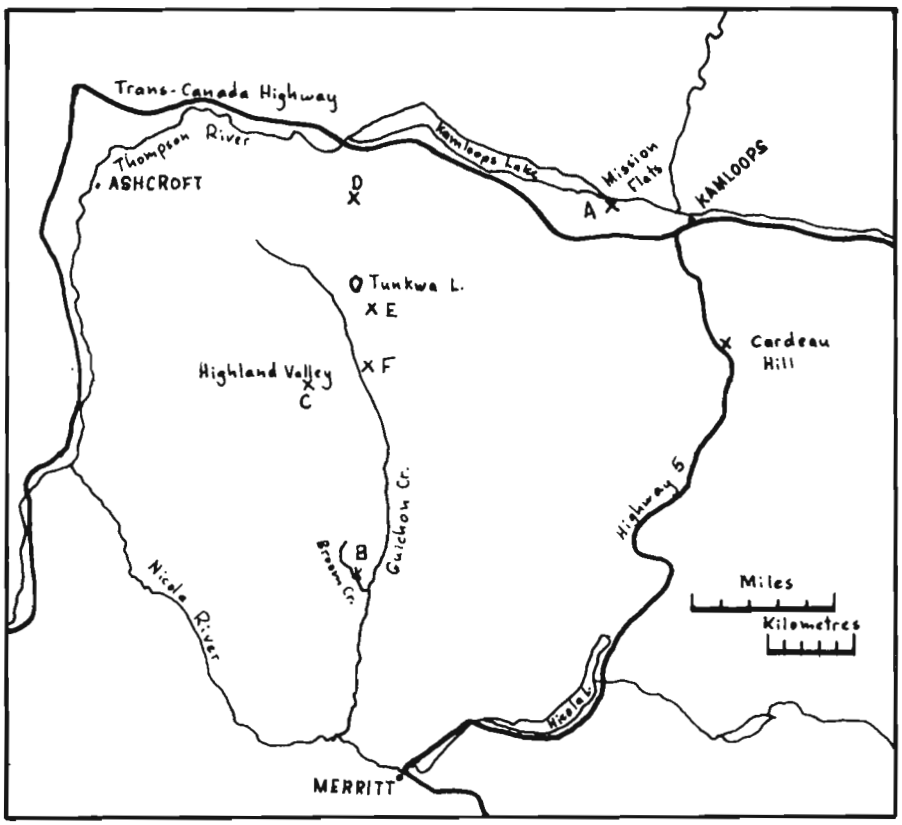

A - weathered basalt, Cardeau Hill-weathered greenstone

B - weathered granite (*see* Fig. 16.2)

C, D - weathered till

E, F - weathered unconsolidated sediments

Figure 16.1. Location map.

[1] A ped is a naturally formed unit of soil structure.

Figure 16. 2. Exposure of granite on Broom Creek that has been effected by spheroidal weathering (GSC 116429).

powder when rubbed between the fingers and has virtually no grit when crushed between the teeth. At the top of the exposure the interior of the peds is a strong brown colour (7. 5YR5/6), and the area between peds is pale yellow (5Y7/3). When moistened the material becomes sticky, and when worked it has a clayey consistency. Locally in the altered material coherent core stones of bleached basalt and thin (up to 2 mm) veinlets of quartz or chalcedony persist.

The distribution of altered and unaltered material is irregular. Knobs of completely unaltered rock lie a few metres to the west and north of the main exposure, and cuts to the east expose small areas of altered and unaltered rock. Natural outcrops of coherent but fractured basalt lie to the east and south of the exposure. Recent road-cuts at the base of these outcrops expose small pockets of altered rock; in one area the road exposes what appears to be talus, which is derived from the basalt and which has been altered in a fashion similar to that described above. One obvious characteristic of the natural exposures is an abundance of open fractures that extend from the top to the base of many outcrops (in some place a vertical distance of up to 5 m). Below natural ground level these fractures are occupied by up to 2 cm of altered material indicating that even coherent bedrock has been subjected to weathering that has developed clay-rich alteration products along fractures.

This weathering of bedrock is thought to have occurred during an interglacial period that preceded the last (Olympia Interglaciation) main nonglacial interval. The Quaternary sediments overlying the weathered rock include nonglacial deposits containing freshwater shells that have been radiocarbon dated as older than 35 500 years B. P. (GSC-413, Dyck *et al.*, 1966). The interglacial sediments are directly overlain by Kamloops drift (Fulton, 1975), deposited during the last glaciation (Fraser Glaciation of Armstrong *et al.*, 1965). They overlie glacial lacustrine silts that are considered to have been deposited as Okanagan Centre Glaciation (Fulton, 1975) ice retreated from the area. Basal beds of the Interglacial succession and upper layers of the glacial lacustrine sequence contained admixtures of the altered rock material. Hence the period of bedrock alteration occurred before Okanagan Centre Glaciation (more than 43 800 years B. P.) If the basalt is correctly placed in the Kamloops Group, it is of Middle Eocene age (Mathews, 1964). The period of uplift that permitted incisions of these volcanics did not occur until Pliocene or Pleistocene (Mathews, 1968); hence the Thompson Valley, in which the altered bedrock occurs, probably could not have been cut to its present dimensions before early Pleistocene and the rock weathering must have taken place at a later time.

South of Kamloops

What appears to be weathered rock is exposed in one or two cuts and occurs in the till in a number of places on Highway 5 between the junction with Trans-Canada Highway and Cardeau Hill about 15 km (10 miles) south of Kamloops (Fig. 16. 1). The rock underlying this area (Cockfield, 1948) is part of the Nicola Group and here consists of a dark green metavolcanic containing prominent pyroxene phenocrysts. The unweathered rock appears to derive much of its green colour from chlorite, and where altered by weathering the rock appears to consist largely of chlorite. The altered material does not seem to be as soft or poorly consolidated as the altered basalt, but it has an extremely slippery, greasy feel even when dry. Where altered rock was seen it was overlain in place by till and a good developmental profile was not found. In general so much of this material was incorporated in the overlying till that the contact between the two was gradational and the till took on properties similar to those of the weathered rock.

The age of the alteration is unknown but at one locality the overlying till is marked by a weathering profile that is considered to be an Olympia Interglaciation paleosol (Fulton, 1975). The major period of bedrock alteration therefore occurred more than 43 800 years ago. No evidence exists that points to this being a Quaternary weathering phenomena, but because it occurs near the present surface and is near Kamloops where there appears to be other evidence for a Quaternary weathering period, it is tentatively correlated with the same time period that developed the weathering profile on the basalt at Mission Flats.

Its slippery, clay-rich nature gives this alteration unit a significance from a geotechnical point of view. The performance of these materials can be seen at Cardeau Hill, 15 km (10 miles) south of Kamloops where the highways department has had great difficulty stabilizing fill that contains and overlies this material;

a series of slumps has occurred in till that is rich in this altered material at the small creek valley south of Kamloops at the junction of the Trans-Canada Highway and Highway 5.

Altered Granite

Another site that contained altered rock that might be due to Quaternary weathering is located on Broom Creek about 3 km (2 miles) upstream from its junction with Guichon Creek, 55 km (35 miles) southwest of Kamloops (B of Fig. 16.1). The rock affected is a coarse granitic phase of the Guichon Batholith, and it has been altered by spheroidal weathering to the point where it outcrops as loose grus[1] surrounding core stones (Fig. 16.2). Till overlies the rock but there is no other limitation on the age of this alteration.

Weathered granite overlain by till also is exposed in a cut about 20 km (12 miles) east of Ashcroft on the Highland Valley road. At this place the alteration product consists of granitic rubble set in a dark brown clay-rich matrix which also contains an admixture of grus. The only thing that can be said about the age of this weathering is that it preceded the last glaciation.

Altered Unconsolidated Materials

Altered unconsolidated materials of possible Quaternary age were noted at several localities. At two sites (C and D of Fig. 16.1) the material present is till, and the alteration takes the form of red-brown and grey-green veins that preserve the till structure. The greenish altered material is very clay rich and contains pebbles that can be easily cut with a knife. The red-brown material commonly lies between relatively unaltered till and the greenish material and appears to be an oxidized transition phase. Only about 2 m of the material is exposed and there is no noticeable change in the degree of development of the veins throughout the exposure. Unaltered till, deposited during the last glaciation, overlies the older till.

Sand, silt, and diamicton that have been altered outcrop in several road-cuts south of Tunkawa Lake 40 km (25 miles) southwest of Kamloops (E and F of Fig. 16.1). At these localities the outcrops consist of a yellowish, brownish red or greenish material that appears to consist largely of clay sized particles at present, even though the sediment appears to have consisted of sand or even diamicton at the time of deposition. These sections have not been studied in detail and could be flat-lying Tertiary material; however the diamicton that is present in at least one of the exposures might be a till, in which case the sediment, and consequently the weathering, could be of Quaternary age.

[1] An accumulation of waste consisting of coarse-grained fragments.

Conclusion

Detailed studies have not been made of any of the localities mentioned, nothing is known of the chemical nature of the alteration, and only field information is available on the physical differences between the altered and unaltered material. It is not possible to speculate on the nature of climate at the time weathering occurred; it is possible that some alteration at different localities occurred at different times and that in places the alteration may be due to processes other than weathering associated with a land surface. It was felt worthwhile mentioning the possible existence of a buried Quaternary land surface, which had been subjected to relatively deep weathering in the interior of British Columbia, in view of the significance that these materials could have in a geotechnical sense and of the importance that this weathering period could have on mineral exploration.

References

Armstrong, J.E., Crandell, D.R., Easterbrook, D.J., and Nobel, J.B.
1965: Late-Pleistocene stratigraphy and chronology in Southwestern British Columbia and Northwestern Washington; Geol. Soc. Am., Bull. 76, p. 321-330.

Cockfield, W.E.
1948: Geology and mineral deposits of Nicola map-area, British Columbia; Geol. Surv. Can., Mem. 249, 164 p.

Dyck, W., Lowdon, J.A., Fyles, J.G., and Blake, W. Jr.
1966: Geological Survey of Canada radiocarbon dates V; Radiocarbon, v. 8, p. 96-127.

Fulton, R.J.
1975: Quaternary geology and geomorphology, Nicola-Vernon area, British Columbia, 82 L W½ and 92 I E½; Geol. Surv. Can., Mem. 380.

Fulton, R.J. and Halstead, E.C.
1972: Quaternary geology of the south Canadian Cordillera; Int. Geol. Congr., Guideb. Field Exc. AO2, Montreal, 49 p.

Mathews, W.H.
1964: Potassium-argon age determinations of Cenozoic volcanic rocks from British Columbia; Geol. Soc. Am. Bull., v. 75, no. 5, p. 465-468.

1968: Geomorphology, southwestern British Columbia; *in* Guidebook for Geological Field Trips in Southwestern British Columbia, Rept. no. 6, Dept. Geol., Univ. Brit. Columbia, p. 18-24.

17. THE TERRAIN MAPPING AND EVALUATION SYSTEM ADOPTED FOR THE EASTERN QUEEN ELIZABETH ISLANDS

Project 720081

D. A. Hodgson
Terrain Sciences Division

Introduction

Another variant of the Terrain Sciences Division Quaternary mapping system (T. S. system) has been introduced (Hodgson and Edlund, 1975), and this note seeks to explain the development and function of this variant, as well as to justify continued experimentation. There is a similarity of approach in current northern Quaternary reconnaissance mapping projects, with the exception of the integrated interdisciplinary mapping project carried out on Melville Island (Barnett *et al.*, 1975).

The basic T. S. system as used in British Columbia, Labrador, and Mackenzie Valley has been described by Fulton *et al.* (1974, 1975). To summarize it, maps showing surficial materials and landforms are compiled at a scale between 1: 50 000 and 1: 125 000. At the core of the system are the materials-genetic terms which describe about ten general groups of materials. Each group, which normally can be recognized on 1: 60 000 scale air photographs, has a similar genesis, range of materials (which includes stratigraphy and geotechnical properties), and perhaps morphology. The term may be defined further by adding a textural (grain size) modifier. When morphology is simple, a term to describe it may be added to the materials-genetic term; morphology also may be the basis for subdividing units. If the areas of two or more groups are inseparable at the scale of the compilation map, then complex units may be formed.

Terrain units thus are constructed from a variety of land attributes and are intended to provide base data for a number of land uses. An expanded legend commonly is added, in which characteristics of each materials group are described in more detail. Information on vegetation, soils, geotechnical properties, potential engineering problems, etc. also may be added to the legend. This information is grouped around the materials-genetic terms out of convenience in presentation, though the system then assumes some of the rigidity of format and generalization in content inherent in the 'landscape approach' to terrain mapping, as exemplified by the Australian C. S. I. R. O. land research maps (*see* Mabbutt, 1968).

Eastern Queen Elizabeth Islands

The variant scheme has been developed mainly in west-central Ellesmere Island (Hodgson, 1975, Fig. 1). There were no strictly defined land use objectives, and it is hoped that the maps will provide base data necessary for land management in general. The impetus for the project, however, was provided by oil and gas exploration and by the commensurate need for environmental impact studies and land use regulation of such activities as overland seismic vehicle travel, construction of winter and all-weather roads and airstrips, site activities, and any subsequent pipeline construction; therefore information relevant to these specific uses also is provided.

The most significant attributes of the land were considered to be: properties of surficial materials and their spatial variations, morphology (or surface geometry) at all scales, geomorphological processes (active, inactive, potential), drainage, and vegetation. Particular difficulties in the area mapped include: a) the great variety and rapid spatial changes in surficial materials, a consequence of much of the material being *in situ* weathered bedrock derived from a large number of complexly folded and faulted lithologies; b) the presence of discontinuous veneers of glacial and marine sediments, which may be significantly different from underlying and adjacent materials but are not always identifiable on air photographs; c) the presence of ground ice, a significant surficial material, with origins and distribution poorly understood; d) the variations in relief from macroscale (up to 1000 m/km) to microscale (gullying, ice growth, and thaw structures); e) the range of geomorphological processes which are poorly understood, especially those controlled by the thermal regime of the ground and directly by massive ground ice. A further problem to be resolved is the uncertainty over which parameters should be investigated, as there has been little 'feedback' from potential or actual users of those maps that have been completed.

With the number of variables and unknowns present, the author felt unable, at least at the reconnaissance stage, to recognize in the landscape a finite number of repeating patterns in which the relationships between significant attributes could be clearly stated. For geotechnical purposes in particular, it is important to display all the information available, and parameters should not be absorbed into a generalized repeating-pattern unit. An alternative 'parametric approach' defines units on the basis of quantitative values for each parameter considered; obviously such data are difficult to collect in a reconnaissance survey, although this is the most promising direction for development, as it does not require subjective or arbitrary grouping of parameters into supposedly cohesive units. The T. S. system provides the basis for a workable compromise where an area of similar attributes may be described without foreknowledge of, or reference to, other areas and using whatever information is available.

A major modification made to the T. S. system is that only surficial materials (and consequently to a

Figure 17.1. Part of biophysical regions map for Baumann Fiord (NTS 49 C).

degree, genesis) are described. Processes and morphology are considered in a second series of (biophysical) maps; both attributes are too complex to be easily linked with surficial materials. Obviously certain conclusions about morphology may be drawn from a depositional materials-genetic term; however erosional bedrock-controlled landscapes dominate in the field area. Gross relief may be determined from contours (200- or 500-foot intervals) on the topographic base for the surficial materials map. Photomosaics were rejected as base maps for this area because radial displacement due to relief precludes precise registration with topographic maps and thus accurate description of the location of points.

Surficial Materials (variant scheme)

Materials maps are compiled at 1: 125 000 scale (no example of materials map per se reproduced, but information displayed as screened background on the biophysical map example, Fig. 17.1). Figure 17.2 shows a legend panel explaining the system; Figure 17.3 shows part of a surficial materials legend. Each map or group of maps placed on Open File has a legend with the same format, but with descriptions of the local facies of materials-genetic units and bedrock lithologies. About twenty materials-genetic terms are used, and new, local terms are introduced when it is felt that the materials and genesis of an area are not described adequately by the standard terms. The 'lithologies' described are in fact rock-stratigraphic formations, although it is fully recognized that lithic rather than formational units should be used (*see* Fig. 17.2). Up to thirty different formations may outcrop in a single map-area. The textural modifier identifies material grain size; information is gained from observations and by inference from the materials-genetic term as identified on air photographs. If sufficient data were available, the Unified Soil Classification System would be preferred. Use of the process modifier has been restricted to describing the manifestation of segregated ice on the surface, through changes in the thermal equilibrium of the ground (ice-wedge polygon troughs, thaw flow slides, thermokarst ponds, etc.).

As with the basic T. S. system, the potential exists for each unit on the map to have a unique designation, and hence there is a problem in appending information about each distinct unit to an expanded/interpretative legend of reasonable length. The solution described earlier of using the materials-genetic terms as the key was rejected as this cancels out the benefits of the flexible system and also does not permit description of complex units. Furthermore, morphology and processes were not taken into account in defining the materials units. It also was felt that a description of vegetation, which is closely related to geological and geomorphological attributes and is a significant criterion in environmental impact studies, should be included. Therefore a new series of maps and legends was drawn, complementing the materials maps.

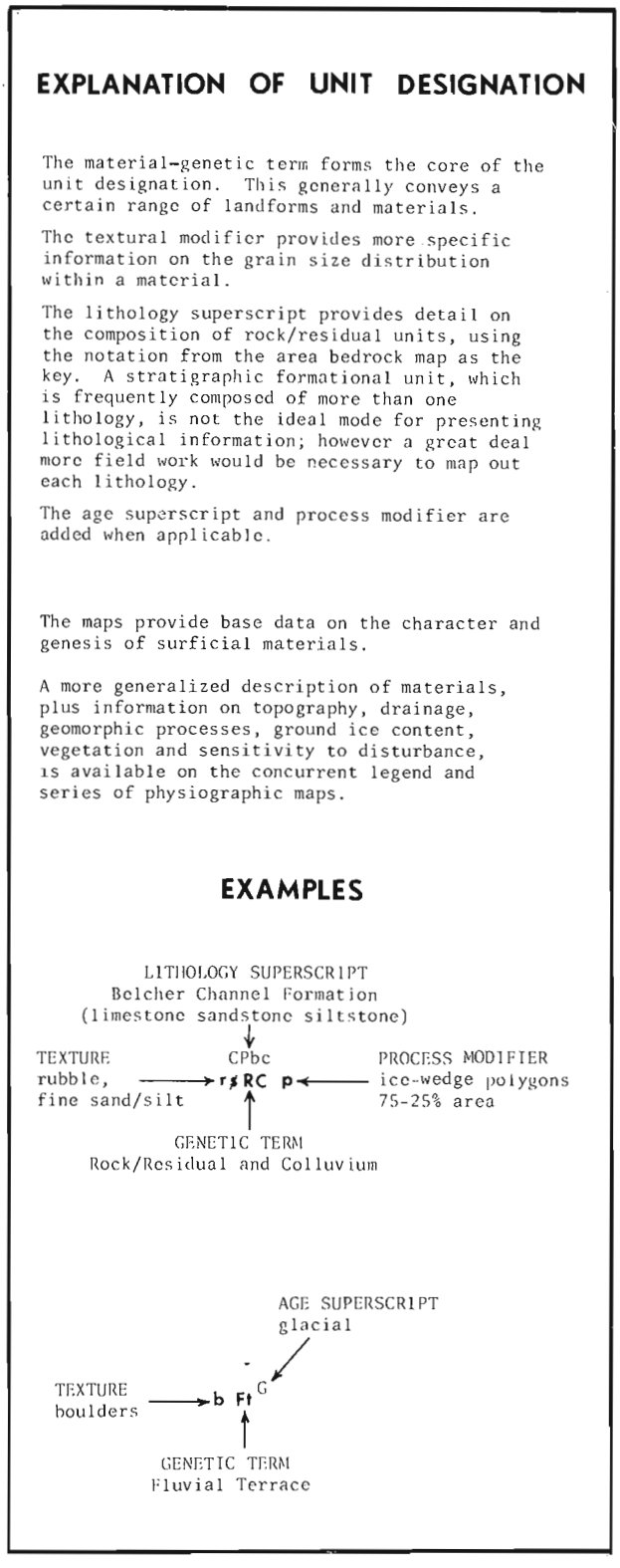

Figure 17.2. Explanation of surficial materials unit designations; panel from surficial materials legend shown as Fig. 17.3.

LEGEND TO ACCOMPANY SURFICIAL MATERIALS MAPS 49 C (Baumann Fiord) AND 59 D (Graham Island)

For explanation of designations see panel in lower left.

Compiled by D.A. Hodgson. Information derived from field work in 1974 with the assistance of A.C. Lord and M.G. Green, and from airphoto interpretation 1974-75.

TEXTURAL MODIFIER

Summary of grain size classes

The textural description of a map-unit is drawn from scattered field observations and occasional laboratory checks of samples, from estimates of the composition of depositional landforms identified on air photographs, and from estimates of the probable weathering products of source rocks.

In many units, materials are composed of more than one grain size class. In this case, classes are combined into a broader group (e.g., fines), or listed in the order of their occurrence.

c clay (<.002 mm)

si silt (.063-.004 mm)

y silt and clay undifferentiated (<.063 mm)

d silt and fine sand, undifferentiated (.25-.004 mm)

f fines: clay, silt and fine sand present in unknown proportions (<.25 mm).

s sand, including fine sand if present (2-.063 mm)

g gravel (2-256 mm) little or no fines

b boulders (>256 mm)

r rubble: angular rock fragments >2mm in size; commonly up to 25% of the total mass is represented by sand or fines either in the fragment interstices, or concentrated locally by frost action.

Note that the character of rubble is dependent on the source rock; e.g., indurated sandstone produces fragments and sand, shale produces platy fragments and silt-clay. Refer to the rock/residual superscript and key to determine the lithology of source rocks.

Rubble on resistant formations often represents a veneer derived from mass-wasting of competent bedrock

o outcrop: exposed bedrock surface little altering by weathering; refer to rock/residual superscript and key to determine lithology

p peat

EXPLANATION OF UNIT DESIGNATION

The material-genetic term forms the core of the unit designation. This generally conveys a

MATERIAL-GENETIC TERM

Identified from air photographs and field observations.

Fp Fluvial plain

Active stream channels and their associated floodplains. There are normally one or two main channels, plus a secondary network of braided channels which contain the excess discharge during snowmelt or following heavy or extended rainfall.

A fluvial plain will only partially reflect the material through which a stream is passing, as the coarser fraction from it is emphasized; it frequently also carries a coarse bedload derived from an upstream source.

Ft Fluvial terrace

Inactive floodplain

Fpt Floodplain and terrace indivisible at the **Ftp** scale of the map.

Ff Fluvial/Alluvial fan

Cone or fan-shaped deposit of stream sediments on land, usually at a point where the gradient abruptly decreases.

Provides a heterogeneous mixture of materials, though with a tendency for grading from coarser to finer from apex to toe.

Fd Fluvial delta

Sediment deposited where a stream enters the sea or a lake. Commonly divisible into coarse topset beds, finer foresets, and fine bottomset beds; i.e., coarse material overlying fine. Fine-grained "St. Elmore" deposits at the margins.

As most deltas in the map-area are adjacent to tidewater, their form has been modified by the (relatively) falling postglacial sea level to provide multiple terraces, in addition to an active braided surface. Deltas with inactive surfaces extensive enough to be mapped as a unit or partial unit, can be identified by the "1" (inactive) superscript.

m Marine plain

Sediments deposited by nearshore marine processes; or re-worked older deposits.

In the map-area, characteristically low surface gradient (<10); dominantly silt to fine sand, deposited in a low energy environment.

A combination of poor drainage and raised-rim ice-wedge troughs often leads to the development of thermokarst ponds.

mv Marine veneer

Veneer of marine deposits <1 m thick. Often derived from underlying material rather than being transported from elsewhere on the coast.

Thermokarst ponds less frequent than on a marine plain.

mb Marine beaches

Flights of well-developed ridges and swales, raised by postglacial isostatic uplift. Commonly found where higher energy conditions exist (e.g., headlands), and where a source of coarse material is available.

Ridges are normally sand or gravel, 0.5 to 1.5 m high; swales are underlain by a finer fraction with a thin veneer of organic material.

M Moraine

ROCK/RESIDUAL LITHOLOGY SUPERSCRIPT

Descriptions of the bedrock are based mainly on members, formations and groups described by Greiner (1963), Kerr (1968a, 1968b), Kerr and Thorsteinsson (1971), Thorsteinsson (1974) and Tozer (1963). Typical weathering products in the bedrock units were examined in the field in 1974.

If more than one weathering product is listed, the finer fraction will generally be more in evidence on gentle slopes than on steep slopes.

Kle Eureka Sound Formation

Siltstone, sandstone, shale, minor conglomerate and coal. Poorly cemented and readily eroded.

Weathers to loose silt and sand, clay, minor gravel. Develops "badland" topography.

K Cretaceous, undifferentiated, on Graham Island

Little areal information available (see Greiner, 1963). The island is underlain by Kanguk, Hassel, and possibly Christopher Formations, of Cretaceous age.

For the purposes of surficial mapping, the following lithologies are recognized:

K1 (Kanguk). Shale; fissile, minor siltstone, diabase dykes. Weathers to small platy fragments and fines (mainly silt). May include areas of K3.

K2 (Kanguk-Hassel?). Siltstone; shale, fine-grained sandstone. Weathers to silt, fine sand, and minor clay.

K3 (Kanguk?). Shale; fused by combustion. Weathers to lightweight, white-grey-pink-red blocks and platy fragments.

K4 (Hassel?). Sandstone; friable fine- to medium-grained; minor silt-stone shale. Weathers to sand, silt, minor rubble.

Kl Isachsen Formation

Medium-bedded to massive and commonly cross-bedded quartzose sandstones, fine to coarse-grained. Minor shale beds.

Generally poorly cemented, and exposed as a loose sand. Easily gullied, especially in moderate to strong relief.

J Jurassic (undivided Awingak and Sverdrup Formations)

Sandstone, siltstone and shale. Generally friable, some indurated beds.

Weathers to silt, sand and log rubble.

Kh Heiberg Formation

Succession of sandstone, siltstone, with minor shale, especially near the base. Generally friable, some indurated beds.

Weathers to sand, silt, fine sand, sandstone/siltstone fragments, with minor clay. Where beds are moderately to strongly dipping, differential weathering and erosion leads to a succession of minor and major scarps.

The formation is less resistant to weathering than the Triassic formations below.

Ks Schei Point Formation

Calcareous siltstone and sandstone, shale, and minor limestone. Generally friable, some indurated beds.

Weathers to silt, sand and sandstone fragments. Differential weathering and erosion as with the Heiberg Formation.

Tb Bjorne Formation

Quartzose sandstone, grey to orange, red weathering; minor siltstone clay and conglomerate ranges from well-cemented to poorly-cemented.

Dobl$_{1b}$ Okse Bay Formation: Lower Sandstone Member-upper beds

Quartz sandstone, massive to thick-bedded, well cemented, yellow to orange weathering.

Weathers to boulders and rubble.

Dobl$_{1a}$ Okse Bay Formation: Lower Sandstone Member-lower beds

Quartz sandstone (as above) and recessive red shale beds.

Weathers to rubble and fines.

Dob Okse Bay Formation (undivided)

Dbi$_2$ Bird Fiord Formation: Upper Member

Quartz sandstone, partially calcareous.

Weathers to rubble

Dbi$_1$ Bird Fiord Formation: Lower Member

Limestone, shale, sandstone

Weathers to rubble and fine sand, silt

Dbl$_2$ Blue Fiord Formation: Brown Limestone Member

Limestone, medium- to thick-bedded.

Weathers to rubble.

Dbl$_1$ Blue Fiord Formation: Limestone and Shale Member

Light grey limestone and recessive calcareous shale.

Weathers to rubble and silt.

De Eids Formation

Shale, siltstone, minor limestone, gypsum. Poorly consolidated and very fissile, to unconsolidated.

Weathers to silt-clay, minor platy siltstone and shale fragments.

Slopes and stream channels adjacent to quartz members, other resistant formation, or pre-glacial gravel deposits may have up to 50% rubble or gravel incorporated in the active layer. Hashed areas include a discontinuous veneer of gravel. Presence of scattered erratic boulders indicates discontinuous morainal deposits.

De$_1$ Eids Formation: Quartz Sandstone Member

Resistant sandstone; weathers to rubble.

Dcp Cape Phillips Formation

Shale, siltstone, minor limestone. Dark, fissile to thin-bedded.

Weathers to fines and platy fragments.

Oao Allen Bay Formation

Very resistant dolomite, minor limestone, shale.

Weathers to rubble, minor fines.

Oci Irene Bay Formation

Limestone, shaly interlayers; thin-bedded

AGE SUPERSCRIPT

A Active forming processes

e.g., Fd^A deltaic sediments currently being deposited.

I Inactive forming processes

e.g., Fd^I delta forming processes inactive.

G Glacial: forming processes associated with an ice mass, not currently active unless specified.

Non-morainal supra-, intra-, sub-, and pro-glacial deposits.

Usually applied to fluvial processes. e.g., Ft^G glacial fluvial terrace.

As late-glacial conditions produced larger volumes of water and higher energy conditions than exist at present, deposits are normally coarser and more extensive than Holocene fluvial deposits.

Where terms are used in combination, the leading letter is dominant.

PROCESS MODIFIER

Identifies important processes which may modify the texture and form of materials.

If a modifier is added, then the process affects >75% of the unit.

If a bar (-) is placed over the modifier, then 25% to 75% of the unit is affected.

p Ice wedges

Ice-wedge polygon troughs identified from air photographs or in the field, indicating a substantial volume of surficial material (ca. 10-20% in the upper 2m) is wedge ice.

Not all polygon areas have been identified, as a large ice wedge may have only a weak surface expression.

k Thermokarst

Local depression of the ground surface following thawing of ground ice. Mainly on the marine plains, which now have a close pattern of small ponds. The ponds could also occupy poorly-drained depressed-centre polygons. The ponds are floored by a thin veneer of fines and organics.

pk Ice-wedge troughs + thermokarst melting, thaw ponds.

Wedges over which greater than average amount of thawing has taken place, resulting in deep (>1m) broad troughs, often containing standing water for at least part of the summer.

Figure 17.3. Part of surficial materials legend for map-areas NTS 49 C and 59 D.

GROUP/UNIT[1]	MATERIALS DESIGNATOR[2]	TOPOGRAPHY, LANDFORM GENESIS[3]	DRAINAGE, ACTIVE LAYER PROCESSES AND MICRORELIEF	SURFICIAL MATERIAL[4]	GROUND ICE[5]	VEGETATION[6]	SENSITIVITY[7]	TRAFFICABILITY[8]
							Magnitude Form	Roughness Traction
8 Baumann Fiord	Mainly: r, rb $^{Dob}_{RC}$ r,rf $^{Dob}_{3,4*RC}$ f, r $^{Dob}_{2*}$ RC, CR Minor: b, g $^{G}_{Fp}$ I	Altitude: 0-3600' (0-110 m) Hilly to rolling upland, mainly long slopes (to 10 km) at 2-10°. Greatest elevations are to the south, where the 'Holtedahl Ice Cap' is superimposed on the highland. The E half of the group is dissected by steep-sided, north flowing valleys. The same valley lineation is apparent in the W, but rivers are tributary to a broad NE trending valley. Residual weathered bedrock, lesser colluvium, local glacio-fluvial sediments, are underlain by a series of clastic rocks folded into a broad E-W trending syncline. The more resistant beds (quartz sandstone) have to more rugged relief, the recessive shales are more subdued.	Drainage good on coarse-grained materials and outcrop, via unconfined seepage. Drainage fair on finer materials, poor on flats or gentle slopes, via seepage lines (sorted and nonsorted stripes). Solifluction processes very evident. Stripes, solifluction lobes on all except wholly rubble slopes. Lobes of large dimensions common (toe heights to 4 m). Ice-wedge polygons rare, or have indiscernible surface expression, except on coarse fluvioglacial deposits. Active layer depth maximum 20-60 cm, or higher in rubble.	Material varies from coarse grained (boulders, gravel) residual weathered mantle on resistant beds, to fine-grained colluvium and weathered mantle on recessive beds. Group is mainly underlain by a succession of argillaceous sandstones, shales, siltstones, mudstones. Mainly resistant beds under 8.1, recessive under 8.2. Massive quartzose sandstones in the SW, weather to blocks from which boulders to gravel-size glaciofluvial material derived. Fluvial deposits mainly gravel, sand.	No observations of ground ice, however segregated ice expected in rubble interstices. Segregated ice also predicted in thick residual weathered bedrock and colluvial deposits which contain appreciable quantities of fines. Ice-wedge polygons discontinuous, except general in very coarse fluvioglacial deposits (8.5).	Substantial areas of this region, both bedrock and active fluvial areas, are devoid of vegetation. Saxifrage based communities are common on this region, on dry sorted sands and dry gravels. On boulder fields, a Rhacomitrium-Alectoria community is common in the interstices of the boulders. Crustose lichens are often found on the exposed faces. Localized mesic gravels carry a Dryas-Salix vegetation with a Carex-Eriophorum marsh vegetation in seepage zones and in areas where ponding occurs.	1-2 variable	2-3 - Roughness difficult-mainly steep grades especially on rock scarps; boulder size material.
8.1	r, rfo, rf $^{Dob}_{1,2*RC}$	0-3000' (0-910 m) E-W chain of hills, broken by deep N-S valleys. Slopes 1-10°, but steeper to deep valleys. Slopes broken by outcropping rock ledges, and by gully-like rock-cut glacial drainage channels. Residual weathered bedrock, lesser colluvium, minor outcrop; underlain by quartz sandstone, siltstone, shale. More resistant than 8.2.	See 8. Drainage moderate to good, on predominantly coarse-grained materials; poor on fine-grained slope segments overlying recessive beds.	Sandstone rubble and boulders over 50% of unit. Minor sand fines, outcrop. Residual weathered mantle, lesser colluvium, underlain by quartz sandstone, siltstone, shale.	See 8.	Most of the area is devoid of vegetation,* especially at the highest elevations. Sorted materials Fine sands: <1% Luzula-Saxifrage barrens. Papaver Draba and Cryophyllaceae occasional. Interstices of boulders: 10-20% (locally to 50%) Rhacomitrium-Alectoria barrens. Cetraria, Thamnolia, Peltigera, Cladonia, Dactylina, and Polytrichum sp. present. Boulder faces: Crustose lichens (To 75% on exposed localized gravelly moraine). dry: <5% Saxifraga-Luzula barrens, with occasional dwarf shrub component. mesic: 5-25% Dryas-Salix barrens. Lower stratum of moss and patina may be present locally to 75%. Luzula nivalis and Carex nardina tussocks frequently occur. Local snowbeds: Cassiope and Rhacomitrium, locally dense.	1 C*	2 2/1
8.2	fr, fro $^{Dob}_{2,3*RC, CR}$	0-3000' (0-910 m) Slopes and low hills of finer-grained, more recessive deposits than adjacent unit 8.1. Slopes 1-10°, less rugged than 8.1, except where bedrock outcrops. Weathered mantle and colluvium, minor outcrop; underlain by shale, siltstone, sandstone.	See 8. Drainage moderate to poor, on predominantly fine-grained materials.	Silt, clay, fine sand; minor gravel, rubble, outcrop. Residual weathered mantle and colluvium underlain by a succession of argillaceous sandstones, shale, siltstone, mudstone. Mainly recessive beds.	See 8. Note segregated ice probable as appreciable fines present.	Sorted boulder, cobbles and fines:* boulders: crustose lichens may be present to 75%. interstices of boulders: 10-50% Rhacomitrium-Alectoria barrens. fines: <5% Saxifraga oppositifolia barrens. Localized fine grained veneer: dry: <5% Saxifraga oppositifolia barrens. mesic: 5-20% Salix-Dryas (* Carex nardina) to 70% moss-patina saturated: 10% Alopecurus-Carex stans (* Salix) 75% moss	2 A*B*C*	2 3/2
8.3	rb, r $^{Dob}_{m}$ R	0-3600' (0-1100m) Mountain massif trending E-W, divided into a series of N-S ridges by narrow steep-sided valleys. Underlain by massive quartzose sandstone, weathered to blocks. Dissected by systems of close-spaced steep-sided glacial drainage channels, except for the tops and S-facing slopes.	No organized postglacial drainage systems. Seepage through block interstices to channel floors i.e. drainage excellent.	Quartzose sandstone, gravel to boulder size, underlain by same sandstone. Local areas of gravel to boulder size material, minor sand, morainal deposits.	See 8. Coarse-textured deposits	Sorted boulders and fines:* boulders: crustose lichens (to 75% of exposed faces) interstices: 10-40% Rhacomitrium-Alectoria barrens. fines: <5% Saxifraga-Luzula barrens (localized).	1	3 1/1
8.4	r, rf $^{Dob}_{RC}$	1200-3000' (370-910 m) Hills and ridges, divided by steep-walled glacially-modified valleys. Adjacent to 8.3, but underlain by less resistant clastics and carbonates, mantled with residual weathering products and colluvium.	See 8. Drainage moderate to good, on predominantly coarse materials	Rubble, gravel; minor fines, outcrop. Residual weathered mantle and colluvium underlain by sandstone, limestone, shale.	See 8. Mainly coarse-textured deposits.	<1% Saxifraga oppositifolia barrens.*	1	3 2/1
8.5	b, g $^{G}_{Fp}$	100-200' (300-610 m) Flat to gently sloping surface (<2°), steepening adjacent to 8.3. Glaciofluvial deposits derived from and underlain by unit 8.3, and to a lesser degree, 8.4.	See 8.3 for drainage. Areas with boulder/block (but not gravel) cover have a network of ice-wedge polygons, with troughs 1-2 m broad, to 1 m deep.	Quartz sandstone blocks, 10-50 cm diameter, adjacent to 8.3. Limestone and sandstone gravel adjacent to 8.4 Depth to competent bedrock unknown.	See 8. Ice-wedges general in boulder/block size deposits.	faces of boulders: crustose lichens to 90% of exposed faces. Rinodina, Parmelia and Umbilicaria species present. Interstices of boulders: (rare) Alectoria-Rhacomitrium barrens.	1 B*	2-3 1/1
8.6	f g $^{Dob}_{1,2(3)}$	0-400' (0-120 m) Low rolling, slopes 0-5°, exceptionally 15°. Marine colluvium and recessive weathered bedrock.	Drainage moderate to poor. Seepage lines (sorted and nonsorted stripes), shallow gullying where slopes >2°. Solifluction general. Local dessication cracks/hummocks. Rare flowslides. Ice-wedge polygon networks discontinuous.	Silt and clay; minor gravel, rubble. Marine reworked colluvium and residual weathered mantle, 1-3 m thick, overlying siltstone, shale, sandstone.	See 8. Note segregated ice probably widespread. Ice-wedge polygons discontinuous.	Exposed bedrock: <5% Saxifraga oppositifolia-Luzula nivalis barrens. Silty veneer: mesic: 10% Salix arctica-Carex nardina * 75% moss-patina Polygonum, Potentilla, Dryas frequently present. seepage zones: 10-20% Carex stans-Eriophorus (* Salix) 90% moss (hummocks) Alopecurus, Arctagrostis, Dupontia frequently present.	3 A B C	1 3/2
8.7	gfM & fr CR	800-1200' (240-370 m) Low rolling morainal deposits and colluvium. Dissected adjacent to main river.	See 8.1.	Sandstone gravel, minor fines: in morainal deposits and colluvium.	See 8.	faces of boulders: crustose lichens (to 90% of exposed faces) interstices of boulders: Rhacomitrium-Alectoria barrens. fines: Sparse Saxifraga oppositifolia barrens.	2 A B C	2 3/2
8.8	g, a F	0-800' (0-240 m) Braided fluvial floodplains and terraces, sufficiently extensive to be mapped separately. Inter-terrace bluffs 1-10 m in height.	Well drained terraces. Ice-wedge polygons on inactive surfaces.	Mainly gravel, lesser sand; minor silt in slack-water zones.	Ice-wedge polygon on inactive surfaces.	Active fluvial surfaces are devoid of vegetation.* on fine sands, 10% Puccinellia tussocks occasionally occur.	1 B*	1-2 1/1
8.9	I	1400-3600'(430-1100 m) Glacial ice. Mainly glacier tongues on N side of 'Holtedahl Ice Cap', plus scattered smaller caps. Glacier gradients ca. 3°, but steeper at margins, where parabolic profile may reach the vertical at the base.	Supra-glacial drainage by narrow vertically-sided channels to 10 m deep. Crevasses rare. Shear moraines locally thrust above ice surface.	Ice, snow, very local rubble at margins.		Devoid of vegetation.*	- -	1-3

Figure 17.4. Biophysical regions legend for group no. 8, Baumann Fiord (NTS 49 C).

Biophysical Regions

Map-units based on surficial materials, topography, drainage characteristics, and vegetation serve as a framework for an interpretative legend. The system has two tiers: groups of units or regions identified by whole numbers and described in the first entry in each legend panel (Fig. 17.4); the individual 'biophysical' units identified by decimal fractions after the group number. Though assembly of units and groups of units is based on an appreciation of land attributes, these units are regarded as essentially a convenience for handling data; the regional boundaries, in particular, should not be thought of as enclosing 'natural' geographical areas, other than perhaps at a broad reconnaissance scale. Extreme diversity of land attributes may occur within regions, and where gradational changes occur or data is sparse, regional boundaries may be somewhat arbitrary. As already noted, surficial materials was one of the main criteria used in defining units, and thus biophysical and materials boundaries commonly coincide (Fig. 17.1).

As well as descriptions of significant landscape attributes (prose can be more informative than an inadequate number of quantitative values for complex areas), semiquantitative ratings for 'sensitivity' and 'trafficability' are provided for each unit. Sensitivity is considered to be the susceptibility of an area to disturbance, where disturbance is a man-initiated change in surface characteristics. Ratings for magnitude (probability of disturbance occurring and the degree to which it occurs) and the probable form which disturbance will take are given. Trafficability is an assessment of terrain in terms of performance of Arctic tracked vehicles. Ratings for surface roughness and traction are given.

Summary

A variant of the basic T.S. Quaternary mapping system has proved workable for reconnaissance mapping of surficial materials in the High Arctic and as a source of geotechnical information. The mnemonic alphabetic notation is useful both in compiling and in using the map; other geotechnical parameters (e.g., U.S.C.S.) can be added. If this notation becomes too unwieldy for machine processing, then designations can be encoded as ciphers. This system is not, however, suitable for recording complex attributes such as morphology, poorly defined parameters such as ground ice, or site-specific information such as soil bearing ratios, ground ice content as recorded in cores, etc. A second system of units therefore has been adopted complementing materials maps, which is partly derived from surficial materials and partly using other landscape attributes. The finite number of units, with numeric labels, is keyed to a descriptive and interpretative legend. This second series, which has similarities with the landscape or integrated approach, is regarded as a temporary solution until either an alternative more systematic scheme is devised, or sufficient data is assembled for a parametric approach to be used. The latter approach seems preferable in place of both biophysical and surficial materials maps; it does not require fusing of complexly related, or even unrelated, parameters into units.

Acknowledgment

Information on vegetation and concomitant advice on boundaries of biophysical units has been provided by S.A. Edlund.

References

Barnett, D.M., Edlund, S.A., and Dredge, L.A.
1975: Interdisciplinary environmental data presentation for eastern Melville Island: an approach; *in* Report of Activities, Pt. B, Geol. Surv. Can., Paper 75-1B, p. 105-107.

Fulton, R.J., Boydell, A.N., Barnett, D.M., Hodgson, D.A., and Rampton, V.N.
1974: Terrain mapping in northern environments; *in* Canada's Northlands: proceedings of technical workshop to develop an integrated approach to base data inventories for Canada's Northlands; April 17-19, 1974, Toronto, Lands Directorate, Environment Canada, p. 16-60.

Fulton, R.J., Hodgson, D.A., and Minning, G.V.
1975: Inventory of Quaternary geology, southern Labrador: an example of Quaternary geology – terrain studies in undeveloped areas; Geol. Surv. Can., Paper 74-46, 14 p.

Hodgson, D.A.
1975: Surficial geology, geomorphology, and terrain disturbance, central Ellesmere Island (49 C, D, E, F, 59 D); *in* Report of Activities, Pt. A, Geol. Surv. Can., Paper 75-1A, p. 411.

Hodgson, D.A. and Edlund, S.A.
1975: Surficial materials and biophysical regions, eastern Queen Elizabeth Islands: Part I; Geol. Surv. Can., Open File 265.

Mabbutt, J.A.
1968: Review of concepts of land classification; *in* Land Evaluation, ed. G.A. Stewart, Melbourne, Macmillan, p. 11-28.

18. INTERPRETATION OF SEISMIC SHOTHOLE DATA FROM WESTERN BANKS ISLAND, DISTRICT OF FRANKLIN

Project 740065

C. M. Tucker
Terrain Sciences Division

Introduction

As a continuation of the Banks Island Surficial Deposits Inventory Mapping Project (Vincent *et al.*, 1975), during February 1975 efforts were made in conjunction with Elf Oil Exploration and Production Canada, Ltd. to obtain detailed textural and stratigraphic information in surficial unconsolidated deposits along the west coast of the island from Sea Otter Harbour to Lennie River (Fig. 18.1). Elf Oil planned seismic operations covering a distance of 177 km of line at a density of 600 per cent (6 shotpoints per 1.6 km, 268 m apart). Normally seismic programs do not record shothole stratigraphy, thus the opportunity to acquire subsurface data for the western lowlands of Banks Island was invaluable since the surface is blanketed with an undetermined thickness of glacial material and solifluction debris, and exposures are scarce. It also presented

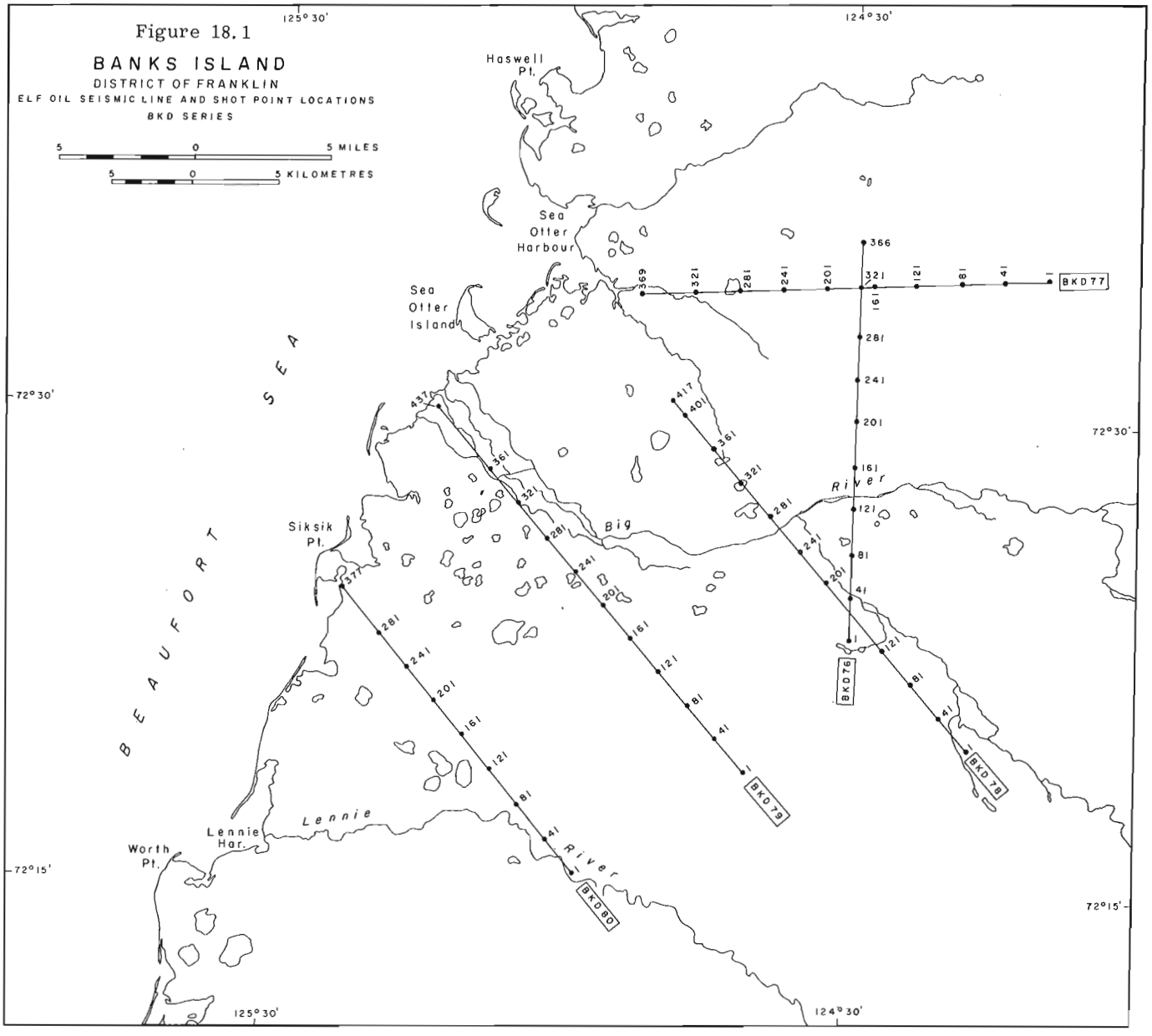

Figure 18. 2. Flextrac Nodwell with Gardner-Denver air drill.

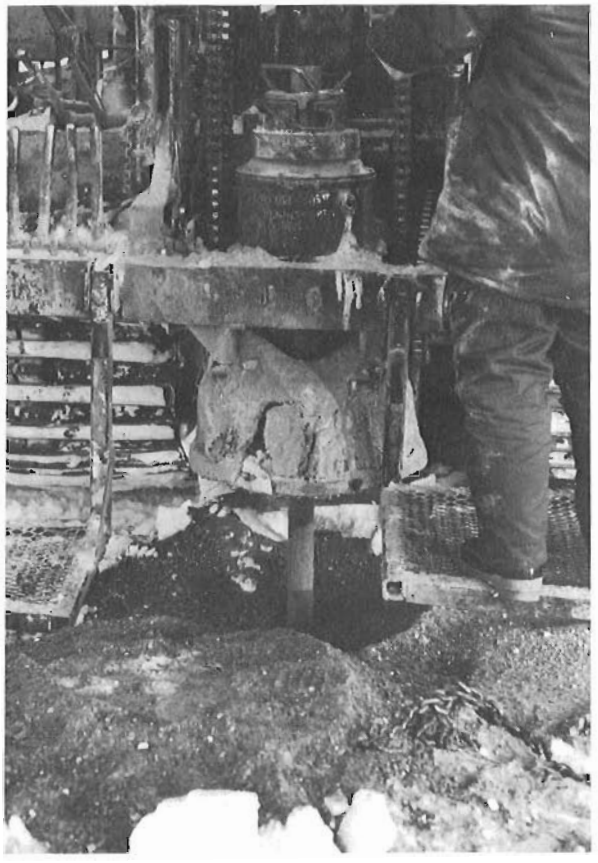

Figure 18. 3. Drill stem, apron, and rotary table.

an opportunity to enter and collect information from Banks Island Migratory Bird Sanctuary No. 1 which is closed for a large portion of the summer field season.

During a similar project in the winter and spring of 1973-1974 samples were obtained from various seismic operations on Banks Island and were shipped frozen to the Institute of Sedimentary and Petroleum Geology in Calgary for detailed laboratory work.

For 1975, it was hoped that by directly involving a member of the Banks Island Surficial Mapping Project, who was familiar with the surface materials, and by increasing the degree of sample interpretation at the drill site, a saving could be realized both in manpower and time.

Procedure

A Gardner Denver air drill mounted on a Flextrac Nodwell was used (Fig. 18. 2). Holes were bored to a depth of 27. 4 m using 4. 6 m sections of stem. Depending on terrain and drilling conditions, holes were completed in 30 to 60 minutes each. Since the Elf operation used seven drill rigs, it meant that ideally one person could log holes and collect samples at approximately 1. 8-km intervals. The field method involved observing drill cuttings for colour or textural variations and recording the stem depth to the nearest 0. 3 m. Cuttings were retrieved as significant changes occurred or as anomalous material appeared, rather than at specific intervals. To minimize the risk of contamination, samples were collected from just below the stem apron (Fig. 18. 3), before being deflected to the ground by uphole air pressure. They were packaged in 0. 5-litre waxed containers and were labelled. Representative frozen samples later were put in polyethylene sample bags and vacuum sealed for future detailed laboratory analysis.

From an interpretative standpoint, there are several shortcomings to the procedure. Since no core is obtained, information must be acquired from disturbed cuttings. Coarser sediments tend to be pulverized by the drill bit and the original texture commonly is altered. Well rounded fluvial gravels are recovered as angular fragments with rounded individual faces. More important is the risk of contamination from caving and infilling. For example, if the drill goes from a coarse, well sorted gravel to a pure, fine to medium sand, there is a chance that pebbles from the overlying material will be incorporated in the cuttings as they are blown out of the hole. Similarly, unless the perimeter of the drill site is kept clean, there is a danger of old cuttings re-entering the hole and contaminating fresh bottom-hole sediment. The risk of incorrect interpretation can be minimized by inspecting the frozen cuttings to ensure that they incorporate pebbles with texture and lithology

similar to the loose material. A third weakness of the procedure is that the original moisture content of materials is not always preserved. If the drill has been cutting through a hard, well sorted gravel for an extended period, the bit and lower stem tend to heat up. Any fine sediments with a high water content that immediately underlie it may be ejected in a semi-liquid state or with water covering the cuttings. Assuming that this is the only point at which moisture content may be modified, the loss can be reduced if samples are collected below the first few centimetres of penetration into the finer material.

For detailed bedrock information, the reader is referred to Miall (1974). Till on the western lowlands of Banks Island is generally Beaufort-derived; L.V. Hills (pers. comm.) states that it may be readily identified by the presence of carbonates, granite, or diabase. Texturally it need not vary greatly from its source material. Colluvium was distinguished on the basis of local situation, degree of sorting, and an increase in the content of fragmented peat.

Results

Since much of the data obtained from Elf Oil remains confidential, only general observations will be outlined in this report. Detailed stratigraphic profiles are being constructed from the shothole data and elevations are being recorded to the nearest 0.01 m by Elf Oil; results will be documented in future publications.

Line BKD 76

Generally, the drill points crossing Big River Plain (S.P. 50 to 125) show sequences of well sorted, brown-grey, Beaufort-derived alluvial gravels containing light to dark grey cherty and quartzite pebbles up to 2 cm in diameter. Shotpoints 161-205 cross an area of undulating terrain with westerly oriented meltwater channels. The line runs parallel to and about 3 km west of what may have been a pre-late Wisconsinan ice stand (Fyles, 1962), which can be readily identified by a change in meltwater channel orientation and north-south trending morainal ridges. Till up to 3 m thick overlies grey quartzite Beaufort gravels and Eureka Sound sediments (Miall, 1974) that appear to have been glacially reworked some time prior to the last glaciation. The Eureka Sound material consists of medium to dark grey shaly-silty clay, interbedded with light grey quartzose silts, fine sands, and quartzite granules. Till is Beaufort-derived and of a grey, silty, sandy gravel composition with subangular pebbles and fragments of light and dark grey quartzites, minor cherts, and diabase. From shotpoints 241 to 349, till increases in thickness (up to 9 m) and overlies glacially reworked Eureka Sound silts and clays.

Line BKD 77

Shotpoints 1 to 165 are similar; all contain 2 to 9 m of light grey-brown silty, gravelly till with light and dark grey quartzite granules and pebbles as well as varying percentages of peat. This is underlain by thin Beaufort gravels and reworked Eureka Sound material. At the cross point of lines BKD 77 (S.P. 165) and BKD 76 (S.P. 317), till up to 8 m thick overlies a band of light brown, very fine sand and silt, 2 to 4 m thick, which in turn overlies alternating sequences of grey Eureka Sound clays, silts, and quartzite gravel lenses. The light brown silts are anomalous and possibly indicate ice-contact deposits or minor glaciolacustrine ponding at some stage. From S.P. 165 to 341 till cover thins to the west and is <2 m thick at S.P. 321.

Line BKD 78

Shotpoints 413 to 345 are located on hummocky terrain 30 to 64 m a.s.l. The general stratigraphy includes up to 1.5 m of grey sandy colluvium with chert and quartzite fragments. This overlies about 15 m of Beaufort-derived till, which in turn covers Beaufort sands and gravels. Between S.P. 325 and 285 near the northwestern escarpment of Big River, till thins out and drill cuttings consist of reworked Beaufort silts, sands, and gravel covering distorted Eureka Sound dark grey silts, gravel lenses, and woody peat. Shotpoints 261 to 209 contain alluvial gravels over reworked Eureka Sound sediments. Discontinuous lenses of compact dark brown woody peat <0.5 m thick occur at depths of 26 to 27 m; these belong to the Eureka Sound Formation. From S.P. 209 to the southeastern termination of BKD 78, the surface is covered by up to 10 m of colluvium and grey-brown silty till with quartzite and cherty granules as well as varying percentages of peat. The till covers at least 20 m of Eureka Sound sediment.

Line BKD 79

The northwestern end of BKD 79 is located on the present flood plain at the mouth of Big River. A general sequence of materials from S.P. 353 to 281, which are located on an abandoned thermokarst modified flood plain, includes <1.5 m of grey-brown sandy sediment with quartzite granules and peat overlying Beaufort-derived alluvium. As elevations increase near S.P. 241, the stratigraphy changes to coarse gravelly till with salt and pepper, medium to coarse grained sand and silt, pebbles of rounded quartzites, diabase, and limestone, with some peat. Over 16 m of Beaufort gravels underlie the till. From S.P. 169 to 149 till is similar to that previously described, except that it is slightly siltier, reflecting the underlying grey shaly silts and dark quartzite gravel lenses. From S.P. 113 to 61 delineation of formation boundaries is difficult since bedrock structure varies considerably from one shotpoint to the next. The holes contain reworked medium grey Eureka Sound shales and silt interbedded with Beaufort sands and gravels. Till thickens at the southeastern end of line BKD 79 to a total of 23 m at S.P. 13.

Line BKD 80

Materials sampled on line BKD 80 are similar to those of the southern half of line BKD 79. Thin veneers

(∿2 to 6 m) of silty Beaufort-derived till overlie Beaufort sands and gravels. At S.P. 89, located near the top of a northeast-southwest trending ridge, 3 m of light brown silty-sandy till and 13.5 m of reworked Beaufort sands, quartzite pebbles, and minor wood fragments cover an unknown thickness of very fine brown silts and quartzose sands. The genesis of the silt has not been determined because caving prevented further penetration. Near Lennie River (S.P. 65 to 45) thin veneers of silty till cover Beaufort sands and fine, well sorted gravels.

Conclusions

Results show that till cover on western Banks Island is patchy and in many cases difficult to separate from its source material. It is generally thickest as a residue on ridge crests and is underlain by varying depths of glacially disturbed Beaufort gravels as well as Eureka Sound clays and silts.

The 1975 Elf seismic program on Banks Island indicates that such operations provide an excellent opportunity to obtain subsurface data from areas that, for various reasons, lack suitable exposures. Since major expenses for a seismic operation are established prior to start-up, the added cost of obtaining shothole samples and stratigraphy is minimal and worthwhile.

Acknowledgments

The author would like to thank the following for their help and advice: Dr. H. Evers, Elf Oil Exploration and Production Canada Ltd., Calgary, Alberta, and Dr. L.V. Hills, Dept. of Geology, University of Calgary, Calgary, Alberta.

References

Fyles, J.G.
1962: Physiography; *in* Banks, Victoria, and Stefansson Islands, Arctic Archipelago, ed. R. Thorsteinsson and E.T. Tozer; Geol. Surv. Can., Mem. 330, p. 8-17.

Miall, A.D.
1974: Subsurface geology of western Banks Island; *in* Report of Activities, Pt. B, Geol. Surv. Can., Paper 74-1B, p. 278-281.

Vincent, J-S., Tucker, C.M., and Edlund, S.A.
1975: Surficial geology inventory, Banks Island, District of Franklin; *in* Report of Activities, Pt. A, Geol. Surv. Can., Paper 75-1A, p. 431-434.

19. DEPOSITIONAL SETTING OF THE MEGUMA GROUP, NOVA SCOTIA

Project 730083

I. M. Harris
Atlantic Geoscience Centre, Dartmouth

This report presents an interpretation of the sedimentology of the Lower Paleozoic Meguma Group of Nova Scotia, based on the results of recent field work (Harris, 1975) and previous studies by Schenk (1970, 1973) and Harris (1971). These authors (Harris and Schenk, 1975) have incorporated the account that follows in a field manual prepared for the 1975 field trip of the Eastern Section, S. E. P. M. The general geology of the Meguma outcrop area and the conclusions of earlier workers regarding the sedimentology of the Meguma Group are summarized in the abovementioned articles, and are not repeated here.

The Meguma Group comprises two conformable and partly coeval formations. The lower, the Goldenville Formation, consists of alternating layers of greywacke-sandstone and finer grained beds having the characteristics of sandy flysch, and the upper, the Halifax Formation, consists of slate, siltstone and minor sandstone with both distal turbidite and non-turbidite characteristics. The thickness of the Goldenville Formation is unknown because the base is nowhere exposed; the greatest thickness recorded is 5600 m (Faribault, 1914). The Halifax Formation is about 4400 m thick in the northwest and thins to 500 m in the south (Taylor, 1967).

The salient sedimentary characteristics of the Meguma Group are as follows: (1) The Goldenville Formation comprises sandy flysch, as noted above. The Halifax Formation is composed of several facies of dominantly fine grained sediments, of which shaly flysch is probably predominant. The shaly flysch is distinguished from other facies of the Halifax Formation by the preponderance of beds displaying the Bouma sequence of structures, mainly CDE and BCDE. (2) Graded bedding is generally weakly developed in the thick sandstone beds that make up much of the Goldenville Formation. However, a few of the thick beds display excellent, continuous grading. Normally, grading is restricted to the upper few centimetres of sandstone beds; the main part of the bed typically has a uniform distribution of grain sizes, and generally either is structureless or has diffuse parallel lamination. This lamination is distinct from the sharply defined, planar lamination that occurs towards the tops of many beds (i. e., the Bouma B division). The Bouma C, ripple-laminated division is widely developed in parts of the Halifax Formation and in relatively thin beds of the Goldenville Formation, but is generally restricted in development or missing altogether in the upper portions of thick sandstone beds. (3) Lenses and layers of conglomeratic material occur in some beds mainly composed of sandstone, particularly in the lower parts of the beds. Beds made up entirely of conglomerate or conglomeratic sandstone are rare. (4) Intraformational clasts (mudstone-siltstone rip-ups) are components of many of the Goldenville beds. They occur preferentially in thick beds, and probably were derived from the undercutting of channel walls. (5) Groove markings are abundant on the undersurfaces of beds in the Goldenville Formation, but are relatively uncommon in the Halifax Formation. (6) Flutes are especially abundant in the transitional zone between Goldenville and Halifax lithosomes (where the sand/shale ratio is close to unity), and are common but less abundant than grooves in the Goldenville sandy flysch. (7) Channels that eroded up to four metres into the pre-existing layers are evident at many outcrops. Larger channels, although present, are generally too large for their whole shape to be viewed in outcrop. (8) Load structures are very abundant in the Goldenville Formation. Many are associated with asymmetrical flame structures formed by sand foundering into fine grained material during the deposition of the bed. Load-balls (pseudonodules) are locally well developed in the shaly flysch of the Halifax Formation. (9) Fluid-escape structures are abundant. These include sand volcanoes at upper bedding surfaces and vertical pillar structures within sandstone beds. (10) Trace fossils are present at many outcrops, but generally not in great numbers. Vertical shafts, some twinned (presumably U-tubes), are the most visible biogenic structures in the Halifax Formation, and the trails of organisms are conspicuous at the base of some sandstone beds in the Goldenville Formation. A small proportion of the sand volcanoes and vertical pillar structures may have been produced by organisms.

Schenk (1970) used a 3- by 4-km grid as a guide for selecting outcrops throughout the Meguma area, at which he collected sedimentologic data. These data provided the basis for an evaluation of the regional variations of directional, textural, and compositional properties, illustrated by trend-surface and moving-average maps. Analyses of directional measurements of current structures at each outcrop indicate that the paleocurrent trend is axial, and turns 90 degrees from due north in the southwest to due east in the eastern part of the area. This paleocurrent pattern persists through all horizons of the Meguma. The paleocurrent trend appears to "contour" the scalar properties — i. e., currents trend along, not across contours of such properties as grain size, layer thickness, per cent lithic clasts, etc. Stated another way, the paleocurrent trend is almost at right angles to the dispersal direction inferred from the lateral variations in sandstone grain-size and composition, maximum and average bed thickness, and other sedimentologic properties. To explain these characteristics of Meguma sedimentation, Schenk proposed that the sediments were moved into the area mainly by turbidity currents, slump and creep, but were reworked by contour-following bottom currents that flowed northwards in the southwestern part of the area and hooked right to flow eastward in the

northeast. According to this view, directional structures indicate the direction of the last current, whereas other structures and the texture and composition give the initial downslope path. Schenk compared the depositional environment with that of the present continental rise of the western North Atlantic, where contour-flowing bottom currents are an important agent of sediment transport and deposition (Heezen *et al.*, 1966). This model agreed with the interpretations of workers who invoked normal ocean currents, rather than turbidity currents and related processes, to explain flysch sedimentation in other areas where the relationship between paleocurrents and the apparent paleoslope is seemingly anomalous (e.g., Hubert, 1966, 1968; Klein, 1966; Scott, 1966). Later work by Harris (1971, 1975) and Schenk (1973) and reinterpretation of the comparable situations in other flysch basins (e.g., Walker, 1970) suggest that this model does not satisfactorily explain the Goldenville sandy flysch, but nevertheless may be valid for the non-turbidite part of the Halifax Formation.

Harris (1971, 1975) carried out a bed-by-bed study of sedimentary structures in the Goldenville Formation in an area of good coastal exposures near the village of Sheet Harbour, approximately 55 miles (90 km) northeast of the city of Halifax. This work brought to light the following characteristics of the Goldenville sediments in that area: (1) Sandstone (dominantly fine- to medium-grained) constitutes at least 70 per cent of the formation and occurs in beds 1 cm to more than 50 m thick. To explain the predominance of fine grained sandstone, Harris suggested that the Goldenville sediments were transported by turbidity currents down submarine channels, and that portions of both the coarse and fine fractions were left behind in 'upstream' areas. According to this view, some of the argillaceous material accumulated in interchannel areas and on a prograding continental rise, ultimately to form a part of the Halifax Formation. (2) The sandstone beds, when traced along strike from outcrop to outcrop over a distance of several kilometres, commonly appear either to be discontinuous or to become segregated into a number of thinner beds or to become amalgamated into thicker beds. In vertical sequence, the sandstone beds form thickening-upward, large-scale megarhythms (the vertical extent of each megarhythm is from 200 to 700 m). Harris suggested that these characteristics of the beds indicate deposition in a prograding submarine fan system. Both thickening-upward and thinning-upward megarhythms are present on a smaller scale as well. The average small-scale megarhythm has a vertical extent of approximately 25 m. Flysch studies in other areas in recent years have demonstrated that such megarhythms may be attributed to channel-fill (generally thinning-upward) and unchannelled (generally thickening-upward) deposition in the 'suprafan' areas of submarine fan complexes (*see* reviews by Walker and Mutti, 1973; Mutti, 1974). (3) Analyses of numerous measurements of directional sole markings, coupled with good structural control, indicated that the mean paleocurrent direction is closely parallel to the trend of the major folds, substantiating Schenk's finding that the regional paleocurrent trend is axial. A possible explanation is that the currents flowed parallel with the long axis of a tectonically-controlled trough, and that later the folds developed axial to the trough. Harris favoured another interpretation, however. He surmised that the paleocurrents determined the geometry or 'grain' of the sandstone beds, which, in turn, controlled the early development of the main folds. He suggested that the early folds were later steepened and rotated into a stable tectonic position. However, the amount of horizontal rotation that may have been involved is unknown. (4) Many of the sandstone beds have deeply-tooled groove markings on their undersurfaces, commonly associated with scour depressions that in numerous instances are deformed by loading. Intrabed scour-and-fill structures are prominent in some beds, and outside intraformational clasts (>1 m in length) are present in others. These features suggest the action of high-energy currents. (5) Dewatering structures, such as sand volcanoes, pillar structures and sheet structures (the latter are described by Laird, 1970), are present in about half of the sandstone beds. These features indicate that the sand was highly water-laden, apparently as a result of rapid deposition from currents highly charged with suspended sediments. Abundant slump structures and slide markings further attest to the unstable and presumably water-laden conditions of the sediments. (6) The mean direction of slide markings is parallel to the mean paleo-current direction, suggesting that both the currents and slides moved downslope. However, the slope may have been controlled by the configuration and siting of the main depositional lobes of the submarine fan complex rather than by the regional bathymetry.

Descriptions in recent years of both modern deep-sea fans and inferred ancient deep-sea fans (*see* reviews by Walker, 1970, 1973; Walker and Mutti, 1973; Mutti, 1974; Nelson and Kulm, 1973; and Nelson and Nilsen, 1974) have contributed greatly to an improved understanding of flysch (and hence Meguma) sedimentology. The application of recent work on megarhythyms to the Goldenville Formation was noted above. Schenk (1973) drew attention to the striking similarity of the Goldenville and Halifax lithologies to present, abyssal plain turbidites and continental rise contourites of the western North Atlantic, as described by Horn *et al.* (1971). This comparison supports the concept that the Meguma sediments accumulated in a deep-marine setting. In the region of the Hatteras Abyssal Plain (off the east coast of the United States), channellized turbidites are being deposited by turbidity currents that move in the same general direction as the contour-following currents that transport and deposit the fine-grained sediments of the adjacent continental rise, and both flow approximately parallel with the continental margin. The continental rise sediments presumably are prograding outwards over the Hatteras Abyssal Plain transverse to the direction of the depositional currents. The sedimentation and regional paleocurrent pattern of the Goldenville and Halifax formations may have developed in a similar manner. The paleocurrent directions of the Halifax and Goldenville formations are mutually parallel, and some of the fine grained sediments of the

Halifax Formation are possible contourites that prograded laterally over the Grenville sandy flysch. Schenk's (1970) analyses of the Meguma paleocurrents indicate that they probably flowed more or less parallel with the ancient continental margin. A ramification of the theory of plate tectonics is that the principal folds that developed during diatrophism of a eugeoclinal succession juxtaposed with an ancient continental margin may have a tendency to be aligned subparallel with the ancient margin, and in the case of the Meguma, therefore, subparallel with the regional paleocurrent trend.

Middleton and Hampton (1973) described and classified the bed-forms that result from deposition by four possible mechanisms of sediment gravity (mass) flows, namely, (1) turbidity currents, (2) fluidized sediment flows, (3) grain flows and (4) debris flows. The great majority of sandstone beds in the Goldenville Formation have bedding characteristics that indicate deposition by turbidity currents, fluidized sediment flows, and grain flows. However, relatively few of the beds can be categorized as exclusively the product of any one of these three mechanisms. The sequence of sedimentary structures in most beds suggest that more than one of the mechanisms operated simultaneously or successively during the process of deposition. I speculate that the sediments were moved into the area primarily by turbidity currents, and that fluidized sediment flow and grain flow became important immediately before and during deposition of the majority of the sandy beds. The delayed grading that characterizes many of these beds suggests that turbidity-current action prevailed during the final phase of deposition in such cases.

According to the facies classification of Walker and Mutti (1973), the bulk of the Goldenville Formation corresponds to Facies B2 (massive sandstones without dish structure) and Facies C (mainly Bouma AE, proximal turbidites), with subordinate Facies A2 (organized conglomerates), A4 (organized pebbly sandstone), and B1 (massive sandstones with dish structures). Occurrences of Facies A1 (disorganized conglomerates) and A3 (disorganized pebbly sandstones) are rare. Facies D ("classical" distal turbidites of Walker, 1967) and minor Facies G (pelagic and hemipelagic muds and silts) are present as intercalations from tens of centimetres to hundreds of metres thick within the Goldenville Formation. Walker and Mutti equate this association of facies with mid-fan deposition in submarine fan systems.

The Halifax Formation is composed of Facies D and G, with minor Facies C. A number of environments of deposition are probably represented – the outer fan and basin plain; the interchannel areas of the inner fan; and the areas between major channels and canyons on the rise and slope. Upper Halifax strata that grade vertically into neritic deposits of the White Rock Formation probably represent outer shelf deposits that accumulated in relatively shallow water (Lane, 1975).

In the light of these considerations, the conventional view of the Meguma Group as composed of two time-stratigraphic formations identified solely on the basis of lithology (i.e., the sandy Goldenville and the slaty Halifax) is clearly inappropriate. In this report, the Meguma is envisaged as a complex of interfingering lithosomes. Zones of fine grained sediments up to 1 km thick within the Goldenville are interpreted as facies-equivalent to Halifax sediments with comparable sedimentologic characteristics. In broad aspect, the Goldenville and Halifax sediments are at least partly and may be wholly, coeval. However, the knowledge of facies relationships in the Meguma is far from complete at the present time.

References

Faribault, E.R.
1914: Greenfield and Liverpool Town map-area, Nova Scotia; Geol. Surv. Can., Summ. Rept. 1912, p. 334-340.

Harris, I.M.
1971: Geology of the Goldenville Formation, Taylor Head, Nova Scotia; unpubl. Ph.D. thesis, Univ. Edinburgh, 224 p.

1975: Sedimentological study of the Goldenville Formation, Nova Scotia; *in* Report of Activities, Pt. A, Geol. Surv. Can., Paper 75-1, pt. A, p. 171-174.

Harris, I.M. and Schenk, P.E.
1975: The Meguma Group; *in* Guidebook for the Eastern Section, Society of Economic Paleontologists and Mineralogists Field Trip (1975); Marit. Sediments, v. 11, in press.

Heezen, B.C., Hollister, D.C., and Ruddiman, W.F.
1966: Shaping of the continental rise by deep geostrophic contour currents; Science, v. 152, p. 502-508.

Horn, D.R., Ewing, M., Horn, B.M., and Delach, M.N.
1971: Turbidites of the Hatteras and Sohn Abyssal Plains, western North Atlantic; Marit. Geol., v. 11, p. 287-323.

Hubert, J.F.
1966: Sedimentary history of Upper Ordovician geosynclinal rocks, Girvan, Scotland; J. Sediment. Petrol., v. 36, p. 677-699.

1968: Currents and slopes in flysch basins: a discussion; J. Sediment. Petrol., v. 38, p. 1390-1393.

Hubert, J.F., Scott, K.M., and Walton, E.K.
1966: Composite nature of Silurian flysch sandstones shown by groove moulds on intra-beds surfaces; Peebleshire, Scotland; J. Sediment. Petrol., v. 36, p. 237-241.

Klein, G.D.
1966: Dispersal and petrology of sandstones of the Stanley-Jackfork boundary, Ouachita fold belt, Arkansas and Oklahoma; Am. Assoc. Pet. Geol., Bull., v. 50, p. 308-326.

Laird, M. G.
1970: Vertical sheet structures — a new indicator of sedimentary fabric; J. Sediment. Petrol., v. 70, p. 428-434.

Lane, T. E.
1975: Stratigraphy of the White Rock Formation; *in* Guidebook for the Eastern Section, Society of Economic Paleontologists and Mineralogists Field Trip (1975); Marit. Sediments, v. 11, in press.

Middleton, G. V. and Hampton, M. A.
1973: Sediment gravity flows: mechanisms of flow and deposition; *in* Turbidites and deep-water sedimentation; Society of Economic Paleontologists and Mineralogists, Pacific Section, Los Angeles, Short Course Notes, p. 1-38.

Mutti, Emiliano
1974: Examples of ancient deep-sea fan deposits from circum-Mediterranean geosynclines; *in* Dott, R. H. and Shaver, R. H. (eds.), Modern Ancient Geosynclinal Sedimentation; Society of Economic Paleontologists and Mineralogists, Spec. Publ. 19, p. 92-105.

Nelson, C. H. and Kulm, L. D.
1973: Submarine fans and deep-sea channels; *in* Turbidites and deep-water sedimentation; Society of Economic Paleontologists and Mineralogists, Pacific Section, Los Angeles, Short Course Notes, p. 39-70.

Nelson, C. H. and Nilsen, T. H.
1974: Depositional trends of modern and ancient deep-sea fans; *in* Dott, R. H. and Shaver, R. H. (eds.), Modern and Ancient Geosynclinal Sedimentation; Society of Economic Paleontologists and Mineralogists, Spec. Publ. 19, p. 69-91.

Schenk, P. E.
1970: Regional variation of the flysch-like Meguma Group (Lower Paleozoic) of Nova Scotia compared to Recent sedimentation off the Scotian Shelf; Geol. Assoc. Can., Spec. Paper 7, p. 127-153.

1973: Nova Scotia, Morocco and continental drift; *in* Earth Science Symposium on Offshore Eastern Canada; Geol. Surv. Can., Paper 71-23, p. 219-222.

Scott, K. M.
1966: Sedimentology and dispersal pattern of a Cretaceous flysch sequence, Patagonian Andes, Southern Chile; Am. Assoc. Pet. Geol., Bull., v. 50, p. 72-107.

Taylor, F. C.
1967: Reconnaissance geology of Shelburne map-area, Queens, Shelburne, and Yarmouth Counties, Nova Scotia; Geol. Surv. Can., Mem. 349, 83 p.

Walker, R. G.
1970: Review of the geometry and facies organization of turbidites and turbidite-bearing basins; *in* Lajoie, J. (ed.), Flysch Sedimentology in North America; Geol. Assoc. Can., Spec. Paper 7, p. 219-251.

1973: Mopping up the turbidite mess; *in* Ginsburg, R. N. (ed.), Evolving Concepts in Sedimentology; John Hopkins Univ. Press, Baltimore, p. 1-37.

Walker, R. G. and Mutti, E.
1973: Turbidite facies and facies associations; *in* Turbidites and deep-water sedimentation; Society of Economic Paleontologists and Mineralogists, Pacific Section, Los Angeles, Short Course Notes, p. 119-157.

20. STELLATE NODULES FROM THE UPPER DEER BAY FORMATION (VALANGINIAN) OF ARCTIC CANADA

Project 550004
E. Kemper and H. H. Schmitz[1]

Introduction

The Deer Bay Formation, a sequence of shale-siltstone beds, was deposited in the Sverdrup Basin during an interval ranging from the late Upper Jurassic (Volgian Stage) to the early Lower Cretaceous (Upper Valanginian) (Kemper, 1975). The beds of the formation, which are equivalent to the younger part of the lower Valanginian and the older and middle parts of the upper Valanginian, contain great quantities of peculiar aggregates of crystals. They are named here "composite euhedra" or "euhedral aggregates" but the popular descriptive term "hedgehog" concretions could also be applied to them. "Polar euhedra" is a possible genetic term. It is impossible to overlook the presence of these euhedral aggregates when studying the Valanginian part of the Deer Bay Formation. Although characteristic of the beds of the upper Deer Bay Formation, they also occur in impressive quantities in the Aptian-Albian Christopher Formation.

The "hedgehogs" are particularly impressive for those workers, who are familiar with the contemporary sediments of other regions, as they are totally absent in the Boreal and in the Luisitanian-Mediterranean faunal realms. To date "hedgehogs" are unknown in the Cretaceous of the Canadian mainland (J. A. Jeletzky, oral comm., December 12, 1974), in USSR, and even in East Greenland. However, they do occur in the Valanginian of Spitzbergen (Pchelina, 1965; Kemper, 1975). The absence of "hedgehogs" in sediments of definitive warm and temperate latitudes and their occurrence in regions which are Arctic according to specialists on continental drift (e. g. Bullard *et al.*, 1965; Dietz and Holden, 1970) leads to the conclusion that they formed under cold water, high latitude conditions. They are, therefore, believed to be indicators of cold water marine environments.

In the following sections the writers have assembled such data on the "hedgehogs" as were available to them. Further data, as for example those dealing with the value of "hedgehogs" for correlation, those outlining the scope of the project, and those defining the report-area, and the studied localities are available in Kemper's (1975) paper.

The tasks involved in the compilation of this paper have been divided as follows: E. Kemper is responsible for the field work, paleontology, and the organization of relevant data while H. H. Schmitz is responsible for the mineralogy.

J. A. Jeletzky, Geological Survey of Canada, Ottawa kindly translated the original German text into English and made valuable critical comments. Dr. N. Schulgina of the Soviet Institute of Arctic Geology in Leningrad provided valuable information and literature data.

Geological Aspects: Occurrence, Distribution, and Morphology of Euhedral Aggregates

Euhedral aggregates ("hedgehogs") of the Deer Bay Formation are interpreted as calcite pseudomorphs after thenardite (Na_2SO_4). Their coarser varieties, at least, are indistinguishable from crystal aggregates reproduced in Conybeare and Crook (1968, Pl. 58) and interpreted by these workers as "glendonite" [= siderite pseudomorphs of glauberite, $Na_2Ca(SO_4)_2$]. These glendonites occur in Upper Permian marine Ulladulla mudstones of New South Wales, Australia (David *et al.*, 1905; Brown, 1925). According to Conybeare and Crook (1968), the original aggregates formed in muddy marine sediments because of glauberite crystallization during a chilling of marine water to temperatures below 0°C. There is other evidence (e. g. erratics and cold water fauna) indicating a glacial environment of the sedimentation. This inferred genesis of glendonites was not accepted by Brown (1925, p. 29) although he did not clarify the exact relationships between the glendonites and the fauna.

David *et al.* studied glendonites with remarkable thoroughness. They undertook comprehensive comparisons with analogous crystalline aggregates, taking into consideration even the oldest literature. The identification of crystalline aggregates solely on the basis of the literature is, however, extremely difficult and mostly quite impossible because of their extremely complex nature. This is true even of the comparison of the well described glendonites with our composite euhedra. This uncertainty must be taken into account when evaluating our conclusions. There is no doubt that the above cited authors had compared rather heterogeneous material. Similar, but nevertheless not identical, crystalline aggregates can arise under very different conditions.

David *et al.* made two most important observations bearing on the problem of origin of glendonite. These are, the presence of pseudomorphs (recent composite euhedra?) on the bottom of the White Sea and the association of barite with glendonites. The latter observation is supported by suggestions of the precipitation of barite in recent polar seas described in recent literature (e. g. Hermann, 1974). The Australian authors are also responsible for the suggestion that the glendonite is a pseudomorph after glauberite.

In spite of the publication of David *et al.* (1905), the name "glendonite" and other problems connected with it have been almost completely neglected by subsequent geologists. In spite of all efforts, we did not succeed in finding the name "glendonite" in any geological handbook or treatise, although it is listed in mineralogical treatises of Palache *et al.* (1951) and Hey (1962).

[1]Bundesanstalt für Geowissenschaften und Rohstoffe, Hannover, Federal Republic, Germany.

"Hedgehogs" differ from glendonite in composition and size of aggregates. Furthermore, the identity of the outer shapes had to be recognized solely on the basis of illustrations and descriptions available. This prevented us from making a quite positive identification, although there is a high probability of identity. Therefore, we do not use the name "glendonite" in this paper but prefer the descriptive terms "composite euhedra" or "euhedral aggregates" for the Canadian crystal aggregates.

To date composite euhedra have not been treated in any detail in the literature concerned with Arctic regions. We know of only two descriptive mentions of euhedral aggregates where the Valanginian occurrences are concerned. Heywood (1957, p. 9) stated when describing Deer Bay Formation: "Numerous calcite concretions and rosettes occur throughout the formation....." and Pchelina (1965) considers: "stellate nodules of anthracolite..." as very characteristic for the Valanginian rocks of Spitzbergen. The term "anthracolite" is identical with that of anthraconite and may be interpreted as calcite (Hey, 1962).

Test *et al.* (1962, p. 36, fig. 10) mention "hedgehogs" from Bajocian beds of the Lena Region as "calcite crystals" but do not attempt any interpretation of their genesis. F. G. Young (written comm. June 3rd, 1975) found "hedgehogs" in the Upper Jurassic Husky Formation in northern Yukon Territory.

The sedimentary units of the Arctic Valanginian containing euhedral aggregates are mostly thick, ranging between 2 and 20 m. The distance between the individual aggregates is relatively great, which results in a relatively low density of occurrence. The distances separating individual euhedral aggregates fluctuate between several tens of centimetres and several metres. The aggregates are irregularly distributed, as a rule, and apparently do not form layers. Their spectacular accumulations result from the erosion of the surrounding argillaceous matrix. Our euhedra are, in common with the glendonites of the Ulladulla Formation, confined to argillaceous rocks; they are absent in sands.

The mineralogical composition of clay minerals of claystones containing euhedra is like that of the highest (i.e. superimposed) beds of the Deer Bay Formation devoid of euhedra. However, the two differ in the content of plant particles. The beds containing aggregates are almost devoid of plant particles, in contrast to the highest beds of the Deer Bay Formation. However, this fluctuation of the content of plant material could have been effected by the gradually increasing proximity of land because of a gradual upward increase of sandy and silty inclusions (Dr. H. Hufnagel; internal report; *see* Table 20. 1).

The diameter of Valanginian euhedral aggregates of the Sverdrup Basin averages between 5 and 8 cm. The external appearance of these radially fibrous aggregates is most variable. It ranges from spinose spheres with slender, sharp crystals to tabular aggregates with coarse crystals. The morphology of the bulk of the aggregates is confined between these extremes. Most aggregates have a distinctly flattened basal surface where crystal growth was inhibited. The unhindered expansion of crystal aggregates was only possible in the lateral and upward directions.

The euhedra formed by means of slow, radial crystallization of primary minerals in the upper layers of the argillaceous sediment deposited on sea bottom. The mud was pressed aside by the crystallization instead of being incorporated into the precipitated crystalline matter.

It is the origin of the primary mineral that is decisive for the interpretation of the "hedgehog" nature. It was thenardite in the case of the Valanginian aggregates of the Sverdrup Basin (*see* next section), and it appears to be highly probable that it was the thenardite and not the glauberite that occurred as the primary mineral also in the Ulladulla Formation. However, the nature of the original mineral does not affect the genesis of the structures. Such a development of large, slowly growing crystals of sodium sulphates in seawater is, in the writers' opinion, only conceivable in overcooled waters in marginal basins or embayments which have limited water exchange with the principal Arctic basins.

The kind of secondary material now present in euhedra is only of subordinate importance; its precipitation depends on still unknown processes in the muddy environment. Glendonites consisting of dark calcium-carbonate have been mentioned from Australia by Brown (1925), although the majority of concretions consist of siderite. Furthermore, siderite-pseudomorphs seem also to be present in the Arctic regions (e.g. Spitzbergen?).

The metasomatic replacement of primary mineral by calcitic or sideritic secondary minerals probably occurred in the early diagenetic stage. Details of the segregation processes in a mud environment under cold marine, presumable Arctic conditions remain largely unknown. The concentration of calcite in euhedra is so far inexplicable. Only small quantities of finely dispersed siderite are observable in the surrounding argillaceous rocks. Calcite is completely absent in the surrounding rock (*see* analyses at the end of the paper). The solubility of calcium in the Arctic and high-Boreal waters remains equally problematic. The opinion about an easy solubility of calcium in cold seas, which is widespread in text books, cannot be valid in such a generalized form. For example, MacIntyre and Platford (1964) have found in the Labrador Sea an oversaturation with calcium carbonate. Furthermore, calcareous concretions can form in cold water surroundings, as it is proved by the "imatra stones" Pettijohn (1957, p. 203). Our knowledge of these processes is still rather fragmentary.

The observations made on Valanginian euhedra are very important because of the above considerations. They prove, in conjunction with the Permian Ulladulla glendonites, that the rosette-like carbonate aggregates of crystals can form in the marine argillaceous rocks of high Boreal to polar areas. These calcite- or siderite-euhedra, which formed in a pseudomorphic fashion, must be strictly separated from sand-crystals or rosettes of warm regions. The latter do not have anything in common with euhedra where genesis, chemistry, and crystal form are concerned.

X-Ray diffraction analysis:

1) Claystone of the upper Valanginian, Ellesmere Island, Blackwelder Mountains. Layer with euhedral aggregates.

Method: Microscopic and fluorescent-photometric study of a polished plate of a concretion corner. Determination of the capacity for microscopic reflection. Conditions of measurement: objective 60: 1, oil, 546 mm; diameter of the measured spot about 1.3μ; glass-standard 1.01% R; 50 measurements; distribution maximum of the average reflection.

Results: Silty claystone, no recognizable bedding. Pyrite as fine grained globulith, mostly scattered but occasionally combined into larger accumulations.

The organic inclusions consist of grey, low reflectory, commonly porous grains and small lamellae. These inclusions consist not of a vitrinitic but of bituminous matter. According to the capacity for macroreflection (0.46% R) this matter can be tentatively determined – according to Jacob's nomenclature – as belonging to the group of grahamite-glance pitch-albertite. The luminous, liptinitic components are quantitatively prevalent, however. They consist mostly of a very fine grained liptodetrinite, occasionally also of algenite and skin-like, presumably animal-derived remnants. A definitive sporinite and cutinite were not seen. Inertinite occurs only rarely. Alongside these definitively recognizable organic particles a brown, transparent substance, which is very probably also of organic origin occurs relatively commonly.

Contrary to the claystone from the highest beds of Deer Bay Formation (early upper Valanginian), the organic material of which is largely derived from the terrestrial plants, it is impossible to demonstrate a terrigenous origin of the organic material of the rock that surrounds euhedral aggregates. This organic material may have been derived, for the most part, from a marine environment. It is impossible to obtain more detailed data on the basis of an analysis of a solitary sample.

2) A sample from the claystone of the upper Valanginian (Axel Heiberg Island, south of Buchanan Lake), which is superimposed on the beds containing euhedral aggregates and was deposited under warmer climatic conditions.

The X-Ray diffraction analysis produced:

Quartz – principal component
Kaolinite, Muscovite-Illite, Pyrite – secondary components
Gypsum, feldspar, siderite, montmorillonite? – traces.

The organic substance of this sample consists of very fine, finely scattered, detrital, mostly 20-30μ particles. The groundmass is vitrinitic; it contains, otherwise, strongly luminescent liptinites (i.e. spores, also cuticulae and grains of pitch) and subordinated inertinite. Vitrinite and inertinite occasionally exhibit a definitive plant cell structure. Pyrite, which occurs also as a globulith, is relatively common.

X-Ray fluorescence analyses (by Dr. Raschka, BGR-Hannover):

1) Claystone with euhedral aggregates (upper Valanginian, Blackwelder Mountains, Ellesmere Island).

2) Claystone without euhedral aggregates (uppermost Valanginian, south of Buchanan Lake, Axel Heiberg Island).

3) Euhedron (upper Valanginian, Blackwelder Mountains, Ellesmere Island).

	1.	2.	3.
SiO_2	59.36	47.09	1.79
Al_2O_3	15.84	21.40	1.35
Fe_2O_3	5.61	7.50	1.03
MnO	0.05	0.04	0.16
MgO	1.63	1.96	1.10
CaO	0.98	0.85	49.60
Na_2O	0.59	0.28	0.12
K_2O	2.80	2.62	0.05
TiO_2	0.91	0.90	0.04
P_2O_5	0.26	0.22	0.42
SO_3	0.66	0.63	0.00
LOI	11.00	16.68	42.75
Total or Sum	99.67	100.17	98.52

Mineralogical Studies

Composition

The composite euhedra of Deer Bay Formation consist of calcite (Figs. 20.1, 20.2, and 20.3). However, the appearance of crystals does not correspond at all to that of a trigonal symmetry, even if the first, superficial impression is that of a scalenohedron. The euhedra are, therefore, pseudomorphs of calcite after another mineral. It seems feasible to suggest the replacement of previously existing glauberite crystals also in this instance (i.e. similar to that described by David, *et al.* 1905 in the case of Australian glendonites). Glauberite [$Na_2Ca(SO_4)_2$] belongs to the monoclinic prismatic class, space group C_{2h}^6 – C2/c. According to Hintze (1930), the external appearance of the crystals is caused mostly by the relationship of the two most frequently occurring forms {111} and {001}. If {111} is dominant, the crystals are usually elongated along the rim {111} : {111}; they acquire thereby a prismatic character. If the basal pinacoid {001} is prevalent, the crystals are correspondingly tabular-shaped. Figures 20.4, 20.5 and 20.6 show the principal shapes of glauberite. Figure 20.9 is a photograph of a natural glauberite crystal taken by scanning electron microscope. A comparison of the crystals with pseudomorph shapes of calcite of the aggregates makes it obvious that a different (i.e. as compared with that of glauberite) crystalline system forms their basis.

Macroscopical studies

Figures 20.1, 20.2 and 20.3 give an idea concerning the size and appearance of euhedral aggregates. The pyramidal appearance of individual crystals and their quadrangular cross-section, are clearly recognizable in many specimens. Their size fluctuates from a minimum of 0.5 cm to a maximum of about 4 cm. The crystals average about 1 cm. All concretions are flattened on their undersides and, if present at all, the crystals are reduced on this surface. The colour of concretions varies from dirty white through grey to red-brown. The facetted, mosaic-like, rough, characteristically non-reflective faces do not permit a crystallographic measurement with a double-circle-reflection goniometer. Therefore it was only possible to carry out approximate measurements of angles on larger crystals, which were mostly less satisfactorily preserved. The measurements of the angle of pyramid (111) Λ (111) produced values between 55 and 60 degrees.

The result is the same as that obtained using scanning electron microscope (*see* below), namely, the external appearance of crystals does not correspond at all to the trigonal class of symmetry but either to the tetragonal or to the orthorhombic system.

Study in thin section

One thin section of a pseudomorph was studied to try to elucidate the nature of the original mineral using the internal texture. The material is a mosaic-like aggregate of small particles which have commonly a flaser-like or flame-like appearance. Their size averages 180μm. The largest crystals measure 200 by 400μm. The internal structure is typically pseudomorphic with individual crystals not showing any consistent orientation. The investigated crystals are, without exception, calcite; they are coloured light brown because of ferruginous impurities. Twinning of crystals, because of the influence of pressure, occurs only occasionally. Whenever present, it could have also been caused by the preparation of thin section. The filling of the space is not complete, as the aggregates are porous. A clay mineral occurs in some interspaces. This mineral is kaolinite as it was confirmed by X-Ray analysis.

Studies with scanning electron microscope.

The scanning electron microscope is most suitable for photographic reproduction of smallest particles because of its greater depth of focus. Figures 20.7 and 20.8 are photographs of small areas of concretions. It is clearly visible that the crystals are pyramidal shapes with a rectangular cross-section. The top of the pyramid occasionally forms a cutting edge. Very steep (Fig. 20.7) as well as more corpulently-shaped (Fig. 20.8) crystals occur in the studied areas. Re-entrant angles indicate the presence of either twinning or parallel intergrowths.

As in the binocular microscope study, it was only possible to recognize the faces which are reproduced in the photographs. Neither pinacoids nor prismatic faces occur, but exclusively faces {111} of the basic pyramid. The habit of crystals definitely does not correspond to that of a trigonal class of symmetry but either to that of the tetragonal or to that of the orthorhombic system.

X-Ray and fluorescent-photometric studies

X-Ray diffraction of our crystal aggregates resulted in recognition of their calcitic composition. The surfaces of the crystal aggregates have yielded, in view of the absence of other analyses, enough clay material for some further analyses. The clay surrounding the concretion consists of (Sample 74/8):

Quartz – principal component
Kaolinite – secondary component
Siderite, pyrite – secondary components or traces
Muscovite-illite, feldspar – traces

The absence of calcite is remarkable as is only the minor siderite content. An investigation of Dr. H. Hufnagel (BRG – Hannover) provides information about the organic substances present in the clay (*see* Table 20.1)

Discussion of mineralogical results obtained from euhedra

Because of the above special studies, it is possible to rule out glauberite as the original crystals of the euhedra. However, there are other minerals that can form under similar conditions, the crystalline appearance of which is either similar to or identical with that

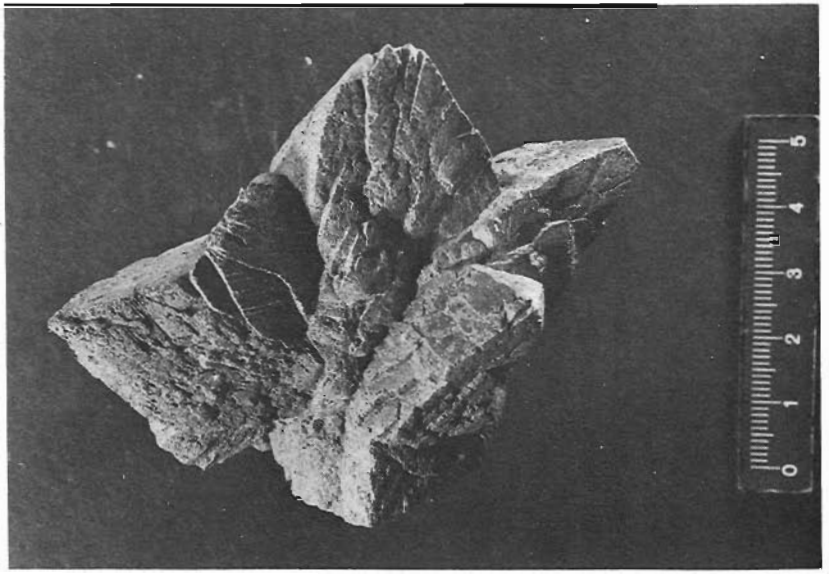

Figure 20. 1

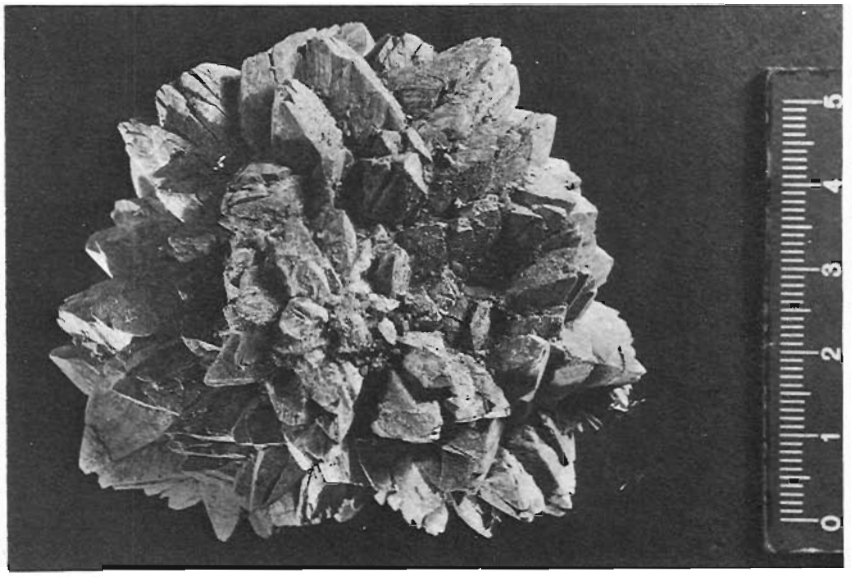

Figure 20. 2

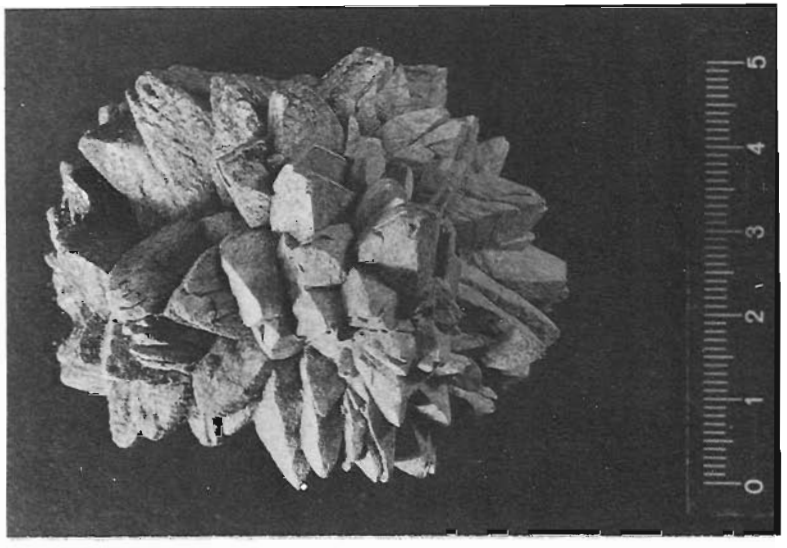

Figure 20. 3

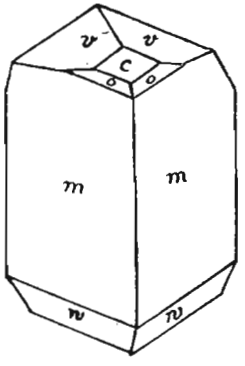

Figure 20. 4

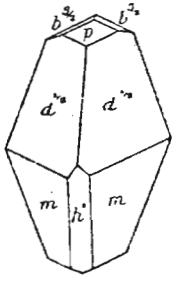

Figure 20. 5

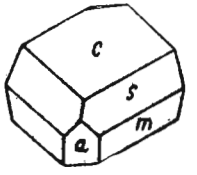

Figure 20. 6

Figures 20. 1-3: Composite euhedra or euhedral aggregates ("hedgehogs") from the Valanginian part of Deer Bay Formation. Blackwelder Mountains, Ellesmere Island, locality 5 of Kemper (1975).

Figure 20. 4: Glauberite crystal with prominent prismatic faces parallel to C {hko}. From Hintze (1930).

Figure 20. 5: Glauberite crystal with prismatic faces having the most common habit {hkl}. From Goldschmidt (1918).

Figure 20. 6: Tabular glauberite crystal which has a basal pinacoid habit {001}. From Philipsborn (1967).

of the here discussed calcite pseudomorphs. These minerals are: gaylussite (natrocalcite; $CaNa_2(CO_3)_2 \cdot 5H_2O$) and thenardite ($Na_2SO_4$).

David *et al.* (1905) pointed out the existence of a certain relationship between the Australian pseudomorphs and gaylussite or thinolite. However, there remained some differences and they preferred to give the new name glendonite to these pseudomorphs.

Gaylussite crystallizes in the monoclinic-prismatic class C_{2h}^6 or C2/c. The shape of crystals is mostly extended-columnar toward {001}, octahedron-like through {110} and {011} or tabular toward {001}. Their faces are, as a rule, uneven, rough, or even striated (compare Fig. 20.12) (Hintze, 1930). Pseudomorphs of calcite after gaylussite are known under the name "barley corn". According to Klockmann (1967), they can be found: "in the bottom of swamps of Schleswig, in Dollart, in Southwest Africa and elsewhere." Hintze (1930) described the occurrence of Obersdorf bei Sangerhausen, where the individual crystals, commonly as many as four or more specimens, grow through each other in a cross- or star-shape. Gaylussite is supposed "to form only under the influence of sufficiently concentrated solution of soda on $CaCO_3$ when the temperature is not too high". However, there still remain some unanswered questions about the exact conditions of the formation and those of the pseudomorphs. It is striking that nearly all described occurrences were found in young sediments. Only in Japan were "Gaylussite-calcite-pseudomorphs" described from the Tertiary (Hintze, 1930). Some crystal shapes of gaylussite are shown in Figures 20.10, 20.11 and 20.12. The last figure is a photograph by scanning electron microscope of crystals from Obersdorf near Sangerhausen. A comparison of the crystals (Figs. 20.10, 20.11) with the pseudomorphs of our composite euhedra (Figs. 20.1 – 3, 7, 8) attests to the presence of much greater morphological similarities than in the case of glauberite. However, the striation, the size of crystals, the mode of formation of aggregates, and also the respective ages, make an affinity unlikely in our opinion.

Thenardite crystallizes in the rhombic-dipyramidal class, space group D_{2h}^{24} or Fddd. According to Hintze (1930), the habit of thenardite crystals is determined, in most instances, by a solitary, or at least prevalent, appearance of the basic pyramid {111}. The twinning occurs preferably along {101} and the vertical faces form an angle of 102°02'. Some simple and twin forms are reproduced in Figures 20.13-17 after Goldschmidt.

Our knowledge of the conditions under which thenardite is formed is fragmentary and even contradictory. Hintze (1930) provided the following information. On the one hand Van't Hoff and Saunders in Hintze (1930) indicated that the minimum temperature at which thenardite precipitates from NaCl – containing solution appears to lie at 17.9°C. However, in Spain at Salinas de'Espartines, near Madrid thenardite crystals with faces {111} and {001} appear to form in winter from the brine. The crusts with 52.3 per cent of thenardite from a creek bed in Greenland is the third known occurrence of the mineral. These observations permit the conclusion that, under certain natural conditions the details of which remain obscure, thenardite can precipitate at very low temperatures.

Figures 20.13 and 20.14 show dipyramidal crystals of thenardite. The characteristic steepness of the planes of the pyramids corresponds to crystals of our pseudomorph, as it is shown in the photographs of the scanning electron microscope. Figure 20.15 shows a dipyramid with a cutting edge replacing the tip. Figures 20.16 and 20.17 reproduce the most common kind of twinning of thenardite. If the twinning affects an unlimited number of thenardite crystals, hedgehog-like aggregates result.

A comparison of the crystal shapes of thenardite with the photographs of our euhedra produced by the scanning electron microscope, and the comparison of its twin crystals with the photographs of the euhedral aggregates (Figs. 20.1-3) is impressive in indicating a clear agreement of the two. The evaluation of all data leads us, therefore, to the conclusion, which is a probability merging on the certainty, that the calcite of our euhedral aggregates formed after thenardite.

Chemical analysis

As a supplement to the above studies one chemical analysis was made of the claystone of the euhedra-bearing layers (column 1), of the stratigraphically higher (early late Valanginian) claystone devoid of euhedra (column 2), and of the pseudomorphs themselves (column 3). The results are presented in Table 20.1.

With the exception of differing SiO_2 and Al_2O_3 values, the analyses of shales are more or less identical. The greater roasting loss by the claystone of the highest studied Valanginian beds (column 2) reflects a higher content of organic matter. The chemical result corresponds to the minor nature of the differences of mineralogical composition.

Simultaneously with the fluorescence analysis of carbonate, an unsuccessful attempt (*see* Table 20.1) was made to deduce the nature of the residues of the original substance of euhedra.

Megafauna of the Beds with Composite Euhedra

An analysis of fauna is very important in connection with the hypothesis of Arctic depositional environment of euhedral aggregates proposed herein. However, there arise some problems. On the one hand it is difficult to define the regions characterized by Arctic faunas as there are all possible transitions to the Boreal province. On the other hand comparisons with recent models can be only undertaken to a limited extent, as the Early Cretaceous species are extinct. Furthermore a general ecological analysis is difficult because of an active involvement of many factors acting against each other. In spite of these difficulties, a cautious interpretation of the evidence produces many important hints about the Valanginian environment of Sverdrup Basin which Jeletzky (1971) placed in his "North American Boreal Province".

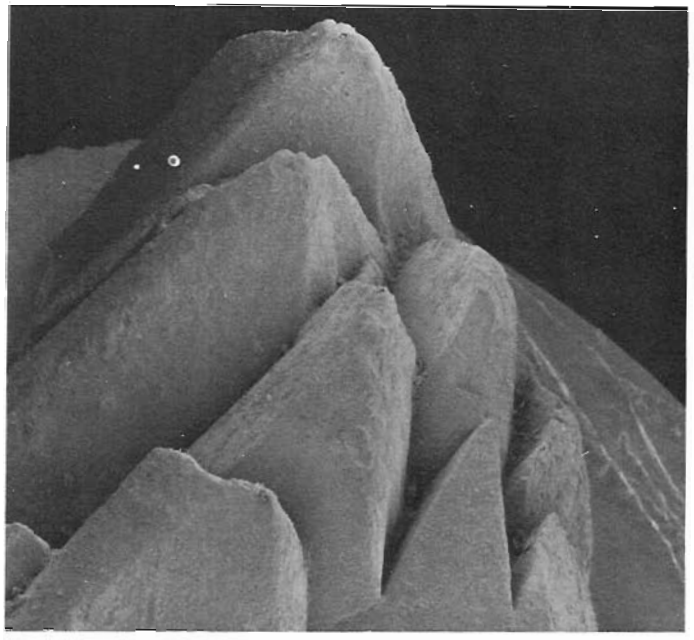

Figure 20. 7

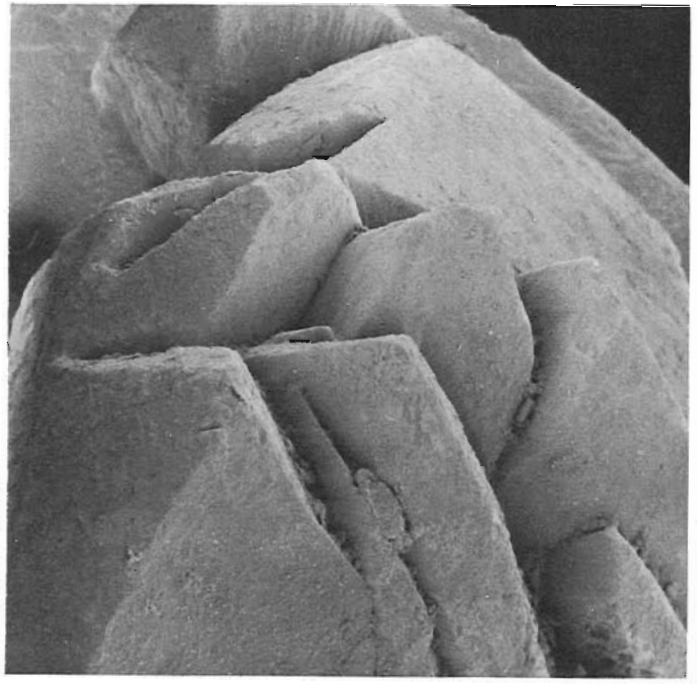

Figure 20. 8

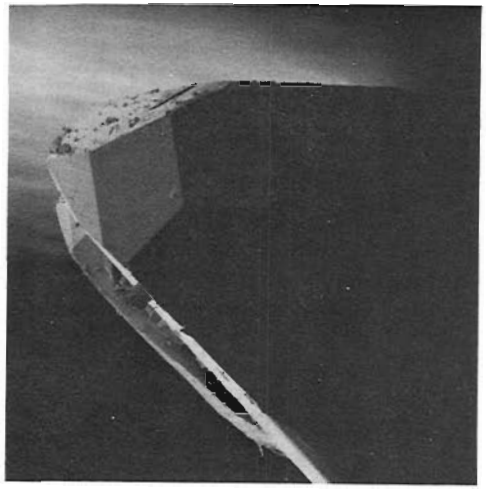

Figure 20. 9

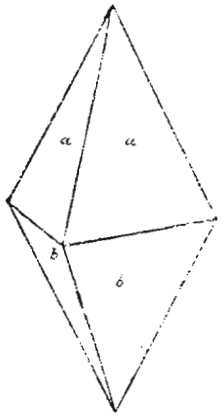

Figure 20. 10

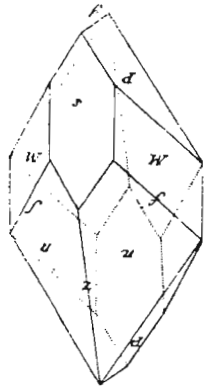

Figure 20. 11

Figures 20. 7, 8: Larger scale photographs of euhedral aggregates. The same locality as for those in Figures 20. 1-3. Scanning electron microscope photographs by E. Knickrehm. The variation of steepness of crystals is clearly visible and so are the spicular or edge-like shapes of crystals. Basal pinacoids are not present. Magnifications: Figure 20. 7, X 19; Figure 20. 8, X 19.

Figure 20. 9: Natural glauberite crystal from Ciemhozuelos near Madrid, Spain. The crystal, which is macroscopically scalenohedron-like, corresponds to the glauberite of Figure 20. 5. A scanning electron microscope photograph by E. Knickrehm, X 120.

Figures 20. 10, 11: Crystal forms of gaylussite after Goldschmidt (1918).

A few remarks of a general nature, and those dealing with the recent Arctic faunas, must be made first. As with all extreme climatic conditions, the Arctic environment is characterized by a great abundance of only a few species. The existence of this situation in the Canadian Lower Cretaceous has already been noted by Jeletzky (1971, p. 14). At present, large numbers of representatives of only a few species (e.g. *Arca glacialis, Pecten groenlandicus, Ophiura nodosa)* are known from the Arctic seas of Eastern Siberia. This phenomenon is most strongly expressed in the restricted marine basins where the layering of the water is most pronounced, with the resulting average yearly temperatures of under 0°C (e.g. White Sea).

The benthonic organisms are decisive for evaluating the environment, as they cannot evade unfavourable conditions but must adapt to them. The cold influences the development of eggs and larvae especially strongly. Many planktonic larvae can only complete their development and settle on the ground within the required time limit if the temperature exceeds a certain minimal value (Hertling, 1953). The cold results, furthermore, in a general slowing down of the development and in a lengthening of life processes and in a prolongation of growth. This is one of the reasons for the large size of animals characteristic for the polar regions.

The elements of recent cold water faunas are *Yoldia arctica* (<4°C), *Pecten groenlandicus* (<0°C), *Chlamys islandica, Macoma* species, and large carnivorous gastropods (Buccinidae), which prey on pelecypods. Furthermore, these faunas include Echinodermata, especially Ophiuroidea and Asteroidea. The existence of recent cold water dibranchiate cephalopods is also notable.

If the preceding comments concerning the recent Arctic province are applied to the data obtained in the Valanginian of the Sverdrup Basin, a striking similarity emerges. The composite profiles of Reptile Creek, north of Eureka weather station (Kemper, 1975) are most informative.

There is no doubt about the paucity of species and the abundance of individuals in the Valanginian faunas of Sverdrup Basin. Fossils are usually completely absent from the units bearing composite euhedra. If the fauna is present, it consists of especially large *Buchia* species and the associated large gastropods. Both groups of fossils are invariably squashed and are not identifiable as to species.

The fauna is relatively more diversified specifically and richer in individuals in the units of claystone devoid of euhedral aggregates. In addition to the still prevalent *Buchia* species, it includes ammonites, belemnites, and pectinid bivalves (e.g. *Boreionectes* sp.). In the highest exposed segment of the profile the character of fauna changes from a *Buchia*-gastropod community to a *Buchia*-pectinid fauna with ophiuroids and crinoids. These beds are most likely referable to the *Homolsomites* cf. *quatsinoensis*-Zone, the fauna of which is notable for its pronounced southern affinities (Kemper, 1975). This fauna must be, nevertheless, evaluated as high Boreal to Subarctic. The still-present depauperation of this fauna is evident when it is compared with the mid-European fauna. The comparative tables of Zacharov (1966, Table 3) are significant in this connection. They demonstrate conclusively how the rich Upper Jurassic pelecypod faunas of North Siberia become depauperated in the Berriasian and Valanginian. However, the extreme conditions of the Sverdrup Basin are not nearly approached in this region; the euhedral aggregates are still absent there.

Of course, an extreme depauperation of species combined with a great number of individuals of every taxon present alone may have different reasons: e.g. decrease of salinity (not here as all occurring fossils are stenohaline), excessive muddiness of the water etc. But in combination with giant size and other features indicating cold water conditions the depauperation favours our interpretation.

The outstanding feature of the Boreal to Arctic Valanginian of the northern hemisphere is the prevalence of *Buchia* species which may result in a monotypic fauna in many beds. *Buchia* is an extremely typical fossil of the northern Valanginian seas with an extraordinarily wide geographic range. It is very rare in middle Europe, as its principal habitat was situated to the north. Many *Buchia* species appear to be cold-eurythermal. It is assumed that the large *Buchia* forms of the beds with composite euhedra, which may be up to 10 cm long, belong to a special Arctic species or variant. They are too poorly preserved for a definitive decision on the subject. Jeletzky (1971, p. 21) recognized a progressive differentiation of *Buchia* faunas in the Valanginian which: .... "supports the conclusion about the persistence of climatic distinctions between the Boreal and North Pacific provinces of Canada".

The Oxytomidae (e.g. *Arctotis* etc.), which occur in the early Lower Cretaceous of Siberia, were not observed in the Sverdrup Basin. They are, however, present in the Valanginian of the Canadian mainland (e.g. northern Yukon; J.A. Jeletzky, pers. comm., May 21, 1975) and so are probably only high Boreal to Subarctic forms. The complete absence of oysters in the Valanginian of Sverdrup Basin is much more important as they were widespread and common in the Luisitanian-Mediterranean Realm and in many regions of the Boreal Realm in the early Lower Cretaceous. The adverse influence of the cold upon the physiology and reproduction of oysters is well known (e.g. Hertling, 1953). The absence of representatives of Trigonidae has already been pointed out by Jeletzky (1971).

In conclusion, it must be stated that the faunal communities of shales with composite euhedra of the Sverdrup Basin, and those of the beds intercalated with them, strongly resemble the present day Arctic faunas, in spite of their specifically different composition. The cold water character of these faunas is stressed even more by the paucity of species and the abundance of individuals, as well as by the gigantic size of some species and the absence of more moderately Boreal elements. The fauna has, therefore, a cold water character and can be assigned only to the Subarctic to Arctic climatic province.

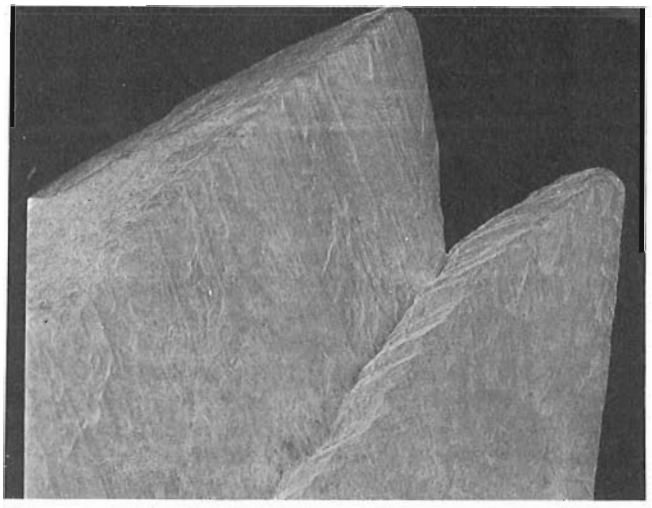

Figure 20. 12. Gaylussite from Oberdorf near Sangerhausen. Scanning electron microscope photograph by E. Knickrehm. Striation of crystalline faces is clearly visible X 25.

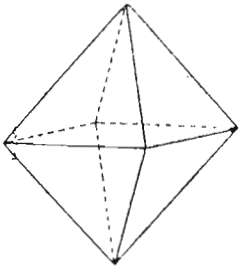

Figure 20. 13

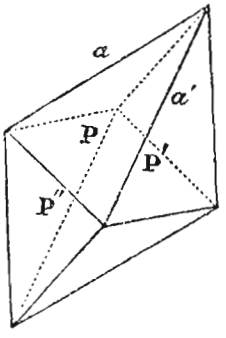

Figure 20. 14

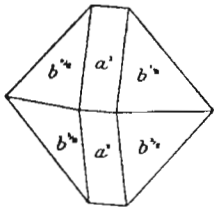

Figure 20. 15

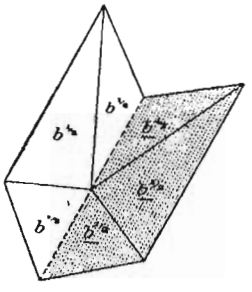

Figure 20. 16

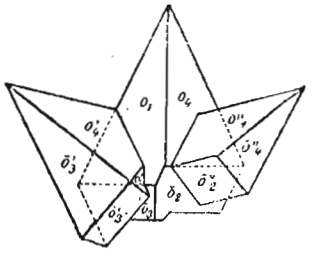

Figure 20. 17

Figures 20. 13-15: Thenardite crystals, after Goldschmidt (1918). The figures show dipyramid with faces of a different steepness. Crystals reproduced in Figures 20. 13 and 20. 14 are pointed while that shown in Figure 20. 15 has an edge termination.

Figures 20. 16-17: Twinning of thenardite crystals, after Goldschmidt (1918). These habits are the same as the crystal forms of euhedral aggregates (*see* Figs. 20. 1-3).

An exact comparison of the Valanginian fauna of Sverdrup Basin with that of the Ulladulla Formation is impossible because of the scarcity of data provided by Brown (1925). Furthermore, the Permian fauna is too different to permit such a comparison.

General Conclusions: Euhedral Aggregates are Indices of Polar Water Environment

The suggestion made here that euhedral aggregates can be utilized as indices of polar and, in our particular case, Arctic conditions is confirmed by all the observations of the authors. It goes without saying that some of the observations summarized below (e.g. abundance of driftwood or depauperation of fauna), when considered individually, could be interpreted in other ways, but regarding all in combination they strongly favour the conclusions reached in this paper. The principal arguments and conclusions are summarized below:

1. Comparison with contemporary sediments of other regions. Euhedral aggregates are absent from all unquestionable tropical and boreal provinces of Valanginian time, including North Siberia (Zacharov, 1966) and East Greenland. Therefore, they must be products of extreme conditions which, under the circumstances could only represent the cold, polar extreme.

2. Comparison with results of various Australian workers obtained from study of the Upper Permian Ulladulla mudstone of the Permian Polar Province in New South Wales (a good summary provided by Brown, 1925). The closely similar, probably identical "glendonites" are associated there with glacial erratics and a cold water fauna. The neglect of "glendonites" in the international geological literature is symptomatic. The crystal aggregates of the glendonite-group are, indeed, absent everywhere, except for the polar regions. Therefore, they are only significant for these regions, which include the Permian of the southern hemisphere, the Middle Jurassic of Lena-Province, and the Valanginian and Albian of Sverdrup Basin and Spitzbergen.

3. The megafauna exhibits all characters of a cold water community. Namely it is characterized by a peculiar composition, paucity of species, and abundance of individuals combined with a gigantic size of some species and an absence of stenothermal benthonic species of the moderate belt (for instance oysters).

4. Coincidence of the areas of distribution of so far identified euhedral aggregates with those of the early Cretaceous polar belt as identified by the students of continental drift (e.g. Bullard, Everett and Smith, 1965; Dietz and Holden, 1970; Kemper, 1975).

5. An exceptionally wide distribution and abundance of driftwood presumably caused by a weakness or absence of biological decomposition (Kemper, 1975). Trees did not have to grow necessarily in the vicinity of the coast. They could have been transported by rivers over large distances. The presence of trees, and that of remains of rapidly swimming marine reptiles, in the units devoid of euhedral aggregates are therefore not an argument against the polar hypothesis advanced herein.

The cooling of seawater to below 0°C is postulated herein as the condition of growing of euhedral aggregates. Such as condition is feasible, either exclusively or principally, in those parts of the Arctic Ocean which existed as more or less secluded basins, but not in open ocean itself. The Sverdrup Basin is believed to have been such a semi-isolated marine basin. The present White Sea was already named as a contemporary example which is characterized by subzero temperatures the year around. What appears to be a recent example of euhedral aggregates was most appropriately found in the White Sea by fishermen from Arkhangel'sk (according to P.W. Jeremeyev; cited in David, *et al.*, 1905). These crystal aggregates are most probably identical with our euhedral aggregates described herein, as the replacement material has, in our opinion, no meaning for the interpretation of the origin of euhedra.

In the Sverdrup Basin, the youngest known Valanginian euhedral aggregates were observed approximately in the middle of *Prodichotomites* beds of the upper Valanginian (Kemper, 1975, Fig. 2). A warming trend set in the youngest upper Valanginian. This was paralleled by shallowing and reduction of size of the basin and therefore by an increase in size of the adjoining landmass. This development found its clearest expression in the deposition of Isachsen Formation (latest Valanginian-Barremian ? and early Aptian). The deposition of dark grey claystones with euhedral aggregates was then resumed in the Aptian-Albian Christopher Formation.

It is still impossible to account for the warming up episode that occurred during the time of deposition of Isachsen Formation during an apparently constant position of the Pole. However, this episode did not need to be pronounced. The formation of swamps and the deposition of peat (i.e. of coal measures of the Isachsen Formation) could take place at relatively low temperatures.

6. The growth mechanism of euhedra. Because of the evidence presented in the preceding sections and summarized above, the development of large, slowly growing crystals of sodium-sulphates from a watery solution is, in the writers' opinion, only conceivable in the environment of overcooled marine water. It is to be expected under such conditions, even if the actuogeological observations are not yet positively demonstrative (however *see* above).

References

Berggren, W.A. and Hollister, C.D.
1974: Paleogeography, paleobiogeography and the history of the circulation in the Atlantic Ocean. *In:* Studies in Paleo-Oceanography (W.W. Hay, ed.), Soc. Econ. Paleontol. Mineral.; Spec. Publ. No. 20, p. 126-186, 22 figs., Tulsa, Oklahoma.

Brown, I.A.
1925: Note on the occurrence of glendonites and glacial erratics in Upper Marine Beds at Ulladulla, N.S.W.; Proc. Linn. Soc. N.S.W., v. 50 p. 25-31, Sydney.

Bullard, E., Everett, J.E., and Smith, A.G.
1965: The fit of the continents around the Atlantic; R. Soc. Lond., Philos. Trans., Ser. A, v. 258, No. 1088, p. 41-51, 8 figs., London.

Conybeare, C.E.B. and Crook, K.A.W.
1968: Manual of Sedimentary Structures; Aust. Dept. Nat. Develop., Bur. Min. Res., Geol. Geophys., Bull. 102, 1-327, 5 figs., pl. 1-108, Canberra.

David, T.W.E., Taylor, T.G., Woolnough, W.G., and Foxall, H.G.
1905: Occurrence of the pseudomorph glendonite in New South Wales; Rec. Geol. Surv. N.S.W., v. 8, 1905, p. 161-179, 3 figs., pls. 24-30, Sydney.

Dietz, R.S. and Holden, J.C.
1970: The break-up of Pangea; Sci. Am., no. 223 (4), p. 30-41, 10 figs., San Francisco, California.

Goldschmidt, V.M.
1918 and 1922: Atlas der Kristallformen, v. 4 and 5 (text and plates), Heidelberg (Carl Winter).

Gordon, W.A.
1973: Marine life and ocean surface currents in the Cretaceous; J. Geol., v. 81, p. 269-284, 6 figs., Chicago.

Herman, Y. (Ed.)
1974: Marine geology and oceanography of the Arctic Seas; 1-397, Springer-Verlag, Berlin – Heidelberg – New York.

Hertling, H.
1953: Einführung in die Meeresbiologie; 1-215, 79 figs., Berlin (Duncker & Humblot).

Hey, M.H.
1962: Chemical Index of Minerals; Br. Mus. (Nat. Hist.).

Heywood, W.W.
1957: Isachsen Area, Ellef Ringnes Island, District of Franklin, Northwest Territories; Geol. Surv. Can., Paper 56-8, p. 1-36, 21 figs., 9 pls., 1 map, Ottawa.

Hintze, C.
1930: Handbuch der Mineralogie; v. 1 (3rd division, 2nd half: 1.3.2), p. 3657-4565, figs. 1197-1519, Berlin und Leipzig (W. de Gruyter).

Jeletzky, J.A.
1971: Marine Cretaceous biotic provinces and palaeogeography of Western and Arctic Canada: illustrated by a detailed study of ammonites; Geol. Surv. Can., Paper 70-22, p. 1-92, 20 figs., 11 tab., Ottawa.

Kay, M. (Ed.)
1969: North Atlantic geology and continental drift; Am. Assoc. Pet. Geol., Mem. 12, p. 1-1082, Tulsa, Oklahoma.

Kemper, E.
1975: Upper Deer Bay Formation (Berriasian-Valanginian) of Sverdrup Basin and biostratigraphy of the Arctic Valanginian; *in* Report of Activities, Pt. B, Geol. Surv. Can., Paper 75-1B, p. 245-254.

MacIntyre, W.G. and Platford, R.F.
1964: Dissolved calcium carbonate in the Labrador Sea; Can. Fisheries Res. Board J., v. 21 (6), p. 1475-1480, table, map.

Palache, C., Berman, H. and Frondel, C.
1951: Dana's System of Mineralogy, Vol. II, Seventh Edition; J. Wiley and Sons, Inc.

Pchelina, T.M.
1965: Stratigraphy and composition of the Mesozoic deposits in central Westspitzbergen; *In:* Sokolov, V.N. (Ed.): Geology of Spitzbergen, 1965, v. 1, p. 131-154 (in translation of National Lending Library), 1 fig., Leningrad.

Pettijohn, F.J.
1957: Sedimentary Rocks; Second edit., p. 1-718, 773 figs., 40 pls., New York (Harper & Brothers).

Philipsborn, H. von
1967: Tafeln zum Bestimmen der Minerale nach äusseren Kennzeichen; p. 1-319, Stuttgart (E. Schweizerbart).

Smith, A.G., Briden, J.C., and Drewery, G.E.
1973: Phanerozoic world maps; *In:* Organisms and Continents through Time (N.F. Hughes, Ed.), Spec. Papers in Palaeontology, No. 12, Pal. Assoc. Lond.), p. 1-42, 21 figs., London.

Test, B.J., Osipova, Z.V., and Sychev, V. Ja.
1962: Mesozoic deposits of the Zigansk area; Arbeiten des wissenschaftlichen Forschungs-Institutes für die Geologie der Arktis. Vom Ministerium für Geologie und Schutz der Bodenschatze, v. 131, p. 1-120, 36 figs., 4 tab., Leningrad (Russian).

Zacharov, V.A.
1966: Pozdneyurskie i rannemelovye dvustvorchatye mollyuski severa Sibiri i uslovija ich suschestvovanja (Otriad Anisomyaria); Akad. Nauk SSR, p. 1-189, 23 figs., 3 tab., 46 pl., Moskau (Russian).

PROJECT APPALACHIA (Reports 22-29)

Project 720097

G. B. Leech
Regional and Economic Geology Division

Project Appalachia seeks to develop and apply methods of combining information and concepts on regional geology, mineral deposits, and mathematics in computer-aided regional mineral resource appraisal. The Canadian Appalachian region was selected as the base for experiments because its geology is relatively well known and because of the number, variety, and distribution of its mineral deposits.

Design of the regional geological data base was the initial and critical step in the project. The objective was to represent Canadian Appalachian geology with a scope broad enough and in units suitable enough to test or reveal relationships between mineral deposits and features of their geological environment at genetic as well as empirical levels. The units had to be applicable through the range of information levels about the various parts of the Appalachians, had to represent the features of recognized or possible metallogenic significance, and had to be suitable for statistical analysis.

The ensuing legend has strong tectonic connotations. For example, among the basic master lithologic units for sedimentary strata, three are for carbonate lithologies and represent the facies characteristic of platformal, intermediate, and deep waters respectively. After selection of the 20 basic lithological units, came the selection of age parameters which, when combined with lithological units, made up "geological" or "litho-age" units. The ages and age-spans were selected to accord with Canadian Appalachian stratigraphy so that the mappable "stratigraphic packages", with their tectono-genetic implications, would be describable in terms of the legend. To avoid broad age-spans, e.g. – Lower Paleozoic, which are unsatisfactory for statistical use, age assignments were applied on a best judgment basis to several rock units whose actual ages were uncertain. Part of the data base is thus subjective, a geological hazard that is difficult to avoid.

Computerization of regional geological information involves quantification of two main factors: extent and location. This necessitates measuring the areas underlain by the various geological units and the lengths of linear features, and recording the positions of the areal, linear, and point data. This quantification of geological information is best done from maps. For geomathematical purposes, it is necessary that units of the data base be rateable at the "present or absent" level over the entire study region. Units that locally are distinguished separately but disappear elsewhere into grosser undivided ones are unsuitable. Hence, data bases derived from ordinary geological maps are limited by the lowest common denominator effect imposed by the least detailed maps from which input is required.

To avoid this limitation, and to enrich the data base with information not generally recorded on the available maps, a series of maps amended and augmented for the purposes of this project, was developed in a "precoding" stage. This required the advice of experienced geologists. These maps were used for quantification. The quantification was basically by point-counting methods (*see* Report 22, this publication). Automated digitization would be used more extensively now, but colour-scanning methods for measuring areal and linear features would require considerable redrafting of precoded maps.

The mineral information file is linked to the regional geological file by the location co-ordinate system and by litho-age unit terms. The host rocks of the deposits are described in the terms used in the source reference and again in terms of the litho-age units of Project Appalachia. Two separate mineral deposit classification schemes are used. One is basically morphological and objective. The other is basically genetic and therefore subjective but is, we hope, the result of as consistent an application of the chosen criteria as available data permit. It is a useful "handle", but not a necessary tool in analytical use of the file.

Data on about 1000 deposits and occurrences that contain Cu, Zn, and/or Pb are entered. About 900 additional deposits and occurrences of other mineral commodities are also recorded (identifier and location only), on the premise that they are components of the regional geology and that their presence and distribution may, in some instances, relate to environmental conditions that influenced the formation of the deposits of main interest. Similarly, the plan positions of Cu, Zn, and Pb deposits relative to igneous contacts and certain unconformities and other stratigraphic contacts are recorded. The rationale is that the data base input should not be guided exclusively by current metallogenic concepts if unsuspected relationships are to be revealed.

The initial experiments proved the feasibility of manipulating the complex data base to generate list printouts and map plots of individual items and combinations of components. These included experiments designed to reproduce the obvious, i.e. – to corroborate the correctness of the operational systems. Examples of ways in which data can be re-ordered and correlated appear in succeeding papers. These and associated papers contain examples of the kinds of statistical techniques used to process the data further. For simplicity of explanation, most of the examples involve only a single or a few geological variables, e.g. – the example of the derivation of a "probability" of occurrence of a mineral deposit, in which volcanic rock is the only geological parameter mentioned. Combinations of these techniques can be applied to successively more complex sets of geological data.

The earlier, larger experiments were based on the entire Canadian Appalachian region, using stepwise

multiple regression procedures applied to a linear mathematical model developed earlier by Agterberg for the Abitibi region. These led to concentration on one deposit-type in a single area, namely stratabound volcanic-associated massive sulphide deposits in the Eastern Townships of Quebec. The gross objective here was to "predict" (reproduce) the distribution pattern of the deposits in one half of the area using the other half as a data base. These experiments tested the relative leverages or sensitivities of various geological parameters, singly and in combination, and the effects of varying the control areas in a "mosaic" model (each unit areal cell of the control and target areas is a mosaic of litho-age units). Some of these experiments are noted in reports 23 and 24 of this publication.

These experiments led to application of individual statistical techniques to specific parts of the data base, as building blocks for eventual larger models. The principles of the techniques of classification analysis, cluster analysis, and canonical correlation analysis are described in reports 26, 27 and 28 of this publication.

At present, we are in a learning stage of communication between geology and mathematics. For example, trials of certain combinations of geological parameters have produced geologically meaningless results because of unexpected (by the geologists) statistical leverages in the mathematical models. The geologists were unaware of certain built in statistical assumptions and limitations in the mathematical models, whereas the mathematics part of the team were aghast at some of the "maybe" aspects of the geological models we were attempting to couple with them.

Transformation of descriptive geological models into mathematical ones should involve weighting factors that reflect the relative importances of the various geological features. The features are ranked qualitatively first e.g. - critical, important, subsidiary, possibly significant. Critical features are "yes-no" or "go-no-go" elements; the others receive absolute values. In practice, even qualitative ranking is uncertain for most geological models, especially in view of the likelihood of feed-back effects, i.e. - that the values of combinations are not simply the sums of the values of their parts. Quantitative weighting factors are therefore speculative, at best. Experiments in computer modelling stimulate better definition of conceptual models of geological processes.

22. A DATA BASE FOR MINERAL POTENTIAL ESTIMATION IN THE APPALACHIAN REGION OF CANADA

Project 720097

A. G. Fabbri, S. R. Divi, and A. S. Wong
Regional and Economic Geology Division

Introduction

This paper deals with the creation of the data base for Project Appalachia. A computerized data base for regional geological and base metal deposit information has been completed in order to express quantitatively various parameters which may directly or indirectly control the location of mineral deposits. Previous experience in file building for projects of this kind had been attained through work in other areas of Canada, mainly Precambrian terranes of the Canadian Shield, for which the geological input was of a more generalized nature (Agterberg *et al.*, 1972; Fabbri, 1975).

A large part of the initial data collection and coding for the project was performed by temporary personnel hired as part of the special governmental summer and winter assistance programs during the summer 1972 and winter 1972-1973, and through contracts mainly during summer 1973. These activities were closely supervised by permanent staff members. An initial unpublished documentation of the Project Appalachia data base was prepared after the completion of these activities (Fabbri *et al.*, 1973). In total, 50 man-months were spent on the project by the temporary personnel between June 1972 and August 1973, when most of the data collection and coding took place. Later, 16 man-months of assistance by casuals were needed to complete the file building phase and for further improvements.

The complexity of the Canadian Appalachian region is reflected by its great variety of lithologies. In addition to facies changes, the rocks exhibit features indicating polyphase deformation, metamorphism and intrusion. For this reason, the geological parameters were initially separated into three broad sets of "areal" parameters, namely, lithological, structural and metamorphic variables. The regional geological legend, reflecting different sedimentary, structural and metamorphic "regimes" was designed by W. H. Poole. Some "linear" parameters, e.g. selected geological contacts, were also categorized.

D. F. Sangster and R. V. Kirkham proposed the type and number of parameters to be quantified for deposits and occurrences of copper, lead and zinc, and for "indicators". For the purpose of this project, the term "deposit" was used to indicate (a) ore deposits for which base metal grade and tonnage figures were available (for production or reserves), or (b) deposits which could be considered as potentially exploitable although relatively little development work might have been done on them to date. The term "occurrence" was used instead of "deposit" to indicate ore deposits for which grade and tonnage figures were not available but for which a limited amount of development reflected the presence of copper, lead, or zinc mineralization. The term "indicator" was used for occurrences of commodities other than copper, lead, or zinc, which, although not necessarily having any recognizable genetic relation to the base metal deposits considered, might nevertheless have some bearing on the larger metallogenic environment.

The regional geological information was collected and coded on the basis of cells according to a network covering the entire Appalachian region. On the other hand, the base metal deposit information was collected for points representing the locations of the deposits. Because of this difference in method of location, two separate computer files have been constructed for the project which are the regional geological file and the mineral deposit file, and were designed to be complementary and are linked through parameters for location and also by means of litho-age units.

Regional Geological File

In total, thirteen basic lithological units were defined to represent sedimentary and volcanic rocks, and six for intrusive rocks. Twenty-two age units were also defined covering the time span of the "stratigraphic packages" that occur in the Appalachians. As not all lithologies are represented in each age unit, only 79 "litho-age units" resulted (*see* Table 22.1). In addition, these parameters were quantified: four classes of structural parameters (intense, intermediate, low and undeformed), and four grades of regional metamorphism (amphibolite facies; biotite, chlorite and subchlorite zones (Table 22.1)). The linear parameters coded include selected stratigraphic contacts, selected intrusive contacts, selected unconformities, and iron-formations.

These seven sets of geological parameters were initially compiled on 82 "base maps" selected to cover the entire Appalachian region. The scale is 1 inch to one and two miles for maps of Quebec, Nova Scotia and New Brunswick, and 1 inch to four miles of Newfoundland. As most of the base maps did not contain all of the geological information available for the area covered, and the geological legend of these base maps often could be directly correlated with the geological parameters selected for coding, it was necessary to acquire and compile additional information for each base map from other sources. Such additional detailed information was acquired from published and unpublished material and in consultation with Geological Survey geologists and other experts with a personal knowledge of the base map area. The uneven distribution of the quality and quantity of the information for the region as a whole required a variable amount of generalization and careful extrapolation of some types of information across base map boundaries. These 82 base maps and the information entered before coding have been kept as a

Figure 22. 1.

Two data blocks for the regional geological file of Project Appalachia: (a) Mainland block (2555 cells) and (b) Newfoundland block (1409 cells). In total, there are 3964 cells in the Appalachian region.

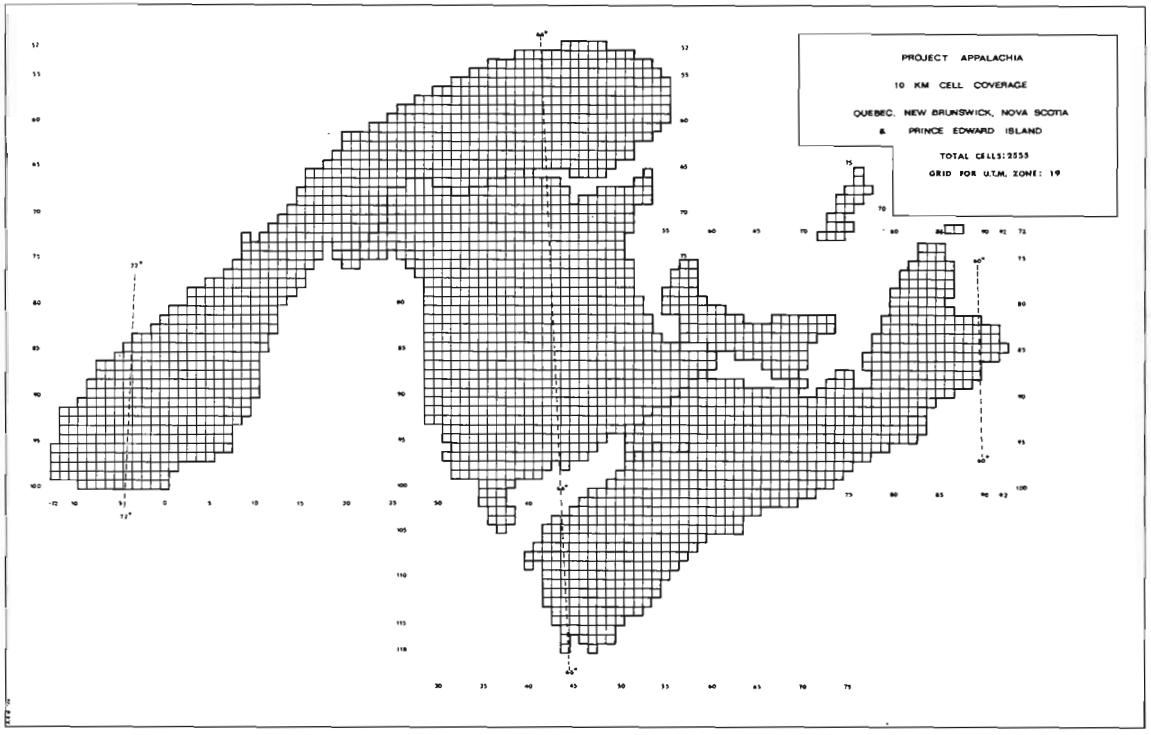

a

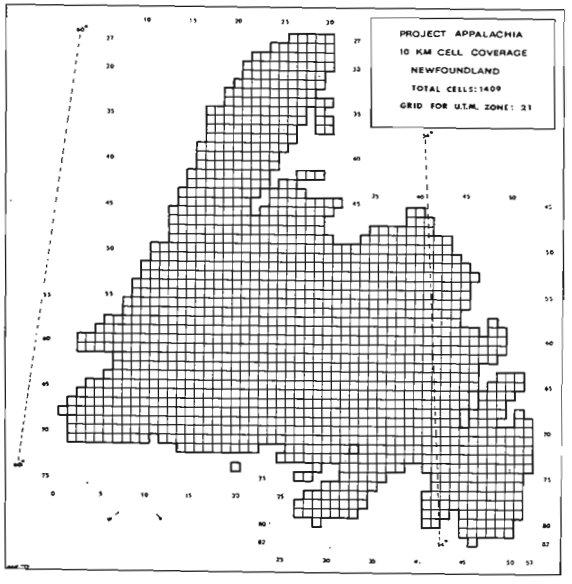

b

documentary file. They have been consulted frequently during the interpretation of results derived by statistical analysis of the data in the geological data file.

The unit record selected for coding the regional geological parameters was a cell of 10 by 10 km, the size of the Universal Transverse Mercator Grid (Fig. 22.1). A unit cell of this size is convenient for expressing, in quantitative terms, the regional geological patterns in the Appalachian region. The regional geological parameters have been quantified from the base maps for each of the 3964 unit cells occurring in the study area.

On a global scale, the UTM co-ordinate system consists of 60 zones each 6^{o} of longitude wide, but the grid system for a given zone can be extended across adjacent zones on both sides. This has been used to let the data block for a specific zone extend into other zones in areas where it was undesirable to interrupt the continuity of the geological and geographical pattern. For the Mainland Block (Fig. 22.1a), the grid of UTM zone 19, has been extended into zone 18 in Quebec, and into 20 to the east of the 66th meridian. For the data block of the Island of Newfoundland (Fig. 22.1b), zone 21 was extended into zone 22 east of the 54th meridian.

The position of a point in the UTM system is specified by zone number, by easting (metres east of the standard meridian of the zone) and by northing (metres north of the equator). For convenience, individual cells have been labelled according to the number systems shown in Figure 22.1. The UTM co-ordinates of the centre of the cell labelled "O,O" are 305 000 m E and 5 985 000 m N for the two data blocks of Mainland (zone 19) and Newfoundland (zone 21). The centre of a cell labelled "(x, y)" has easting equal to (10x + 305) km, and northing equal to (5985 - 10y) km.

Litho-age units, structural and metamorphic parameters were coded by estimating the areas occupied by each variable in individual 10-km cells by point counting. Use was made of graticules drawn on transparent film by means of which a cell was either subdivided into 400 subcells of 500 m on a side, or represented as 400 points corresponding to the midpoints of these subcells, Fabbri (1975). Cumulative counts, totalling 400 per cell, were entered on specially designed coding forms for key punching. Linear parameters such as lengths of contacts were measured using dividers and map scales.

A full record for a cell consists of its co-ordinates (Fig. 22.1) followed by a string of numbers (no more than 3 digits) for each of the following geological parameters: 79 litho-age units, 2 parameters for Quaternary and water covered areas; 4 structural parameters; 4 metamorphic parameters; 20 granitic contacts of different types; 6 parameters for the length of particular unconformities, 1 parameter for the length of the Windsor-Horton contact; and 4 parameters on the length of iron-formations. In addition, the record for each cell includes identification of the base map on which the point counting was carried out and of other sources of information used during the geological compilation for that cell. For convenience, the regional geological file is being kept available on two separate sets of magnetic tapes, one for mainland Appalachia and one for Newfoundland. Other computer files can be derived from these tapes for specific data management and computing purposes.

Areas underlain by each of the lithologic units, and structural and metamorphic parameters are expressed in Table 22.1 as percentages of the entire area of compilation (3964 x 100 = 396 400 km^2). Sedimentary rocks (58.20 per cent), volcanic rocks (7.75 per cent), and plutonic rocks (16.12 per cent) cover 82.06 per cent of the area with the remainder of the study area (17.75 per cent) occupied by drift and water.

Mineral Deposit File

Selected information on 180 base metal deposits (with tonnage and grade figures), 844 base metal occurrences, and 695 indicators, has been entered in the second type of file (Mineral Deposit File) which is complementary to the file for regional geological data. The parameters coded for the mineral deposit file are shown in Table 22.2. Seven groups of data items have been distinguished: (a) identification, (b) location, (c) geological position in terms of distances from specific intrusions and unconformities, (d) immediate host rocks, (e) mineralogy, (f) classification according to morphologic and genetic types, and (g) tonnage of each of the commodities copper, lead, and zinc. Information of this last group on tonnages could not be coded for occurrences. Only groups on identification and location were coded for indicators.

Individual data items are shown by sequence number in Table 22.2 and by means of the abbreviated names used for computer file management. More details for the coded parameters will be given, followed by a survey of the contents of the file.

Each deposit is identified (Items 1-6, Table 22.2) by number, name, exploitation status, listings of the commodities in production and in reserves, and other commodities present.

Location data (Items 7-15) include Province, National Topographic System (NTS) designation, latitude and longitude, UTM co-ordinates, and the grid co-ordinates of the cell containing the deposit have been coded. For some deposits, the distance from an intrusive contact or an unconformity is coded (Data Items 16-21).

In recording host rocks (Items 22-24), the litho-age terms used are those used in the regional geological file. A distinction is made between "map host" and "host rocks" of a deposit; the former is the litho-age unit shown at the deposit site on the map used in coding the regional geology; and the latter is the specific litho-age unit or units that enclose the deposit. Map host may differ from host rock; e.g., when the deposit is in an area designated on the map as "basic volcanics with minor acid volcanics" and it is the acid volcanics, which are not distinguished separately on the map, that contain the deposit. The mineralogy entry (Item 25) consists of a list of up to 20 minerals that are present in the ore or in the gangue.

Each deposit is classified according to two separate sets of terms (Items 26-27). The first classification is in terms of morphology and geometric relations to

Table 22.1

Definitions and frequencies of litho-age units selected for coding geological information from maps in the Appalachian region. Frequencies of occurrences of areas covered by structural and metamorphic parameters and their definitions are shown

AGE UNITS	LITHO-UNITS																				
	Sedimentary and Volcanic Rocks													Plutonic Rocks						Drift	Water	TOTAL in %
Period Series Stage	Pred	Cp	Pcred	Pc	O	Ci	Pgngy	Cd	Pel	Gw	Va	V	Vb	Gr	GNA	GrGNA	Um	GD	Agr	QDAU	W	
																					G81	15.23
Quaternary																				G80		2.52
Triassic	G01												G02									0.68
Post-Visean	G04						G03						G05									11.26
Visean	G06		G08	G07																		1.50
Frasnian-Tournaisian	G10						G09				G11	G12	G13									2.55
Devonian														G14	G15							10.67
M. Devonian	G16											G17										0.34
L. Devonian						G18	G23		G22		G21	G19	G20									7.82
Silurian					G27		G26		G25	G24	G28	G29										1.79
U. Silurian	G33					G30			G32	G36		G34	G35									2.14
M. Silurian	G38				G40	G31	G37															0.49
L. Silurian	G43					G39	G42		G41		G44	G46										2.35
Pre-Silurian														G51			G52	G53	G54			3.26
U. Ordovician								G50														1.57
M.-U. Ordovician									G45	G47	G49	G48										7.14
M. Ordovician		G57			G55				G56													1.73
L. Ordovician		G59							G58	G60	G61	G63	G62									12.16
Cambrian		G66			G68				G64	G65	G70		G67									5.94
Latest Hadrynian					G69																	0.02
Late Hadrynian	G72						G71		G75		G73	G74										6.28
Early Hadrynian		G76			G77				G78													0.18
Pre-Early Hadrynian																G79						2.39
TOTAL areas in Appalachian region in %	9.76	1.76	1.19	.05	1.55	1.68	9.42	1.57	13.36	17.85	3.32	3.08	1.35	12.47	0.82	2.39	0.26	0.36	0.002	2.52	15.23	100.0

Structural (S) and Metamorphic (M) parameters		Areas covered in % of total
Intense	S1	15.78
Intermediate: Dips >50°	S2	29.65
Low : Dips 50°-20°	S3	13.92
"Undeformed": Dips <20°	S4	22.90
Amphibolite Facies	M1	5.39
Biotite Zone	M2	4.10
Chlorite Zone	M3	14.23
Sub-chlorite - Unmetamorphosed	M4	58.54

ABBREVIATIONS

Pred =Proto-sandstone, pelite, conglomerate; dominantly red.
Cp =Carbonate; platform type.
Pcred=Proto-sandstone, pelite, conglomerate, and carbonate, gypsum, anhydrite, salt; dominantly red.
Pc =Proto-sandstone, pelite, conglomerate, and carbonate, gypsum, anhydrite, salt; dominantly green-grey, grey.
O =Orthoquartzite, siltstone, conglomerate; clean, marine transgression.
Ci =Carbonate; intermediate, "dirty", mainly Silurian-Devonian.
Pgngy=Proto-sandstone, pelite, conglomerate; dominantly green-grey, grey.
Cd =Carbonate, thin bedded argillaceous limestone; deep water.
Pel =Pelite (marine) with or without minor siltstone and carbonate.
Gw =Greywacke-pelite, turbidite; deep water.
Va =Acid volcanics greater than 50%.
V =Basic volcanics; minor acid volcanics.
Vb =Basic volcanics; no reported acid volcanics.
Gr =Granite.
GNA =Gabbro, norite, anorthosite.
GrGNA=Granite, gabbro, norite, anorthosite.
Um =Ultramafic.
GD =Gabbrodioritic.
Agr ="Associated" granite.
QDAU =Quaternary, drift, alluvium, unmapped.
W =Water-covered areas where geology cannot be extrapolated.

Table 22.2

Sequence number, name and description of data items used in Project Appalachia mineral deposit file. Same sequence numbers are used in Figure 25.2 of Wong, Chung and Fabbri (this publication, report 25)

No.	Data Item Name	Description	Group
1	MDNO	Deposit number.	(a) Identification
2	NAME	Name of the deposit.	
3	STATUS	Status of the deposit.	
4	PROCOM	List of up to 8 commodities in production.	
5	RESCOM	List of up to 8 commodities in reserves only.	
6	OTHCOM	List of up to 8 other commodities.	
7	PROVINCE	Political province of the deposit.	(b) Location
8	NTSNO	National Topographic System (quadrangles).	
9	LATITUDE	Latitude in degrees, minutes and seconds.	
10	LONGITUDE	Longitude in degrees, minutes and seconds.	
11	UTM	Universal Transverse Mercator grid zone.	
12	NORTHING	UTM northing in metres.	
13	EASTING	UTM easting in metres.	
14	X	X-co-ordinate of 10-km cell.	
15	Y	Y-co-ordinate of 10-km cell.	
16	DINT	Distance (metres) to nearest intrusion.	(c) Geological position
17	GVB	Intrusive litho-age unit.	
18	DUNC	Distance (metres) to Carboniferous unconformity.	
19	UVB	Parameter of Carboniferous unconformity.	
20	DCNT	Distance (metres) to Windsor-Horton contact.	
21	CVB	Parameter of Windsor-Horton contact.	
22	MAPHOST	Litho-age unit at deposit location.	(d) Host rocks
23	HROCK	Litho-age unit hosting the ore.	
24	RKNAME	Names of the host rocks.	
25	MINERALS	List of up to 20 minerals present in the ore or in the gangue.	(e) Mineralogy
26	NATDEP	Morphologic nature of the deposit.	(f) Classifications
27	GEOGRP	Genetic geological grouping of the deposit.	
28	TONGRD	Tonnage and grade of the 6 commodities.	(g) Size
28a	COM	Commodity described in the order of Cu, Pb, Zn, Ag, Au and Ni.	
28b	TONMIL	Total tons of ore produced.	
28c	PGRADE	Grade of production (% or oz/ton).	
28d	PMETAL	Short tons or troy ounces of metal produced.	
28e	FYEAR	First year of production.	
28f	LYEAR	Last year of production.	
28g	TONRES	Total tons of ore reserves.	
28h	RGRADE	Grade of reserves (% or oz/ton).	
28i	RMETAL	Short tons or troy ounces of metal in reserves.	
28j	RYEAR	Year of reserves estimation.	
28k	TMETAL	Total short tons or troy ounces of metal in production and reserves.	
28l	TGRADE	Average grade of ore in production and reserves.	

is in terms of morphology and geometric relations to enclosing rocks; the second is genetic. This part of the file building was carried out by economic geologists with knowledge of the deposits.

The content ("Tonnage", Item 28) of the deposits is expressed in terms of estimated tonnages and grades of "ore" and quantities of contained metals. Cumulative production, reserves, and cumulative production plus reserves are expressed separately for the commodities copper, lead, zinc, silver, gold and nickel. The reserve figures have been obtained from published material or other public sources of information. For each deposit, a single tonnage reserve value with corresponding average grade value was entered into the file for each metal contained in the ore, rather than using separate categories of reserves. The latter have been recorded in a documentary file if the reserves had been categorized for a deposit. For mines that contain a number of separate orebodies, separate figures were assigned to each of these orebodies.

The mineral deposit file is linked to the regional geological file through the UTM cell co-ordinates and also through the host rock designations of the individual deposits. The latter is possible because the host-rock part of the mineral deposit file and the regional geological file use the same lexicon for litho-age units, making it possible to rate various geological formations according to the types and amounts of mineralization known to occur in them.

A number of selective retrievals are shown in Table 22.3, which contains counts or frequencies of all deposit records of particular types. The purpose of Table 22.3 (a and b) is to illustrate some of the ways in which individual categories of data in the file can be cross-correlated. In Table 22.3a, the geological grouping (subjective genetic classification) of deposits is compared with their morphological classification (upper part of table), and also with the litho-age classifications of their host rocks (lower part of table).

In Table 22.3b, many of the parameters of the deposits are intercorrelated. The top line of figures represents totals of various deposits in the file classified in different categories, e.g. 39 are in Quebec, 74 have the status of past-producers, 15 are skarns, 28 are "size A" in terms of copper, etc. The remainder of this part of the table can be read in the manner similar to a mileage chart for road maps. For example, of the 39 deposits in Quebec, 23 are past-producers (PP) and 7 are skarn type deposits (SK). The size ranks A to E in Table 22.3b have been arbitrarily chosen for display purposes.

Set theory, as remarked by Agterberg (1974, p. 153), is important because it uses a logic which is compatible with that used for the programming of digital computers. The logic of Boolean algebra applies very well to the problem of selective retrieval of information stored in large geological data banks. Elementary set theory notations will now be used to facilitate the formulation of the retrievals presented in Table 22.3 (a and b).

Let T be defined as the set of all 180 records of deposits in the file. If S represents a subset of T, also written as $S \subset T$, n(S) is defined as the number of elements contained in S or in the cardinal of S. The following examples (1 to 4) contain definitions of subsets and also illustrate the calculation of frequencies of occurrence of events by random selection of records out of T with n(T) = 180. The frequencies derived in these examples correspond to the numbers (1) to (4) in Table 22.3b.

(1) $NB = \{x \in T:$ Province of x is New Brunswick$\} \subset T$, where x indicates an arbitrary element, and $\in$ means "belongs to". In Table 22.3b, it is shown that n(NB) = 72. Hence the relative frequency of deposits in New Brunswick is (72/180) = 0.40 or 40 per cent. Likewise, $R = \{x \in T:$ Status of x is Reserves$\}$ has n(R) = 79, with relative frequency of (79/180) = 0.44.

(2) $NB \cap R = \{x \in T: x \in NB$ and $x \in R\} = \{x \in T:$ Province of x is New Brunswick and Status of x is Reserves$\}$. Here, $\cap$ means "intersection" of the two sets which, in computer terminology, is equivalent to the Boolean .AND.. It follows that $n(NB \cap R) = 48$, with relative frequency (48/180) = 0.27.

(3) $CuA \cup CuB = \{x \in T: x \in CuA$ or $x \in CuB\} = \{x \in T:$ Size Cu of x is A or Size Cu of x is B$\}$. Here, $\cup$ means "union" of the two sets which is equivalent to the Boolean .OR.. Since the subsets CuA and CuB are disjoint with $n(CuA \cap CuB) = 0$ (Table 22.3), $n(CuA \cup CuB) = 28 + 48 = 76$. The relative frequency of the combined event is therefore (76/180) = 0.42.

(4) $VMS = \{x \in T:$ Geological Grouping of x is Volcanogenic Massive Sulphide$\} \subset T$, with cardinal n(VMS) = 108, and relative frequency (108/180) = 0.60. Let VMS^c represent the subset of all deposits which are not volcanogenic massive sulphides, where the superscript ^{c} means "complement". Then, from Table 22.3b, it follows that $n(VMS^c) = 180 - 108 = 72$, with relative frequency (72/180) = 0.40.

Some general conclusions concerning the content of the mineral deposit file which can be drawn from Table 22.3 (a and b) are: (1) most deposits in the Appalachian region are either past producers (74) or deposits with reserves only (79). There are also some potential deposits without estimated reserves which are believed to contain considerable mineralization. (2) The majority of deposits in the file are of the volcanogenic massive sulphide type; no deposits were classified as magmatic in Nova Scotia or Newfoundland. (3) Of 180 deposits, 127 have tonnage and grade figures for copper, 66 for lead, and 78 for zinc. (4) Size differences for the combined presence of Cu-Pb, Cu-Zn, and Pb-Zn, reflect progressively increasing grades going from copper to lead and zinc. (5) A comparison of the two classifications of deposits called "Nature of Deposit" and "Geological Grouping of Deposit" in Table 22.3a shows that most volcanogenic massive sulphide deposits are concordant massive, and that the skarn deposits are discordant irregular. (6) Finally, the genetic classification of the deposits, and their host rocks combined into 17 litho-age groupings in Table 22.3a indicates that most (84) volcanogenic massive sulphide deposits occur in Ordovician volcanic rocks, skarn deposits occur in various pre-Carboniferous

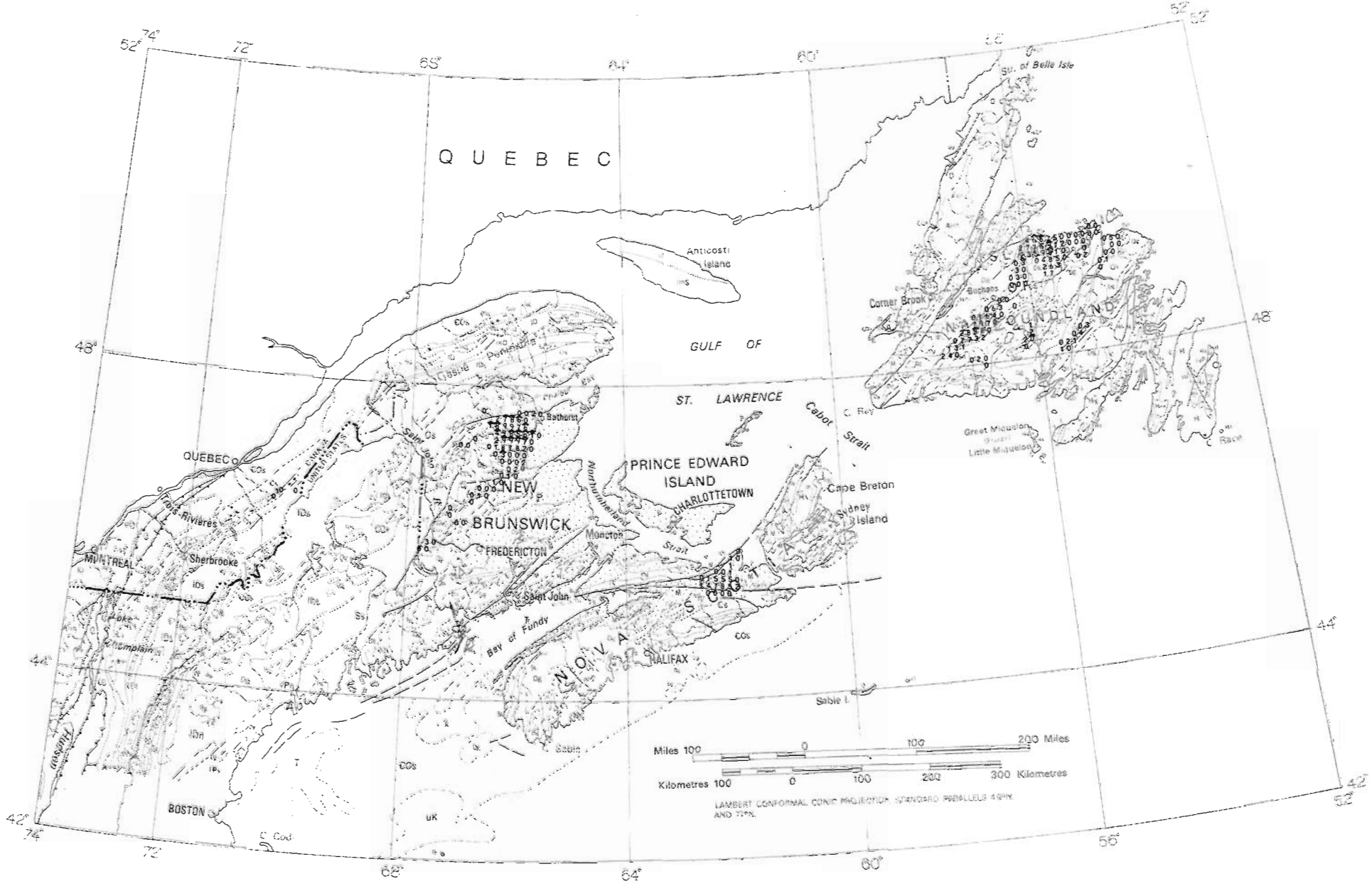

Figure 22. 2. Distribution of Middle-Upper Ordovician volcanic rocks in the Appalachian region. Cells with volcanogenic massive sulphide deposits are indicated by hats.

Table 22.3 (a and b)

Counts or frequencies of occurrences of deposits (records) in the Project Appalachia mineral deposit file, classified according to the values of main parameters coded. Numbers (1) to (4) in b refer to set theory expressions used in the text.

PROVINCE STATUS

QUE	NB	NS	NFD
39	72(1)	16	63

PP	P	R	PT
74	14	79(1)	13
23	4	12	-
10	6	48(2)	8
7	-	7	2
34	4	12	3

GEOL. GROUPING

SK	VMS	VR	SD	MG	UD
15	108(4)	31	13	7	6
7	21	2	5	2	2
5	41	17	1	5	3
2	1	6	6	-	1
1	45	6	1	-	-
-	52	13	7	-	2
3	10	1	-	-	-
9	45	9	6	7	3
3	1	8	-	-	1

Cu SIZE

A	B	C	D	E
28	48(3)	42	7	2
7	12	11	-	2
9	17	16	5	-
3	5	1	-	-
9	14	14	2	-
19	22	15	2	-
-	1	8	2	2
9	25	19	3	-
*	*	*	*	*
1	3	4	-	2
17	33	20	7	-
6	3	3	-	-
1	6	2	-	-
1	3	2	-	-
2	-	1	-	-

Pb SIZE

A	B	C	D	E
4	25	24	11	2
-	7	1	-	-
2	11	14	6	1
-	-	3	1	1
2	7	6	4	-
2	11	9	3	-
-	-	2	5	1
2	14	13	3	1
*	*	*	*	*
-	-	-	-	-
-	17	19	10	1
4	4	3	-	-
-	2	2	1	1
-	-	-	-	-
-	2	-	-	-
4	1	-	-	-
-	14	13	-	-
-	1	9	7	-
-	-	-	3	1
-	-	-	-	-

Zn SIZE

A	B	C	D	E
3	17	38	17	3
-	6	7	-	-
2	4	20	8	3
-	1	3	2	-
1	6	8	7	-
1	11	11	3	1
-	-	2	4	2
2	6	25	10	-
*	*	*	*	*
-	-	1	1	-
-	9	31	12	3
3	3	3	2	-
-	2	2	2	-
-	2	-	-	-
-	1	1	-	-
-	4	2	-	-
-	7	21	2	-
-	2	9	10	-
-	-	-	2	3
-	-	-	-	-
3	-	-	-	-
-	11	11	-	-
-	1	18	5	-
-	-	-	9	2
-	-	-	-	1

GEOL. GROUPING OF DEPOSITS

		SK	VMS	VR	SD	MG	UD	Total	
NATURE OF DEPOSIT	CM	-	79	-	2	1	-	82	concordant massive
	CD	3	2	-	10	3	2	20	concordant disseminated
	CU	-	6	-	-	-	-	6	concordant unclassifiable
	DSV	-	1	17	-	-	-	18	discordant simple vein
	DVS	-	-	11	-	-	1	12	discordant vein sets, stock (work)
	DI	9	-	-	-	-	-	9	discordant irregular
	DU	2	3	1	-	-	-	6	discordant unclassifiable
	UK	1	17	2	1	3	3	27	unknown setting
	Tot.	15	108	31	13	7	6	180	Total No. of deposits in file
LITHO-AGE GROUPING FOR HOST ROCKS	T	-	-	2	-	-	-	2	Triassic rocks
	CS	-	-	1	6	-	-	7	Carboniferous sediments
	CV	-	-	3	-	-	-	3	Carboniferous volcanics
	DIT	-	-	1	-	5	-	6	Devonian intrusive
	LDS	3	-	-	-	-	2	5	Lower Devonian sediments
	LDV	1	1	-	-	-	-	2	Lower Devonian volcanics
	SS	1	-	2	-	-	1	4	Silurian sediments
	SV	2	17	1	-	-	1	21	Silurian volcanics
	PSIT	1	-	1	-	2	1	4	Pre-Silurian intrusives
	MUOS	4	-	11	2	-	1	18	Middle & Upper Ordovician sediments
	MUOV	-	46	-	-	-	1	47	Middle & Upper Ordovician volcanics
	LOS	1	-	-	1	-	-	2	Lower Ordovician sediments
	LOV	-	38	3	-	-	-	41	Lower Ordovician volcanics
	CBS	1	-	-	3	-	-	4	Cambrian sediments
	CBV	-	5	-	-	-	-	5	Cambrian volcanics
	HS	1	-	1	1	-	-	3	Hadrynian sediments
	HV	-	1	5	-	-	-	6	Hadrynian volcanics

(a)

Definition of selected parameters for deposits

QUE	Quebec	
NB	New Brunswick	
NS	Nova Scotia	
NFD	Newfoundland	
PP	past producer	
P	producer	
R	reserves only	
PT	potential deposit (no size estimate)	
SK	skarn, contact metasomatic	
VMS	volcanogenic massive sulphide (includes alteration)	
VR	vein and replacement (exclusive of skarn).	
SD	sedimentary Pb-Zn & Cu	
MG	magmatic	
UD	undifferentiated	
Cu size	A	between 1 and 999 short tons of metal
	B	.....1000 and 9999.....
	C	....10000 and 99999.....
	D	...100000 and 999999.....
	E	over 1000000 short tons of metal
Pb size	A	
	B	
	C	see classes for Cu above
	D	
	E	
Zn size	A	
	B	
	C	see classes for Cu above
	D	
	E	

(b)

Table 22.4

Selected retrieval from the mineral deposit MARS VI computer file for all deposits of the set $(VMS \cap G^{48}) \cup (VMS \cap G^{49})$ for volcanogenic massive sulphide deposits in undivided Middle and Upper Ordovician volcanic rocks. PROCOM refers to commodities produced, RESCOM to commodities in reserves only; and OTHCOM to commodities present in the mineralization, but without tonnage and grade figures.

X	Y	NAME OF DEPOSIT	PROCOM	RESCOM	OTHCOM	PROVINCE
38	72	THIRD PORTAGE LAKE (RESTIGOUCHE M) (GOWGANDA)		ZNPBAG		NEW BRUNSWICK
39	72	MURRAY BROOK (KENNCO)		PBZNCUAUAG		NEW BRUNSWICK
39	73	DEVIL'S ELBOW MINES LTD.		CU	PBZNCO	NEW BRUNSWICK
40	71	ANACONDA CARIBOU (CARIBOU-CHALEUR MINES LTD.)	CUZNPBAGAU			NEW BRUNSWICK
40	74	HALF MILE LAKE (BAIE COPPER),(CONWEST)		ZNPBCU	AUAG	NEW BRUNSWICK
40	74	HALF MILE LAKE (KEEVIL MINING GROUP),(TECK)		ZNPBCUAG	AU	NEW BRUNSWICK
40	74	LITTLE BALD MOUNTAIN (TEXAS GULF)		ZNPBCU	AUAG	NEW BRUNSWICK
40	76	CHESTER (CLEARWATER) MINES LTD. (1)		CUPBZN	AGCDBI	NEW BRUNSWICK
40	76	CHESTER (CLEARWATER) MINES LTD. (2)		CU		NEW BRUNSWICK
41	71	NEW CALUMET (ORVAN BROOK) MINES LTD.		ZNPBCUAUAG		NEW BRUNSWICK
41	71	ROCKY TURN		ZNPBCUAUAG		NEW BRUNSWICK
41	73	CANOE LANDING (CLEARWATER NO.3 PROPERTY)		CUPBZNAGAU		NEW BRUNSWICK
41	73	WEDGE MINE	CUAUAG		PBZN	NEW BRUNSWICK
41	74	HEATH STEELE (LITTLE RIVER) MINES LTD. "C"-6		ZNCUPBAGAU		NEW BRUNSWICK
41	74	HEATH STEELE (LITTLE RIVER) MINES LTD. "C"-4		ZNCUPBAGAU		NEW BRUNSWICK
41	74	TOMOGONOPS (STRATMAT 61,MAIN ZONE)		PBZNCUAG		NEW BRUNSWICK
41	74	TOMOGONOPS (STRATMAT 61,WEST ZONE)		CU	PBZN	NEW BRUNSWICK
42	71	ANACONDA (ARMSTRONG "A" ZONE)		PBZNCUAUAG		NEW BRUNSWICK
42	71	ANACONDA (ARMSTRONG "B" ZONE)		ZNPBCUAUAG		NEW BRUNSWICK
42	73	MOSHER "C" (NEPISIGUIT "C")		ZNPBCUAG		NEW BRUNSWICK
42	73	NEPISIGUIT "A"		PBZNCUAG		NEW BRUNSWICK
42	73	NEPISIGUIT "B"		PBZNCUAG		NEW BRUNSWICK
42	73	NINEMILE BROOK (SMITH OR SMYTH GROUP)		ZNAGAU		NEW BRUNSWICK
42	74	HEATH STEELE (LITTLE RIVER) MINES LTD. 'C'5/6	ZNCUPBAGAU			NEW BRUNSWICK
42	74	HEATH STEELE (LITTLE RIVER) MINES LTD. "A"	ZNCUPBAGAU			NEW BRUNSWICK
42	74	HEATH STEELE (LITTLE RIVER) MINES LTD. "B"-1	ZNCUPBAGAU			NEW BRUNSWICK
42	74	HEATH STEELE (LITTLE RIVER) MINES LTD. "B"-2	ZNCUPBAGAU			NEW BRUNSWICK
42	74	HEATH STEELE (LITTLE RIVER) MINES LTD. "B"-3	ZNCUPBAGAU			NEW BRUNSWICK
42	74	HEATH STEELE (LITTLE RIVER) MINES LTD. "B"-4	ZNCUPBAGAU			NEW BRUNSWICK
42	74	HEATH STEELE (LITTLE RIVER) MINES LTD. "C"-1	ZNCUPBAGAU			NEW BRUNSWICK
42	74	HEATH STEELE (LITTLE RIVER) MINES LTD. "C"-5	ZNCUPBAGAU			NEW BRUNSWICK
42	74	HEATH STEELE (LITTLE RIVER) MINES LTD. "D"	ZNCUPBAGAU			NEW BRUNSWICK
42	74	HEATH STEELE (LITTLE RIVER) MINES LTD. "E"		ZNCUPBAGAU		NEW BRUNSWICK
43	72	BRUNSWICK NO. 12 (ANACON-LEADRIDGE)	CUZNPBAG			NEW BRUNSWICK
43	73	AUSTIN BROOK		PBZNAGFE	CUCDSBCOBISN	NEW BRUNSWICK
43	73	BRUNSWICK NO.6	ZNPBCUAGFE		SNCDSBCOBI	NEW BRUNSWICK
43	73	PABINEAU RIVER (HEADWAY RED LAKE G.M.L.)		CUAGZNPB		NEW BRUNSWICK
43	74	CAPTAIN MINES LTD.		CUAGAU	COPBZNBISN	NEW BRUNSWICK
44	73	MIDDLE LANDING (NEW LARDER U) (ANACON LEAD)		ZNPBCUAG		NEW BRUNSWICK
18	61	TULK'S BROOK		ZNPBCU		NEWFOUNDLAND
26	53	GULLBRIDGE MINES LTD.	CU		PBZN	NEWFOUNDLAND
26	63	GREAT BURNT LAKE		CU		NEWFOUNDLAND
28	50	CRESCENT LAKE MINE	CUAG			NEWFOUNDLAND
29	50	PILLEYS ISLAND MINE	CU		ZN	NEWFOUNDLAND
30	51	LOCKPORT MINE		CU		NEWFOUNDLAND
30	52	NORANDA PROPERTY		ZNCU	AGAUPB	NEWFOUNDLAND

--- END OF RETRIEVAL ---

rocks, and vein and replacement deposits are not restricted to any particular litho-age grouping. Of the 180 deposits, Ordovician and Silurian volcanic rocks, and Middle and Upper Ordovician sedimentary rocks host 127 deposits; Ordovician rocks singly host 180 deposits; and all volcanic rocks host 127 deposits.

Considerations of this type, which at times appear elementary, are important for understanding the content of the data base, as well as for editing, planning, and statistical modelling. They are important because, by feedback, they can generate redefinitions of parameters for further coding in order to produce an improved problem-oriented data base.

An Example of Further Usage of the Data

The regional geological data bank created for Project Appalachia can be considered as a numerical expression of a geological compilation map. All features occur as numbers in the data bank so that they can be manipulated by means of the digital computer and used for statistical analysis. The main purpose of a statistical analysis of this type is to compare patterns of different parameters which can be extracted from the data bank in order to detect a correlation between patterns of combinations of parameters with patterns of various types of mineralization. For example, a map (Fig. 22.2) shows the combined areas of outcrop of acid and intermediate volcanics of undivided Middle and Upper Ordovician age (litho-age units G49 and G48 in Table 22.1). Using set notation, let G be the set of all cells in the regional geological file and $G_k = \{x \in G:$ nonzero value of k-th litho-age unit of $x\}$, for $k = 1, 2, \ldots, 81$. The set of all cells with litho-age units G48 and G49 in the file can be expressed as $G_{48} \cup G_{49}$. The total number of these cells is $n(G_{48} \cup G_{49}) = n(G_{48}) + n(G_{49}) - n(G_{48} \cap G_{49}) = 186 + 59 - 35 = 210$.

This map in digital form consists of single digit numbers expressing the percentage of each cell occupied by these volcanic rocks (0 = 1-9%, 1 = 10-19%, 2 = 20-29%, etc.) and plotted by the EAI-430 flat bed plotter for display purposes on a geological map (GSC Map 1250A, scale 1:5 000 000). In Figure 22.2, the cells containing one or more volcanogenic massive sulphide deposits

hosted by Middle-Upper Ordovician basic volcanic rocks with minor acid (G48) and acid (G49) volcanic rocks are indicated by hats. For routine purposes, similar data displays can be produced at less cost on the line-printer of the computer.

Names and some other parameters of the deposits within these cells were retrieved from the deposit file by searching for the set $(VMS \cap G^{48}) \cup (VMS \cap G^{49})$, where VMS = {x∈T: Geological Grouping of x is Volcanogenic Massive Sulphide}, G^{48} = {x∈T: Host Rock of x is G48}, and G^{49} = {x∈T: Host Rock of x is G49}. This information is listed in Table 22.4 for the 46 deposits of the resulting subset. The examples of Table 22.4 and Figure 22.2 have been given in order to stress the complementary character of the two files, one of the main guiding principles for construction of the data base.

In order to test for similarities in terms of occurrence of Cu-bearing deposits, the volcanic rocks considered for this example in Quebec (Beauceville Group), New Brunswick (Tetagouche Group), Nova Scotia (Browns Mountain Group), and Newfoundland (Exploits and Gander Lake groups) can be assigned relative frequencies or probability values. Several examples based on different assumptions are noted here.

Of the 210 cells, 22 contain deposits with copper classified as volcanogenic massive sulphide deposits, and with an average of (22/210) = 0.10 for the relative frequency or "probability" of occurrence of a deposit with copper in a cell with G48 or G49 volcanic rocks chosen at random in the region. If, however, the volcanic rocks in New Brunswick (71 cells) are considered as representative of this type of mineralization, the probability is (15/71) = 0.21 which is larger than the preceding value 0.10. Using deposits for Newfoundland (113 cells), the probability becomes (7/113) = 0.06. For the interpretation of the latter two probabilities, it should be kept in mind that there are 15 and 7 cells with Cu-bearing deposits in New Brunswick and in Newfoundland, respectively.

A similar type of reasoning can be applied to the areal amount in square kilometres of volcanic rocks present in a cell. The total area of G48 or G49 volcanic rocks in cells with copper deposits amounts to 1112 km^2; and the total area of these rocks in the Appalachian region is 5514 km^2. Hence (1114/5514) = 0.20 or 20 per cent of the area occupied by volcanic rocks under consideration (G48 and G49) occurs in cells with copper deposits. The ratio of (43/5514) = 0.008 deposits/1 km^2 of G48 or G49 volcanic rocks represents a relative frequency which can be considered as an estimator of the probability of occurrence of a single deposit per unit of area (1 km^2).

Most of the preceding considerations apply to 10 by 10 km cells only, because these were used as units for coding. Similar expressions could be developed for cells of different sizes. Fabbri (1975) reviewed the use of cells of different sizes and shapes used in the past for the quantification of regional geological data. Obviously, it is relatively easy to compute probabilities for multiples of the unit cells used for coding; in particular, probabilities for 20 by 20 km, 30 by 30 km and 40 by 40 km cells can be readily obtained from our file for the Appalachian Region.

Concluding Remarks

The construction of the data base for Project Appalachia has shown that it is feasible to quantify large amounts of information from existing geological maps and documents on mineral deposits, by involving specialists in the fields of regional geology, mineral deposits, and geomathematics. Data banks of the type described here can also contribute to the definition of geological standards, thereby improving geological communication.

It is also possible to perform many kinds of elementary statistical operations resulting in useful tabulations and displays of selected variables in map-form. Correlations of deposits retrieved from the mineral deposit file with parameters retrieved from the regional geological file can be performed by defining various kinds of probabilities which aids to the evaluation of regional mineral potential.

Acknowledgments

We are grateful to the following persons for their assistance during the preparation of the data bank for Project Appalachia: R.A. Adamick, J.J.O. Carvenali, V. Doyle, A. Edwards, J. Laurier, C.A.M. McCann, G.C. McDonald, R.G. Newbury, D.P. Nundy, L.O. Ross, J. Traill, and J. Wright.

References

Agterberg, F.P.
1974: Geomathematics: Mathematical background and geo-science applications; Amsterdam-New York, Elsevier, 596 p.

Agterberg, F.P., Chung, C.F., Fabbri, A.G., Kelly, A.M., and Springer, J.S.
1972: Geomathematical evaluation of copper and zinc potential of the Abibiti area, Ontario and Quebec; Geol. Surv. Can., Paper 71-41, 55 p.

Fabbri, A.G.
1975: Design and structure of geological data banks for mineral potential evaluation; Can. Min. Metall., Bull., v. 69, p. 91-98.

Fabbri, A.G., Divi, S.R., Wong, A.S., and Carrara, A.
1973: Project Appalachia: A data base on geological and mineral deposit parameters. Unpublished report.

Leech, G.B., Agterberg, F.P., Fabbri, A.G., Kirkham, R.V., Poole, W.H., and Sangster, D.F.
1974: Project Appalachia; *in* Report of Activities, Part A, Geol. Surv. Can., Paper 74-1A, p. 135.

Project 720097
F. P. Agterberg, C. F. Chung, and S. R. Divi
Regional and Economic Geology Division

Introduction

The purpose of the computer runs to be described here was to develop and test, on Project Appalachia data (Fabbri *et al.*, the publication, Report 22), a flexible computer-based system to express expectancies for occurrence of mineral deposits of specific types in terms of the parameters systematically coded for the geological framework. This report summarizes results of a sequence of statistical experiments performed mainly during October, 1973, and June-August, 1974. During these two periods, the mineral deposit file was in preparation and the regional geological file was being edited.

For every experiment described here, a specific set of data selected from the mineral deposit file was correlated with a usually much larger set of data retrieved from the regional geological file. Because of improvements and amplifications periodically applied to the data base, these statistical experiments have been performed in different data sets. A single experiment or set of similar experiments involves a variable amount of computer programming and consists of several separate stages for data selection, statistical analysis, representation in map-form and interpretation of results. Experiments such as those described here cannot, at this time, be performed rapidly, on a routine basis. They may take up to a month in time and require the collaboration of several persons with a detailed knowledge of the statistical method, computing procedures and the geology.

Therefore, it was not practical to repeat all previous experiments after the latest revision of the data base. Moreover, further revisions are likely to be made when new data become available, and new experiments can normally be better designed than earlier experiments. The results listed here, however, are of a general nature and, on the whole, are not strongly affected by later revisions applied to local geological environments or individual deposits. This is also suggested by the results of a few statistical experiments which were repeated after major revisions of the data base (e. g. Runs 1, 11, and 33 in Tables 23. 1 and 23. 2).

Correlation Between Sulphide Deposits and Litho-Age Units

Figure 23. 1 corresponding to Run 33 in Table 23. 2 provides a typical example of one of the experiments. It is based on data for the entire Canadian Appalachian Region. The 78 dots in Figure 23. 1 indicate the "control cells" for this run, each of which contains one or more sulphide deposits with at least 100 tons of "ore" (with copper, lead, or zinc; cumulative production or reserves). This effectively eliminated small occurrences or showings and confined the test to well-established deposits. Genetic or morphological type of the sulphide deposits was not considered separately for this run. The control cells measure 10 km on a side like the other cells used for coding.

In total, 60 of the 79 litho-age units distinguished in the regional geological file (*see* Table 22. 1 in Fabbri, *et al.*, this publication, report 22) are present in one or more of the 78 control cells; the litho-age units so recognized may or may not be host rocks to the deposits in the control cells. In this run, as well as in the other runs of Tables 23. 1 and 23. 2, variables not occurring in any of the control cells for a run were eliminated at the start of the statistical analysis . The 60 variables for Run 33 were taken as the "independent" variables (X_i, i=1, 2, . . . , 60) with which the "dependent" variable of the yes-no type for occurrence of deposits (Y) was correlated using the stepwise multiple regression technique. The multivariate statistical methodology has been described elsewhere by Agterberg *et al*, (1972).

Table 23. 1
Applications of general linear model of least squares: October (1973) runs *)

Run No.	Independent Variables	R^2	F
1	Litho-age units	0. 1195	2. 55
2	Lithologies only	0. 0403	4. 26
3	Paired lithologies	0. 1251	2. 69
4	Ages only	0. 0200	5. 24
5	New age variables	0. 0039	6. 75
6	Structural + metamorphic variables**)	0. 0229	5. 04
7	Structural variables	0. 0072	6. 56
8	Metamorphic variables	0. 0148	5. 64
9	Lithologies + structural + metamorphic variables	0. 0549	3. 73
10	Litho-age units + structural + metamorphic variables	0. 1240	2. 46

*) In the general linear model of least squares used for stepwise regression, it is assumed that occurrence of deposits depends on a linear combination $\Sigma B_i X_i$ of the p variables X_i, i=1, 2, . . . , p. In Run 1, for example, each X_i represents cell area underlain by the i-th litho-age unit.

**) + indicates that the linear combination $\Sigma B_i X_i$ is defined as

$$\sum_{i=1}^{p} B_i X_i \equiv \sum_{i=1}^{m} B_i U_i + \sum_{i=m+1}^{m+n} B_i V_i, \text{ where } U_i \equiv X_i$$

$(i=1, \ldots, m)$, and $V_i \equiv X_i$ $(i=m+1, \ldots, m+n)$ represent the variables of the two groups being combined with one another.

Table 23.2. Applications of general linear model of least squares: Summer (1974) runs

Run No.	Deposit Type	Independent Variables	R^2	F	Number of Control Cells	Number of Variables *)
11	All	Litho-age units	0.1880	2.07	78	65
12	Ditto, Nfld.		0.1788	1.89	23	22
13	Ditto, Mainland**		0.2443	1.84	55	53
14	Massive Sulphide	Litho-age units	0.2690	1.53	44	40
15	Ditto, Nfld.		0.2304	1.57	18	17
16	Ditto, Mainland**		0.3611	1.33	26	32
17	Skarn	Litho-age units	0.0267	4.31	9	26
18	Skarn	Paired litho-age units	0.2952	2.22	9	79
19	Vein and replacement	Litho-age units	0.0691	3.83	7	23
20	Sedimentary	Litho-age units	0.0178	5.40	10	18
21	30x30km cells	Litho-age units	0.4628	-	52	83
22	30x30km cells	Litho-age units	0.4204	-	53	82
23	All	Structural + metamorphic	0.0304	5.45	78	8
24	All	Structural	0.0099	7.43	78	4
25	All	Metamorphic	0.0163	6.80	78	4
26	All	Metamorphic (modified)	0.0115	7.35	78	4
27	All	Litho-age units + metamorphic	0.1889	2.06	78	69
28	All	Litho-age units + metamorphic (mod.)	0.1890	2.06	78	69
29	All	Litho-age units x metamorphic ***)	0.2533	1.85	78	149
30	All	Litho-age units x metamorphic (mod.)	0.2913	1.86	78	105
31	All	Litho-age units + sextic polynomial	0.1968	1.90	78	92
32	All	Sextic polynomial	0.0217	4.91	78	27
33	Revised Geology	Litho-age units	0.1611	2.28	78	60
34	Revised Geology	Massive Sulphide Litho-age units	0.2311	1.72	44	35

*) Represents number of independent variables present in one or more control cells.

**) Mainland consists of Quebec, Nova Scotia and New Brunswick.

***) x indicates that the linear combination $\Sigma B_i X_i$ is defined as $\sum_{i=1}^{p} B_i X_i \equiv \sum_{j=1}^{n} \sum_{i=1}^{m} B_{(i-1)n+j} U_i V_j$.

The squared multiple correlation coefficient (R^2) for the pattern of Figure 23.1 amounts to $R^2 = 0.1611$. R^2 provides a measure of the strength of the linear relationship between Y and the X_i, i=1, 2, ..., 60. This linear relationship is of the type $Y = B_0 + B_1X_1 + B_2X_2 + \ldots + B_{60}X_{60}$, where the B_i, i=0, 1, ..., 60, represent weighting factors or regression coefficients. Because of the usage of a stepwise method, the 60 variables expressing amounts of litho-age units in a cell were included successively, in order of importance measured according to their contribution to R^2. In most stepwise multivariate runs of this type, a number of variables are eliminated as redundant or irrelevant when their contribution is much less than the variables initially selected; these variables receive coefficients B_i equal to zero.

In the specific kind of regression run resulting in Figure 23.1, the variables X_i represent a number of nonoverlapping fields or subcells on the geological map. In that situation, the coefficients B_i and the values Y_k as calculated from the coefficients for all 3964 cells (labelled k with k = 1, 2, ..., 3064) can be interpreted as "probabilities" in the following sense.

Among the litho-age variables, the stepwise procedure assigned greatest importance to variable No. 49 (Middle-Upper Ordovician acid volcanics) followed by No. 48 (Middle-Upper Ordovician mixed volcanics), No. 62 (Lower Ordovician basic volcanics), and No. 44 (Lower Silurian acid volcanics). The corresponding coefficients B_i finally assigned to these four variables were: $B_{49} = 0.00196$; $B_{48} = 0.00071$; $B_{62} = 0.00069$; $B_{44} = 0.00071$. The fact that the latter three coefficients are almost exactly the same is believed to be fortuitous. The values of X_i are counts for subcells of which there occur 400 in a 10 by 10 km cell. Suppose, for example, that a cell is fully underlain by variable No. 49, then $X_i = 400$ and the probability (Y_k) that it is a control cell (or contains one or more deposits) is equal to $Y_k = B_{49} \times 400 = 0.00196 \times 400 = 0.784$ or 78 per cent.

A similar probabilistic interpretation can be given to the other coefficients B_i and all values Y_k. Suppose

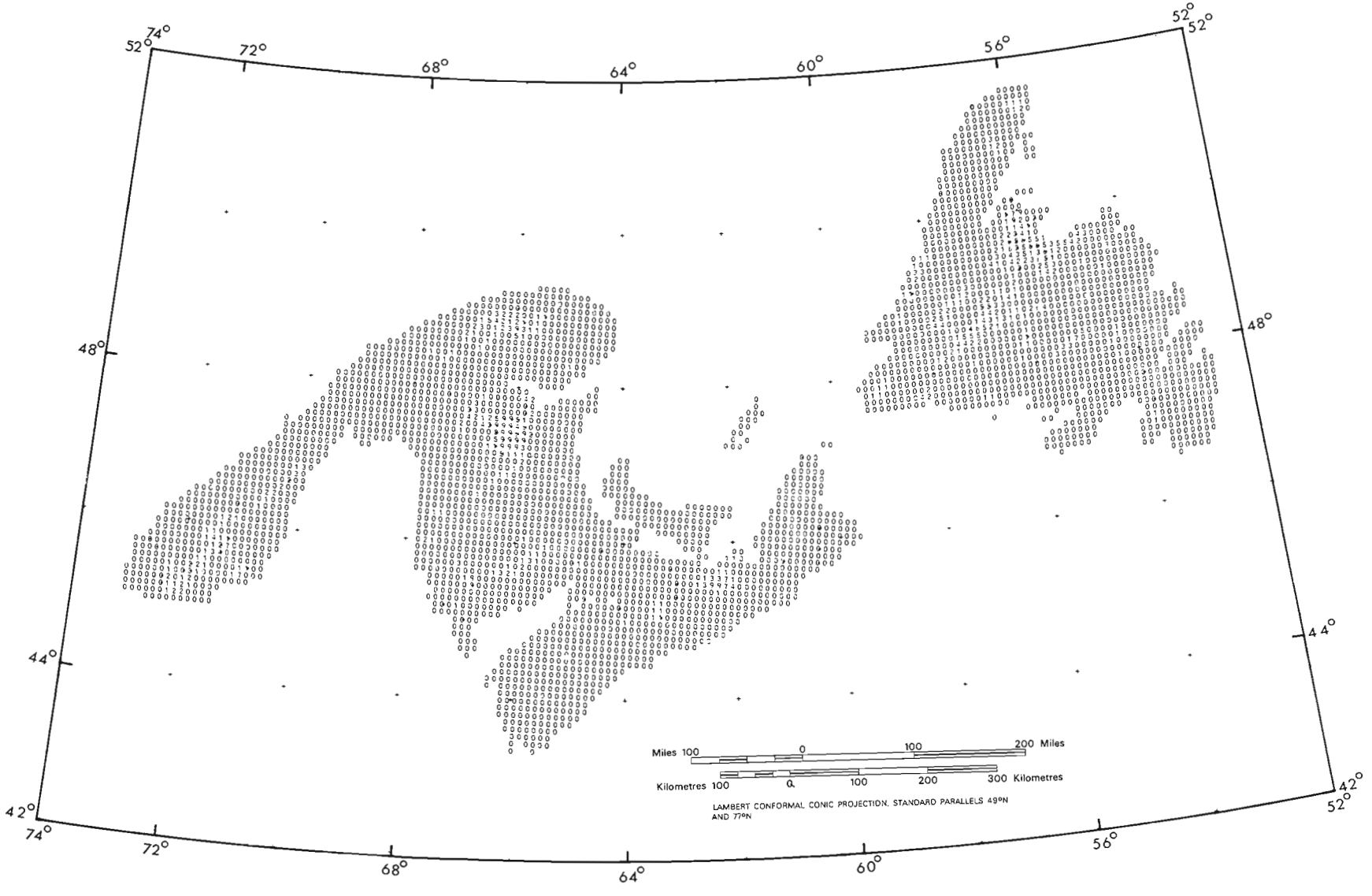

Figure 23.1: Plot of values calculated for Run 33. Occurrence of 78 control cells (indicated by dots on the map) has been related to litho-age units. Each value for a cell is a weighted sum of the amounts for the litho-age units present in that cell. (Map obtained on EAI-430 plotter, using program GEOPLOT.)

that a cell is underlain 50 per cent by X_{49} and 50 per cent by X_{48}, then its value Y_k satisfies Y_k = 0.00196x200 + 0.0071x200 = 0.534 = 53 per cent.

The preceding four coefficients (B_{49}, B_{48}, B_{62}, B_{44}) and also many of those not listed here, are related to the occurrence of volcanogenic massive sulphide deposits, the most abundant type of sulphide deposit in the Appalachian region. It is noted that selection of a variable by the multivariate statistical technique used here does not necessarily mean that this variable actually hosts deposits. It merely indicates that these litho-age units occur in the same cells as the deposits.

Values proportional to the value Y_k, computed for each individual cell are shown in Figure 23.1. The value actually printed is 10 by F by Y_k, truncated to integer value and set equal to 9 for all values greater than or equal to 9. Negative values that can occur locally are shown as zeros. The correction factor F is a number, greater than one, and equal to the number of control cells (n) divided by the sum of the calculated values Y_k^c in a "control area" ($F = n/\Sigma Y_k^c$). For all runs of Tables 23.1 and 23.2 this control area consisted of all the control cells used for a run and, for each control cell, the eight cells surrounding it, excluding overlap. Thus, for an isolated control cell, the resulting control area is 900 km^2 (nine 10 by 10 km cells). In Figure 23.1 there are n = 78 control cells, and the control area consists of 452 cells. The corresponding value of F satisfies F= 2.28. The constant F-1 (=1.28) provides a crude measure of the total area elsewhere in the Appalachian region which is similar in terms of the independent variables used for the model, to the control area that consists of the "immediate vicinities" of the known deposits. F can be regarded as a scaling factor because it does not change the pattern of the calculated values Y_k. A good reason for defining it on the basis of a control area is that the general linear model necessarily results in values Y_k which satisfy ΣY_k=n when added for the entire region. However, the sum of the modified values $Y_k^* = FxY_k$ is equal to ΣY_k^* = Fxn for the entire area, and equal to $\Sigma Y_k^{*c} = n$ for the control area. Thus, for the purpose of interpretation in terms of probabilities, it is usually better to consider the value Y_k^* for a cell. The calculated value Y_k is then interpreted as the product of f x Y_k^* where f = 1/F represents the "probability of discovery". According to the model applied here, all deposits are assumed to have been discovered in the control area (with F = 1). It should be appreciated that these definitions, although they are simple and easily applied, are related to a rather specific statistical model which is, at best, approximately satisfied in reality.

The coefficients R^2 and F are listed for all runs of Tables 23.1 and 23.2. They are not independent of one another. Normally, F decreases to 1 when R^2 increases. On the other hand, F reaches its largest value in the situation of "randomness" when it is assumed that there is no correlation (or $R^2 = 0$) between occurrence of deposits and the regional geological variables. Suppose that the control cells are randomly distributed, then the area outside the control area is "similar" to that inside the control area. For the situation of Figure 23.1, this would give F = 3964/452 = 8.77. This computation is consistent with the previous formula $F = n/\Sigma Y_k^c$ because, in the case of randomness, $\Sigma Y_k^c = 78 \times f$, with f = 452/3964 merely representing the fraction of the total area designated as control area.

The variables 49 and 48, which were selected by stepwise regression for Run 33 (Fig. 23.1), have relatively high weighting factors B_{49} and B_{48} because, in the Tetagouche Group of the Bathurst-Newcastle area, they contain a relatively large number of volcanogenic massive sulphide deposits. This is also the area with most of the large values (Fig. 23.1). However, Middle-Upper Ordovician mixed volcanics occur elsewhere, e.g. in central Nova Scotia (Browns Mountain Volcanics), and this accounts for the smaller area of large values here. Because of their similarity in lithology and age classification to the volcanics of the Bathurst-Newcastle area, the computer assigned the Browns Mountain Volcanics a considerable hypothetical mineral potential in Run 33.

In a pattern such as Figure 23.1, although many factors are considered simultaneously, it constitutes a direct representation of the information contained in the regional geological file. All variables in the data base have been weighted. The determination of the weighting factors is performed in two ways: (1) Choice of mathematical equations and variables; (2) Computation of weighting factors such as B_i, i=0, 1, . . . , 60, by means of the objective method of least squares. Of course, the second stage (least squares) could be deleted completely if it were possible to guess the weighting factors in a subjective manner. Much depends on the first choice (mathematical model). For example, in the model underlying Figure 23.1, a number of variables in the data base such as metamorphic grade were not considered. This does not mean that these variables are not relevant. When a variable is included in the mathematical equation, it is done in a specific manner which is not necessarily best. For example, the weighting factor (B_{49}) for Middle-Upper Ordovician acid volcanics in Run 33 applies to that variable only. Because variable No. 49 has both specific age and lithology, its weighting factor will not apply to any other variable or to places where Middle-Upper Ordovician acid volcanics are absent. Another example of the importance of the form in which variables are entered in the mathematical equation, to be discussed in more detail later, consists of the addition of the metamorphic variables to the litho-age units in Runs 27 and 29, respectively. In Run 27 (+ sign in Table 23.2), this addition had little effect, whereas Run 29 (x sign in Table 23.2) resulted in an entirely different pattern.

The remainder of this paper contains brief descriptions of other preliminary experiments, each of which is characterized by a different choice of variables for the mathematical equation. Otherwise, the procedure of weighting them is the same as that described above for Run 33.

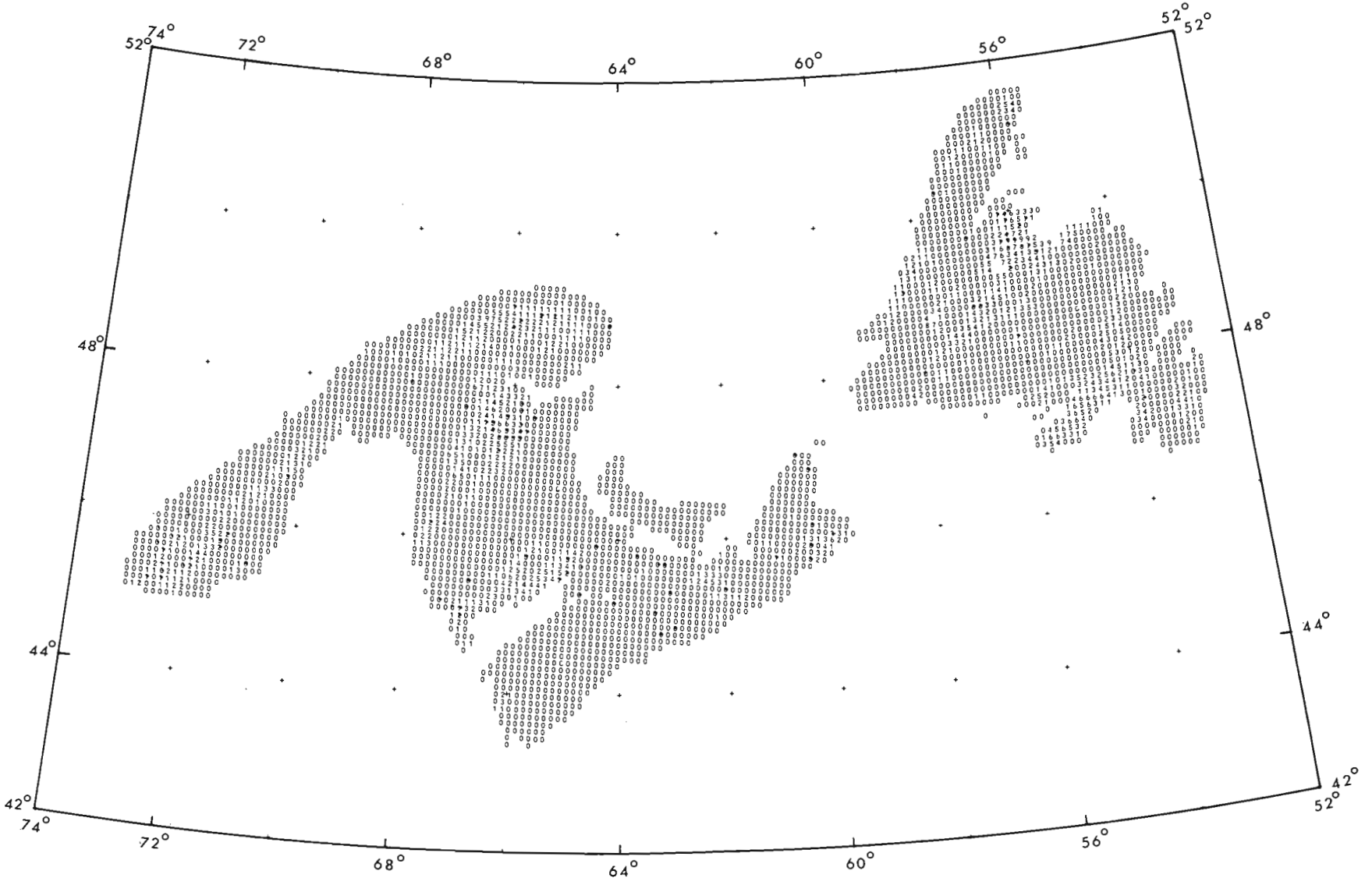

Figure 23. 2. Plot of values calculated for Run 2. Occurrence of 89 control cells (indicated by dots on the map) has been related to 14 generalized lithological variables.

Correlations Between Sulphide Deposits and Lithology, Age, Regional Metamorphism and Structural Style

The first 10 experiments (Table 23.1) were performed in October, 1973, using a preliminary set of 89 control cells (shown in Fig. 23.2) and a geological data base from which post-Devonian rocks had been excluded. The setup for Run 1 is the same as that for Run 33 described above and performed in August, 1974. The second experiment (Run 2) disregarded the age of the litho-age units. Only 14 lithological variables were considered for this run with the final pattern shown in Figure 23.2, which differs considerably from that of Figure 23.1. For example, in Figure 23.2 there occur many large values on the Avalon Peninsula, southeastern Newfoundland. This is because volcanic rocks are abundant in this area, and these obtained their weighting factors in other parts of the Appalachian region (e.g. Bathurst-Newcastle area) where similar volcanic rocks contain many volcanogenic massive sulphide deposits. The reason that the acid volcanics on the Avalon Peninsula are not reflected in Figure 23.1 is that they are Late Hadrynian in age, and volcanics of this age elsewhere in the Canadian Appalachians seem almost devoid of sulphide deposits. Two exceptions are the Teahan and Lumsden deposits in southern New Brunswick which occur in Hadrynian volcanic rocks.

Run 2 is equivalent to a run on lithological variables for the Abitibi area on the Canadian Shield previously described by Agterberg (1973, Fig. 6). In that situation, the rocks were all Archean in age, but the degree of fit could be improved by considering all possible pairs of rock types. Thus, the presence of acid volcanics in a cell was qualified by the presence of basic volcanics and acid intrusives in the same cell. Such interactions of variables can be expressed by incorporating variables of the type X_iX_j $(i \neq j)$ in the mathematical equation. Run 3 was based on the 14 variables on Run 2 and the 91 product-variables for all possible pairs of the 14 lithologies. It was found that the area of high values on the Avalon Peninsula virtually disappeared in the pattern of Run 3 (not shown). This is because the rocks with which the acid volcanics here are associated are different from those occurring with many of the volcanics with which massive sulphide deposits are associated, e.g. in the Bathurst-Newcastle area.

As a corollary to Run 3, differences in lithology were ignored in Run 4 and the age of the litho-age units was the only variable considered. The R^2 value for Run 4 is 0.020 which is less than the value of 0.040 for Run 3. This indicates that, in the Appalachian region on the whole, the occurrence of sulphide deposits is more strongly controlled by lithology than by age.

In Runs 1 and 4 no consideration was given to the chronological ordering of ages in the geological time table. It could be that this order is of metallogenic importance if younger rocks were to have a memory for mineralization in older rocks. In order to test this possibility, the ages were number 1, 2... from the pre-Early Hadrynian (1) to the Middle Devonian (19). After making a few changes in this numbering sytem to account for overlapping ages of some units, a polynomial of degree 10 was fitted to the resulting new age variable. This run (No. 5 in Table 23.1) has a very low R^2 value (=0.004). Its pattern shows a gradational increase in frequencies of occurrence of sulphide deposits from the Hadrynian onward with a peak during the Ordovician followed by a decrease in the Silurian and Devonian. This pattern can be considered as a smoothed version of the simple histogram obtained by plotting frequency of deposits against geological time intervals.

The remaining runs of Table 23.1 made use of the structural and metamorphic variables. These variables (Run 6) have a slightly greater R^2 than age (Run 4). The 4 variables for metamorphic grade (Run 8) are better correlated with the occurrence of sulphide deposits than the 4 variables for extent of structural deformation (Run 7). These variables caused only a little change in the overall patterns if they were added (with their own coefficients) to the lithological variables (Run 9) or litho-age units (Run 10). It may be concluded that in the Canadian Appalachians the occurrence of sulphide deposits is mainly controlled by lithology followed by age, regional metamorphism and structural style, in order of decreasing importance.

Experiments Involving Separate Deposit Types, Larger Cells and Other Factors

Runs 11 to 34 were performed during the summer of 1974 (Table 23.2). They made use of some or all of the 78 control cells shown in Figure 23.1. This pattern of 78 cells differs from the pattern of 89 control cells shown in Figure 23.2. This accounts for differences in R^2 and F values for some runs in Table 23.2 which were otherwise similar to the corresponding runs in Table 23.1. An example of this is Run 11 which repeated Run 1, and is also equivalent to Run 33 (Fig. 23.1). The Appalachian Region was divided into two parts (Newfoundland and mainland Appalachia), and Run 11 was also repeated on the two smaller regions yielding Runs 12 and 13.

Volcanogenic massive sulphide deposits, as a separate deposit type, were correlated with the litho-age units in Run 14. This experiment was repeated on data from Newfoundland and mainland Appalachia separately (Runs 15 and 16). It may be concluded from these results that taking the volcanogenic massive sulphide deposits separately as a group, results in a better correlation with the litho-age units. The patterns of values plotted for cells (not shown here) were also improved because some spurious influences by other types of deposits had been eliminated by not considering the other deposits in these runs.

Skarn deposits, which occurred in 9 control cells only, were also correlated with the litho-age units (Run 17). The results are shown in Figure 23.3 for part of the area (Newfoundland had 1 control cell only and very few non-zero values). This pattern illustrates that most of the relatively high values on the Gaspé Peninsula (Fig. 23.1), and also in a smaller area in

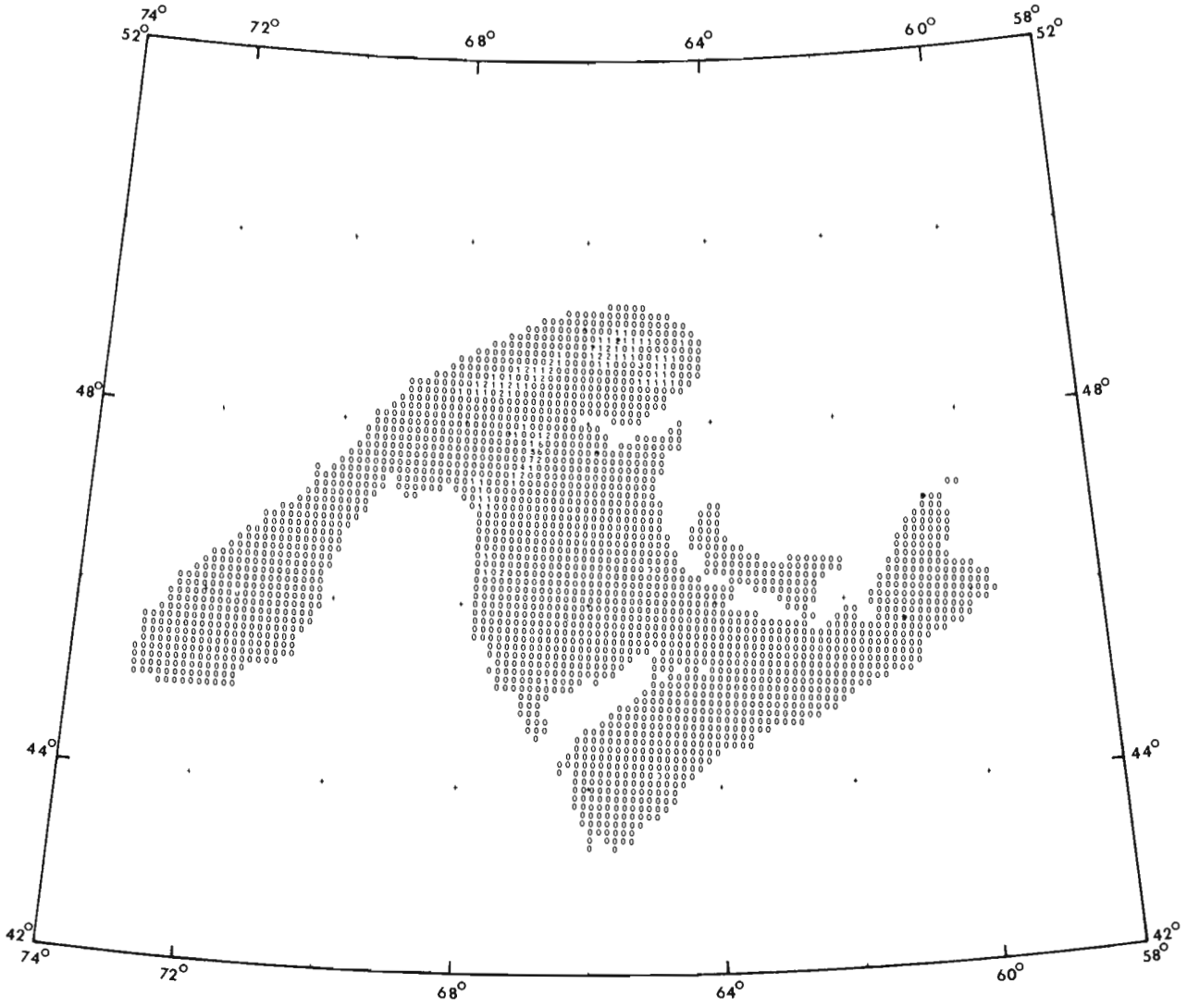

Figure 23.3: Plot of values calculated for Run 17. Occurrence of 9 control cells (8 of these are indicated by dots on map, Newfoundland not shown) for skarn deposits has been related to litho-age units.

north-central New Brunswick, are caused by variables related to the occurrence of skarn deposits rather than to the volcanogenic massive sulphide deposits which account for most of the higher values in runs such as illustrated in Figure 23.1 where the deposits were not subdivided into types. The three variables selected first by the stepwise regression method in Run 17 are No. 26 (shale), 18 and 50 (both carbonates).

In total, 26 litho-age units occurred in the 9 control cells for Run 17. All possible pairs of these were considered, and 53 of the pairs for coexisting variables occur in at least 1 of the 9 control cells. These 79 (26 + 53) variables were used for Run 18. It increases R^2 by a factor of more than 10 which reflects the fact that the pattern of the calculated values for Run 18 more closely resembles the pattern for skarn mineralization consisting of 9 control cells only. It is noted that a high value of R^2 or a close correspondence between observed and calculated pattern does not necessarily imply that a model is good because irrelevant variables may have been included in a situation of this type.

Runs 19 and 20 were for "vein and replacement" and "sedimentary" type deposits related to the litho-age units.

Runs 21 and 22 repeated Run 11 but all data had been related to 30 by 30 km cells by combining the 10 by 10 km cells into squares each consisting of 9 cells. Of course, it is possible to form 9 different arrays of 30 by 30 km cells out of an array of 10 by 10 km cells. Runs 21 and 22 represent results for only 2 of these 9 possible arrays. They have higher R^2-values than Run 11 for smaller cells because the multiple correlation coefficient increases with cell size when a punctual pattern (pattern consisting of points) of deposits is correlated with a regional geological pattern (Agterberg, 1974).

Runs 23 to 25 repeated Runs 6 to 8 for the different set of control cells.

For Run 26, every cell was assigned a single variable representing the metamorphic grade occupying the most area within the cell. This process yielded 4 modified metamorphic variables of the yes-no type that are either present or absent in a cell.

Run 27 was for litho-age units plus the 4 ordinary metamorphic variables; and Run 28 repeated Run 27 using the 4 modified metamorphic variables.

For Run 29, every litho-age unit was replaced by 4 new variables resulting from multiplying each litho-age variable by each of the 4 ordinary metamorphic variables. Run 30 repeated Run 29, using the 4 modified metamorphic variables.

From the results of Runs 25 to 30, it may be concluded that (1) modified metamorphic variables and ordinary metamorphic variables gave approximately the same results; and (2) the degree of fit increases significantly if the litho-age units are qualified by means of the metamorphic grade.

For Run 31, a sixth degree of sextic polynomial (27 terms) was added to the linear expression for the litho-age units. This experiment and Run 32, which was for a sextic polynomial only, repeated experiments described by Agterberg (1971) for a preliminary evaluation of the mineral potential of the Province of British Columbia.

During the summer of 1974, the regional geological data base was revised significantly. The last two experiments (Runs 33 and 34) were performed after this major revision and repeated Runs 11 and 14. Run 33 was discussed in detail earlier in this paper. The revised data show a slightly smaller R^2-value, whereas F is greater (Table 23.2).

A probable reason for this is that several litho-age units occurring in relatively few cells and previously considered separately were eliminated by lumping them with other, more abundant litho-age units during this revision. The phenomenon that lumping, as well as decreasing the cell size, may decrease R^2 has been illustrated for several other experiments of Tables 23.1 and 23.2. This is contrary to the usual situation, in other applications of multiple regression analysis, where a higher multiple correlation coefficient (R) is desirable because it signifies a better fit. In our situation, however, a smaller value of R^2 may be the result of a more realistic geological model.

Concluding Remarks

The experiments described in this paper indicate that it is feasible to manipulate very large arrays of numerical geological data, to perform multivariate statistical analyses, and to represent the results automatically in map-form. The runs performed on the entire Project Appalachia Data Base have been listed in Tables 23.1 and 23.2, and a few of these runs have been discussed in detail. All results are preliminary because they can be refined significantly by employing improved mathematical methods and by dealing with separate areas, selected geological variables and specific types of mineral deposits.

References

Agterberg, F.P.

1971: A probability index for detecting favourable geological environments; Can. Inst. Min. Met., Spec. Vol. 12, p. 82-91.

1973: Probabilistic models to evaluate regional mineral potential; *in* Mathematical Methods in Geoscience: Symposium held at Pribram, Czechoslovakia, October, 1973, p. 3-38.

1974: Geomathematics: Mathematical background and geoscience applications; Elsevier, Amsterdam-New York, 596 p.

Agterberg, F.P., Chung, C.F., Fabbri, A.G., Kelly, A.M., and Springer, J.S.

1972: Geomathematical evaluation of copper and zinc potential of the Abitibi area, Ontario and Quebec; Geol. Surv. Can., Paper 71-41, 55 p.

Fabbri, A.G., Divi, S.R., and Wong, A.S.

1975: A data base for mineral potential estimation in the Appalachian region of Canada; *in* Report of Activities, Part C, Geol. Surv. Can., Paper 75-1C.

Project 720097

C. F. Chung and S. R. Divi
Regional and Economic Geology Division

Introduction

This study of methods contributing to regional evaluation of mineral potential was undertaken to conduct some new statistical experiments and to repeat some of the experiments done earlier on the entire Appalachian region, applying them this time to a smaller, geologically more coherent area. Interpretation of the interrelations among variables within each analysis for a specific model, and comparisons of different results between different models, are easier to appreciate for such a selected area. This is particularly convenient during preliminary studies, when a number of experiments are carried out, and new geological and statistical models are being tested.

In the previous paper, it was pointed out that the regression coefficients computed for the litho-age units, and the calculated values for cells based on the regression coefficients, can be interpreted as probabilities. During a discussion of these preliminary results, it was suggested by economic geologists participating in the project that a similar study be carried out for the Eastern Townships subregion an area containing a number of volcanogenic massive sulphide deposits and also some sulphide deposits stratabound in sediments.

This subregion was selected because it consists of a number of rather well-defined geological belts. The Eastern Townships case history study was carried out during the fall of 1974.

The geological and mineral deposit setting in the area is described. A statistical model based on the concepts of "map host" and "host rock", and not used earlier, is then outlined and with this background, some of the pertinent results are discussed.

Geological and Mineral Deposit Setting

Sedimentary and volcanic rocks ranging in age from Hadrynian to Devonian form stratigraphic – structural belts, which trend northeast in the Eastern Townships. Six such belts were distinguished by St. Julien (1972) extending southeasterly from Logan's Line. Because the ages of some of the rocks in these belts are uncertain, and in view of the specific objectives of Project Appalachia, some interpretation had to be applied during our compilation.

On the northwest, Hadrynian (volcanics G74), Cambrian (shales, G64; quartzites, G68), Lower Ordovician (greywackes, G60) and Middle Ordovician (argillaceous limestones, G57; calcareous shales, G56) sequences occur in a series of nappes, imbricated thrust slices, and klippen. The second belt, known as the Serpentine Belt, includes polyphase deformed Cambrian metasediments (greywackes, G65; quartzites, G68), Lower Ordovician metasediments (greywackes, G60) and mixed metavolcanics (G63). The distinctive feature of this belt is the presence of Lower Ordovician ophiolite series (G52, G53, G54). To the southeast lies the next belt, known as the St. Victor Synclinorium, comprising Middle Ordovician greywackes (G47) and rhyolites (G49). The fourth belt, including Stoke Mountain, is formed of Lower Ordovician shales (G58) and volcanics (G61, G63). The fifth belt, forming part of the Gaspé – Connecticut Valley Synclinorium, is composed mainly of Middle Silurian carbonates (G31) and Lower Devonian volcanics (G19), which are intruded by a number of small bodies of Devonian granitic (G14) and gabbroic (G15) plutons. Lastly, the southeastern-most belt, comprising the Boundary Mountain Anticlinorium, is underlain by Lower Ordovician greywackes (G60).

Within the Eastern Townships area, the presence of plate margins, involving accretion and consumption, has been postulated (Bird and Dewey, 1970; Poole, 1974). In or near the loci of these interpretative features, there are 29 sulphide deposits for which grade and tonnage figures are available. Attention to the importance of such a tectonic – metallogenic association

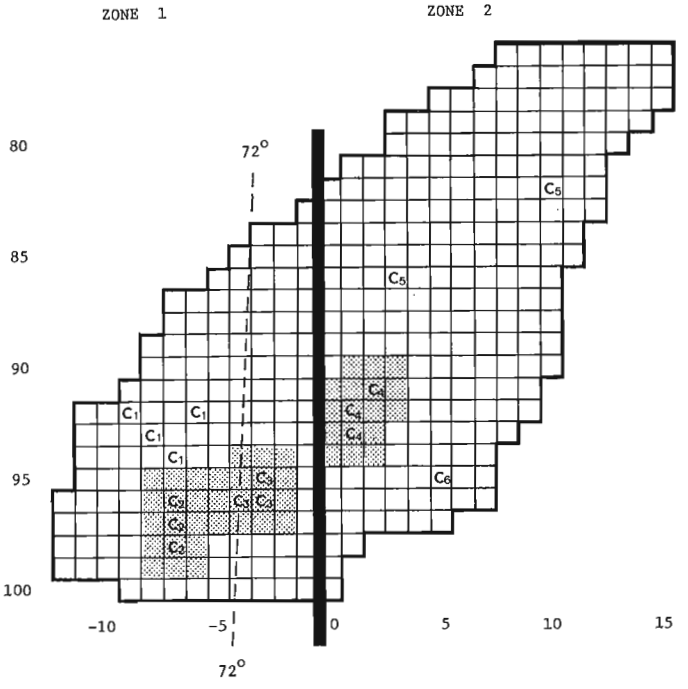

Figure 24.1. Eastern Townships subarea; zones 1 and 2; cells C are control cells with subscripts denoting group numbers. Control area used for Runs A, B, and C (Figure 2a-c) is shown by stippled pattern.

has been noted recently elsewhere in the Appalachians (Strong, 1974).

The Eastern Townships part of the regional geological file for Project Appalachia consists of 384 cells. Only 25 of the litho-age units in the Appalachian file occur in this subregion. For comparison purposes, it was divided transversely into two zones (Fig. 24.1) both containing the first five belts. Zone 1 contains 153 cells and zone 2 contains 231 cells. The 29 sulphide deposits are distributed among 16 of the cells. These are termed control cells, i.e. a control cell is defined as a cell with one or more deposits. Twenty of the deposits are in zone 1 (the southwestern zone) the remainder are in zone 2. The deposits were divided into 6 groups based on their genetic type and the age of their host rocks. Three groups (1 to 3) occur in zone 1 and three (4 to 6) in zone 2. Although groups 2 and 3 in zone 1 are both volcanogenic deposits, they were separated to admit the possibility that the geological environment of group 2 reflects a zone of crustal accretion (ophiolite assemblage), whereas that of group 3 represents a zone of crustal consumption (calc-alkaline assemblage), according to the plate tectonic model (Poole, 1974), and that this difference has a bearing on the larger metallogenic environment. In zone 2, group 6 which is represented by the Clinton deposit only, was separated from group 4 on the basis of a younger age of its host rocks (Lower Devonian).

As shown in Figure 24.1 and also in Table 24.1, each deposit group consists of a number of control cells and each control cell contains one or more deposits. The grouping of deposits was done with the objective of delineating a single geological regime common to the deposits in any one group, so that such a regime can be used for prediction purposes.

Method of Computations

Three different models (general linear model of least squares, map host model and host rock model) were used for the prediction of occurrence of deposits from several sets of data in the Eastern Townships area. The results for only the 16 control cells are shown in Table 24.2, although values are computed for all 384 cells for each run. Runs A, B, and C in Table 24.2 are also

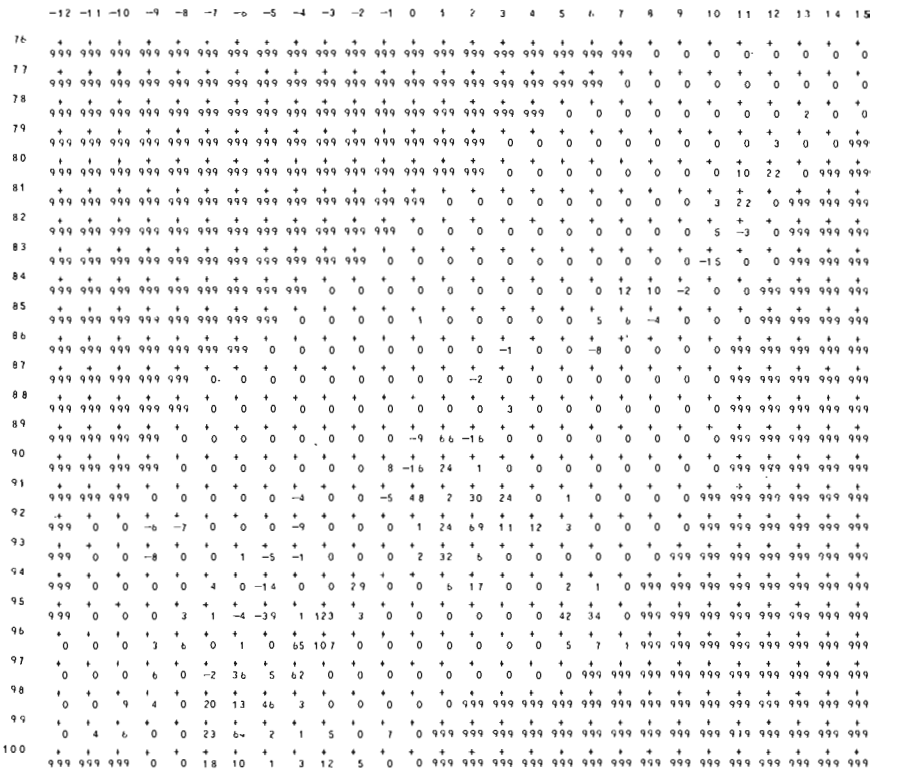

Figure 24.2a

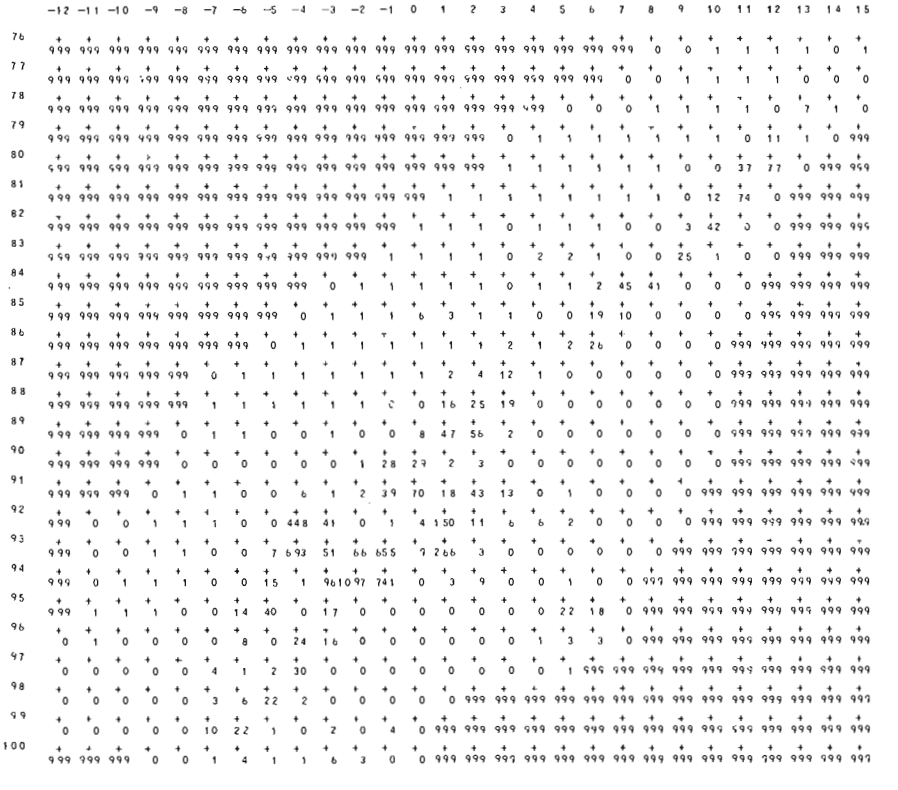

Figure 24.2b

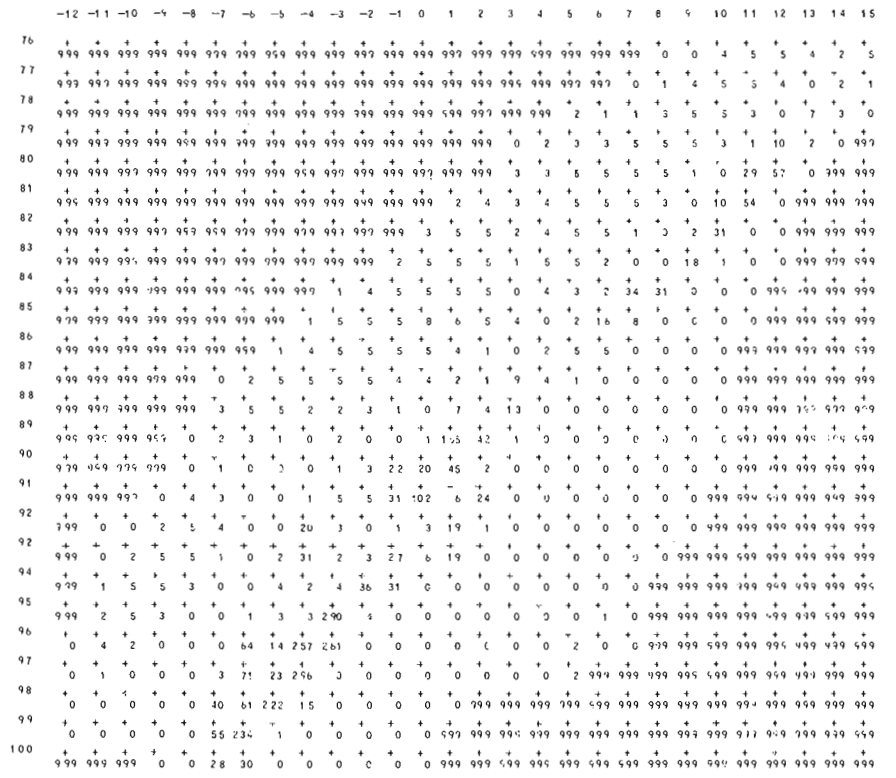

Figure 24. 2a, b, c.

Eastern Townships area (compare to Fig. 24. 1). Results for Runs A, B, and C are shown in Figures a, b, and c, respectively. Values calculated by regression (2a), and values $\hat{n}_S(x, y)$ computed by Eq. (7) for map host (2b) and host rock (2c) model were multiplied by 100 for display purposes.

represented in Figure 24. 2a-2c. These experiments will be discussed in more detail in the next section. The statistical models are discussed first.

A linear least squares model, based on the presence or absence of a deposit of a given type, was used by Agterberg (1971, 1973) to construct probabilistic models for mineral potential. An application of this model to data from all cells in the Appalachian region is described in the previous paper. Using this model, we estimated the probabilities that cells in the Eastern Townships area contain one or more deposits of a given type on the basis of the litho-age units. In the first model, an important role is played by the litho-age units occurring in the control cells. These have been listed in Table 24. 1.

The other two models (map host model and host rock model) are described here in more detail. From a computational point of view, these two models are identical but they are based on different geological assumptions.

The "map host" model is based on the litho-age units at the sites of the mineral deposits according to the geological compilation map used for coding the regional geological file. Every deposit was plotted as a single point on this map and was assigned a single "map host" only. On the other hand, the "host rock" model is based on the litho-age units at these sites according to the most detailed available maps and descriptions but expressed in terms of the litho-age unit scheme used for the regional geological file. Map hosts and host rocks for the 29 deposits are shown in Table 24. 1. In cases of deposits with two host rocks, half the deposit is assigned to one host and half to the other for statistical purposes.

For a given area R, suppose that R consists of m disjoint (not overlapping) litho-age units (g^R_i) for each i = 1, 2, ..., m. Let us assume that a total of N deposits of a given type occurs in R, some discovered and others undiscovered and let N_i be the number of the deposits that are "associated with" i-th litho-age unit g^R_1 (i = 1, 2, ..., m).

It is assumed that with each g^R_1, there is associated an average (or expected) frequency λ_i that indicates the expected number of deposits per unit of area of g^R_i. The term "associated with" refers to a geological association. The two models are distinguishable on the basis of their different geological parameters.

Since N_i deposits occur in g^R_i units in R, the average frequency is

$$\lambda_i = \frac{N_i}{g^R_i} \quad \text{for each } i = 1, 2, \ldots, m. \qquad (1)$$

When (1) all λ_i (i = 1, 2, ..., m) are known, (2) the N_i deposits are randomly distributed according to a simple Poisson distribution, and (3) all g^R_i (i = 1, 2, ..., m) are statistically independent, the expected number n_S of deposits of a given type within a subarea S in R may be expressed as

$$n_S = \sum_{i=1}^{m} \lambda_i \, g^S_i \qquad (2)$$

Table 24.1

Deposits, control cells and deposit groups used for Eastern Townships case history study (*see* also Figure 24.1)

Deposit Group	No. of Deposits	Control Cells	Litho-Age Units in Control Cell	Map	Host	Host Rock[o]	
1	4 (a-d)	(-9,92)	G53,G56,G57,G60	a	G57	a*	G59(G57)
		(-8,93)	G53,G60	b	G60	b*	G66(G59)
		(-7,94)	G56,G64,G65,G68, G74	c	G65	c*	G66
		(-6,92)	G56,G65,G68,G74	d	G56	d[x]	G66(G57)
2	3 (a-c)	(-7,96)	G52,G60,G65,G68, G74	a	G60	a	G62,G52
		(-7,97)	G52,G60,G63,G65, G68	b	G60	b	G62,G52
		(-7,98)	G52,G53,G60,G63, G65,G68	c	G60	c	G58,G53
3	13 (a-m)	(-4,96)	G47,G58,G63	a	G58	a-c	G49(G61)
				b-d	G63	d	G61
		(-3,95)	G31,G47,G51,G58, G63	e	G63	e	G61,G60
		(-3,96)	G31,G58,G63	f-j	G58	f-l	G61
				k-m	G63	m	G62
4	4 (a-d)	(1,92)	G14,G22,G31,G61, G62	a	G62	a	G61,G14
		(1,93)	G14,G22,G31,G54, G61,G62	b	G61	b	G49(G61)
		(2,91)	G14,G22,G23,G31, G62	c,d	G62	c,d	G61
5	4 (a-d)	(3,86)	G52,G60,G65,G68, G74	a	G65	a*	G64
		(10,82)	G47,G52,G53,G60, G62,G65	b-d	G47	b*	G46
						c,d[+]	G46,G52
6	1	(5,95)	G14,G19,G22,G23, G60		G19		G19

[o]) After conducting Runs 1-51 of Table 24.2, the host rock was revised for a number of deposits; new host rock numbers are given in brackets in this column. Run C (Fig. 24.2c) was based on the revised host rock data;

[*]) indicates sedimentary type deposit;

[x]) deposit type unknown;

[+]) magmatic deposit (all other deposits listed are of the volcanogenic massive sulphide type).

where g_i^S is the i-th geological variable in S for i = 1, 2, ..., m.

However, N (the total number of deposits) is obviously unknown and all we can observe is P, the number of discovered deposits, and P_i which are the numbers of known deposits associated with the geological variables g_i^R for i = 1, 2, ..., m. Thus, the λ_i (i = 1, 2, ..., m) are unknown and presumably differ from place to place. In order to simplify the problem, let us assume that all g_i^R are statistically independent and that the N_i deposits are randomly distributed in g_i^R (i = 1, 2, ..., m). The problem then consists of estimating optimum numerical values for the λ_i.

The following statistic ($\hat{\lambda}_i$) can be considered as an estimator of λ_i:

$$\hat{\lambda}_i = \frac{P_i}{g_i^R} \tag{3}$$

It is obvious that $\hat{\lambda}_i \leq \lambda_i$ since $P_i \leq N_i$ for each i = 1, 2, ..., m. That means $\hat{\lambda}_i$ always underestimates λ_i; this bias was called "regular bias" by Agterberg (1971) who introduced a "correction factor" to reduce this type of bias.

The theoretical correction factor F_i is defined as:

$$F_i = \frac{N_i}{P_i} \qquad \text{for each } i = 1, 2, \ldots, m. \tag{4}$$

To estimate the correction factor, we first have to establish a control area C (Agterberg, 1971) which is presumed to have been completely explored so that no undiscovered deposits exist here. It usually is defined in such a manner that it contains all P known deposits. Let us define a statistic $\hat{F}_C$

$$\hat{F}_C = \frac{P}{\sum_{i=1}^{m} \frac{g_i^C P_i}{g_i^R}} \tag{5}$$

where g_i^C denotes the i-th geological variable in the control area C. $\hat{F}_C$ was used as an estimator of all F_i in this study where the control area was defined as the control cells plus the 8 surrounding cells. In the case that the whole area R is chosen for the control area, the correction factor $\hat{F}_R = 1$. However, if we choose a very small area containing all P known deposits, the correction factor would be very large. Thus, it is clear that $\hat{F}_C$ depends on the size of the control area chosen.

For each cell S(x, y), the expected number $n_{S(x,y)}$ of deposits of a given type is estimated by

$$\hat{n}_{S(x,y)} = \hat{F}_C \sum_{i=1}^{m} \hat{\lambda}_i g_i^S \tag{6}$$

It implies, by substituting (3) and (5) into (6), that

$$\hat{n}_{S(x,y)} = P \frac{\sum_{i=1}^{m} g_i^S q_i}{\sum_{i=1}^{m} g_i^C q_i} \tag{7}$$

where $q_i = P_i / g_i^R$ for each i = 1, 2, ..., m.

For every cell S (x, y) in the Eastern Townships region, $\hat{n}_{S(x,y)}$ was computed. These values were plotted on the map for the two new models (Fig. 24.2b, c).

A common weak point of the estimators $\hat{\lambda}_i$, and $\hat{F}_C$ is that they depend on the selection of a control area. Statistical properties of the estimators have not been investigated in detail. Further drawbacks of the two models, from a statistical point of view, are not only the difficulty of estimating λ_i's, but also the fact that the two assumptions of random distribution of deposits and independence of the geological variables may be violated. In fact, the optimality of estimators of λ_i and F_C depends on the latter two assumptions. In the Eastern Townships area, a model that accounts for spatial clustering of deposits such as the negative binomial distribution fits the data better than the simple Poisson distribution for individual deposits assumed for this study.

Discussion of Statistical Experiments

The three models were applied 18 times, and some results for each run are shown in Table 24.2. Patterns of calculated values, using a correction factor F_C, are shown in Figure 24.2a-c, for Runs A, B, and C in Table 24.2.

Run A is based on the 9 control cells of groups 2, 3 and 4 which contain volcanogenic massive sulphide deposits only. The computational procedure followed for Run A is the same as that used previously for the patterns shown in Figures 24.1-24.3 of the preceding paper. Runs B and C are both based on the 20 deposits in groups 2, 3 and 4, instead of on the 9 control cells used for Run A. However, the control area used for estimating $\hat{F}_C$ for these two runs was kept the same as that for Run A.

The interpretation of the pattern of Figure 24.2a differs from that of Figure 24.2b, c. Disregarding the multiplicative factor of 100 in Figure 24.2, which was applied in all three patterns to represent the values with more precision, the values in Figure 24.2a are estimates of the number of control cells per cell, whereas the values in Figure 24.2b, c estimate the number of deposits per cell. A single control cell in the Eastern Townships area contains from 1 to 8 individual deposits (*see* Table 24.2). For the input of Run A, a cell is either a control cell or not a control cell. In the corresponding output (Fig. 24.2a), the values (for number of control cells per cell) are nearly all less than unity, and we prefer to refer to each of these values as the "probability" that a cell will be a control cell, or that it will contain one or more mineral deposits.

A possible advantage of using control cells instead of individual deposits is that less weight is assigned to the individual deposits in the more populated clusters such as group 3 which contains as many as 13 deposits within a relatively small area. In Run A, groups 2, 3 and 4 received equal weights, but in Runs B and C, the relative weights assigned to the groups were 15% (group 2) 65% (group 3) and 20% (group 4), with group 3 dominating the results of the statistical analyses.

The x-signs for control cells in Table 24.2 have the following meaning. For every run, one or more groups were related to the litho-age units either in the zone containing the groups, or in the entire area (zone 1 + 2). Values were calculated for every cell in the entire area, without making use of a correction factor (except for Runs A, B, and C), and these were compared with a cell average as follows. The cell average for a run is the number of control cells or deposits used for control divided by the total number of cells contained in the zone (or zone 1 + 2) to which it was related. Cell values above the cell average are represented by x-signs in Table 24.2. For example, the control for Run B consisted of groups 2, 3 and 4 in zone 1 + 2. Values above the cell average occurred in 7 of the 9 control cells (*see* Table 24.2). Cells (-7, 96) and (-7, 97) had values below average and were left blank in Table 24.2. They also show relatively low values in the pattern of Figure 24.2b.

The remainder of this section contains a more detailed discussion of some of the results for the runs listed in Table 24.2.

In the regression model, all the litho-age units in a control cell influence the definition of a favourable geological environment for the occurrence of mineral deposits in a cell. On the other hand, only a single "map host" and usually a single "host rock" are influential in the "map host" model and "host rock" model, respectively. Results for Runs A, B, and C based on the 3 different models but using the same 9 control cells (of deposit groups 2, 3 and 4), have been displayed in Figure 24.2a-c for comparison purposes. For Run A, the order of importance and corresponding final values of the regression coefficients for the litho-age units occurring in the Eastern Townships area are: (1) Lower Ordovician mixed volcanics (G63), 0.00569; (2) Lower Ordovician pelite (G58), 0.00155; (3) Devonian granite (G14), 0.00081; and (4) Cambrian greywacke (G65), 0.00022. The high values in the area of deposit group 3 (cells -4, 96; -3, 95; -3, 96) are well displayed. These high values appear to continue in a southwesterly direction, following the belt of Ascot-Weedon volcanics (G63) and Brompton pelites (G58). But the high values in the region of group 4 (cells 1, 92; 1, 93; 2, 91) are not due to the presence of Lower Ordovician volcanics but to Devonian granite, which attained a relatively high regression coefficient because of its relatively high frequency of occurrence in the control cells (*see* Table 24.1). To the northwest of the cells belonging to group 4, the Caldwell volcanics (G63) display some relatively high values. Outside the control cells used, the Clinton deposit coincides with a high value in Figure 24.2a. As in the case of group 4 deposits, this high value is caused by the presence of litho-age unit G14. No high values occur in the regions of deposit groups 1 and 5, because these occur in a sedimentary environment without any of the variables with larger coefficients in the control cells (groups 2-4) used for this experiment (Run A).

In Run B using the map host model (Fig. 2b) the litho-age units with high $\hat{\lambda}_i$ are: (1) G63 ($\hat{\lambda}_{G63}$ = 0.00832); (2) G58 ($\hat{\lambda}_{G58}$ = 0.00729); (3) Lower Ordovician basic volcanics, G62 ($\hat{\lambda}_{G62}$ = 0.00157); and (4) Lower Ordovician acid volcanics, G61 ($\hat{\lambda}_{G61}$ = 0.00119). Since G63 and G58 occur 6 and 7 times as map host of deposits in group 3 (also *see* Table 24.1), the control cells of group 3 and other cells with G63 or G58 acquired high values. In Run A, as discussed above, G63 and G58 also attained high coefficients, but for different reasons. Unlike the regression model, where the Devonian granite has a high coefficient because of its frequent presence in control cells, it has zero $\hat{\lambda}_i$ in this model because it is never actually the map host for deposits. Thus, the high values in Figure 24.2a in the control cells of groups 4 and 6 are eliminated in Figure 24.2b. The high values north of group 4 are influenced by the presence of G63 in this region. As in Run A, no high values occur in the region of groups 1 and 5 which contain sedimentary type deposits.

The litho-age units with high $\hat{\lambda}_i$ in Run C, based on the "host rock" model (Fig. 2c) are: (1) G61 ($\hat{\lambda}_{G61}$ = 0.03576); (2) G62 ($\hat{\lambda}_{G62}$ = 0.00262); (3) pre-Silurian ultrabasic rocks, G52 ($\hat{\lambda}_{G52}$ = 0.00218); and (4) G58 ($\hat{\lambda}_{G58}$ = 0.00091). As can be seen, these litho-age units with high $\hat{\lambda}_i$ are different from those in the "map host" model. This is because the "host rocks" are identified on the basis of very detailed information commonly available for the immediate vicinities of mineral deposits, whereas the "map host" was taken directly from the regional litho-age unit map. In Run C, the control cells of group 4 attained high values, as in Run A, but because of G61 rather than G14, although G14 was counted as half a host rock for one of the deposits (group 4, deposit a in Table 24.1). Litho-age unit G52 belonging to the ophiolite series is indicated, in Run C only, as an important litho-age unit associated with the presence of volcanogenic sulphide deposits. Although the dominant host rock of group 3 is G61, no high values occur in the control cells of group 3, because in this region the relatively thin belts of G61 in the volcanics were not distinguished on the geological compilation maps used for coding; all volcanics here were designated as G63. To avoid this problem of different scales of observation, some runs (not shown in Table 24.2) were made combining litho-age units G61 and G63 because both contain acid volcanics. The high values in the two regions, north of group 2 and northeast of group 3, reflect the presence of acid volcanics (G61) in the Caldwell Group and Ascot-Weedon belt, respectively.

The other 51 runs shown in Table 24.2 (Runs 1-51) consist of a set of 17 runs repeated for each of the three basic models considered. The 17 runs include 4 runs using deposit data for the 3 groups in zone 1, treating

Table 24. 2

Values predicted for 16 control cells (from the 6 groups) according to Runs A, B, C and Runs 1-51; only above average values are shown as x.

Run No.	Model	Zone No.	Group No.	Zone No.	1									2					
				Group No.	1				2			3			4			5		6
				No. of cells / Cell	(-9,92)	(-8,93)	(-7,94)	(-6,92)	(-7,96)	(-7,97)	(-7,98)	(-4,96)	(-3,95)	(-3,96)	(1,92)	(1,93)	(2,91)	(3,86)	(10,82)	(5,95)
1	Regression	1	1	4	x		x	x	x	x	x							x		
2			2	3			x	x	x	x	x		x	x				x		
3			3	3							x	x	x	x						
4			1,2,3	10	x		x	x	x	x	x	x	x	x				x		
5		2	4	3										x	x	x			x	x
6			5	2	x		x	x	x	x					x	x	x	x	x	
7			6	1											x	x	x			x
8			4,5,6						x	x					x	x	x	x	x	x
9		1+2	1	4	x		x	x												
10			2	3				x	x	x	x		x	x				x		
11			3	3							x	x	x	x						
12			1,2,3	10	x		x		x	x	x	x	x	x				x		
13			4	3										x	x	x			x	x
14			5	2				x	x	x	x				x	x	x	x	x	
15			6	1											x	x	x			x
16			4,5,6	6											x	x	x		x	x
A(Fig.2a)			2,3,4	9				x	x	x	x	x	x	x	x	x	x	x	x	x
17			1 - 6	16	x		x		x		x	x	x	x	x	x	x	x	x	
				No. of Deposits																
18	Map Host	1	1	4	x			x	x	x	x							x		
19			2	3	x	x					x									
20			3	13							x	x	x	x						
21			1,2,3	20	x						x	x	x	x						
22		2	4	4											x	x	x		x	
23			5	4					x	x	x	x	x					x	x	
24			6	1																x
25			4,5,6	9					x	x		x	x		x	x	x	x	x	x
26		1+2	1	4	x		x	x	x	x	x							x		
27			2	3	x	x														
28			3	13							x	x	x	x						
29			1,2,3	20	x						x	x	x	x						
30			4	4											x	x	x		x	
31			5	4					x	x	x	x	x					x	x	
32			6	1																x
33			4,5,6	9								x	x		x	x	x	x	x	x
B(Fig.2b)			2,3,4	20							x	x	x	x	x	x	x		x	
34			1 - 6	29	x						x	x	x	x	x	x	x		x	x
				No. of Deposits																
35	Host Rock	1	1	4																
36			2	3	x					x	x	x	x	x	x	x	x	x	x	
37			3	13											x	x	x		x	
38			1,2,3	20								x			x	x	x		x	
39		2	4	4											x	x	x			x
40			5	4						x	x							x		
41			6	1																x
42			4,5,6	9						x					x	x	x			x
43		1+2	1	4																
44			2	3	x					x	x	x	x	x	x	x	x	x	x	
45			3	13											x	x	x		x	
46			1,2,3	20								x	x	x	x	x	x		x	
47			4	4											x	x	x			x
48			5	4			x			x	x							x		
49			6	1																x
50			4,5,6	9			x			x					x	x	x			x
C(Fig.2c)			2,3,4	20								x	x	x	x	x	x		x	x
51			1 - 6	29			x					x	x	x	x	x	x		x	

the groups separately and combined, and using zone 1 geology only; 4 similar runs for deposits in the 3 groups in zone 2, and using zone 2 geology only; and 9 runs using the geology of zones 1 and 2 together. In cases where the geology of only one zone is used, the prediction is extrapolated to the next zone. Runs 1-8 and 9-16 are identical except that the former set (Runs 1-8) used zone 1 or zone 2, whereas the latter set (Runs 9-16) used the geology of the combined area of zones 1 and 2.

In the series of runs for group 1 only (Runs 1, 9, 18, 26, 35, and 43 in Table 24.2), Middle Ordovician carbonate (G57) is strongly correlated with the occurrence of deposits in both the regression and map host models. It caused a high value in control cell (-9, 92) for Runs 1, 9, 18 and 26, mainly because the distribution of G57 on the regional litho-age unit map is almost entirely restricted to cell (-9, 92) only.

In contrast, no values were created anywhere in Runs 35 and 43 for the "host rock" model, because the host rocks of the deposits do not appear on the litho-age unit map used for the regional geology file.

Run 36, using the host rock model for deposits of group 2 related to the litho-age units of zone 1, yielded relatively high values in the vicinity of groups 4 and 5. This is because of the presence of Lower Ordovician basic volcanics (G62) and pre-Silurian ultrabasic rocks (G52) which follow the Serpentine Belt.

Runs for deposit group 3 using the regression and "map host" models (Runs 3, 11, 20, 28), indicate high values in the control cells and in their vicinity following the belt of Ascot-Weedon volcanics and Brompton pelites. On the other hand, in the "host rock" model (Runs 37, 45), the high values occur mainly outside the control cells, where Lower Ordovician and acid volcanics (G61) are abundant. In the runs for deposit groups 1-3 combined, some high values occur in cells containing litho-age units G63 and G57, which have high coefficients in the regression (Runs 4, 12) and map host (Runs 21, 29) models.

In the runs for group 4, high values appear in the control cells of group 4 itself, and in their vicinity, for each of the three models when zone 2 is considered (Runs 5, 22, 39). These values are reduced considerably when the combined area of zones 1 and 2 is considered (Runs 13, 30, 47).

The runs for group 5 lack high values in all three models (Runs 6, 14, 23, 31, 40, 48), probably because of a poor geological grouping of the deposits in group 5.

The runs for group 6 using the regression model (Runs 7, 15) exhibit high values in the control cells of groups 4 and 6. These values are caused by G14 in the region of group 4, and by G14 and G19 in the region of group 6. The other two models (Runs 24, 32, 41, 49) did not give any significant values. Runs for deposit groups 4-6 combined gave high values in the region of deposit group 4 for regression and "host rock" models, when zone 2 is considered (Runs 8, 42). The other runs (16, 25, 33 and 50) did not result in any exceptionally high values. Runs 17, 34 and 51, for all deposits combined, provided values which are more or less sums of values previously obtained by relating individual groups to the litho-age units in the entire area (zone 1 + 2). Because cells with "sedimentary" and volcanogenic type deposits were combined for these runs, the resulting pattern is less distinct than patterns for a single type of deposits only.

Concluding Remarks

The experiments conducted in this study were intended to probe some aspects of multivariate statistical analysis used for mineral prediction purposes. On the whole, there was a good correspondence between results based on the regression and "map host" models, respectively. This is not surprising because both models made use of the same regional geological data base.

The "host rock" model, on the other hand, yielded significantly different results in a number of cases. The weighting factors for this model were computed from a data base that included more detail on the immediate vicinities of the mineral deposits. The differences in the results reflect this greater level of detail in the data base.

Detailed evaluations of statistical results, in terms of the local geology, are desirable because they may indicate (1) possible shortcomings in the mathematical model initially used for computing weighting factors, and (2) discrepancies between the geological settings of the mineral deposits as determined from the maps used for quantification of the regional geological framework, and those determined from the more detailed data used for the definition of host rocks.

Additional studies are needed of some problems indicated during this study. These include (1) a possible redefinition of control cells, centring them around individual deposits or clusters of deposits, instead of using the random grid of 10- by 10-km cells; and (2) improved utilization of detailed information on the immediate environments of mineral deposits in models for regional mineral potential evaluation which are based primarily on data systematically quantified for the geological framework of large regions.

References

Agterberg, F.P.

1971: A probability index for detecting favourable geological environments; Can. Inst. Min. Met., Sp. Vol. 10, 1970, p. 82-91.

1973: Probabilistic models to evaluate regional mineral potential, *in* Mathematical methods in geoscience: Symposium held at Pribram, Czechoslovakia, October, 1973, p. 3-38.

Bird, J.M. and Dewey, J.F.

1970: Lithosphere Plate-Continental Margin tectonics and the evolution of the Appalachian Orogen; Geol. Soc. Am. Bull., v. 81, p. 1031-1060.

Poole, W. H.
1974: Stratigraphic framework of volcanogenic massive sulphide deposits, Northern Appalachian Region; *in* Report of Activities, Pt. B, Geol. Surv. Can., Paper 74-1B, p. 11-17.

St. Julien, P.
1972: Appalachian tectonics in the Eastern Townships of Quebec; Inter. Geol. Cong. 24th, Excursion B-21, 21 p.

Strong, D. F.
1974: Metallogeny and plate tectonics: A Guidebook to Newfoundland mineral deposits, NATO advanced studies Institute, May 1974, 171 p.

25. DATA MANAGEMENT AND DISPLAY FOR PROJECT APPALACHIA

Project 720097

A. S. Wong, C. F. Chung, and A. G. Fabbri
Regional and Economic Geology Division

Introduction

The contents of the regional geological file and the mineral deposit file have been described in a preceding paper (report 22, this publication). This paper describes computer usage, file organization and structure, and methods of graphical display used for the Project Appalachia data. The computer was used for manipulating, editing and displaying the data in order to avoid manual handling, which, for large data sets, would require too much time.

Methods of display in map-form are particularly important for representing results of statistical analysis. Examples of this have been given in the three preceding papers and several additional examples will be presented later in this paper.

Because of the structural complexity of the information collected for the mineral deposit file, it was believed necessary to utilize MARS VI, a file management system implemented on the CYBER 74 at the Departmental Computer Science Centre. This system was chosen because it was readily available, relatively simple to use, and practical for the provision of inputs to statistical analysis.

File Organization

The procedures followed for building the two files in the data bank for Project Appalachia are illustrated in the flow chart of Figure 25. 1. Because of differences in (1) types of unit records, (2) types of information contained in the records, and (3) file structures, the two files have been assembled separately. Both files were organized in such a way that the parameters quantified could be accessed, retrieved, and updated easily by computer, and would be useful for statistical modelling. Three stages which can be distinguished for file organization are coding, editing and manipulating.

The coding stage included collection and compilation of information under the guidance of regional and commodity geologists, and the design of special coding forms for the quantification of the parameters.

In the editing stage, the information quantified was key-punched and stored on magnetic tapes and discs. As illustrated in Figure 25. 1, a series of FORTRAN computer programs have been written for the project, particularly for the purpose of editing the regional geological data. This was done because of the complexity of organizing, quantifying, coding and inputting the individual values for the large number (3964) of records of which there is one for every cell. Use has been made of fixed format for these values most of which were equal to zero because any one cell contains only a fraction of all features coded for the entire region. A number of 80-column cards were needed to contain the litho-age units information. It was necessary to key-punch card sequence numbers (called FLAG in Fig. 25. 1) and to include the UTM 10-km cell co-ordinates in every card. The computer programs written for this purpose are as follows.

Program SUM was used to check the total count of 400 points per cell, the sequence of the six cards used per cell record, and to display for text editing purposes the references entered in code for every record.

Program STAR was used to check every cell record for duplications of cards or of co-ordinates.

Program LIST was used in order to produce an orderly list of all the information in each cell record.

Program VAR was used to produce, on the line-printer, a digital map for each parameter. On such a map, the digits 0 to 9 represent 10 percentage intervals (0-10%, 10-20%, ... , 90-100%) for a given parameter.

The file consisted at first of two tapes; one for litho-age units, and the other one for structural and metamorphic parameters. Program COMPARE was used to check the sequence of cell co-ordinates and also the counts for Quaternary- and water-covered areas, which should be the same in these two tapes.

The two tapes were then merged into a single tape by the means of program COMBINE. The resulting tape, after the elimination of duplications of co-ordinates and card sequence numbers, contained most of the information of the regional geological file. For convenience, this information is at present being kept in two separate magnetic tapes: one for the data block of mainland Appalachia and the other for the data block of Newfoundland.

Unlike in the case of the regional geological file, the mineral deposit data were entered onto special purpose coding forms and then stored, retrieved, edited and updated by using MARS VI. The geographical locations of deposits were checked by replotting their positions by means of the plotting program GEOPLOT on the CALCOMP-763 drum plotter.

The manipulating stage, which follows the coding and editing stages, includes data transformations and display in preparation of statistical analysis. Initially, the regional geological file, its structure being relatively simple as shown in Figure 25. 2a, did not demand a file management system. In situations where programs for statistical analysis of large data sets were used, particularly for the regional geological file, it was found more convenient to retrieve the information by the program SELEC from the tapes mentioned above, rather than by using the MARS VI system. However, later a MARS VI file was created for this information also and this MARS VI version of the regional geological file was also found efficient for analyzing the content of the file, and for the production of sub-files with selected information. For a faster handling of the information in the files, extensive use was made of the NCR-320 intercom time-sharing terminal available for the project.

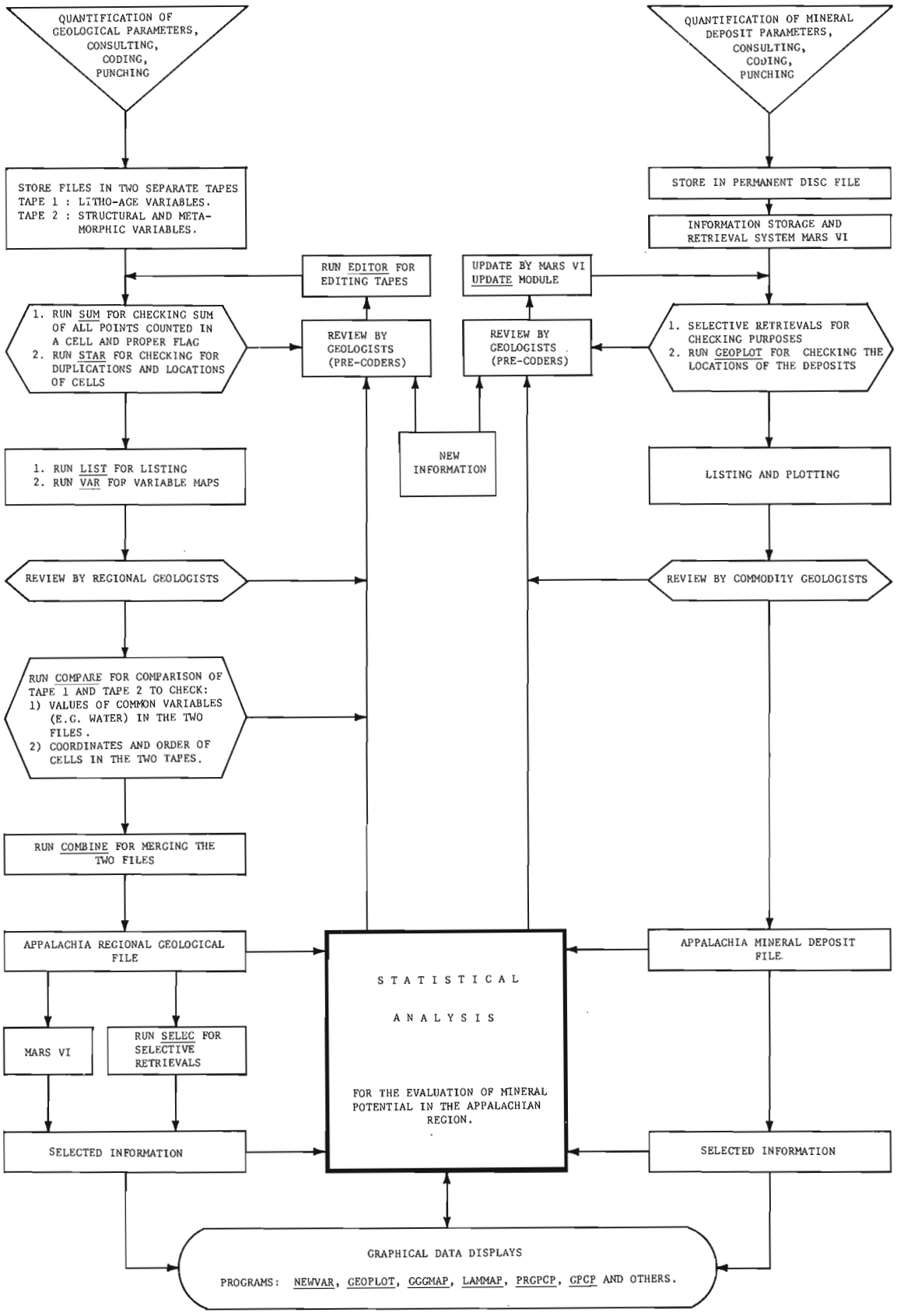

Figure 25.1 Schematic flow chart to illustrate procedures used for building the two files.

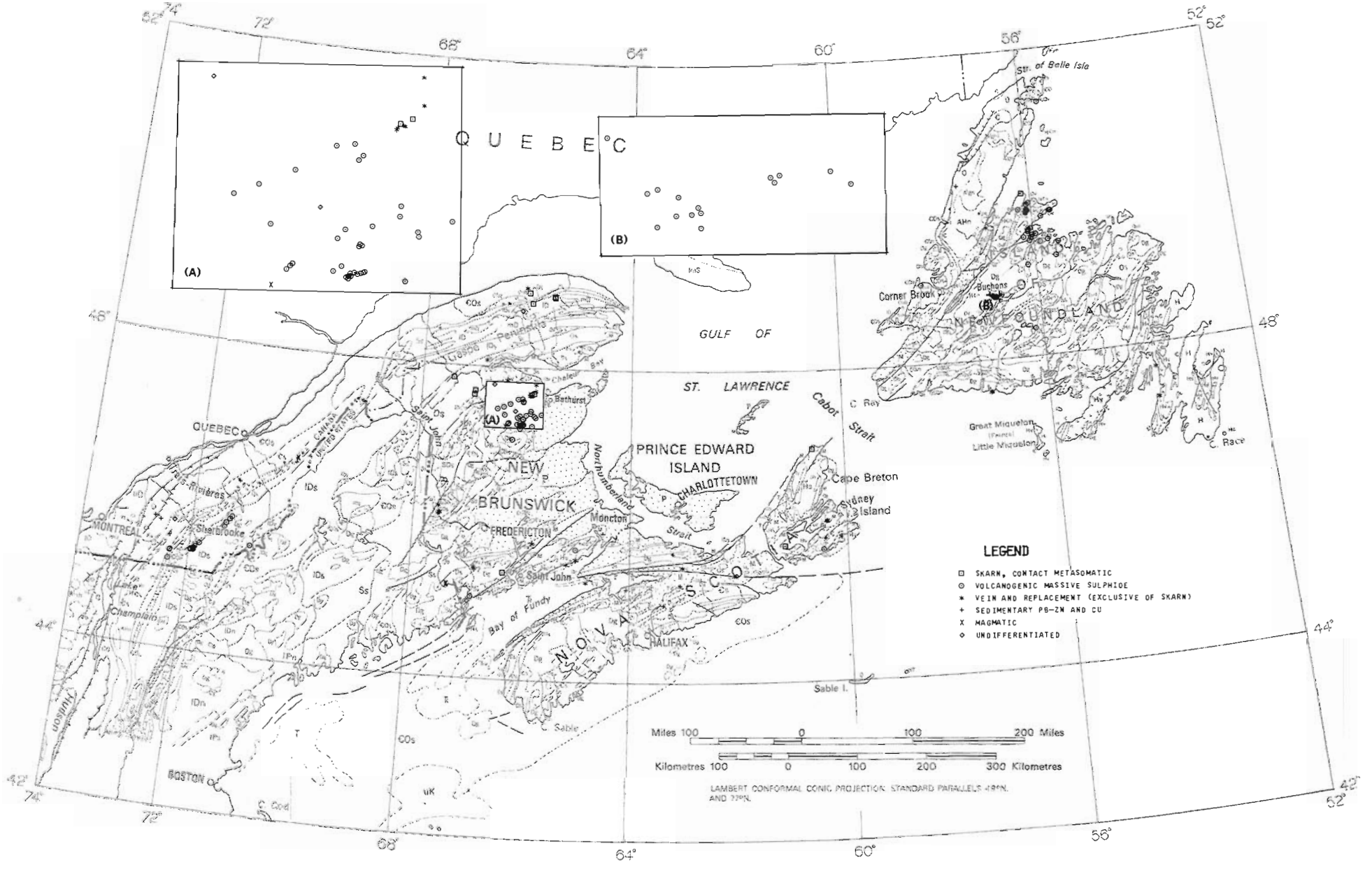

Figure 25. 3. Distribution of the 180 mineral deposits in the Project Appalachia mineral deposit file plotted by the EAI-430 flat bed plotter; (A) pattern for Bathurst area, New Brunswick, was enlarged 5 times; (B) Buchans area, Newfoundland, was enlarged 100 times.

The remainder of the information belonging to the regional geological file (linear parameters for selected intrusive contacts, unconformities and thin banded iron-formations) is kept on separate tapes. So far, this information has not been used for statistical analysis.

File structure

The structures of the two files have been designed so as to be both practical for data management and useful for the production of inputs for statistical analysis.

The description of these structures can be introduced by citing the following definition of a geological data file by Hubaux (1973, p. 161) "A data file may be conceived as a collection of measurements and/or observations pertaining to a given set of properties or characters about a series of geological objects of the same kind. These objects, which serve as basic units in the file may be, e.g. oil wells, mineral deposits, fossils, outcrops, etc.". A data file consists of records each representing a precisely defined entity of description. Every single record in a file has the same specific structure. The structures of the records of the MARS VI-version of the regional geological file and the mineral deposit file are shown in Figure 2.

The smallest unit of information in the data record is the data item which has a name (data item name) and a value (data item value). Data items of the same kind form data groups usually representing parameters of which the values were collected and recorded simultaneously. Data items and groups for the mineral deposit file have been given in Table 2 of report 22, this publication. For example, the data group "Location" contains 9 separate data items (7-15) representing, in turn, 5 different methods of location. The same data items are now shown in Figure 25.2 (lower part).

In a file management system, data item names are used to retrieve data item values. The latter comprise all numbers and words originally entered into the

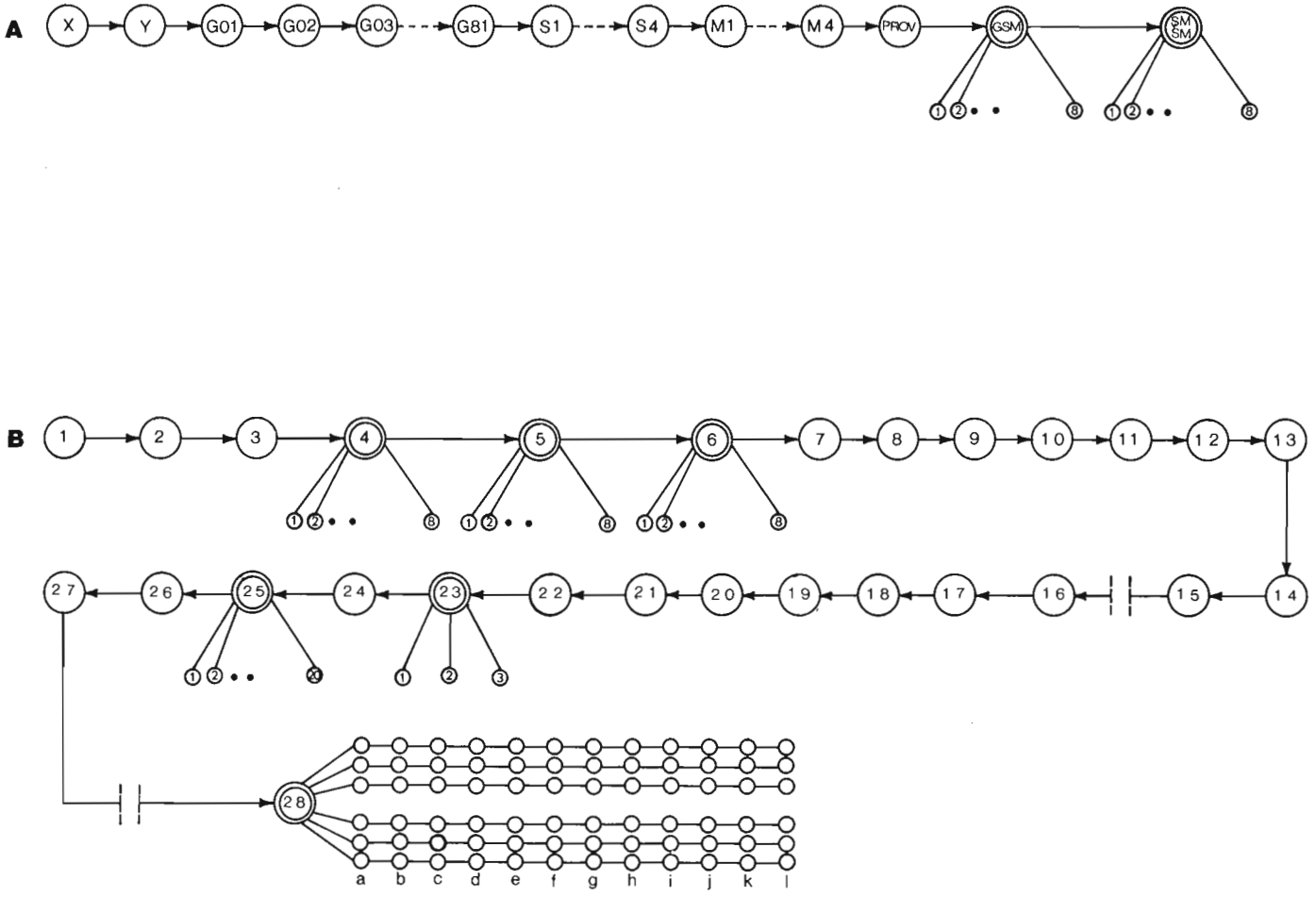

Figure 25.2. Data file structures. (A) Structure of MARS VI version of regional geological file; Data items X and Y represent 10-km cell co-ordinates, G01-G81 are litho-age units, S1-S4 are structural parameters, M1-M4 are metamorphic parameters, PROV is province, GSM is for up to eight references for litho-age units, SMSM is for up to eight references for structural and metamorphic parameters. (B) Structure of mineral deposit file; Data items and their sequence numbers are as in Table 22.2 of Fabbri, Divi and Wong (this publication); 1-6 = Identification; 7-15 = Location; 16-21 = Geological position; 22-23 = Host rocks; 25 = Mineralogy; 26-27 = Classifications; 28a-l = Size

Figure 25. 4

Example of output of GGGMAP for line-printer; values are part of pattern of Figure 2a in Chung and Divi (report 24, this publication).

	-9	-8	-7	-6	-5	-4	-3	-2	-1	0	1	2	3	4
87	999	999	0	0	0	0	0	0	0	0	0	-2	-0	0
88	999	999	0	0	0	0	0	0	0	0	-0	0	3	0
89	999	0	0	0	0	0	0	0	0	-9	66	-16	0	0
90	999	0	0	0	0	0	0	0	8	-16	24	1	0	0
91	0	0	0	0	0	-4	0	-0	-5	48	2	30	24	0
92	-6	-7	0	0	0	-9	0	0	0	1	24	69	11	12
93	-8	-0	0	1	-5	-1	0	0	0	2	32	6	0	0
94	0	0	4	0	-14	0	0	29	0	0	6	17	0	0
95	0	3	1	-4	-39	1	123	3	0	0	0	0	0	0
96	3	6	0	1	0	65	107	0	0	0	0	0	0	-0
97	6	0	-2	36	5	62	0	0	0	0	0	0	0	0
98	4	0	20	13	46	3	0	0	0	0	0	999	999	999
99	0	0	23	64	2	1	5	0	7	0	999	999	999	999
100	0	0	18	10	1	3	12	5	0	0	999	999	999	999

specially designed coding forms. In Figure 25. 2, the data items are represented as open circles connected by arrows; they are linked to one another in a logical order by a chain.

In some situations, it is convenient to make use of the concept of a "repeating data item". In Figure 25. 2, repeating data items are radiating downward from so-called nodes represented by double circles. For example, GSM in the regional geological file represents a repeating data item which can be repeated up to eight times. It means that the list of references for the cell, to which the record applies, can contain up to eight entries. The form of each repeated item is the same but its content (data item value) is different.

In other situations, a larger segment of the chain connecting all data items has to be repeated more than once. This is called a repeating data substring. The only example of a repeating data substring in Figure 25. 2 is TONGRD (No. 28) for tonnage and grade values of the six different metals (Cu, Pb, Zn, Au, Ag, and Ni) in the mineral deposit file.

The basic structure of each record in the MARS VI-version of the regional geological file, shown in Figure 2a, consists of values for the 81 litho-age units, followed by values for the 4 structural and 4 metamorphic parameters.

The regional geological file is the larger of the two files. Each of its 3964 records occupies five 80-column cards, for a total of 19 820 card images. The entire string of a record consists of 94 data items, including two repeating data items. All data item values are integer numbers ranging from 0 to 400, except the data items GSM and SMSM each of which consists of 8 different sets of 6 alphanumeric characters. This file structure was designed to simplify access to individual data items and to leave the greatest possible freedom to the user for regrouping of the items according to different geological models. It also allows easy sorting of data item values and, when the MARS VI data management system is used, the usage of MARS VI arithmetic functions such as SUM and AVG to give total counts or average counts, respectively, for a given item value for a study area.

Three separate subfiles can be distinguished in the mineral deposit file containing the 180 mineral deposit records, 844 mineral occurrence records, and 695 records for indicators, respectively. In total, this file consists of 6926 80-columns cards: 12 for each individual deposit, 4 per occurrence and 2 per indicator. The basic structure of the mineral deposit file consists of 28 data items and is shown in Figure 25. 2b. For practical reasons, the structure of the three subfiles has been designed so that they could be merged into the single structure of Figure 25. 2b. However, only part of the information coded for a mineral deposit is contained in records of the occurrence subfile, and even smaller amounts of the information are contained in the records of the indicator subfile. The three sub-files were assembled separately. Two parallel broken line segments indicate in Figure 25. 2b the portions of structures applicable to the occurrence and indicator records, respectively.

The following remarks regard the usage of repeating data items and the structure of the repeating substring in the mineral deposit record (*see* Fig. 25. 2b). For items 4 (PROCOM), 5 (RESCOM), 6 (OTHCOM) and 25 (MINERALS), no implied order exists for the values entered in the record. This means that a search can

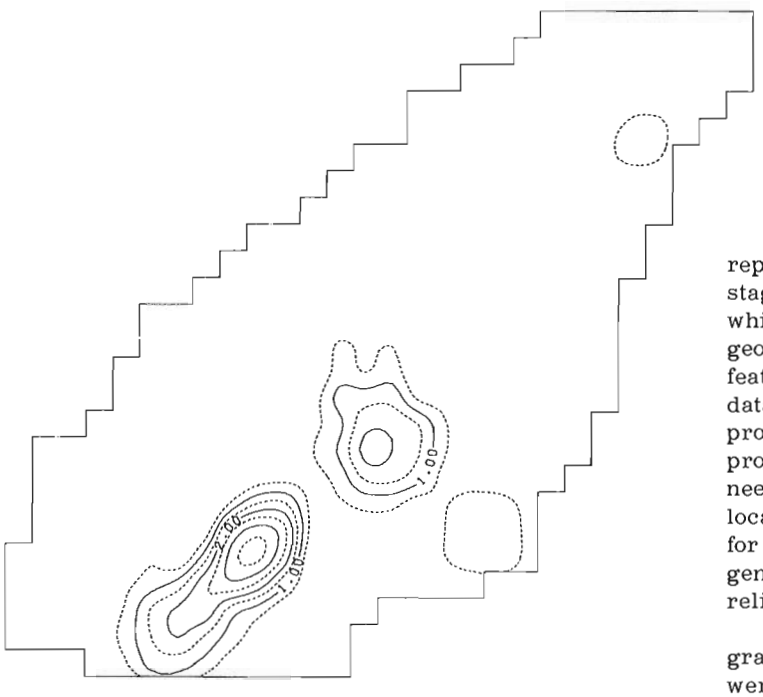

Figure 25.5

Example of output of PRGPCP for CALCOMP-763 plotter; outline of Eastern Townships area; contour values are 9-point moving averages (multiplied by 9) of values of Figure 2a in Chung and Divi (this volume).

be made by comparing a given value for the data item to all values occurring anywhere within the set of repeating items. This may represent a limitation in practice. The repeating substring 28 (TONGRD) contains data on tonnage, grade, and other data, for each of the commodities Cu, Pb, Zn, Ag, Au, and Ni, in that order. The logical sequence of the different items is also fixed for these metals. The implied order of the data items within a substring, and of the substrings within the repeating set, allows a great flexibility, making it possible to retrieve any item value by specifying the data item name and a subscript between (1) and (6). For example, the grade of Zn in total ore produced can be retrieved by asking for PGRADE(3). This substructure was designed to allow quick comparisons between values for all commodities occurring in a record and to facilitate automatic counting and tabulation of data items contained in the file.

The item values of each record in both files have been carefully checked for uniformity. Parameters such as location in UTM co-ordinates, host rocks in terms of the litho-age units, classification of the deposits into morphologic and genetic types, and sizes and grades of the deposits have to be subjected to stringent standards before they are fully comparable from record to record.

Computer graphic displays

Computer graphic displays have been extensively used for editing the data and displaying the results of statistical analysis for Project Appalachia. This section contains a discussion of how computer graphics were used in the project and a more detailed description of several programs for computer graphics which can also be used independently on data other than those contained in the Project Appalachia files.

Graphic displays are important especially for representing the geological data, during the editing stage and later, and the results of statistical analyses which in most cases are to be plotted on topographic or geological maps for comparison with known geological features. In situations where it is necessary that the data be plotted according to a specific cartographic projection, such as the Lambert Conformal Polyconic projection, lengthy mathematical computations are needed in order to plot a given point at its proper location. Such plotting cannot be performed extensively for a large data set without using a computer. In general, computer graphics are more accurate and reliable than results of manual plotting.

In the early stages this project, two computer graphic programs, STAR and VAR (also see Fig. 25.1) were used for editing the regional geological data. Maps produced on the line-printer by the program VAR were particularly useful to precoders and regional geologists for checking the patterns of variables defined earlier because printed patterns of many different variables selected from the data file could be quickly and inexpensively reproduced in the editing stage.

Figure 25.2 in report 22, this publication was plotted by program NEWVAR which is a modified version of VAR. It uses the EAI-430 flat-bed plotter instead of the line-printer and plots according to the Lambert Conformal Polyconic projection used for small-scale compilation maps (e.g. at scale 1:5 000 000).

The program GEOPLOT was utilized to plot the locations of mineral deposits and to check the measurements of either the UTM co-ordinates of the latitudes and longitudes of locations in the file. This program was designed to be flexible so that it can be utilized for many different purposes. Some features of GEOPLOT are as follows:

1. The co-ordinates of the points to be plotted can be specified either as decimal degrees of latitude and longitude or as UTM eastings and northings in metres.
2. The scale of the output is specified in the input.
3. Input points can be plotted according to the Lambert Conformal Polyconic projection with given standard parallels (south and north) or according to the UTM projection with given central meridian of the UTM zone.
4. The output map can be produced either on the EAI-430 plotter or on the CALCOMP-763 plotter.
5. Up to 6 different centred symbols can be used for different objects which are to be located. The size of these symbols can also be controlled in the input. Identifications of up to 10 characters in length can be printed or drawn beside each centred symbol.

Figure 25. 3 was plotted by program GEOPLOT using the EAI-430 plotter. The operations required to produce this plot jointly took less than 30 minutes; they were performed by means of the NCR-320 time-sharing terminal, where they consisted of (a) a series of MARS VI retrievals from the mineral deposit file to produce a subfile for the data to be used, (b) preparation of the input for GEOPLOT, and (c) linkage of the data subfile with GEOPLOT. The two enlarged insets shown in Figure 3 (A and B) were produced later, after plotting the initial map. A further documentation of GEOPLOT is in preparation.

In order to display the results of multivariate statistical analysis, three subprograms or subroutines have been written, GGGMAP, LAMMAP and PRGPCP, and these have been frequently used. Subprogram GGGMAP was added to most main programs for statistical analysis of which the output contained maps produced on the line-printer. An example of output for GGGMAP is shown in Figure 4 which corresponds to part of Figure 25. 2a in the preceding paper. The latter figure, and also Figures 25. 2b, c in that same paper dealing with the Eastern Townships, were produced by NEWMAP on the EAI-430 plotter instead of on the line-printer. NEWMAP is a modification of GGGMAP and is used for publication purposes only.

The program LAMMAP was written in order to plot the results of statistical analyses of data from large regions on Lambert Conformal projection maps. Figures 23. 1 - 23. 3 were produced by LAMMAP on the EAI-430 plotter.

Program PRGPCP was written to prepare input for GPCP (General Purpose Contouring Program), a contouring package available on the CYBER 74 computer using the CALCOMP-763 plotter. PRGPCP was applied to the data of Figure 25. 4 for the Eastern Townships area with the result shown in Figure 25. 5. Each of the values automatically contoured in Figure 25. 5 is the sum of 9 values forming a square of 30 km on a side. An option of PRGPCP is that it can compute sums for squares consisting of 1, 4, 9, 16, 25 (etc.) values. The boundaries of the study area are also drawn according to input specifications.

The programs described in this paper have been specially designed for Project Appalachia and in this context they have greatly facilitated the task of organizing, editing, displaying and analyzing simultaneously the large data sets.

Acknowledgment

During the preparation of the computer programs described in this paper, we have been assisted by the following summer students: Judith M. Ross (1973), Frank P. Regimbald (1974) and Raymond D. Martin (1975). Help by Cassie McCann during 1973-74 is also gratefully acknowledged.

Reference

Hubaux, A.
1973: A new geological tool - the data; Earth Sci. Rev., v. 9, p. 159-196.

Project 720097

C. F. Chung
Regional and Economic Geology Division

Introduction

This paper will outline an application of classification analysis to aid in predicting mineral potential from geological maps. Application of classification analysis, also known as discriminant analysis or pattern recognition, has been studied as part of the development of multivariate statistical models for the evaluation of mineral potential. The technique is in the development stage and the results presented in this paper are preliminary.

The general procedure of classification will be discussed followed by a more detailed description of the linear discriminant function which is based on the concept of two multivariate normal populations. An application of discriminant analysis to the Eastern Townships area in the Appalachian region will then be presented.

General Procedure for Classification

Given two populations π_1 and π_2 each consisting of individuals, the problem of classification is how to assign an individual to one or the other of the two populations π_1 and π_2 on the basis of measurements on a p-component vector $\underline{x} = (x_1, x_2, \ldots, x_p)$ on that individual. Let R be the p-dimensional region in which the point of observation $\underline{x}$ falls. We have to divide this region R into two subregions R_1 and R_2 by some suitable optimum method depending on the vector of measurements $\underline{x}$. If the observation $\underline{x}$ falls in R_1, we classify it as coming from population π_1, and if $\underline{x}$ falls in R_2, it is assigned to π_2. With such a procedure, two kinds of errors can occur in the classification. The procedure may assign an individual to π_2 when it really belongs to π_1, and vice versa. A good classification procedure should control and minimize these kinds of errors in classification.

Suppose that $f_1(\underline{x})$ and $f_2(\underline{x})$ are the probability density functions of $\underline{x}$ in the two populations π_1 and π_2, respectively. Then the probability of misclassifying an individual from π_1 as from π_2 (the first type of error in classification) is

$$\alpha_1 = \int_{R_2} f_1(\underline{x})\, d\underline{x}$$

and the probability of misclassifying an individual from π_2 as from π_1 is

$$\alpha_2 = \int_{R_1} f_2(\underline{x})\, d\underline{x} .$$

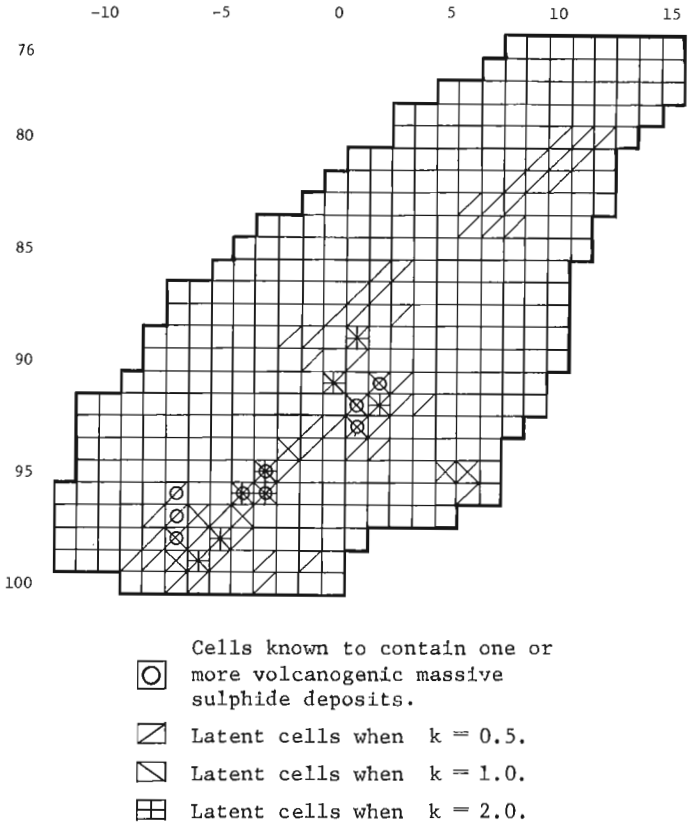

Figure 26. 1. Distribution of latent cells and non-latent cells for volcanogenic massive sulphide deposits in the Eastern Townships area.

The total probability of misclassification is $\alpha = \alpha_1 + \alpha_2$.

Let the cost or penalty of misclassifying an individual from π_1 as from π_2 be c_1 and let the cost of misclassifying an individual from π_2 as from π_1 be c_2. Then the problem is to divide R into R_1 and R_2 such that

$$\alpha = \int_{R_2} f_1(\underline{x})\, d\underline{x} + \int_{R_1} f_2(\underline{x})\, d\underline{x}$$

is minimized subject to the condition,

$$c_1\alpha_1 = c_2\alpha_2 \qquad \text{or} \qquad \alpha_1 = \frac{c_2}{c_1}\alpha_2$$

A solution of this minimization problem is provided by the Neyman-Pearson lemma (Rao, 1965). The solution is as follows. The best subregions R_1 and R_2 are chosen according to the criteria:

$$R_1 : \frac{f_1(\underline{x})}{f_2(\underline{x})} \geq k$$

$$R_2 : \frac{f_1(\underline{x})}{f_2(\underline{x})} < k \quad \text{where} \quad k = \frac{c_2}{c_1} . \tag{1}$$

Linear Discriminant Function

In practice, the probability functions $f_1(\underline{x})$ and $f_2(\underline{x})$ are usually estimated from samples from the two populations π_1 and π_2, respectively. For the preliminary analysis, let us suppose that the π_1 and π_2 are two multivariate normal populations with equal covariance matrices, namely, $N(\underline{\mu}(1), \Sigma)$ and $N(\underline{\mu}(2), \Sigma)$ where $\underline{\mu}(i) = (\mu_1(i), \mu_2(i), \ldots, \mu_p(i)$ is the mean vector of the i-th population (i = 1, 2) and Σ is the common convariance matrix of the two populations. Then the density function of i-th population (i = 1, 2) is

$$f_i(\underline{x}) = \frac{1}{(2\pi)^{\frac{1}{2}p}|\Sigma|^{\frac{1}{2}}} \exp\{-\tfrac{1}{2}(\underline{x}-\underline{\mu}(i))'\Sigma^{-1}(\underline{x}-\underline{\mu}(i))\}$$

The ratio of density functions is

$$\frac{f_1(\underline{x})}{f_2(\underline{x})} = \frac{\exp\{-\frac{1}{2}(\underline{x}-\underline{\mu}(1))'\Sigma^{-1}(\underline{x}-\underline{\mu}(1))\}}{\exp\{-\frac{1}{2}(\underline{x}-\underline{\mu}(2))'\Sigma^{-1}(\underline{x}-\underline{\mu}(2))\}}$$

$$= \exp\{\underline{x}'\Sigma^{-1}(\underline{\mu}(1)-\underline{\mu}(2)) - \tfrac{1}{2}(\underline{\mu}(1)+\underline{\mu}(2))'\Sigma^{-1}(\underline{\mu}(1)-\underline{\mu}(2))\} \tag{2}$$

Substitution of (2) into (1) yields the best subregions R_1 and R_2, and

$$R_1 : \underline{x}'\Sigma^{-1}(\underline{\mu}(1)-\underline{\mu}(2)) - \tfrac{1}{2}(\underline{\mu}(1)+\underline{\mu}(2))'\Sigma^{-1}(\underline{\mu}(1)-\underline{\mu}(2)) \geq \log_e k$$

$$R_2 : \underline{x}'\Sigma^{-1}(\underline{\mu}(1)-\underline{\mu}(2)) - \tfrac{1}{2}(\underline{\mu}(1)+\underline{\mu}(2))'\Sigma^{-1}(\underline{\mu}(1)-\underline{\mu}(2)) < \log_e k \tag{3}$$

In the case of the unknown parameters $\underline{\mu}(1)$, $\underline{\mu}(2)$ and Σ these must be also inferred from samples. In such a case, Anderson (1958) suggested using the sample mean vectors $\underline{\bar{x}}(1)$ and $\underline{\bar{x}}(2)$ and the sample covariance matrix S instead of $\underline{\mu}(1)$, $\underline{\mu}(2)$ and Σ, respectively. Let $\underline{x}^1_1, \underline{x}^1_2, \ldots, \underline{x}^1_{N_1}$ be N_1 random samples from π_1 and let $\underline{x}^2_1, \underline{x}^2_2, \ldots, \underline{x}^2_{N_2}$ be N_2 random samples from π_2 where $\underline{x}^i_j = (x^i_{j1}, x^i_{j2}, \ldots, x^i_{jp})$ for all j = 1, 2, ..., N_i and i = 1, 2. Then the sample mean vectors $\underline{\bar{x}}(i)$ (i = 1, 2) and the sample covariance matrix S are defined by

$$\underline{\bar{x}}(i) = (\bar{x}^i_1, \bar{x}^i_2, \ldots, \bar{x}^i_p)$$

$$\bar{x}^i_k = \frac{1}{N_i}\sum_{j=1}^{N_i} x^i_{jk} \qquad \text{for all } k = 1, 2, \cdots, p \text{ and } i = 1, 2 \tag{4}$$

$$S = \frac{1}{N_1+N_2-2}\left\{\sum_{j=1}^{N_1}(\underline{x}^1_j-\underline{\bar{x}}(1))(\underline{x}^1_j-\underline{\bar{x}}(1))' + \sum_{j=1}^{N_2}(\underline{x}^2_j-\underline{\bar{x}}(2))(\underline{x}^2_j-\underline{\bar{x}}(2))'\right\} .$$

Substitute these estimates in (4) for the parameters in (2) to obtain the following estimate of the likelihood ratio in (1):

$$\widehat{\left(\log_e \frac{f_1(\underline{x})}{f_2(\underline{x})}\right)} = \underline{x}'S^{-1}(\underline{\bar{x}}(1)-\underline{\bar{x}}(2)) - \tfrac{1}{2}(\underline{\bar{x}}(1)+\underline{\bar{x}}(2))'S^{-1}(\underline{\bar{x}}(1)-\underline{\bar{x}}(2)) \tag{5}$$

This is known as the sample linear discriminant function or as Anderson's classification statistic. The procedure (3) of classification now becomes:

$$\hat{R}_1 : \underline{x}'S^{-1}(\bar{\underline{x}}(1)-\bar{\underline{x}}(2)) - \tfrac{1}{2}(\bar{\underline{x}}(1)+\bar{\underline{x}}(2))'S^{-1}(\bar{\underline{x}}(1)-\bar{\underline{x}}(2)) \geq \log_e k$$
$$\hat{R}_2 : \underline{x}'S^{-1}(\bar{\underline{x}}(1)-\bar{\underline{x}}(2)) - \tfrac{1}{2}(\bar{\underline{x}}(1)+\bar{\underline{x}}(2))'S^{-1}(\bar{\underline{x}}(1)-\bar{\underline{x}}(2)) < \log_e k \qquad (6)$$

The statistical properties of Anderson's statistic have been described in detail by Anderson (1958) and Kshirsagar (1972).

Practical Example

The Eastern Townships area in the Appalachian region is taken for this example and the data for this area have been extracted from the Appalachia regional geological file. The area consists of 384 cells with a size of 10 by 10 km and contains 25 litho-age units (*see* report 24, this publication). Thus, the vector $\underline{x}$ for each individual cell contains 25 components. Among the 384 cells, 9 cells contain one or more known volcanogenic massive sulphide deposits, the type considered in this example.

Let π_1 be the population of cells that contain one or more deposits (discovered and undiscovered) and let π_2 be the population of cells that do not contain any deposit. Suppose that the 9 cells with the known deposits are random samples from π_1 and that the remaining 375 cells are random samples from π_2. Furthermore, let the two populations be two multivariate normal populations with equal covariance matrices. Then the classification procedure in (6) can be applied for classification of cells into the two populations π_1 and π_2.

For each cell, the linear discriminant function, the Anderson's statistic in (5), was computed. However, in order to classify cells according to one of the two populations, the ratio of costs $k(= c_2/c_1)$ was set equal to 2, 1 and 0.5 respectively, with corresponding patterns shown in Figure 26.1. When the Anderson's statistic of a cell $\underline{x}$ is equal to or greater than $\log_e k$ ($\underline{x}$ is in R_1), the cell is classified into π_1; the cell is predicted to have deposits and, in this paper, is called a "latent" cell. When a cell is classified into π_2, the cell is predicted not to have any volcanogenic massive sulphide deposit and it is called a "non-latent" cell. In more explicit terms, k = 2 means that the cost of misclassification of cells with undiscovered deposits as non-latent cells is twice as great as the cost of misclassification of cells without any deposit as latent cells. The reverse holds true for k = 0.5. k = 1 implies that the two costs are equal.

In order to evaluate this technique, let us make comparisons with the results from the regression analysis in the paper by Chung and Divi (report 24, this publication). Figure 24.2a in that paper portrays results from a regression analysis based on the same data. If a pattern is made with cells of which the values in Figure 24.2a are greater than 45, 22 and 4, then this pattern approximately coincides with that in Figure 26.1 of this paper. In fact, even though the two multivariate techniques are based on different assumptions, the two sets of estimates are nearly proportional to each other.

Kshirsagar (1972) has shown that the regression estimates $\underline{x}'\underline{b}$ (Fig. 24.2a), where the $\underline{b}$ is the least squares estimator of the regression coefficients in the regression model, can be expressed in terms of $\bar{\underline{x}}(1)$, $\bar{\underline{x}}(2)$ and S, and

$$\underline{x}'\underline{b} = \frac{N_1N_2\underline{x}'S^{-1}(\bar{\underline{x}}(1)-\bar{\underline{x}}(2))}{(N_1+N_2)(N_1+N_2-2) + N_1N_2(\bar{\underline{x}}(1)-\bar{\underline{x}}(2))'S^{-1}(\bar{\underline{x}}(1)-\bar{\underline{x}}(2))}$$

Also, Anderson's statistic (Fig. 1) can be expressed, using the regression estimates $\underline{x}'\underline{b}$, by

$$\frac{(N_1+N_2)(N_1+N_2-2) + N_1N_2(\bar{\underline{x}}(1)-\bar{\underline{x}}(2))'S^{-1}(\bar{\underline{x}}(1)-\bar{\underline{x}}(2))}{N_1N_2}\,\underline{x}'\underline{b}$$
$$- \tfrac{1}{2}(\bar{\underline{x}}(1)+\bar{\underline{x}}(2))'S^{-1}(\bar{\underline{x}}(1)-\bar{\underline{x}}(2)).$$

Thus, the two analyses provide the same pattern. The two patterns do not coincide exactly because some variables (litho-age units) were eliminated by using the stepwise regression procedure for the regression analysis. In the classification analysis, the boundary point $\log_e k$ can be easily set to classify cells into latent cells or non-latent cells, whereas in the regression analysis, setting the boundary point above which cells potentially contain deposits is more difficult. A possible drawback of this classification procedure is that the assumption of normality can not be satisfied in practice, because only a fraction of the 25 litho-age units are present in any one cell.

References

Anderson, T.W.
1958: An Introduction to multivariate statistical analysis; John Wiley & Sons, New York, Chap. 6, p. 126-153.

Kshirsagar, A.M.
1972: Multivariate analysis; Marcel Dekker, Inc., New York, Chap. 6, p. 187-246.

Rao, C.R.
1965: Linear statistical inference and its applications; John Wiley & Sons, New York, Chap. 7, p. 374-434.

27. PRELIMINARY APPLICATION OF CLUSTER ANALYSIS TO PROJECT APPALACHIA DATA

Project 720097

A. G. Fabbri
Regional and Economic Geology Division

Introduction

The data bank of Project Appalachia has been built for the application of statistical methods, in order to (1) recognize patterns in the geological parameters coded for 10-km UTM cells and for deposits with Cu, Pb or Zn, (2) correlate these patterns with one another, and (3) use this correlation to compute estimates for the probability of occurrence of deposits which have not yet been discovered. This paper is a preliminary description of an application of cluster analysis to the problem of recognizing patterns in the interrelations of the geological parameters contained in selected groups of cells.

The problem is to consider the geological variables in a selected group or population of cells and to classify them according to the values that they assume in the cells. It may then become possible to group the cells and to compare the resulting pattern on the basis of mutual similarity in terms of the geological variables with the distribution pattern of cells containing known deposits.

Cluster analysis consists of a variety of techniques believed to be suitable for this purpose. An example of a preliminary application to a group of cells selected from the regional geological file of Project Appalachia will be presented for illustration.

Cluster Analysis

A general review of the problems to be considered in the application of cluster analysis for pattern recognition has been given by Kendall (1972). During the past 15 years, several hundred papers have been published dealing with theory and applications of this technique. A book on cluster analysis has been written by Anderberg (1973). It contains a large set of computer programs for a variety of clustering methods.

Applications of cluster analysis have been made in many fields including the natural sciences, the social sciences, medicine, information theory, and engineering science. Specific applications have been made by Anderson (1971) in soil science, Collyer and Merriam (1973) in mineral exploration, Wiatr and Stenzel (1974) in the classification of engineering geological environments, and Jaquet *et al.* (1975) for the study of lake geochemical samples. An interesting recent application of clustering to the analysis of polymodal distributions in orientation data is given by Bailey (1975).

Cluster analysis comprises a variety of different techniques all designed to subdivide observations into groups, so that each group is more or less homogeneous and distinct from the others. Consideration should be given to the kinds of data to which cluster analysis can be applied in practice. According to the nature of the

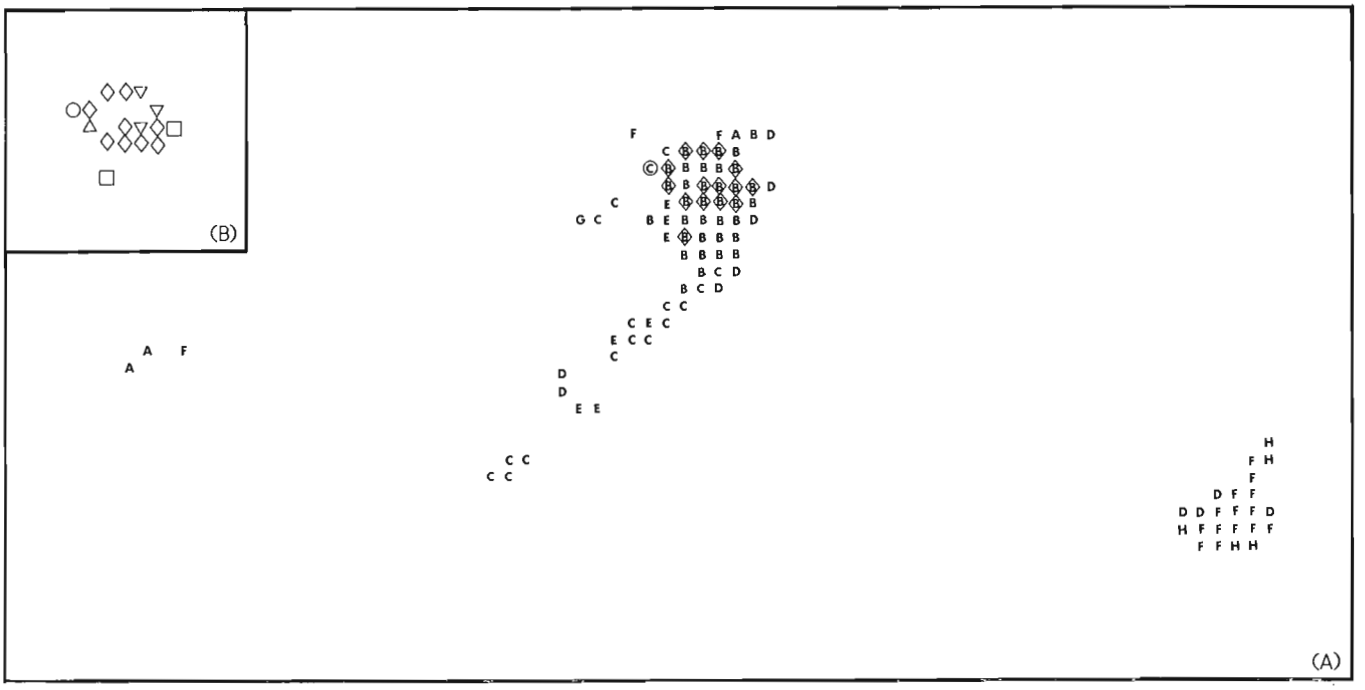

Figure 27. 1. Distribution of clustered cells. 27. 1A shows cells of Figure 27. 2 classified into 7 clusters (A-H) by selecting a similarity level of 0. 6346. Cells with deposits are distinguished by the same symbols used in the dendrogram of Figure 27. 2; 27. 1B shows distribution of the 16 mineralized cells, classified into 5 clusters. In order to compare this pattern to that of 27. 1A and to Figure 27. 2, the clustered cells are distinguished by different symbols.

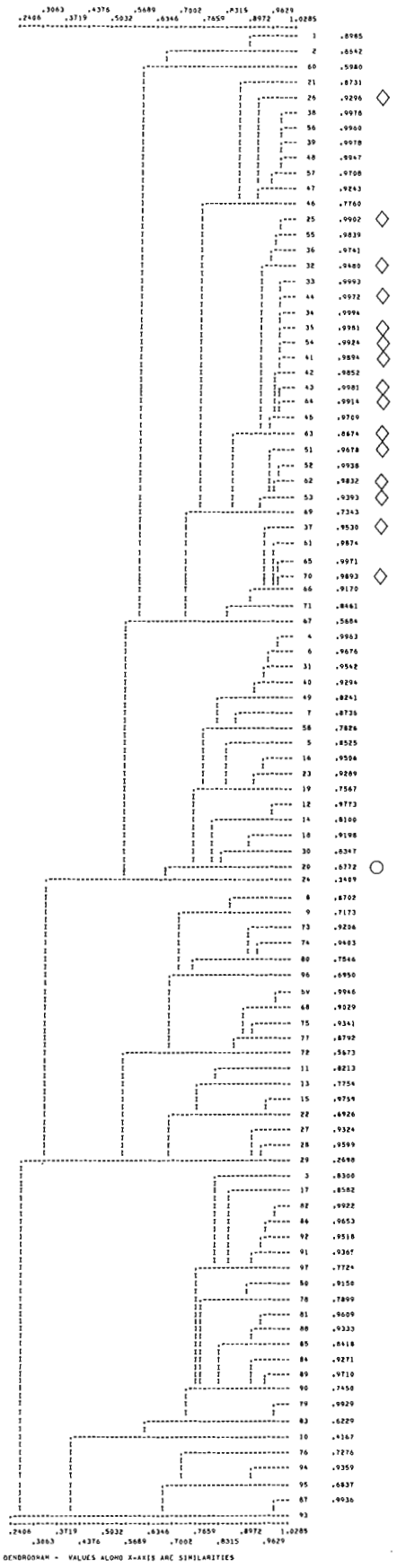

data, variables can be divided into continuous, discrete and binary variables, or, on basis of the scale of measurement, into ratio, interval, ordinal and nominal variables. Different clustering techniques have been developed to transform and analyze variables of different types.

Suppose that n specimens are to be classified, and that m measurements have been made on each specimen. This produces an n x m matrix as the data set. We can compute some measure of the degree of similarity between pairs of specimens (or pairs of measurements).

A variety of similarity coefficients have been developed for this purpose. The ordinary (Pearson product-moment) correlation coefficient r_{ij} and the standardized Euclidean distance d_{ij} in m-dimensional space are among those more commonly used. The latter distance coefficient is computed as $d_{ij} = \sqrt{\sum_{k=1}^{m} (X_{ik} - X_{jk})/m}$, where X_{ik} denotes the k-th variable measured on specimen i and X_{jk} is the k-th variable measured on specimen j.

Other measures of association used in cluster analysis include the cosine theta coefficient, matching coefficients, and cross-association coefficients. A discussion of the similarity coefficients most widely used in geology has been given by Harbaugh and Merriam (1968).

A practical example will now be given in order to show a relatively simple type of application of the technique, which seems particularly suitable for the problem of analyzing data stored in large computerized data banks like the one created for Project Appalachia.

Application to Middle-Upper Ordovician Volcanic Environments

Cell records for this experiment with litho-age units G48 or G49 were retrieved from the mainland Appalachia data block of the regional geological file. These data have also been used for example in a preceding paper where the cells containing Middle-Upper Ordovician basic with minor acid volcanics (G48) and Middle-Upper Ordovician acid volcanics (G49) have been shown in Figure 22. 2.

Of the total number of records (97), 3 occur in Quebec, 71 in New Brunswick and 23 in Nova Scotia. In total, there are 39 variables with nonzero values in one or more of the cells. The numbers (*see* Table 22. 1) of the litho-age units in the 97 cells are 3, 4, 8-11, 14, 15, 20-23, 25, 26, 28, 29, 33, 34, 36-38, 45, 47-49, 51-53, 55, 60, 62. All four structural variables (S1-S4) and 3 (M2-M4) regional metamorphic variables are also represented. Of the latter only the amphibolite facies (M1) is absent from the cells used for example. The 97 cells and their 39 variables comprise a matrix of size (97 x 39).

Figure 27. 2

Computer produced dendrogram for the clustering of 97 10-km UTM cells containing Middle and Upper Ordovician volcanic rocks in the Mainland data block of Project Appalachia regional geological file. Cells are numbered 1 to 97; cells containing volcanogenic massive sulphide deposits are indicated by means of open diamonds and circle.

Sixteen of these 97 cells contain among them a total of 39 volcanogenic massive sulphide deposits. One of these 16 contains 10 deposits, two contain 4 deposits, two contain 3 deposits, four contain 2 deposits, and seven contain 1 deposit. These 16 cells, all of which occur in the Bathurst-Newcastle area, have at least one nonzero value for 20 litho-age units and structural and metamorphic variables numbered 4, 14, 15, 23, 25, 33, 34, 45, 47-49, 51, 53, 55, S1, S2, S4, and M2-M4. The 16 deposit-bearing cells and their 20 geological parameters comprise a second matrix of size (16 x 20).

The example, therefore, consists of two matrices of sizes (97 x 39), and (16 x 20) for cells and variables, respectively. Cluster analysis has been applied using both correlation and distance coefficients in order to obtain patterns of clusters for cells and to compare these patterns with that for the cells that contain volcanogenic massive sulphide deposits. The results for the correlation coefficient and the distance coefficient were not appreciably different, so only the experiments in which the correlation coefficient was employed will be presented.

Use has been made of the clustering program listed by Davis (1973) which has been designed for small data sets and uses a clustering technique called weighted pair-group method with arithmetic average. Figure 27.2 represents the dendrogram printed in the output of this program by means of which the 97 cell records were clustered using the correlation matrix. For the construction of this type of dendrogram, the highest pairwise similarities are calculated first and two specimens are connected only if they have maximum correlation with one another. Next, the correlations with other specimens are averaged in order to obtain a smaller matrix of average correlations. The process is continued until all specimens and clusters of specimens are jointed together and the final result is represented in the dendrogram.

In the dendrogram of Figure 27.2, the second column from the right represents the cells which had been numbered 1 to 97. The last column contains the similarity levels at which the clusters linked to the cells from above join other clusters downwards in Figure 27.2. By sectioning the dendrogram along a vertical line at the 0.6346 similarity level, we can distinguish 8 clusters. One of these, the second one from the top downwards, contains 15 of the 16 cells with deposits; the next cluster contains the remaining cell with deposits. These mineralized cells have been indicated by open diamonds and a circle, respectively. This pattern is represented in map form in Figure 27.1a where the 8 clusters are indicated by the letters A to H. All cells of cluster B could be considered as indicating a geological environment with a relatively high probability of containing volcanogenic massive sulphide deposits. Of particular interest could be those B-cells which are not located in the immediate vicinity of cells containing known deposits. Cluster C would also be of interest.

Increasing the level of similarity in Figure 27.2 above the value of 0.7659, instead of 0.6346 used above, results in the reclassification of cells 26, 37 and 70 into two clusters separate from the cluster that contained them previously. This further separation of clusters can also be observed by using as the sample for cluster analysis the subset of the 16 cells with known deposits and with 20 variables only. The distribution pattern of 5 clusters obtained at a similarity level of 0.9050 for the correlation matrix resulting from that other experiment, is shown in Figure 27.2b in order to compare this pattern with the one for the Bathurst-Newcastle area in Figure 27.1a. In Figure 27.1b, the cell records of the different clusters are distinguished by open triangles that point either upward or downward, squares, diamonds and a circle.

Conclusions

This preliminary application of cluster analysis to cells containing Middle-Upper Ordovician volcanics serves to suggest the potential usefulness of this technique for the classification of geological environments favourable to the occurrence of volcanogenic massive sulphide deposits. Further applications to Project Appalachia data will consider transformation methods by which the variables can be weighted before they are subjected to several, alternative methods of cluster analysis.

References

Anderberg, M.R.
1973: Cluster analysis for applications; New York and London, Academic Press, 359 p.

Anderson, A.J.B.
1971: Numeric examination of multivariate soil samples; Mathematical Geol., v. 3, p. 1-14.

Bailey, A.I.
1975: A method of analyzing polymodal distributions in orientation data; Mathematical Geol., v. 7, p. 285-293.

Collyer, P.L. and Merriam, D.F.
1973: An application of cluster analysis in mineral exploration; Mathematical Geol., v. 5, p. 213-223.

Davis, J.C.
1973: Statistics and data analysis in geology; New York, John Wiley & Sons, 550 p.

Harbaugh, J.W. and Merriam, D.F.
1968: Computer applications in stratigraphic analysis; New York, John Wiley & Sons, 282 p.

Jaquet, J.-M., Froidevaux and Vernet, J.-P.
1915: Comparison of automatic classification methods applied to lake geochemical samples; Mathematical Geol., v. 7, p. 237-266.

Kendall, M.G.
1972: Cluster analysis: in Frontiers of Pattern Recognition (Watanabe, S., editor); New York and London, Academic Press, 359 p.

Wiatr, I. and Stenzel, P.
1974: Application of factor analysis to classification of engineering-geological environments; Mathematical Geol., v. 6, p. 17-31.

28. APPLICATION OF CANONICAL CORRELATION ANALYSIS TO PROJECT APPALACHIA DATA

Project 720097

S. R. Divi
Regional and Economic Geology Division

Interrelationships between sets of variables can be studied by applying canonical correlation analysis (Hotelling, 1936). Application of this technique seems to be particularly useful for Project Appalachia data that consist of different sets of variables which have been coded for each of 3964 10 by 10-km-square cells.

Suppose that we have a sample Z from a p-dimensional space, containing p_1 random variables in set Z_1 and p_2 random variables in set $Z_2 (p_1 + p_2 = p)$. Z_1 may be the predictor or independent variables such as the litho-age units, structural variables, or metamorphic variables, and Z_2 may be the criterion or dependent variables, such as amounts of the commodities Cu, Pb, Zn contained in the deposits of a given type. The objective is to understand the interrelationship between Z_1 and Z_2. If Z_1 and Z_2 each contain a few variables only, the problem can be studied by obtaining the bivariate correlation coefficients for different pairs of variables among the two sets. Or, for the special case in which the number of dependent variables in the second set equals one, the multiple regression technique can be applied. However, when the sets (with either dependent or independent variables) are as large as those in Project Appalachia, as for example the set with 79 litho-age variables, it becomes very difficult to comprehend simultaneously the meaning of the resulting very large number of correlation coefficients, and to generalize the extent and nature of the relationship between the sets. In such cases, the relationship can be summarized and expressed as an index by applying canonical correlation analysis. Detailed derivations and discussions of this technique have been given by Anderson (1958) and Wilks (1962); a brief description follows.

The objective of canonical correlation is to find a maximum correlation between the two sets Z_1 and Z_2. This is done by finding, initially, a linear equation for each of the two sets of variables with

$$U = A'Z_1 \quad ; \quad V = B'Z_2$$

where

$$A = \begin{pmatrix} a_1 \\ a_2 \\ a_3 \\ . \\ . \\ . \\ a_{p_1} \end{pmatrix} \quad ; \quad B = \begin{pmatrix} b_{p_1+1} \\ b_{p_1+2} \\ b_{p_1+3} \\ . \\ . \\ . \\ b_p \end{pmatrix}$$

A and B are selected in such a way that the canonical variates U and V have unit variance and the largest possible correlation between them. The coefficient of correlation between U and V is known as the canonical correlation coefficient or λ_1. Calculation of λ_1, which represents the square of the canonical correlation coefficient, involves partitioning of the correlation matrix R of Z as

$$R = \left(\begin{array}{c|c} R_{11} & R_{12} \\ \hline R_{21} & R_{22} \end{array}\right)$$

where R_{11} and R_{22} are the correlation matrices of Z_1 and Z_2, respectively, and $R_{12} = R'_{21}$ is the matrix for correlations between Z_1 and Z_2. λ_1 can be obtained as the largest eigenvalue of the equation

$$\left| R_{11}^{-1} R_{12} R_{22}^{-1} R_{21} - \lambda I \right| = 0.$$

The smaller values of λ satisfying this equation also correspond to canonical variates. The strength of the link between Z_1 and Z_2 is measured by the larger canonical correlation coefficients, which may be tested for statistical significance; and the nature of the link is indicated by the larger weights (a_i, $i = 1, \ldots . p_1$; and b_j, $j = 1, \ldots . p_2$) assigned to the variables.

As in most other multivariate techniques, and for the purpose of applying statistical tests, the assumption is made that the observed variates are linear functions of the canonical variates and that they are normally distributed.

Canonical correlation analysis can be combined with trend-surface analysis to obtain what are known as canonical trend surfaces. Here, the geographic co-ordinates (or cell co-ordinates for Project Appalachia data) form one set, and the other variables, e. g. litho-age units or commodities, form the second set. The computed canonical trend surface then represents the succinct summarization of the regional trend common to the variables in the second set. Through more complicated computations, it is possible to study the interrelationships between three or more sets of variables (Roy, 1957). It is useful to study and understand the meaning of regional trends common to the variables in both the regional geological file and mineral deposit file for Project Appalachia data. Existing computer programs (Lee, 1969; Dixon, 1972) have been modified to become applicable to the specific types of Project Appalachia data, and studies using the canonical correlation technique are in progress.

References

Anderson, T. W.
1958: An introduction to multivariate statistical analysis; Wiley, New York, Chap. 12, p. 587-590.

Dixon, W. J., (Editor)
1972: BMD Biomedical computer programs (FORTRAN IV), Univ. California Press, Los Angeles: Program BMD09M (by Paul Sampson), p. 269-276.

Hotelling, H.
1936: Relations between two sets of variables; Biometrika, v. 28, p. 321-377.

Lee, P. J.
1969: FORTRAN IV programs for canonical correlation analysis and canonical trend-surface analysis; Univ. Kansas, Computer Contr. no. 32, 46 p.

Roy, S. N.
1957: Some aspects of multivariate analysis; Wiley, New York, 214 p.

Wilks, S. S.
1962: Mathematical statistics; Wiley, New York, p. 576-581.

29. SPATIAL CLUSTERING AND LOGNORMAL SIZE DISTRIBUTION OF VOLCANOGENIC MASSIVE SULPHIDE DEPOSITS IN THE BATHURST AREA

Project 720097

F. P. Agterberg
Regional and Economic Geology Division

Introduction

Volcanogenic massive sulphide deposits often occur in clusters. Several examples of clustering can be seen in Figure 25. 3. Locally, deposits cluster strongly near Sherbrooke in the Eastern Townships, Quebec, and near Buchans, central Newfoundland. In the Bathurst area, New Brunswick, the Heath Steele Mine provides an example of strong localized clustering with 12 separate orebodies occurring within a relatively narrow zone about 6 km long.

Clustering of volcanogenic massive sulphide deposits is a phenomenon that is amenable to statistical analysis. Figure 29. 1 is for the Bathurst area and shows 49 of the 10 by 10 km cells of the UTM grid used for coding. The 40 deposits of Figure 29. 1 occur in the Tetagouche Group of Middle-Upper Ordovician age which consists mainly of acid volcanics, basic volcanics and greywackes. Thirty-two of the 49 cells of Figure 29. 1 are empty, 8 contain 1 deposit, 4 contain 2 deposits, 2 contain 3 deposits, 2 contain 4 deposits, and 1 contains 10 deposits. These observed frequencies are represented in Table 29. 1 (first column) and will be statistically analyzed according to different methods.

In addition to the spatial clustering of the deposits, consideration will be given to their size, measured as total tonnage of ore per deposit, and to the grades of the metals Cu, Pb and Zn contained in this ore.

It seems that specific types of clustering and lognormality of the size-frequency distribution represent characteristic features of volcanogenic massive sulphide deposits.

Sangster (1972) has compared Precambrian volcanogenic massive sulphide deposits in Canada and the Kuroko deposits of Miocene age in Japan. The Paleozoic deposits of Figure 29. 1 can also be regarded as belonging to this general type. For example, the deposits are zoned. In the more or less stratabound massive sulphide lenses, the zinc- and lead-rich parts lie stratigraphically above the copper-rich parts. Copper-bearing disseminated or stockwork ore that cross-cuts the stratigraphy may occur at a stratigraphically lower level.

These deposits are considered to have a volcanic exhalative origin; hydrothermal solutions rose to the surface at the final stage of a cycle of submarine, calc-alakali type volcanism and precipitated sulphides at or near the seabottom. A single volcanic cycle generally commenced with the formation of basalt lavas; near the end of the cycle, extensive acid volcanism occurred with formation of rhyolites and pyroclastics, particularly near the volcanic centres. Upon completion of a cycle, a new cycle may have started or sedimentary rocks may have been deposited. Many of the deposits in the Bathurst area are enclosed by sedimentary rocks,

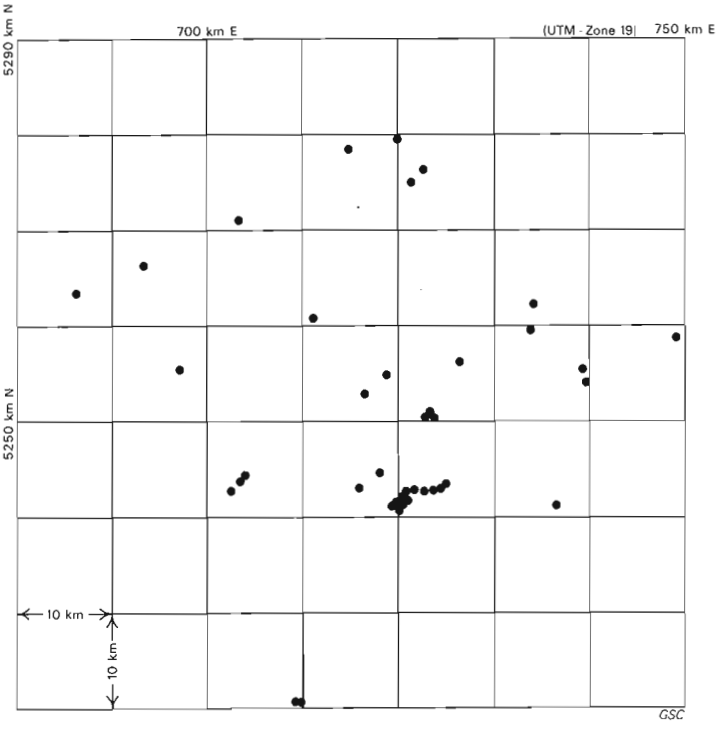

Figure 29. 1. Pattern of volcanogenic massive sulphide deposits in Bathurst area with superimposed UTM-grid; compare to Figure 25. 3 of Wong, Chung, and Fabbri (this publication).

mainly greywackes, at or near the contact with acid volcanic rocks.

According to D. F. Sangster (1974, pers. comm.), the Bathurst area probably contains at least three volcanic centres with abundant rhyolites and associated volcanic exhalative mineral deposits. Clusters of deposits can occur at a variable distance from the major volcanic centres with which they may be genetically associated. Later in this paper, a stochastic point process model of the Neyman-Scott type will be applied to explain this clustering of deposits. It should then be kept in mind that the centres of clusters of deposits to be considered in the stochastic model do not necessarily coincide with volcanic centres.

Spatial Clustering

The simplest model for points randomly distributed in two dimensions is the simple Poisson stochastic point process model (Fisher, 1972). This model actually provides a natural definition of randomness of points

Table 29.1

Observed frequencies and calculated frequencies for Poisson model (Equations 1-2 in text) and Negative Binomial model (Equations 3-5 in text) for cells of Figure 29.1. Subcells containing one or more deposits measure 2.5 km on a side. Last columns (Deposits, 36 cells) are for smaller area with 13 empty cells deleted (*see* text).

		Deposits (49 cells)			Subcells (49 cells)			Deposits (36 cells)		
		Obs.	Calc. Pois.	Calc. Neg. Bin.	Obs.	Calc. Pois.	Calc. Neg. Bin.	Obs.	Calc. Pois.	Calc. Neg. Bin.
	Mean	0.82	0.82	0.82	0.57	0.57	0.57	1.11	1.11	1.11
	var.	2.88	0.82	2.69	0.82	0.57	0.93	3.60	1.11	3.20
No. events/cell	0	32	21.7	32.1	32	27.7	31.4	19	11.9	19.3
	1	8	17.7	7.9	9	15.8	11.1	8	13.2	7.4
	2	4	7.2	3.7	5	4.5	4.1	4	7.3	3.9
	3	2	2.0	2.0	3	0.9	1.5	2	2.7	2.2
	4	2	0.4	1.2	0	0.1	0.6	2	0.8	1.3
	≥5	1	0.1	2.1	0	0.0	0.3	1	0.2	1.9

in Euclidean space because any point can occur anywhere with the same probability. The number of points contained in a cell or subregion is a random variable K with Poisson distribution. The probability that the cell contains exactly k deposits is given by

$$P(K=k) = \lambda^k e^{-\lambda}/k! \qquad (1)$$

The parameter λ is constant for constant cell size. Actually, λ = constant $^{o}m(A)$ where m(A) represents the area (as Lebesgue measure) of cell A.

A pattern of points created by the simple Poisson process will exhibit a certain amount of clustering of points. However, this clustering is random. Actual clustering constitutes a departure from randomness and occurs only if locally the points lie anomalously close to one another. A point pattern can be tested for randomness in many different ways. Some of these tests will now be applied to the pattern of Figure 29.1.

The observed frequencies of deposits per 10 x 10 km UTM cell are shown in Table 29.1. Since there are 40 deposits in n = 49 cells, the sample mean is m= 40/49 = 0.82. The average squared deviation from m amounts to var = 2.88 and will be used as an estimate of variance. The Poisson distribution has the property that its mean E(K) is equal to its variance σ^2 (K) with

$$E(K) = \sigma^2(K) = \lambda \qquad (2)$$

For a random point pattern $\hat{\chi}$ (n-1) = n. var/m is distributed as χ^2 with (n-1) degrees of freedom (Bliss and Fisher, 1953). We have for Figure 29.1a, $\hat{\chi}^2$ (48) = 172 to be compared with $\chi^2_{0.05}(48) = 65$ or $\chi^2_{0.01}(48) = 74$. Obviously, the hypothesis that the points in Figure 29.1 are randomly distributed should be rejected.

Theoretical frequencies calculated by Eq. (1) after setting λ = m = 0.48 are also shown in Table 29.1. The fit with the observed frequencies is rather poor although not as bad as might have been expected on the basis of the result of the χ^2- test. The reason for this is that the variance (var) is very sensitive to anomalously large observed frequencies. A procedure proposed for reducing the effect of strong localized clusters (Agterberg, 1974) consisted of replacing the individual deposits by other "events" comprising one or more deposits.

In order to evaluate the influence of strong localized clustering in the situation of Figure 29.1, such "events" were defined as follows. Each 10 x 10 km cell was divided into sixteen $2\frac{1}{2}$ by $2\frac{1}{2}$ km subcells. A subcell was counted as an "event" when it contains one or more deposits. This yields a new set of observed frequencies with mean of 0.57 and variance 0.82 also shown in Table 29.1. Application of the χ^2- test now gives $\hat{\chi}^2(48) = 70.5$; hence, the hypothesis of randomly distributed "events" should be rejected but not so readily.

The simple Poisson model can be generalized in several ways. The so-called "simple coloured map model" which can be used to interpret the patterns of values in Figures 23.1-23.3 provides an example. The map consists of disjointed sub-regions (e.g. lithoage units) coloured according to a specific scheme. The occurrence of "events" is believed to be controlled by a number of simple Poisson stochastic point processes one for each colour, with different parameters λ_i for the p different colours i (i = 1, 2, ..., p).

Other multivariate generalizations can be made. These have the advantage that a new λ can be determined for each cell or combination of cells on the map. The probability distribution for number of deposits in the cell or larger region remains given by Eq. (1) because of a unique property of the Poisson distribution (Plackett, 1974).

Another type of generalization is as follows. We can assume that λ is a random variable. It means that this parameter, which uniquely defines the random variable for occurrence of points in a cell, is itself a random variable which assumes different values in different cells. If λ then satisfies the gamma-distribution, which is known to be very flexible, the actual frequencies for deposits per cell will satisfy the negative binomial distribution. The probability $P(K = k)$ that a cell contains exactly k deposits is now given by:

$$P(K=k) = \binom{r+k-1}{k} p^r q^k \qquad (3)$$

where $p + q = 1$. Mean and variance satisfy:

$$E(K) = rq/p; \quad \sigma^2(K) = rq/p^2 \qquad (4)$$

It can also be derived that:

$$P(K=0) = p^r; \quad P(K=k+1) = \frac{r+k}{k+1} q \cdot P(K=k) \qquad (5)$$

Substitution of $m = 0.82$ and $var = 2.88$ into Eq. (4) gives $p = 0.29$, $q = 0.71$, $r = 0.33$. This simple method of substitution is not the best method for fitting a negative binomial. Bliss and Fisher (1953) have developed the maximum likelihood method for this case. Our computer program for this method is a slightly modified version of the program written by Ondrick and Griffiths (1969). The maximum likelihood estimates for deposits in Figure 29.1 are $p = 0.30$, $q = 0.70$ and $r = 0.35$. Use of Eq. (4) now gives $E(K) = 0.82$ (as before), but $\sigma^2(K) = 2.69$.

Calculated frequencies obtained by the maximum likelihood method are shown in Table 29.1 for deposits in Figure 29.1, subcells, and deposits in an area of 36 cells instead of 49 cells. The fit is excellent in every case. It reflects the flexibility of the negative binomial model. In the third example in Table 29.1, it was fitted to deposit frequencies for the 36 cells in the Bathurst area which are mainly underlain by rocks of the Tetagouche Group. This experiment was performed in order to base the analysis on a better approximation of the outcrop pattern of the Tetagouche Group.

A disadvantage of the negative binomial is that its parameters (p, q, and r) depend on cell size. Unlike in the cases of the simple Poisson model and the simple coloured map model, parameters computed for a single size of cells cannot be readily extended to compute probabilities for numbers of deposits in larger regions. The main reason for this is that the boundaries of the cells used for counting may intersect clusters as shown in Figure 29.1. As a result, frequencies for adjacent cells are not stochastically independent, a condition that would have to be fulfilled for extrapolation to larger areas.

Neyman-Scott Model

Stochastic point process models of the Neyman-Scott type are also very flexible and, theoretically at least, they can be used to overcome the disadvantage of the simpler negative binomial model. Neyman and Scott (1972) have discussed several applications of their model including some in mathematical ecology and astronomy.

The three basic assumptions of the Neyman-Scott model are as follows: (1) The points occur in clusters and the cluster centres are randomly distributed according to the simple Poisson process. (2) The number of points per cluster is a random variable. (3) If a cluster centre is known to occur at a location denoted by the vector u, the points belonging to this cluster are randomly distributed around u, according to a probability distribution $f(x \mid u)$ where x denotes distance from the cluster centre.

The preceding three basic assumptions are rather general and several further assumptions are needed for practical application of the Neyman-Scott model. One possible application to the pattern of Figure 29.1 is as follows. Suppose that there are 10 cluster centres in the area of 49 cells. The simple Poisson process controlling occurrence of cluster centres then has $\lambda = 10/49 = 0.204$.

It is further assumed that each cluster has K deposits with probabilities according to the negative binomial model with $p = 0.037$; $q = 0.963$ and $r = 0.153$. By using Eq. (5), this yields for the probabilities: $P(K = 0) = 0.603$ or 60 per cent; and the sequence 0.089, 0.049, 0.034, 0.026, 0.021, 0.017, 0.015, 0.013, 0.011, 0.010, ..., for k = 1, 2, ..., 10, ... It implies that we admit a 60 per cent probability that a cluster centre has no deposits associated with it. There is a 20 per cent probability that it has 1, 2, 3 or 4 deposits, and also a 20 per cent probability that it has 5 or more deposits associated with it. Consequently, only a few clusters of deposits would actually occur in the Bathurst area and if they occur, they can contain many deposits.

For the probability distribution $f(x \mid u)$, an isotropic 2-dimensional Gaussian distribution with $\sigma = 9.8$ km is assumed. This model was chosen because it showed a reasonably good fit with the two-dimensional autocorrelation function estimated for the data of Figure 29.1. According to this model, the probability that a deposit occurs decreases in all directions away from a cluster centre. The probability that a deposit occurs within 9.8 km is 39 per cent; and the probability that it occurs within 19.6 km is 63 per cent. It implies that the clusters are rather large and would overlap one another within the Bathurst area.

A more extensive discussion of the assumptions underlying the preceding results has been given in Agterberg (1975b). The main purpose of presenting the model here is to provide an alternative to the other, better known, generalizations of the simple Poisson model, which are either using a general linear model of multivariate analysis, or the negative binomial model for cell frequencies.

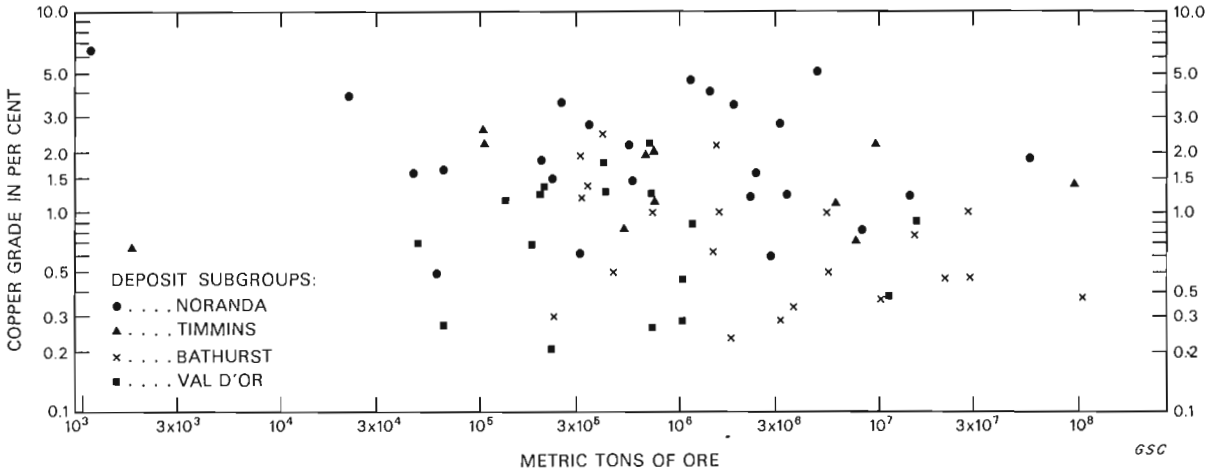

Figure 29. 2. Comparison of size- and copper grade figures for volcanogenic massive sulphide deposits from 4 subareas (from Agterberg, 1975a).

Lognormal Size- and Grade Distributions

Size of deposits has only rarely been considered in conjuction with multivariate Poisson models such as the simple coloured map model. It has more often been combined with the negative binomial distribution model for points in two dimensions. Examples of applications include Uhler and Bradley (1970) to oil deposits occurring in 5 by 5 mile cells in Alberta and DeGeoffrey and Wu (1970) to total dollar values for mines in 10 by 10 mile cells on the Canadian Shield.

Published size and grade figures were available for only 23 of the 40 deposits shown in Figure 29. 1. The median size value for these 23 deposits is 1. 54 million metric tons of ore. The extreme positive skewness of the size distribution is indicated by the fact that the largest size value on file is 104. 7 million metric tons (for New Brunswick No. 12); this is 68 times as large as the median value.

Most of the 23 deposits with size figures have reported grade values for all of the three metals, copper, lead and zinc. In total, the mineral deposit file contains 21 grade values for copper, 17 values for lead, and 18 values for zinc. Median grades for all 23 deposits can be estimated if it is assumed that a missing value for a metal in a deposit represents a grade below the median estimated from the grade data available. These median grades are 0. 55% copper, 1. 0% lead, and 4. 5% zinc. Taking each metal separately, the largest grade values are 2. 5% Cu, 4. 6% Pb and 8. 2% Zn; they reflect the fact that the individual grade distributions are only moderately skew.

The 21 deposits from the Bathurst area with reported copper values are shown as crosses in Figure 29. 2 with the copper grade plotted against the size (in metric tons of ore), using logarithmic scales along the two co-ordinate axes. It is well known that the Bathurst deposits contain more lead-zinc relative to copper than the Precambrian massive sulphide deposits on the Canadian Shield (Sangster, 1972). The three subgroups of deposits to which the Bathurst deposits are compared in Figure 29. 2 represents three geographically coherent subareas in the Abitibi volcanic belt of the Superior Province. The deposits of the Noranda subgroup originate from a subarea of 49 (10 by 10 km) cells, equal in size and shape to the area of Figure 29. 1. The Val d'Or subgroup and the Timmins-Kirkland Lake subgroup represent polymetallic massive sulphide deposits from larger, irregularly shaped, subareas. The median grade values for 25 volcanogenic massive sulphide deposits occurring within the Noranda subarea of 49 cells are 1. 7% Cu, 0. 0% Pb, and 2. 3% Zn. The reason for restricting most of the present comparison to copper is that fewer grade values for zinc were available and almost no grade values for lead in the Abitibi volcanic belt.

A more detailed account of these results, the data, and additional statistical tests are given in Agterberg (1975a). Subject to the limitations of the data used, the following conclusions can be drawn:

(1) There is no systematic relationship between size of deposits and copper grade in the deposits shown in Figure 29. 2. Neither does such a relationship exist within the subgroups.

(2) The size-frequency distribution can be regarded as approximately lognormal and the same for all four areas compared with one another. The only significant difference between the size-distributions is that the Bathurst size-distribution has no values less than 2.4×10^5 metric tons like the other distributions (*see* Fig. 29. 2). This effect is probably of an economic nature and does not signify that the size-distributions for ore in large deposits (before mining) are statistically different.

(3) The copper grade-distributions for the four subareas show differences that are statistically significant. For example, in Figure 29. 2, the cloud of solid circles for Noranda deposits occurs at a higher level than the cloud of crosses for the Bathurst deposits. The opposite

holds true for lead and zinc of which the concentration is higher in the Bathurst deposits (*see* median grade values listed previously in this section).

Considerations on sizes and grades such as those given here are important for prediction purposes. Suppose that we can predict the number of "events" or deposits in a region by means of one of the generalized Poisson models discussed in previous sections. Then the problem remains of how to predict the amounts of ore in the deposits and the amounts of the metals contained in the ore.

The size (in metric tons of ore) of the 73 volcanogenic massive sulphide deposits of Figure 29.2 is lognormally distributed with logarithmic mean (base 10) equal to 6.0 and logarithmic variance of 0.9. The median is almost exactly 1 million metric tons of ore, and the population includes two giants (New Brunswick No. 12 and Kidd Creek Mine) with a size of about 100 million metric tons of ore. Contrary to the grade-distribution, the size-distribution seems to be independent of location. It means that a precise quantitative prediction of regional mineral potential along these lines is not possible, because the total amount of ore in a region is mainly determined by the occurrence of very few giants with a size of the order of 100 million metric tons of ore. For this reason, predictions of regional mineral potential should be presented in probabilistic terms in order to express the great uncertainty in estimates of amounts of ore in deposits not yet discovered.

References

Agterberg, F.P.
1974: Automatic contouring of geological maps to detect target areas for mineral exploration; J. Mathematical Geol., v. 6, p. 373-395.

1975a: Statistical models for regional occurrence of mineral deposits; Proc. 13th Intern. Symp. on Computers and Mathematics in Mineral Industries, Clausthol. Fed. Rep. Germany, October 1975 (in press).

Agterberg, F.P. (cont.)
1975b: New problems at the interface between geostatistics and geology; Proc. NATO. A.S.I. on Geostatistics, Rome, October 1975 (in press).

Bliss, C.I. and Fisher, R.A.
1953: Fitting the negative binomial distribution to biological data and note on the efficient fitting of the negative binomial; Biometrics, v. 9, p. 176-200.

DeGeoffroy, J.G. and Wu, S.M.
1970: A statistical study of ore occurrences in the greenstone belts of the Canadian Shield; Econ. Geol., v. 65, p. 496-509.

Fisher, L.
1972: A survey of the mathematical theory of multidimensional point processes; *in* P.A.W. Lewis, Editor: Stochastic point processes, Wiley, New York, N.Y., p. 468-513.

Neyman, J. and Scott, E.L.
1972: Processes of clustering and applications; *in* P.A.W. Lewis, Editor: Stochastic point processes, Wiley, New York, N.Y., p. 646-681.

Ondrick, C.W. and Griffiths, J.C.
1969: FORTRAN IV computer program for fitting observed count data to discrete distribution models of binomial, Poisson and negative binomial; Kans. Geol. Surv., Comput. Contr., 35, 20 p.

Plackett, R.L.
1974: The analysis of categorical data; Griffin's Statistical Monographs and Courses, 35, Hafner Press, New York, N.Y., 159 p.

Sangster, D.F.
1972: Precambrian volcanogenic massive sulphide deposits in Canada: A review; Geol. Surv. Can., Paper 72-22, 44 p.

Uhler, R.S. and Bradley, P.G.
1970: A stochastic model for petroleum exploration over large regions; J. Am. Statist. Assoc., v. 65, p. 623-630.

30. CAVENDISH GEOPHYSICAL TEST RANGE, ONTARIO (NTS 31 D/16 W): HISTORICAL BACKGROUND (Reports 31-33)

Peter J. Hood
Resource Geophysics and Geochemistry Division

As a contribution to mark Canada's Centennial, it was decided that a conference on mining and groundwater geophysics should be held in Niagara Falls during October 1967. It was felt, however, that the educational value of such a conference would be enhanced if members of the geological surveys or their equivalent organizations in the developing nations could also attend. Accordingly, the Canadian International Development Agency was approached and after some discussion it was decided to hold a pre-conference field seminar on mining geophysics which would enable the delegates to obtain first hand experience in the use of Canadian geophysical equipment and techniques in addition to attending the conference at Niagara Falls.

Fortunately, about 90 miles northeast of Toronto, two EM conductors were known to exist in Cavendish Township and these were used by various geophysical instrument companies in Toronto to test their geophysical equipment. The conductors cross the Salmon Lake Road (Fig. 30. 1), which intersects Highway 507 about 675 miles by road south of Gooderham. For the seminar a survey grid consisting of 5 lines spaced 40 feet apart was laid out to cover the conductors with survey pegs spaced at 100 foot intervals along the lines. A base line was also laid out at right angles to the main survey lines. The elevations at the survey pegs are given in Figure 30. 2.

The seminar, held during the period October 9 to 21, 1967, was attended by 24 delegates from 17 developing nations who were lodged in cabins at the Hospitality Inn near Minden. A series of orientation lectures were held, and these were followed by field exercises on the survey grid in which the delegates themselves took readings along the survey lines and compiled the data into map form. In addition demonstrations of more

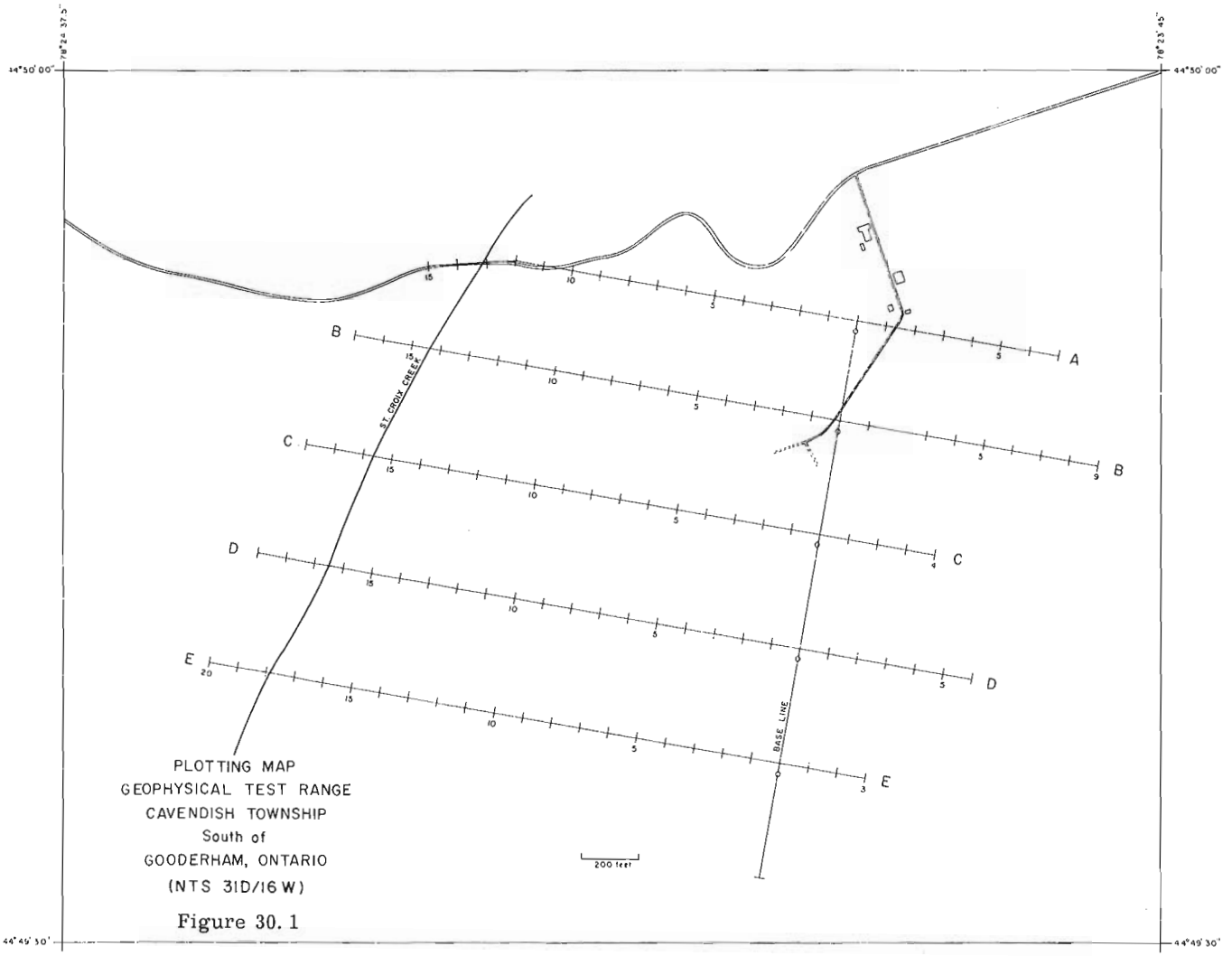

Figure 30. 1

Figure 30. 2 Topographic map for the Cavendish geophysical test range.
The elevations of the survey stations are given in feet above mean sea level.

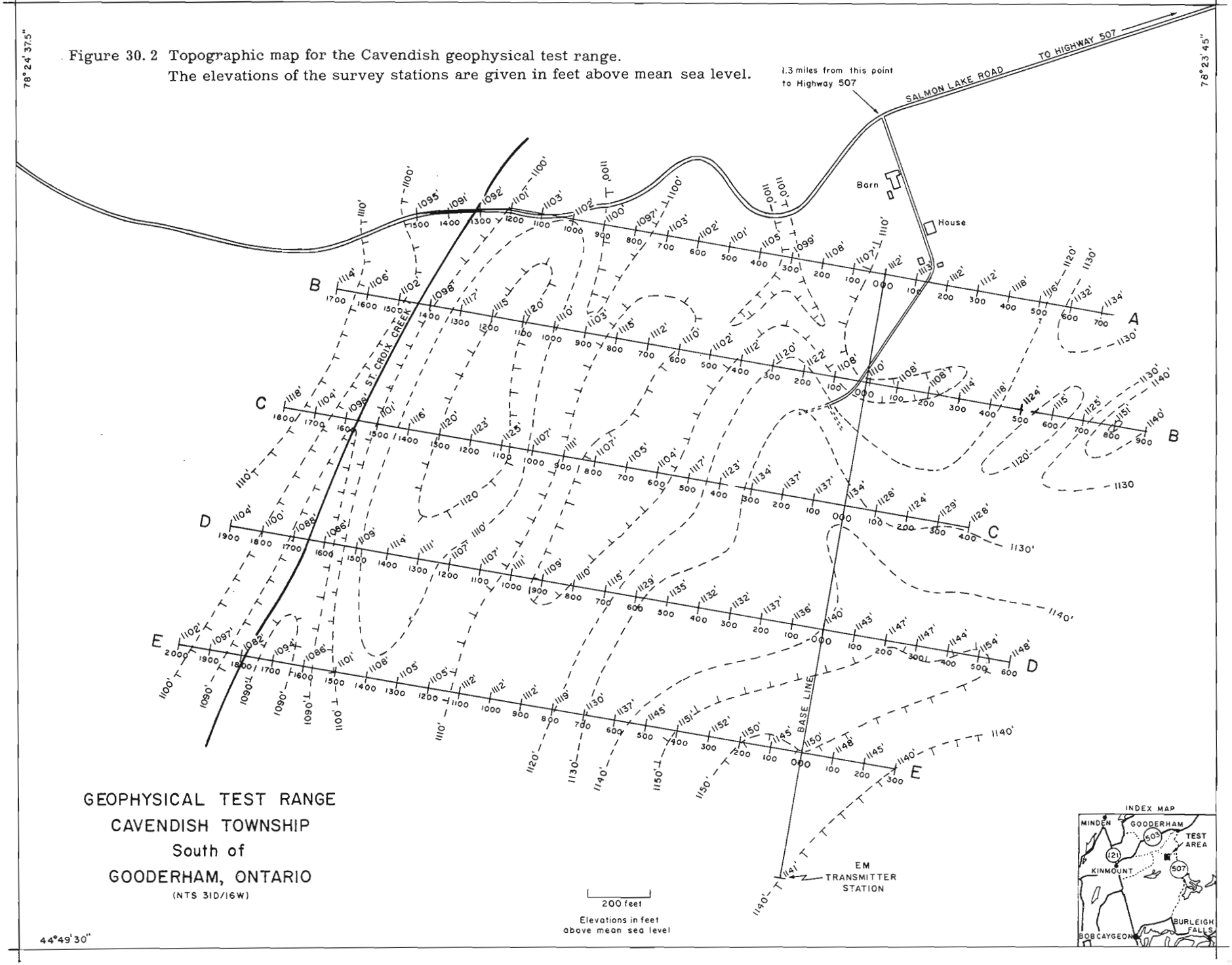

complicated equipment which could not be operated by a single person, such as the induced polarization type, were carried out by the various instrument companies in Toronto and two half-days were set aside for expositions on case histories.

Subsequent to the seminar, the Cavendish geophysical test range has continued to be used by the geophysical instrument companies, universities and government organizations and groups have actually travelled long distances to use the range. For this reason, it was thought worthwhile to publish three papers (Reports 31, 32, 33) describing gravity, magnetic and hammer seismic surveys which were carried out at the time of the 1967 seminar. A complementary paper was also published in 1975 by Williams *et al.* presenting diamond drilling results obtained in 1973.

The Cavendish geophysical test range is a particularly valuable one for experimental and calibration purposes to the mining geophysical community for the following reasons. The mineralization consists of a mixture of pyrrhotite and pyrite which is continuous enough to produce electromagnetic anomalies in two zones (Zones A and B) which cross the survey lines at a high angle. The mineralization ranges in content up to 10 per cent sulphides (Williams *et al.*, 1975) and therefore produces induced polarization anomalies because of its disseminated nature. Because of its magnetic properties, the pyrrhotite produces noticeable magnetic anomalies, and these are augmented by the presence of magnetite. Unfortunately the sulphides do not produce enough density contrast in the country rock to produce distinctive gravity anomalies. Thus the Cavendish geophysical test range may be used to test most of the commonly used geophysical equipment employed in mineral exploration programs. Coincidentally it bears the name of a famous geophysicist (and noted misogynist!!) of the eighteenth century who utilized an early form of torsion-balance to determine the mean density of the earth and Newton's gravitational constant (Cavendish, 1798).

Acknowledgments

Acknowledgment is made to John Ratcliffe of Phelps Dodge Corporation of Canada Ltd. who was the co-convenor (with P.J. Hood) for the seminar and to Hugh MacAulay of the Resource Geophysics and Geochemistry Division who was responsible for surveying the Cavendish geophysical test range. Acknowledgment is also made to the various members of the Resource Geophysics and Geochemistry Division and the Canadian geophysical instrument companies too numerous to mention individually by name who contributed to the success of the seminar.

References

Cavendish, H.
1798: To determine the density of the earth; Phil. Trans. Proc. Roy. Soc., London, v. 88, p. 388-408.

Charbonneau, B.W. and McGrath, P.H.
1975: Cavendish geophysical test range, Ontario (NTS 31 D/16 W): ground magnetic surveys; *in* Report of Activities, Part C, Geol. Surv. Can., Paper 75-1C.

Hobson, G.D.
1975: Cavendish geophysical test range, Ontario (NTS 31 D/16 W): hammer refraction seismic survey; *in* Report of Activities, Part C, Geol. Surv. Can., Paper 75-1C.

Sobczak, L.W. and Jacoby, W.R.
1975: Cavendish geophysical test range, Ontario (NTS 31 D/16 W): gravity survey; *in* Report of Activities, Part C, Geol. Surv. Can., Paper 75-1C.

Williams, D.A., Scott, W.J., and Dyck, A.V.
1975: Cavendish Township geophysical test range: 1973 diamond drilling; Geol. Surv. Can., Paper 74-62, 14 p.

L. W. Sobczak and W. R. Jacoby
Gravity Division, Earth Physics Branch

Introduction

The Canadian Centennial Conference on Mining and Groundwater Geophysics was held at Niagara Falls in 1967. In connection with the conference, a detailed gravity survey of the Cavendish geophysical test range was made (Fig. 31.1). The survey served as a demonstration of the use of the gravity method in mineral exploration to delegates of 17 countries who had attended the conference. Other geophysical and geological techniques were also tested on the range (this publication, reports 32, 33 and McPhar Geophysics, 1967). The test range lies between the Anstruther and Glamorgan granite gneisses in southwestern Ontario in the Grenville province of the Canadian Shield.

The Gravity Survey

Field Work

In 1967 the Earth Physics Branch established 123 gravity stations over the Cavendish geophysical test range. Two gravimeters, a temperature controlled WORDEN and a CANADIAN with scale constants of

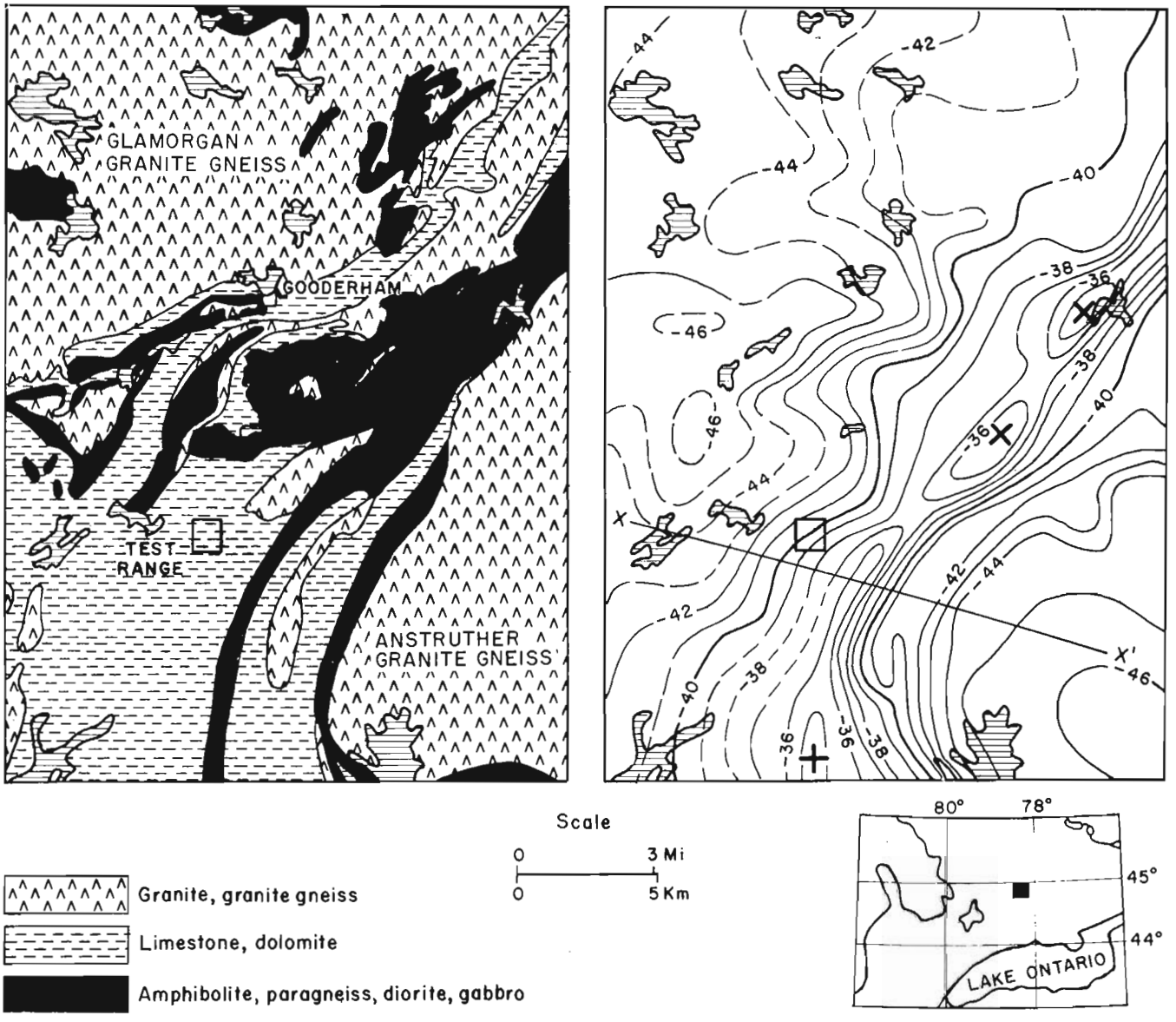

Figure 31.1. Regional geology and Bouguer anomaly field (contours 1 mgal) over the Gooderham map sheet (NTS 31D/16W).

Figure 31. 2. L. W. Sobczak (left) demonstrating the Canadian and Worden gravity meters to W. Mahanga (Tanzania), A. D. Nasuation (Indonesia) and V. Gopal (India), who is partly hidden.

Figure 31. 3. Survey group taking readings at survey peg 100W on line E. Left to right: H. Yoshikawa (Japan), L. W. Sobczak of Earth Physics Branch, S. Padmanagara (Indonesia), D. B. Craig (Jamaica) who is noting the readings and D. N. Rimal (Nepal).

0. 39940 and 0. 10154 mgal/div respectively, were used by two small field parties (Figs. 31. 2 and 31. 3). The readings were made within 2 feet of the station markings established by the Geological Survey of Canada. Five control stations were observed by base looping with both gravimeters along the base line (Figs. 31. 4, 31. 5, 31. 7 and 31. 8). Within the Gooderham map sheet (NTS 31D/16W) which surrounds the area there are about 125 gravity measurements at a station spacing of about 2 km. These were made by the Earth Physics Branch during the period of 1961 to 1967 with various gravimeters and are sited mainly along existing roads.

Reductions

The gravity data are presented as Bouguer anomalies. The observed gravity values g_o, corrected for drift, assuming linear variation with time, contain the following effects.

1. The gravity change with latitude on the earth's ellipsoid — from the International Elipsoid of 1930 the theoretical gravity γ is given in gals by $\gamma = 978.049\ (1 + 0.00528838 \sin^2\theta - 0.00000587 \sin^2 2\theta)$.
2. The gravity change with elevation h — the vertical gradient $\partial g/\partial h$ is -0. 09406 mgal/ft or -0. 3085 mgal/m.
3. The gravity effect of the topographic mass between sea level and the land surface — it is sufficient to approximate this by an infinite slab of rock of the thickness h. The Bouguer effect of the slab is $2\pi G\rho h$, where $G = 6.67 \times 10^{-8}$ cgs and $\rho = 2.67$ g/cm^3.
4. The effects of buried mass inhomogeneities, including zones of mineralization, and other lithological variations.

Removal of effects (1) to (3) from the observed gravity values, g_o, gives the Bouguer anomalies Δg_B which then mainly contain effect (4). The formula is:

$$\Delta g_B = g_o - \gamma \frac{\partial g}{\partial h} h - 2\pi G\rho h.$$

The values of the Bouguer anomalies at the stations in the test range are shown in Figure 31. 4.

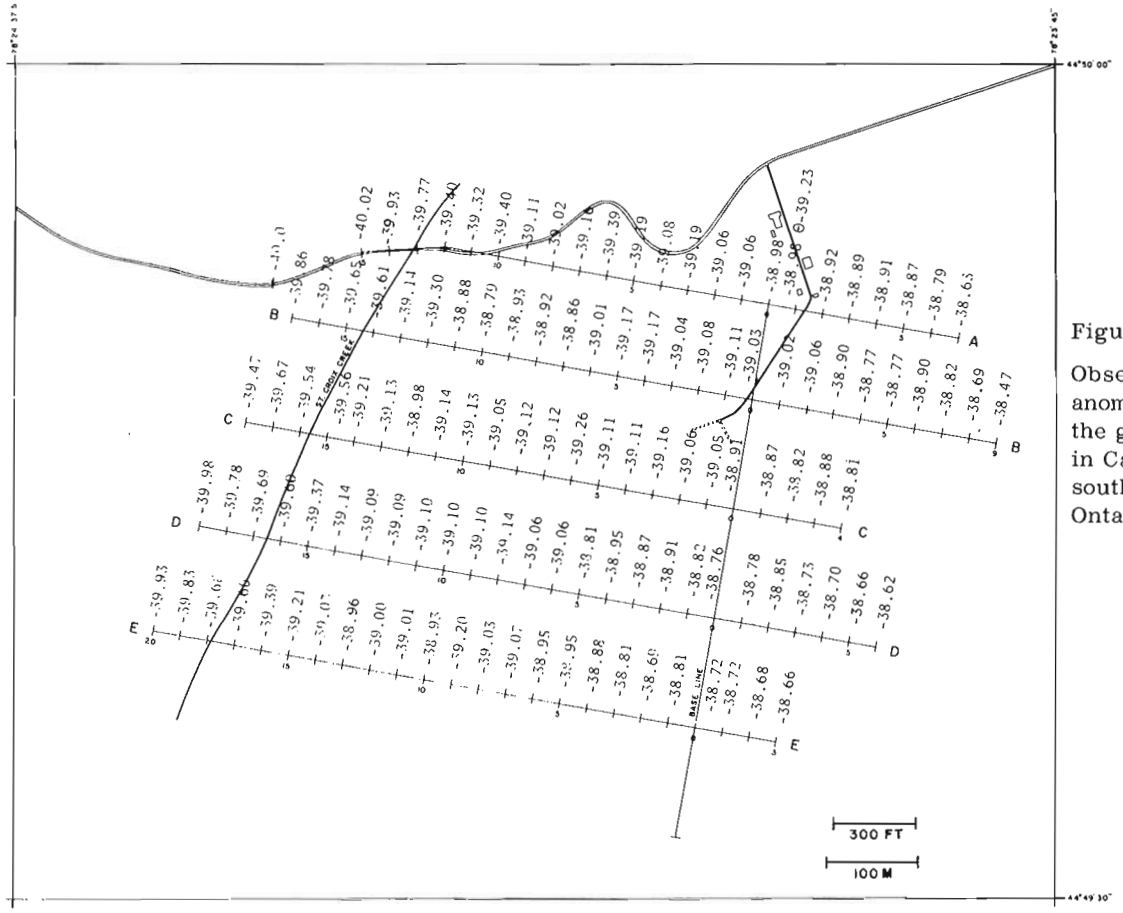

Figure 31. 4

Observed Bouguer anomalies (mgal) over the geophysical test range in Cavendish Township south of Gooderham, Ontario.

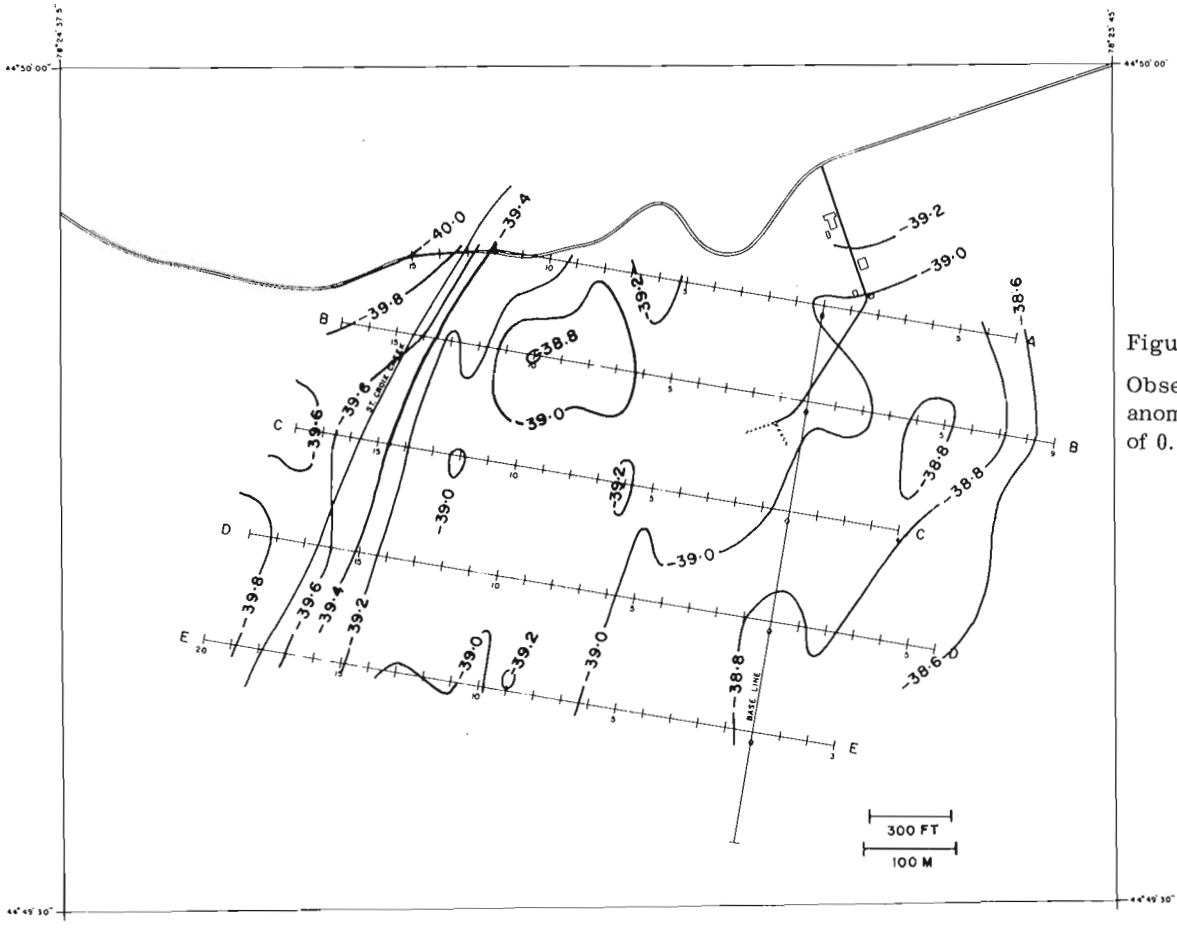

Figure 31. 5

Observed Bouguer anomaly field (isogals of 0. 20 mgal).

TABLE 31. 1

Density measurements

Rock Type	Number of Samples	Density Range g/cm^3	Mean Density g/cm^3	Standard Deviation g/cm^3
Granitic Gneiss	17	2. 56 - 2. 68	2. 61 ± . 01	± 0. 03
Biotite Gneiss	20	2. 56 - 2. 85	2. 72 ± 0. 02	± 0. 07
Hornblende Gneiss (Amphibolite)	29	2. 74 - 3. 05	2. 92 ± 0. 01	± 0. 07
Limestone (marble)	16	2. 56 - 2. 84	2. 74 ± 0. 02	± 0. 08

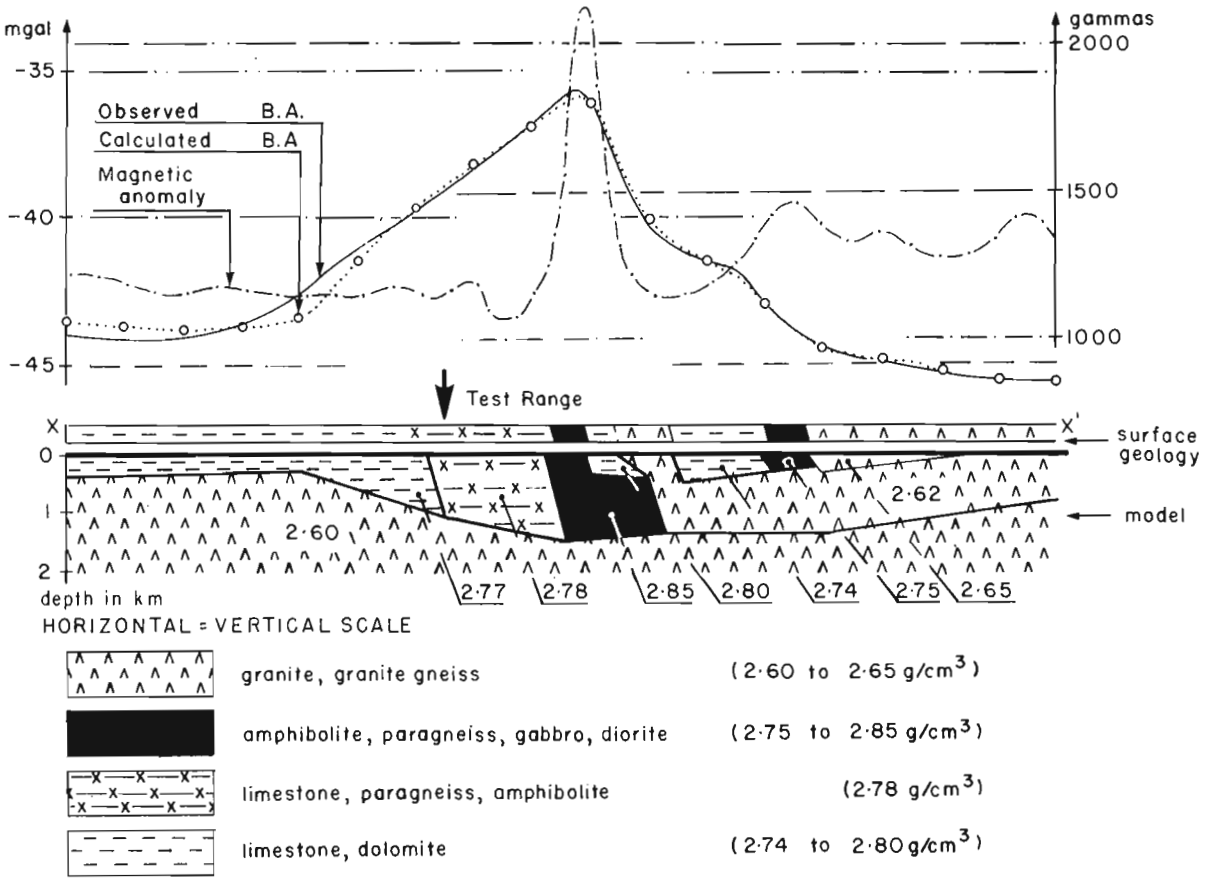

Figure 31. 6. Regional profile X -X shows the observed and calculated gravity anomalies, the surface geology, the model corresponding to the calculated gravity anomaly and the total magnetic field anomaly.

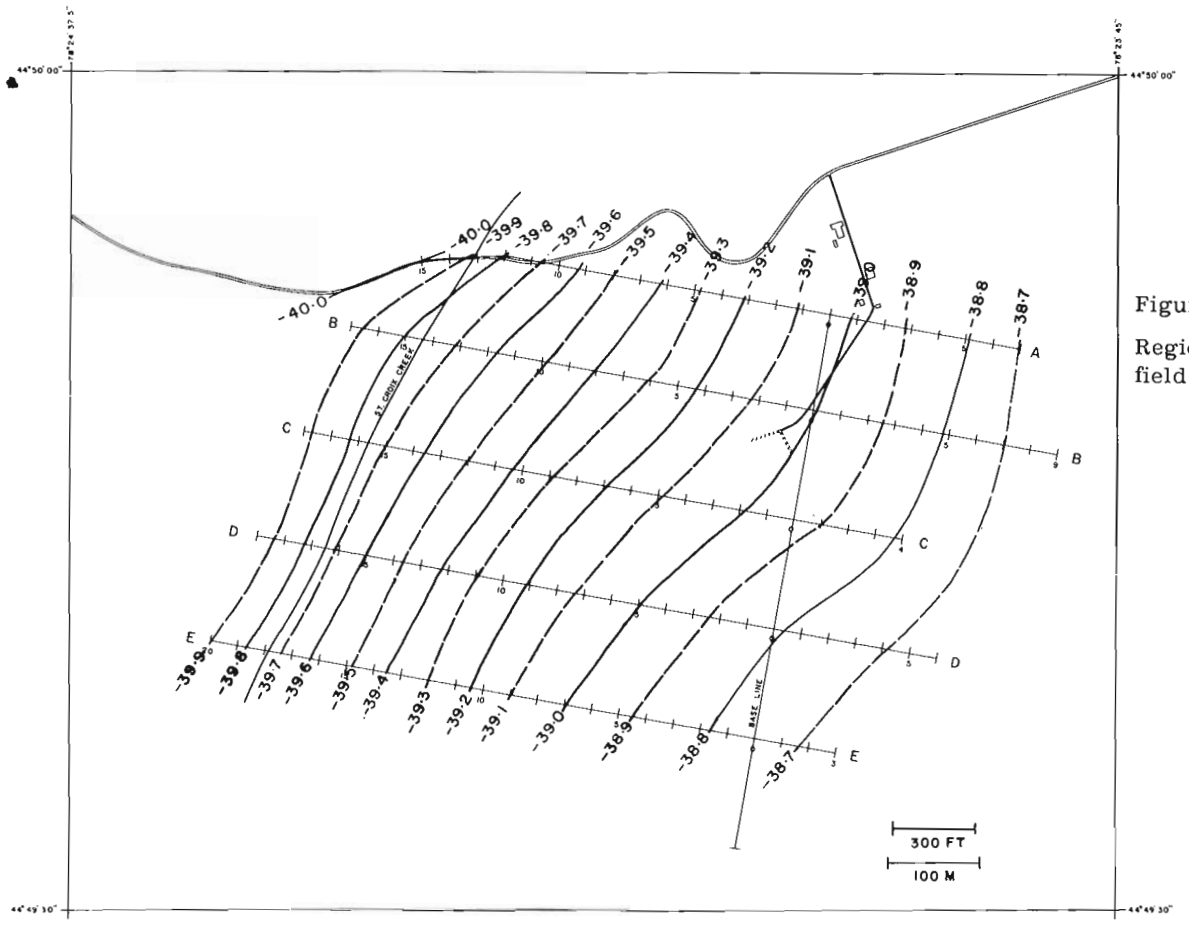

Figure 31. 7

Regional Bouguer anomaly field (isogals of 0. 10 mgal).

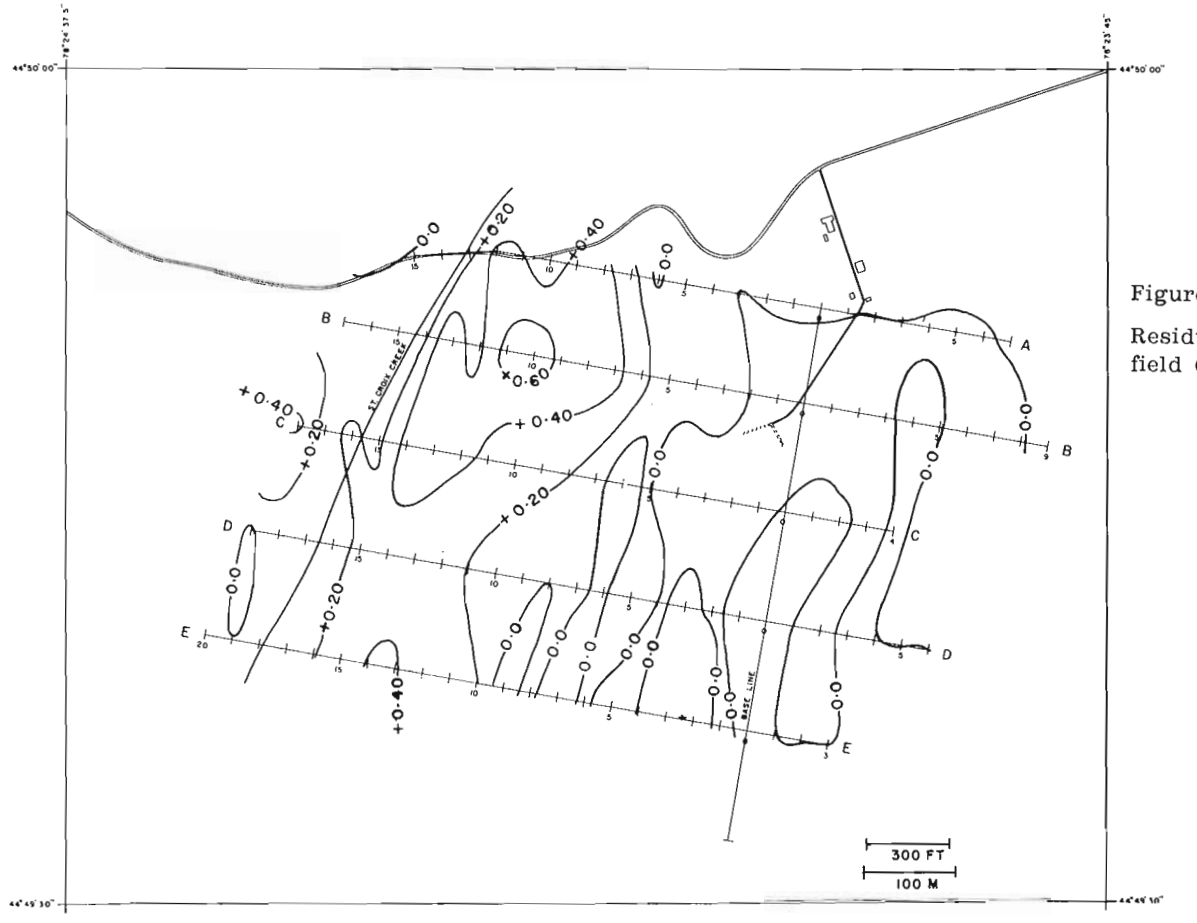

Figure 31. 8

Residual Bouguer anomaly field (isogals of 0. 20 mgal).

Accuracy of the Bouguer Anomalies

Mineral exploration by the gravity method can locate only those shallow bodies, which differ in density from the surrounding rocks. The corresponding gravity effects usually have short wavelengths and small to moderate amplitudes. It is therefore essential to evaluate the relative accuracy of the Bouguer anomalies. Errors come from different sources and are discussed briefly.

The standard deviation of a single gravity observation is estimated to be less than ± 0.04 mgal for stations on solid ground and about ± 0.08 mgal for stations on less stable ground (e.g. muskeg). The uncertainty in the heights of the stations measured by spirit levelling is less than ± 1 ft corresponding to ± 0.06 mgal in the Bouguer anomalies. The elevations in the test range vary by ± 36 ft and the rock densities vary by 0.15 g/cm^3 so that the use of an assumed density (2.67 g/cm^3) in the Bouguer reduction results in errors of up to ± 0.07 mgal. The departures of the terrain from a level plain are small and have an average effect of only 0.01 mgal.

The uncertainty of the Bouguer anomalies from all sources is in the order of 0.1 mgal, which allows the results to be contoured at intervals of 0.2 mgal with confidence.

Geology and Rock Densities

The test range is located near the centre of a north-northeast striking band of metasediments, comprising limestone, dolomite, amphibolite and paragneiss, intruded by small bodies of diorite, gabbro and some granitic gneiss. This band of metasediments separates the Anstruther and Glamorgan granite gneisses (Fig. 31.1, based on Map 1957b, Haliburton-Bancroft area, Ontario Dept. of Mines).

A knowledge of the densities of the rocks in the area is necessary for the interpretation of the gravity data. Eighty-two rock samples representative of the major lithological units were collected for density measurements during the gravity survey, and by L.J. Kornik during detailed geological mapping of the test range. The results are listed in Table 31.1. The mean value is 2.76 g/cm^3 weighted according to the areal distribution of the different rock types in the test range. The densities of biotite gneiss (2.72 g/cm^3) and of marble (2.74 g/cm^3) do not deviate much from the mean density; the amphibolite has a considerably higher density (2.92 g/cm^3) and the granite gneiss (2.61 g/cm^3) occurring only at the western boundary of the range has a distinctly lower density than the mean.

Interpretation of the Regional Gravity Field

The location of the test range in relation to the regional geology and the regional gravity field is shown in Figure 31.1. There is a good correlation between the regional gravity field and geology. A north-northeast-trending belt of relatively positive anomalies ranging from -40 to -36 mgal, is underlain by a band of metasediments and amphibolite which is locally intruded by diorite and gabbro. The belt of positive anomalies separates two extensive gravity lows to the northwest and southeast; these lows, which have minimum values of -46 mgal, are underlain by the Glamorgan and Anstruther granite gneisses. Steep gravity gradients coincide with the contact between the granite gneisses and metasediments particularly on the southeastern flank of the high. Gravity, magnetic and geological profiles across the band of metasediments X-X', Fig. 31.1) are shown in Figure 31.6. A model, consistent with the surface geology and measured rock densities was constructed and a good correspondence between the observed and calculated gravity profiles was obtained. The gravity high is interpreted as the combined effect of the metasediments and amphibolites which range in density from 2.77 to 2.85 g/cm^3 in this locality. Granite gneiss (2.60 to 2.65 g/cm^3) underlies the metasediments which reach a maximum thickness of 1.5 km below the peak anomaly. A local magnetic high coincides with the gravity maximum and appears to be related to the amphibolites as shown in Figure 31.6.

The gravity data can be used to define the subsurface boundary between the metasediments and the granite gneiss. The depth of this boundary may have some control over the possible occurrence of mineralized zones within the metasediments. Moreover, the coincidence of the local gravity and magnetic highs (Fig. 31.6) and the shallow depth to the granite gneiss may be interpreted as indicative of conditions favourable to mineralization and further exploration may be warranted.

The Bouguer anomaly field in the test range was separated into two components, the regional and residual gravity anomalies. The regional component as shown in Figure 31.1 is the smooth gradient already discussed on the western flank of the major belt of gravity highs. This local trend (Fig. 31.7) was subtracted from the total field in the test range (Fig. 31.5) to give the residual anomalies shown in Figure 31.8. These residual anomalies are discussed in the next section.

Interpretation of the Gravity Field over the Test Range

The residual Bouguer anomalies in the test range vary locally from -0.10 mgal to a maximum of 0.70 mgal in the northwest of the range (Fig. 31.8). The general north-northeast trend of the contour lines follows the geological strike. The dominant feature of the residual anomaly field is a positive belt between 600 and 1400 feet west of the baseline. This positive belt, which strikes north-northeast with a maximum value of more than 0.7 mgal on line B, exceeds 0.3 mgal on all lines and correlates well with a band of dense amphibolite (Fig. 31.9 II and III). The gradients on the west flank of this anomaly are steeper than on the east flank suggesting that the amphibolite band dips to the east. Zero anomaly is reached in a distance of 500 to 1000 feet on both sides of the positive anomaly which indicates that the anomalous mass is only a few hundred feet wide. In the eastern half of the area the values are fluctuating

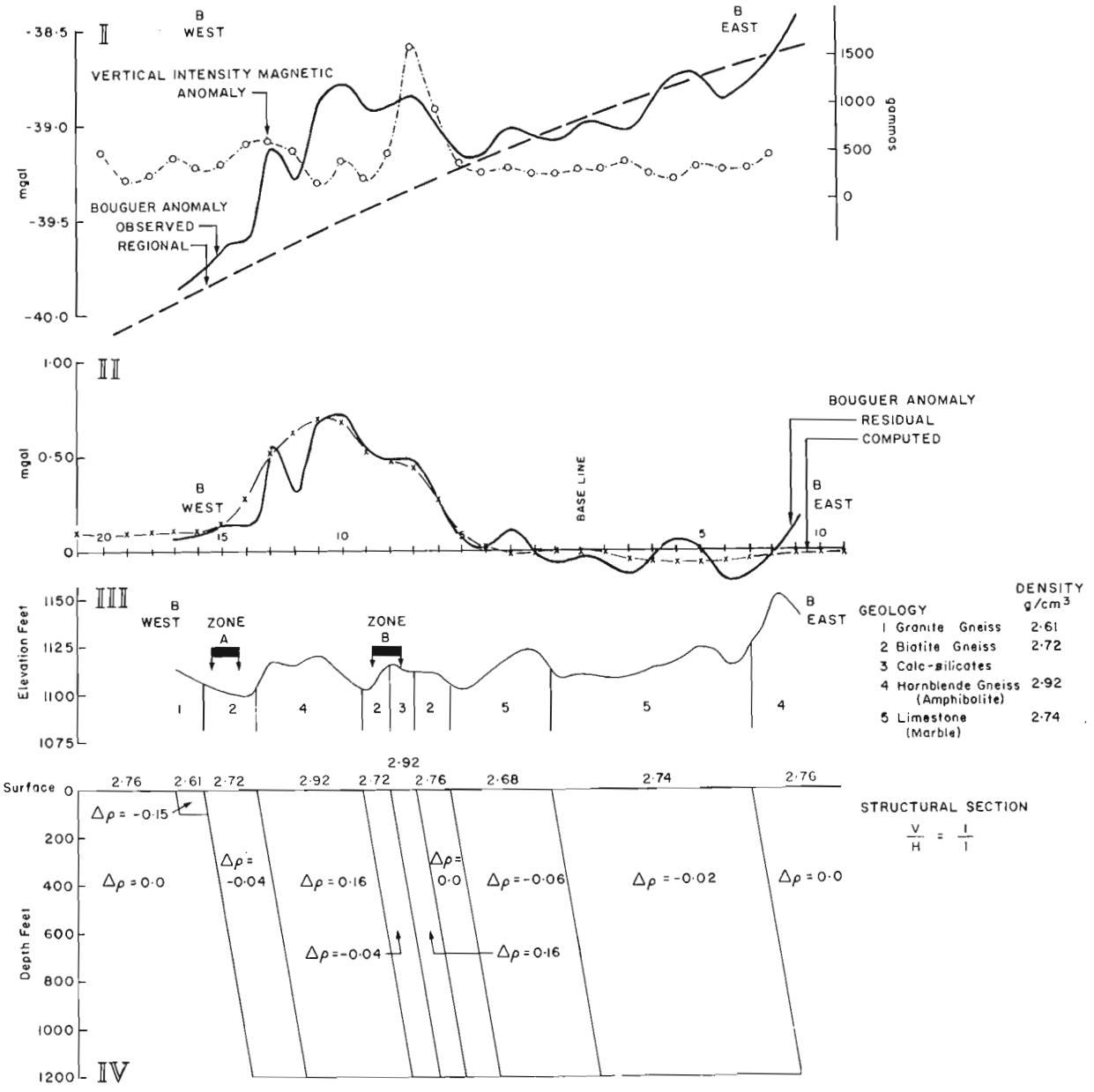

Figure 31. 9. Profile along line B showing detailed surface geology and model interpreted from Bouguer and magnetic anomalies.

zero (± 0. 1 to 0. 2 mgal). These small variations have a wavelength of only a few station intervals and may be due to (1) random errors in the Bouguer anomalies discussed earlier, (2) variations of the thickness of overburden (± 10 feet may account for ± 0. 1 mgal) and (3) minor density variations within the lithological units.

Two anomalous zones, A and B, were detected by most of the geophysical methods applied by McPhar Geophysics (1967); massive sulphides were found by drilling in zone A. The mineralization is located on either side of the amphibolite band and hence on the flanks of the local gravity anomaly. The direct effect of the mineralization on the gravity field is masked by the effect of the amphibolite band.

A gravity profile across the strike of the residual anomaly at its maximum was chosen for interpretation along line B (Fig. 31. 9 I and II). A cross-section (Fig. 31. 9 IV) consisting of steep easterly-dipping layers of different densities (Table 31. 1) was constructed from surface geology (Fig. 31. 9 III and IV). The gravity effect of this model was calculated using a line integral method (Morgan and Grant, 1963; Nagy, 1964). It fits the residual Bouguer anomaly satisfactorily if the density of the calc-silicates is assumed to be 2. 92 g/cm^3 and if the background density is 2. 76 g/cm^3 i. e. the mean value of the densities of Table 31. 1 mentioned above. On these assumptions, the amphibolite band is at least 1200 feet thick. Other

models differing from the one given in Figure 31. 9 IV could also account for the gravity anomaly, but the given model is in agreement with the observed geology and measured densities.

The direct gravity effect of the mineralized zones cannot be differentiated from the small variations of the gravity field discussed above. However the correlation of the gravity and magnetic anomalies at zone B (Fig. 31. 9 I and III), may indicate that more mineralized material lies under zone B than under zone A. A rough estimate of the amount of ore near the surface is possible if it is assumed that the small positive variation of the gravity field near zone B is entirely due to heavy minerals. If the total mass excess is considered to be condensed on a horizontal line the anomalous mass can be estimated from the formula from Jung (1961, p. 218):

$$M = m\,\ell = \frac{g_{max} X_{\frac{1}{2}}}{2G}\,\ell,$$

where G is the gravitational constant, ℓ is the strike length of the mass line, g_{max} is the maximum gravity value and $X_{\frac{1}{2}}$ is the half width. For $X_{\frac{1}{2}} = 50$ m, $\ell = 250$ m and $g_{max} = 0.1$ mgal the anomalous mass is estimated to be 4 metric tons/cm of strike length. The total mass excess is 10^5 metric tons.

Conclusion

The gravity data give useful information about the geological structure and the possible occurrence of mineralization in the area under study, from both the regional and the local point of view. Insufficient accuracy of the gravity data and disturbing effects of overburden and other sources tend to obscure the gravity anomalies due to the mineralized zones. In the present case, a gravity survey has extended our knowledge of the geology to greater depth and has proven that the sulphides that are present are of rather limited tonnage.

References

Morgan, N. A. and Grant, F. S.
1963: High speed calculation of gravity and magnetic profiles across two-dimensional bodies having an arbitrary cross-section; Geophy. Prospect., v. 11, p. 10-15.

Nagy, D.
1964: The gravitational effect of two-dimensional masses of arbitrary cross-section; Unpublished manuscript, Gravity Division, Dominion Observatory, Ottawa.

McPhar Geophysics Ltd.
1967: A geophysical case history: Cavendish Township, Ontario, Canada; McPhar Geophysics Ltd., Toronto, Ontario, 14 p.

Jung, K.
1961: Schwekraftverfahren in der angewandten Geophysik (Gravity methods in applied geophysics); Leipzig.

32. CAVENDISH GEOPHYSICAL TEST RANGE, ONTARIO (NTS 31 D/16 W): GROUND MAGNETIC SURVEYS

B. W. Charbonneau and P. H. McGrath
Resource Geophysics and Geochemistry Division

Magnetic surveys of the Cavendish geophysical test range were carried out by participants (Fig. 32. 1) in the Seminar which preceded the Conference on Mining and Groundwater Geophysics held in Niagara Falls in October 1967. Actually it was planned to survey the property with four different magnetometers but because of inclement weather the surveys were completed with only two of the fluxgate instruments, namely the Sharpe (now Scintrex) MF-1 and the Sharpe PMF-3. In addition, McPhar Geophysics completed an independent survey of the range with their M-700 fluxgate magnetometer. A Barringer GM-102A proton free-precession instrument was also available but the survey was not completed with it. Each of the lines was surveyed by a different person, and the resultant data has been compiled into vertical force maps (Figs. 32. 2 and 32. 3).

For the survey the instruments were set to zero at a base station at a large boulder north of the farm house on the northeast part of the range (Fig. 32. 1). This is a relatively low gradient area and provides a good location for the zero station. Each line was surveyed with the operator facing west along the line and holding the instrument sensing head directly over the station stake. After each line was surveyed the operator returned directly to the base station to check the zero.

The two maps (Figs. 32. 2 and 32. 3) show the relative magnitude of the vertical intensity of the Earth's magnetic field contoured at 500 gamma intervals. The anomaly pattern established differs very little from that found in the McPhar survey in which the magnetometer employed was a McPhar M-700. This latter survey can be found in the geophysical case history published by McPhar Geophysics (1967).

The regional magnetic pattern in the area of the range can be found on GSC aeromagnetic map 146 G (Gooderham) as a north-northeast-trending magnetic grain varying in relative intensity from 1100 gammas in the southeast of the range to 1250 gammas in the northwest. This grain parallels the strike of geological formations in the area.

One minor and one major magnetic zone were outlined by the ground survey, and these are referred to as Zones A and B respectively. The minor magnetic zone (Zone A) is a rather discontinuous north-trending zone of anomalies of approximately 1000 gammas peak amplitude. This zone lies approximately along St. Croix Creek at the west of the test range. The axis of the zone trends through A 1300 W, B 1400 W, C 1600 W, is not found on line D and through E 1800 W.

The major magnetic zone (Zone B) is a continuous north-trending belt some 200 feet in total width with peak amplitude of approximately 4500 gammas. The belt has an axis trending through survey stations A 600 W, B 700 W, C 900 W, D 900 W and E 900 W. In addition minor anomalies of approximately 700 gammas peak amplitude at A 900 W, C 1300 W and E 1500 W and these may constitute an additional zone. A weak trend extends from 1700 W on line B to 1800 W on line C. An isolated anomaly of approximately 1000 gammas occurs on line C at 400 W.

Figure 32. 1. Participants in the 1967 seminar held at the Cavendish geophysical test range. Left to right: L. D. G. Black (Jamaica) is reading Sharpe MF-1 fluxgate magnetometer standing on the boulder used as the base station. In the centre, W. Mahanga (Tanzania) is carrying a Barringer GM 102A proton precession magnetometer. At right, A. D. Nasuation (Indonesia) holds the sensor for the Barringer GM 102A magnetometer whilst wearing a Sharpe PMF-3 fluxgate magnetometer.

A geological survey of the range was made by L. J. Kornik at the time of the seminar and his data was incorporated into a report by Williams *et al.* (1975). In general terms the lithologies within the range from west to east are a granite gneiss which is in contact with a quartz-plagioclase-biotite-amphibole gneiss along a line approximately through A 1500 W, B 1600 W, C 1700 W, D 1800 W and E 1900 W. The quartz-plagioclase - biotite gneiss is in contact with a marble unit along a line approximately through A 400 W, B 600 W, C 800 W, D 800 W, E 900 W.

Figure 32. 2. Vertical force magnetic survey of the Cavendish geophysical test range. The instrument used was a Sharpe (now Scintrex) MF-1 fluxgate magnetometer.

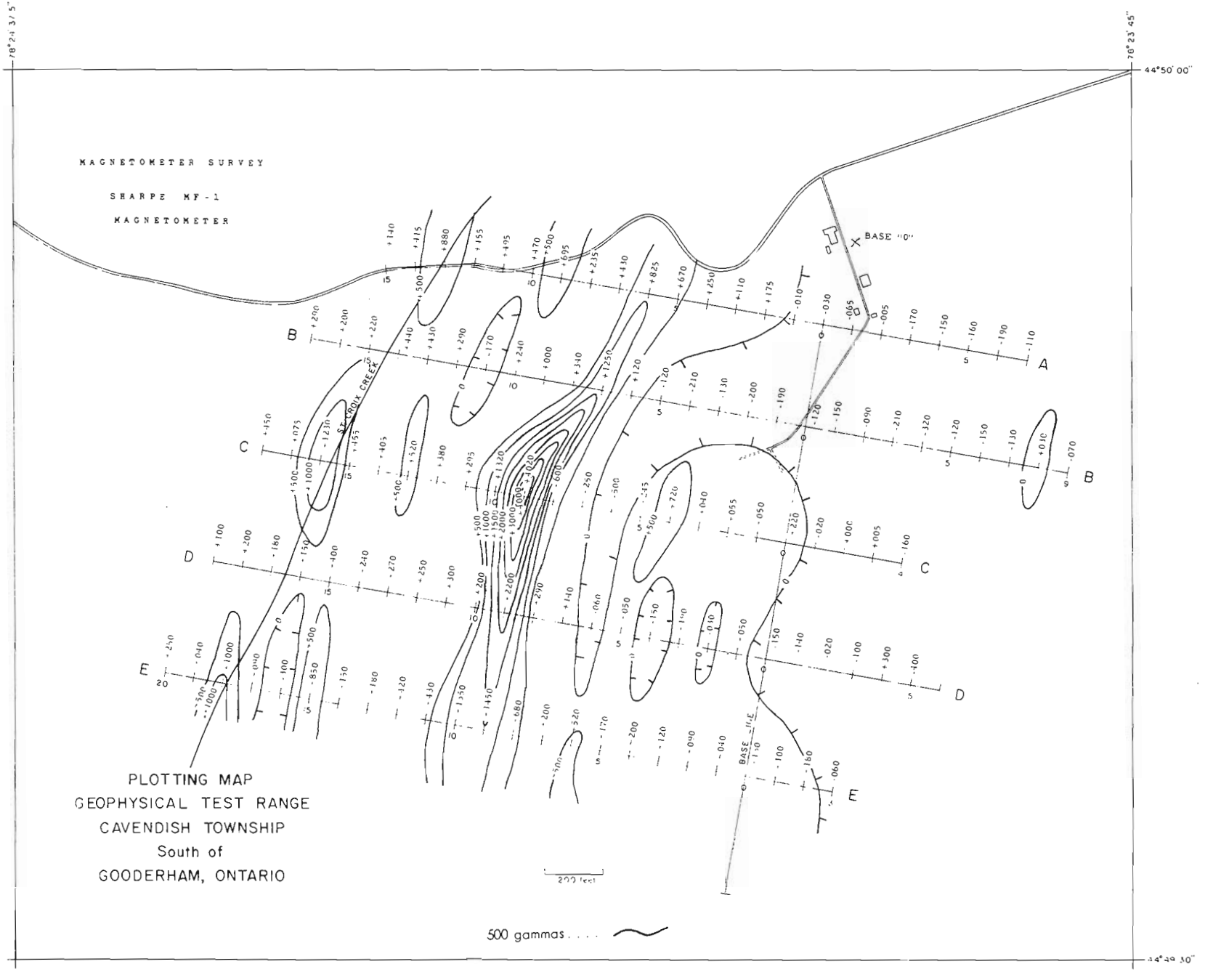

Figure 32. 3. Vertical force magnetic survey of the Cavendish geophysical test range. The instrument used was a Sharpe (now Scintrex) PMF-3 fluxgate magnetometer.

The magnetic expression over the marble is flat with the exception of the 1000 gamma anomaly at C 400 W which is unexplained because of lack of outcrop in that area. The magnetic pattern over the quartz-plagioclase-biotite gneiss is variable and it is this geological unit which contains the major and minor magnetic zones outlined above. The eastern boundary of the quartz-plagioclase-biotite gneiss and the marble is approximately defined by the 500 gamma magnetic contour, immediately east of the major magnetic zone. Not enough of the area underlain by the granite gneiss was surveyed to enable much to be deduced about the pattern over this unit but it appears that it is quite flat with minor magnetic highs.

Magnetic susceptibilities were determined in the laboratory with the Sharpe SM-4 magnetic susceptibility meter on crushed portions of some of the geological samples. It appears from the few determinations made that the magnetic pattern can be explained by the contrasting magnetic susceptibilities of the rock formations alone. The determinations from all three geological units excluding the anomalous zones in the quartz-plagioclase-biotite gneiss unit were quite low, averaging 70 x 10^{-6} cgs units. Four determinations were made on specimens from the major magnetic anomaly zone within the quartz-plagioclase-biotite gneiss. At C 900 W values of 225 and 250 x 10^{-6} cgs units were obtained. However at D 1000 W a value of 800 x 10^{-6} cgs units was measured and at D 900 W a measurement of 5000 x 10^{-6} cgs units was obtained. The fact that the samples from the central part of the major magnetic anomaly at C 900 W did not give as high susceptibility values as the samples from an area of the anomaly where the magnetic intensity was not as great is explained by either assuming the samples from C 900 W are not representative or that the major source of magnetization here is not at the surface. The former seems the most likely explanation for the apparent discrepancy.

Both the major and minor magnetic zones are caused by disseminated pyrrhotite and magnetite which was observed in section. Both magnetic belts carry considerable sulphides, upwards of 2 per cent pyrite being observed at C 900 W in a quartz-plagioclase-biotite-tremolite gneiss that also contains chlorite and epidote.

References

McPhar Geophysics Ltd.
1967: A geophysical case history: Cavendish Township, Ontario, Canada; McPhar Geophysics Ltd., Toronto, Ontario, 14 p.

Williams, D.A., Scott, W.J., and Dyck, A.V.
1975: Cavendish Township geophysical test range: 1973 diamond drilling; Geol. Surv. Can., Paper 74-62, 14 p.

33. CAVENDISH GEOPHYSICAL TEST RANGE, ONTARIO (NTS 31 D/16 W): HAMMER REFRACTION SEISMIC SURVEY

G. D. Hobson
Polar Continental Shelf Project

A hammer refraction seismic survey was conducted along the five lines originally cut to establish a geophysical test range in Cavendish Township, about five miles south of Gooderham, Ontario, which was used in the seminar organized for delegates sponsored by the Canadian International Development Agency to the Conference on Mining and Groundwater Geophysics held in Niagara Falls in October 1967. This survey was undertaken to determine the thickness of drift overlying bedrock thus permitting the construction of a bedrock map and geological sections along each grid line.

A Huntec model FS-3 facsimile seismograph (Fig. 33.1) was used to record all seismic data. A 16-lb sledge hammer struck against a steel plate on the ground provided the seismic energy. Explosives were not used as a source of energy.

Figure 33.2 shows the locations of the seismic profiles surveyed over the test range. Profiles were not obtained at locations at which the bedrock outcrop had been mapped by L. J. Kornik (pers. comm.). Fourteen reversed refraction profiles and 18 unreversed or single-ended refraction profiles were obtained. Reversed profiles were surveyed wherever topography and terrain permitted this procedure. A few low-lying very wet areas were omitted from the program.

Surface elevation at each station had been determined earlier when the grid was established. Surface elevation varies between +1151 feet at the east end of line

Figure 33.1. G. D. Hobson (centre) explaining the operation of the Huntec FS-3 hammer seismograph to S. Samaniego (Philippines) and R. Bellety (Guyana), while C. M. H. Jennings (Botswana) strikes a steel plate with a sledgehammer to produce the seismic energy waves.

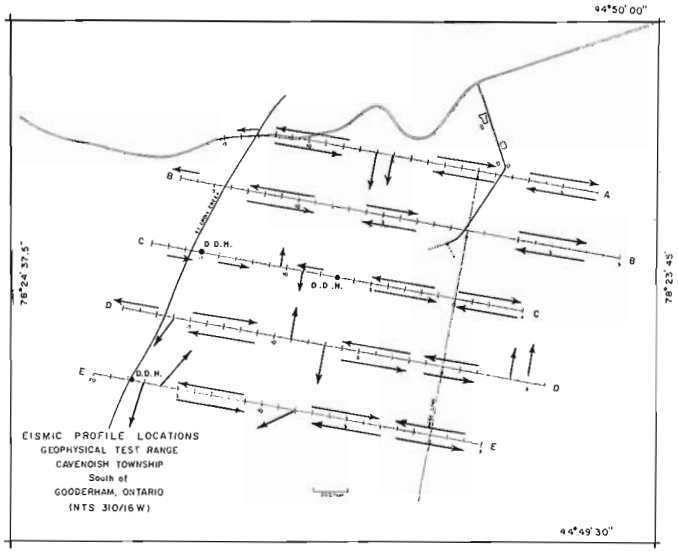

Figure 33.2. Seismic profile locations, geophysical test range, Cavendish Township, Ontario.

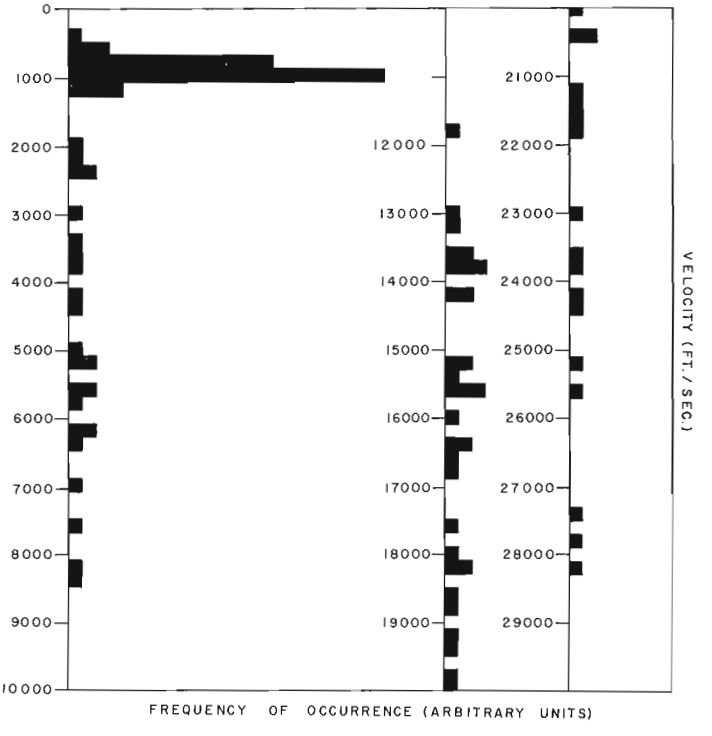

Figure 33.3. Histogram of observed velocities, geophysical test range, Cavendish Township, Ontario.

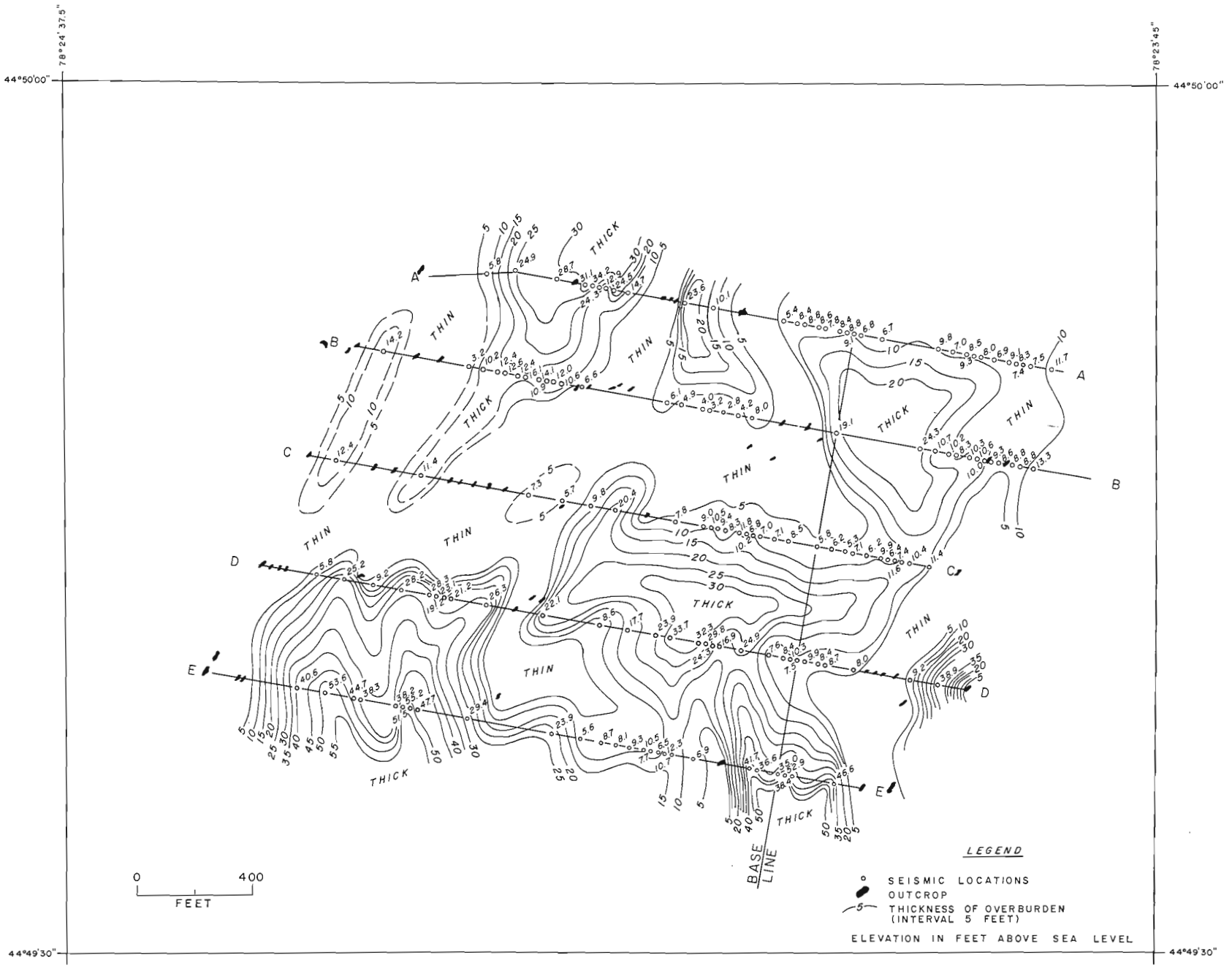

Figure 33. 4. Thickness of overburden, geophysical test range, Cavendish Township, Ontario.

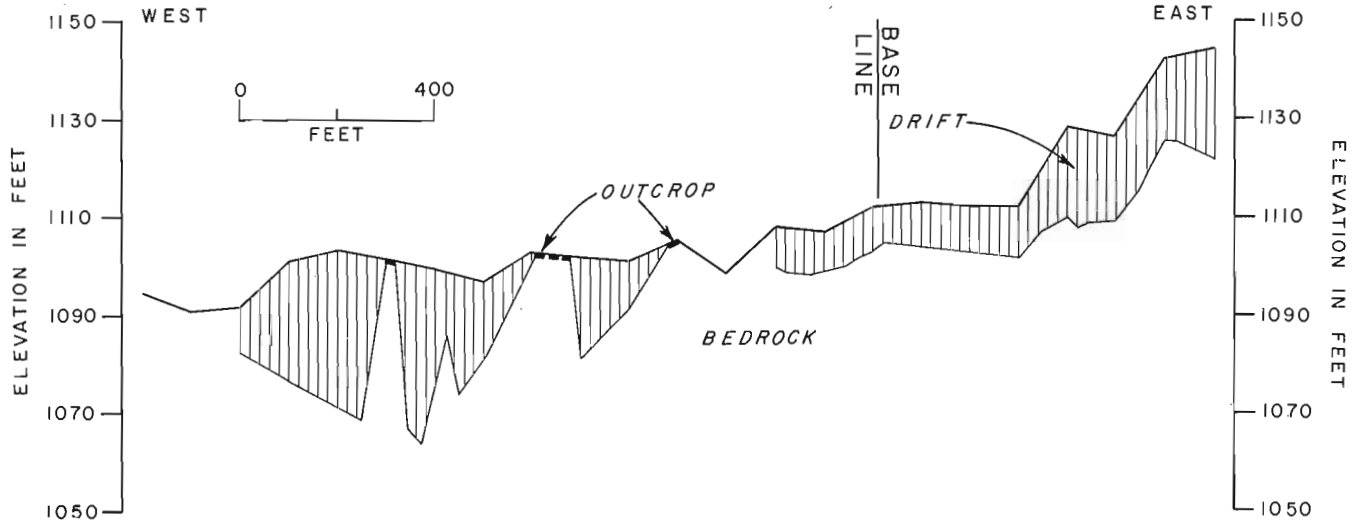

Figure 33. 5. Cross-section line A, geophysical test range, Cavendish Township, Ontario.

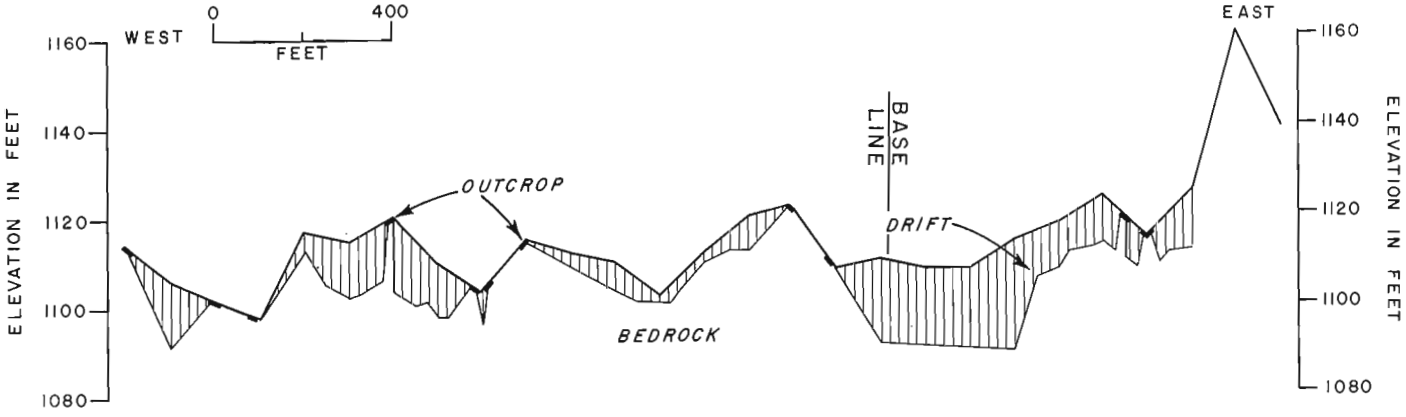

Figure 33. 6. Cross-section line B, geophysical test range, Cavendish Township, Ontario.

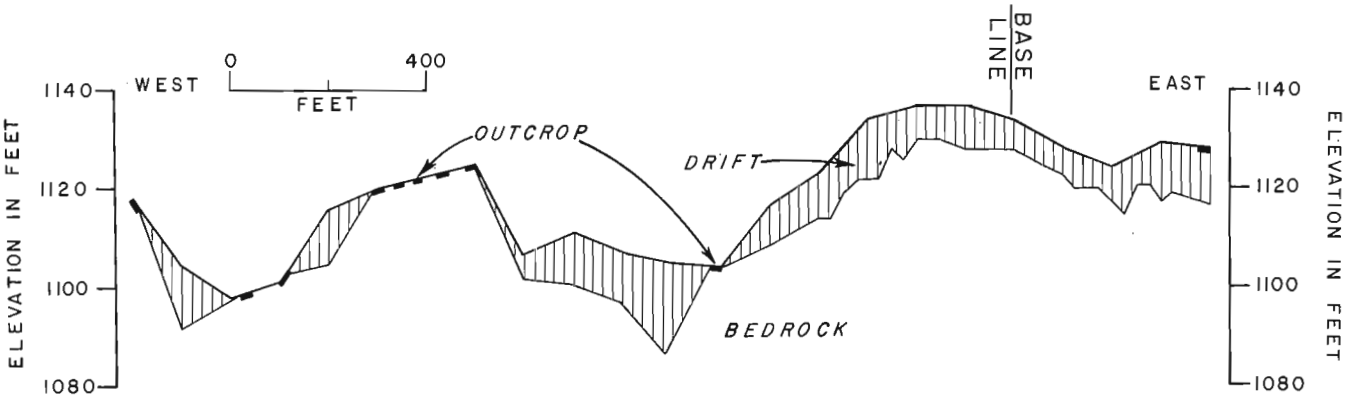

Figure 33. 7. Cross-section line C, geophysical test range, Cavendish Township, Ontario.

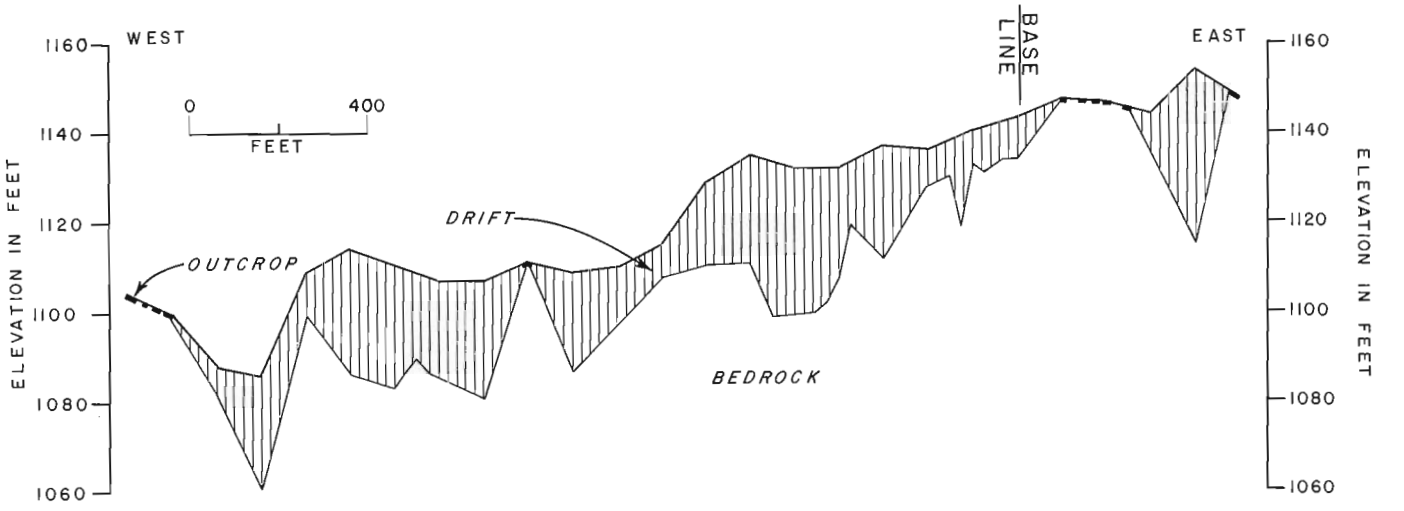

Figure 33.8. Cross-section line D, geophysical test range, Cavendish Township, Ontario.

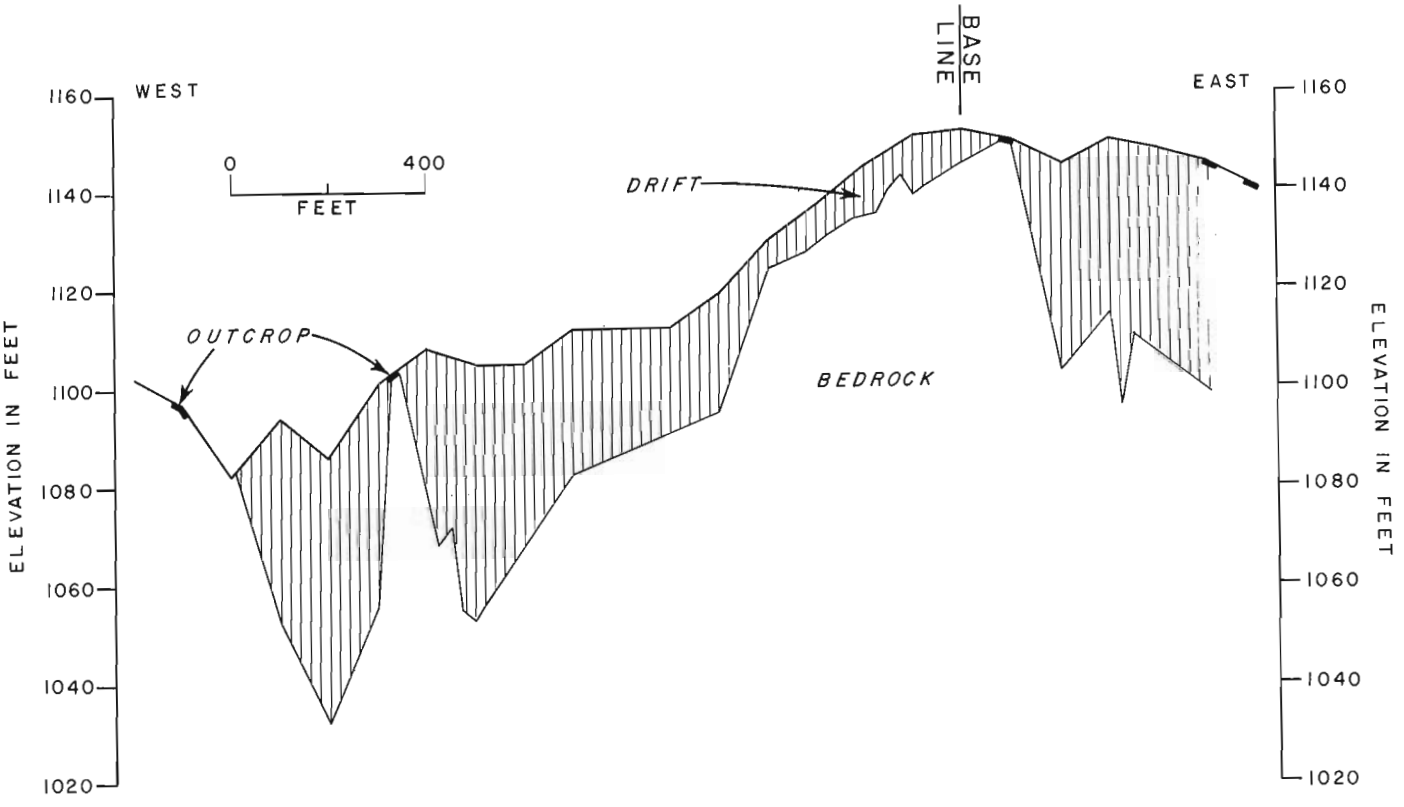

Figure 33.9. Cross-section line E, geophysical test range, Cavendish Township, Ontario.

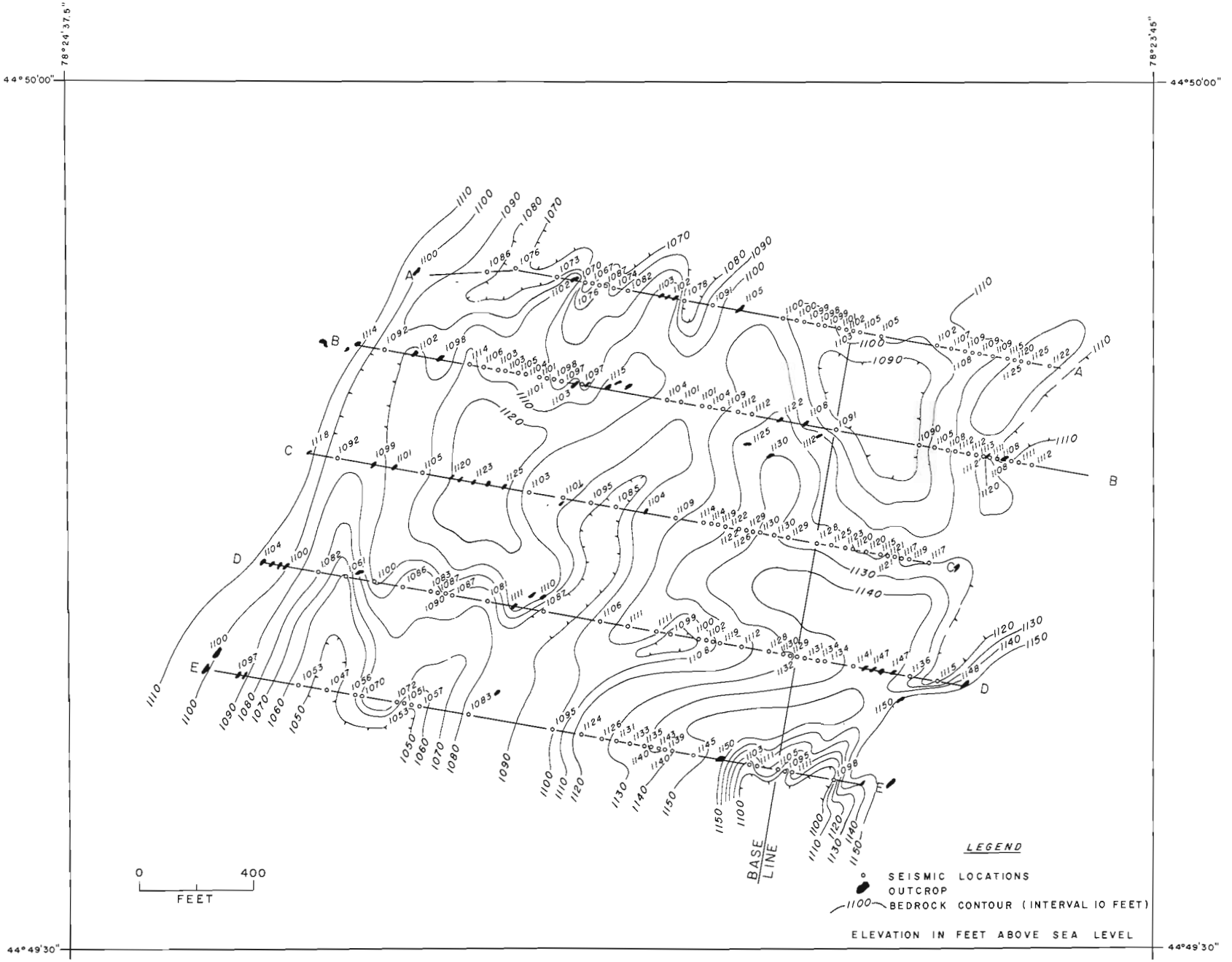

Figure 33.10. Bedrock topography, geophysical test range, Cavendish Township, Ontario.

B and + 1082 feet at St. Croix Creek at the west end of line E. The eastern one-third of the test range is relatively-open gently-rolling terrain recently abandoned as farmland. The western parts of the range are covered with deciduous and evergreen growth with many low-lying wet swampy areas. Access to all parts of the test range is good. A contoured topographic map is presented by Hood (this publication, report 30).

Results

Velocities

Figure 33.3 is a histogram of observed seismic velocity versus frequency of occurrence. The velocities are as observed and are not corrected for dip. The surface layer of soil is represented by velocities between 300 and 1300 feet per second, while velocities within the overburden range between 2000 and 8500 feet per second, and the velocity within bedrock is in excess of 12 000 feet per second. Bedrock lithology cannot be defined on the basis of seismic velocities in this area.

Overburden thickness

Maximum overburden cover is to be found on line E of the test range; 53 feet of overburden has been detected at the east end of that line and 55 feet in the western part of the line. Figure 33.4 is a contoured map of the test range showing thickness of overburden in feet. There does not appear to be any obvious trends to the thickness of overburden covering the area.

Bedrock

Figures 33.5, 33.6, 33.7, 33.8 and 33.9 are cross-sections depicting rock outcrop, overburden thickness and bedrock topography for grid lines A, B, C, D, and E on the geophysical test range. The two velocity strata detected within the overburden have been combined and represented graphically as one stratum. Significant topographic relief is obvious on the bedrock surface. Since all formations in the bedrock are vertical in attitude such sharp relief is to be expected.

Figure 33.10 is a contoured map of the bedrock surface. One hundred feet of relief is indicated over the extent of line E whereas the relief on bedrock is not so severe on the other four lines. Definite trends, particularly of the bedrock "lows", are discernible.

Conclusions

Thickness of overburden over this geophysical test range is readily procured using portable hammer seismograph instrumentation without resorting to explosives as a source of energy.

The magnetic, SP, EM, AFMAG and IP anomalies outlined by McPhar Geophysics Ltd. (1967) in the western half of the test range are generally associated with thin overburden except on line E. The westerly of the two principal anomalies is associated with a bedrock depression while the other anomaly is not associated with any bedrock feature.

References

Hood, P.
1975: Cavendish geophysical test range, Ontario (NTS 31D/16W): historical background; *in* Report of Activities, Part C, Geol. Surv. Can., Paper 75-1C.

McPhar Geophysics Limited
1967: A geophysical case history, Cavendish Township, Ontario, Canada; McPhar Geophysics Ltd., Toronto, Ontario, 14 p.

34. RESIDUAL AEROMAGNETIC ANOMALIES ASSOCIATED WITH THE MEGUMA GROUP OF NOVA SCOTIA AND THEIR RELATIONSHIP TO GOLD MINERALIZATION

G. W. Cameron and Peter J. Hood
Resource Geophysics and Geochemistry Division

Introduction

In 1970, P. H. McGrath indicated that pyrrhotite and pyrrhotite-altered to magnetite were the cause of dominant linear and quasi-circular magnetic anomalies over the Meguma Group. The close association of structural features containing gold deposits to these magnetic features indicated that a quantitative study of spatial relationships would be worthwhile. The paper therefore presents a correlation of gold occurrences with geological and magnetic data for the Meguma Group of Nova Scotia in an attempt to demonstrate the existence of a gold-pyrite-pyrrhotite relationship.

The Meguma Group

The metasedimentary Meguma Group of Nova Scotia is the largest single rock mass of the Atlantic provinces (Schenk, 1970). Two large areas constituting approximately 30 per cent of mainland Nova Scotia are underlain by the Meguma Group. These are separated in the Halifax district by a tongue of the main granite batholith of Nova Scotia (Fig. 34. 1).

Constituent formations of the Cambro-Ordovician Meguma Group are the upper, thinly stratified slate-siltstone-argillite Halifax Formation (Halifax slates) conformably overlying the thin to thickly stratified lithic greywacke and feldspathic-quartzitic Goldenville Formation (Goldenville quartzites). The Halifax-Goldenville formational contact is the only recognizable marker horizon in the Meguma (Taylor and Schiller, 1966; Schenk, 1970). The Halifax slates are estimated to be 14 500 feet thick and contain subordinate amounts of quartzite. The Goldenville quartzites are estimated to be 16 000 feet thick and contain a subordinate amount of interbedded slates (Cameron, 1947). It is common to find isolated sheets and lenses of slate in the midst of metamorphosed sandstone (Woodman, 1899).

The Meguma Group sediments were compressed into a set of asymmetric to isoclinal folds in Devonian times during the Acadian orogeny (Poole, 1967) and were subsequently altered by regional and contact metamorphism. The grade of regional metamorphism is a greenschist facies and an almandine-amphibolite facies produced as a result of the following sequence of dynamic-thermal metamorphism (Taylor and Schiller, 1966):

1. deformation producing major folds and associated secondary structures such as schistosity;
2. contemporaneous low-grade metamorphism with local areas of higher grade metamorphism;
3. after the folding had ceased, there was a major period of metamorphism closely followed by
4. granite intrusion; Schenk (1970) speculates that anatexis of the lower parts of the Meguma Group led to emplacement of the Devonian granodioritic batholiths into the metamorphosed Meguma Group;
5. a later minor deformation which produced slip-shear features in some localities, such as in the Guysborough District.

Gold Occurrences in Nova Scotia

Gold was discovered in Nova Scotia more than a century ago. Consequently the literature dealing with gold areas and individual large and small occurrences is extensive. Early studies (Woodman, 1889; Faribault, 1911) and more recent investigations (Nova Scotia Dept. Mines, 1966) indicated that the majority of gold occurrences in Nova Scotia are within either of the constituent formations of the Meguma Group, many of them at or near the Halifax-Goldenville contact (Fig. 34. 1). Detailed geological settings of the gold occurrences were presented on maps compiled by E. R. Faribault and others. Interbedded and cross-cutting auriferous quartz veins are located on the limbs and axes of major fold features or within subordinate folds. Cameron (1947) indicated that veins occur in the interbedded slates of the Goldenville quartzites, though some are found in the Halifax slates. Lang (1970) noted that gold mining was carried on in slates, generally along the crests of anticlines. Gold is also found in quartz boulders, as placer deposits, along fault or fracture planes, and in association with other minerals.

Woodman (1899), Faribault (1929) and Lang (1970) all noted the association of gold with sulphides. Woodman stated that pyrite is the most abundant sulphide, occurring in both veins and sediments. Faribault noted the occurrence of gold mainly in association with pyrite, though in a few cases the richest ores were associated with pyrrhotite-bearing rocks. Lang indicated that the gold in some placer districts may have existed in the oxidized upper parts of sulphide deposits. Lang also indicated that sulphide minerals may carry specks of gold too small to be seen even with a hand lens.

Gold-quartz veins in Nova Scotia are located mainly in areas underlain by greenschist facies rocks (temperature and pressure conditions of 300°C to 500°C and P_{H_2O} ~ 3000 to 8000 bars (Turner and Verhoogen, 1960), though unconfirmed gold-bearing veins in the almandine-amphibolite facies (500°C to 750°C; P_{H_2O} ~ 4000 to 8000 bars (Turner and Verhoogen, 1960) have been reported (Taylor and Schiller, 1966). Evidence that metamorphism may have had a control in concentrating gold is indicated by a northwest-trending line of gold occurrences commencing just east of Halifax. This line of occurrences runs approximately parallel to the edge of the granitic intrusion (Fig. 34. 1). It is thought that mineralization is associated with the late phases of

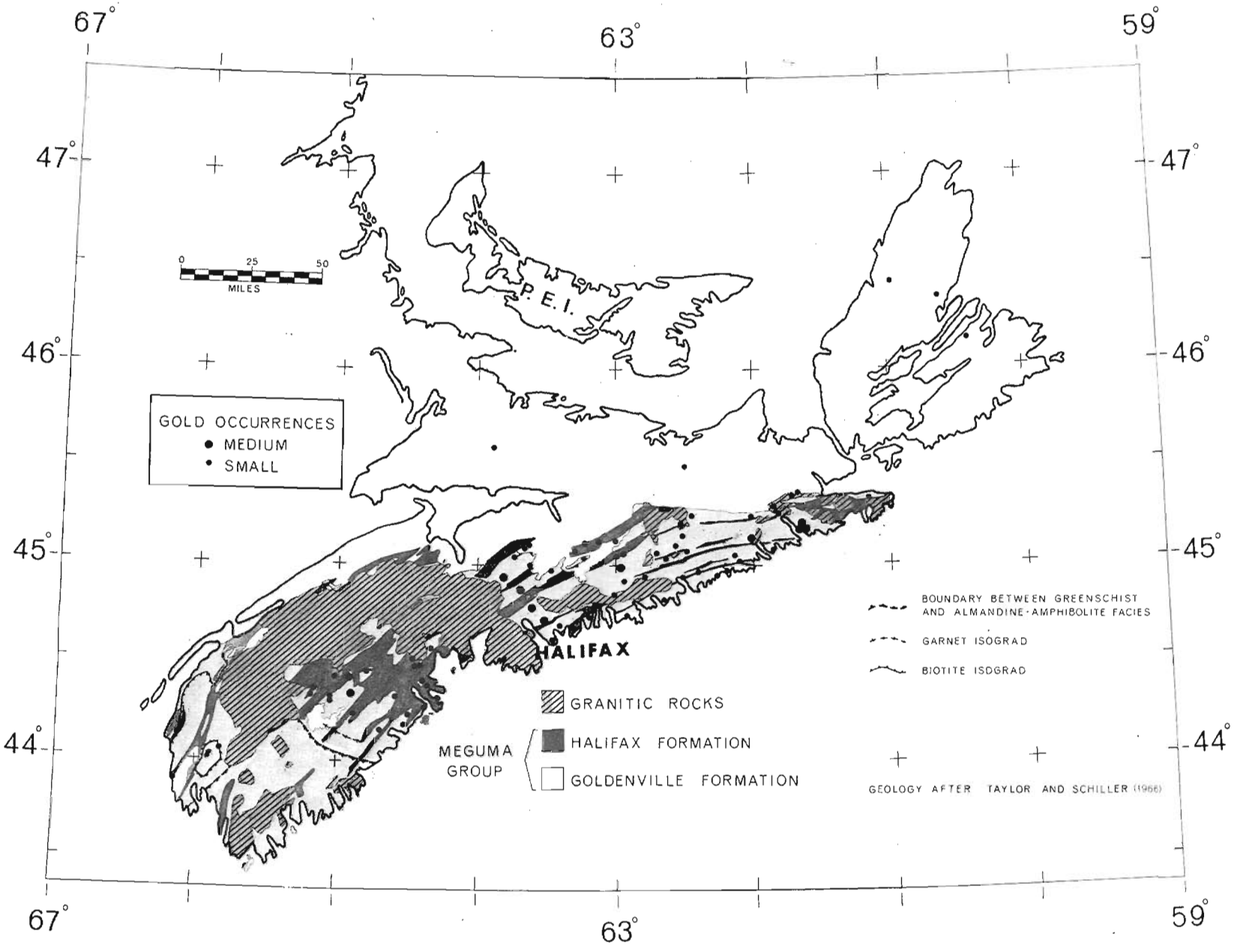

Figure 34.1. Gold occurrences and general geology, Meguma Group, southern Nova Scotia.

cooling of the granite (Douglas, 1948). It is interesting to note that the Curie temperature of the Meguma pyrrhotite (Schwarz, 1973) falls within the temperature limits for the metamorphic zone in which pyrrhotite is the predominant magnetic mineral. A similar relationship holds for magnetite.

Geological Statistics for Meguma Gold Occurrences

Numerous gold occurrences in Nova Scotia are located in the area between 44°30'N and 45°00'N and between 62°W and 64°W. This area was chosen for a statistical study relating the position of quartz veins and auriferous quartz veins to geological contacts. The positions of most of the veins considered in the area are shown in Figure 34.2. Geological maps of the area (at a scale of one inch equals one mile) compiled by Faribault and others, show the position and length of quartz and auriferous veins. Using these maps, the distance from the centre of a mapped quartz vein to the nearest geological contact was measured and recorded. Because the centre of a vein is used, if the vein was not parallel to a contact, quite often one end of the vein was closer to the contact than the recorded distance to its centre. If several veins occurred close together and parallel to each other, they were considered as one vein and the distance from a geological contact to the centre of the group of veins was measured. From the recorded data, histograms of frequency (number of veins) versus distance from geological contacts were drawn (Fig. 34.3 and 34.4).

Percentages calculated from data used to compile the histograms indicate that of the total (210) veins considered, 26.2 per cent (55) were auriferous. Other notable percentages are presented in Table 34.1. All percentages are with respect to the total number of veins considered (210). Note in particular that 52.8 per cent of the veins occur within one mile of a geological contact and 30.5 per cent are within one mile of a quartzite-slate contact.

Percentage calculations for Figure 34.2E indicate only a minor percentage of veins are related to quartzite-limestone or slate-limestone contacts.

From the histograms and tabulated percentages, indications are that, from a geological contact approach, the probability of finding quartz veins in general and auriferous veins in particular is greatest in close proximity to a quartzite-slate contact in either the Goldenville (quartzite) or Halifax (slate) formations. These conclusions are similar to those reached in a report published by the Nova Scotia Department of Mines (1966).

Residual Magnetic Field in Nova Scotia

The magnetic field recorded by a magnetometer at or near the earth's surface receives contributions from two sources. The larger contribution of the magnetic field has its origin in the earth's core and is usually referred to as the main earth's field. The smaller contribution of the magnetic field is due to the induced and remanent magnetization of the rocks forming the earth's

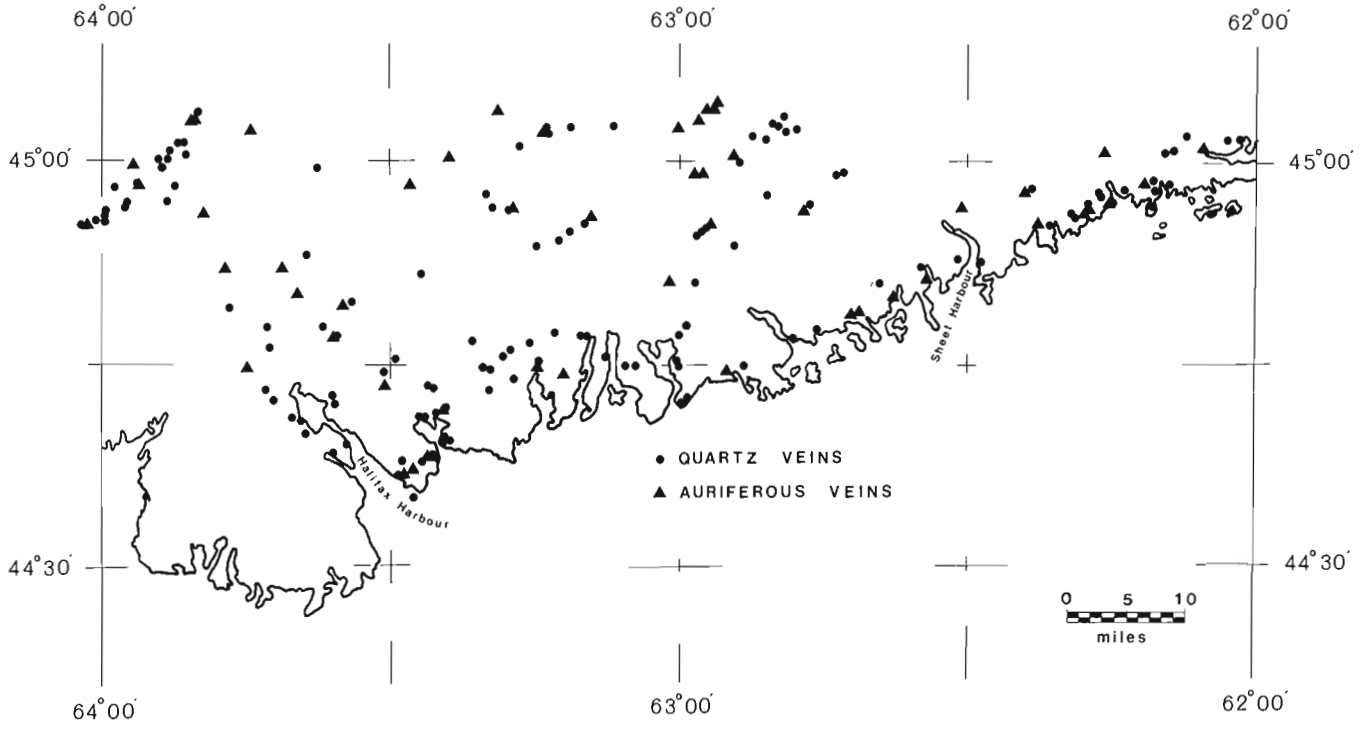

Figure 34.2. Location of most quartz and auriferous veins in area chosen for statistical study relating vein occurrences to geological and magnetic contacts.

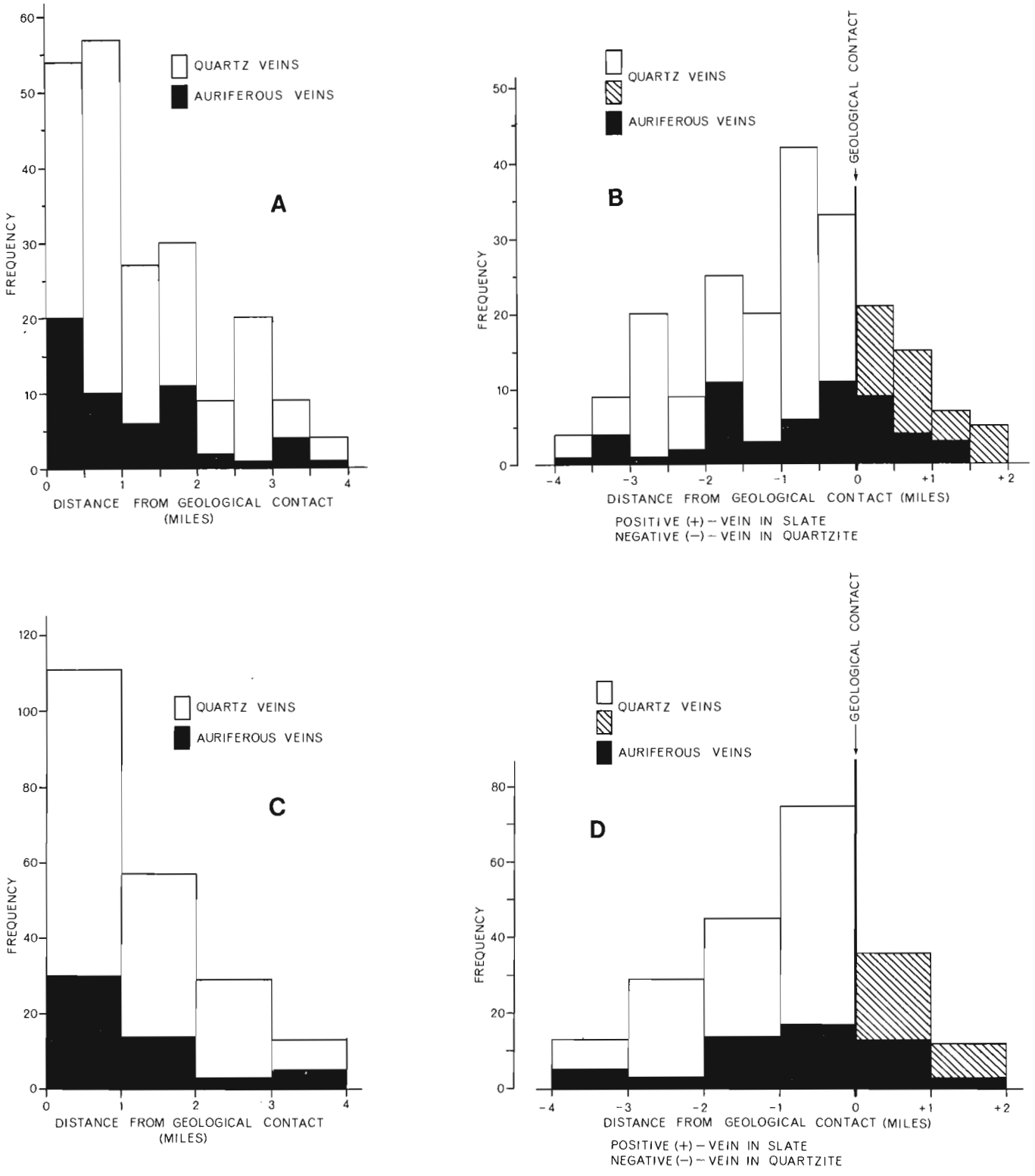

Figure 34. 3. Histograms of frequency of veins versus distance from any geological contact. B and D indicate the number of veins occurring in slate or quartzite whereas A and C represent the combined totals. A and B at 0. 5 mile increments; C and D at 1. 0 mile increments.

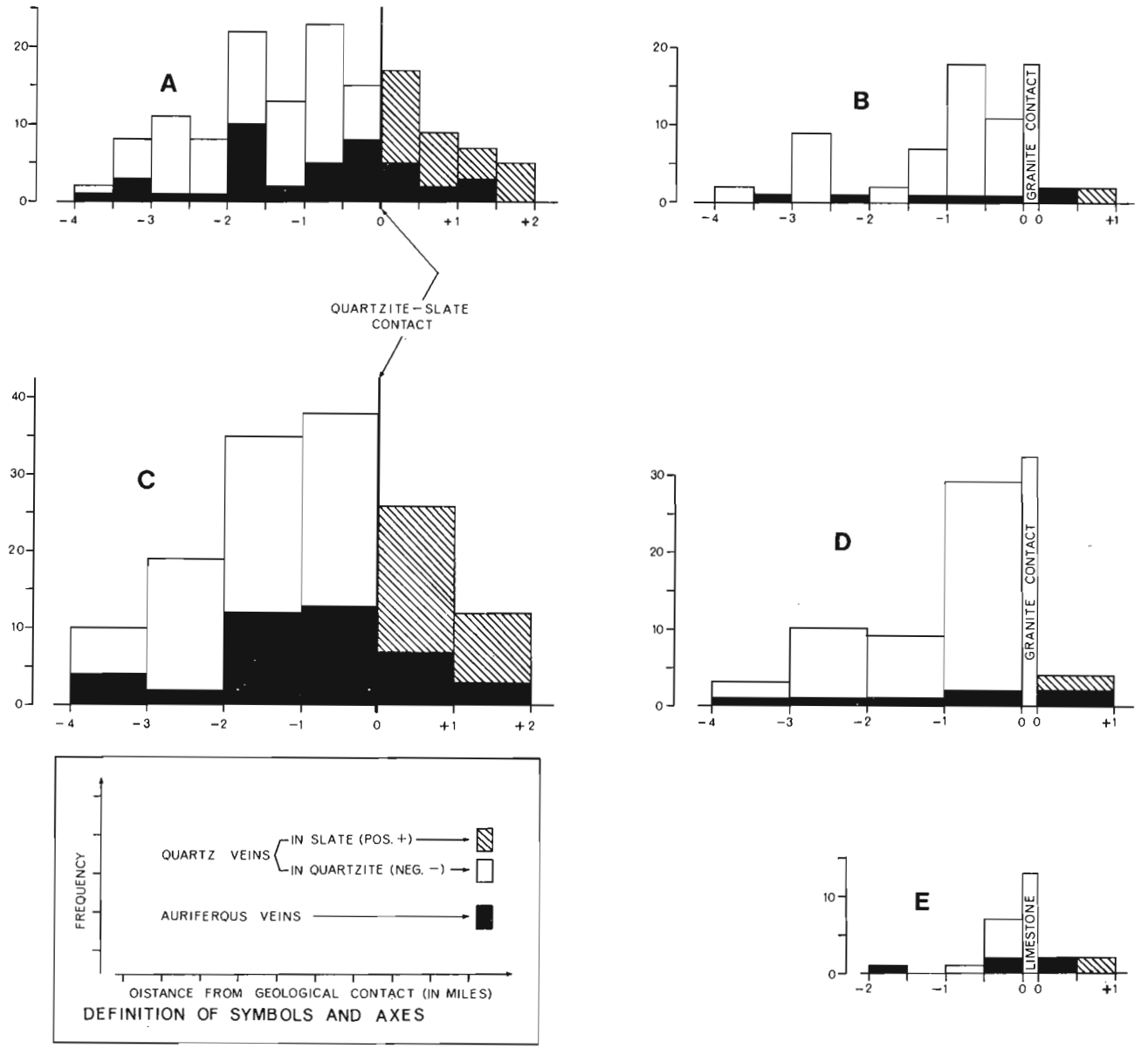

Figure 34. 4. Histograms of frequency of veins versus distance from a particular geological contact. The nearest geological contact is indicated on the diagrams. A, B and E at 0. 5 mile distance increments; C and D at 1. 0 mile increments.

crust. If the magnetic gradient of the main earth's field across an area is large, the anomalies due to crustal features, which may only be a few hundred gammas in amplitude, tend to be masked by the dominating effect of the parallel contours representing the gradient of the core field. Thus a better resolution of magnetic anomalies due to near-surface causative bodies can be obtained by removing the predominating effect of the main earth's field. The resultant map is usually called a residual magnetic anomaly map.

The international Geomagnetic Reference Field (IGRF) is a mathematical model intended to represent that part of the earth's main magnetic field which has its origin in the earth's core. Removal of this core-generated field from total field values on aeromagnetic and shipborne magnetometer maps provides residual magnetic data. Negative residual values are below the IGRF value for a particular location and positive values are greater than the IGRF value. Thus the resulting contoured residual magnetic anomaly map represents the variations of the total magnetic field which are caused solely by the crustal rocks of the earth.

Aeromagnetic maps for Nova Scotia (published during the 1950's) show numerous linear magnetic zones paralleling the strike of the Meguma Group

(Fig. 34.5). These magnetic zones show sharp positive anomalies some 400 gammas or so in amplitude separated by areas of relatively flat magnetic relief. In Nova Scotia, the relatively steep gradient of the main earth's field amounts to 3.8 gammas per kilometre; i.e. about 2000 gammas from the eastern tip of Cape Breton Island to the provincial boundary line with New Brunswick (Fig. 34.6 reproduced from the 1965.0 total field map for Canada published by the Geomagnetic Division of the Earth Physics Branch). Removal of the degrading influence of the gradient due to the core generated field and subsequent compilation of a residual

TABLE 1

Percentage of quartz and auriferous veins within 0.5 mile and 1.0 mile of geological contacts

DISTANCE FROM NEAREST GEOLOGICAL CONTACT (IN MILES)	GEOLOGICAL CONTACT	PERCENTAGE OF AURIFEROUS VEINS			PERCENTAGE OF NONAURIFEROUS VEINS			TOTAL PERCENTAGES		
		IN QUARTZITE	IN SLATE	TOTAL	IN QUARTZITE	IN SLATE	TOTAL	IN QUARTZITE	IN SLATE	TOTAL
⩽ 0.5	———	5.2	4.3	9.5	10.5	5.7	16.2	15.7	10.0	25.7
⩽ 1.0	———	8.1	6.2	14.3	27.6	10.9	38.5	35.7	17.1	52.8
⩽ 0.5	QUARTZITE-SLATE	3.8	2.4	6.2	3.3	5.7	9.0	7.1	8.1	15.2
⩽ 1.0	QUARTZITE-SLATE	6.2	3.4	9.6	11.9	9.0	20.9	18.1	12.4	30.5
⩽ 0.5	GRANITE	0.5	1.0	1.5	4.7	0.0	4.7	5.2	1.0	6.2
⩽ 1.0	GRANITE	1.0	1.0	2.0	12.8	1.0	13.8	13.8	2.0	15.8

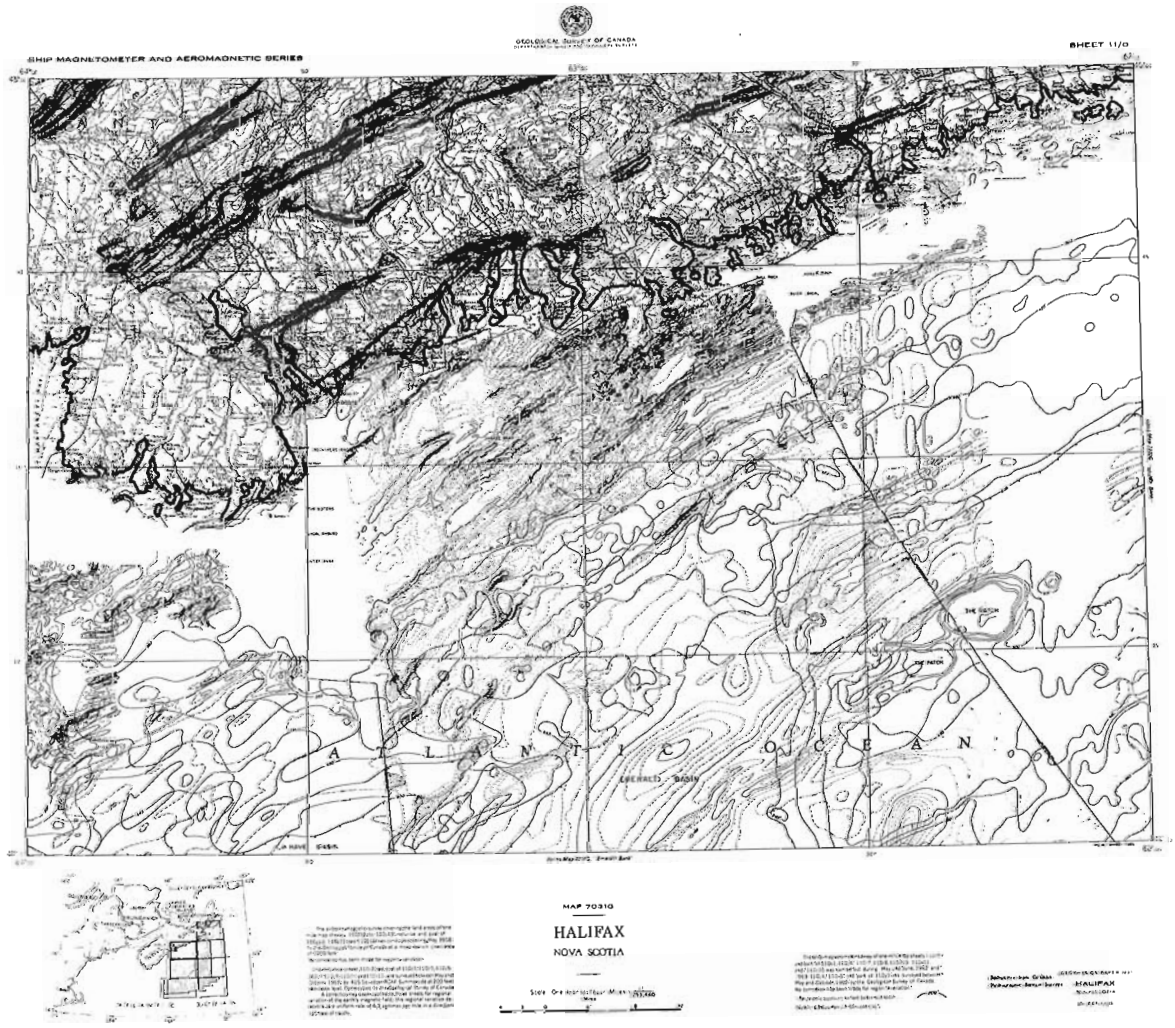

Figure 34.5. Halifax Aeromagnetic Sheet.

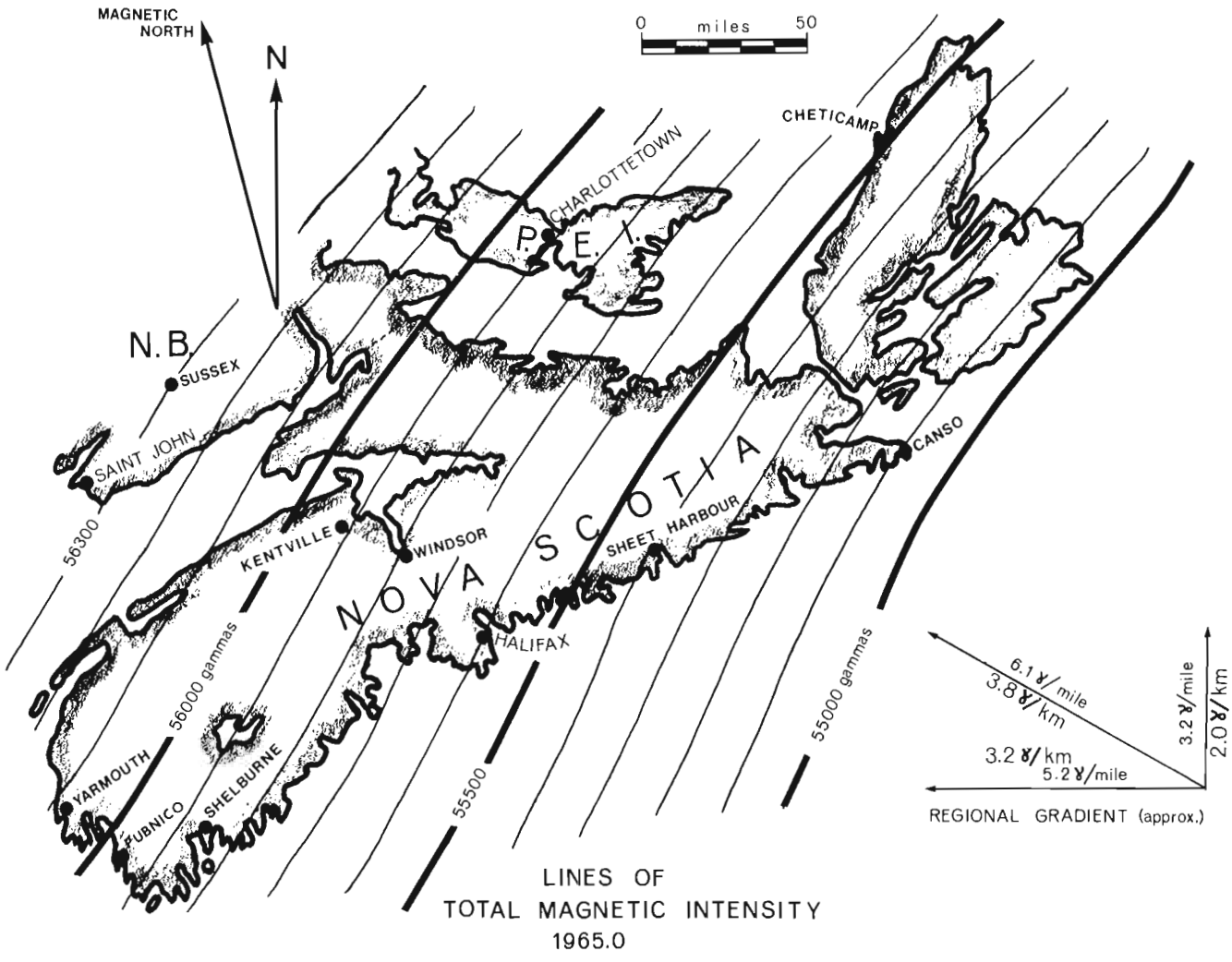

Figure 34.6. Regional Magnetic Field (1965.0), Nova Scotia.

magnetic anomaly map for Nova Scotia yields a better correlation of the magnetic anomalies of Figure 34.5 to outcropping and near-surface causative features of the anomalies.

Figure 34.7 is a residual magnetic anomaly map of Nova Scotia (with the location of some gold occurrences added). It is part of a preliminary 1:1 000 000 residual magnetic anomaly map of the Maritimes compiled by the Magnetic Methods Section of the Geological Survey of Canada. The 1965.0 International Geomagnetic Reference Field values, corrected for secular variation to the year a particular magnetic survey was carried out, were removed from the total field values on the aeromagnetic and shipborne magnetometer maps by a graphical technique. The 1965.0 IGRF values were used because all surveys were flown prior to 1965.

Three main wavelengths are apparent on the residual magnetic anomaly map of the Maritimes. The longer wavelength is of the order of 225 km. The shorter wavelengths vary between less than 12 km in length to greater than 50 km in length (with an average of approximately 30 km). It is the shorter wavelength (hereafter called 12-km or 50-km anomalies) anomalies that are of interest in Nova Scotia. The 12-km anomalies are associated mainly with rocks of the Meguma Group whereas the 50-km anomalies are associated with rocks other than those of the Meguma.

Magnetic Expression of the Meguma Group and General Relationship to the Geology

This report relates geological features of the Meguma Group to aeromagnetic and residual magnetic anomaly patterns on magnetic anomaly maps of the Maritimes. Before reading the detailed magnetic-geologic correlation, the reader should be aware of the experimental error to be expected in the preparation of a residual magnetic anomaly map. It is estimated that, due to levelling and other compilation procedures, and the inaccuracy of the IGRF itself, the values of the residual magnetic contours as presented in Figure 34.7 could be ± 50 gammas in error. Therefore, the spatial

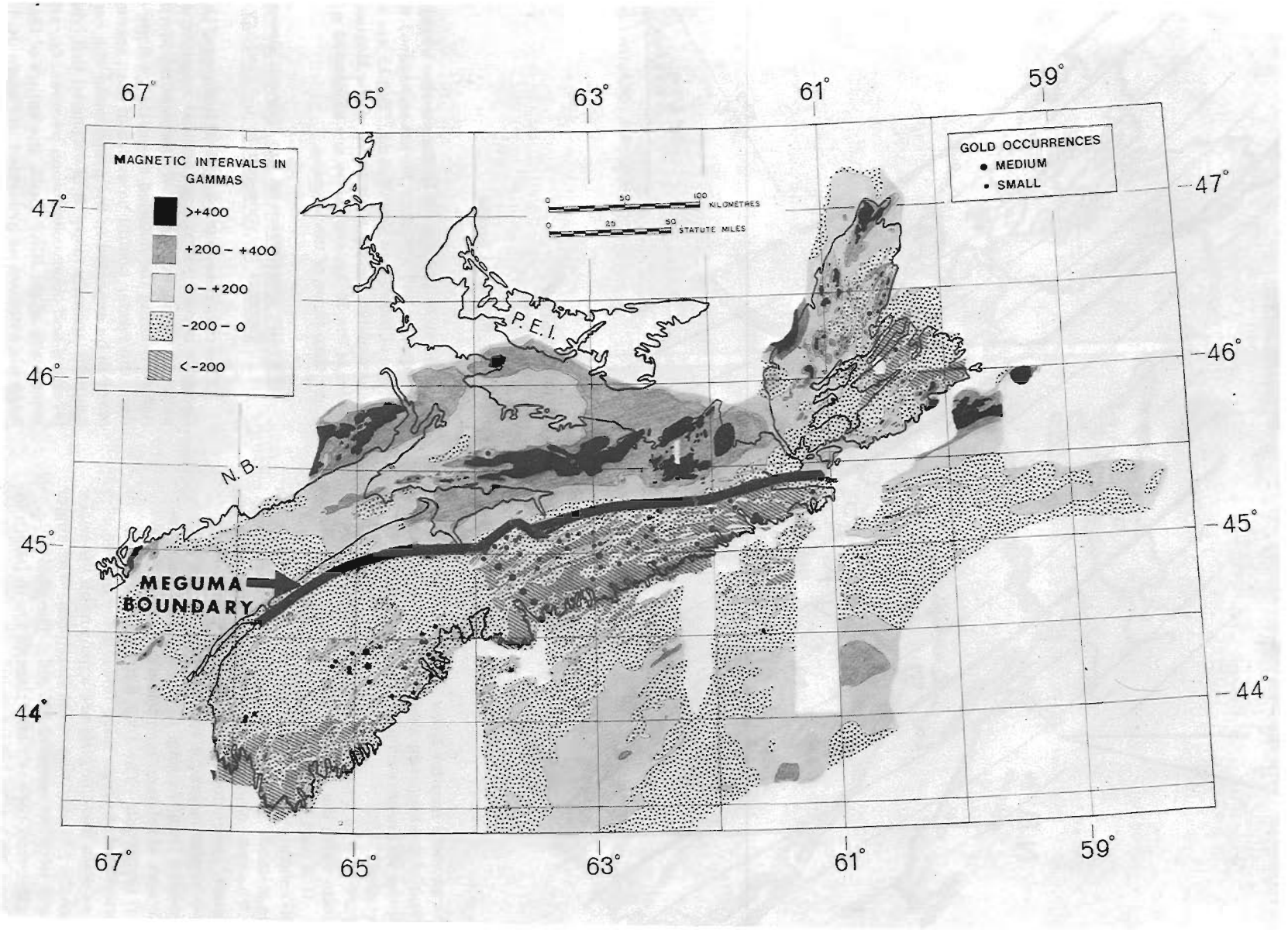

Figure 34.7. Residual Magnetic Anomaly map of Nova Scotia.

relationships of geological features to particular magnetic contours presented in this paper do have a small experimental error. Nevertheless, the main conclusions are valid even though the statistical determinations may change slightly as the IGRF is refined.

Many of the positive magnetic anomalies (aeromagnetic data) of Figure 34.5 are coincident with the axes of major structural features in the Meguma Group (Fig. 34.8). Similarly, since residual magnetic data are the result of graphically filtering aeromagnetic data and yield a better correlation of magnetic anomalies to causative features of the anomalies, the same relation holds for residual magnetic data. It is readily evident from a superposition of the mapped axes of major anticlines and synclines in the Meguma Group on the residual map that many of these major fold features are coincident or nearly coincident, with the residual magnetic anomalies. The 12-km wavelength anomalies on the residual map form linear magnetic zones that appear to be related to the major structural features whereas the 50-km wavelength anomalies form broad, nonlinear magnetic zones of flat magnetic relief which are in general associated with granitic intrusions. Linear and nonlinear magnetic zones are also present over the Scotian Shelf which is strong evidence that the Meguma Group extends offshore (Hood, 1966). Coincidence of magnetic and structural features accentuates the marked parallelism of linear magnetic zones to the regional Appalachian trend.

Many magnetic features of Figure 34.7 are also directly associated with individual geological formations (Halifax and Goldenville) of the Meguma Group. Linear magnetic zones (12-km anomalies) in the 0 gamma to + 200 gamma range, frequently with isolated 'peaks' along their length in the + 200 gamma to + 400 gamma range, are produced by the Halifax Formation. The boundaries of these zones are approximately coincident with Halifax-Goldenville (slate-quartzite) contacts. Scattered zones containing values greater than + 400 gammas, such as near Pubnico in the southwestern part of the province and in the Kentville, Etna and Windsor areas in the west-central part of the province are also directly associated with the Halifax Formation. Negative magnetic zones, in the 0 gamma to less than -200 gamma range are, in general, caused by the Goldenville Formation or by granitic intrusions. Most of the zones in the 0 to -200 gamma range are broad and appear to represent the background level for the residual magnetic anomaly map. Several zones with residual magnetic field values less than -200 gammas are elongated parallel to the regional Appalachian trend.

Cause of Magnetic Anomalies in the Meguma Group

The widespread occurrence of pyrite (FeS_2) in the Meguma has been noted by several authors (Woodman, 1899; Faribault, 1911; Taylor 1967; McGrath, 1970). Pyrite in the Meguma Group occurs within facies bands parallel to the folded bedding (McGrath, pers. comm.) and in auriferous veins controlled by the bedding. Under stress and mild heating, pyrite (FeS_2) loses sulphur resulting in the crystallization of platy, pseudohexagonal pyrrhotite (Fe_7S_8) (Schwarz and McGrath, 1973), which is the most magnetic form of pyrrhotite. Regionally, pyrite crystals in the Halifax Formation are altered to pyrrhotite within sheared slates whereas in nonsheared slates pyrite is generally unaltered (McGrath, 1970).

Linear magnetic zones associated with the Halifax slates are due to the presence of up to 5 per cent (by volume) of this single pyrrhotite type (Fe_7S_8). The ferromagnetic pyrrhotite (Curie temperature ~ 315°C) was formed from pyrite as small lenses along the schistosity planes during the Acadian Orogeny (E. G. Schwarz and P. H. McGrath, pers. comm., 1973). Negligible amounts of pyrrhotite are visible at the surface (due to weathering) but drill cores reveal many subsurface lenses approximately 2.5 cm (one inch) in length (McGrath, pers. comm). The relative abundance of pyrrhotite increases considerably towards the axes of the magnetic zones.

Magnetic features associated with the Goldenville quartzite are caused by a single phase of almost pure magnetite (Fe_3O_4) (McGrath, 1970).

Granitic stocks are often associated with quasi-circular magnetic aureoles on aeromagnetic maps (Hood, 1966). Magnetic anomalies associated with these granitic intrusions are caused by magnetite (Curie temperature ~ 585°C), not pyrrhotite (Schwarz and McGrath, 1973). However, the magnetite within the aureoles around granitic bodies is derived from pyrrhotite which had been altered by the intruding granites (McGrath *et al.*, 1973).

In the Guysborough area, disseminated magnetite and ilmenite form up to 5 per cent (by volume) of andalusite-bearing rocks interbedded with greenschist facies rocks (Taylor and Schiller, 1966), thus producing well-defined magnetic anomalies.

Magnetic Statistics and Relation of Magnetic Features to Gold Occurrences

The residual magnetic anomaly map of the Meguma Group is contoured at 200 gamma intervals. In order to establish a quantitative relationship between the occurrence of a quartz and/or auriferous vein and the magnetic contour interval (range) within which the veins occur, a statistical study relating the distance from the centre of a quartz and/or auriferous vein to the nearest 200 gamma residual magnetic contour was undertaken.

The same area used for the geological statistics was used for the magnetic statistics (44°30'N to 45°00'N; 62°W to 64°W). The residual magnetic map of the area was compiled at a scale of 1:250 000. The detailed geological maps (scale of 1:63 360) compiled by Faribault and others were reduced to a scale of 1:250 000 and vein occurrences superimposed on the residual magnetic data. This reduction of geological data reduced the distance between several of the quartz vein occurrences to a negligible amount. Thus veins which were separated enough to be considered individual occurrences for the geological statistics now occurred

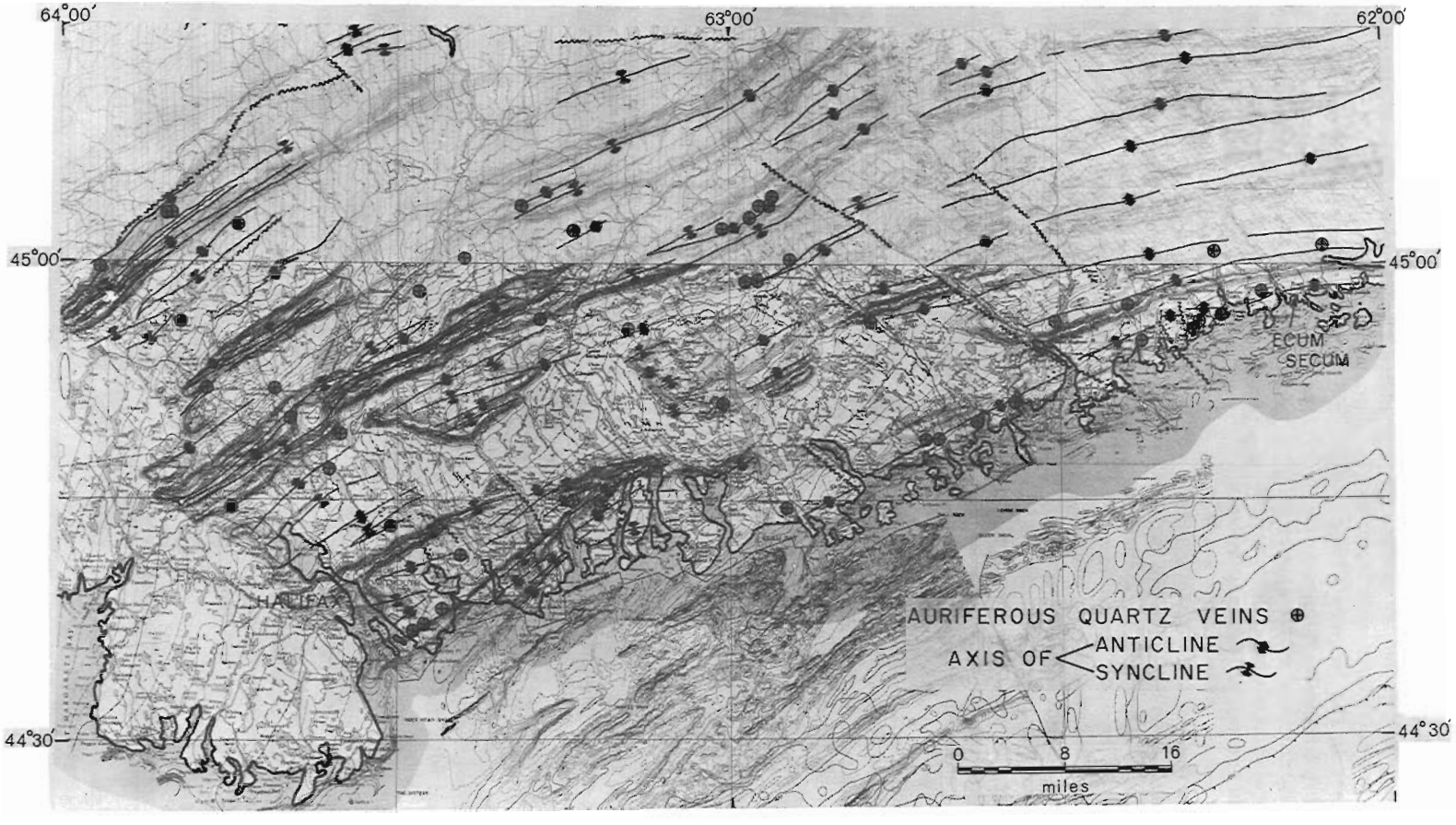

Figure 34. 8. Location of gold deposits and axes of major structural features superimposed on Geological Survey aeromagnetic map-sheets for central Nova Scotia (7031G and 7035G).

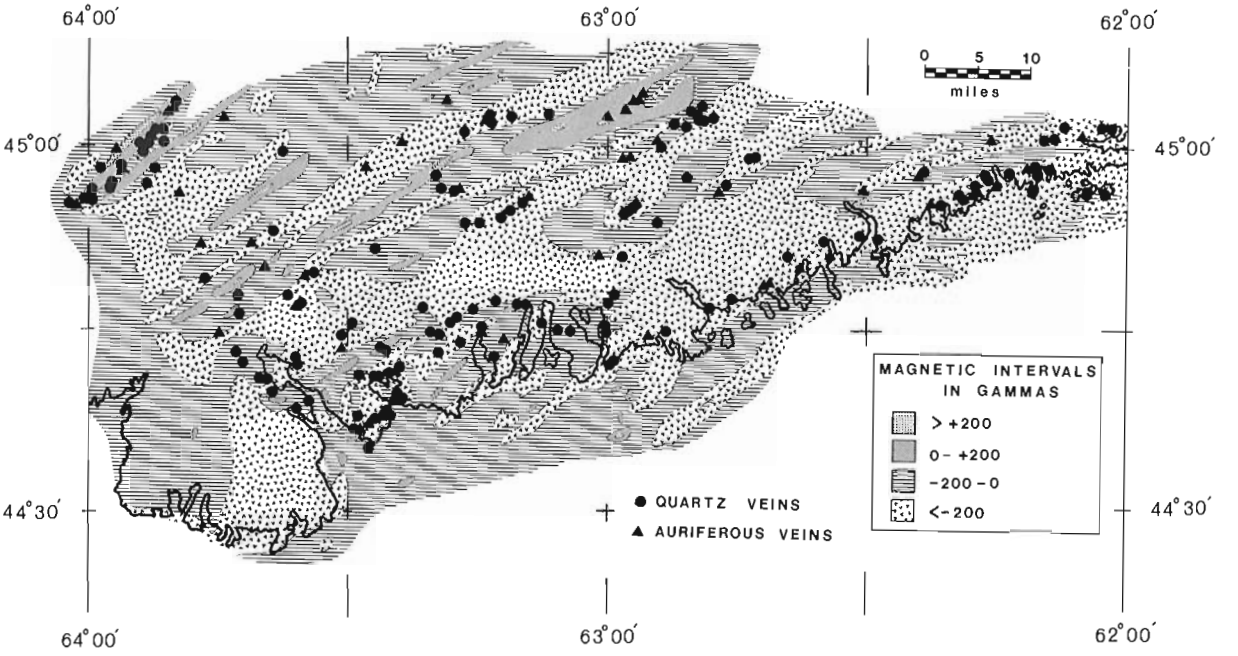

Figure 34. 9. Section of residual magnetic map of Nova Scotia showing the location of quartz and auriferous veins with respect to magnetic "contacts".

TABLE 2

Percentages of quartz and auriferous veins within 0. 5 mile and 1. 0 mile of a particular residual magnetic contour

DISTANCE (MILES) FROM NEAREST RESIDUAL MAGNETIC CONTOUR	NEAREST RESIDUAL MAGNETIC CONTOUR	RANGE →	PERCENTAGE OF AURIFEROUS VEINS			PERCENTAGE OF NONAURIFEROUS VEINS			TOTAL PERCENTAGES		
			<-200γ	-200γ → 0γ	0γ → +200γ	<-200γ	-200γ → 0γ	0γ → +200γ	<-200γ	-200γ → 0γ	0γ → +200γ
≤ 0.5	-200γ		2.1	7.4		21.0	10.5		23.1	17.9	
		TOTAL % →	9.5			31.5			41.0		
≤ 1.0		64.1% within 1.0 miles of -200γ residual magnetic contour (17.5% auriferous; 46.6% nonauriferous)									
≤ 0.5	0γ			2.6	1.1		3.2	4.7		5.8	5.8

as a group close enough together to be considered just one occurrence. Consequently, the total number of veins considered in compiling the statistics relating vein occurrences to 200 gamma residual magnetic contours was reduced to 190 from 210. The number of auriferous veins (55) remained the same. This caused a minor increase in the total percentage of auriferous veins: (i. e.) 28. 9 per cent of all veins considered in the magnetic statistics were auriferous compared to 26. 2 per cent in the geological statistics.

Figure 34. 9 is an enlargement of Figure 34. 7 for the area considered and shows the location of quartz and auriferous veins (also *see* Fig. 34. 2) with respect to residual magnetic contours. The distance from the centre of a vein to the nearest 200 gamma residual magnetic contour was measured and histograms of frequency (number of veins) versus distance from the nearest 200 gamma residual contour drawn. These histograms are shown in Figures 34. 10 and 34. 11. Figure 34. 10 indicates the frequency-distance relationships for the total number of veins in the noted ranges, whereas Figure 34. 11 represents the same relationship and indicates which 200 gamma residual contour is the closest. Percentage calculations related to the histograms are presented in Table 34. 2. Calculations indicate that 64. 1 per cent of all veins (17. 5 per cent auriferous; 46. 6 per cent nonauriferous) occur within one mile of the -200 gamma residual contour. The histograms tend to verify the relationship that many gold occurrences in the Meguma that are associated with Halifax-Goldenville contacts appear to be associated with the zero gamma and -200 gamma residual magnetic contours.

The residual magnetic map of Nova Scotia shows both linear and broad magnetic zones. The edges of the linear zones produced by rocks containing pyrrhotite can be considered a magnetic 'contact' with the broad zones produced by rocks consisting of a very small percentage of magnetite. Since the short wavelength magnetic patterns reflect the near-surface geology, a number of these magnetic contacts are therefore pyrrhotite-magnetite (Halifax-Goldenville or Halifax-granite) boundaries.

As noted previously, many of the linear magnetic zones are coincident with the axes of structural anticlines and synclines. Since many of the anticlinal and synclinal structures in the Meguma have gold deposits associated with them, it follows that the magnetic features related to structural features also have gold deposits associated with them (Fig. 34.8). The linear magnetic zones are often the resultant of magnetic patterns created by the composite effect of several closely-spaced fold features. Each individual fold containing pyrrhotite

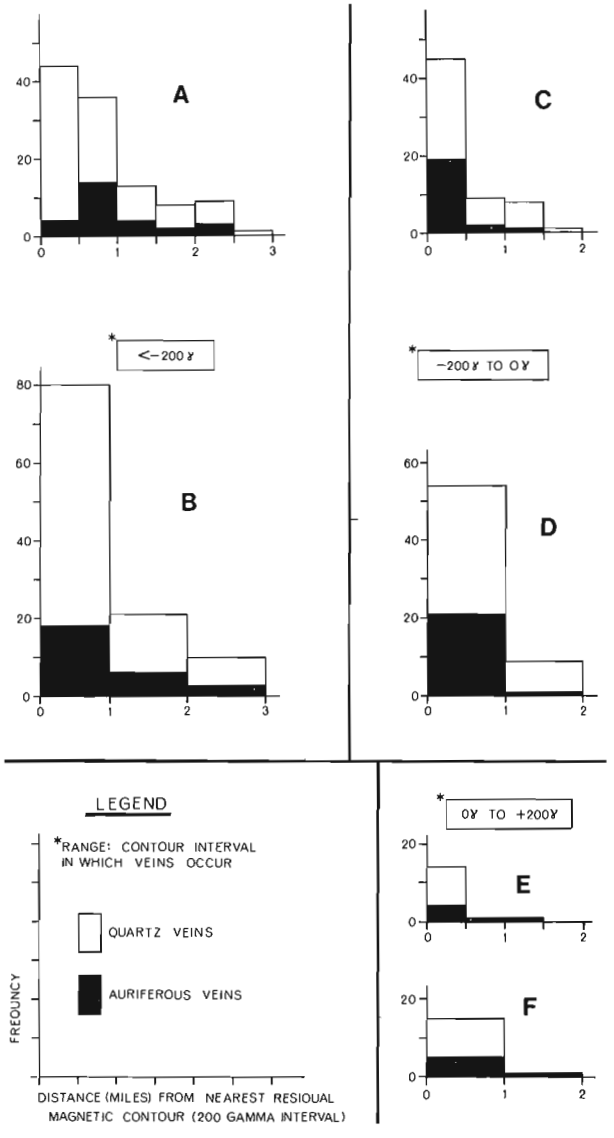

Figure 34.10. Histograms relating the distance of quartz and auriferous veins within a 200 gamma contour interval (range) to the limiting contours of the interval. A, C, E and F at 0.5 mile increments; B and D at 1.0 mile increments.

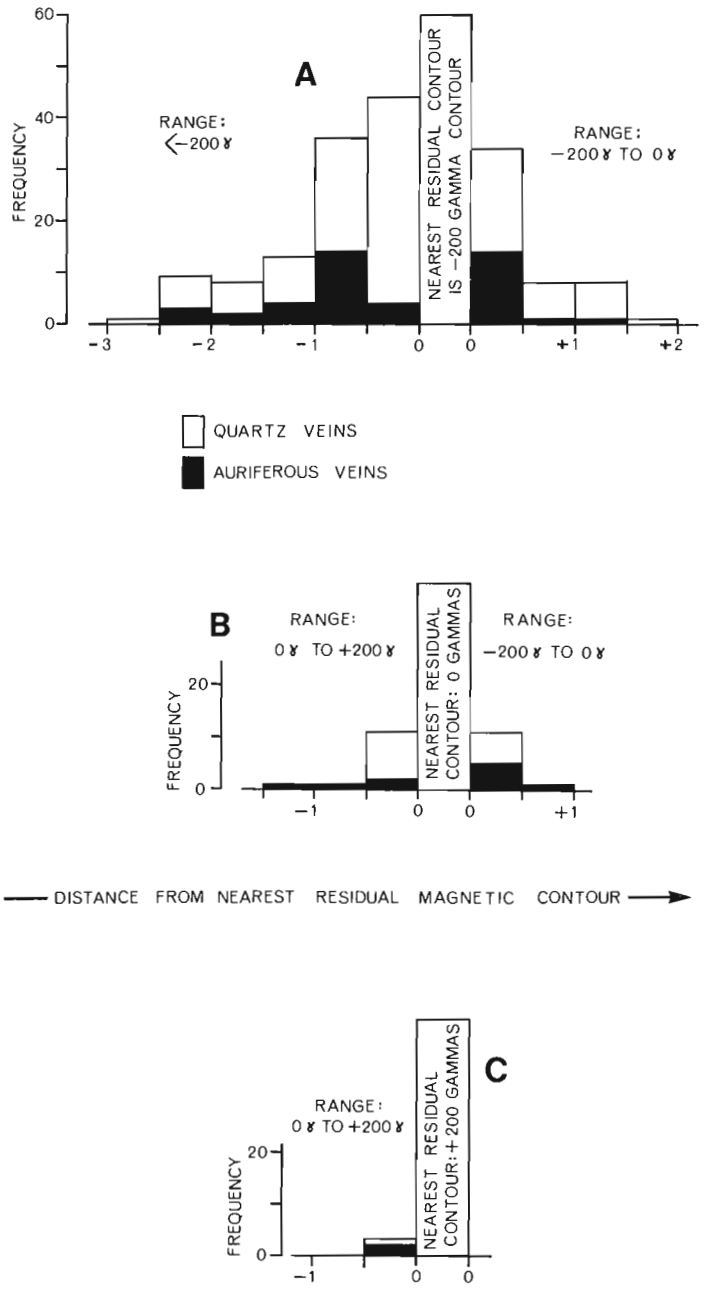

Figure 34.11. Histograms relating the distance of quartz and auriferous veins within a 200 gamma contour interval to the nearest limiting contour of the interval. A, B and C at 0.5 mile increments.

produces a separate magnetic anomaly. In the case of a series of closely-spaced parallel folds the individual magnetic anomalies due to the individual folds are not resolved at the survey altitude of 1000 feet and results in a single composite anomaly parallel to the regional trend. Consequently gold occurrences within each fold which might normally be associated with the edge of an individual anomaly would appear along the axis of the resultant composite linear magnetic zone. Better resolution of individual causative features could be obtained by a ground magnetic or airborne gradiometer survey.

Gold deposits outside the Meguma Group are, in general associated with high value positive magnetic zones. The high positive magnetic zones in the Cheticamp area are probably caused by pyrrhotite. The ores in this area consist of sulphides, of which pyrrhotite is one, occurring as lenses and irregular-shaped tabular masses lying in the schistosity planes (Faribault, 1929). A gold deposit near Barachois Harbour on Cape Breton Island is an example of at least one gold occurrence outside the Meguma Group that can be associated with magnetic zones of similar amplitude to those over the group.

From a consideration of the histograms, percentage calculations for the data relating quartz veins to magnetic data, and the location maps themselves, it is apparent that most gold occurrences in Nova Scotia can be associated with the edges of magnetic zones which are caused mainly by pyrrhotite related to pyrite. Pyrite is disseminated through the same facies of the host rock as pyrrhotite and frequently occurs in auriferous veins. Gold occurrences near granitic intrusions are related to magnetic features caused by magnetite altered from pyrrhotite. The probability of finding quartz veins in general and auriferous veins in particular is higher in areas where the magnetic field is below the IGRF value in close proximity to the linear anomalies produced by pyrrhotite. Areas of particular prospecting interest in the Meguma are bounded by the -200 gamma contour.

Other Gold-Pyrite-Pyrrhotite Occurrences

Taylor and Schiller (1966) noted that other gold deposits in Canada show the same relationship to regional metamorphism as do gold deposits in Nova Scotia. Some of these gold deposits occur in greenschist facies volcanic rocks as opposed to the metasediments of the Meguma Group. If the assumption is made that the initial geochemical environment and subsequent regional or local metamorphism of gold-bearing areas was similar to that of the Meguma Group, then many gold deposits should exhibit a gold-pyrite-pyrrhotite relationship.

A gold-pyrite-pyrrhotite association within metasedimentary and volcanic rock domains in other gold-bearing areas is known. Published material related to deposits noted by Taylor and Schiller (McLaren, 1947; Lumbers, 1964); related to deposits associated with greenstone belts in Manitoba (Davies, 1960; Davies *et al.*, 1962) and related to deposits associated with other metasedimentary environments (McLaughlin, 1949; Monnette, 1949; Tigert, 1949; Giguere, 1972; Sawkins and Rye, 1974), strongly indicate the existence of a gold-pyrite-pyrrhotite relationship. Boyle and Gleeson (1972), Coats (1970), Jones (1958) and Price and Bray (1948) present other examples where gold is found in association with pyrite and pyrrhotite. Hence the results of the present study should be worthwhile in outlining primary areas in Nova Scotia to prospect for gold.

Summary and Conclusions

A gold-pyrite-pyrrhotite relationship exists in the Meguma Group of Nova Scotia.

Pyrite in the Meguma Group of Nova Scotia occurs within facies bands parallel to the folded bedding and in quartz veins. In sheared slates, pyrite is altered to ferromagnetic pyrrhotite by dynamic and thermal metamorphism (greenschist facies). This pyrrhotite causes linear magnetic zones on aeromagnetic maps which are coincident with the axes of many of the major structural features. A number of the structural features have gold deposits associated with them. Thus magnetic anomalies associated with these structural features also have gold deposits associated with them.

Compilation of residual magnetic anomaly maps better resolves the extent of the causative features of the anomalies on aeromagnetic maps. In the Meguma Group, linear magnetic zones produced by pyrrhotite and broad magnetic zones produced by magnetite are evident on the residual anomaly map of Nova Scotia.

The linear residual magnetic anomalies, in general, have gold mineralization associated with their boundaries. This relationship of gold deposits to magnetic zones indicates areas where prospecting could be worthwhile in both the Goldenville quartzites and the Halifax slates. The probability of finding auriferous veins is highest in areas where the magnetic field is below the IGRF value and in close proximity to the linear anomalies produced by pyrrhotite. As the minerals causing the magnetic features are related to a particular facies, it is apparent that further prospecting along a particular facies band in the bedding could also prove worthwhile. Further field studies using a ground magnetometer and/or airborne gradiometer should be carried out to determine if these instruments would better resolve causative features of the anomalies and delineate more precisely areas where ore grade material could be found.

Other gold-bearing areas appear to have a similar gold-pyrite-pyrrhotite relationship. The major difference between these deposits and the Meguma Group are the host rocks: (i. e.) some of the other gold-bearing areas are within low-grade metamorphosed volcanic rocks as opposed to the metasediments of the Meguma Group. Detailed laboratory and field studies of several other areas to determine in a more definitive way the initial mineralogical and structural conditions leading to the emplacement of the gold, pyrite and pyrrhotite might prove worthwhile.

Acknowledgments

The authors would like to thank L. J. Kornik and P. H. McGrath for reviewing and suggesting improvements in this paper. Gratitude is also expressed to E. J. Schwarz and R. V. Kirkham for the time taken to discuss relevant material and to D. G. Benson and L. M. Cumming for reference material.

References

Alcock, F. J.
1949: Geological map of the Maritime Provinces; Geol. Surv. Can., Map 910 A.

Boyle, R. W. and Gleeson, C. F.
1972: Gold in the heavy mineral concentrates of stream sediments, Keno Hill area, Yukon Territory; Geol. Surv. Can., Paper 71-51.

Cameron, H. L.
1947: Structural control of orebodies in Nova Scotia Gold districts; *in* Can. Inst. Min. Met., Trans., v. 50, p. 1-14.

Coates, M. E.
1970: Geology of the Killala-Vein lakes area; Ont. Dept. Mines, GeoI. Rept. 81, 35 p. (accompanied by maps 2191 and 2192).

Davies, J. F.
1960: Massive sulphide deposits in Manitoba; *in* Can. Inst. Min. Met., Bull., v. 53, no. 515, p. 141-144.

Davies, J. F., Bannatyne, B. B., Barry, G. S., and McCabe, H. R.
1962: Geology and Mineral Resources of Manitoba; Man. Dept. Mines Nat. Resour.

Douglas, G. V.
1948: Structure of the gold veins in Nova Scotia; *in* Structural Geology of Canadian Ore Deposits: A symposium; Can. Inst. Min. Met. Jubilee Volume, p. 919-926.

Dunbar, W. R.
1948: Structural relations of the Porcupine ore deposits; *in* Structural Geology of Canadian Ore Deposits: A symposium; Can. Inst. Min. Met. Jubilee Volume, p. 442-456.

Faribault, E. R.
1911: Gold bearing series of the basin of Medway River, Nova Scotia; *in* Summary Report of the Geological Survey Branch, Geological Survey of Canada, Summary Report, 1911, Sessional Paper No. 26, p. 334-340.

Geol. Surv. Can. Maps. 551 (1895), 565 (1896), 611 (1897), 624 (1898), 700 (1906), 807, 908, 985 (1907), 1019, 1036, 1043 (1908), 1025 (1909), 150 A (1916), 1981 (1924), 2153 (1929), 2259 (1931).

Faribault, E. R., Armstrong, P., and Wilson, J. T.
Geol. Surv. Can. Maps. 435 A, 436 A, 437 A, 438 A, 439 A, 440 A (1938), 531 A, 532 A (1939).

Fletcher, H. and Faribault, E.
Geol. Surv. Can. Maps 382 (1893), 1037 (1909).

Geological Survey of Canada.
Aeromagnetic Maps 7030G, 7031G, 7032G, 7033G, 7034G, 7035G, 7036G, 7291G, (1965, 1966, 1968)

: Unpublished photographically reduced composites of Aeromagnetic Maps 11G, 12G, 14G, 15G, 16G, 68G, 69G, 95G, 96G, 97G, 8390G.

: Unpublished Residual Magnetic Map of the Maritimes, compiled in Magnetic Methods Section of the Resource Geophysics and Geochemistry Division (1973).

Giguere, J. F.
1972: Geology of the Granitehill Lake area, Districts of Algoma and Thunder Bay; Ont. Dept. Mines Northern Affairs, Geol. Rept. 95, 33 p. (accompanied by map 2219).

Hood, P. J.
1966: Magnetic surveys of the Continental Shelves of Eastern Canada; *in* Continental Margins and Island Arcs; Geol. Surv. Can., Paper 66-15, p. 19-32.

Jones, W. A.
1948: Hollinger Mine; *in* Structural Geology of Canadian Ore Deposits: A symposium; Can. Inst. Min. Met. Jubilee Volume, p. 464-482.

Lang, A. H.
1970: Prospecting in Canada; Geol. Surv. Can., Econ. Geol. Rept. no. 7, 308 p.

Lumbers, S. B.
1964: Preliminary report on the Relationship of Mineral Deposits to Intrusive Rocks and Metamorphism in Part of the Grenville Province of Southeastern Ontario; Ont. Dept. Mines, Prel. Rept. Pr. 1964-4, 37 p.

Malcolm, W. and Faribault, E. R.
1929: Gold Fields of Nova Scotia; Geol. Surv. Can., Mem. 156.

McGrath, P. H.
1970: Aeromagnetic Interpretation Appalachia, New Brunswick and Nova Scotia; *in* Report of Activities, Part A, Geol. Surv. Can., Paper 70-1A, p. 79-82.

McGrath, P. H., Hood, P. J., and Cameron, G. W.
1973: Magnetic surveys of the Gulf of St. Lawrence and Scotian Shelf; *in* Earth Science Symposium on Offshore Eastern Canada, Geol. Surv. Can., Paper 71-23, p. 339-358.

McGrath, P.H.
1973: Personal Communication.

McLaren, D.C.
1947: McKenzie Red Lake Gold Mines: Brief outline of geology, mining and milling; *in* Can. Min. J., v. 68, no. 4, p. 235-241.

McLaughlin, D.H.
1949: The Homestake Mine; *in* Can. Min. J., v. 70, no. 12, p. 49-53.

Monette, H.H.
1949: Geological outline of Pickle Crow; *in* Can. Min. J., v. 70, no. 11, p. 99-105.

Nova Scotia Department of Mines
1966: Metallic mineral occurrences recorded in the Province of Nova Scotia (accompanied by a Mineral Map of Nova Scotia).

Poole, W.H.
1967: Tectonic evolution of Appalachian Region of Canada; *in* Geol. Assoc. Can., Spec. Paper no. 4, p. 9-51.

Price, P. and Bray, R.C.E.
1948: Pamour Mine; *in* Structural Geology of Canadian Ore Deposits: A symposium; Can. Inst. Min. Met. Jubilee Volume., p. 558-564.

Sawkins, F.J. and Rye, D.M.
1974: Relationship of Homestake-type gold deposits to iron-rich Precambrian sedimentary rocks; *in* Inst. Min. Metall., Trans., v. 83, Sect. B, p. B56-N69.

Schenk, P.E.
1970: Regional variation of the flysch-like Meguma Group (Lower Paleozoic) of Nova Scotia, compared to recent sedimentation off the Scotian Shelf; *in* Geol. Assoc. Can., Special Paper no. 7, p. 127-153.

Taylor, F.C. and Schiller, E.A.
1966: Metamorphism of the Meguma Group of Nova Scotia; *in* Can. J. Earth Sci., v. 3, no. 7, p. 959-974.

Taylor, F.C.
1967: Reconnaissance geology of Shelburne map-area, Queens, Shelburne and Yarmouth Counties, Nova Scotia; Geol. Surv. Can., Mem. 349, 83 p.

Tigert, T.T.
1949: Geology of Central Patricia Mine; *in* Can. Min. J., v. 70, no. 12, p. 49-53.

Turner, F.J. and Verhoogen, J.
1960: Igneous and metamorphic petrology; McGraw-Hill Book Co., Toronto.

Woodman, J.E.
1899: Studies in the Gold-Bearing Slates of Nova Scotia; *in* Proc. Boston Soc. Nat. Hist., v. 48, no. 15, p. 375-407.

35. GAMMA-RAY SPECTROMETRY INSTRUMENTATION

Project 700087; Uranium Reconnaissance Program

Q. Bristow
Resource Geophysics and Geochemistry Division

The first phase of a two-phase project to update the high sensitivity airborne gamma-ray spectrometry system is now complete. This involved replacing the all important signal conditioning electronics with units designed in terms of the newer and more sophisticated linear integrated circuits which are now available. Specifically the original emitter follower preamplifiers for each of the twelve 9" x 4" sodium iodide detectors have been replaced with ones containing FET operational amplifiers connected as charge amplifiers, one for each photomultiplier tube with provision for adjusting their individual contributions to an output buffer stage thereby allowing for tube gain matching. A new summing amplifier has been designed with differential inputs for the twelve detectors, pole zero cancellation, a two-stage active filter using operational amplifiers, and base line restoration circuitry. It provides unipolar gaussian-shaped pulses via a high power buffer output stage suitable for driving any standard pulse height analysis equipment. Front panel controls are provided for gain adjustment of the twelve detectors.

The result has been a dramatic improvement in the resolution of the system, which despite some aging detectors is now 11.8 per cent for the total volume of 3050 cubic inches.

In order to facilitate this work a transportable multichannel analyzer was assembled by interfacing a standard commercial pulse height analysis ADC to a Texas Instruments 960A minicomputer. An elementary D/A converter was incorporated in the system to provide a spectrum display capability using any laboratory oscilloscope. A program was written incorporating a variety of features which no hardwired multichannel analyzer would normally have, but which were found very valuable during the course of this and other work. For example, the system was taken to Uplands Airport (Ottawa at various times between June and August 1975) in order to verify the operation of four different airborne gamma-ray spectrometry systems designed for use on contract surveys. The system operated satisfactorily from a gas driven 1 kilowatt generator and enabled some vital checks to be made quickly and reliably by tapping into the detector signals from the aircraft spectrometer systems. These include: -

- Recording a complete spectrum from each system over each of the five calibration pads for immediate display and storage on cassette tape.
- Integration of counts over the standard spectral windows in these spectra, for comparison with the values obtained by the single channel analyzers in the aircraft system.
- Obtaining figures for overall detector resolution on the standard $^{137}C_s$ isotope peak.

In all but one case these tests revealed discrepancies (some serious) which enabled adjustments or modifications to be made to bring the performance into line with the contract specifications thereby ensuring as far as possible that uniform results would be obtained from the surveys.

The recorded spectra were subsequently transmitted via an acoustic coupler and office telephone to the E.M.R. Computer Science Centre, where a program written by M.T. Holroyd of the Digital Methods Section automatically produced titled and annotated plots for permanent records. This approach is a demonstration of the author's philosophy that minicomputers should be used for data acquisition and elementary processing, while more sophisticated number crunching, plotting etc. should be carried out on a larger more powerful machine with a library of statistical software and peripheral equipment.

The spectra shown on the succeeding pages were recorded from the Geological Survey's high sensitivity system using this technique over the calibration pads, following installation of the redesigned signal conditioning electronics described above. These are now considered as reference spectra for airborne gamma spectrometry systems and illustrate the quality of results which can be obtained from a well designed spectrometer of this type.

The computer-based analyzer is currently being used to record complete spectra from borehole probes *in situ*, where once again defects in the commercial equipment that is being used were soon revealed, enabling corrective action to be taken. The spectra so far recorded make it very clear that the efficiency of the necessarily small sodium iodide detectors for gamma radiation above 1 MeV is so low, that peaks lower down in the spectrum, e.g. ^{214}Bi 609 Kev and ^{208}Tl 910 KeV, should be investigated for routine logging with separate potassium, uranium and thorium profiles.

A brief extract from the documentation of the program that was written for the minicomputer based analyzer is given below, to illustrate the field capability that is available with such a system.

A Pulse Height Analysis Program for Acquisition of Gamma-Ray Spectra Using the Texas Instruments 960A Minicomputer

General

This program is a stand-along module which does not require the Program Support Monitor (P.S.M.). It is designed to acquire 1024 channel gamma-ray spectra via a Nuclear Data Inc., model N.D.- 560 Analogue/digital converter (A.D.C.), interfaced to a

Figure 35.1

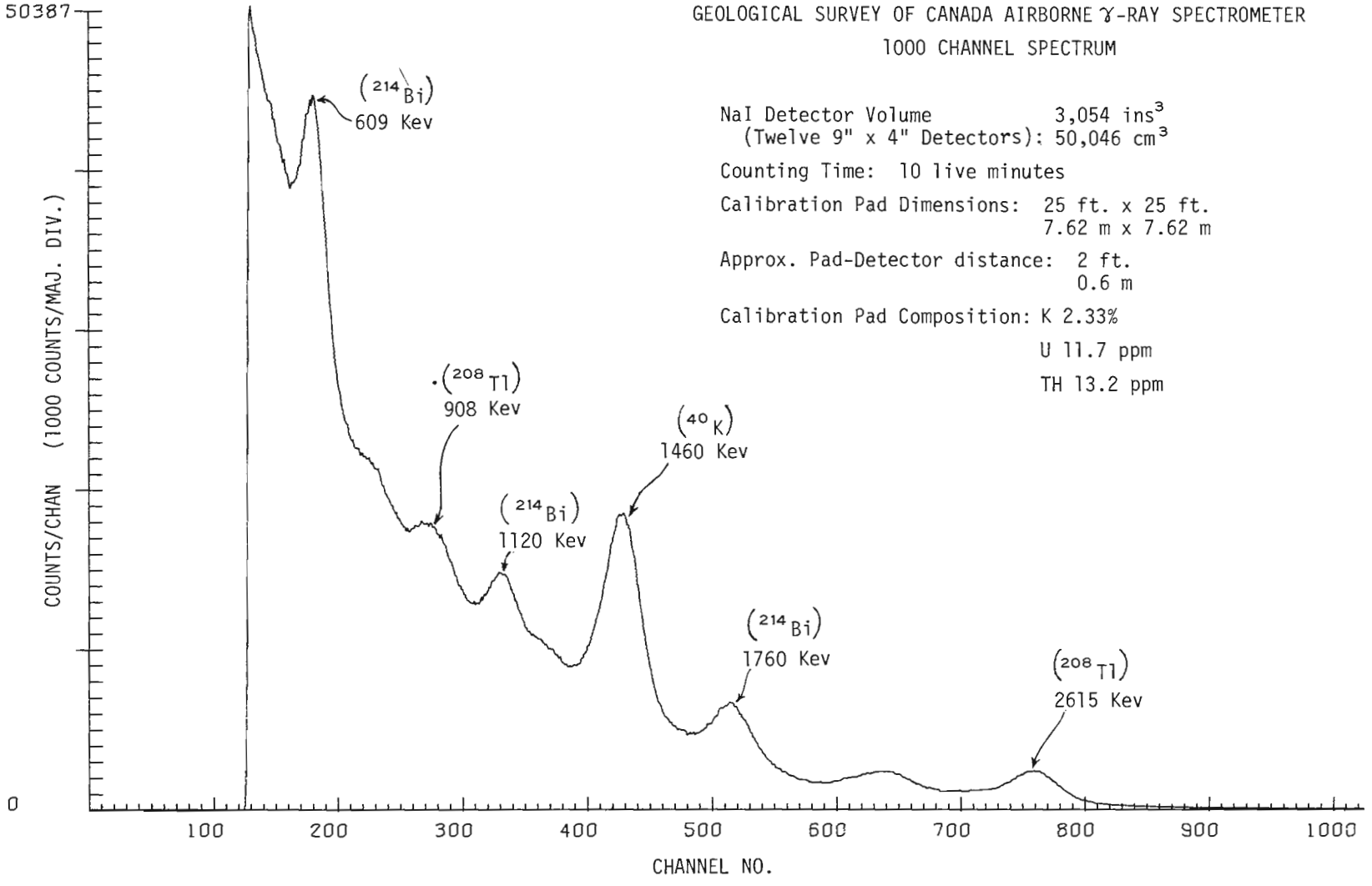
GEOLOGICAL SURVEY OF CANADA AIRBORNE γ-RAY SPECTROMETER
1000 CHANNEL SPECTRUM
NaI Detector Volume 3,054 ins³
(Twelve 9" x 4" Detectors): 50,046 cm³
Counting Time: 10 live minutes
Calibration Pad Dimensions: 25 ft. x 25 ft.
7.62 m x 7.62 m
Approx. Pad-Detector distance: 2 ft.
0.6 m
Calibration Pad Composition: K 2.33%
U 11.7 ppm
TH 13.2 ppm
50387
0
COUNTS/CHAN (1000 COUNTS/MAJ. DIV.)
(214 Bi) 609 Kev
(208 Tl) 908 Kev
(214 Bi) 1120 Kev
(40 K) 1460 Kev
(214 Bi) 1760 Kev
(208 Tl) 2615 Kev
100
200
300
400
500
600
700
800
900
1000
CHANNEL NO.

Figure 35.2

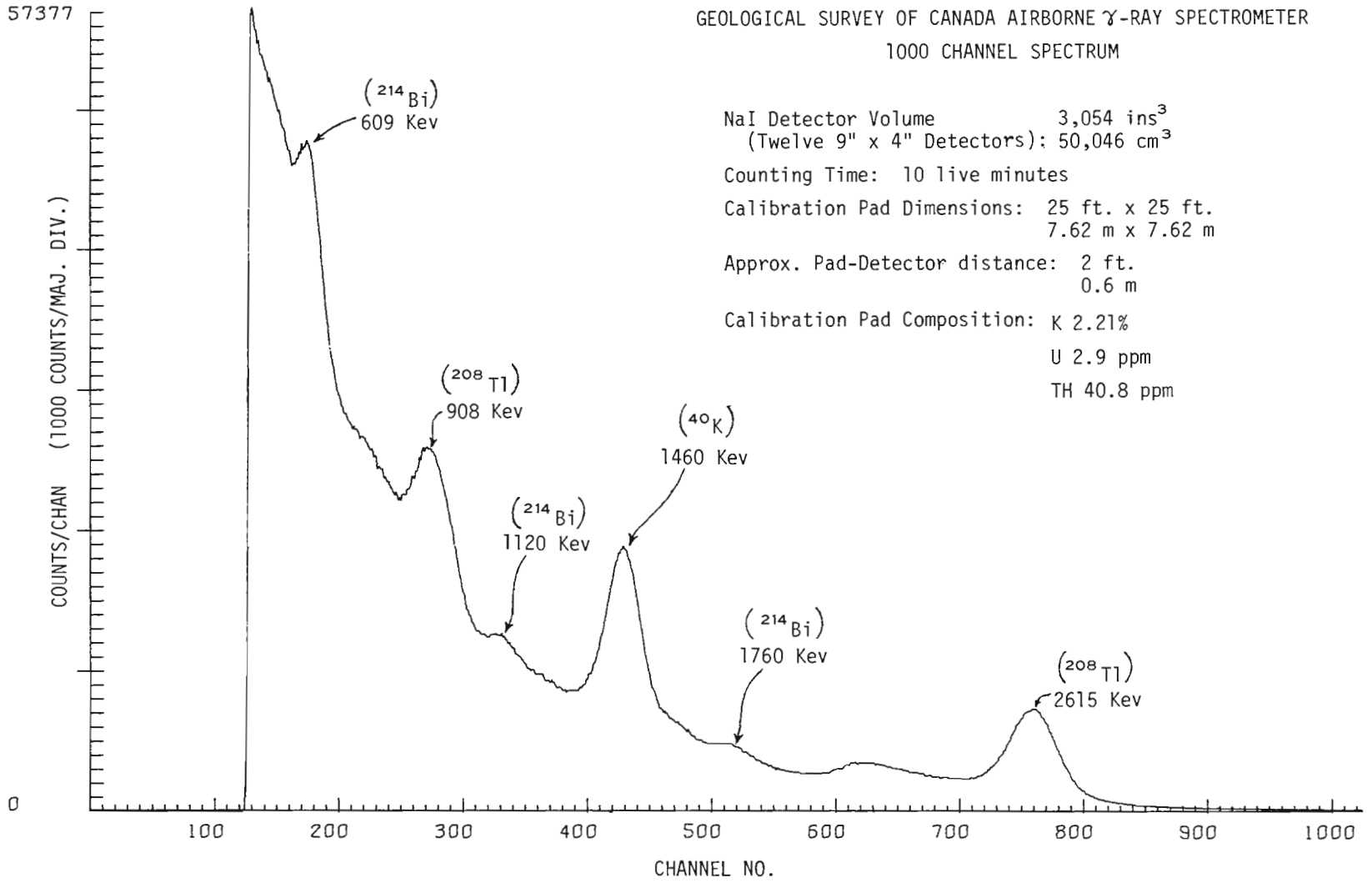
GEOLOGICAL SURVEY OF CANADA AIRBORNE γ-RAY SPECTROMETER
1000 CHANNEL SPECTRUM
NaI Detector Volume 3,054 ins³
(Twelve 9" x 4" Detectors): 50,046 cm³
Counting Time: 10 live minutes
Calibration Pad Dimensions: 25 ft. x 25 ft.
7.62 m x 7.62 m
Approx. Pad-Detector distance: 2 ft.
0.6 m
Calibration Pad Composition: K 2.21%
U 2.9 ppm
TH 40.8 ppm
57377
0
COUNTS/CHAN (1000 COUNTS/MAJ. DIV.)
(214 Bi) 609 Kev
(208 Tl) 908 Kev
(214 Bi) 1120 Kev
(40 K) 1460 Kev
(214 Bi) 1760 Kev
(208 Tl) 2615 Kev
100
200
300
400
500
600
700
800
900
1000
CHANNEL NO.

Figure 35.3

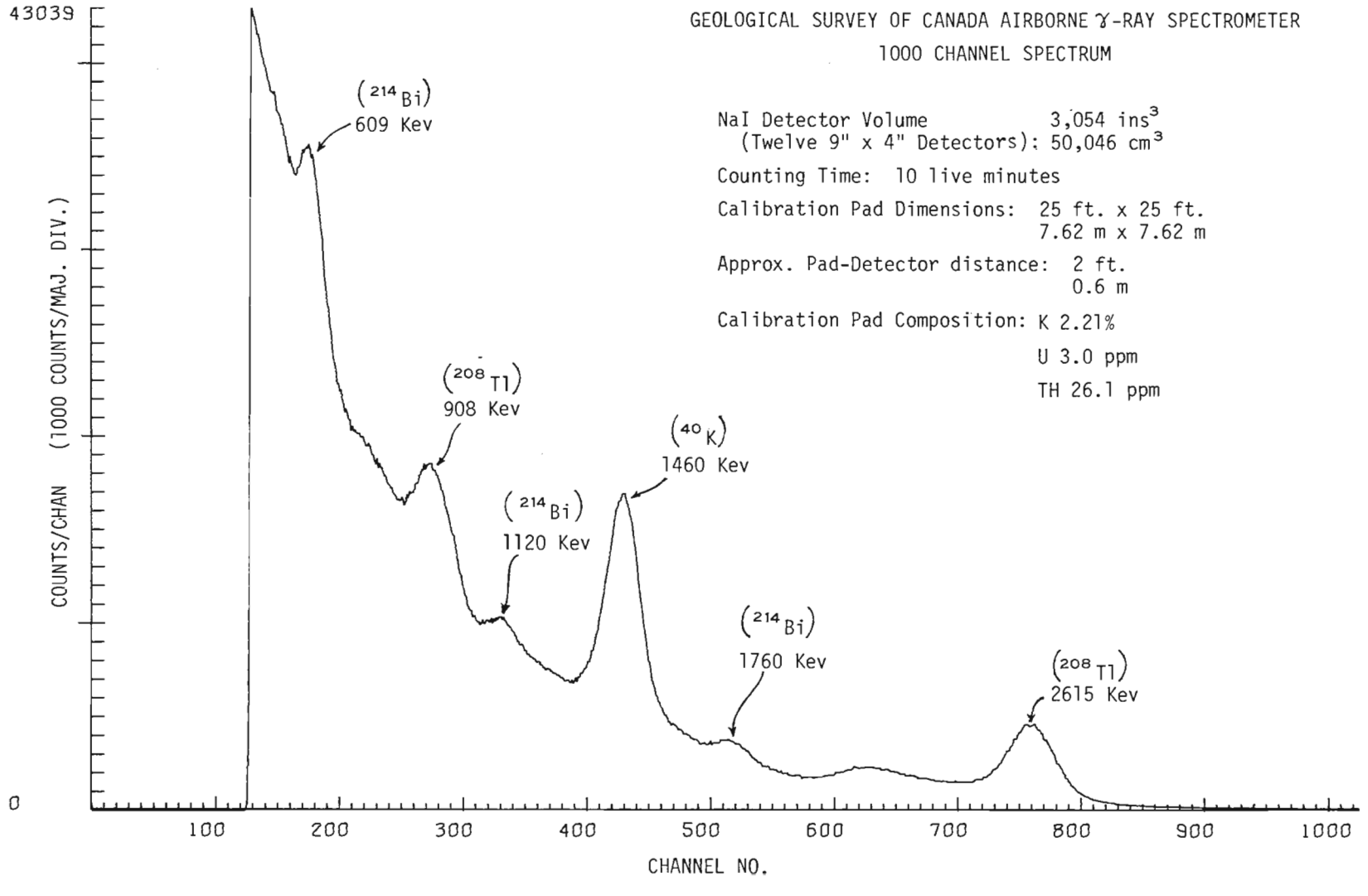
GEOLOGICAL SURVEY OF CANADA AIRBORNE γ-RAY SPECTROMETER
1000 CHANNEL SPECTRUM
NaI Detector Volume 3,054 ins³
(Twelve 9" x 4" Detectors): 50,046 cm³
Counting Time: 10 live minutes
Calibration Pad Dimensions: 25 ft. x 25 ft.
7.62 m x 7.62 m
Approx. Pad-Detector distance: 2 ft.
0.6 m
Calibration Pad Composition: K 2.21%
U 3.0 ppm
TH 26.1 ppm
(214 Bi) 609 Kev
(208 Tl) 908 Kev
(214 Bi) 1120 Kev
(40 K) 1460 Kev
(214 Bi) 1760 Kev
(208 Tl) 2615 Kev
43039
0
COUNTS/CHAN (1000 COUNTS/MAJ. DIV.)
100
200
300
400
500
600
700
800
900
1000
CHANNEL NO.

Figure 35.4

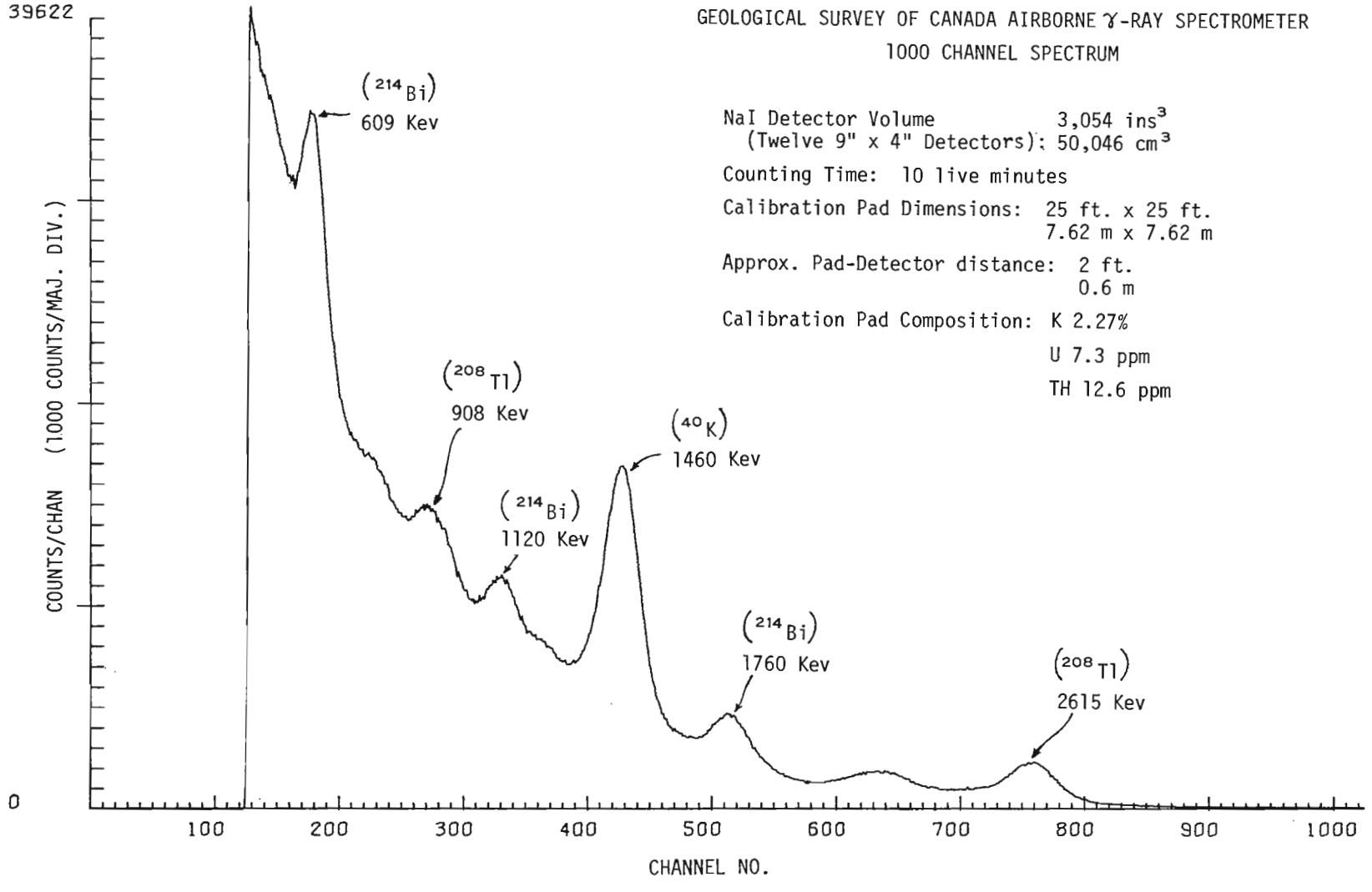
GEOLOGICAL SURVEY OF CANADA AIRBORNE γ-RAY SPECTROMETER
1000 CHANNEL SPECTRUM
NaI Detector Volume 3,054 ins³
(Twelve 9" x 4" Detectors): 50,046 cm³
Counting Time: 10 live minutes
Calibration Pad Dimensions: 25 ft. x 25 ft.
7.62 m x 7.62 m
Approx. Pad-Detector distance: 2 ft.
0.6 m
Calibration Pad Composition: K 2.27%
U 7.3 ppm
TH 12.6 ppm
39622
0
COUNTS/CHAN (1000 COUNTS/MAJ. DIV.)
(214 Bi) 609 Kev
(208 Tl) 908 Kev
(214 Bi) 1120 Kev
(40 K) 1460 Kev
(214 Bi) 1760 Kev
(208 Tl) 2615 Kev
100
200
300
400
500
600
700
800
900
1000
CHANNEL NO.

Figure 35.5

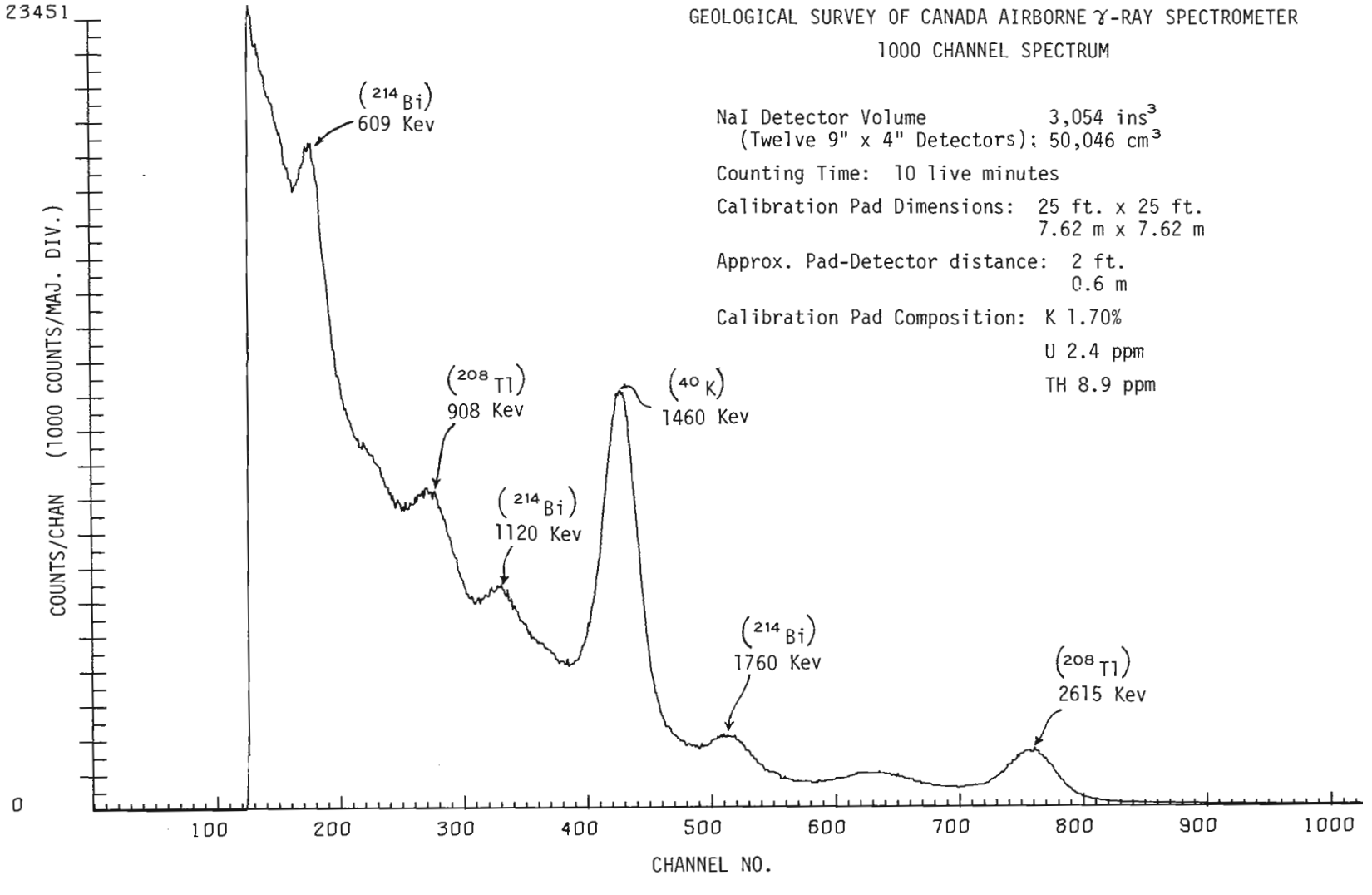
GEOLOGICAL SURVEY OF CANADA AIRBORNE γ-RAY SPECTROMETER
1000 CHANNEL SPECTRUM
NaI Detector Volume 3,054 ins³
(Twelve 9" x 4" Detectors): 50,046 cm³
Counting Time: 10 live minutes
Calibration Pad Dimensions: 25 ft. x 25 ft.
7.62 m x 7.62 m
Approx. Pad-Detector distance: 2 ft.
0.6 m
Calibration Pad Composition: K 1.70%
U 2.4 ppm
TH 8.9 ppm
(214 Bi) 609 Kev
(208 Tl) 908 Kev
(214 Bi) 1120 Kev
(40 K) 1460 Kev
(214 Bi) 1760 Kev
(208 Tl) 2615 Kev
23451
0
COUNTS/CHAN (1000 COUNTS/MAJ. DIV.)
100
200
300
400
500
600
700
800
900
1000
CHANNEL NO.

standard T.I. 960A 16 I/O module plugged into C.R.U. slot F60. An elementary 8 bit D/A converter connected to the same module provides a spectrum display capability using any laboratory oscilloscope.

Program features are as follows: -

- Single keyboard character for each command
- Live counting times specified by keyboard entry
- Automatic print out of peak channels and energies following end of counting time
- Continuous cycling feature allows for repeated acquisition and peak channel print out of spectrum from same source for long term stability checks
- Automatic display of spectrum concerned following execution of any command
- Provision for display of any portion of a spectrum specified by keyboard entry
- Provision for storage and manipulation of 5 spectra
- Calibration of system by keyboard entry of one peak channel and corresponding energy
- Computation and print out of per cent resolution of any peak specified by keyboard entry
- Addition and subtraction of stored spectra as specified by keyboard entry
- Generation of error messages if channel overflow occurs during counting or spectrum addition
- Listing of channel contents between specified limits
- Integration of counts between specified channels or energies
- Provision for recording spectra with descriptive title on 733ASR cassette tape in ASCII
- Provision for reading back recorded spectra into memory blocks specified by keyboard entry
- Automatic generation of artificial spectrum with triangular peaks on command from keyboard, for checking program function and calibrating display

Program Length

X '2A37' Hexadecimal, 10 807 decimal locations

T.I. Hardware Prerequisites

- 960A or 960B C.P.U. with 12 K memory
- Silent 700 data terminal with at least one cassette transport and remote device with 1200 baud option connected to C.R.U. slot F00
- 16 I/O module in C.R.U. slot F60 (*see* section on interfacing for further details)
- Real time clock module in C.R.U. slot F30
- ± 15 V regulator board

Software Prerequisites

- Bootstrap loader; nothing else required

Program Command Summary

There are twelve commands consisting of single character keyboard entries identified as follows:

C Initiate counting into one of five 1024 channel data blocks for a specified live time

E Calibrate system in terms of Kev/channel using a peak of known energy in a known channel

F Find and list the peak channel numbers and the corresponding energies in Kev.

R Print out the resolution in % (F.W.H.M.) of a peak in a specified data block and channel number

D Display the spectrum in a specified block between specified channels

L List channel contents in a specified block between specified channels

I Integrate channel contents in a specified block between specified channels or energy limits

S Subtract spectrum stored in one data block from that stored in a second and deposit the difference in a third

A Add a spectrum in one data block to that stored in a second data block

T Record a spectrum from a specified data block with a descriptive title on cassette tape in ASCII

P Read a spectrum from cassette tape into a specified data block

G Generate the artificial spectrum for program function verification and display calibration

36. A BURIED BEDROCK CHANNEL OUTLINED BY THE SEISMIC METHOD NEAR BEAUCEVILLE, QUEBEC, 21 L/2 EAST HALF

Project 630434

G. D. Hobson[1]
Resource Geophysics and Geochemistry Division

Introduction

A seismic survey was conducted to demonstrate the feasibility of locating and outlining, by the hammer seismic refraction technique, bedrock channels buried under loose sediments in the Beauceville, Quebec area. The Beauceville project is only one such project undertaken in recent years to demonstrate the versatility of the seismic method in similar problems. In this project area, one geologic section had been established by diamond drilling by a mining company and a buried channel system had been suggested from airphoto interpretation. The objective of the study was to determine (1) the probability of locating and outlining buried preglacial channels, (2) the profiles of the channels, and (3) the types of loose sediments which fill them.

Location of Area and Profiles

The survey was carried out in the Beauceville map-area (21 L/2 east half), in the Rigaud-Vaudreuil seigniory. The area lies within the Chaudière basin and on the east side of the Chaudière River which rises at the International Boundary (near the State of Maine) and enters the St. Lawrence River at Quebec City. Beauceville is about 60 miles southeast of Quebec City, and is the principal town near the project area (Fig. 36.1). One traverse was run across Bolduc stream to the northeast of the village of Rivière Gilbert, nine traverses in the area of St.-Simon-les-Mines and the Gilbert River, five in the area of Cumberland Mills, and three traverses across the Famine and Abenakis rivers.

History of Mining in the Area

Chalmers (1897), Tyrrell (1915), and MacKay (1921) have given the most complete descriptions of mining operations in this area. Chalmer's description is most detailed. The first indication of placer gold in this area was in 1823 or 1824 when a woman first discovered gold in the Chaudière Valley near the mouth of the Gilbert River. In 1847, the Chaudière Mining Co. mined gold on the Gilbert and Des Plantes rivers having leased the mining rights from the de Lery family. Very little scientific mining was done in the early days; shafts were dug by hand to mine deposits. The attempts made to mine the gravels met with varying degrees of success. The first mining operations were confined to shallow placers but as these deposits became exhausted the gold was followed upstream where the mining of shallow placers led directly to the deeper and richer gravels lying on bedrock. Although the origin of the gold has never been determined it is known that it has not been carried any great distance. In total, to the end of the century, about $2 000 000 worth of gold had been extracted from the gravels of the Gilbert River Valley.

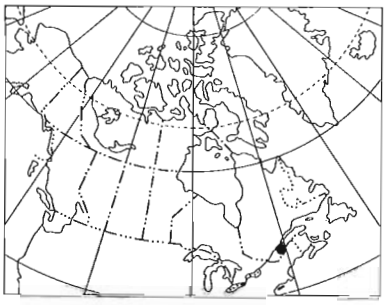

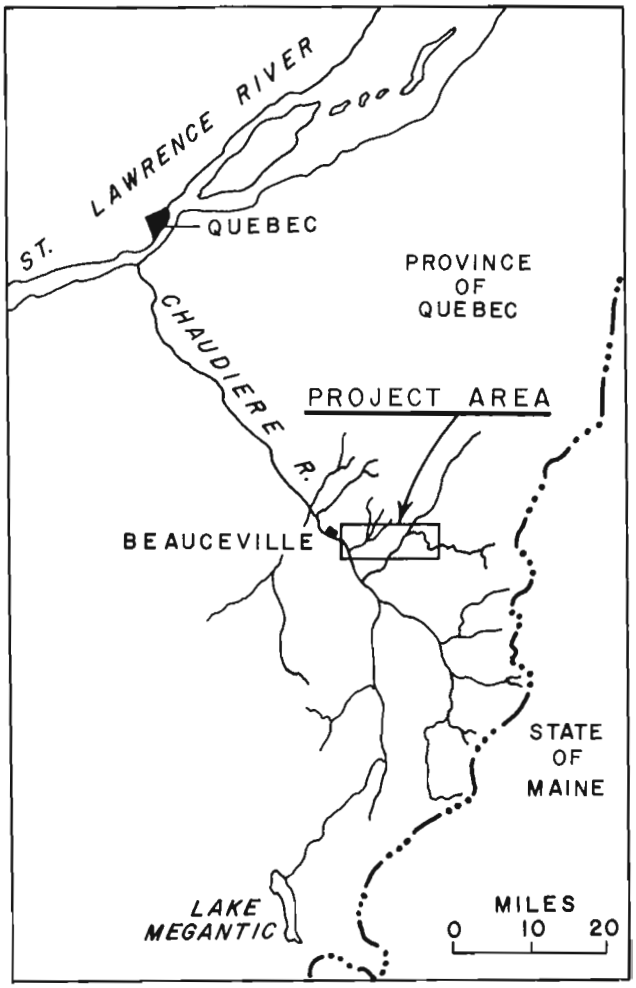

Figure 36.1. Project location map.

[1]Polar Continental Shelf Project

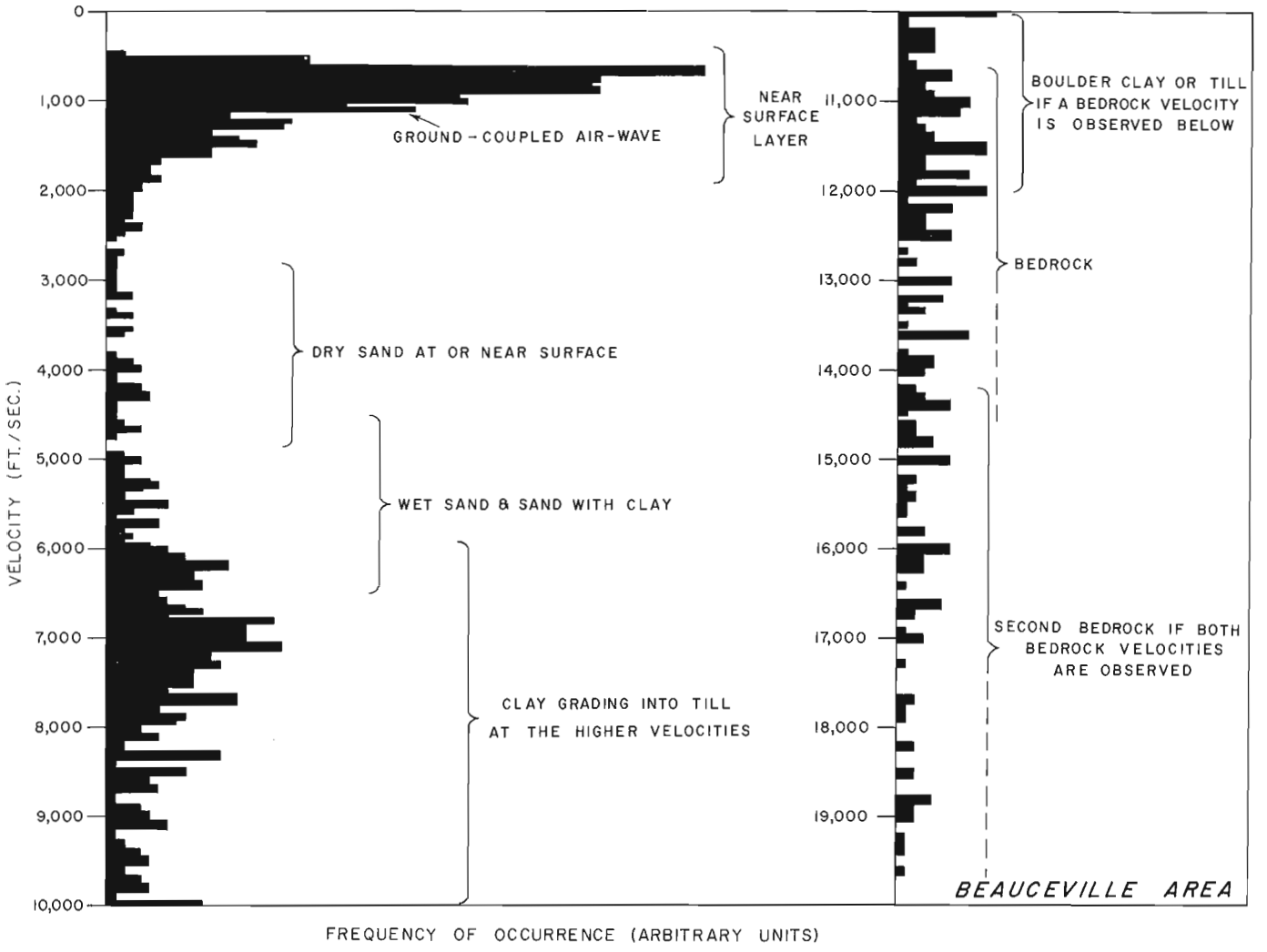

Figure 36. 2. Histogram of observed seismic velocity versus frequency of occurrence, Beauceville, Quebec.

Mining operations almost ceased from about 1886 until about 1910 when hydraulic type operations were undertaken on Meule Creek. This lasted for only 2 years. The most important streams in the area for placer gold have been the Gilbert River, Rivière du Loup, Meule Creek, Rivière des Plantes, and the Famine River. The Gilbert River has been the most important of these.

Very little gold has been taken out of the creeks and rivers since the turn of the century. Some old prospectors have eked out a living by panning the stream gravels but nothing on a commercial scale had been undertaken until 1962. In that year Beauce Placer Mining Co. Ltd. moved a modern dredge into the Gilbert River and commenced operations. Due to operational difficulties this venture was shut down in the fall of 1962 and was not re-opened during 1963. During 1964, mechanical and operational changes were made in order to overcome the unusual clay handling problem. Mining operations by dredge were undertaken again in 1965.

Brief Description of Geology

Bedrock of the Beauceville area has been described in part by MacKay (1921) and was restudied during the summer of 1963 by the Quebec Department of Mines and Natural Resources. Gadd (1964) studied the Pleistocene geology and briefly reviewed the glacial history of the area.

The area lies wholly within the Appalachian Province and exhibits a topography characteristic of that physiographic province. Outcrops are of the Beauceville sediments (conglomerates, quartzites, and slates) and Beauceville volcanics (acid tuffs, rhyolite flows, and agglomerates), both of which MacKay (1921) identified as Ordovician in age. The Beauceville series is very closely folded and faulted so that, at times, it is very difficult to distinguish between sediments and volcanics. The Beauceville map-area, which is much more extensive than this project area, is covered by

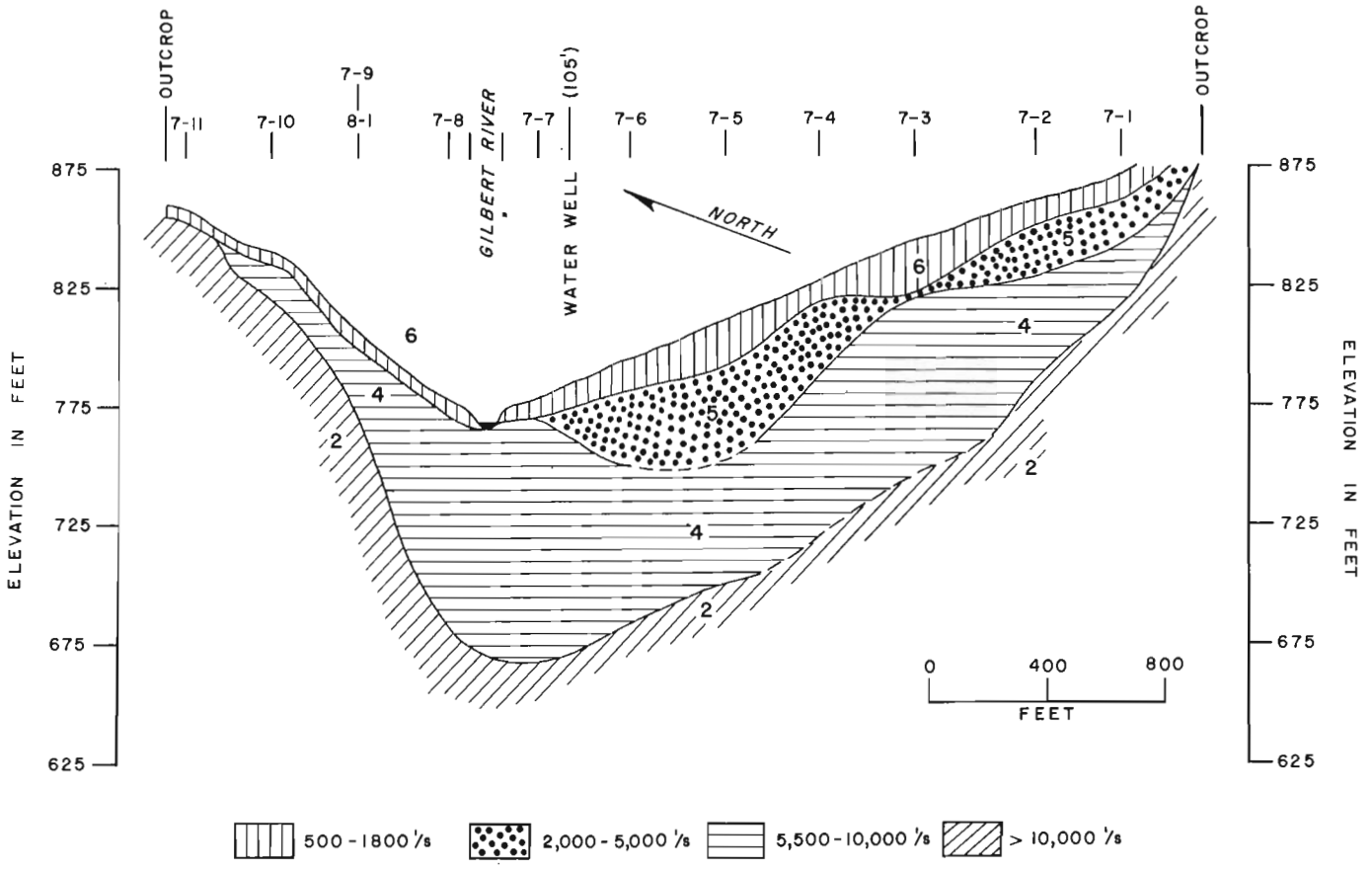

Figure 36. 3. A typical section from a seismic traverse, Beauceville, Quebec.

Precambrian to Devonian strata which at various times have been highly folded, faulted, and intruded by igneous rocks. Dips of the beds are seldom less than 60 degrees and strike is generally southwest-northeast. Therefore, bedrock ridges with considerable local relief generally strike perpendicular to the south-southeast movement of the Laurentide glaciers.

The development of the present topography took place in several successive stages. In the first place, several orogenic movements preceding and following the deposition of the Devonian sediments have elevated these Devonian beds and the underlying formations. The folding and faulting characteristic of definite movements in the Appalachian geosyncline took place during the Taconic and Acadian orogenies. In the second principal stage there has been peneplanation giving a plateau character to the high ground. The third stage is a general uplifting of the region and active erosion so that the plateau has become very dissected and reduced to the "valloneux" state or one of valleys and hills.

The region was glaciated at least twice (Gadd, 1964). Till of the earlier glaciation has been observed by Gadd and in all exposures observed it is dark grey or nearly black in colour, calcareous, very compact and hard, and lies immediately above bedrock. In general this till contains local rocks but may also contain numerous granite and granite gneiss boulders. A nonglacial episode is represented in the Pleistocene section by a relatively thick sequence of sands and gravels. In several places, these have been observed to rest on the till of the first glaciation and to be overlain by the younger till. In much of the area with which this survey is concerned the youngest sediment, river gravel, rests on all older sediments, but particularly on the bedrock. In summary the Pleistocene section is as follows: gravel in the bottom of the present streams in which some gold has been found, overlying a till or boulder clay which is the youngest in the region, overlying sands and gravels of the nonglacial period which may be up to 115 feet thick, overlying unassorted and unstratified boulder clay or till of the first glaciation which may be as much as 100 feet thick, overlying thin beds of stratified gravel which average from one to two and a half feet in thickness but in certain locations may attain fifteen feet, overlying bedrock.

In Beauce county, many of the preglacial channels have been preserved from the action of glacial ice because they were oriented at right angles to the movement of the glaciers. The Chaudière Valley itself was at right angles to the direction of glacial flow. Therefore, the bases of these channels have not been disturbed or washed so that the original channel materials are still in place. This explains why this area is interesting from an economic point of view. Placer gold deposits, if present, have been undisturbed by glaciation and it

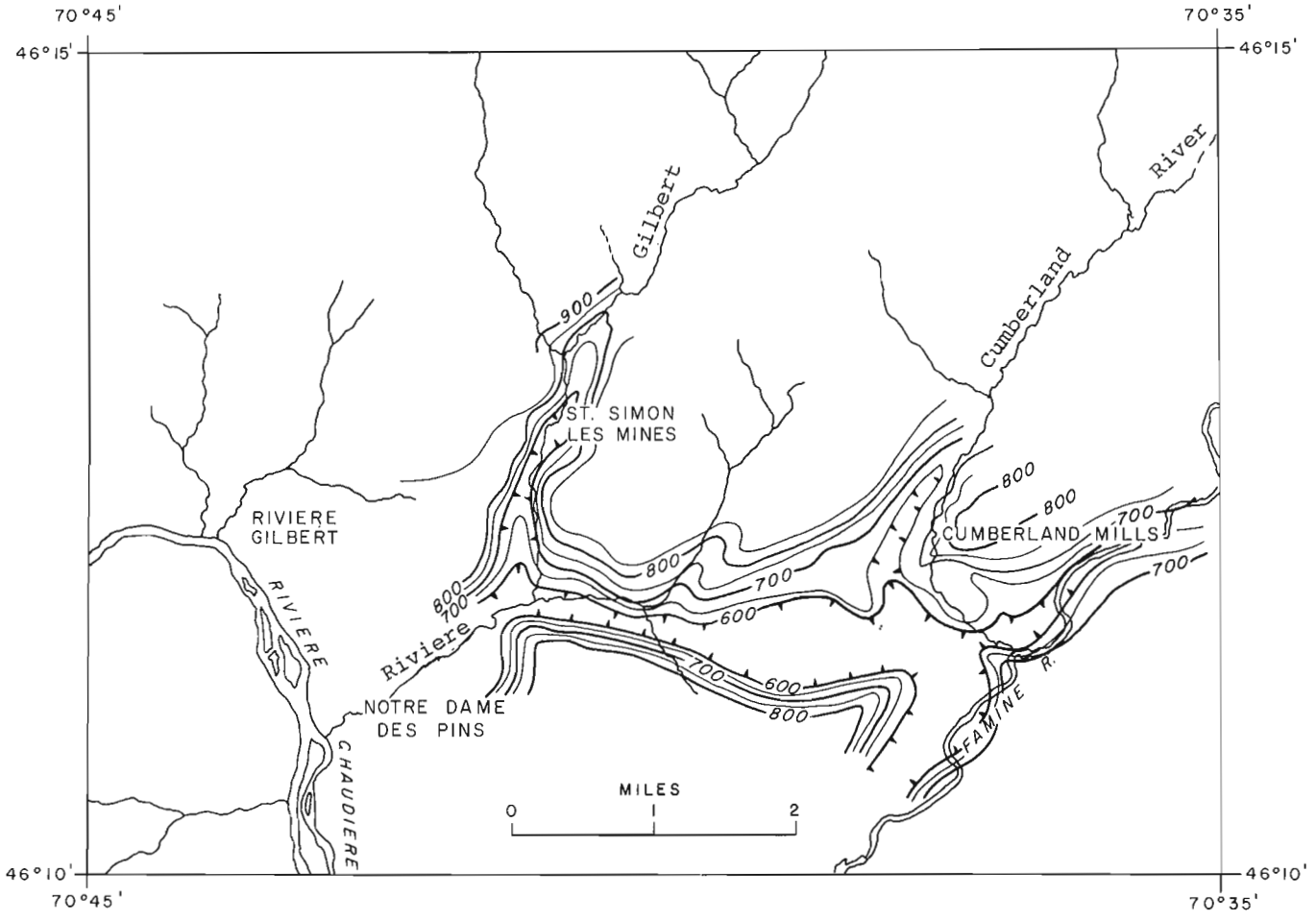

Figure 36.4. Topography of the buried bedrock channel against a sea level datum, Beauceville, Quebec.

is in the bedrock gravels that the concentrations of gold are to be found. The buried channels containing the placer golds are definitely preglacial.

Whether or not all the buried and potential gold-bearing gravel channels in the area have been discovered will not be discussed since the aim of the project was not to delineate the complete channel system but rather only to test the feasibility of the method. There may be other bedrock channels in the map-area that could be delineated.

Instrument and Field Procedure

A Model MD-1 hammer refraction seismograph was used to determine depths to bedrock. A 10-pound sledge hammer striking against an 8" by 8" by 1" steel plate resting on the ground was the energy source. No explosives were used.

Completely reversed profiles, that is data acquired in both directions over each profile, were surveyed along all traverses and in a continuous manner to yield sections in greater detail than is usually acquired.

Topography

The Beauceville map-area exhibits the general relief and mature topography characteristic of the Appalachian physiographic province. Maximum elevation in the surveyed area is about 1125 feet while the lowest elevation is 525 feet above sea level. There is an adequate network of good secondary roads permitting access to almost all parts of the area. Cross-country profiles can be surveyed readily since there is very little thick bush to impede progress. Although there may be considerable topographic relief over adjacent profiles, the relief on individual profiles does not present problems to the computation procedure.

Control Points

One water well drilled late in 1962 in a new housing subdivision within the survey area, and one other hole drilled as a water well, were the prime control points at the time of the survey. Also, several diamond-drill holes had been drilled by Beauce Placer Mining Co. Ltd. south of the Gilbert River and this line of boreholes was

Table 36. 1

A comparison of known and seismically computed depths to bedrock at selected locations in the survey area.

Location	Computed depth feet	Known depth feet	% Error
1-8	82	80	- 2.5
7-7	120	150	-12.5
15-2	93.1	132	+29.5
15-3	93.2	115	+19.1
15-4	69.0	77	+10.4
11-7	16.0	16	± 0.0

traversed. The accuracy attained during this project by comparing known and computed depths to bedrock is set out in Table 36. 1.

Seismic Velocities and their Relationship to Lithology

The velocity of seismic waves travelling through different materials varies appreciably and must not be considered to be unique but rather to vary between certain flexible limits which can be broadly defined. One method of defining these limits is to construct a histogram of observed velocity versus frequency of occurrence as in Figure 36. 2.

The overburden in the Beauceville area is heterogeneous in that there is little continuity of strata in the drift. Seismic velocities vary considerably over a single traverse to a point that disagreement or at least difficulties arise in the interpretation of data. Recent side-hill cuts in the overburden have exposed sections indicating a succession of sedimentary deposits varying appreciably in thickness and continuity. Furthermore, the periods of glaciation have left obvious traces in the form of immense erratic boulders on surface and in the near-surface materials. It is obvious to the geophysicist that the great size of some of these erratics will affect subsurface seismic velocities.

The average thickness of the surficial aerated or weathered zone over the entire project area is 7. 1 feet which is relatively thin compared with other areas in Canada.

Bedrock is very altered at the contact with the overburden and the amount of this penetration of weathering into the bedrock is not known. An error, one of the principal errors in the application of the seismic method in the Beauceville area, is introduced since the path of the refracted wave within the bedrock is not known. It is known, however, that this path is within the bedrock and not at the drift-bedrock interface because the weathered bedrock layer probably exhibits a seismic velocity comparable to that of the lower clay and boulder clay horizons. Secondly, since the sedimentary formations of the Appalachian geosyncline have been strongly folded and faulted and now dip between 45° and 85° over a horizontal distance of one half or one mile, a seismic wave may penetrate several formations of different lithology and therefore different physical properties. Because of this considerable dip and because these same formations have been cut again by dykes and other small lava intrusions varying from acidic to basic, it is inconceivable that there should be any consistent and well-defined seismic velocity within the bedrock. This is clearly indicated by the broad spread of bedrock velocities on the histogram of Figure 36. 2 with no definite peak or peaks of velocities.

The correlation between the various seismic velocities observed and the Pleistocene and bedrock lithology has been attempted from a consideration of the seismic histogram, the actual drillhole logs acquired from Beauce Placer Mining Co. Ltd. and local water well information. The decision to set out interfaces and label subsurface materials has been complicated in this area by the heterogeneity of the overburden rather than by poor data. The overlapping of velocity ranges representative of the various Pleistocene and bedrock materials is well displayed in the histogram. Figure 36. 3 is a typical section from a seismic traverse setting out surface and subsurface topography and the definition of subsurface materials based upon the velocity of seismic waves through the various media.

The Bedrock Channel System

Fourteen of the 20 traverses surveyed indicate or confirm the suspected existence of a buried bedrock channel. The bedrock channel system is shown in Figure 36. 4 setting out the topography of the bedrock surface using a sea level datum. There appears to be one principal east-west channel with a side-channel beneath the present course of the Gilbert River through St. -Simon-les-Mines and other side-channel immediately west of Cumberland Mills partially underlying the present Cumberland River. The main depression does not appear to correlate with any present day drainage pattern except on the eastern limits of the project where the Famine River channel may be controlled by subsurface topography. The western limits of the bedrock channel are poorly defined; however, seismic traverses seem to indicate that the channel system does not extend in that direction. This would indicate therefore that the depression possibly terminates in the Chaudière River Valley near Notre-Dame-des-Pins and confirmation of this, if desirable, could readily be obtained by a line of control on the secondary road about one mile east of that settlement. The traverse across the Plantes River also reveals the existence of a buried channel. This channel has advantages over the system of St. -Simon-les-Mines in that it is not as deep and there is an almost total absence of erratic boulders. These conditions would permit easier extraction of any placer deposits using floating dredge equipment. The direction of flow of water in the preglacial channel is difficult to determine from the data available. Figure 36. 4 clearly indicates that both side-channels poured their waters into the main channel but the data do not clearly determine whether water in this channel system then flowed

westward or eastward. The normal conclusion is that it flowed westward into the Chaudière River Valley but some interesting implications might be made if an easterly flow was indicated. To the author's knowledge, the general direction of water movement prior to glaciation has not been determined for this region.

Aquifers

From a study of the individual traverses, it is obvious that there is no scarcity of locations under which water might be found. There are good possibilities of locating water under those locations at which a second velocity has been observed in the range of 3500 to 5500 feet per second, or in low-velocity sand or clay materials infilling a depression in the bedrock. Many possibilities may be outlined and it need not be pointed out that the entire east-west main channel (Fig. 36.4), is a potential aquifer of immense proportions.

Conclusions

1. A preglacial drainage system can be outlined using the seismic method and portable hammer seismic refraction instrumentation.
2. The profiles obtained, some verified by geological data and drillhole control, have revealed the presence or absence of bedrock channels as prognosticated from geomorphological studies.
3. Seismic velocities can be correlated with lithology in the Beauceville area to permit a distinction between Pleistocene materials and to determine depth to bedrock. Time-distance graphs used to compute strata thicknesses are good to excellent in quality.
4. Areas that may provide supplies of water for household and light industrial needs can be outlined by an interpretation of seismic velocities.
5. Accuracy of depth determinations by the seismic refraction method in this area is probably about 10 per cent and the error will be in the shallow direction.
6. One main bedrock depression with two side features form a bedrock channel system the extremities of which are undefined by this survey.
7. In some areas, two bedrock horizons can be observed pointing up the complexity of the underlying bedrock strata. Bedrock lithology cannot be correlated with seismic velocities because of such complexity.
8. The presence of immense erratic boulders on the surface and throughout the overburden makes the interpretation of data more difficult but does not present an insurmountable barrier.

References

Chalmers, R.
1897: Report on the surface geology and auriferous deposits of southeastern Quebec; Geol. Surv. Can., Ann. Rept., v. 10, pt. J.

Gadd, N.R.
1964: Surficial geology, Beauceville map-area, Quebec (21 L/2); Geol. Surv. Can., Paper 64-12.

MacKay, B.R.
1921: Beauceville map-area, Quebec; Geol. Surv. Can., Mem. 127.

Tyrrell, J.B.
1915: Gold-bearing gravels of Beauce County, Quebec; Trans. Am. Inst. Min. Eng., v. 51, p. 672-683.

Project 670074

G. D. Hobson[1] and R. M. Gagne
Resource Geophysics and Geochemistry Division

A seismic refraction survey consisting of 1909 single-ended profiles was conducted in the eastern portion of the Niagara Peninsula from the Welland Canal to the Niagara River and from Lake Erie to Lake Ontario (Fig. 37.1). The project was designed to complement the studies associated with the development of the new Welland Canal, and to complete the mapping of the bedrock topography of the area.

Figure 37.2 is a histogram of the observed seismic velocities versus the frequency of occurrence for all locations surveyed. In general, the histogram shows three major velocity groupings, which may be correlated with three layers: these are, a thin surface layer, a more compacted layer of gravels and clay, and bedrock which is identified with a velocity in excess of 10 000 feet per second or 3000 metres per second.

A typical cross-section from seismic data is shown in Figure 37.3 with an interpretation of the surficial materials. Intermediate velocities were not recorded at all locations. Drilling of bore holes in the area disclosed two distinctive till layers in part of the area; these two till layers are not defined clearly on the histogram of Figure 37.2.

Figures 37.4, 37.5 show generalized contours on the bedrock surface of the study area based upon seismic and borehole data. The necessity for different contour intervals on these two maps has been dictated by the fact that a 20-foot-interval is too tight for the scale of the northern map, Figure 37.5.

The general tightening of the contour interval between 540 and 600 feet a.s.l. in the southern half of Figure 37.4 may be interpreted as a north-facing scarp formed by subcropping of the resistant Devonian Oriskany sandstone.

The generally high ridge across the southern half of this figure, i.e. elevations above 600 feet a.s.l., may also be outliers of this same formation. The considerable relief shown on the bedrock surface between Welland and Port Colborne (west side of Fig. 37.4) is explained by the fact that this area was originally contoured on 1:25 000 scale as a contribution to Owen, 1972.

The general east-west strike of the bedrock topography contours of Figures 37.4, 37.5 is in complete agreement with the strike of the geological formations comprising the bedrock.

The buried St. Davids Gorge set out by Hobson and Terasmae (1969) is not readily discernible in Figure 37.5; the generalized contour interval does not permit the clear definition of that previously outlined prominent bedrock feature. There is, however, a very definite bedrock depression indicated south and east of the city of St. Catharines extending into Lake Ontario. The

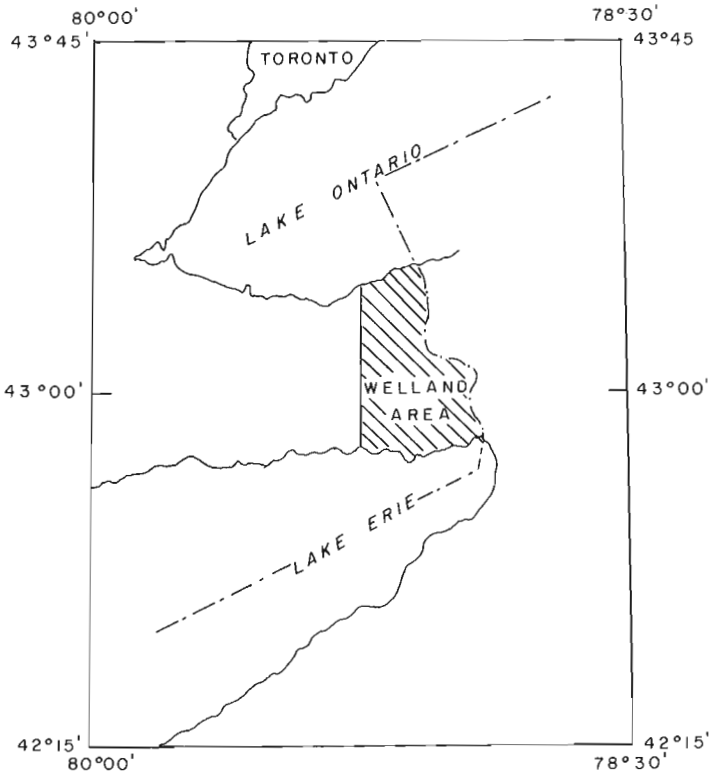

Figure 37.1. Location map, eastern Niagara Peninsula, Ontario.

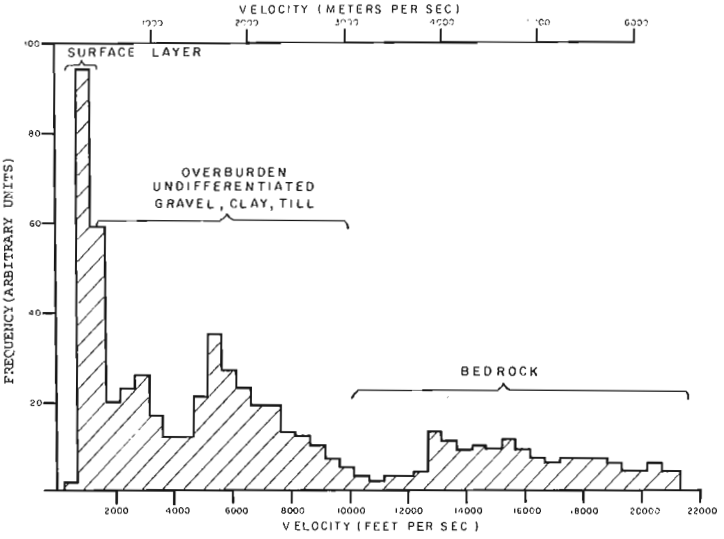

Figure 37.2. Histogram of observed seismic velocity versus frequency of occurrence, eastern Niagara Peninsula, Ontario.

[1]Polar Continental Shelf Project

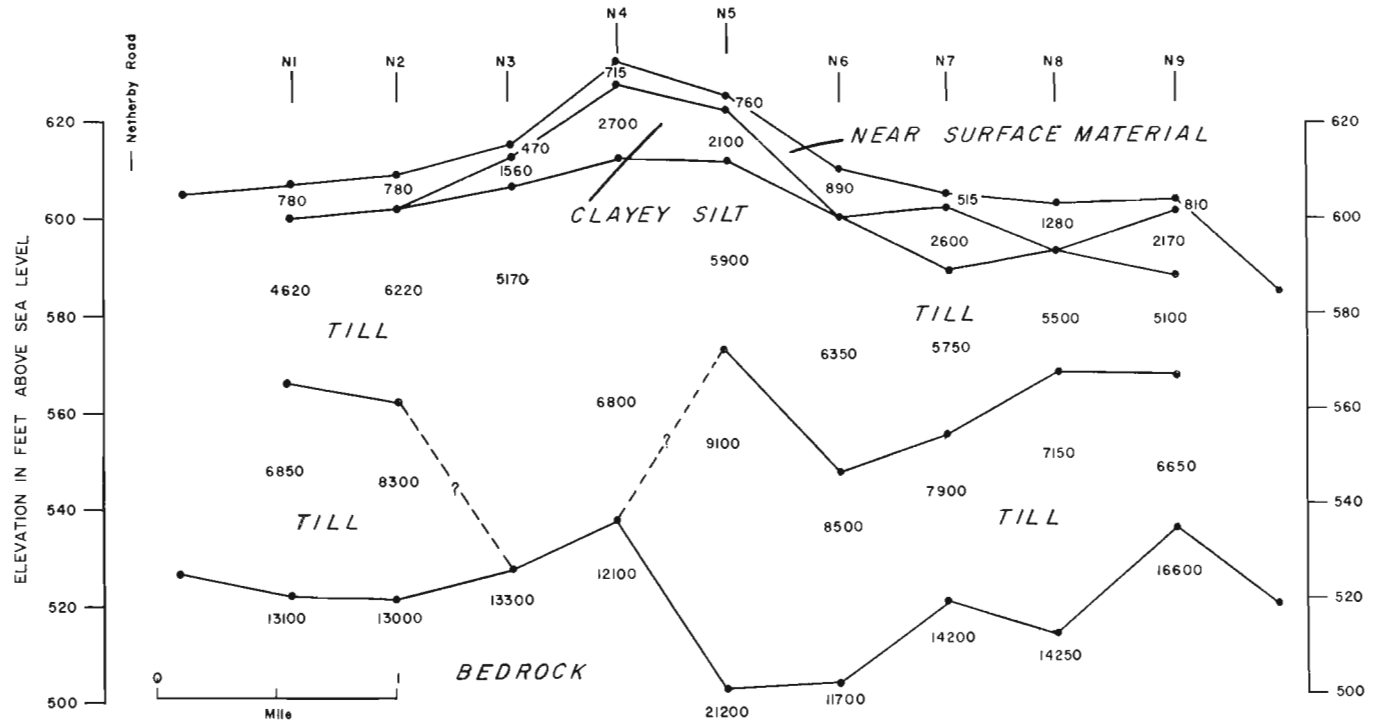

Figure 37. 3. A typical seismic cross-section, along railroad relocation at Welland, Ontario.

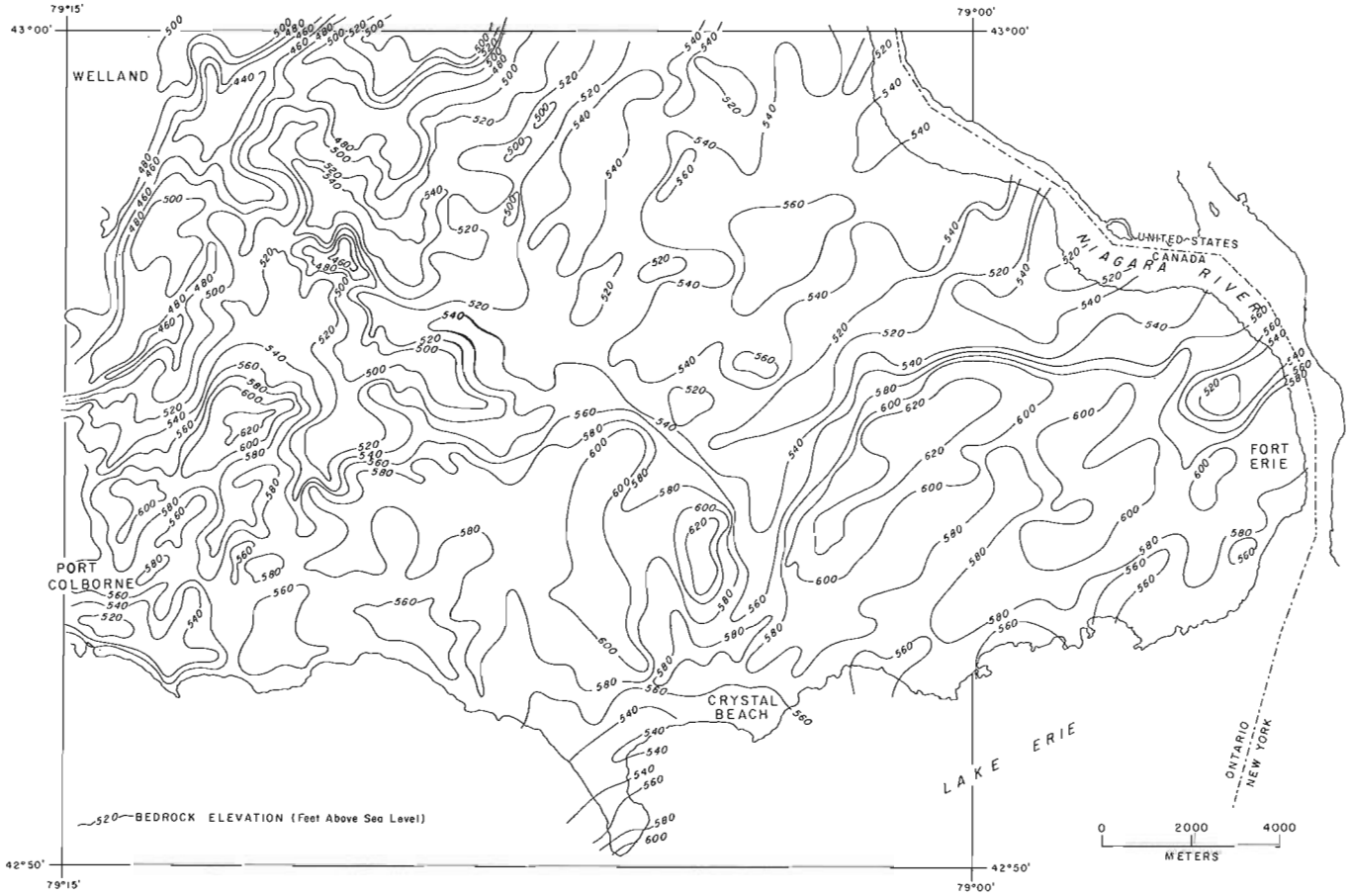

Figure 37. 4. Bedrock topography with reference to sea level datum, contour interval 20 feet, southern half of eastern Niagara Peninsula, Ontario.

Figure 37.5

Bedrock topography with reference to sea level datum, contour interval 50 feet, northern half of eastern Niagara Peninsula, Ontario.

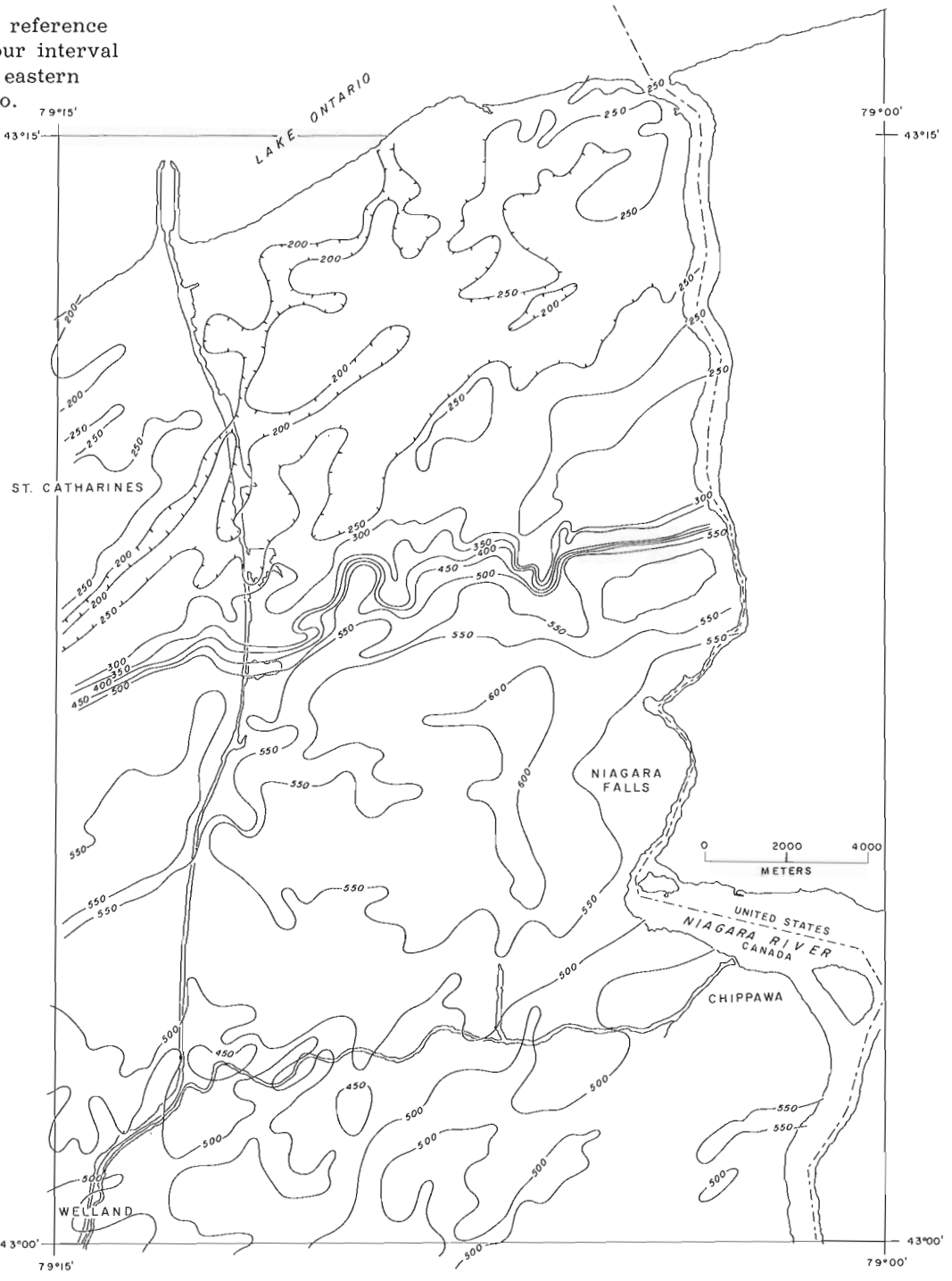

Niagara escarpment is very evident on Figure 37.4 as would be expected.

All seismic and well data have been located on U.T.M. grid, coded and placed on computer cards and is available in that format upon request to the Director General, Geological Survey of Canada.

References

Hobson, George D. and Terasmae, J.
1969: Pleistocene geology of the buried St. Davids Gorge, Niagara Falls, Ontario: Geophysical and Palynological studies; Geol. Surv. Can., Paper 68-67.

Owen, E.B.
1972: Geology and engineering description of the soils in the Welland-Port Colborne area, Ontario; Geol. Surv. Can., Paper 71-49.

SELENIUM IN SULPHIDES FROM SOME CANADIAN BASE METAL DEPOSITS

Projects 730043 and 740107

I. R. Jonasson[1] and D. F. Sangster[2]

This report forms part of a series to be presented on trace metal levels found in sulphides from Canadian ore deposits and occurrences.

A more complete report is available for Hg (Jonasson and Sangster, 1974) and this summary for Se continues the release of data for such trace elements of interest

Table 38.1

Selenium in sulphides from some Canadian base metal deposits

VOLCANOGENIC TYPES	AGE	SPHALERITE	CHALCOPYRITE	PYRITE	GALENA
Hackett River	Archean	20(3)	-	37(3)	-
High Lake	Archean	144(1)	159(3)	-	-
Mattabi	Archean	17(1)	-	-	-
Kidd Creek	Archean	205(2)	-	-	-
Normetal*	Archean	42(8)	232(8)	-	-
Lac Dufault*	Archean	108(5)	339(5)	-	-
Coniagas*	Archean	2(1)	-	-	11(2)
Manitou-Barvue*	Archean	22(5)	380(4)	-	68(5)
Mattagami Lake*	Archean	201(8)	537(8)	-	-
Orchan*	Archean	116(5)	345(5)	-	-
Poirier*	Archean	-	436(4)	-	-
West Macdonald	Archean	0(1)	-	-	-
Horne*	Archean	-	260(6)	-	-
Joutel*	Archean	-	412(4)	-	-
Tetrault	Proterozoic	44(2)	-	-	-
New Calumet	Proterozoic	25(2)	-	-	-
Flin Flon*	Proterozoic	152(1)	240(2)	133(2)	-
Fox Lake*	Proterozoic	323(1)	321(2)	198(1)	-
Errington	Proterozoic	13(2)	-	-	-
Snow Lake*	Proterozoic	-	198(1)	-	-
Eustis*	Phanerozoic	-	140(1)	-	-
Western*	Phanerozoic	-	8(1)	-	-
PORPHYRY TYPES					
Granisle*	Phanerozoic	-	249(3)	-	-
Coast Copper*	Phanerozoic	-	125(4)	-	-
MAGMATIC TYPES					
Lynn Lake*	Archean	-	102(1)	128(2)	-
MISCELLANEOUS					
Icon Sullivan*	Proterozoic	-	48(8)	-	-
Opemiska*	Archean	-	69(5)	-	-
Campbell-Chibougamou*	Archean	-	64(9)	-	-
Patino*	Archean	-	62(5)	-	-

Notes:
1. *Samples are (monthly) composite mine concentrates; except pyrite.
2. All others are grab samples.
3. All values in ppm.
4. Numbers of samples analyzed, in parentheses.

[1]Resource Geophysics and Geochemistry Division

[2]Regional and Economic Geology Division

to resource geologists and environmental geologists alike.

Se was determined by a colorimetric method which utilizes the reagent, 3.3'-diamino-benzidine. Limit of detection for the procedure used was 1 ppm.

Table 38.1 contains data for 29 deposits, some defunct, some working and some as yet undeveloped. Some effort has been made to obtain mine concentrate composites which better reflect the true abundance of Se in a given deposit; otherwise carefully selected hand specimens have been separated into constituent sulphides and analyzed.

The data have been sorted by deposit type; most are derived from volcanogenic massive type Cu-Pb-Zn ores. Inspection suggests that Se is more abundant in chalcopyrite than in sphalerite in both grab samples and mine concentrates. At present there is insufficient information available for other constituent sulphides, particularly pyrite which is the most important sulphide discarded from the mined ores.

Reference

Jonasson, I.R. and Sangster, D.F.
1974: Variations in the mercury content of sphalerite from some Canadian sulphide deposits; *in* Geochemical Exploration-1974; Proc. 5th Internat. Symp. Geochem. Explor., Vancouver. Eds. Elliot, I.J., Fletcher, K., Publ. Elsevier, Amsterdam, p. 313-332.

39. FURTHER STUDIES OF HYDROGEOCHEMISTRY APPLIED TO MINERAL EXPLORATION IN THE NORTHERN CANADIAN SHIELD

Project 730009

E.M. Cameron and C.C. Durham
Resource Geophysics and Geochemistry Division

Introduction

In 1974 hydrogeochemical studies were carried out in eastern and northern parts of the Slave Province (Cameron and Lynch, 1975; Cameron and Ballantyne, 1975). The Slave Province has been a principal area used by the Geological Survey for the development of methods of lake sediment geochemical reconnaissance. In part, the hydrogeochemical studies were initiated to gain an understanding of the processes of secondary dispersion in this permafrost terrain. Such knowledge is essential for the proper interpretation of lake sediment data. In addition, these studies showed that hydrogeochemical sampling might be of value in its own right for mineral exploration or assessment in the region. While lake sediment surveys appear to be the method of choice for broad scale reconnaissance, lake water sampling has many advantages for more detailed programs (i.e., one sample per 2 square miles to four samples per square mile) such as that carried out by the exploration industry (Cameron and Ballantyne, 1975). The principal advantages result from the speed and relative simplicity of water sampling, preparation, and analysis, plus, in the northern Shield, the great abundance of lakes. This allows areas of 1000 square miles or more to be covered rapidly with the results, provided by field laboratories, being available within a day or so of sampling. Targets that are outlined by lake water anomalies can be more closely defined by analysis of spring or seep waters.

One of the principal objectives of the 1975 program was to test more efficient methods of water sampling using helicopters. Of equal importance was the testing of concepts and procedures on which hydrogeochemical sampling in the northern Shield is based. This includes seasonal changes in water chemistry; the choice of sampling interval; and the effects on trace element chemistry of filtering, acidification and storage of the water samples. One further objective was to refine the techniques and logistics of field laboratories set in the barren lands, in particular to reduce the weight and complexity of equipment which must be air transported.

The 1975 field program can be subdivided as follows:

1. Hydrogeochemical sampling for uranium over the Hornby Bay sandstones and the underlying rocks of the Wopmay Subprovince in the Lac Rouvière-McGregor Lake areas. This work is described elsewhere (Durham and Cameron, this publ., rept. 54).
2. Study of temporal variation in lake water chemistry in the Agricola Lake and Hackett River areas of the eastern Slave Province. The analytical work for this project is in progress.
3. A hydrogeochemical survey for Zn and Cu in a 1300 square mile area of the northern Slave Province (centred on High Lake). This area is being actively explored by mining companies for massive sulphide mineralization in Archean metavolcanic rocks. The preliminary results of this project are summarized in this report.

Sampling Apparatus

In 1974, lake water sampling was accomplished in simple fashion by the sampler leaning from the helicopter float, immersing a bottle in the water, and allowing it to fill. At that time it was felt that even a modest increase in sophistication would increase the sampling rate, with the additional benefit of easing the work of the sampler; perhaps even adding to the credibility of the technique. Since pH and, more obviously, temperature are subject to change if measurement is delayed, it was desirable to measure these parameters *in situ*, or as soon after sampling as possible.

The basis for the design was to collect a fairly large water sample as quickly as possible on the lake surface. Then, en route to the next site, some of the sample could be bottled for future analysis, while the remainder was used to measure pH, conductivity and temperature, before being dumped prior to the next landing.

A small, high capacity, immersible plastic pump connected to the helicopter power supply was fixed to the skid of the helicopter, just below the front portion of the float. In this position it draws water from a depth of approximately 20 cm and lifts it through plastic tubing into three plastic containers, each of 500 ml capacity, situated in the rear compartment of the Hughes 500 helicopter. The first container (right, Fig. 39.1) is used to fill a 500 ml plastic sample bottle, the second holds a pH electrode, and the third (left, Fig. 39.1) contains temperature and conductivity probes. The pump motor switching, the flushing, filling and draining of the three containers, and the labelling of the sample bottles are carried out by an operator in the rear compartment (Fig. 39.1). An electronic console in the front compartment of the helicopter provides digital readings of pH, conductivity, and temperature. A navigator sitting to the right of the pilot (Fig. 39.2) records these measurements and the locations of the sample sites. The sampling apparatus was constructed by Viking Helicopters Ltd. The electronic console was designed by Q. Bristow and built in the Geochemistry Section instrumentation laboratory by J.J. Parker.

Using the apparatus it was possible to collect at least 30 samples per hour, only 8 to 12 seconds being spent on the lake surface. Under these conditions sampling rates are determined by the speed, acceleration,

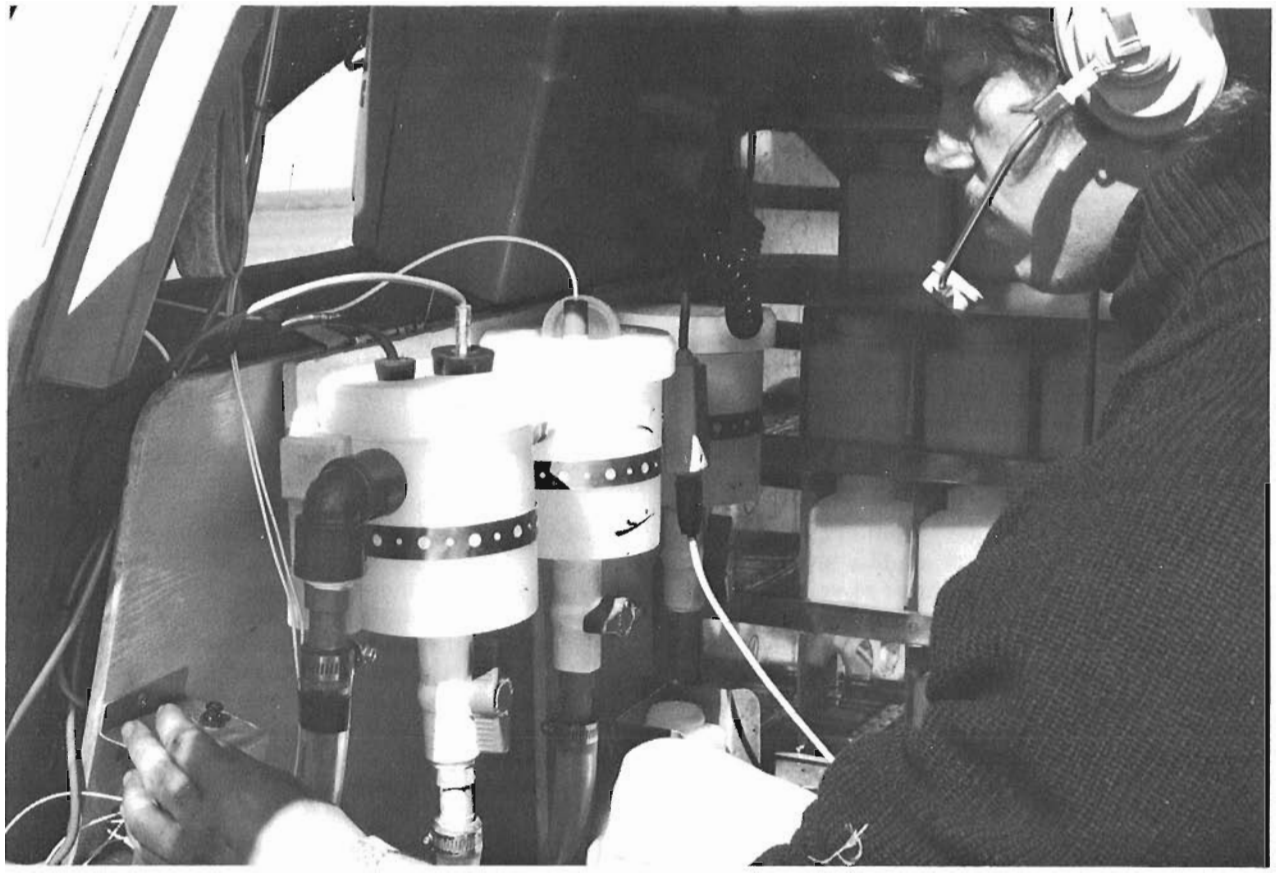

Figure 39. 1. Rear compartment of water sampling helicopter. The three plastic containers are (left to right): for temperature and conductivity measurement; for pH measurement; and for filling sample bottles. Operator's left hand is on pump motor switch. In background is a rack with capacity for up to 200 500 ml sample bottles.

and manoeuvreability of the helicopter and by the skill of the pilot, navigator and sampler. In most respects the small, turbine-powered Hughes 500 helicopter is an ideal aircraft for this work. Although "start-up" problems restricted the number of temperature and conductivity readings, satisfactory pH measurements were obtained throughout the summer.

To test possible sample to sample contamination by the apparatus a very highly anomalous lake was sampled (High Lake). This was immediately preceded by a sampling of a nearby lake with background contents of Zn and Cu and immediately followed by three successive landings and samplings of the same background lake. The chemical data from this test are shown in Table 39. 1. They indicate that contamination is satisfactorily low--in the range 1-3%.

Field Analysis

Water samples were analyzed in the field laboratory for Zn and Cu. The analytical method used was similar to that described for the 1974 program (Horton and Lynch, 1975). Fifty ml of unacidified and unfiltered water are extracted with APDC-MIBK and the extract is aspirated into the air-acetylene flame of an atomic absorption spectrometer. In order to improve extraction efficiency, mechanical shaking of the separatory funnels was used in 1975. All analytical equipment and supplies, plus the three analysts involved, were carried in one load of a Twin Otter aircraft (∿2500 lb,). The facility was accommodated in one longhouse tent (12 feet by 14 feet). Two, sometimes three, analysts measuring Zn and Cu kept pace with the 150 samples that could comfortably be collected each day. Detection limits for the method are 0. 5 ppb for both Zn and Cu.

Table 39. 1

Successive water sampling to estimate contamination caused by helicopter sampling system

SAMPLE	LAKE TYPE	Zn ppb	Cu ppb
2829	Background	<0. 5	<0. 5
2830	Anomalous	235	90. 2
2831	Background	3. 5	2. 5
2832	Background	<0. 5	<0. 5
2833	Background	<0. 5	<0. 5

Figure 39. 2

Front compartment of water sampling helicopter. The electronic console fitted in front of the navigator's position measures the pH, temperature and conductivity of the water.

Notes on Sampling and Preparation Procedures

One of the most attractive features of the hydrogeochemical approach that was apparent during the 1974 studies was the relative simplicity of sampling and preparation methods. For example, it was shown (Cameron and Ballantyne, 1975) that for the two lakes tested, surface waters are very homogeneous in Zn and Cu content within a given lake. Also, it was not found necessary to filter or acidify samples prior to analysis. As well as saving time, particularly under field conditions, possible contamination of the sample is avoided.

Workers studying waters from different environments have frequently found filtering and/or acidification essential to successful analysis of the samples. In order to provide a firmer basis for the procedures used some samples were analyzed in the field after filtering and/or acidification and compared with analyses made on the same untreated waters. Analysis of these samples will be continued during the 1975 winter to estimate the effects of acidification and filtering on the storage properties of the samples.

Table 39. 2 gives data on the analysis of High Lake waters in the field to estimate the effects of sample treatment. This is a highly anomalous lake adjacent to a Cu-Zn massive sulphide body (*see* Cameron and Ballantyne, 1975 for location of the site). Each value given is the mean of one determination on each of 4 bottles of High Lake water. Acidification consisted of adding 1 ml concentrated HNO_3 per 500 ml water.

The data given in Table 39. 2 indicate that acidification has little effect on analyses of High Lake water made within a few days of collection. Filtering has no noticeable effect on the measured content of Zn in this water, but does cause a slight decrease in the Cu content.

Table 39. 2

Sample treatment comparisons, High Lake waters

TREATMENT	Zn ppb	Cu ppb
Untreated	229	78. 9
Acidified	235	77. 2
Filtered 0. 45μ	227	65. 1
Filtered 0. 22μ	235	66. 4
Filtered 0. 45μ and Acidified	233	67. 2
Filtered 0. 22μ and Acidified	235	65. 7

High Lake Hydrogeochemical Survey

In 1974, an area of 1000 square miles, centred on High Lake, N. W. T. was sampled at a density of one sample per 3. 5 square miles (9 km^2). Data on pH, Zn and Cu for these samples has since been published,

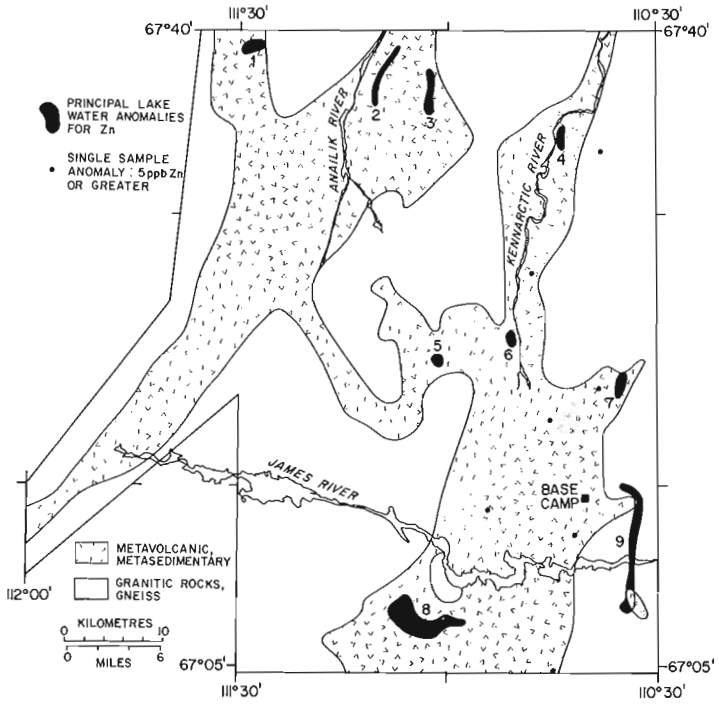

Figure 39. 3. Lake water geochemical survey, High Lake area, N. W. T., 1975. Geology after Fraser (1964).

along with similar data for lake waters from the Hackett River massive sulphide camp to the southeast (Cameron and Ballantyne, 1975). The results were of sufficient interest to encourage further study of the High Lake area. In 1975, a 1300-square-mile (3367 km^2) area was sampled an area that includes a majority of the previously mapped metavolcanic rocks within 1: 250 000 NTS sheet 76M (Fig. 39. 3). The sample density employed was one sample per square mile. Previous lake sediment or lake water surveys in the northern Shield have employed wider sample intervals up to one per 10 square miles. The rationale for using these wide intervals is that the ubiquitous massive sulphide mineralization of the Archean tends to occur in clusters, rather than as single, isolated bodies (Cameron, 1975). To detect such clusters it is not necessary to choose a sample interval capable of identifying each body within the cluster. The relatively close sample interval used for this 1975 work was chosen to test this clustering concept in an area that is believed to have good massive sulphide potential.

The area studied in 1975 is the scene of moderately intensive exploration activity. While this region of the Slave Province has seen sporadic mineral exploration during the past several decades, this work increased sharply in 1974 and again in 1975. Despite the earlier work, exploration is still largely in the reconnaissance phase. During 1975, the principal exploration activities were geological mapping, airborne E. M. surveys, and some lake sediment sampling, with a limited amount of drilling on previously defined targets. On the basis of information kindly provided by exploration geologists, it was possible to judge the probable usefulness of lake water surveys at this stage in exploration.

The High Lake area has a rugged local relief of up to 300 feet. Although there is a general south to north dip to the land surface, much of the area sampled lies close to the 1000-foot contour. Only along the northern boundary of the survey area is there a rapid drop to the shores of Coronation Gulf. There is an abundance of lakes in the area, that would allow a much higher sample density than one per square mile to be used, if such was necessary. Overburden is generally thin. The area is far north of the treeline and is on the zone of continuous permafrost. Gossanous outcrops, in places spectacular, are common throughout the area underlain by metavolcanic rocks.

As the results for Zn and Cu became available, it was apparent that the close sample density of the 1975 survey was outlining the same anomalies previously defined in 1974. There is an apparent lack of smaller targets that can only be discovered by the closer-spaced sampling.

Another feature of the 1975 data was the lower level of Zn in waters from background (non-anomalous) areas. In 1974, the median Zn content was 8. 8 ppb for 285 waters, and <1. 0 ppb for Cu. For 1975 median values were <0. 5 ppb for both Zn and Cu. The reasons for this difference in Zn for the two years was not at first apparent. However, after a number of tests it is now clear that it was caused by slight but consistent contamination from the sample bottles used in 1974. These were formed from linear polyethylene. In 1971 and 1972 tests were carried out on similar bottles in the course of collecting waters from the Slave Province (Allan *et al.*, 1972). These showed that negligible contamination of Zn and Cu was contributed by the plastic bottles, even with acidification of samples. Similarly, the linear polyethylene bottles used for the 1975 sampling contribute nil contamination of Zn or Cu. Only the first waters collected in any of the 1974 bottles became contaminated. In 1974 the available bottles had to be reused several times. Thus, the published data for Hackett River (Cameron and Ballantyne, 1975) and for Agricola Lake (Cameron and Lynch, 1975) are not affected by contamination.

The principal lake water anomalies shown in Figure 39. 3 are based on a number of samples within the same area containing 5 ppb Zn or more. Some samples within the areas may contain 100 ppb Zn or more and anomalous results for Zn are often accompanied by anomalous values for Cu. However, only in one case did the Cu content of an anomalous water exceed the Zn content. Lake waters containing 5 ppb or more of Zn are relatively rare away from the principal anomalies (Fig. 39. 3).

Anomalies 1, 2, 3, 5, 6 (High Lake), and 8 (Canoe Lake) are associated with felsic volcanic rocks. Anomalies 4, 7 and 9 appear to be associated with mainly metasedimentary strata. Because of inclement weather at the end of the season this could not be checked for anomaly 4 by ground traversing. Although the area occupied by anomaly 9 is shown as being mainly granitic on Figure 39. 3, metamorphosed greywacke and argillite

are the dominant rock types in the immediate area of the anomaly.

As noted above, gossans are common throughout the area underlain by metavolcanic rocks. In the case of the anomalies associated with felsic volcanics (1, 2, 3, 5, 6, 8) gossans are present. A limited number of samples were taken from these gossans. In the case of the anomalies associated with the metasedimentary rocks (4, 7, 9) there were no gossans observed in the immediate area. The elongate anomalies (2, 3, 8, 9) are oriented parallel to the strike of the associated metavolcanic or metasedimentary rocks.

There appears to be an interesting spatial distribution to the anomalies. Anomalies 1, 2, 3 and 4 occur along an east-west trend that is roughly perpendicular to the strike of the metavolcanic-metasedimentary belt. Similarly, anomalies 5, 6 and 7 are along an east-west axis and anomaly 9 is to the east of the Canoe Lake area anomaly. The separation of these three east-west axes is roughly equidistant at an approximate interval of 17 miles (27 km). It should be noted that the anomalies associated with metasedimentary rocks (4, 7, 9) occur lateral to the anomalies associated with the felsic volcanic rocks. In the Slave Province metavolcanic rocks generally occur along the margin of the greenstone belts, where they form the base of the volcanic-sedimentary sequence of the belts. The axial portion of the belts are composed of metamorphosed flysch facies sediments. To the present there has been insufficient geological work carried out in the northern part of the Slave Province to define the structural relationships between the Archean volcanic and sedimentary rocks. However, in the north-northwest trending Beechey Lake belt to the southeast, volcanic rocks are along the western flank of the belt and metasediments in the axial portion. In this belt there is a well developed base metal lake sediment and water anomaly in the Agricola Lake area that is associated with felsic volcanic rocks (Cameron and Durham, 1974; Cameron and Lynch, 1975). Eight miles (13 km) to the east, within the metasedimentary portion of the belt, is another well developed base metal anomaly. The cause of this anomaly is unknown for, like those associated with metasediments in the High Lake area, there are no gossans present or other obvious signs of base metal mineralization. This phenomenon requires further study.

Most of the anomalies shown in Figure 39. 3 were confirmed by resampling the anomalous lakes and by more detailed sampling. These data will be given in a later paper. A limited number of seep waters were collected in order to more closely define the source base metals for anomalous lakes. The very dry summer of 1975 was not, however, conducive to this follow-up work.

For exploration in this and similar regions, hydrogeochemical methods can probably play an important role in mineral exploration. They provide targets of limited areal extent within which geological, geophysical and geochemical studies can be focussed. The more anomalous base metal values can probably only be derived from actively oxidizing sulphide bodies, so that the effects of glacial transport of metal-rich overburden are reduced. Compared to lake sediment surveys, sampling is simpler, faster and more economical. It is practical to analyze the waters under field conditions. As noted in a previous paper (Cameron and Ballantyne, 1975) anomalies in lake sediments may be recognizable further from the source than those in lake waters. This, together with the uncertainty over the extent of temporal variation in lake water chemistry, and the restriction in the application of hydrogeochemistry to the more mobile elements, determines that lake sediment surveys are presently more suited to broad scale reconnaissance in the northern Shield. But for more detailed surveys of restricted application, such as might be required for exploration for massive sulphides within a given volcanic belt, these disadvantages are of little consequence. In this case the advantages of hydrogeochemical methods noted above may become dominant.

Acknowledgments

The field analytical facilities were capably organized and operated by Ms. G.E.M. Aslin, Ms. A.I. McLaurin and Ms. E. Ruzgaitis. The efforts of our pilot, Mr. Gene Vinet, and the sampler, Mr. J. Thomas, greatly contributed to the operation. We are grateful for the assistance of Mr. L. Camphaug during the design and construction of the sampling system.

References

Allan, R.J., Cameron, E.M., and Durham, C.C.
1973: Lake geochemistry--a low sample density technique for reconnaissance geochemical exploration and mapping of the Canadian Shield; *in* Int. Geochem. Explor. Symp., Proc., 1972, M.J. Jones (ed.), Inst. Min. Metall., p. 131-160.

Cameron, E.M.
1975: Geochemical methods of exploration for massive sulphide mineralization in the Canadian Shield; *in* Geochemical Exploration, 1974, Fifth Int. Geochem. Explor. Symp., Proc., p. 21-49.

Cameron, E.M. and Ballantyne, S.B.
1975: Experimental hydrogeochemical surveys of the High Lake and Hackett River areas, Northwest Territories; Geol. Surv. Can., Paper 75-29, 19 p.

Cameron, E.M. and Durham, C.C.
1974: Geochemical studies on the eastern part of the Slave Province, 1973; Geol. Surv. Can., Paper 74-27, 20 p.

Cameron, E.M. and Lynch, J.J.
1975: Hydrogeochemical studies in the Agricola Lake area, 1974; *in* Report of Activities, Part A, Geol. Surv. Can., Paper 75-1A, p. 203-207.

Durham, C. C. and Cameron, E. M.
1975: A hydrogeochemical survey for uranium in the northern part of the Bear Province, Northwest Territories (this publ., rept. 54).

Horton, R. and Lynch, J. J.
1975: A geochemical field laboratory for the determination of some trace elements in soil and water samples; *in* Report of Activities, Part A, Geol. Surv. Can., Paper 75-1A, p. 213-214.

Fraser, J. A.
1964: Geological notes on northeastern District of Mackenzie, Northwest Territories; Geol. Surv. Can., Paper 63-40, 20 p.

40. A GEOCHEMICAL ORIENTATION SURVEY FOR URANIUM AND BASE METAL EXPLORATION IN SOUTHWEST BAFFIN ISLAND

Project 750052; Uranium Reconnaissance Program

Y. T. Maurice
Resource Geophysics and Geochemistry Division

Introduction

Uranium and thorium mineralization occurs sporadically in the Proterozoic (Aphebian) rocks of southwest Baffin Island. Interesting showings are located on Foxe Peninsula at 11 and 28 miles northeast of Cape Dorset (*see* Fig. 40. 1); these have been described along with other occurrences by Laporte (1974). The radioactive minerals are found in coarse grained to pegmatitic granite sills and dykes and in associated metasediments, and their presence in these rocks is often marked by the characteristic yellow staining of secondary uranium ore minerals.

To date, exploration for radioactive minerals in southern Baffin Island has been strictly a geophysical effort. Companies using airborne radiometric methods at a reconnaissance scale have been relatively successful in Foxe Peninsula where the topography is relatively flat. However, in other parts of southern Baffin Island, particularly east and south of Frobisher Bay, the usefulness of airborne radiometric techniques may be considerably reduced due to a more hilly relief.

The work performed during the 1975 field season was carried out under the Federal-Provincial Uranium Reconnaissance Program (Darnley *et al.*, 1975). It was aimed primarily at investigating the applicability of various geochemical techniques for uranium exploration in southern Baffin Island. In addition to radioactive minerals, a geochemical approach will permit the examination of the potential of the region for other mineral commodities such as base metals and pegmatite minerals. This orientation survey is the preparatory phase for a more extensive coverage that may be undertaken by contract at a later date.

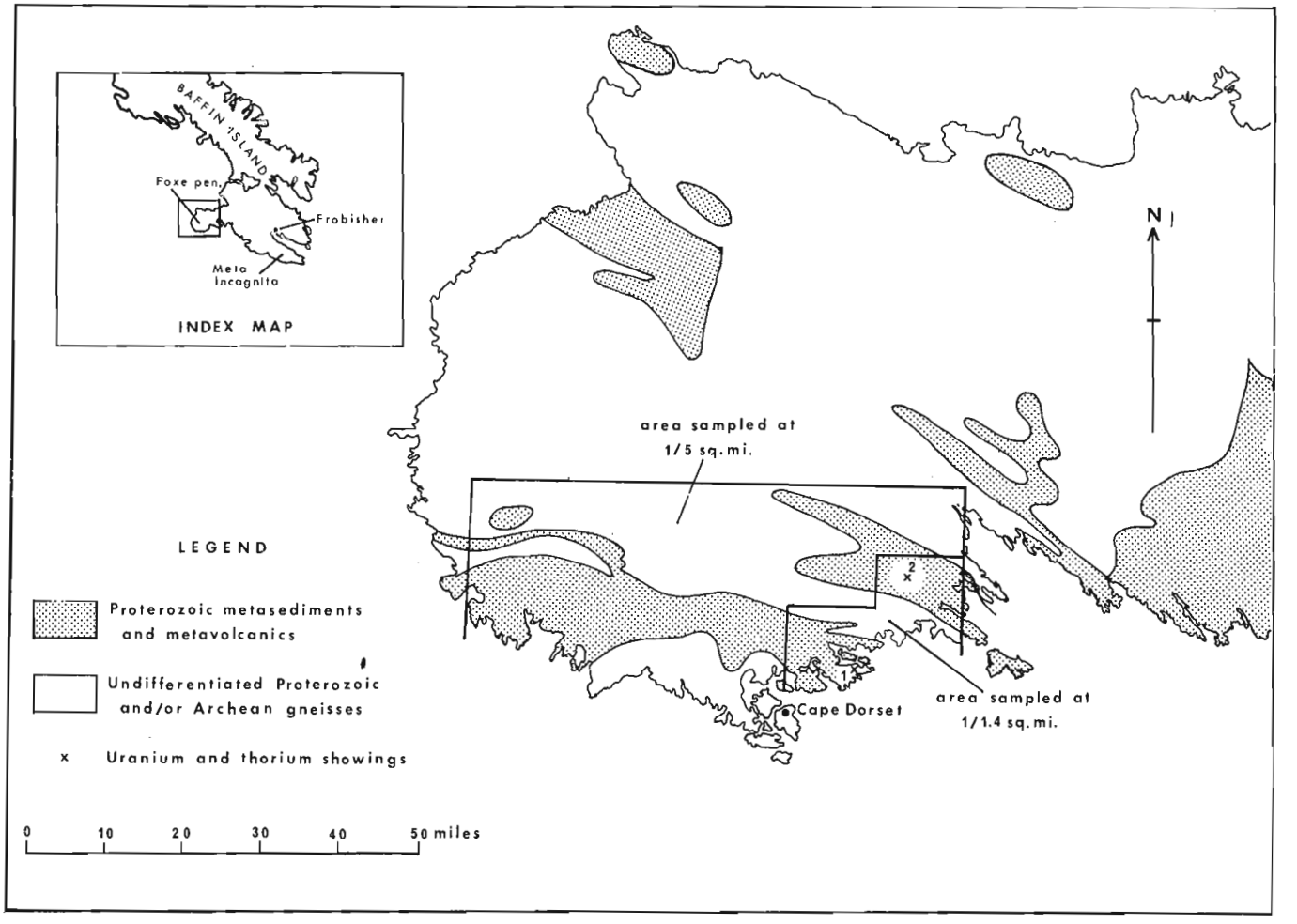

Figure 40. 1. Outline of geology and location of study area.

Detailed Surveys

In order to gain geochemical information on the uranium sources and to recognize the mechanisms involved in the secondary dispersion of metals from these sources, much of our attention was concentrated in the two areas where exposed mineralization was reported (Fig. 40. 1). Near-surface soils were sampled at 50- or 100-foot intervals along several traverses across the mineralized zones. The samples will be analyzed for a suite of elements that will identify those that are enriched and thus indicate potential pathfinders. The results will also be examined against radiometric data obtained in the field with a portable scintillation counter.

To complement these data, several rock samples were selected from mineralized outcrops and will be analyzed for the same elements as the soils. It is interesting to note that molybdenite was found closely associated with radioactive pegmatites at both showings. Consequently, not only has molybdenum some potential as an indicator of uranium, but its distribution in the secondary environment compared to that of uranium may enable us to differentiate areas of pegmatite uranium mineralization from other areas where other types of uranium occurrences may be present.

In addition to the soil and rock surveys, sediment and water samples were collected from all streams, lakes and ponds that could be located within a one-mile radius of the showings. Hopefully, the results of this survey will contribute further to our knowledge of secondary dispersion of uranium and associated elements under the conditions prevailing in southern Baffin Island.

An experiment to evaluate the use of radon in soil-air as an exploration tool for uranium under arctic conditions was also carried out. Radon counts in soil-air were taken at 50-foot intervals along traverses that intersected overburden-covered prolongation of mineralized zones. Preliminary examination of the results tends to indicate that radon in soil-air has some potential as a follow-up tool in uranium exploration in arctic regions.

Reconnaissance Surveys

As shown on the 1: 250 000 topographical maps of southern Baffin Island, both lake density and lake sizes seem generally adequate for reconnaissance lake geochemistry at a density of one sample per five square miles. In most areas, however, a higher density could be achieved if required.

A helicopter-supported lake water and sediment sampling survey was undertaken during the month of August in a 1500-square-mile area of southern Foxe Peninsula underlain by Proterozoic metasedimentary rocks and undifferentiated Proterozoic or Archean gneisses (*see* Fig. 40. 1). Sampling was carried out at a density of one sample per five square miles in much of the area surveyed, but the density was increased to one sample in 1. 4 square miles (one sample from every lake shown on the 1: 250 000 topographical map) in 100-square-mile areas around each one of the two main showings.

The main objectives of this work were:

1. To evaluate the feasibility of lake water and sediment sampling in that area, and to gather basic information such as depths of lakes, nature and abundance of sediments, pH and specific conductivities of waters, presence or absence of suspensions in waters, etc.
2. To complete our research on the secondary dispersion of uranium and associated elements in proximity to exposed mineralization initiated with the detailed surveys.
3. To determine certain geochemical parameters such as background and threshold levels, correlations, etc. for various elements in areas of different geological environments in order to identify the most meaningful elements to be examined during the regional contract survey.

A conclusion with respect to the second and third objectives will not be reached until analytical data are available. As far as the technicalities of lake sampling are concerned, both the abundance of sediment in most lakes and the generally shallow depths make lake bottom sediment sampling a relatively easy task. The Hornbrook-designed tube sampler attached to a 30-metre ¼ inch sash-cord was efficient in most situations. For very shallow lakes (less than three metres) however, the Ponar jaw sampler was preferred. Lake water sampling using the Viking Helicopter-designed system (*see* Cameron and Durham, this publication, report 39) was very reliable. Sampling rate (waters and sediments) was in the order of 10 to 12 per hour.

On Meta Incognita Peninsula (southeast Baffin Island) the relief is considerably higher and more accentuated than in Foxe Peninsula resulting at times in very deep and wide valleys with steeply-rising walls. Although this is not generally the case, it happens that in areas of such topography, the number of lakes is insufficient and that streams would have to be sampled in order to maintain a one-in-five square mile sample density.

An orientation survey to assess the feasibility of stream water and sediment sampling as a complement to lake geochemistry was carried out in a 250-square-mile area on Meta Incognita Peninsula about 40 miles southwest of the town of Frobisher Bay. The streams were remarkably accessible as the helicopter pilot was generally able to land his aircraft in the valleys, within a few feet of the water, resulting in a sampling time equivalent to the time required to sample lakes. It was also found that the majority of the streams that are shown on the 1: 250 000 topographical maps were flowing in mid-August (supposedly the dryest period of the year) and that water samples were readily obtainable. Because two samplers were available, it also became practice to land the aircraft near stream intersections so that two streams could be sampled with no increase in the sampling time. Sediments however were generally difficult to collect and often non-existent due to the bouldery nature of many stream beds.

Summary

An orientation survey designed to evaluate the potential of exploration geochemistry in southern Baffin Island was carried out during the months of July and August, 1975. Two aspects were investigated, namely:

1. The feasibility of helicopter-supported reconnaissance geochemical surveying based on lake sediment and water sampling with occasional stream sampling in areas where lake density is insufficient.
2. The geochemical dispersion of metals in the secondary environment at both regional and detailed scales.

Many of the conclusions will have to await the analytical results but it can be said at this stage that no technical difficulties were encountered with the sampling aspect of the project except perhaps in the case of some streams that had no recoverable sediment. Fortunately, however, this problem affects only a very small proportion of southern Baffin Island.

References

Cameron, E. M. and Durham, C. C.
1975: Further studies of hydrogeochemistry applied to mineral exploration in the northern Canadian Shield; (this publication, report 39).

Darnley, A. G., Cameron, E. M., and Richardson, K. A.
1975: The Federal-Provincial uranium reconnaissance programs; *in* Uranium Exploration 1975; Geol. Surv. Can., Paper 75-26, p. 49-68.

Laporte, P. J.
1974: Southern Baffin Island radioactive showings; *in* North of 60, Mineral Industry Report 1969 and 1970, Volume 2 Northwest Territories east of 104° west longitude, p. 135-139; Can. Dept. Indian and Northern Affairs.

41. THE KEELE ARCH — A PRE-DEVONIAN AND PRE-LATE CRETACEOUS PALEO-UPLAND IN THE NORTHERN FRANKLIN MOUNTAINS AND COLVILLE HILLS

Project 670068

D. G. Cook
Institute of Sedimentary and Petroleum Geology, Calgary

Introduction

A regional paleo-arch about 200 miles long and 75 miles wide extends from Keele River northward at least to Lac des Bois. The arch developed in pre-Early Devonian time and was reactivated in pre-Late Cretaceous time, possibly during the Early Cretaceous.

Erosional truncation on the southern part of the arch in the vicinity of the Shell Keele River L-4 well has been indicated by previous authors (Ziegler, 1969, p. 11, 14; Bassett and Stout, 1967, p. 730, 732, and 736; Gilbert, 1973, p. 228, 231, 232). The extension of the arch northward to Lac des Bois probably is not as well known.

Because the arch is best known near Keele River, and because the deepest paleo-erosion known is recorded in the Shell Keele River L-4 well (Cretaceous rocks overlie Middle Cambrian rocks), the name "Keele Arch" is proposed for this important paleotopographic upland.

The arch is outlined briefly here because the concept of a regional arch may be significant to exploration for hydrocarbons, particularly natural gas, in basal Cambrian sandstone (also *see* Haimila, this publication, report 12).

This report is based mainly on published and unpublished surface geological studies by J. D. Aitken, C. J. Yorath, H. R. Balkwill, M. E. Ayling and the writer (1968, 1969, 1970, 1974) and on the results of exploratory drilling for hydrocarbons by oil companies. Subsurface formation tops have been provided by W. S. MacKenzie or the well operators. Cretaceous age determinations have been provided by W. W. Brideaux and T. P. Chamney. Informal subdivisions of the Franklin Mountain Formation are used following Norford and Macqueen (1975).

Pre-Devonian Keele Arch

In the McConnell Range and the unnamed range containing Mount St. Charles on the eastern flank of the arch, and in Mackenzie Mountains on the western flank of the arch, the Lower Devonian Bear Rock Formation overlies the Ordovician-Silurian Mount Kindle Formation. The broad crest of the arch occurs throughout most of the intervening northern Franklin Mountains and Mackenzie Valley. There, pre-Devonian erosion cut deeper, and the Bear Rock Formation overlies the Cambro-Ordovician Franklin Mountain Formation or older strata (Figs. 2, 4). An interpreted pre-Devonian zero edge of the Mount Kindle Formation is shown on Figure 41.1. Pre-Devonian erosion was deepest along the southern part of the arch (Fig. 41.4) at the latitude of McKay Range. There the Bear Rock overlies the Upper Cambrian Saline River Formation. Due to a northward plunge, the sub-Devonian unconformity overlies progressively younger rocks northward along the arch, so that, at the latitude of Norman Wells, the Bear Rock Formation overlies the Upper Cambrian or Lower Ordovician cherty unit of the Franklin Mountain Formation.

It is not certain how far north the pre-Devonian arch extends because Devonian rocks themselves have been removed by erosion. It may extend to Tunago Lake where an area underlain mainly by the cherty unit of the Franklin Mountain Formation is flanked to the east and west by strata of the Mount Kindle Formation (Cook and Aitken, 1971). The Mount Kindle closes across the arch somewhere in a covered area between Tunago Lake and Lac des Bois (Cook and Aitken, ibid.), but is missing again near Lac Maunoir where the Bear Rock Formation overlies the Franklin Mountain cherty unit. This localized "high" could represent an extension of the Keele Arch or could represent a second arch extending to the north or northwest an unknown distance beneath Devonian cover.

Pre-Late Cretaceous Keele Arch

Following Early and Middle Devonian and possibly younger sedimentation across the arch, a second, pre-Late Cretaceous phase of uplift developed with resultant erosion of Devonian and older strata from the crest of the arch.

The deepest erosion apparently was again in the area of the southern part of the arch. There, Cretaceous strata overlie the Upper Devonian Imperial Formation on the western flank, overlie the middle Cambrian Mount Cap Formation in the Shell Keele River L-4 well approximately on the crest of the arch, and overlie the Middle Devonian Hume Formation on the east flank (Fig. 5). This "deep" erosion was accomplished largely during the pre-Devonian phase, and the younger phase may have eroded little more than Devonian strata.

In the vicinity of Fort Norman, a saddle of Devonian rocks may be continuous across the arch rather than be missing from the crest as interpreted in Figure 41.1.

Northward near Kelly and Mahoney Lakes, the crest is broader (Fig. 41.3) and is marked by the occurrence of Upper Cretaceous, Campanian-Maastrichtian (W. W. Brideaux, pers. comm., 1975) cherty sand and conglomerate, and black shale, overlying the Franklin Mountain cherty unit. On the east flank, east of Mahoney Lake, Lower Cretaceous sandstone and shale overlie Middle Devonian Bear Rock and Hume Formations. On the west flank, in Mackenzie Valley, Lower Cretaceous sandstone and shale overlie the Upper Devonian Imperial Formation. It is uncertain whether Lower Cretaceous strata onlapped the arch, thus requiring that the arch was present at that time, or whether they extended across the arch and subsequently were stripped off during a relatively short early Late

Figure 41.1. The Keele Arch.

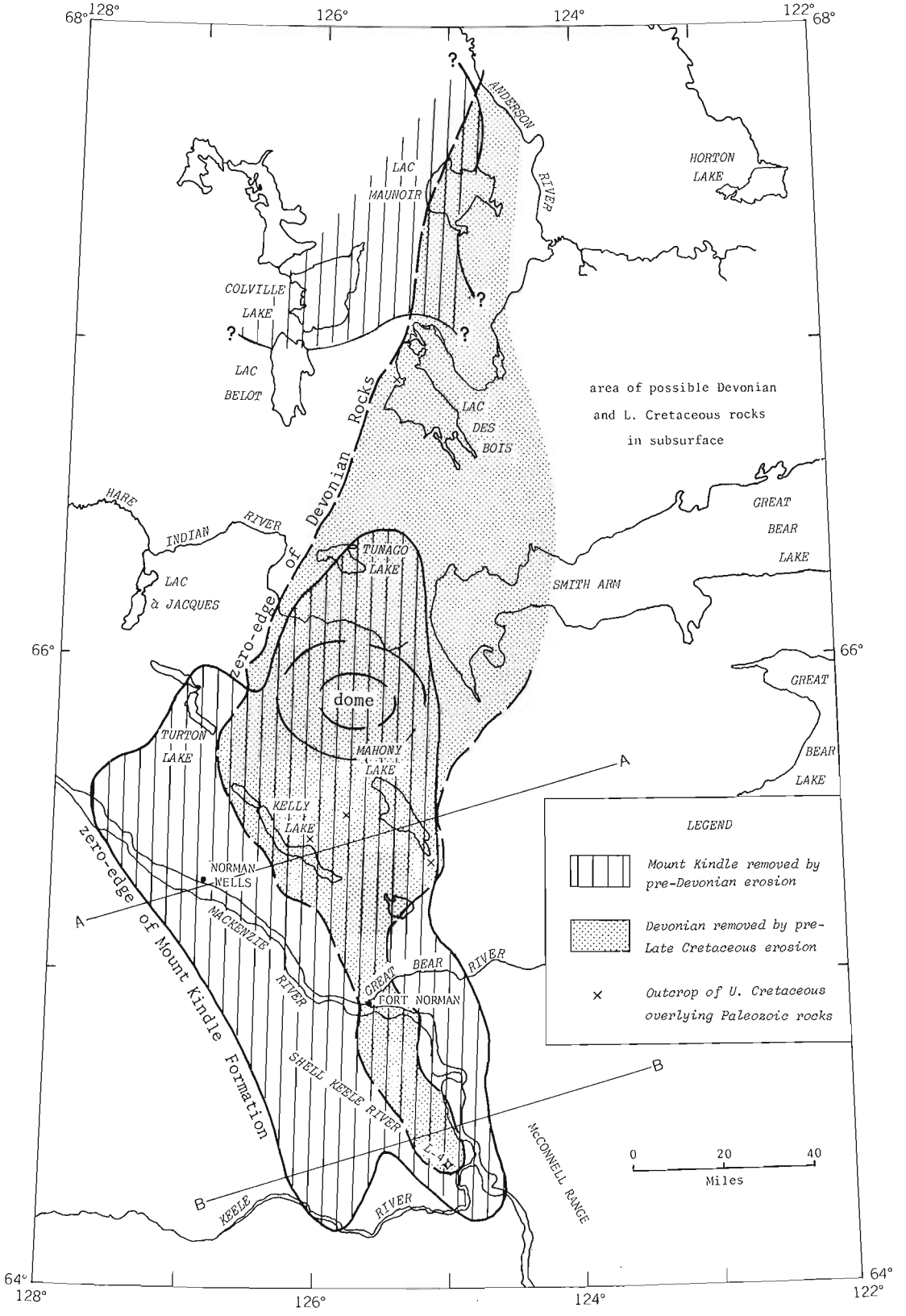

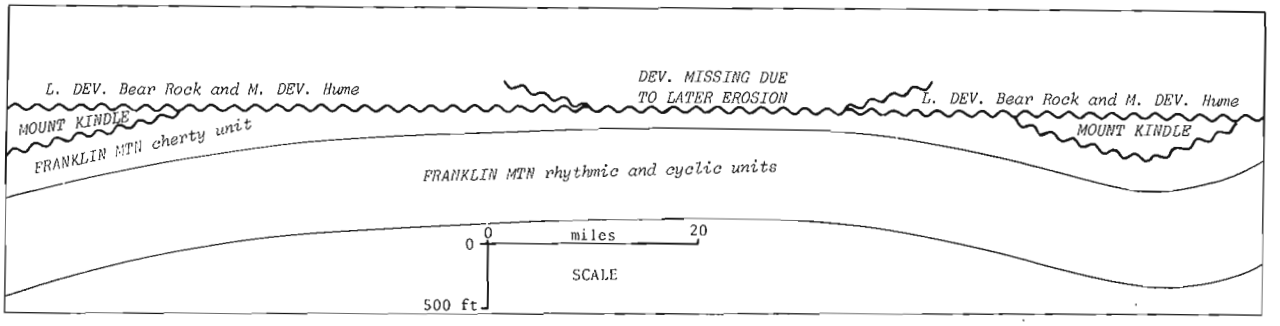

Figure 41.2. Schematic cross-section along AA (Fig. 41.1) showing pre-Devonian truncation of older strata.

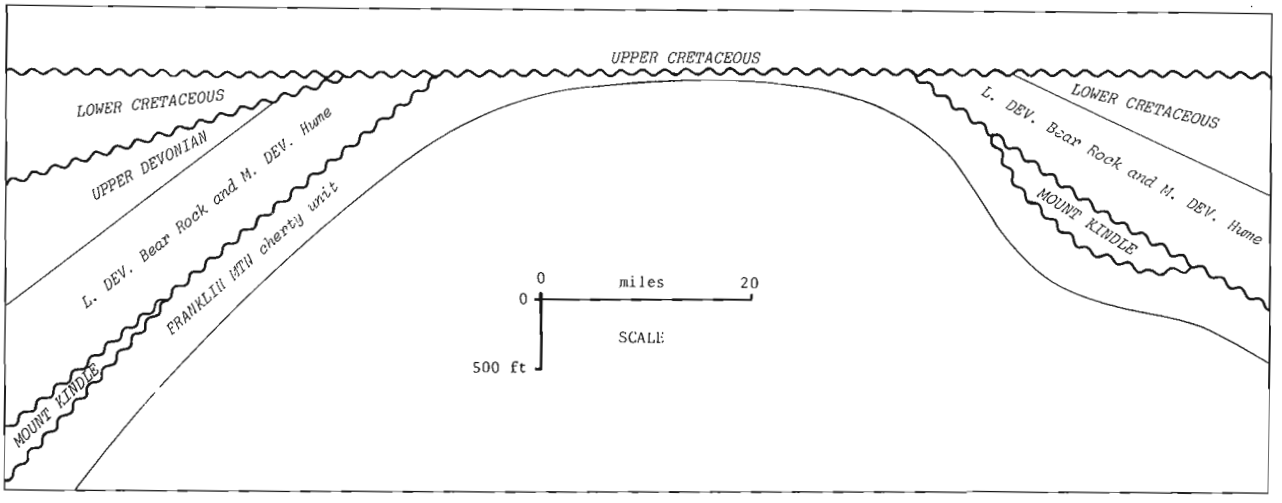

Figure 41.3. Schematic cross-section along AA (Fig. 41.1) showing pre-Late Cretaceous truncation of older strata.

Cretaceous (pre-Campanian) phase of uplift and erosion. Along the southern part of the arch in the Fort Norman area, it is not known whether basal Cretaceous rocks are of Lower or Upper Cretaceous age.

Northward, the crest of the arch can be extrapolated, as it was for the pre-Devonian arch, from Kelly and Mahoney Lakes almost to Lac des Bois along a narrow belt of poorly exposed Franklin Mountain cherty unit with possible outliers of the Mount Kindle Formation. This extrapolation northward is strongly supported by the presence at Lac des Bois of Upper Cretaceous (Turonian) shale which apparently overlies the Mount Kindle Formation (Cook and Aitken, 1971). These Upper Cretaceous beds are flanked to the west and east by Lower Cretaceous rocks.

Gilbert (1973, p. 237) showed a feature named the Lac des Bois High trending from southwest to northeast across Lac des Bois and onto the northern part of Coppermine Arch. The existence of that high apparently is based on the presence at Lac des Bois of Upper Cretaceous (Turonian) beds unconformably overlying Paleozoic rocks. The reason for a southwest-northeast orientation is not clear.

The pre-Late Cretaceous Keele Arch is outlined in the south by the zero-edge of Devonian rocks (Fig. 41.1). Along the northern part of the arch, Devonian rocks are exposed only on the western flank. On the basis of the inferred geometry of the arch, Devonian rocks are to be expected in the subsurface to the east of Lac des Bois.

Economic Geology

A large dome, nearly 50 miles in diameter, appears to exist on the crest of the arch north and northwest of Mahoney Lake (Fig. 41.1). There, rocks of the Franklin Mountain cherty unit with possible outliers of Mount Kindle Formation are topographically high. They must dip eastward beneath Devonian and Cretaceous rocks encountered in wells east of Mahoney Lake, and southward beneath topographically lower Upper Cretaceous rocks west of Mahoney Lake. Control northward is poor, but the entire Keele Arch plunges northward so that the dome should close also in that direction. Progressively younger formations occur westward but the west flank of the dome is disrupted by faulting, and closure there has not been established. This feature is noted by Haimila (this publication, report 12) as one of a number of circular patterns recognizable on satellite imagery, and distributed along the arch.

The best exploration target in the dome and elsewhere along the arch probably is the Mount Clark Formation, a basal Cambrian sandstone. This sandstone was made more attractive as an exploration target by

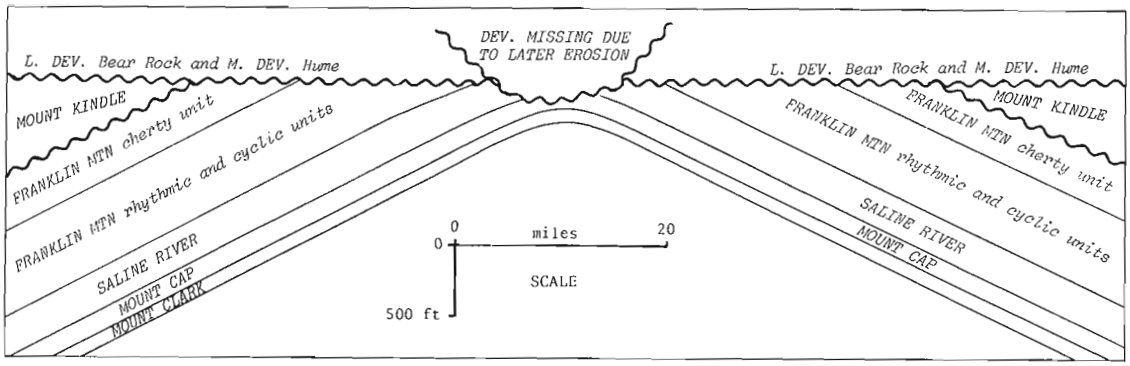

Figure 41.4. Schematic cross-section along BB (Fig. 41.1) showing pre-Devonian truncation of older strata.

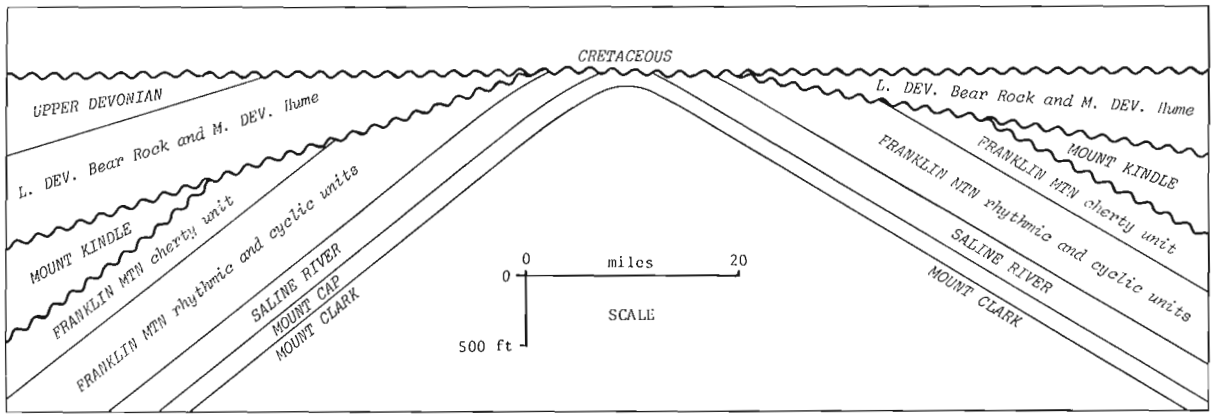

Figure 41.5. Schematic cross-section along BB (Fig. 41.1) showing pre-Late Cretaceous truncation of older strata.

Ashland Oil's gas discovery at Tedji Lake, about 40 miles northwest of Colville Lake (Oilweek, 1974).

Recognition that the arch extends northward to Lac des Bois raises the interesting possibility of a structural basin east of Lac des Bois which could contain Devonian and Lower Cretaceous rocks. Such a basin would be similar to, and possibly an extension of, the depression which occurs east of Mahoney Lake. The potential for a thick Paleozoic and/or Mesozoic section carries with it the potential for trapped hydrocarbons.

References

Bassett, H.G. and Stout, J.G.
1967: Devonian of Western Canada *in* Oswald, D.H. (ed.), International Symposium on the Devonian System, Calgary, 1967; Alberta Soc. Pet. Geol., v. 1, p. 717-752.

Cook, D.G. and Aitken, J.D.
1971: Geology, Colville Lake map-area and part of Coppermine map-area, Northwest Territories; Geol. Surv. Can., Paper 70-12.

Gilbert, David L.F.
1973: Anderson Plain, Northern District of Mackenzie *in* McCrossan, R.G. (ed.), The Future Petroleum Provinces of Canada – Their Geology and Potential; Can. Soc. Pet. Geol., p. 213-244.

Haimila, N.E.
1975: Possible large domal structures along a regional arch in the northern interior plains; this publication, report 12.

Norford, B.S. and Macqueen, R.W.
1975: Lower Paleozoic Franklin Mountain and Mount Kindle Formations, District of Mackenzie: Their type sections and regional development; Geol. Surv. Can., Paper 74-34.

Oilweek
1974: Ashland strikes gas in N.W.T.; Oilweek, v. 25, no. 9, p. 19.

Ziegler, P.A.
1969: The development of sedimentary basins in western and Arctic Canada; Alberta Soc. Pet. Geol.

42. LOWER CRETACEOUS (NEOCOMIAN) SANDSTONE SEQUENCE OF MACKENZIE DELTA AND RICHARDSON MOUNTAINS AREA

Project 710036

D. W. Myhr and F. G. Young
Institute of Sedimentary and Petroleum Geology

Introduction

This paper reviews the major sedimentary facies comprising the Neocomian sandstone sequence ('Parsons sandstone') primarily as observed in borehole cores in the Mackenzie Delta area. Data from the authors' observations (including the 1975 field season) of surface exposures of these rocks west of Mackenzie Delta, and from publications by J. A. Jeletzky, were incorporated to establish a regional correlation framework and were used to construct paleogeographic maps.

The component parts of the Neocomian sandstone wedge are regionally correlative from the west flank of the Richardson Mountains as far east as the subsurface of central Tuktoyaktuk Peninsula (Figs. 42.1 and 42.2). Jeletzky's (1958, 1960, 1961) informally named lithostratigraphic units have been used to describe the stratigraphy in the outcrop area. The informal name 'Parsons sandstone' was introduced recently by Coté *et al.* (1975) for the entire arenaceous wedge in the subsurface east of the modern Mackenzie Delta. Ages of these rocks are less well established, hence the chart is subject to revision.

The major tectonic elements of the study-area that appear to have influenced Lower Cretaceous sedimentation are: Cache Creek Uplift (Fig. 42.12), Rat Uplift (Fig. 42.12), the Eskimo Lakes Fault Zone (Fig. 42.1) all of which are parts of the Aklavik Arch Complex, and the Kaltag-Rapid Fault Array and its offshore extension (Fig. 42.3). The geological map shows the control wells and the extent of Neocomian surface exposures west of Mackenzie Delta (D. K. Norris, pers. comm.).

The sandstone sequence was removed largely in late Hauterivian time over crestal areas of the Aklavik Arch Complex. Neocomian strata are almost completely preserved in three main areas: in the Parsons Lake area; in the northwestern Richardson Mountains; and in the central Richardsons (Figs. 42.1 and 42.3). These areas may have received the bulk of clastic sediment as evidenced by regional thinning of preserved units toward the crests of uplifts (e.g. Fig. 7, *in* Yorath *et al.*, 1975). Highs which appear to have influenced sedimentation include Rat Uplift, Cache Creek Uplift, the flank of Eskimo Lakes Horst, and the Eagle Arch (refer to Paleogeographic Maps, Figs. 42.12 to 42.14). Late Hauterivian right-hand displacements along the Kaltag-Rapid Fault Zone brought a much thinner sequence in contact with the very thick western wedge near Blow River (Young, 1974); the area west of the fault zone, however, also may have been a positive element during Hauterivian time (Fig. 42.3).

Sedimentology

The main lithofacies of the Neocomian arenaceous sequence are defined on the bases of lithology and well-log characteristics. These in turn reflect the depositional environments and processes that were active during early Cretaceous time. Environments recognized include fluvial, delta-plain, subaqueous delta, nearshore, and marine facies.

Offshore and Transitional Facies - Husky Formation

The Upper Jurassic to Lower Cretaceous Husky Formation underlies gradationally the 'Parsons Sandstone'. The uppermost sequence of shale, mudstone and arenaceous units appears to have been deposited in the offshore and lower shoreface (transitional) environments. These facies are nearly identical in texture and sedimentary structures to those described by Bernard *et al.* (1962) and Davies *et al.* (1971) for barrier islands of the Texas Gulf Coast.

Figure 42.4 illustrates the gamma ray log characteristics and thickness variations displayed by the transitional lithofacies. The transitional facies in the subsurface ranges in thickness from 6.1 m (20 ft.) to 39.7 m (130 ft.). At Martin Creek (Fig. 42.12; Lat. 68°12'20", Long. 135°36'), just west of Mackenzie Delta, the facies is approximately 30 to 40 m (98-131 ft.) thick and consists of moderately resistant, alternating arenaceous and shaly beds. In the subsurface, the contact of these facies tracts is obvious from log character in the Gulf Mobil East Reindeer G-04 borehole (Figs. 42.1 and 42.4; Lat. 68°53'15.9"N, Long. 133°46'03.3"W), but in most cases cores are necessary to define the contact with certainty. For example, the offshore facies in core no. 7 (Fig. 42.5) of the IOE Mayogiak J-17 borehole (Fig. 42.1; Lat. 68°26'42"N, Long. 133°48'12"W) consists of silty bioturbated mudstone, devoid of macrofossils. This facies gradationally overlies basinal shales (base of cored interval) and is conformable with the transitional facies (= lower shoreface) above; the latter contact is chosen at the first occurrence of siltstone beds. These strata are predominantly parallel laminated with minor burrowed and ripple cross-laminated upper parts that grade upward into bioturbated mudstone beds. These rhythmic units ("parallel-to-burrowed" sets of Howard, 1972) tend to increase in abundance upsection in conjunction with an increase in the arenaceous component. They may have formed during storms or abnormal tidal conditions when silt was entrained along the sea floor out to the shelf margin by bottom currents generated near the shore (Swift, 1970). This process and others (turbidity currents, rip currents, tsunamis) have been summarized by Goldring and Bridges (1973).

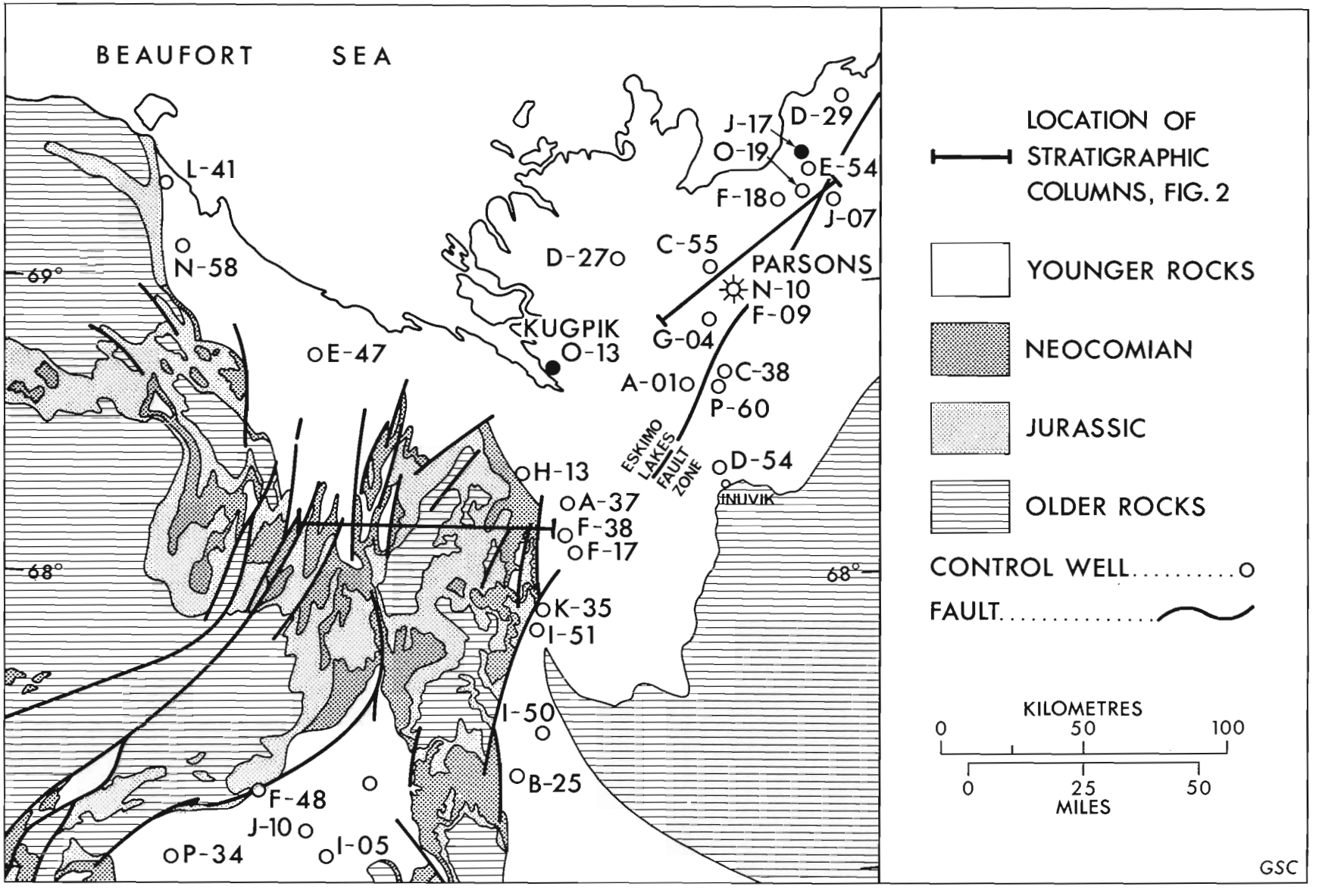

Figure 42.1. Geological map.

At Martin Creek the transition from pelitic rocks of the Husky Formation to the Lower Sandstone division exhibits a gradual change in lithology from mudstone with minor arenaceous beds in the offshore and transitional environments to sandstone of the shoreface environment. The transitional lithofacies consists of interstratified units of completely bioturbated mudstone and less bioturabated, in places fossiliferous, shaly, arenaceous (siltstone and very fine sandstone) beds. The uppermost 5.9 m (19.4 ft.) of the Husky Formation consists of bioturbated mudstone, 2.7 m (8.9 ft.) thick, that grades upward into 3.2 m (10.5 ft.) of thick-bedded, ripple laminated shoreface sandstone, with minor shaly interbeds, 2 to 3 cm thick. This unit is overlain by a resistant cliff of clean, cross-laminated, friable sandstone (Buff Sandstone member, Jeletzky, 1958).

Nearshore Facies

The oldest member of the 'Parsons sandstone', the 'Buff Sandstone member', is variable in thickness due to regional and local (i.e. Parsons Gas Field) unconformities and paleotopographic highs (Fig. 42.4). The unit consists mainly of sandstone which is divisible into middle and upper shoreface facies. These can be identified in cores 4 to 7 inclusive (Figs. 42.6 and 42.7) from the Gulf Mobil Parsons N-10 borehole (Fig. 42.1; Lat. 68°58'34"N, Long. 133°31'33"W).

The middle shoreface sandstone of cores no. 6 and no. 7 (Fig. 42.6) is 11.1 m (32 ft.) thick and tends to be massive at the base and well laminated toward the top of the unit. It exhibits scours, a slump structure, oblique burrows, minor coquina hash, as well as shale beds and partings near the top with rare climbing ripples. The homogeneous fabric at the base may be caused by burrowers re-working the sediment as some burrow mottling is evident. The shaly nature of this facies is recognizable on the gamma ray logs in the Parsons Gas Field (Fig. 42.4).

Structures in the upper shoreface lithofacies (cores no. 4 to 6, Fig. 42.7) include subhorizontal, planar lamination grading to massive at the top, with minor wedge-shaped cross-laminated sets, and coquina laminae. Burrows and ripple-marks are absent. This is the zone within which almost continuous grain movement occurs in wave-generated currents; alternating times of scour and re-deposition occur frequently with passing storms and seasons. The 'Buff Sandstone member' is unconformably overlain by a shaly unit that is easily recognizable from the abrupt change in gamma ray log signature in the Parsons F-09 and N-10 boreholes (Figs. 42.4 and 42.8). The lower part of the 'Parsons sandstone' and upper part of the Husky Formation is considered to have been deposited as a complex of barrier-shoreline deposits. Evidence for individual barriers in the subsurface may improve with additional well control, however, in the outcrop area of Martin Creek and 6 km (4 miles) to the north in "Grizzly Gorge" (Fig. 42.12; Lat. 68°16'N, Long. 135°43'W), the Buff Sandstone member consists mainly of 3 units of resistant to moderately resistant, very fine, well-sorted, and cross-stratified sandstone alternating with less resistant, in places bioturbated, ferruginous and in part fossiliferous argillaceous sandstone. In "Grizzly Gorge", 88 m (288.6 ft.) of Buff Sandstone was measured. These sequences may represent stacked shoreline (?barrier island) deposits in a nearshore setting, where cyclical conditions prevailed in one area for a considerable time.

South of the Aklavik Range, at Treeless Creek (Fig. 42.12; Lat. 67°52'20"N, Long. 135°28"W) the Buff Sandstone member is represented by a delta-plain facies 16.6 m (55 ft.) thick, consisting of pebbly to very fine grained sandstone (fining-upward cycles) interstratified with carbonaceous and argillaceous sandstone, mudstone, and siltstone (flood-basin deposits). Minor amounts of high volatile subbituminous A coal (P.R. Gunther, pers. comm.) and coaly shale are present also. This facies is truncated by the Upper Shale-Siltstone division (Jeletzky, 1960) and is underlain gradationally by transitional (delta-front and shallow marine) deposits of the Husky Formation.

Restricted-Shallow Marine Facies

In the subsurface of Tuktoyaktuk Peninsula, this facies in represented by a 21.2 to 24.4 m (70-80 ft.) thick shale and siltstone (in part sandy) unit that probably was deposited in a restricted, possibly brackish environment (Fig. 42.8). Its lithologic character is variable, as displayed by core no. 2 (Fig. 42.9) from the Gulf Mobil Parsons F-09 borehole (Lat. 68°58'34"N, Long. 133°31'33"W). Brief descriptions of this cored interval are documented in Myhr and Gunther (1974) and Coté *et al.* (1975). There are two sub-lithofacies, one which is completely bioturbated and representative of a lagoon or restricted bay, the other consisting of alternating siltstone and bioturbated mudstone layers with rare cross-laminae and flaser bedding, which suggest tidal flat or back-barrier conditions.

The equivalent lithostratigraphic unit in the subsurface flanking the Aklavik Range (Fig. 42.1; Shell Aklavik A-37, Lat. 68°16'15", Long. 135°07'46", and Shell Beaverhouse Creek H-13, Lat. 68°22'16.4", Long. 135°33'3") consists of dark grey marine shale, interbedded with argillaceous sandstone and mudstone units. Similarly, in Martin Creek a dark grey shale unit (Bluish-grey Shale division equivalents) occurs conformably above the Buff Sandstone member and is 25 m (84 ft.) thick. To the northeast, in the Shell Kugpik 0-13 borehole (Fig. 42.1; Lat. 68°52'50", Long. 135°13'15") the unit is much thicker, and is gradational and interstratified with the underlying Buff Sandstone member equivalents. The age relationships of this unit with the shaly interval previously described from the Parsons Gas Field have been discussed in some detail by Myhr and Gunther (1974). Diachroneity of the unit from west to east has been proposed, based on evidence from palynology (Brideaux, 1975) and stratigraphic relationships (unconformity at the base of the shaly unit) in the Gulf Mobil Parsons N-10 core (Fig. 42.7; and Coté *et al.*, 1975).

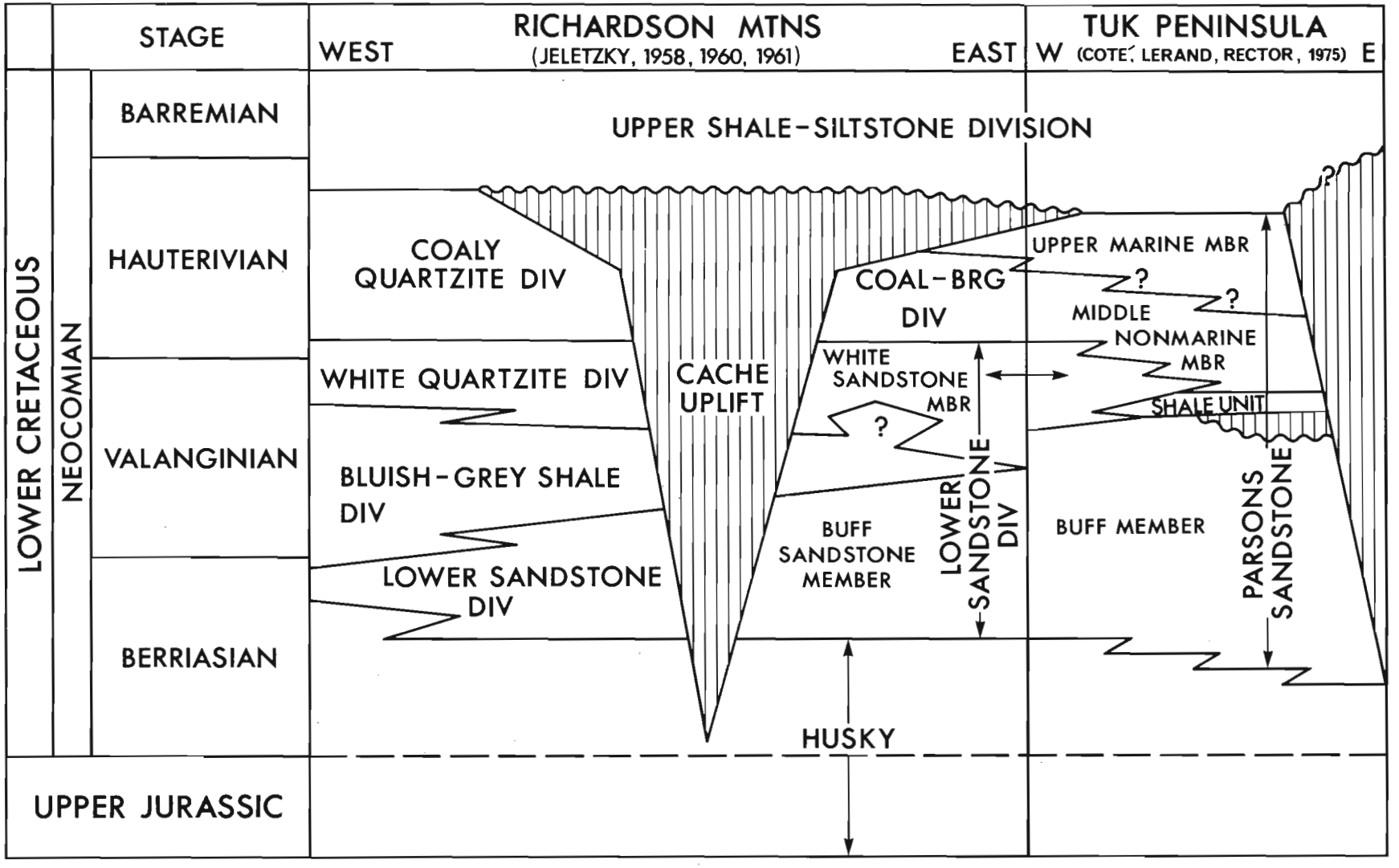

Figure 42. 2. Correlation chart.

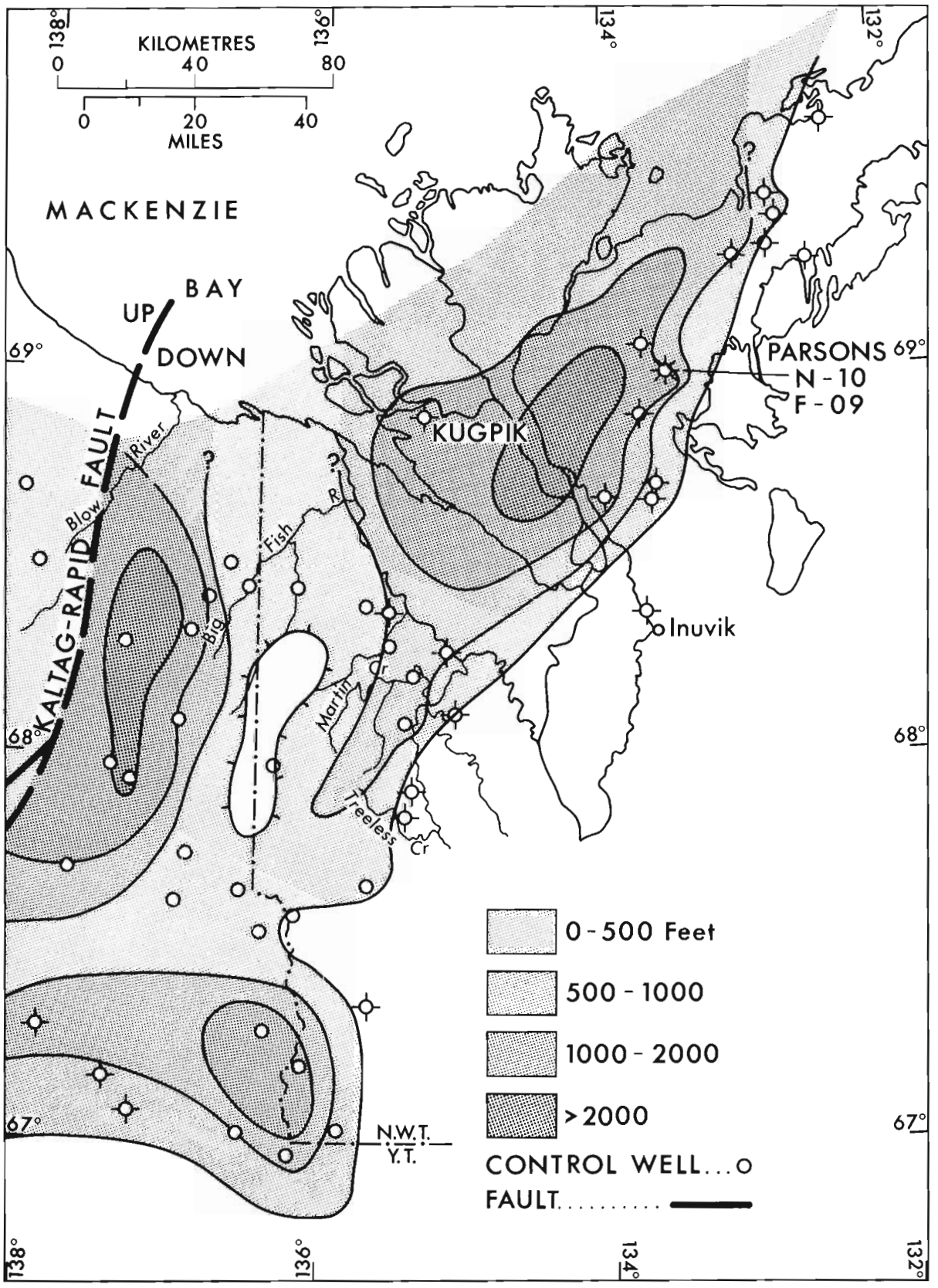

Figure 42.3. "Parsons" isopach map.

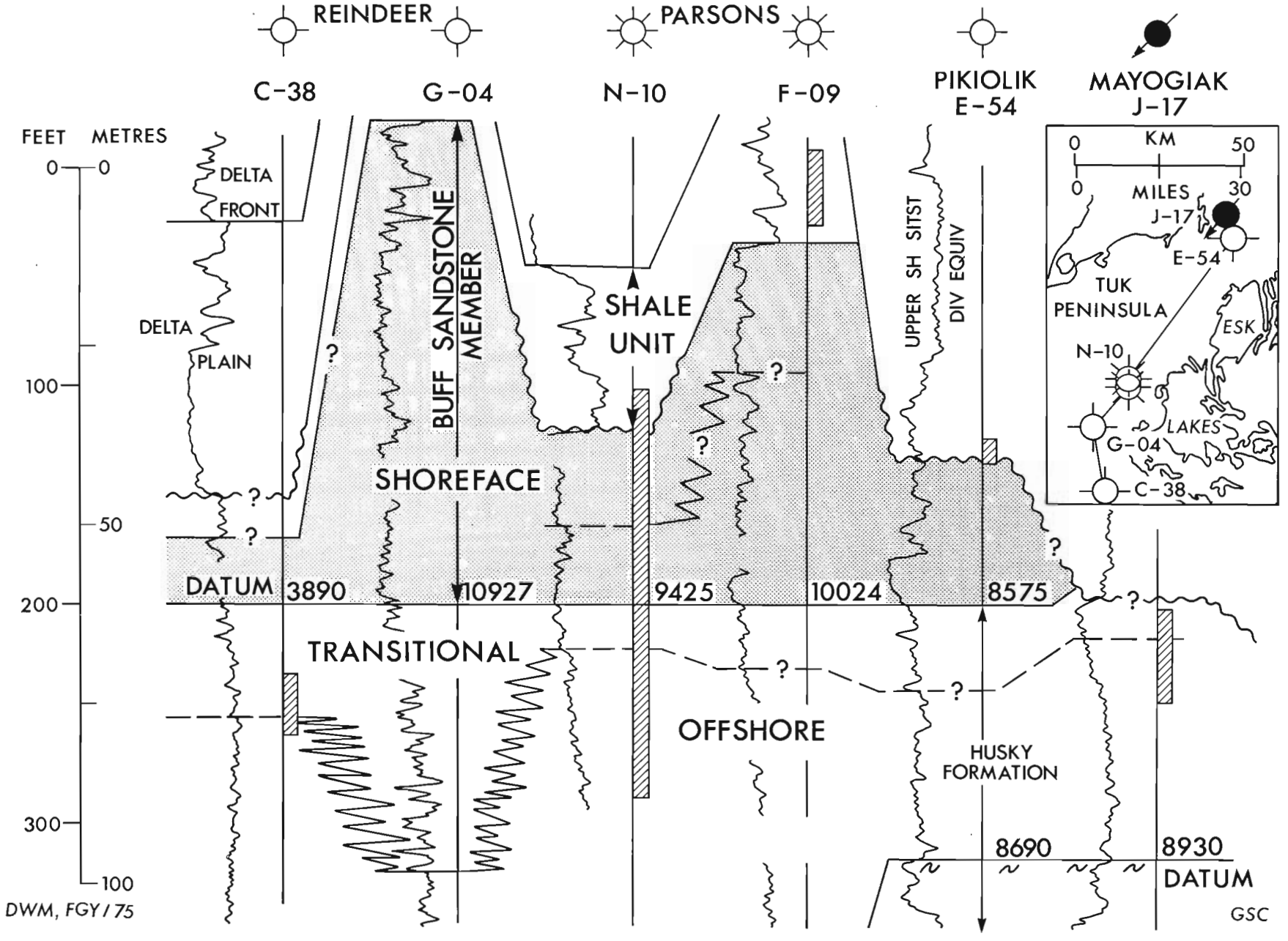

Figure 42. 4. Stratigraphic profile.

Delta Plain (Tuktoyaktuk Peninsula) and Nearshore (Aklavik Range) Facies

The delta-plain facies is characterized by the presence of channel sandstone units and thin coal beds. In the subsurface area of central Tuktoyaktuk Peninsula this facies thickens southwestward from 76.3 m (250 ft.) in the IOE Tuk F-18 borehole (Fig. 42.1, Lat. 69°17'29", Long. 133°04'01") to about 183 m (600 ft.) in Gulf Mobil East Reindeer G-04 and A-01 boreholes (Fig. 42.8). In Gulf Mobil East Reindeer A-01 borehole (Fig. 42.1, Lat. 68°40'13", Long. 134°00'31") the gamma ray log in conjunction with sample cuttings indicates that porous, stacked channel sands interstratified with thin, organic-rich shales occur at the base of the unit, suggesting proximity to a fluvial source as these deposits grade to the northeast into delta-plain deposits in the Gulf Mobil East Reindeer G-04 borehole (Fig. 42.8). Other wells on this profile exhibit a basal porous sandstone unit that has a sharp basal contact, and is overlain by thin coal beds which in the Gulf Mobil Parsons F-09 borehole consist of high volatile C to high volatile A, bituminous coal (Myhr and Gunther, 1974, Fig. 2).

Between channel sands are floodbasin deposits as illustrated by lithologies and sedimentary structures from the lower part (5.2 m, 17 ft.) of core no. 2 (Fig. 42.10) in the Gulf Mobil Parsons N-10 borehole (Shawa and others, Fig. 6 *in* Shawa, 1974). The floodbasin facies consists of a mixture of very fine sandstone, siltstone, mudstone and coal. The sediments contain rootlets, minor burrows, scours, soft-sediment flowage, and both coarsening- and fining-upward cycles; the latter capped by a thin coal bed in core no. 2. The argillaceous component and impervious nature of these lithologies makes them easy to identify on the Gamma Ray-Sonic (Fig. 42.8) and Spontaneous Potential logs.

Distributary-channel sandstones, in part conglomeratic, occur at the top of core no. 2 (Fig. 42.10) and throughout core no. 1 (Fig. 42.8; Gulf-Mobil Parsons N-10). The fluvial facies displays tabular cross-stratification with very coarse grained to conglomeratic laminae and minor ripple-drift cross-lamination in fine-grained sandstone. These sandstones are easily recognized on well-logs by their blocky gamma ray log character and abrupt basal contacts. In core no. 1 mudstone beds containing deformed silt lenses are associated with these fluvial sandstones, and possibly represent levée or overbank deposits.

In Martin Creek (Fig. 42.13) the delta-plain facies is underlain by 38 m (125 ft.) of nearshore deposits (White Sandstone member, Jeletzky, 1958) that consists of light grey weathering, very fine, friable sandstone, with minor ferruginous burrows (horizontal and vertical) and ferruginous sandstone. Bedding thickness is variable (3 cm to 1 m), commonly massive, and in part exhibits faint, low-angle cross-stratification. This member contains near its top a 3-m thick zone of interstratified granular conglomeratic sandstone, black carbonaceous shale, and maroon-weathering, granular sandstone. A thick bed of the latter displays the following in upward sequence: horizontal planar lamination, high-angle cross-lamination (bimodal and bipolar), further planar lamination, gradational into wavy ripple lamination (tidal or estuarine channel). These deposits are conformably overlain by the Coal-bearing division (Jeletzky, 1960 and 1975) which lithologically is representative of a delta-plain lithofacies.

North of Martin Creek, in the eastern part of "Grizzly Gorge" (Fig. 42.13) the White Sandstone member is 27 m (89 ft.) thick and is overlain by the Upper Shale-Siltstone division; the basal 22 m of the latter consists of sandy to silty mudstone with concretionary horizons representing a shale-out of the Coal-bearing division (Jeletzky, 1975, Fig. 8). Moreover, the nearshore deposits grade rapidly westward to estuarine deposits, consisting of limonitic, poorly sorted sandstones, containing rootlets, *Ophiomorpha*, ironstone concretions, dark grey shale, and minor pebble-conglomerate beds.

Delta Front and Prodelta Facies

In the subsurface, the thickness of these facies combined is 27.5 m (90 ft.) to 213.5 m (700 ft.) thick, gradually thickening toward the southwest where it intertongues with delta-plain deposits in the Gulf Mobil East Reindeer A-01 borehole (Fig. 42.8). The delta-front facies contains no coal and much less sandstone than the delta-plain facies, and is overlain by and interfingers with silty mudstone and shale of the prodelta facies.

The delta-front and prodelta to interdeltaic facies consists of alternating arenaceous and shaly units. Sandstone units are very fine to, in places, medium grained, moderately well sorted, laminated and porous (e.g. core no. 1, Gulf Mobil Parsons F-09 borehole, Fig. 42.8). The shaly units tend to be evenly to irregularly bedded, in part bioturbated, and interbedded with laminated siltstone. Many of these beds comprise parallel-to-burrowed sets, common in distal delta-front, shallow, open shelf and lower shoreface environments (Goldring and Bridges, 1973). For example, interbedded arenaceous and pelitic rocks in cores no. 4 and no. 5 from the Gulf Mobil East Reindeer G-04 borehole probably were deposited in a relatively shallow, open shelf environment near an active site of deltaic deposition where brackish to marine conditions prevailed (Myhr, 1974).

Marine - Upper Shale-Siltstone division and equivalents

Following deposition of the arenaceous wedge many of the pre-Mesozoic paleotopographic highs along the Aklavik Arch Complex were uplifted. This erosional interval in late Neocomian time was followed by a regional marine transgression resulting in the deposition of basal arenites, interstratified and grading upward into mudstone and shale. The stratigraphic relationships of this unit were described initially by Jeletzky (1958, 1960) from the Aklavik Range that flanks the modern Mackenzie Delta. Boreholes in this area (Fig. 42.1; Shell Aklavik A-37, and Shell Beaverhouse Creek H-13, Union Aklavik F-17,

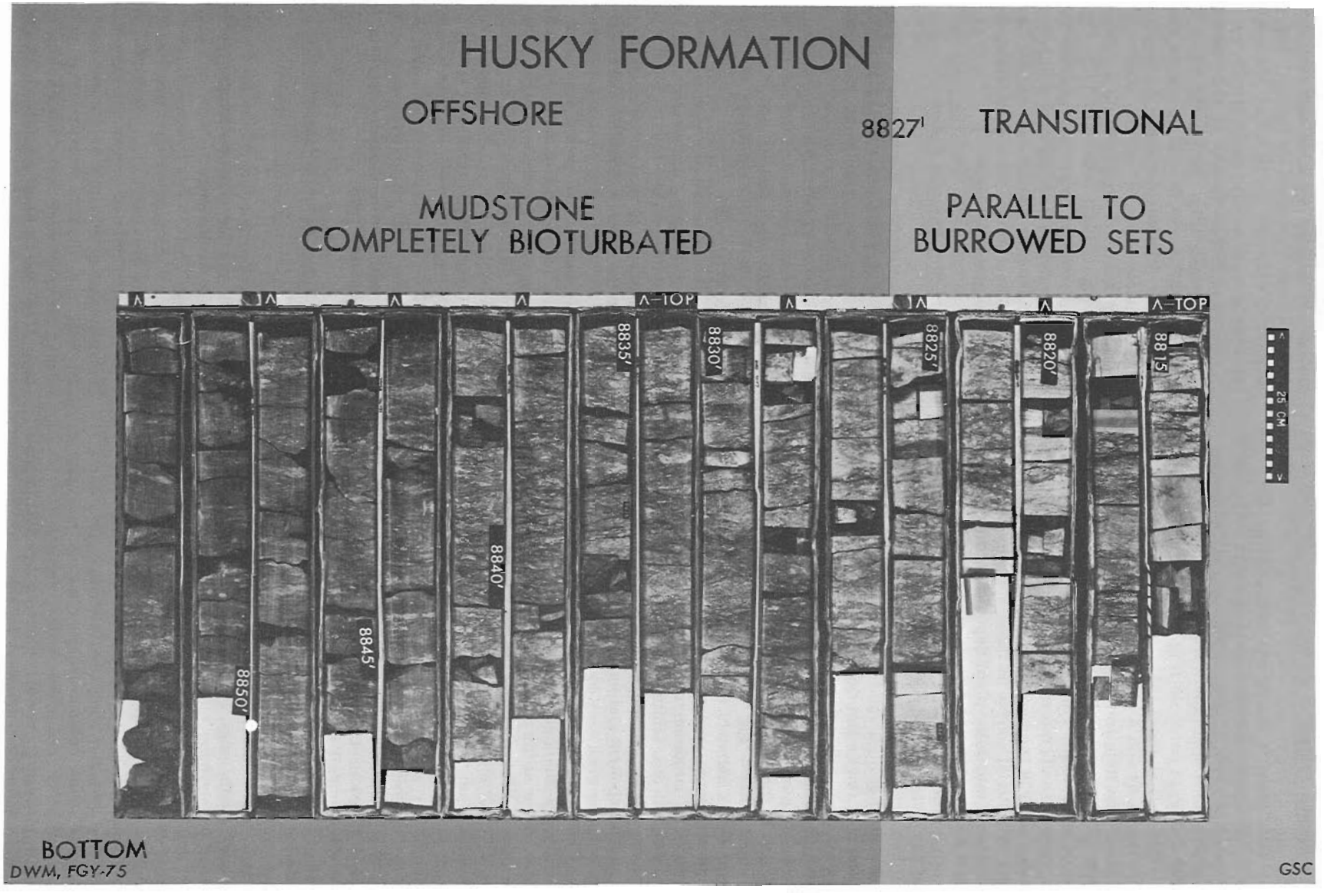

Figure 42.5. IOE Majogiak J-17, Core No. 7.

Lat. 68°06'20", Long. 135°04', and Union Aklavik F-38, Lat. 68°07'15", Long. 135°09'11") may all contain the pre-Upper Shale-Siltstone division unconformity. The evidence for this is tenuous and based only on litho-stratigraphic correlations with near-surface sections and the absence to near-absence of deltaic coal-bearing lithofacies. Conversely, an upward change in facies, expressed by condensation of the Coal-bearing division followed by a possible depositional hiatus, may explain the facies relationships observed in this area. Palynological evidence obtained from sample cuttings of the Banff-Aquitaine-Arco Rat Pass K-35 borehole (Fig. 42.1; Brideaux *in* Barnes, 1974, and Brideaux and Fisher, in press) approximately 25 km (≈16 miles) southwest of the Union Aklavik boreholes indicates that Hauterivian sediments unconformably overlie Upper Jurassic shales and arenites. This stratigraphic relationship is expressed similarly in the Union Aklavik F-17 borehole, based on lithological and well-log evidence.

In the IOE Pikiolik E-54 borehole (Fig. 42.1; Lat. 69°23'15", Long. 132°44'35") the Upper Shale-Siltstone division equivalents rest with angular unconformity on very fine arenites of the Buff Sandstone member (Fig. 42.4). The cored interval (Fig. 42.11) consists of a very fine shoreface sandstone that is cross-laminated and non-bioturbated. The sandstone unit is overlain abruptly by lithic conglomerate and sandstone that grades upward into completely bioturbated, silty mudstone of offshore origin. The age of this facies is Hauterivian-Aptian, possibly no younger than Barremian (W. W. Brideaux, pers. comm., 1974). To the north in the IOE Mayogiak J-17 borehole (Fig. 42.4) and southeast in the IOE Tuktu O-19 borehole (Fig. 42.1; Lat. 69°8'55"N, Long. 132°48'17"W) the Upper Shale-Siltstone division unconformably overlies respectively the transition facies of Late Jurassic age (Chamney *in* Barnes *et al.*, 1974 and Jeletzky *in* Brideaux *et al.*, 1975) and a somewhat older glauconitic, sandy mudstone of the Husky Formation, also of Late Jurassic age (Chamney *in* Barnes *et al.*, 1974).

Paleogeography

The areal distribution of these lithogenetic units is portrayed for three time-stratigraphic intervals. The paleogeographic maps are tentative interpretations, subject to changes necessitated by improvements in paleontologic and lithologic controls.

Berriasian

The oldest interval of the sequence is the Berriasian Stage represented by widespread shoaling following deposition of Upper Jurassic marine mudstone and siltstone over a large area (Fig. 42.12). Well-sorted, very fine and fine grained littoral sandstone of the Lower Sandstone division and Buff member is the characteristic lithofacies. The sand was derived from the head of Vittrekwa Embayment and, in part, from deltaic complexes along the northern flank of Rat Uplift (Treeless Creek area, Jeletzky, 1975, Fig. 11). The sands formed barrier island and strandline complexes around Cache Creek Uplift and shale out farther west and north. An extensive facies belt of bioturbated, argillaceous, silty sandstone (offshore-transitional) was formed basinward of the strandline complexes in northwestern Richardson Mountains.

The Berriasian sandstones consist of about 85 per cent quartz grains and 15 per cent chert and rock fragments over most of the area, and are silica-cemented west of Cache Creek Uplift.

Valanginian

Beginning in the Valanginian Stage, large deltaic complexes were formed along the northwest shelf of the Aklavik Arch Complex, partly in response to tectonic uplifts of the Arch (Fig. 42.13). The locus of deltaic deposition shifted numerous times, and this map reflects only general conditions during this time. The greatest thickness of deltaic sediments appears to have been deposited in the area north of Inuvik, as evidenced by facies and thickness of the Neocomian clastic wedge in the Gulf Mobil East Reindeer A-01 borehole (Fig. 42.8). Thinner deltaic wedges flank Rat Uplift. West of Cache Creek Uplift the bluish-grey Shale division represents open-marine conditions. Uplifts during mid-Valanginian time and westward facies progradation probably caused closure of the strait between Cache Creek Uplift and Rat Uplift, which caused restricted marine or estuarine conditions to develop in the resulting bay.

Sandstones are very fine to very coarse grained and moderately porous in the Parsons area, but generally are fine to very fine grained west of the Aklavik Range and tightly cemented due to quartz overgrowths.

Hauterivian

In Hauterivian time deltaic deposition shifted away from the present area of Tuktoyaktuk Peninsula toward the southwest, with sediments being deposited in the Aklavik Range and Vittrekwa River areas (Fig. 42.14; and Jeletzky, 1975, Fig. 13). It seems likely that further uplifts of Cache Creek Uplift occurred, cutting off one delta depocentre from the other. Thick barrier complexes present in northwestern Richardson Mountains probably were fed by north-flowing currents carrying sand from a southern prograding delta system. The barrier system barred a large lagoon in northern Richardson Mountains, and it periodically received sediments from the southern delta complex, and possibly Cache Creek Uplift.

The "Aklavik" delta system appears to have filled the former embayment with coaly, arenaceous sediments, providing a source for the thick delta-front facies in the Parsons Lake area. The sandstones of the Coal-bearing division are pebbly, and fine to coarse grained, similar to those in the southern deltaic lithotope. They consist of about 80 per cent quartz and 20 per cent chert and other rock fragments and, northward along the western flank of Cache Creek Uplift, they become gradually finer and enriched to almost 100 per cent quartz.

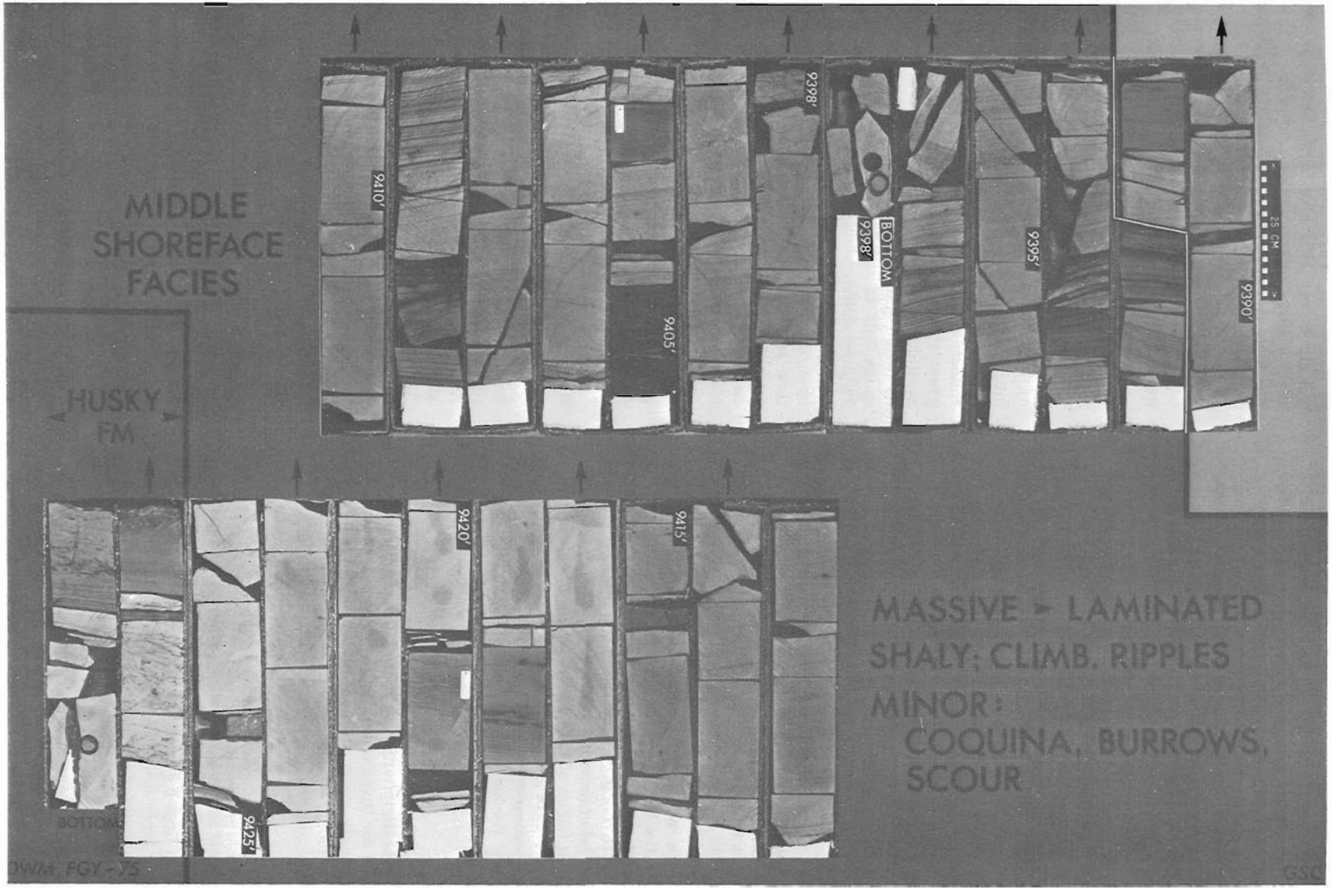

Figure 42. 6. Gulf Mobile Parsons N-10, Core Nos. 6 and 7.

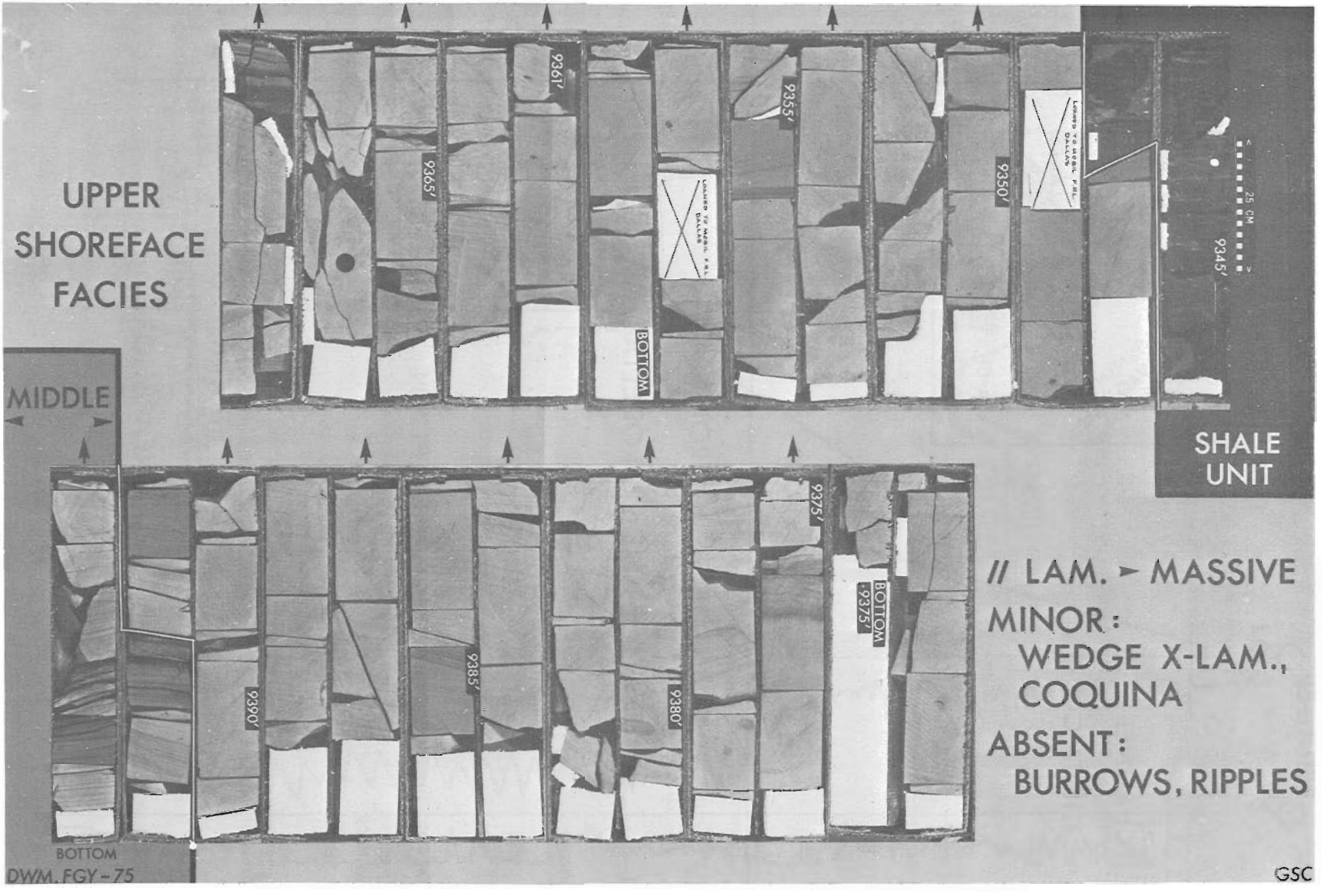

Figure 42. 7. Gulf Mobil Parsons N-10, Core Nos. 4 to 6.

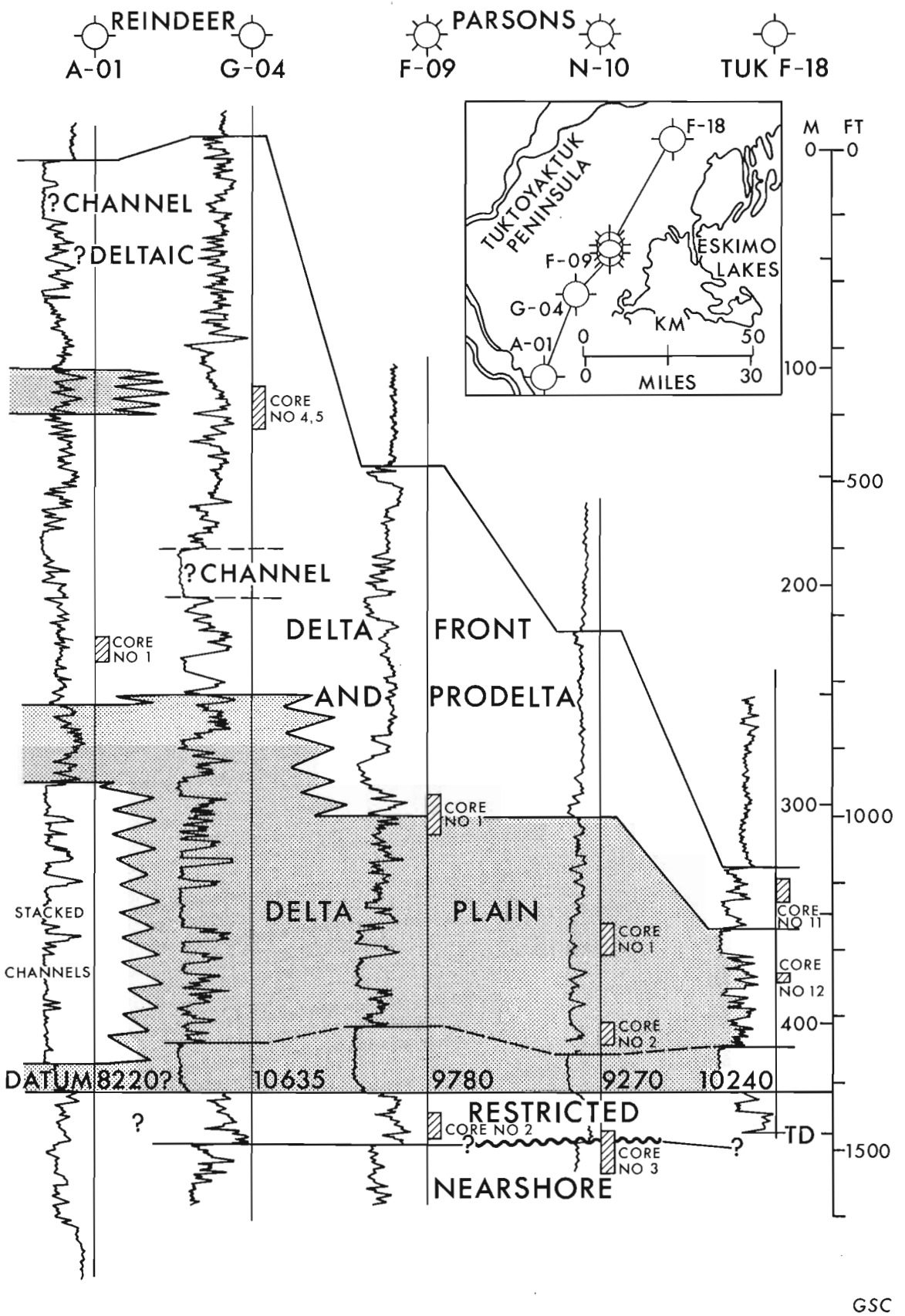

Figure 42. 8. Stratigraphic profile.

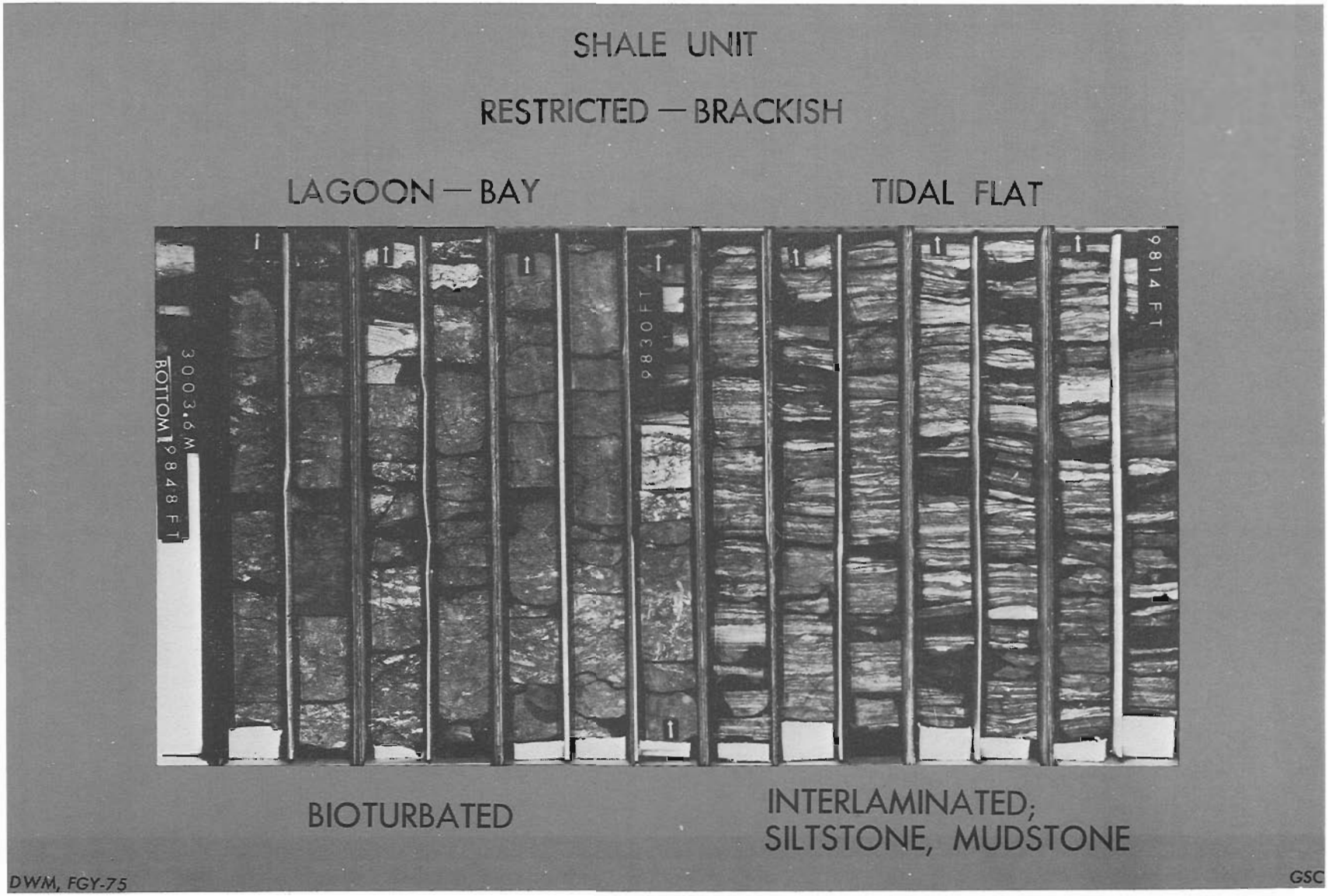

Figure 42.9. Gulf Mobil Parsons F-09, Core No. 2.

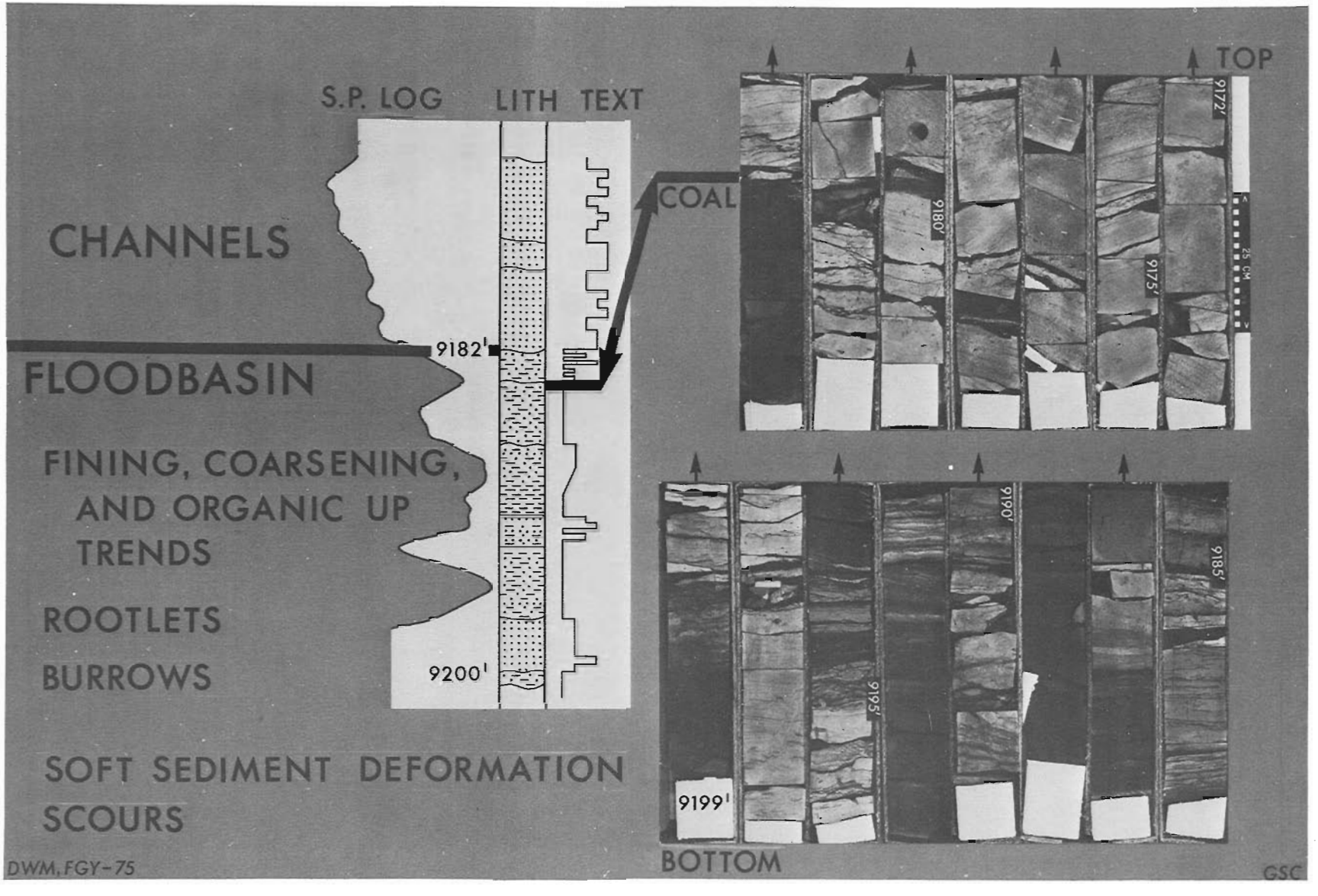

Figure 42.10. Gulf Mobil Parsons N-10, Core No. 2.

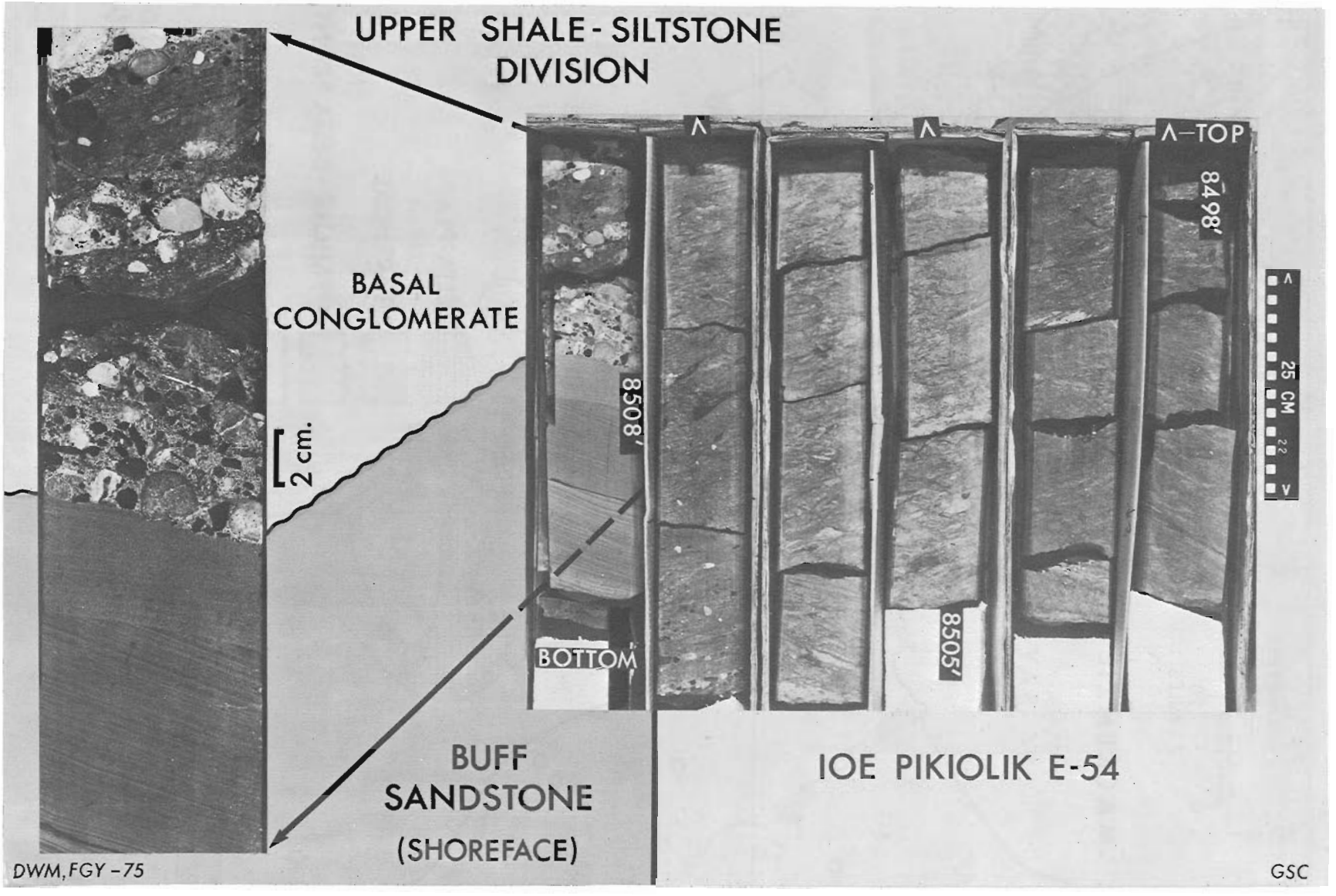

Figure 42. 11. IOE Pikiolik E-54, Core No. 5.

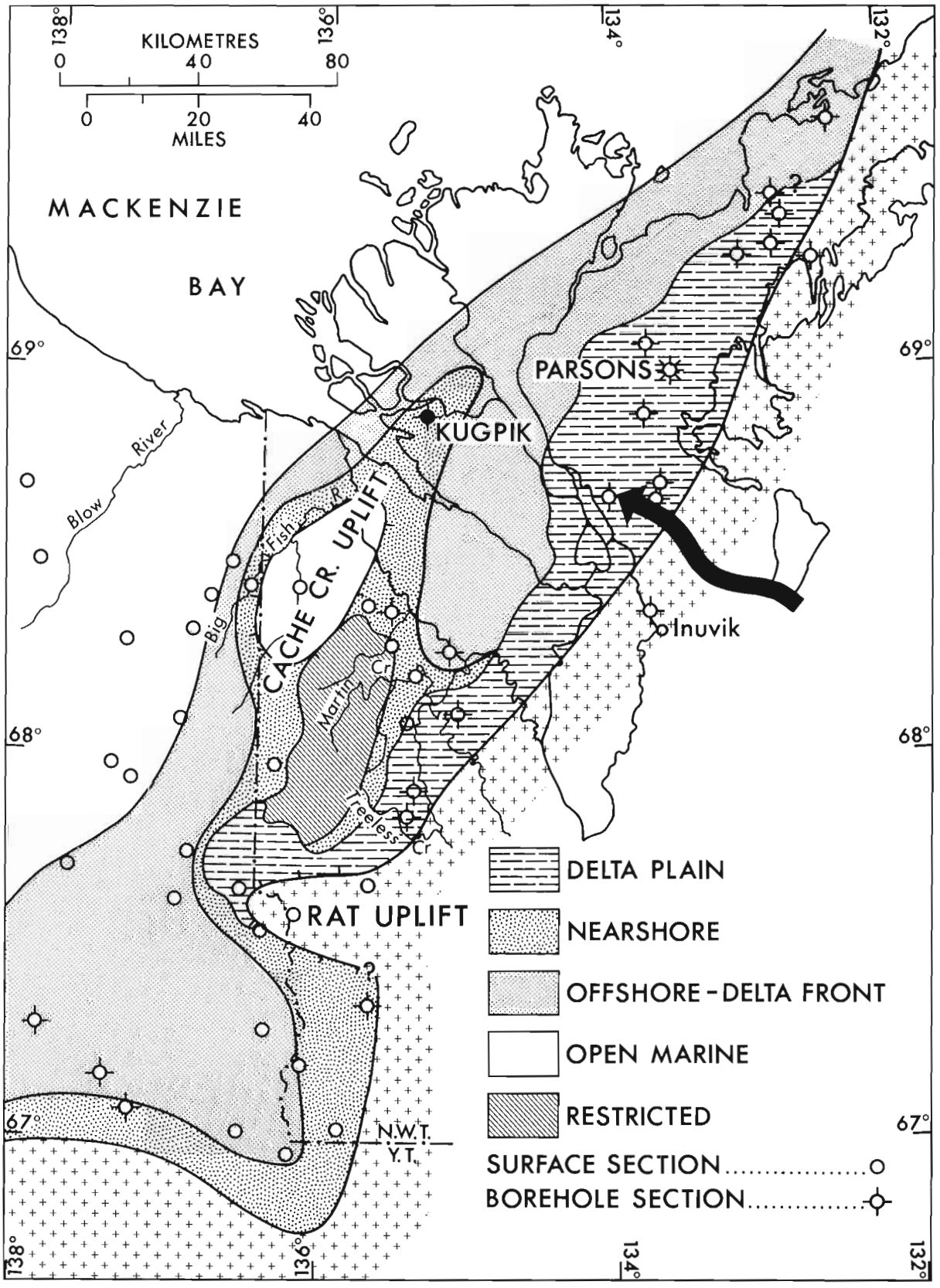

Figure 42. 12. Berriasian paleogeography.

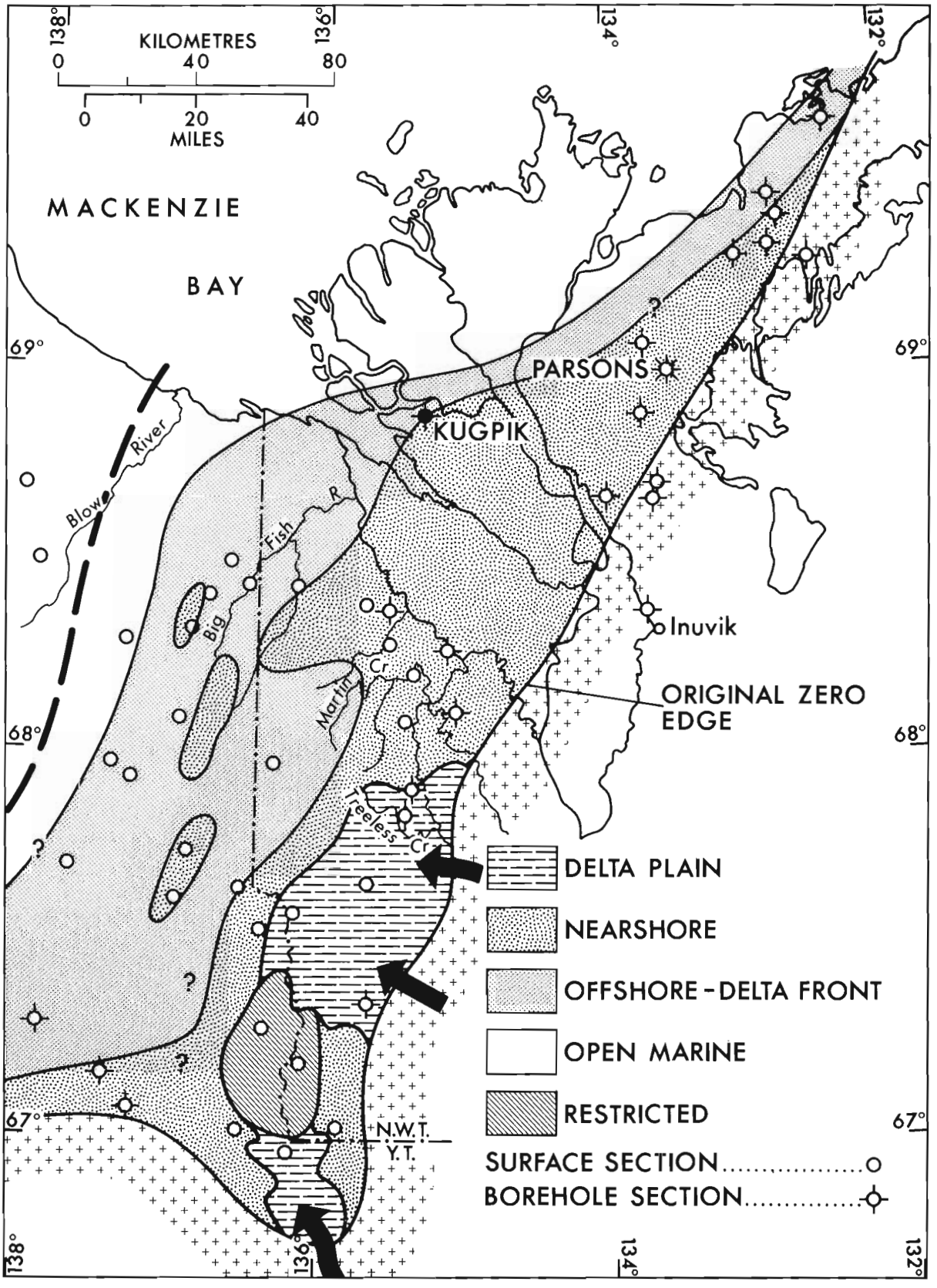

Figure 42. 13. Valanginian paleogeography

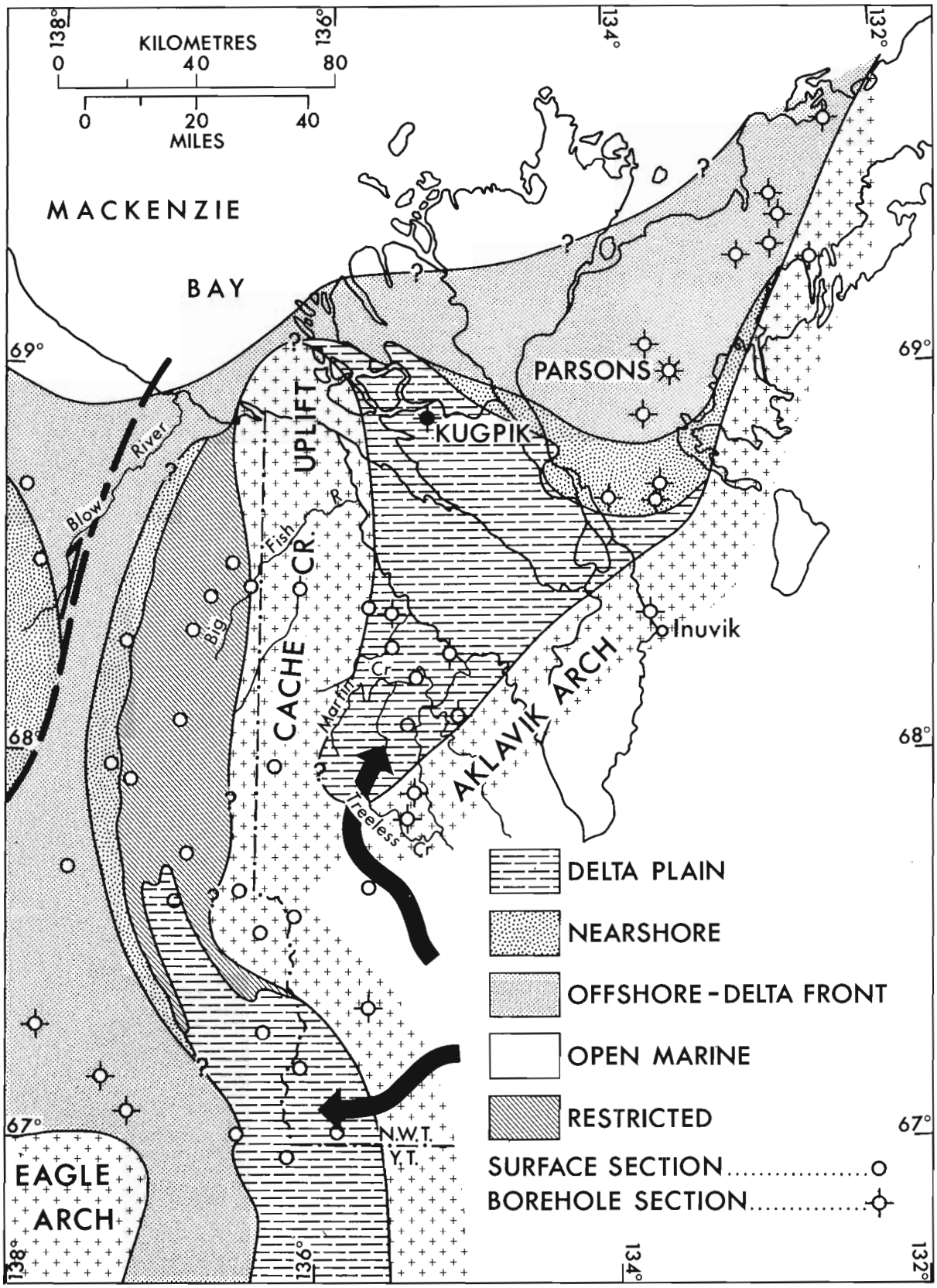

Figure 42.14. Hauterivian paleogeography.

The Kaltag-Rapid Fault Zone appears to have become active during this time interval (Young, 1974), and resulted in uplift of the eastern nose of the Brooks Range Geanticline and a northeastward regression of a shoreline sand complex. The original relationship of this complex with facies in the Richardsons is obscure because of subsequent right lateral movements on the fault, but presumably the two shoal areas were separated by an open marine strait of moderate width for wave development.

Hydrocarbon Prospects

Hydrocarbon prospects in the mountainous areas are negligible because of erosional breaching, tectonism, and supermature organic maturation conditions. Coals in some outcrop areas are of anthracite grade, whereas those in the Parsons F-09 borehole are high volatile bituminous.

Drillstem tests yielded minor gas shows from silty sandstones in the Chevron Ridge F-48 and Chevron Whitefish J-70 boreholes of northeastern Eagle Plain (Fig. 42.1). Further drilling around the Eagle Arch (Young, 1975) may encounter hydrocarbons in porous shoreline sands (Figs. 42.12 and 43.13).

Proven and probable reserves of gas in the Parsons Field have been stated as 1.5 trillion cubic feet by Sproule and Associates (1974). Prospects are good for finding more hydrocarbons beneath Mackenzie Delta and southwestern Tuktoyaktuk Peninsula because of favourable organic maturation conditions, the prsence of cap-rocks, the existence of interfingering deltaic and marine sediments over a large area, and the reported occurrence of faults and established hydrocarbons in the area (Coté *et al.*, 1975).

References

Barnes, C.R., Brideaux, W.W., Chamney, T.P., Clowser, D.R., Dunay, R.E., Fisher, M.J., Fritz, W.H., Hopkins, William S., Jr., Jeletzky, J.A., McGregor, D.C., Norford, B.S., Norris, A.W., Pedder, A.E.H., Rauwerda, J., Sherrington, P.E., Sliter, W.V., Tozer, E.T., Uyeno, T.T., and Waterhouse, J.B.
1974: Biostratigraphic determinations of fossils from the subsurface of the Northwest and Yukon Territories; Geol. Surv. Can., Paper 74-11, p. 6-11, 15-16.

Bernard, H.A., LeBlanc, J.F., and Major, C.F.
1962: Recent and Pleistocene geology of southeast Texas, field excursion No. 3; *in* Geology of the Gulf Coast and central Texas and guidebook of excursions; Geol. Soc. Am., Ann. Meeting Guidebook, p. 175-224.

Brideaux, W.W., Chamney, T.P., Dunay, R.E., Fritz, W.H., Hopkins, William S., Jr., Jeletzky, J.A., McGregor, D.C., Norford, B.S., Norris, A.W., Pedder, A.E.H., Sherrington, P.E., Sliter, W.V., Sweet, A.R., Uyeno, T.T., and Waterhouse, J.B.
1975: Biostratigraphic determinations of fossils from the subsurface of the District of Franklin and Mackenzie; Geol. Surv. Can., Paper 74-39.

Brideaux, W.W. and Fisher, M.J.
1975: Upper Jurassic - Lower Cretaceous dinoflagellate assemblages from Arctic Canada; Geol. Surv. Can., Open File Rept. 253.

Coté, R.P., Lerand, M.M., and Rector, R.J.
1975: Geology of the Lower Cretaceous Parsons Lake Gas Field, Mackenzie Delta, Northwest Territories; *in* Canada's Continental Margins and Offshore Petroleum Exploration, C.J. Yorath, ed.; Can. Soc. Pet. Geol., Mem. no. 4, p. 613-632.

Davies, D.K., Ethridge, F.G., and Berg, R.R.
1971: Recognition of Barrier Environments; Am. Assoc. Pet. Geol., Bull., v. 55, p. 550-565.

Goldring, R. and Bridges, P.
1973: Sublittoral sheet sandstones; J. Sediment. Petrol., v. 43, p. 736-747.

Howard, J.D.
1972: Trace fossils as criteria for recognizing shorelines in stratigraphic record in recognition of ancient sedimentary environments; J.K. Rigby and W.K. Hamblin, eds., Soc. Econ. Paleontol. Mineral., Spec. Publ. No. 16, p. 215-225.

Jeletzky, J.A.
1958: Uppermost Jurassic and Cretaceous rocks of Aklavik Range, northeastern Richardson Mountains, Northwest Territories; Geol. Surv. Can., Paper 58-2, 84 p.

1960: Uppermost Jurassic and Cretaceous rocks, east flank of Richardson Mountains between Stony Creek and lower Donna River, Northwest Territories; Geol. Surv. Can., Paper 59-14, 31 p.

1961: Upper Jurassic and Lower Cretaceous rocks, west flank of Richardson Mountains between headwaters of Blow River and Bell River; Geol. Surv. Can., Paper 61-9, 42 p.

1975: Jurassic and Lower Cretaceous Paleogeography and Depositional Tectonics of Porcupine Plateau, adjacent areas of northern Yukon and those of Mackenzie District; Geol. Surv. Can., Paper 74-16, p. 30-34 and Figs. 8-13.

Myhr, D. W.
1974: A shallow shelf coastal environment interpreted from lithostratigraphy of Lower Cretaceous cores in the Gulf Mobil East Reindeer G-04 borehole, N. W. T.; *in* Report of Activities, Part B, Geol. Surv. Can., Paper 74-1B, p. 282-286.

Myhr, D. W. and Gunther, P. R.
1974: Lithostratigraphy and coal reflectance of a Lower Cretaceous deltaic succession in the Gulf Mobil Parsons F-09 borehole, N. W. T.; *in* Report of Activities, Part B, Geol. Surv. Can., Paper 74-1B, p. 24-28.

Sproule, J. C. and Associates
1974: Submission to the National Energy Board by Canadian Arctic Gas Pipeline Ltd.; Gas Supply Reserves, Section 5, J. C. Sproule Delta Study, p. 23 and 32.

Swift, D. J. P.
1970: Quaternary shelves and return to grade; Marine Geol., v. 8, p. 5-30.

Yorath, C. J., Myhr, D. W., and Young, F. G.
1975: Geology of the Beaufort-Mackenzie Basin; Geol. Surv. Can., Open File Rept. 251, Figs. 2, 3, and 7.

Young, F. G.
1974: Cretaceous stratigraphic displacements across Blow Fault Zone, Northern Yukon Territory; *in* Report of Activities, Part B, Geol. Surv. Can., Paper 74-1B, p. 291-296.

1975: Stratigraphic and sedimentologic studies in northeastern Eagle Plain, Yukon Territory; *in* Report of Activities, Part B, Geol. Surv. Can., Paper 75-1B, p. 309-323.

Young, F. G. and Myhr, D. W.
1975: Lower Cretaceous (Neocomian) Sandstone Sequence of Mackenzie Delta and Richardson Mountains area; *in* Joint CSPG-CSEG Annual Convention, Program and Abstracts, Calgary, 1975, p. 92.

43.

THE PERMIAN BELCHER CHANNEL FORMATION AT GRINNELL PENINSULA, DEVON ISLAND

Projects 680064, 720060

W. W. Nassichuk and G. R. Davies
Institute of Sedimentary and Petroleum Geology, Calgary

Introduction

During the summer of 1974 detailed studies on Carboniferous and Permian rocks in selected areas of Ellesmere and Devon Islands were completed. On Devon Island, Carboniferous and Permian rocks are confined to a rather narrow belt near the northern coast of Grinnell Peninsula (Fig. 43. 1); that belt approximates the southern margin of the Sverdrup Basin. Carboniferous and Permian formations that outcrop on northern Grinnell Peninsula include the Emma Fiord Formation which contains the oldest rocks (Upper Mississippian; Viséan) in the Sverdrup Basin and which is preserved locally in older Paleozoic structural depressions. The Emma Fiord Formation contains mainly thin-bedded nonmarine shale and siltstone and unconformably overlies Ordovician carbonates of the Cape Storm Formation in the Franklinian Geosyncline. The Emma Fiord is, in turn, overlain by a redbed sequence of conglomerate and sandstone belonging to the Middle Pennsylvanian and younger Canyon Fiord Formation. The Canyon Fiord varies in thickness from a feather edge to about 100 m on Grinnell Peninsula and rests unconformably on Devonian or older rocks where the Emma Fiord is absent. The Canyon Fiord Formation on Grinnell Peninsula is overlain invariably by a rather thin (less than 180 m; 700 ft.) succession of thin bedded, Lower Permian sandstone and limestone of the Belcher Channel Formation, the subject of this report. In some places the Canyon Fiord is either absent or is overstepped by the Belcher Channel

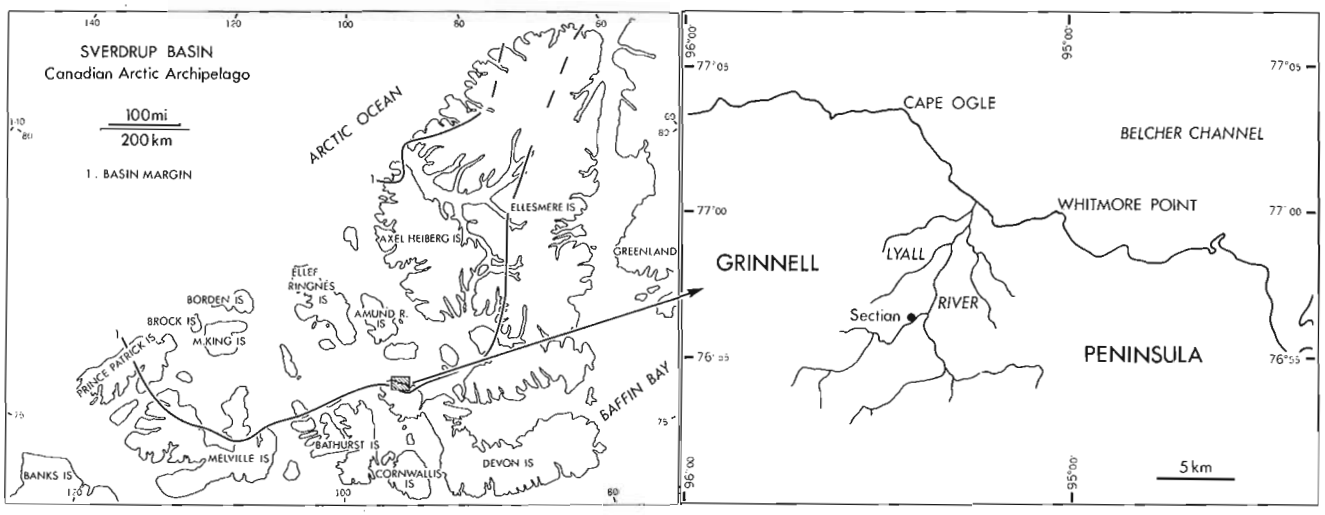

Figure 43. 1. Locality map of the Canadian Arctic Archipelago, with detail of northern Grinnell Peninsula on Devon Island showing location of the measured section of the Belcher Channel Formation described in this paper.

Figure 43. 2

Aerial view of northern Grinnell Peninsula looking eastward from just east of the Lyall River at approximately the same latitude as the measured section (Fig. 43. 1). Beds of the Belcher Channel Formation (BC) and Canyon Fiord Formation (CF), resting unconformably on Ordovician carbonates (Oc), dip northward at 5° to 10° toward the axis of the Sverdrup Basin. Ridges in the distant left also are of Belcher Channel Formation, but contact outlines have not been extended to cover that area because of structural complexities. The more resistant ridges in the Belcher Channel Formation at left foreground are sandy limestones.

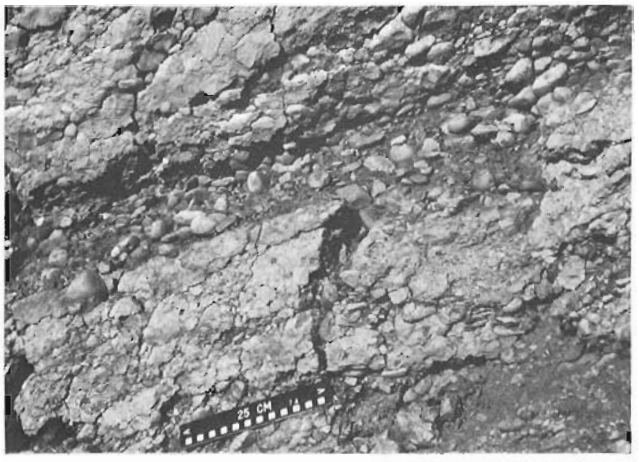

Figure 43. 3.

Coarse, poorly sorted, polymictic conglomerate of the Canyon Fiord Formation on northern Grinnell Peninsula. Clasts mainly are limestone derived from underlying Ordovician rocks. Predominant surface weathering colour of these conglomerates is red.

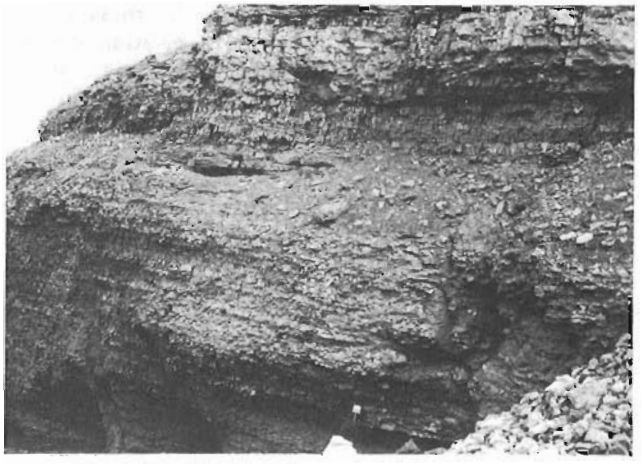

Figure 43. 4.

The upper sandy limestone unit of the Belcher Channel Formation (top of section, Fig. 43. 6) exposed in a creek north of the measured section. The irregular to wavy bedding in this exposure is typical of sandy limestone and purer limestone units in this formation on northern Grinnell Peninsula.

Figure 43. 5.

Aerial view of poorly exposed Belcher Channel Formation at the measured section (Fig. 43. 1). The three more resistant ledges (arrows) are of sandy limestone, and correspond with the three limestone units between 75 and 100 m levels in the measured section (Fig. 43. 6).

Formation which then directly overlies Devonian or older rocks of the Franklinian Geosyncline. Over much of the northern coastal region of Grinnell Peninsula, the Belcher Channel Formation terminates upward as a Recent erosional surface but, locally, in the vicinity of Lyall River, it is overlain conformably by slightly more than 60 m (200 ft.) of loosely consolidated sandstone belonging to the uppermost Lower Permian (Roadian) Assistance Formation. The type section of the Assistance Formation, described by Harker and Thorsteinsson (1960), is directly above the type section of the Belcher Channel Formation at Lyall River. For the present study, exposures of the Belcher Channel Formation were examined about 1. 6 km (1 mile) to the west of the type section; data presented here are designed to complement earlier published descriptions of the Belcher Channel Formation in the type area.

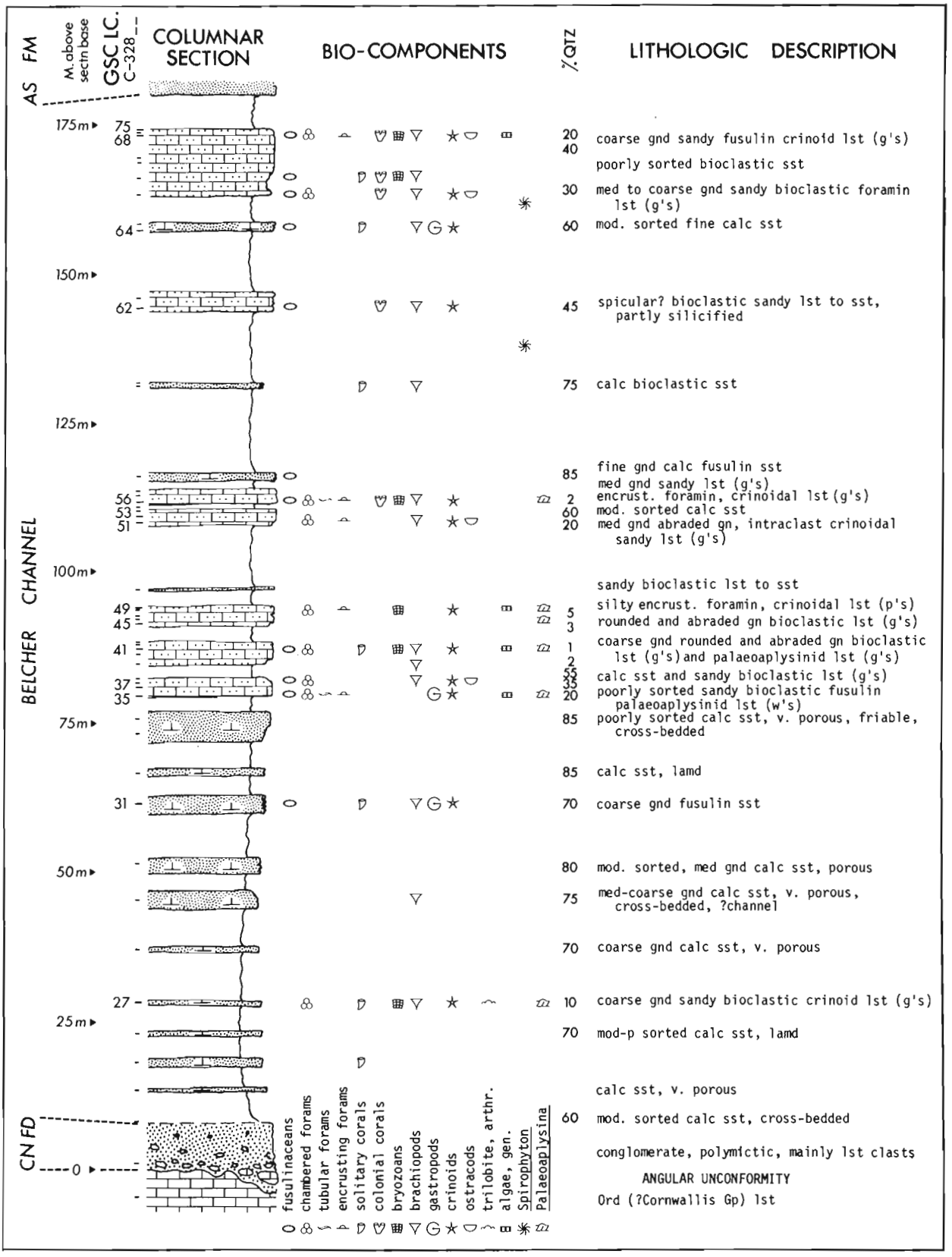

Figure 43.6. Summary of the measured stratigraphic section through the Canyon Fiord Formation (CN FD) and Belcher Channel Formation, into the base of the Assistance Formation (AS). GSC locality numbers are prefixed by C-328 (27 in columnar section = C-32827); unnumbered dashes in same column are samples not referred to directly in this paper. Per cent quartz includes all non-carbonate grains. Covered intervals probably are poorly cemented (non-calcareous) fine grained sandstones. Abbreviations are: w = wackstone, p = packstone, g = grainstone- textural terms of Dunham (1962).

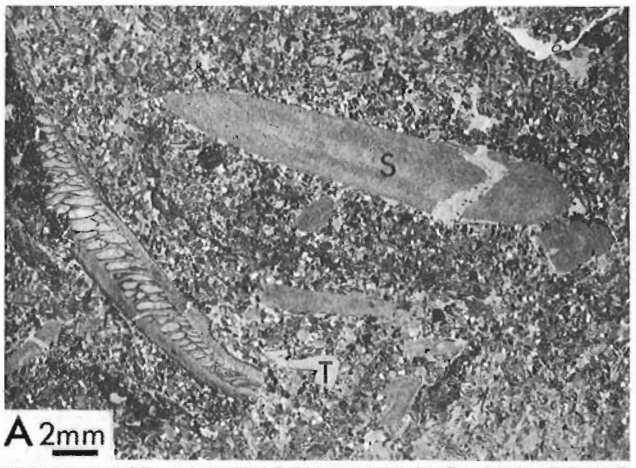

Figure 43. 7A.

Photomicrograph of sandy bioclastic limestone with a variable packstone to grainstone texture. Larger bioclasts include echinoderm spines (s), solitary corals and a fragment of a trilobite or other arthropod (T). Quartz grains form about 10 per cent by volume of the sample. Cement is sparry calcite, often epitaxial on crinoid clasts. GSC loc. C-32827, 21 m above the base of the Belcher Channel Formation.

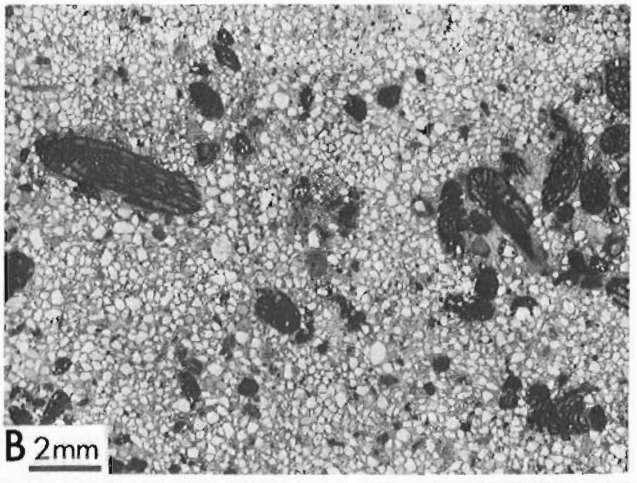

Figure 43. 7B

Photomicrograph of bioclastic fusulinacean sandstone composed of coarse-grained quartz sand and tests of fusulinacean foraminifers. Foraminifers are corroded by post-depositional solution-compaction. Cement is sparry calcite. GSC loc. C-32831, 55 m above base of the Belcher Channel Formation.

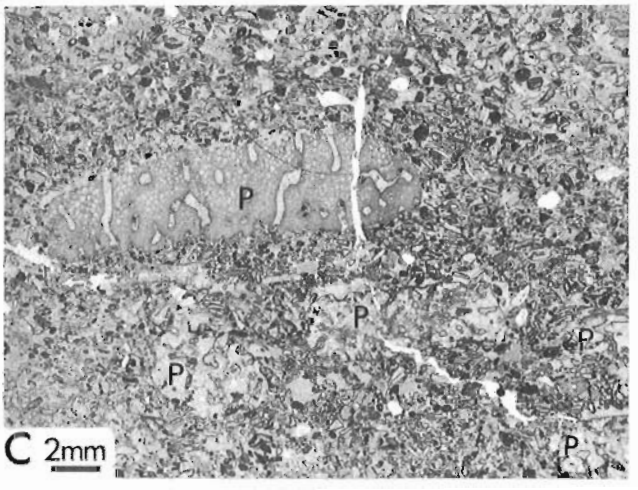

Figure 43. 7C.

Photomicrograph of abraded and micritized grain, palaeoaplysinid grainstone, with many smaller abraded and micritized bioclasts and unidentifiable grains, and larger clasts of the enigmatic organism *Palaeoaplysina* (P). The cellular internal structure and canals of *Palaeoaplysina* (Davies and Nassichuk, 1973) are preserved clearly in the larger clast at left centre. GSC loc. C-32841, 80 m above base of the Belcher Channel Formation.

Belcher Channel Formation - Geological Setting

The Belcher Channel Formation, as defined by Harker and Thorsteinsson (1960), consists of a succession of limestone, sandstone and conglomerate some 6. 4 km (4 miles) upstream from the mouth of Lyall River on Grinnell Peninsula (Fig. 43. 2). Another published description, based on earlier work, was provided by Thorsteinsson (1963) who had studied the type section at Grinnell Peninsula while attached to the Geological Survey of Canada's "Operation Franklin" in 1955. The original definition was modified by Nassichuk (1965), who recognized that reddish-weathering conglomerate (Fig. 43. 3) and sandstone units, that range from only a few feet to a few hundred feet in thickness near the base of the formation in the type area, belong in the Canyon Fiord Formation. The Canyon Fiord was defined on north-central Ellesmere Island by Troelson (1950). Generally it is separated from the Belcher Channel by a prominent disconformity, reflecting nearshore transgressive onlap. Exposures of the Belcher Channel and Canyon Fiord formations are extensive along the eastern and southern margins of the Sverdrup Basin, where they occupy Thorsteinsson's (1974) Marginal Clastic and Carbonate Belt. Whereas the Belcher Channel is particularly thick in eastern regions of the

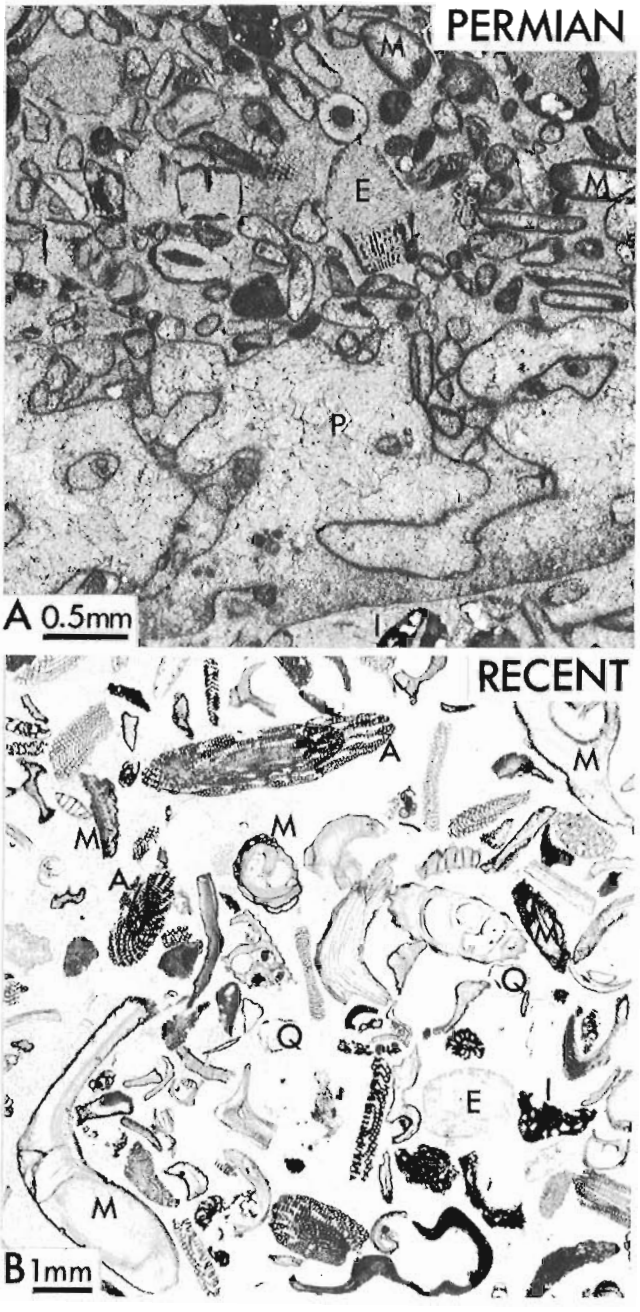

A: Photomicrograph of part of Figure 43. 7C at higher magnification showing abraded and rounded form of most bioclasts, micritized rims on many grains (M), micrite coating on grains including quartz and compound quartz-micrite intraclasts (I), and a large micrite-rimmed clast of *Palaeoaplysina* (P). Although not shown clearly by this photomicrograph, most of the calcite spar cement is developed epitaxially on echinoderm (mainly crinoid) clasts, such as the partly micrite-rimmed and infilled spine base at E.

B: Photomicrograph of plastic-impregnated unconsolidated carbonate sand from the present subtidal environment of Shark Bay, Western Australia. Most of the bioclasts of foraminifers and molluscs (gastropods, bivalves) are broken, abraded, and partly or completely micritized (M); micritization is localized by algal, fungal and other microborings. Quartz grains (Q) have developed thin micrite coatings; others are enclosed in compound intraclastic grains (I; compare with I in Figure 43. 8A). Echinoderm grains (E) show some infilling by mud. Note the fusiform shape of the alveolinellid foraminifers (A); these tests are hydrodynamic analogs for the late Paleozoic fusulinaceans (compare with Figure 43. 10). Like the Paleozoic fusulinaceans, alveolinellids in Shark Bay appear to prefer shallow "shelf" type environments with higher levels of wave and tidal energy.

Figure 43. 8. Comparison between Permian abraded and micritized grain, bioclastic grainstone and Recent unconsolidated abraded and micritized grain carbonate sand from Shark Bay, Western Australia (Davies, 1970).

basin, where it may exceed 600 m (2000 ft.), it is proportionately thinner and more discontinuous along the southern margin. In the type area, where the Belcher Channel is overlain by the Assistance Formation, it is about 180 m (600 ft.) thick. Elsewhere, along the southern margin of the basin, surface exposures of the formation also are relatively thin; at Sabine Peninsula, Melville Island, the Belcher Channel Formation occurs beneath sandstone of the Leonardian Sabine Bay Formation and it is less than 60 m (200 ft.) thick (Tozer and Thorsteinsson, 1964; Nassichuk, 1965). On Helena Island, where the Belcher Channel rests unconformably on the Devonian Griper Bay Formation, it is about 150 m (500 ft.) thick (Kerr, 1974).

As stated previously, the type section of the Belcher Channel Formation, exposed in both the east and west banks of Lyall River, is about 180 m (600 ft.) thick (Nassichuk, 1965). Harker and Thorsteinsson (1960) clearly described the major lithologic components and fossils from the type section. Directly beneath the type section of the Belcher Channel on the east side of Lyall River, the Canyon Fiord Formation is several hundred feet thick and rests with prominent angularity on the lower Paleozoic Cornwallis Group (Fig. 43. 2). About 1. 6 km (1 mile) to the west of the type section at Lyall River, however, the Canyon Fiord Formation is only about 8 m (25 ft.) thick and the Belcher Channel is about 172 m (575 ft.) thick (Figs. 43. 5 and 43. 6); a general view of the upper limestone unit of the Belcher Channel Formation exposed west of Lyall River is shown in Figure 43. 4. At this latter locality, which is 12. 8 km (8. 0 miles) south of Cape Ogle, conglomerates at the base of the Canyon Fiord can be seen filling in depressions on an erosion surface in limestone of the Upper Ordovician Thumb Mountain Formation of the Cornwallis Group. Moderately rounded limestone boulders and pebbles at the base of the Canyon Fiord appear to have been derived locally from the Thumb Mountain.

Biostratigraphy

Newly assembled collections from the Belcher Channel Formation, 1.6 km (1 mile) west of Lyall River, 12.8 km (8 miles) south of Cape Ogle (76°56'30"N, 95°23'W), contain a variety of corals, fusulinaceans and smaller calcareous foraminifers and algae that have been identified at least in preliminary fashion, by several specialists as follows:

Corals, identified by E.W. Bamber

GSC locality C-32860; 123 m (410 ft.) above the base of the Belcher Channel Formation

Bothrophyllum sp. - Note: This species resembles forms referred to *"Caninia" ovibos* Salter by Harker and Thorsteinsson (1960).

Wentzelella sp. [= *Lithostrotion* cf. *L. portlocki* Milne-Edwards and Haime of Harker and Thorsteinsson (1960)]

Age: Early Permian

GSC locality C-32863; 137 m (455 ft.) above the base of the Belcher Channel Formation

Protowentzelella cf. *P. variabilis* Federowski

Age: Early Permian - Note: Typical *P. variabilis* occurs in the Upper Treskelodden Beds in Spitzbergen (Sakmarian sensu lato)

GSC locality C-32872; 162 m (540 ft.) above the base of the Belcher Channel Formation

Protowentzelella cf. *P. variabilis* Federowski

Wentzelella sp.

Age: Early Permian

Fusulinaceans, identified by Charles A. Ross

GSC locality C-32831; 54 m (180 ft.) above the base of the Belcher Channel Formation

Eoparafusulina sp.

Age: Early Permian (Asselian)

GSC locality C-32841; 79 m (262 ft.) above the base of the Belcher Channel Formation

Pseudofusulina sp.

Pseudofusulinella sp.

Age: Early Permian (Asselian or slightly younger, Tastubian)
Note: Fusulinids in this sample have been reworked; specimens are pebbles that have been slightly infilled with glauconitic micrite and that have thin algal overgrowths (or coatings)

GSC locality C-32862; 135 m (450 ft.) above the base of the Belcher Channel Formation

Eoparafusulina? sp.

Schwagerina sp.

Age: Early Permian (Asselian)

GSC locality C-32864; 149 m (495 ft.) above the base of the Belcher Channel Formation

Schwagerina sp. (early form)

Age: Early Permian (late Asselian)

GSC locality C-32868; 164 m (545 ft.) above the base of the Belcher Channel Formation

Schwagerina ex gr. *S. hyperborea* (Salter)

Schwagerina jenkinsi Thorsteinsson

Age: Early Permian (late Sakmarian or early Artinskian)

GSC locality C-32875; 167 m (555 ft.) above the base of the Belcher Channel Formation

Schwagerina spp.

Age: Early Permian (late Sakmarian or early Artinskian)

Calcareous foraminifers and algae, identified by B.L. Mamet

GSC locality C-32835; 72 m (240 ft.) above the base of the Belcher Channel Formation

Beresellaceae

Biseriella sp.

Deckerella sp.

Globivalvulina sp.

Globivalvulina of the group *G. bulloides* Brady

Komia sp.

Orthovertella sp.

Ozawainella sp.

Paradella (Eugonophyllum) sp.

Palaeotextularia sp.

Syzrania sp.

Syzrania bella Rauser-Chernoussova

Schwagerina sp.

Age: Early Permian (Asselian)

Note: This sample contains abundant *Palaeoaplysina* and faunal elements are indicative of an age comparable to other extensive buildups of *Palaeoaplysina* in the Belcher Channel and Nansen Formations elsewhere in eastern and northern regions of the Sverdrup Basin.

In order that faunal and stratigraphic comparisons can be made directly between the section we have examined and the type section 1.6 km (1 mile) to the east at Lyall River, fusulinaceans that were described from the type section by Harker and Thorsteinsson (1960) are listed:

GSC locality 26418, near the base of the type section

Schubertella kingi Dunbar and Skinner

Pseudofusulinella utahensis Thompson and Bissell

Pseudoschwagerina grinnelli Thorsteinsson [= *Pseudofusulina* Dunbar and Skinner (Dunbar *et al.*, 1962)]

GSC locality 26421, 58 m (194 ft.) above the base of the type section

Schwagerina paralinearis Thorsteinsson [= *Monodiexodina* Sosnina (Ross and Dunbar, 1962)] = [*Eoparafusulina* Coogan emend. Skinner and Wilde, 1965 (Ross, 1967)]

GSC localities 26407, 26420, from the Upper 19.5 m (65 ft.) of the type section

Schwagerina jenkinsi Thorsteinsson

Schwagerina hyperborea (Salter)

GSC locality 26419, talus from a position near where *Schwagerina jenkinsi* and *S. hyperborea* were collected from bedrock in the upper 19.5 m (65 ft.) of the type section

Parafusulina belcheri Thorsteinsson

As indicated by Harker and Thorsteinsson (1960) and by Nassichuk and Wilde (in prep.) there is little doubt that all of the fusulinaceans from the type section of the Belcher Channel Formation are of Permian age. Advanced forms of *Pseudofusulina*, such as *P. grinnelli* which occurs near the base of the type section, are confined to the Sakmarian sensu Furnish; 1973 (Wolfcampian). Although *Pseudoschwagerina*, an important index for the Sakmarian Series is absent from the type Belcher Channel, *Pseudoschwagerina* sp. is known to be associated with *Eoparafusulina* sp. low in the Tanquary Formation, south of Mount Bridgeman, Ellesmere Island (Davies and Nassichuk, 1973; Thorsteinsson, 1974). *Pseudoschwagerina* sp. closely resembles *Pseudoschwagerina pavlovi* (Rauser-Chernoussova) which is known from lower Sakmarian (Asselian) strata in the Ural Mountains, and from equivalent strata in the Upper Marine Group, northeast Greenland (Ross and Dunbar, 1962).

Lithology of Belcher Channel Formation

The general aspect of the Belcher Channel Formation (Fig. 43.6) in the section west of Lyall River is practically identical with the type section along strike to the east. Strata dip about 10 degrees to the north and include alternating recessive sandstone and shaly limestone units and more resistant sandstone and skeletal limestone units (Fig. 43.4).

Only about 35 per cent of the measured section of the Belcher Channel Formation west of Lyall River is exposed. The recessive covered intervals between more resistant calcareous sandstone and sandy limestone units (Fig. 43.5) are exposed farther to the east and contain non-calcareous, poorly cemented siltstone and fine grained sandstone; thin beds of poorly exposed yet more resistant beds in these covered intervals usually consist of fine grained calcareous sandstone.

The lower 8 m (25 ft.) of the complete measured section (Fig. 43.6) are composed of red-weathering polymictic conglomerate of the Canyon Fiord Formation (Fig. 43.3). Clasts are of various sizes, but generally decrease in size up-section. These are composed mainly of limestone derived from the underlying and adjacent Ordovician carbonate rocks. Interclast cement is multigeneration sparry calcite with zones of ferroan calcite.

The conglomerates grade upward into buff-brown weathering, coarse to medium grained calcareous sandstone. The base of the Belcher Channel Formation is placed above the uppermost conglomerate bed. The sandstone is friable, porous, and crossbedded. Collected samples are composed of about 60 per cent by volume of quartz sand and other non-carbonate grains, and 40 per cent of detrital sand-size limestone lithoclasts and calcite cement; there are no obvious (primary) bioclasts.

About 11 m (35 ft.) above the base of the Belcher Channel Formation in this section, above a few poorly exposed, thin calcareous sandstone beds, the first marine fossils (solitary corals) were found in a bed of calcareous sandstone. At 21 m (70 ft.) above the base a thin bed of coarse grained sandy bioclastic crinoidal limestone with a grainstone texture (Dunham, 1962) contains about 10 per cent by volume of quartz (mean maximum diameter 250μm), and clasts of crinoids, brachiopods, corals, foraminifers, bryozoans, *Palaeoaplysina*, a possible trilobite, and a number of rounded limestone lithoclasts (Fig. 43.7A)

From 21 to 73 m (70 ft. to 240 ft.) above the base of the formation, the few exposed units are composed of porous, calcite-cemented sandstone with varying proportions of skeletal debris (Fig. 43.7B). Ripple and larger scale crossbed structures are common in these beds. The sandstone units average between 70 and 80 per cent by volume of quartz and other non-carbonate sand- and silt-size grains, with the mean diameter of larger quartz grains ranging from 100 to 300μm. Cement is sparry calcite, often with a late diagenetic ferroan calcite phase. Bioclasts vary in volume from unit to unit, and include fusulinaceans and other foraminifers, crinoid debris, brachiopod valves and spines, gastropods and solitary corals. Many bioclasts are corroded deeply by post-depositional solutional-compactional processes (Fig. 43.7B).

From 73 m (240 ft.) to the top of the formation, exposed units generally are more richly fossiliferous, and include some relatively pure limestone. *Palaeoaplysina* (Fig. 43.7C) is a common and prominent component of several of these units, but apparently is absent about the 140 m (450 ft.) level. *Palaeoaplysina* is associated with a variety of algae, encrusting foraminifers and *Tubiphytes* (?), fusulinaceans, other chambered foraminifers, epimastoporid and other algae, and other skeletal elements. In a few samples at the 73 m (240 ft.) level, *Palaeoaplysina* plates and other larger grains lie in a skeletal micritic wackestone matrix, but in all other samples these components occur as rounded or abraded clasts in a calcite-spar cemented grainstone (Figs. 43.7C and 43.8A). The internal canals of abraded plates of *Palaeoaplysina* (Davies and Nassichuk, 1973) often are filled with micritic calcite with floating quartz grains, unlike the spar matrix enclosing the skeletal clasts.

The more resistant limestone and sandy limestone units in the upper part of the formation are characterized by grainstone textures and are composed of rounded and abraded, often micritized or micrite-coated grains of *Palaeoaplysina*, crinoid debris, fusulinaceans, other foraminifers, algae (particularly epimastoporid forms), bryozoans, brachiopods and gastropods (Fig. 43.8A). Cements are multigeneration sparry calcites, often with a late ferroan calcite phase that commonly is developed epitaxially on crinoid grains (Fig. 43.8A). Quartz sand content of these grainstones varies from a trace to about 5 per cent by volume. The resistant limestone units often are underlain and overlain immediately by poorly exposed, recessive, crudely laminated calcareous sandstone, that may in turn grade into unexposed finer grained detrital sediments in the covered intervals.

From 90 to 150 m (300 ft. to 500 ft.) above the base of the Belcher Channel Formation, the dominant exposed lithology comprises calcareous and bioclastic

sandstone, although most of the section is covered. Large colonial corals (identified by Bamber, this paper) are common in the exposed beds and as float in this interval.

Near the top of the formation, a more resistant sandy limestone unit, 11 m (35 ft.) thick, is composed mainly of coarse grained, sandy, bioclastic grainstones and bioclastic sandstones (Fig. 43.9). Non-carbonate grain volume ranges from 20 to 70 per cent in collected samples; mean size of larger quartz grains ranges from 100 to 200μm. Fusulinaceans and other foraminifers, crinoids, brachiopods, gastropods, bryozoans, solitary and colonial corals and a variety of algae are found in these rocks. Most characteristic of the upper beds are very large schwagerinid fusulinaceans up to 13 mm long by 3 mm diameter (Fig. 43.10).

The ichnofossil *Zoophycos (Spirophyton)* occurs in calcareous sandstone immediately at the base of the uppermost 11 m (35 ft.) thick limestone unit, and also in sandstone float within a thick covered interval about 30 m (100 ft.) lower in the formation.

Discussion

Depositional setting, processes and cyclicity

Because of the incomplete nature of the exposed section of the Belcher Channel Formation in the Lyall River area, a thorough treatment of depositional environment and processes is not given in this paper.

The repetition of resistant, calcareous sandstone and sandy limestone units of basically similar overall composition at irregular intervals throughout the section suggests cyclical or rhythmic controls on sedimentation. If the covered intervals contain mainly non-calcareous, fine, detrital sediments, as is suggested by their recessive profile, they may represent deposition in water deeper than that suggested by the grainstone-textured limestone units. The rare occurrence of the ichnofossil *Zoophycos* in sandstone beds below resistant limestone units and within some covered intervals offers support for this inference, since this trace fossil normally characterizes detrital sediments deposited in deeper water away from shoreface environments.

If this interpretation is correct, a "shallowing upward" sedimentation rhythm or hemi-cycle in these rocks would be composed of a section of fine detrital sediment grading upward into coarser-grained calcite-cemented (that is, originally more porous) sandstone and sandy bioclastic limestone. A reconstructed sequence within the limestone unit would include, at the base, an unsorted sediment composed of more or less intact skeletal grains in a carbonate mud skeletal debris sandy and silty matrix (representing more or less in place accumulation of biogenic sediment) grading upward or abruptly overlain by a moderately well sorted, coarse grained carbonate grainstone composed of rounded, abraded, micritized and coated skeletal grains and intraclasts. The carbonate mud and fine quartz grains filling the internal cavities of some clasts (such as *Palaeoaplysina)* in these grainstones attest to their original deposition in poorly sorted muddy and silty environments.

Abraded and micritized grainstone sediments of this type probably represent a lag deposit of skeletal grains derived by tidal and wave scour of muddy, unsorted bioclastic and detrital sediment accumulating under environment conditions of progressive shallowing, whether controlled simply by sediment accumulation or sea level changes ("regression"). A very similar vertical sequence, culminating in a "regressive", seaward prograding body of penecontemporaneously reworked, abraded and micritized skeletal grains (and larger quartz grains) derived from underlying unsorted bioclastic sediments by wave and tidal scour, is found in Recent carbonate sediments of Shark Bay, Western Australia (Davies, 1970; Fig. 43.8B). Modern examples of this type of sediment also attest to the fact that the presence of abraded, infilled and coated skeletal grains in a rock do not indicate necessarily an extensive time break or hiatus in sedimentation, but may be a normal product of sediment deposition under conditions of progressive shallowing, leading to internal cannibalization.

A lag deposit of this type may mark minimum sea level conditions (maximum regression) and, as a relict sediment, it may mark the onset of renewed transgression and sedimentation.

Cyclicity in this setting, marginal to the basin depositional edge, probably was controlled by shifting environments of detrital sediments derived ultimately from uplifted terrains to the east, south, and west.

Palaeoaplysina

The enigmatic organism *Palaeoaplysina,* assigned by some tentatively to the Hydrozoa (*see* Davies and Nassichuk, 1973), is abundant in Lower Permian (Asselian) shelf carbonate rocks of the Belcher Channel Formation in eastern regions of the Sverdrup Basin (Davies and Nassichuk, 1973) and in contemporaneous shelf limestone of the Nansen Formation in northwesterly regions of the basin. It has not been reported previously from the Belcher Channel Formation along the southern margin of the basin. In both of the former areas, *Palaeoaplysina* is abundant and widespread, and is an important mound builder and limestone component near the outer shelf edge of the Sverdrup Basin. In the Belcher Channel Formation on Grinnell Peninsula, where deposition occurred closer to the shoreline, *Palaeoaplysina* occurs as broken plates, usually abraded, in thin sandy limestone beds.

Palaeoaplysina was first recorded in Canada from a Lower Permian section in the Yukon Territory (Davies, 1971). The overall lithological and paleontological similarities between the Yukon occurrence and the Grinnell Peninsula sequence, both in terms of the general section and more detailed aspects of composition and depositional textures in individual units containing *Palaeoaplysina,* are striking (Davies., Figs. 6B and 8).

Porosity

Although no porosity and permeability analyses have been made for collected samples of the Belcher

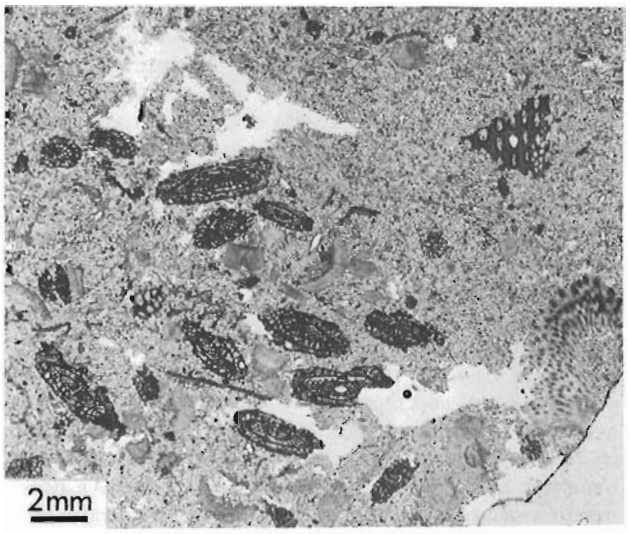

Figure 43. 9.

Photomicrograph of bioclastic fusulinacean-crinoidal sandstone composed of 60 per cent by volume of medium-grained, calcite-cemented quartz sand with localized concentrations of fusulinaceans, crinoids, fenestrate bryozoans and brachiopods. Most bioclasts are corroded by post-depositional solution-compaction. GSC loc C-32864, 150 m above the base of the Belcher Channel Formation.

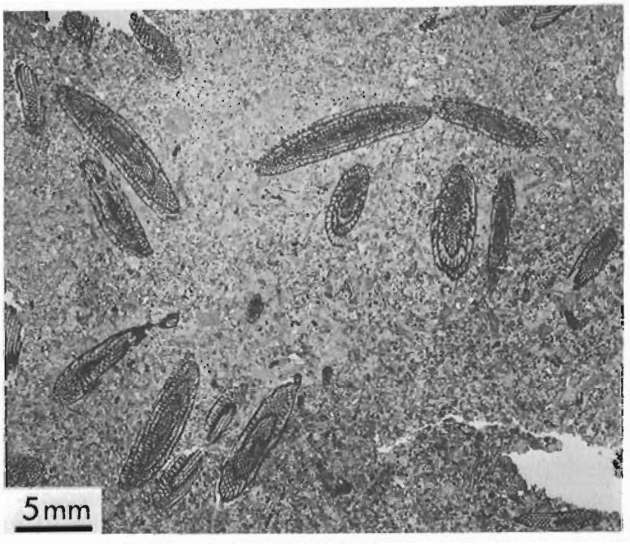

Figure 43. 10.

Photomicrograph of fusulinacean-crinoid grainstone with very large schwagerinid fusulinacean foraminifers that characterize the upper beds of the Belcher Channel Formation. GSC loc. C-32868, 165 m above the base of the Belcher Channel Formation.

Channel Formation, field observations suggest that at least the lower 50 m (160 ft.), and possibly most of the rest of the non-carbonate units in the section (particularly recessive intervals) are porous and permeable. Cementation by calcite is the prime diagenetic agent affecting porosity in these detrital sediments.

References

Davies, G. R.
1970: Carbonate bank sedimentation, eastern Shark Bay, Western Australia; *in* Logan, B. W., and others, Carbonate Sedimentation and Environments, Shark Bay, Western Australia; Am. Assoc. Pet. Geol., Mem. 13, p. 85-168.

1971: A Permian hydrozoan mound, Yukon Territory; Can. J. Earth Sci., v. 8, no. 8, p. 973-988.

Davies, G. R. and Nassichuk, W. W.
1973: The hydrozoan? *Palaeoaplysina* from the upper Paleozoic of Ellesmere Island, Arctic Canada; J. Paleontol., v. 47, p. 251-265.

Dunbar, Carl O., Troelson, Johs, Ross, Charles, Ross, June-Phillips, and Norford, B. S.
1962: Faunas and correlation of the late Paleozoic rocks of northeast Greenland, Part I, General discussion and Summary; Medd. Grønland, Bd. 167, no. 4, p. 1-16.

Dunham, Robert J.
1962: Classification of carbonate rocks according to depositional texture; *in* Classification of Carbonate Rocks, Ham, W. E., ed.; Am. Assoc. Pet. Geol., Mem. 1, p. 108-121.

Furnish, W. M.
1973: Permian Stage names. The Permian and Triassic systems and their mutual boundaries; Can. Soc. Pet. Geol., Mem. 2, p. 522-548.

Harker, P. and Thorsteinsson, R.
1960: Permian rocks and faunas of Grinnell Peninsula, Arctic Archipelago; Geol. Surv. Can., Mem. 309, 145 p.

Kerr, J. Wm.
1974: Geology of Bathurst Island Group and Byam Martin Island, Arctic Canada; Geol. Surv. Can., Mem. 378, 152 p.

Nassichuk, W. W.
1965: Pennsylvanian and Permian rocks in the Parry Islands Group, Canadian Arctic Archipelago; *in* Report of Activities, Field, 1964, Geol. Surv. Can., Paper 65-1, p. 9-12.

Nassichuk, W. W. and Wilde, Garner L.
Biostratigraphic significance of fusulinaceans in the Belcher Channel Formation at Blind Fiord, southwestern Ellesmere Island, Canadian Arctic; Geol. Surv. Can., Paper (in prep.).

Ross, Charles A.
1967: Late Paleozoic Fusulinacea from northern Yukon Territory; J. Paleontol., v. 41, p. 709-725.

Ross, Charles A. and Dunbar, Carl O.
1962: Faunas and correlation of the late Paleozoic rocks of northeast Greenland; Medd. Grønland, Bd. 167, no. 5.

Thorsteinsson, R.
1963: Northern Grinnell Peninsula around Lyall River; *in* Geology of the north-central part of the Arctic Archipelago, N. W. T. (operation Franklin), Fortier, Y. O. *et al.*, Geol. Surv. Can., Mem. 320, p. 250-256.

1974: Carboniferous and Permian stratigraphy of Axel Heiberg Island and western Ellesmere Island, Canadian Arctic Archipelago; Geol. Surv. Can., Bull. 224, 115 p.

Tozer, E. T. and Thorsteinsson, R.
1964: Western Queen Elizabeth Islands, Arctic Archipelago; Geol. Surv. Can., Mem. 332, p. 1-242.

Troelson, J. C.
1950: Contributions to the geology of Northwest Greenland, Ellesmere and Axel Heiberg Islands; Medd. Grønland, Bd. 147, no. 7.

44. SOME METALLOGENIC FEATURES OF THE "D" URANIUM DEPOSIT AT CLUFF LAKE, SASKATCHEWAN

Project 750010

V. Ruzicka
Regional and Economic Geology Division

Uranium and associated polymetallic mineralization have been reported from the region of the Carswell structure at Cluff Lake, Saskatchewan, *in* Glass, ed., (1972).

The region of the Carswell structure is being explored for uranium mainly by Amok Limited. Geological research studies are being carried out by Amok Limited, by the Commissariat à l'Enérgie Atomique, France, and by the Geological Survey of Canada in cooperation with the Physical Sciences Laboratory of CANMET.

Whereas some features of the deposits in this region resemble those found elsewhere in the Canadian Shield, in Northern Territory of Australia, and on the Eurasian continent, the "D" uranium deposit at Cluff Lake represents a distinct type of uranium mineralization.

Criteria derived from study of its metallogenic features, such as source of mineralization, its spatial relationship to unconformity, structural control in localization of mineralization, litho-stratigraphic control in localization of mineralization and mineral assemblage, can be applied in exploration for uranium elsewhere in the Canadian Shield.

The "D" uranium deposit occurs in the Carswell circular structure east of the northern tip of the Cluff Lake (*see* Fig. 44.1).

The Carswell structure comprises several rock units (*see* Table 44.1). The oldest unit belongs to the Basement Complex (Currie, 1969), which forms a central core of the structure and consists of steeply dipping granite gneisses, *lit-par-lit* gneisses and related rocks. Because of its stratigraphic position and lithological composition, the unit can be tentatively correlated with the Tazin Group, which occurs north of Lake Athabasca. The age of this unit may be either Archean or Aphebian.

The Basement Complex is unconformably overlain by the Athabasca Formation, a sequence of rudites, arenites and pelites. Currie (1969) divided the Athabasca Formation within the Carswell structure into two members on the basis of colour and texture: the lower consisting of red, purple or iridescent black rudites and arenites, and the upper represented mainly by white to pale buff homogeneous orthoquartzite. The age of the Athabasca Formation is commonly regarded as Paleohelikian.

Table 44.1

Table of Formations in the Carswell Structure

Era	Period or Epoch	Formation and Thickness (feet)	Lithology
Paleozoic	Ordovician	Cluff Breccias 50±	Red and green angular fragments of the Basement Complex (Tazin Group), Athabasca and Carswell Formations in an igneous matrix.
		Intrusive Contact	
Helikian	Paleohelikian	Carswell Formation 500±	Mainly dolomites
		Douglas Formation ?	Siltstone, marl
		Locally intervening	
		Athabasca Formation 2700±	Basal conglomerate, sandstones, pelites with bituminous matter
		Unconformity	
Archean or Aphebian		Basement (pre-Athabasca) Complex tentatively regarded as Tazin Group ?	Granite gneiss, *lit-par-lit* gneisses, pegmatitic granitoid rocks, leptynite

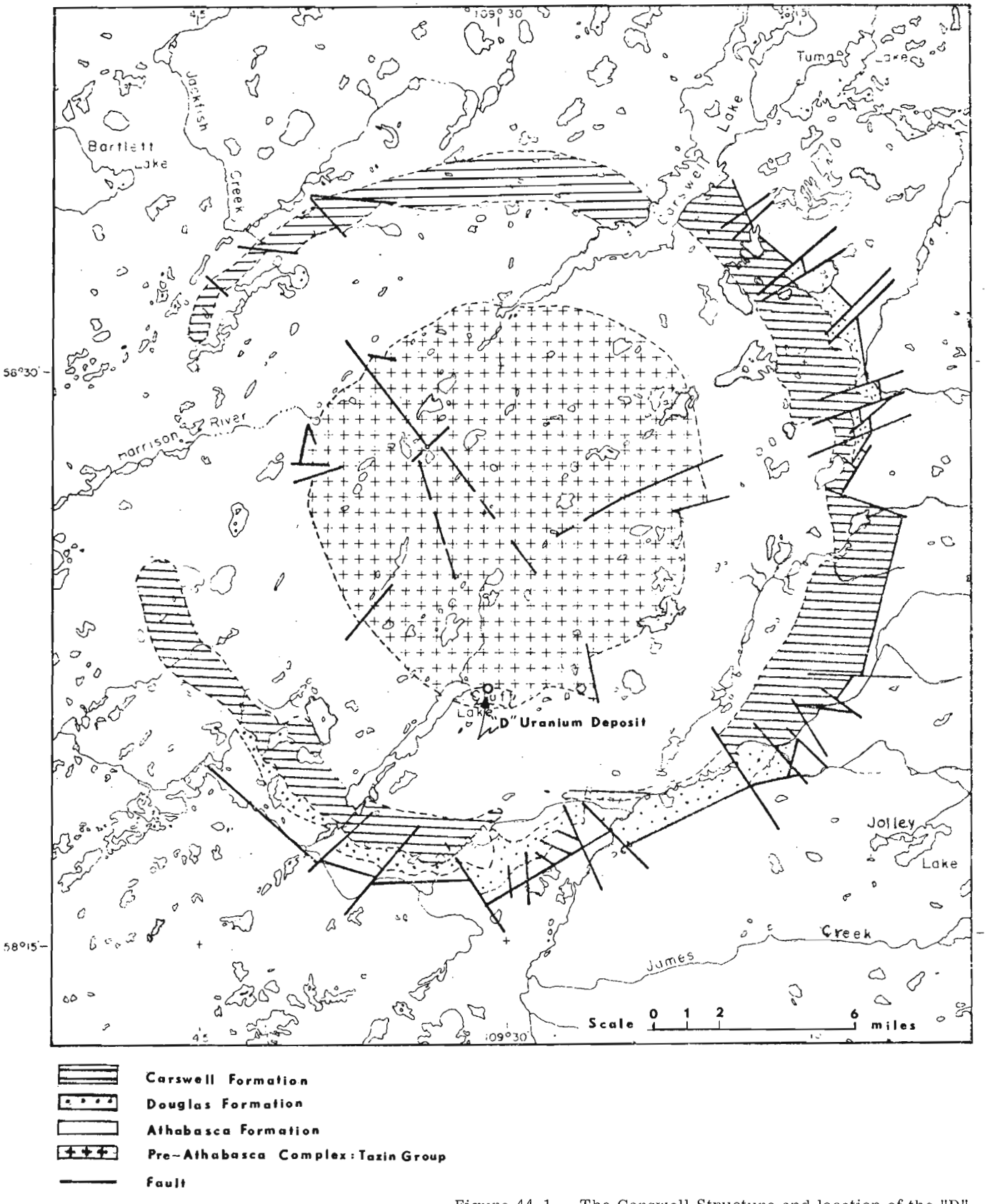

Figure 44.1. The Carswell Structure and location of the "D" deposit. (Compiled after maps of Amok Ltd. and Currie, 1969.)

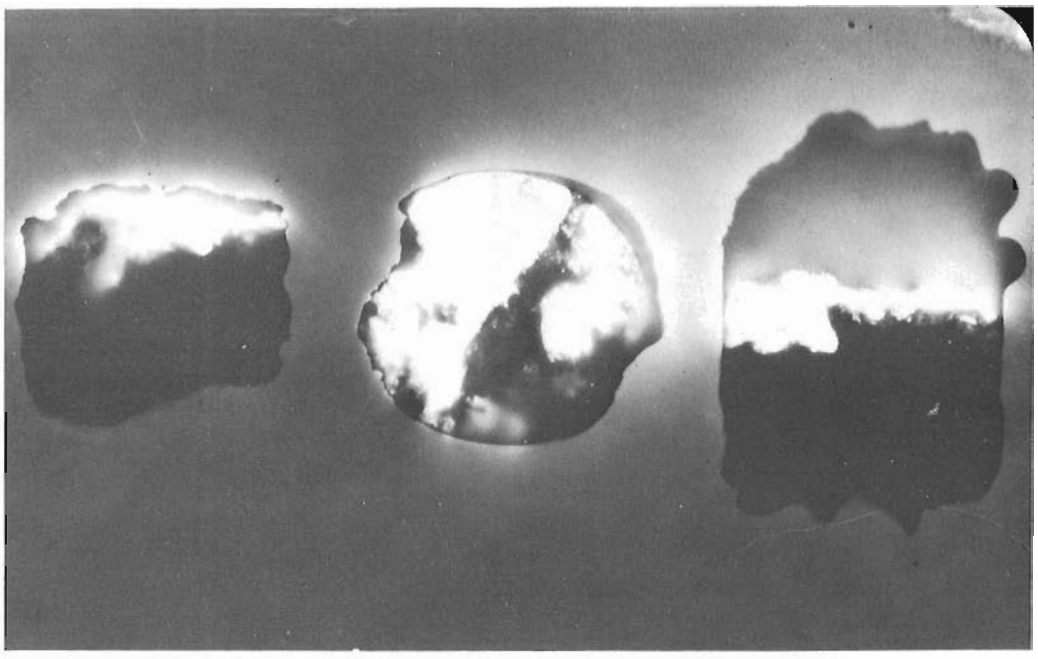

Figure 44. 2.

Autoradiograph of a sample of uranium – polymetallic ore taken approximately from the centre of the "D" deposit. Exposure time: 24 hours.

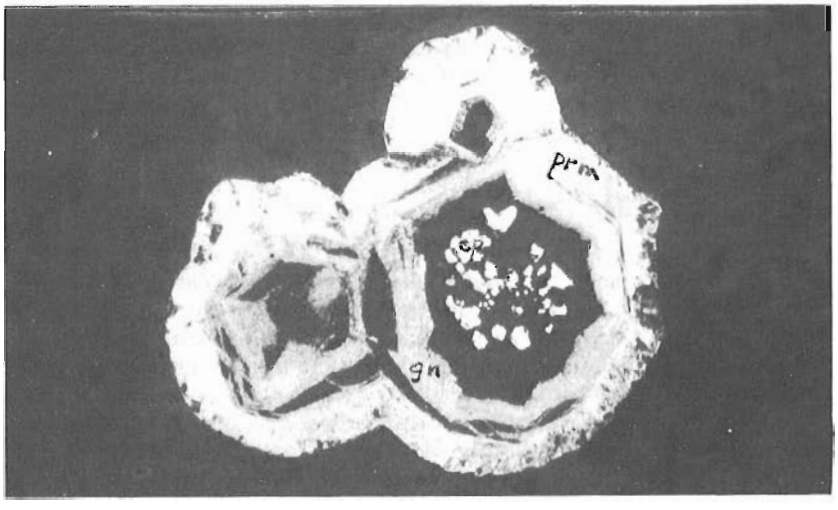

Figure 44. 3.

Microscopic intergrowth showing honeycomb texture. Outer ring is pararammelsbergite, inner ring is galena. Fine grains at core are chalcopyrite occurring in chlorite. X 400. Microphotograph and identification by Kaiman (1975).

The Athabasca Formation is overlain by the Carswell Formation consisting mainly of dolomite. The contact between the Athabasca and Carswell formations is mainly gradational, but locally a slight unconformity or an intervening unit, Douglas Formation, consisting of siltstone and marl, can be recognized.

All the above mentioned units are cut by Cluff breccias (not shown on Fig. 44.1), a series of dykes and irregular bodies composed of brecciated country rocks in an igneous matrix. The Cluff breccias are Ordovician.

Localization of the uranium-polymetallic assemblage in the "D" deposit is apparently controlled by the following factors:

(1) The paleosurface of the Tazin rocks is deeply weathered and has a relatively thick regolith. M. N. Turay of the Geological Survey petrographically investigated a sample collected from the Tazin regolith immediately at the "D" deposit. It consists of approximately 15 per cent quartz, 75 per cent micaceous and clay minerals and 10 per cent of opaque minerals

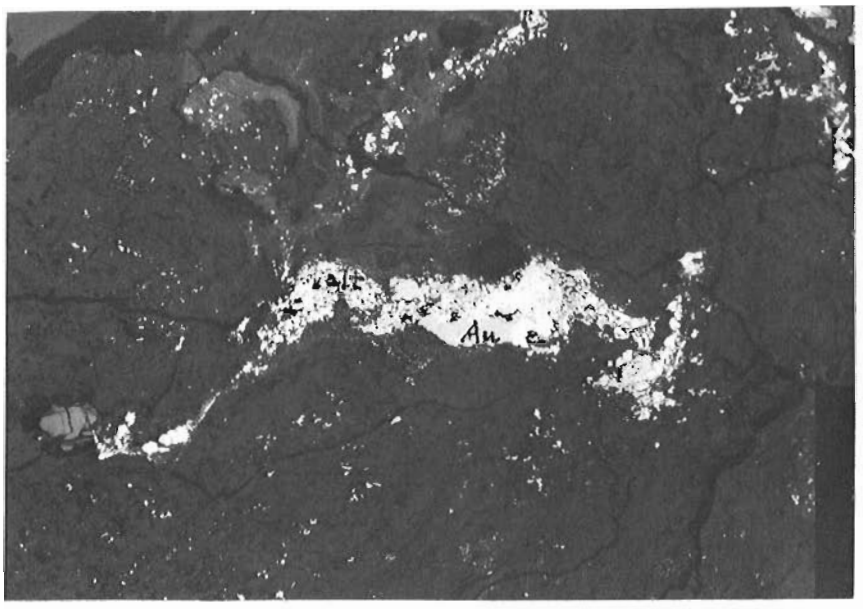

Figure 44.4.

Microscopic intergrowth of gold (Au) and altaite (alt). Microphotograph and identification by Kaiman (1975).

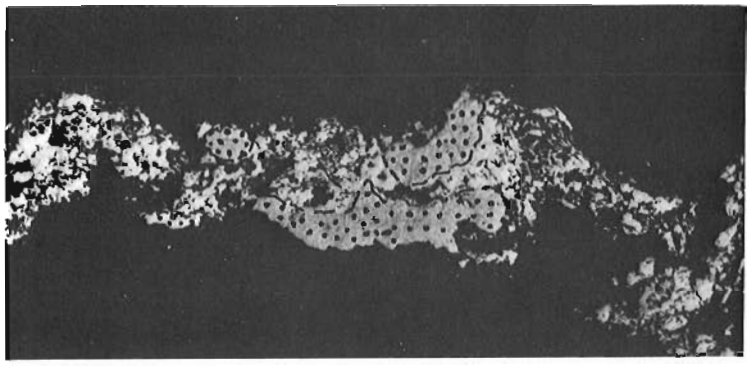

Figure 44.5.

Detail of the same aggregate as in Figure 3. Gold shown by dotted areas. X 200. Microphotograph and identification by Kaiman (1975).

including hematite. The quartz has undulatory extinction and is generally recrystallized in fractures. The hematite is not idiomorphic and together with some of the clay minerals appears to be a product of the alteration of a mafic mineral. An X-ray diffraction pattern of the sample confirms that the regolith is composed of quartz, muscovite, montmorillonite, chlorite and hematite.

(2) The "D" deposit is spatially related to the Athabasca/Tazin unconformity (*see* Fig. 44.1). Uranium-polymetallic mineralization within the deposit is distributed along the faults and fractures at the intersection of three major fracture systems: (a) the northeast — southwest lineament, which appears to be correlatable with the fracture system of the same direction in the Beaverlodge area, (b) the regional northwest — southeast system, which is partly observable within the pre-Athabasca core of the Carswell structure, and (c) the radial fault system genetically related to the origin of the Carswell structure.

(3) The highest uranium concentration occurs in the basal sequence of the Athabasca Formation. This litho-stratigraphic unit generally corresponds with the lower member of the Athabasca Formation in Currie's (1969) classification. However in addition to Currie's description this litho-stratigraphic unit comprises a distinct pelitic facies. J. Geffroy (pers. comm., 1972) recognized two lithological facies controlling uranium mineralization within this sequence: (a) pelites consisting mainly of illite, chlorite and kaolinite, and (b) clastic sediments with rutile, zircon, leucoxene, ilmenite, titanomagnetite, and tourmaline. In the "D" deposit the uranium-polymetallic mineralization is confined almost entirely to bituminous pelites which grade transitionally to sandstones. Locally the base of the Athabasca Formation consists of conglomerate, which, as a rule, is less mineralized. The whole sequence in the area of the "D" deposit is overturned so that the rocks of the Tazin Group rest upon younger Athabasca sediments. The Athabasca/Tazin contact is locally faulted.

(4) The main uranium ore mineral is pitchblende commonly in the form of irregular masses (*see* Fig. 44.2). In the ore mineral succession, the suite of uranium minerals represents the older stage of mineralization with the uraninite being the oldest, pitchblende the

intermediate and most prevalent minerals, and thucholite the youngest of the uranium minerals. Sulphides, selenides, and other minerals represent the younger stage of the ore mineralization (J. Geffroy, Amok Ltd., pers. comm., 1972). Kaiman (1975) examined a sample taken from a drillhole approximately in the centre of the "D" deposit. He commented on the extremely fine grained nature of the polymetallic minerals and their intimate intergrowths. Figure 44.3 shows the microscopic intergrowth of pararammelsbergite, galena, and chalcopyrite in a honeycomb texture. Figures 44.4, 44.5 show the microscopic intergrowth of native gold and altaite.

The above mentioned features can be interpreted and summarized as follows:

(1) The uranium, primarily concentrated in the Tazin rocks, was liberated by deep weathering with the simultaneous formation of a hematite-rich regolith.

(2) Liberated uranium was syngenetically deposited with pelitic sediments either in detrital uraninite, or in massive form (pitchblende), or adsorbed on bituminous substances (thucholite). The depositional environment was also favourable for geochemical concentration of polymetallic compounds and gold.

(3) Subsequent tectonic movements caused remobilization of uranium and other metallic elements and their deposition in lithological and structural traps, among which the overturned Tazin rocks, the Tazin/Athabasca unconformity and the faults were the most effective sites for epigenetic mineralization.

The author acknowledges the permission of Amok Ltd. to use their information in this report.

References

Currie, K.L.
1969: Geological notes on the Carswell circular structure, Saskatchewan; Geol. Surv. Can., Paper 67-32.

Glass, D.J., editor
1972: Excursion C 67: Uranium deposits in Canada; XXIV Internat. Geol. Congress (Little, H.W., Smith, E.E.N., and Barnes, F.Q.).

Kaiman, S.
1975: Mineragraphic identification on sample RAD – 74 – 4; Internal communication; Joint CANMET; Geol. Surv. Can. Publ.

RADIOACTIVE PEGMATITES IN THE RENFREW AREA, ONTARIO

Projects: 720071, 740081; Uranium Reconnaissance Program

B. W. Charbonneau and I. R. Jonasson
Resource Geophysics and Geochemistry Division

Uranium-copper mineralization near South March, Ontario has been reported by the Geological Survey in Ordovician March Formation sandstones in five short papers (Charbonneau, Jonasson and Ford, 1975; Jonasson and Dyck, 1974; Steacy, *et al.*, 1973; Grasty, *et al.* and Charbonneau, *et al.*, 1975). Working on the hypothesis that such occurrences would probably relate to abnormal radioactive levels in underlying Grenville age Precambrian rocks, additional investigations have taken place in nearby basement rocks. The rocks of the Gatineau Park area north of the presently known March Formation occurrences are known to contain some uranium occurrences especially around Meach Lake (Hogarth, 1970) and to be abnormally radioactive. This can be seen on airborne gamma-ray spectrometry maps (Charbonneau, *et al.*, 1975) which overlap part of the Gatineau Park and also on unpublished airborne radioactivity surveys over the Park itself. In addition, further stream sediment geochemical uranium anomalies have been obtained by Jonasson over Paleozoic rocks south of Arnprior, Ontario just west of the boundary of the geochemical uranium map (Charbonneau *et al.*, 1975) and just east of the Renfrew area described

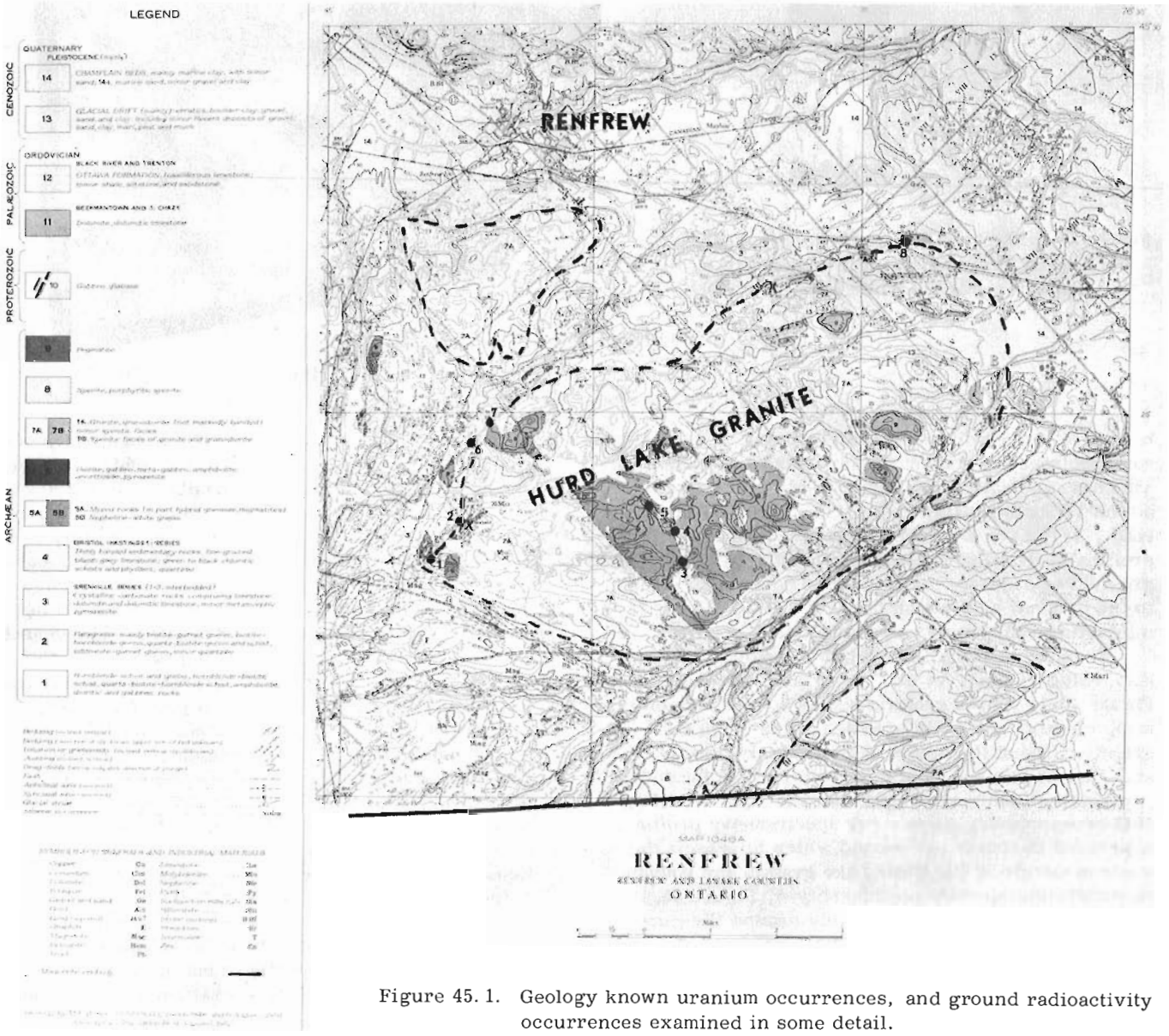

Figure 45. 1. Geology known uranium occurrences, and ground radioactivity occurrences examined in some detail.

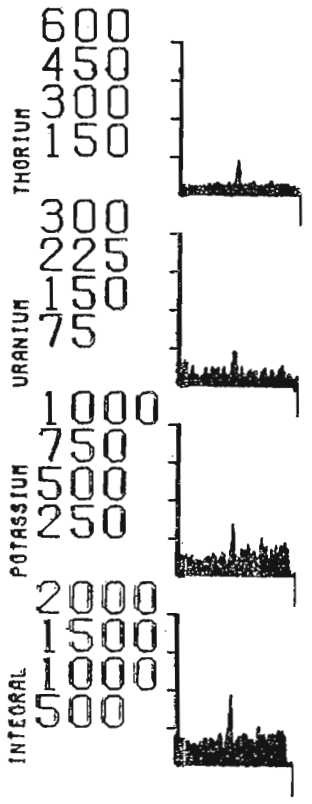

Figure 45. 2. Part of 1972 cross-country radioactivity profile showing radioactivity anomaly at edge of White Lake granite.

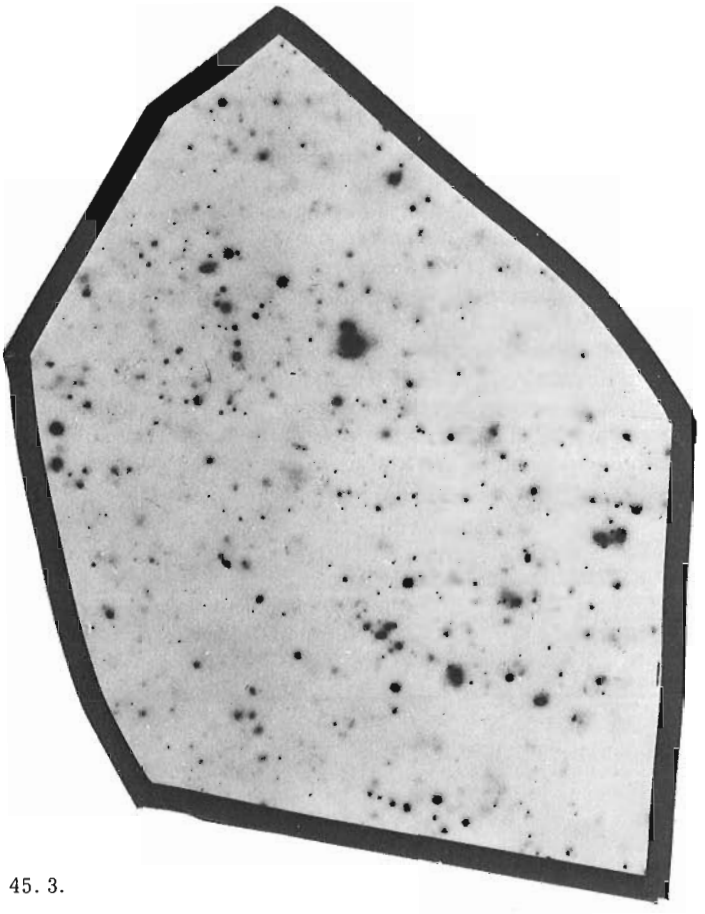

Figure 45. 3.

Autoradiograph of high uranium/thorium ratio pegmatite at locality 1.

here. Moreover, certain cross-country airborne gamma-ray spectrometry profiles which transect the Renfrew area have indicated anomalies one of which can be seen on the 1972 profile (Darnley, *et al.*, 1971; Richardson *et al.*, 1975 have described the 1969, 1970 and 1971 profiles). For the reasons stated above, additional ground radioactivity investigations have taken place in the Renfrew area which has led to the outlining of an interesting radioactive pegmatite zone.

The area of study lies within Geological Survey Map 1046A (Quinn, *et al.*, 1956) and is shown in Figure 45. 1. Three granitic bodies can be seen on this map, the most southerly of which is the White Lake granite. One of the others is centred around Hurd Lake and the smallest and most northerly body is located just south of Renfrew. Figure 45. 2 is a portion of the 1972 cross-country gamma-ray spectrometry profile expressed in counts per second which intersects the western margin of the White Lake granite and reveals an interesting anomaly near locality A, Figure 45. 1. Investigations have centred mainly around the Hurd Lake granite where rather extensive amounts of pegmatite have been mapped by Quinn (1956). These appear as darker masses on Figure 45. 1.

Figure 45. 4 is the aeromagnetic anomaly map of the area (Geol. Surv. Can., Map 67G). Prominent magnetic anomalies of some 500 gammas amplitude relate to zones of hornblende gneiss which dominantly ring the granites. Figure 45. 1 shows the location of some radioactive pegmatites examined and sampled. The central mass of pegmatite has radioactivity levels which average 50 ppm thorium and 10 ppm uranium at the localities 3, 4, 5 by *in situ* gamma-ray spectrometry. The overall average levels for this mass are probably in this general range (3 times normal granite levels, according to Clarke, 1966). The peripheral pegmatite bodies, at localities 1, 2, 6, 7, 8, which dominantly lie within the hornblende gneiss border are much more radioactive. In places, e. g., locality 1, the pegmatite has a high uranium/thorium ratio but generally, as at localities 2, 6, 7, 8, substantial relative thorium levels are found as well. Because of the spotty nature of the concentrations it might be somewhat misleading to quote actual values measured but it is not difficult to find masses of pegmatite which give *in situ* levels in excess of 0. 5% (500 ppm) uranium along the length of the pegmatite belt which follows the northern margin of the Hurd Lake granite. Some radioactive pegmatites are also found along the southern margins of the Hurd Lake granite

and the sites shown are only illustrative of some of the pegmatites examined in more detail. Three occurrences of radioactivity have been previously reported (Lang *et al.*, 1963) from the area and these are marked by "X". Specifically, the Horton occurrence near locality 8 is described as pegmatite with uranothorite and allanite, the Zenith occurrence near locality 2 is described as being associated with molybdenite in pyroxenite (high uranium/thorium ratios measured there suggest the presence of uraninite). Further information on this can be found in Vokes (1963) and Sabina (1970). The Goldyke occurrence is near the Zenith Mine (not marked with a separate X) and is similar in geology; it is reported to contain uraninite, (Lang, *et al.*, 1963). The fact that two out of three of the known radioactive occurrences in this area are associated with molybdenum, which is an important trace metal in the March Formation sandstone occurrences, suggests a genetic relationship between the basement radioactive zones and the Paleozoic stratified sandstone concentrations.

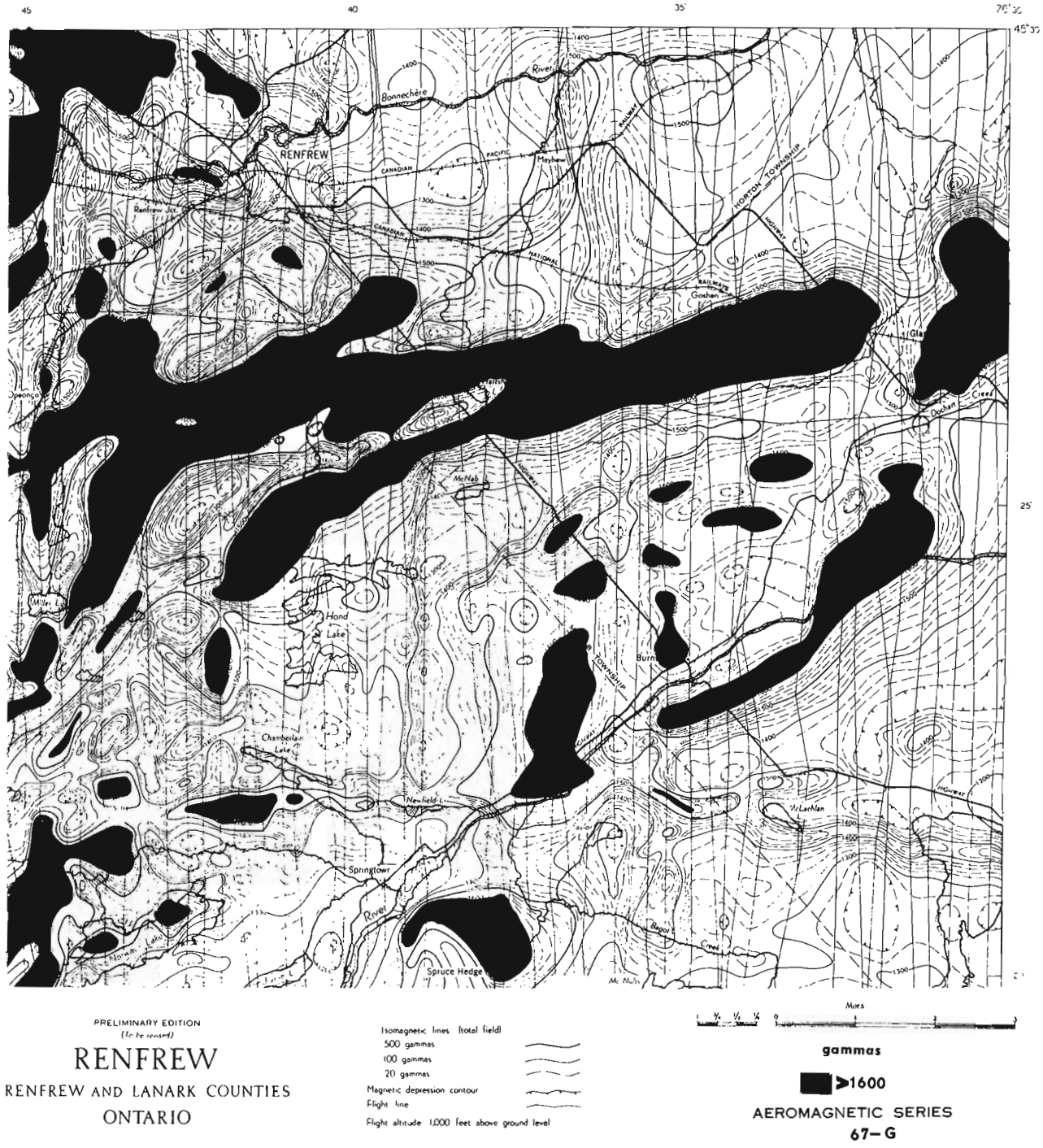

Figure 45. 4. Aeromagnetic anomaly map of Renfrew area.

The pegmatites, where examined, consist of potash feldspar-plagioclase (oligoclase) - quartz ± magnetite ± biotite. The pegmatites are enriched in magnetite near the hornblende gneiss and are more biotite rich near marble. This phenomenon has been observed elsewhere. For example in the Mont Laurier area (Allen, 1971). There is a positive correlation of radioactive levels with magnetite and/or biotite, with magnetite rich pegmatites generally the most radioactive. The pegmatites which have abundant uranium and thorium appear to have uranothorite and allanite as major radioactive minerals. The high uranium/thorium ratio pegmatites, such as the one at locality 1 contains fine grains of uraninite (0.1 mm) with some uranothorite (identified by H.R. Steacy, Geol. Surv. Can.). Figure 45.4 is a seventy-two hour autoradiograph of this sample of granitic rock which contains > 0.1% uranium.

There is an overall resemblance of the Renfrew pegmatite area with the Bancroft uranium district (Satterly, 1957). Both are comprised of a series of granitoid masses with peripheral gneiss into which radioactive granites and pegmatites have been emplaced and the amount of enrichment is usually proportional to the mafic content of the country rock. The similarities in structural style of the area described and the Bancroft district, the pronounced peripheral enrichment in radioelements and the increase in content near mafic

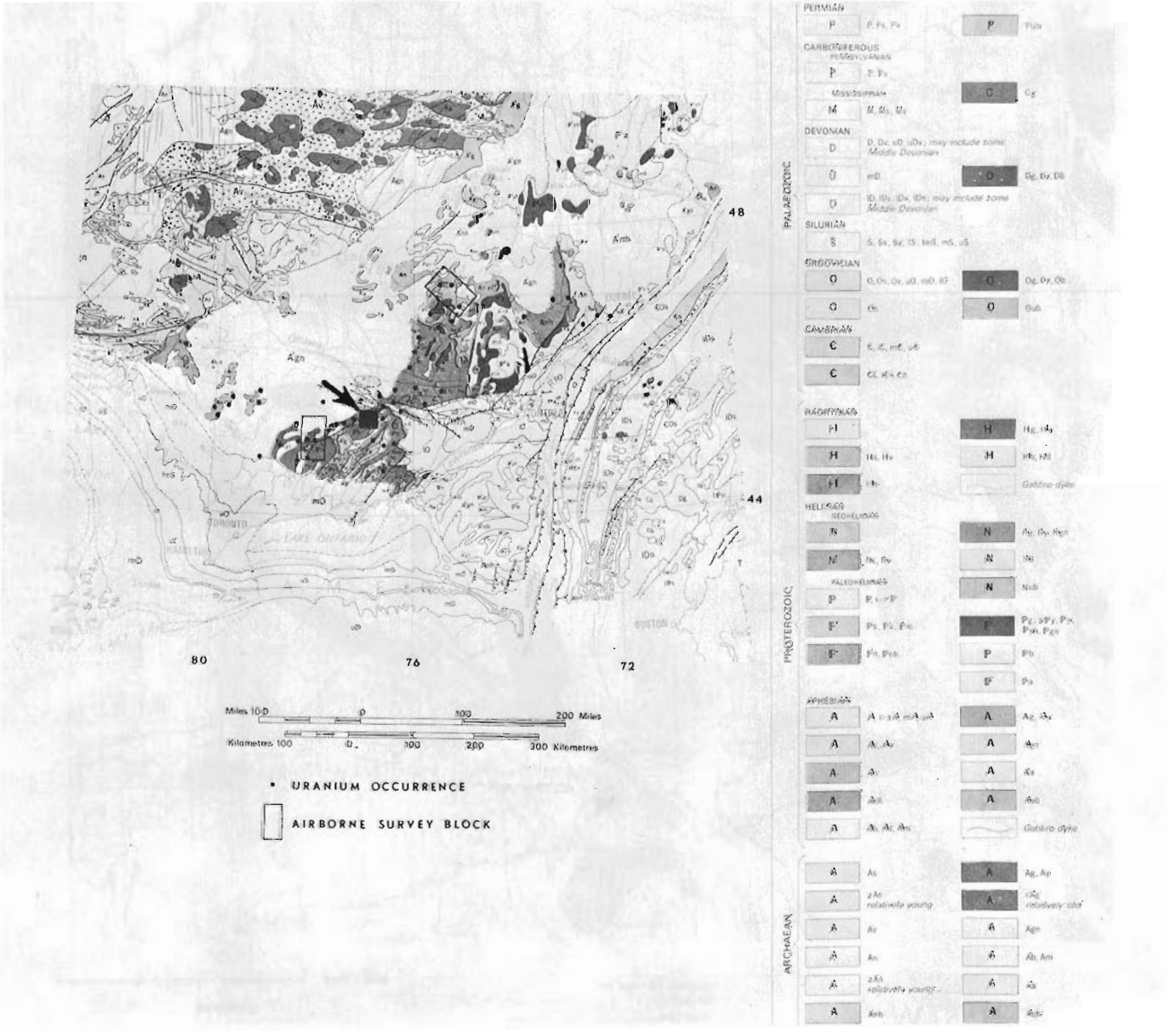

Figure 45.5. Distribution of uranium occurrences in the general area between Bancroft, Ont. (Southwest block) and Mont Laurier, Que. (Northeast survey block). In addition, the Renfrew area described is shown as a black square.

rocks and the length of the enriched contact zones, all combine to make the Renfrew area quite interesting. The fact that zinc, molybdenum and gold occurrences are present along with the uranium concentrations, is an unusual feature of the belt. The structure described above is not meant to preclude the possibility that other pegmatites in the western part of map-area 31F/7 are radioactive. In fact, abnormally high radioactivity levels have been observed in many of them, for example, south of Shamrock.

Figure 45.5 is a compilation of uranium occurrences in the general area between Bancroft and Mont Laurier derived from Allen (1971). The fact that there is a strong tendency for uranium occurrences to scatter along the base of the Grenville Group may indicate partial melting of a lower uraniferous metasediment with subsequent remobilization of radioactive granites and pegmatites as suggested by Allen (1971). The build-up in radioactive levels in the granitoids adjacent to the Grenville Group in the Bancroft area (Darnley and Grasty, 1971) and in the Mont Laurier area (Charbonneau, 1973) may also suggest upwards mobilization of radioelements in the crust during regional metamorphism as suggested by Yermalyev (1973). These radioelements could be concentrated in granites, pegmatites and skarns near and especially just above the unconformity. Whatever the explanation, the regional contact between the Grenville Group rocks and the underlying granitic basement is the locus of radioactive enrichment over more than 300 miles and is certainly worthy of further comprehensive regional exploration interest as the average grade of uranium ore that would be economically tenable drops.

References

Allen, J. M.
1971: The genesis of Precambrian uranium deposits *in* eastern Canada and the uraniferous pegmatites of the Mont Laurier area, Quebec; unpubl. M. Sc. thesis, Queen's Univ., Kingston, Ont.

Charbonneau, B. W.
1973: Ground investigations of the Mont Laurier Airborne Radioactivity Survey; *in* Report of Activities, Pt. A, Geol. Surv. Can., Paper 73-1A, p. 67-78.

Charbonneau, B. W., Jonasson, I. R., and Ford, K. L.
1975: Cu-U mineralization in the March Formation Paleozoic rocks of the Ottawa-St. Lawrence Lowlands; *in* Report of Activities, Pt. A., Geol. Surv. Can., Paper 75-1A, p. 229-233.

Charbonneau, B. W., Jonasson, I. R., Holman, P. B., and Ford, K. L.
1975: Regional airborne gamma-ray spectrometry and stream sediment geochemistry, detailed ground gamma-ray spectrometry and soil geochemistry in an environment of stratabound Paleozoic U-Cu mineralization in the Ottawa-Arnprior area; Geol. Surv. Can., Open File 264.

Clarke, S. P., Jr.,
1966: Handbook of physical constants; Geol. Soc. Am., Mem. 97.

Darnley, A. G. and Grasty, R. L.
1971: Mapping from the air by gamma-ray spectrometry; Can. Inst. Min. Met., Spec. v. 11, p. 485-500.

Darnley, A. G., Grasty, R. L., and Charbonneau, B. W.
1971: A radiometric profile across part of the Canadian Shield; Geol. Surv. Can., Paper 70-46.

Grasty, R. L., Charbonneau, B. W., and Steacy, H. R.
1973: A uranium occurrence in Paleozoic rocks west of Ottawa; *in* Report of Activities, Pt. A., Geol. Surv. Can., Paper 73-1A, p. 286-289.

Geological Survey of Canada
1951: Aeromagnetic map of the Renfrew map-area, 31F/7; Geol. Surv. Can., Map 67-G.

Hogarth, D. D.
1970: Geology of the Gatineau Park area; Geol. Surv. Can., Paper 70-20.

Jonasson, I. R. and Dyck, W.
1974: Some studies of geochemical dispersion about a small uranium showing in March Twp., Ontario; *in* Report of Activities, Pt. A. Geol. Surv. Can., Paper 74-1A, p. 61-63.

Lang, A. H., Griffith, J. W., and Steacy, H. R.
1963: Canadian deposits of uranium and thorium; Geol. Surv. Can., Econ. Geol. Series No. 16, 2nd ed., p. 248 and 264.

Quinn, H. A., Wilson, M. E., and Leech, G. B.
1956: Geology of the Renfrew map-area 31F/7; Geol. Surv. Can., Map 1046A.

Richardson, K. A., Darnley, A. G., and Charbonneau, B. W.
1975: Airborne gamma-ray measurements over the Canadian Shield; 2nd Nat. Radiation Env., Rice Univ., v. 2, p. 681-704.

Sabina, A. P.
1970: Rocks and minerals for the collector. Ottawa to North Bay, Ontario; Hull to Waltham, Quebec; Geol. Surv. Can., Paper 70-50, 130 p.

Satterly, J.
1957: Geological Map of the Bancroft area, Ont. Dept. of Mines; Geol. Map 1957-B, accompanying 65th Ann. Rept., Pt. 6; Radioactive mineral occurrences of the Bancroft area.

Steacy, H.R., Boyle, R.W., Charbonneau, B.W., and Grasty, R.L.
1973: Mineralogical notes on the uranium occurrences at South March and Eldorado, Ontario; *in* Report of Activities, Pt. B., Geol. Surv. Can., Paper 73-1B, p. 103-105.

Vokes, F.M.
1963: Molybdenum deposits of Canada; Geol. Surv. Can., Econ. Geol. Series No. 20, p. 160-161.

Yermolayev, N.P.
1973: Uranium and thorium in regional and contact metamorphism; Transl. from Geokhimiya No. 4, p. 551-558.

Project 670068

R. W. Macqueen
Institute of Sedimentary and Petroleum Geology, Calgary

Introduction

Two sedimentary assemblages make up much of the lower and middle Paleozoic succession of the northern Yukon: the basinal Road River Formation (Middle Cambrian-Early Devonian; Jackson and Lenz, 1962; Aitken *et al.*, 1973; map-unit 6 of Norris *et al.*, 1963), and an unnamed succession of laterally equivalent platform carbonate rocks (map-unit 5, Norris *et al.*, 1963). The distribution of these two assemblages and the fauna and age of the Road River Formation are reasonably well known (Norford, 1964; Lenz, 1972), but the nature, fauna, and age of the equivalent platform carbonate rocks are not. This paper describes the carbonate assemblage reports on the composition of the Road River Formation; and comments on relationships between the two sedimentary assemblages in the Wind River — Wernecke Mountains area (Fig. 46.1). Although this area is only a small part of the region underlain by these rocks in the northern Yukon, it contains excellent exposures of the platform carbonate rocks and of the transition to basinal shale of the Road River Formation. Thus, it is an ideal area for detailed study of sequences and relationships outlined on a regional scale by the earlier work of Norford (1964), Lenz (1972) and others.

The field work was completed by Macqueen in 1973 (Macqueen, 1974) and the subsequent sample studies by several specialists (Table 46.1) and on analytical work, was carried out later at the Institute of Sedimentary and Petroleum Geology, Calgary.

Regional Aspects

During the Ordovician to Early Devonian, and probably Late Cambrian as well, the northern Yukon was characterized by platform areas of carbonate sedimentation and at least one intervening basinal area, the Richardson Trough (Norris, 1973). Carbonate sedimentation was most widespread during Late Cambrian(?) and Early and Middle Ordovician time. Late Ordovician, Silurian, and Early Devonian time saw a progressive onlap of Road River Formation basinal facies rocks over older platformal carbonates, as shown by Norford (1964, Fig. 2, p. 4), and by Lenz's (1972) time-slice maps. Nevertheless, carbonate sedimentation persisted through much of the early and middle Paleozoic time interval in several areas, and is now represented by successions in the Ogilvie, Wernecke and White Mountains, and the Keele Range of northern Yukon Territory. Although the White Mountains succession has been interpreted as a westward extension of the northern Interior Platform (Lenz, 1972) or as a local shallow-water carbonate build-up (Norford, 1964), it seems clear that it is part of the widespread early and middle Paleozoic carbonate suite present in the Ogilvie and Wernecke Mountains and in Keele Range. Lower and middle Paleozoic successions over the northern Yukon are usually considered to be in approximate depositional position relative to one another; the possibility exists, however, that these successions have been displaced by significant strike-slip movements as discussed by Bell (1974).

To the east on the northern Interior Platform, a number of distinctive carbonate units represent the early and mid-Paleozoic time interval, including the Franklin Mountain, Mount Kindle, Delorme, and other formations of the Mackenzie and Franklin Mountains and Interior Lowlands (Aitken *et al.*, 1973; Norford and Macqueen, 1975). Kunst (1973) has extended northern Interior Platform stratigraphic terminology for the carbonate facies into the northern Yukon ("Ronning Group" of Kunst, 1973 = Franklin Mountain,

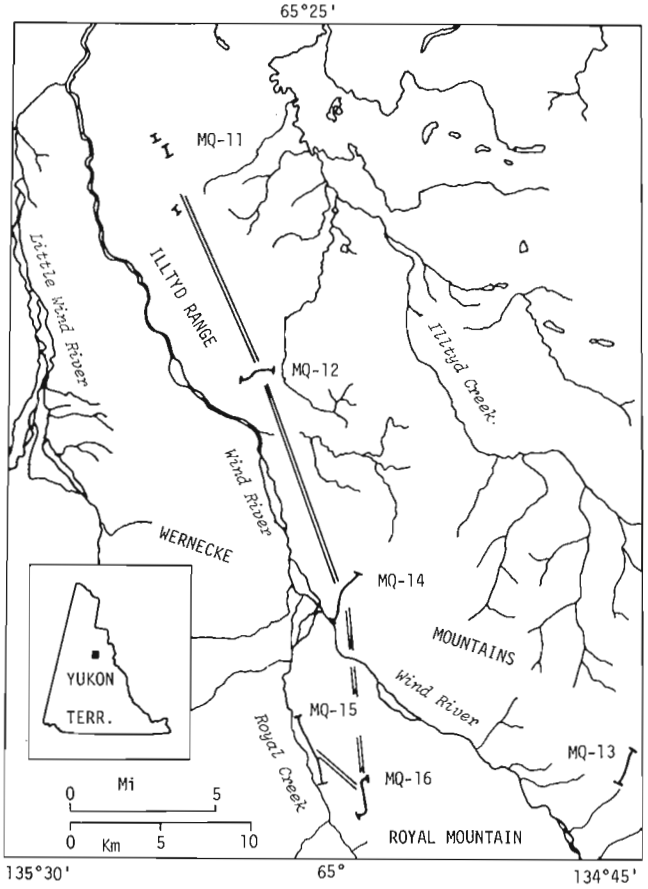

Figure 46.1. Sketch map of Wind River area, Wernecke Mountains, from N. T. S., 1:250 000 sheet 106E, showing section localities and line of cross-section in Fig. 46.2. Inset shows location within Yukon Territory.

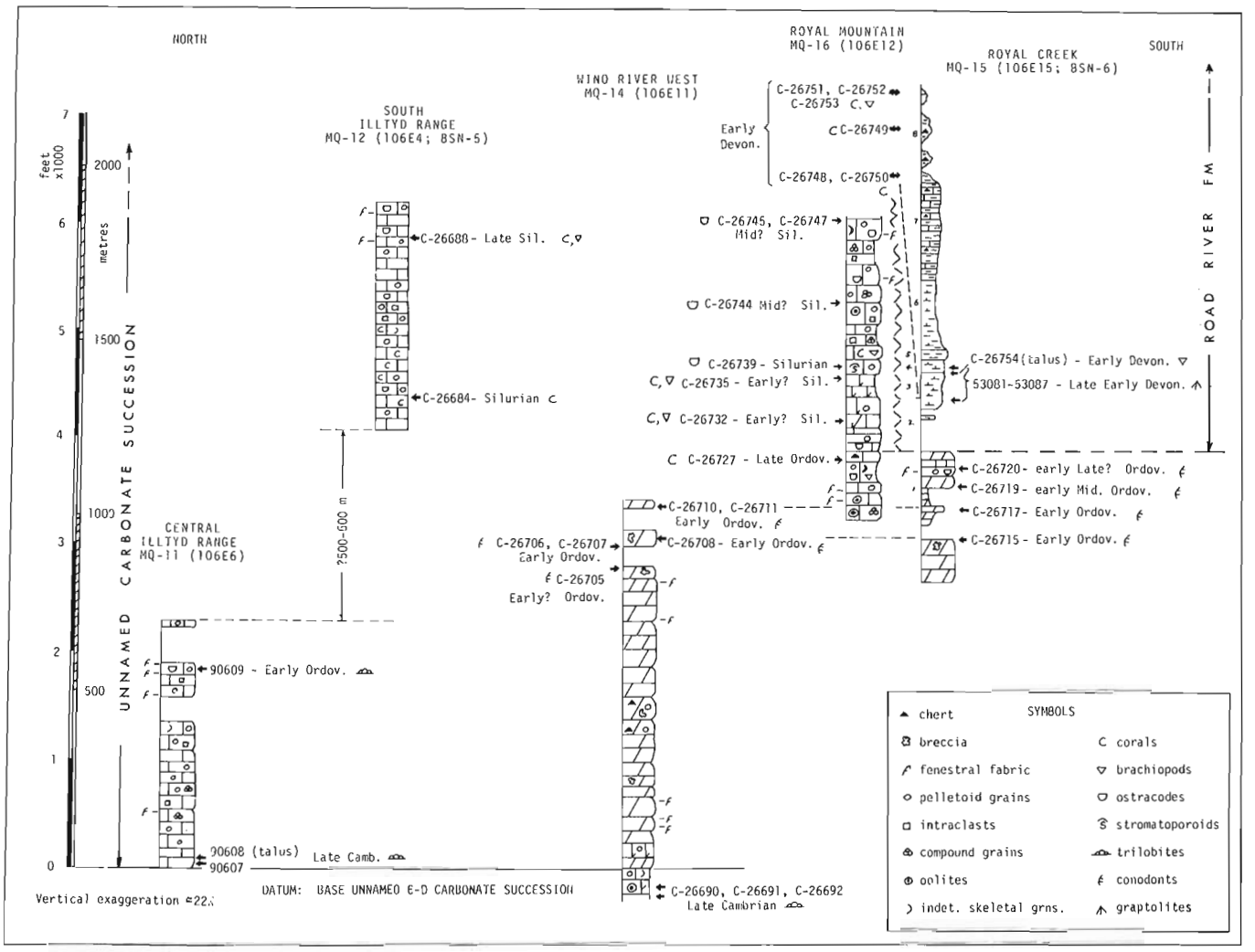

Figure 46. 2. Diagrammatic stratigraphic cross-section, Illtyd Range to Royal Mountain/Royal Creek. See Fig. 46. 1 for location, see text for explanation and Table 46. 1 for additional information on fauna.

Mount Kindle Formations of Norford and Macqueen, 1975). The sequence in the northern Yukon is clearly different as discussed below, however, and requires new stratigraphic terminology not proposed herein. D. C. Pugh of the Institute of Sedimentary and Petroleum Geology currently is conducting a study of subsurface stratigraphy of the Peel Plateau-Eagle Plains area of northern Yukon-northwestern District of Mackenzie. He has traced some borehole log markers from the well established Franklin Mountain-Mount Kindle-Delorme sequence of the Peel Plateau (MacKenzie, 1974; Kunst, 1973) into the subsurface of the Porcupine Plateau-Eagle Plains area (Pugh, pers. comm., 1975). This work should help to clarify relationships between the carbonate successions of the two areas.

To the northwest, in east-central Alaska, a poorly dated carbonate sequence, the ≃ 1040-m-(3400 ft.)-thick Katakturuk Dolomite of possible Cambrian to Devonian age (Dutro, 1970) suggests that shallow-water carbonate sedimentation continued from the northern Yukon into this area as well (*see* also Churkin, 1975).

Platform Carbonates: Unnamed Carbonate Succession

Stratigraphy

The unnamed carbonate succession includes thick to very thick bedded, mostly resistant, light grey weathering limestones or dolomites ranging in age from Late Cambrian to at least Late Silurian, and contains no obvious subdivisions of formational rank. It is underlain, commonly unconformably, by a variety of older Cambrian units in the Wind River-Wernecke Mountains area (Fritz, 1974, Fig. 1; D. K. Norris, 1975); it overlies, with angular unconformity extremely deformed carbonates and phyllites of Proterozoic age immediately to the south in Larsen Creek map-area (Green, 1972).

The Wind River-Royal Mountain-Royal Creek area contains excellent exposures of the carbonate facies and carbonate-shale relationships (Fig. 46. 1); the geology of this area was reviewed by Norris, (1975) and Lenz and Pedder (1972). Three stratigraphic sections provide

details (Fig. 46.2). These are MQ-14, 15, 16: the numbers 106E-11 etc. refer to these stratigraphic sections on a 1:250 000 scale geological map of Wind River (NTS 106E) by D.K. Norris (1975). There the carbonate facies is more than 1860 m (6100 ft.) thick; age range is from at least Early Ordovician to at least Middle Silurian and very likely Early Devonian. This thickness is incomplete, since the top of the carbonate sequence on Royal Mountain above section MQ-16 is inaccessible. A northwest-trending contraction fault between Wind River west (MQ-14) and Royal Creek/ Royal Mountain sections (southwest side up; D.K. Norris, 1975) provides overlap between the upper part of Wind River west section and the lower part of Royal Creek section (MQ-15, Fig. 46.2). Corelation between two sections is established by similarity of conodont faunas identified by C.R. Barnes (C-26708 fauna resembles that of C-26715; C-26710 and C-26711 fauna resembles that of C-26717; Barnes, pers. comm., 1975). The Silurian and younger platform carbonates of Royal Mountain give way abruptly northwestward to Road River shales between Royal Mountain and Royal Creek (Fig. 46.2; note that section MQ-16, Royal Creek, is northwest of section MQ-15, Royal Mountain); beds of Early Devonian age transitional between carbonate and shale facies were examined on the west flank of Royal Mountain between the two sections (GSC fossil localities C-26748 to C-26753, Fig. 46.2). The Royal Creek section is also that described by Norford (1964, section 6) and in part by A.W. Norris (1968). The Wind River west section is almost entirely dolomite; stratigraphically equivalent beds at Wind River east (MQ-13, Fig. 46.1) are limestones in part.

In Illtyd Range, exposed rocks of the unnamed carbonate succession comprise a total interval of more than 1235 m (≈ 4050 ft.) in thickness, and range from Late Cambrian to Late Silurian in age (sections MQ-11, MQ-12, Fig. 46.2). The stratigraphic gap of about 550 m between the two sections shown is estimated from the more complete sections at Wind River-Royal Mountain-Royal Creek. Central Illtyd Range section herein is also partly shown as section 6 of Fritz (1974, Fig. 1); south Illtyd Range herein is also Norford's (1964) section 5.

Obvious evidence of unconformities within any of these carbonate sections is lacking. For 1:250 000 scale geological mapping no subdivisions of formational rank are clearly recognizable within the unnamed carbonate succession in the Wind River-Wernecke Mountains area. Although the stratigraphic interval shown in Figure 46.3 belongs to the lower part (probably early Orodovician) of the unnamed carbonate succession in central Illtyd Range, the overall field character is indistinguishable from that of Silurian strata of the southern Illtyd Range.

Petrography and sedimentology

The most common rock type in the unnamed carbonate succession is a grain-supported, pelletoid grain limestone (Figs. 46.4-46.6). Pelletoid grains (peloids of some authors) are sub-angular to well-rounded, structureless grains of lime-mudstone, generally in the fine to coarse sand size, and of diverse origin (Bathurst, 1971). Pelletoid grain limestone is particularly common in the Illtyd Range sections, which appear to represent interior positions on a shallow-water carbonate bank perhaps of Bahama Banks type. Other types of grains, not obviously of skeletal origin, include intraclasts (angular, redeposited fragments of lithified sediment; Fig. 46.6), compound grains (Figs. 46.6, 46.9), and oöids (Fig. 46.9). Skeletal material, relatively uncommon except in the upper part of the Royal Mountain section (Silurian and probably Devonian), includes mollusc, brachiopod, echinoderm and ostracode shells and fragments, and coral and calcareous algal colonies and fragments. A particularly distinctive feature of these rocks is the fenestral fabric (Bathurst, 1971) which occurs in rocks of Late Cambrian to at least Late Silurian age, identified on sections in Figure 46.2, and illustrated in Figures 46.4 and 46.5. Internal sediment occurs in some fenestral fabric (Fig. 46.5). Similar fabrics, known variously as shrinkage pores, sheet cracks, laminar vugs, desiccation vugs, birdseyes, dismicrites, etc. are widely interpreted as of intertidal origin (e.g. Shinn, 1968). It has yet to be demonstrated, however, that this fabric is exclusively of intertidal origin. In fact, the absence in this succession of other features of probable subaerial origin such as supratidally dolomitized beds, flat-pebble conglomerates, mud cracks, channel fillings, erosion surfaces, unconformities, vadose zone features, and others, many of which are well developed in the Upper Cambrian and Lower Orodovician Franklin Mountain Formation to the east (Norford and Macqueen, 1975, p. 7, 8), argues against an intertidal origin for fenestral fabric in these rocks.

In bedding character, colour, and resistance to weathering, the Silurian-Devonian strata at Royal Mountain resemble older, underlying beds at Royal Mountain and elsewhere. In detail, however, the Royal Mountain sequence contains abundant corals, brachiopods, molluscs, and stromatoporoids (Figs. 46.7 and 46.8). Thus the section appears typical of a carbonate bank margin. Pelletoid grain limestones and fenestral fabrics also are present in this section.

Pure carbonates, the dominance of non-skeletal grains throughout the succession, and the occurrence of sessile organisms (corals, stromatoporoids, calcareous algae) in Late Ordovician and younger parts suggest that the unnamed carbonate succession accumulated on shallow-water carbonate banks during a considerable interval of time and under remarkably stable conditions. A possible analogue is the Bahamas Platform where over 4400 m (≈ 14 500 ft.) of shallow-water carbonates have accumulated since early Cretaceous time (Goodell and Garman, 1969), an interval of approximately 140 million years. There, however, four major cycles of deposition can be recognized, each terminated by a period of erosion and dolomitization (Goodell and Garman, 1969). Although parts of the unnamed carbonate succession are dolomitized, there is no obvious cyclicity to dolomitization. Oddly enough, the interval of time from the base of the Cretaceous to the present about equals that from the base of the Upper Cambrian Franconian stage to the top of the Lower Devonian

Emsian stage (Van Eysinga, 1975). At 4400 m, the known Bahamian succession is over twice as thick as the unnamed carbonate succession of the Wind River-Wernecke Mountains area.

Fauna, age, gaps

With the exception of the Silurian part of the Royal Mountain section, fossils are relatively scarce in rocks of the unnamed carbonate succession. Ages determined from diagnostic collections of trilobites, corals, brachiopods, ostracodes, graptolites, and conodonts are shown in Figure 46. 2 and Table 46. 1. In Illtyd Range, the unnamed carbonate succession ranges from Late Cambrian (Franconian, *Elvinia* Zone) to Late Silurian, whereas in the Wind River-Royal Mountain-Royal Creek area the range is from at least Early Ordovician to Middle(?) Silurian and probably to Early Devonian.

At present, the succession is too poorly dated to identify gaps which may exist, although none is known having obvious stratigraphic expression. Most of the lower part of the succession at Wind River east and west remains undated. In conodont work, no early Middle Ordovician age material was encountered, and C. R. Barnes (pers. comm., 1975) questions whether at Royal Creek a hiatus exists between Early Ordovician beds at C-26717 and early Middle Ordovician beds about 60 m (197 ft.) higher at C-26719. Higher in the succession, Middle Silurian (Wenlockian) beds are tentativley identified at Royal Mountain by an ostracode fauna. Late Silurian and Early Devonian strata are only inferred to be present in the continuous carbonate succession above section MQ-16 on Royal Mountain. There is thus much room for refinement of dating of the succession.

Possible faunal breaks are suspected elsewhere in the unnamed carbonate succession. Studies of trilobites and conodonts were completed by W. T. Dean and T. T. Uyeno, respectively, from collections made in the Keele Range, located about 350 km (200 miles) to the northwest of the Wind River-Wernecke Mountains area. These studies suggest a faunal break in the section, with upper Arenig (uppermost Lower Ordovician) and lowest Llanvirn (lowermost Middle Ordovician) rocks missing through erosion associated with a presumed disconformity between units 2 and 3 (Dean, 1973, p. 2, 25). Only a limited number of samples were available for study, however. Higher in the sequence, no proven Wenlockian (Middle Silurian) sediments have been recognized in the carbonate successions of northern Yukon and adjacent District of Mackenzie.

Comparison with other Late Cambrian-Early Devonian carbonate sequences

The northern Yukon, unnamed, carbonate succession seems unique in its uniformity. As noted above, no obvious divisions of formational rank are evident in the Wind River-Wernecke Mountains area (Fig. 46. 2). In the Keele Range to the northwest, a lower division (units 1, 2, *in* Dean, 1973, p. 2) and an upper division (units 3-6, Dean, 1973) can be mapped separately

Figure 46. 3. View from helicopter of upper part of Central Illtyd Range section. Showing monotonous, thickly bedded sequence of light grey weathering limestones, probably Early Ordovician, dipping gently north. Interval a-b = ≃ 200 m, about 170 to 370 m above base of unnamed carbonate succession.

Figure 46. 4 - 46. 9 (opposite)

Thin section photomicrographs, plane light, bar scale = 2 mm. Figures 4-6, Central Illtyd Range section; Figures 47. 7-47. 9, Royal Mountain section.

4 Fenestral fabric in pelletoid grain packstone/ wackestone. Oriented. 564 m above base of unnamed carbonate succession. Early Ordovician.

5 Mudstone and peletoid grain wackestone (dark grey; medium grey areas are microspar) with irregular sparry calcite-filled cavities (white), many floored by internal sediment. Oriented. 506 m above base of unnamed carbonate succession. Early Ordovician?

6 Bimodal pelletoid grain, compound grain, and intraclast grainstone with sub-horizontal sparry calcite-filled cavities. Oriented. 138 m above base of unnamed carbonate succession. Late Cambrian or Early Ordovician.

7 Skeletal grain limestone, mostly molluscan material with minor ostracode, brachiopod, and calcareous algal detritus. Dark grey matrix is micrite, peletoid grains, and delicate skeletal material. Oriented. 141 m above base of section. Early Ordovician

8 Intraclast, compound grain, and skeletal limestone of bank margin facies. Unoriented. 463 above base of section. Silurian.

9 Oolite grainstone, scattered compound grains and sparry calcite-filled cavities. Unoriented. 10 m above base of section. Early Ordovician.

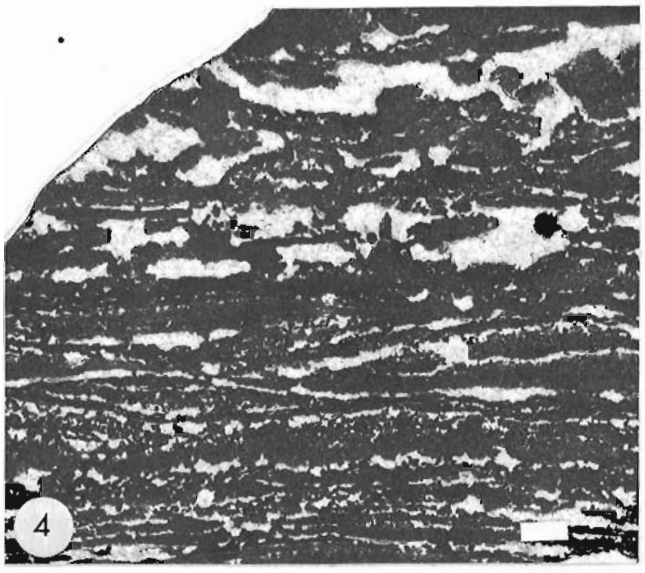
4

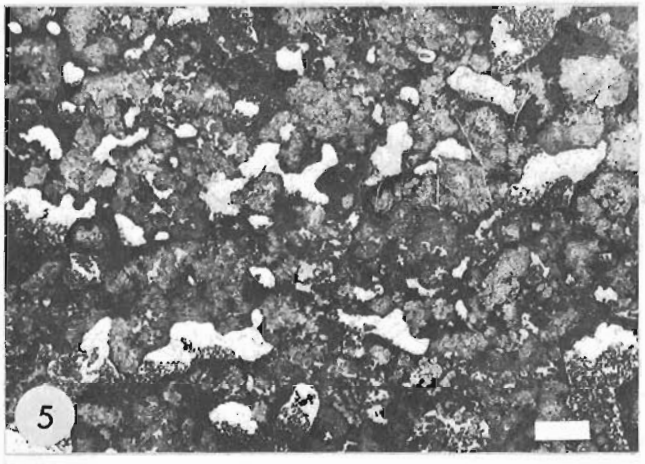
5

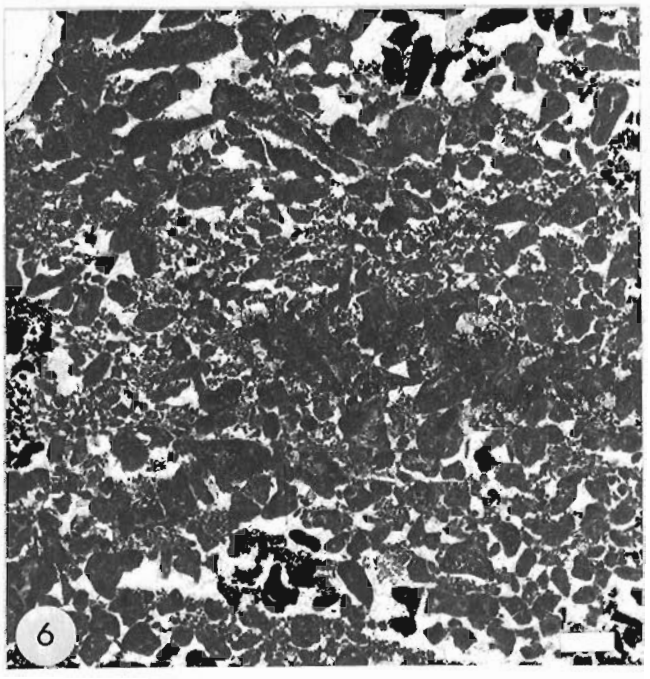
6

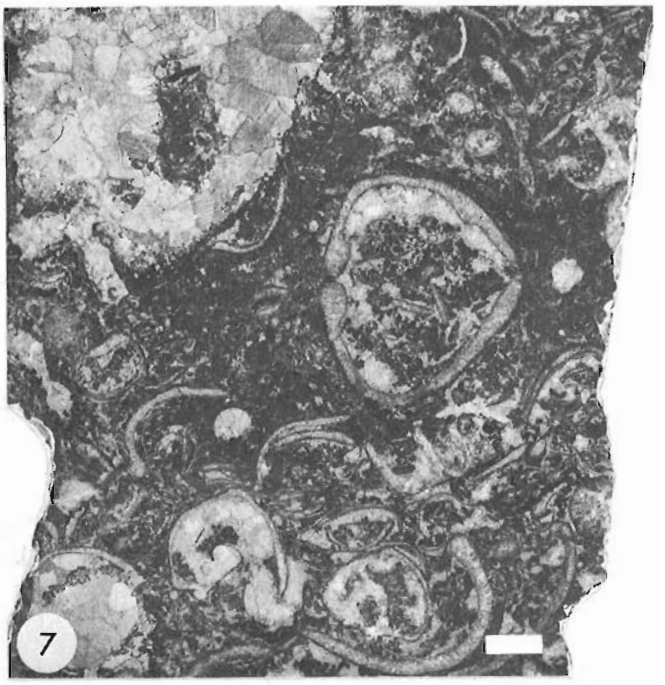
7

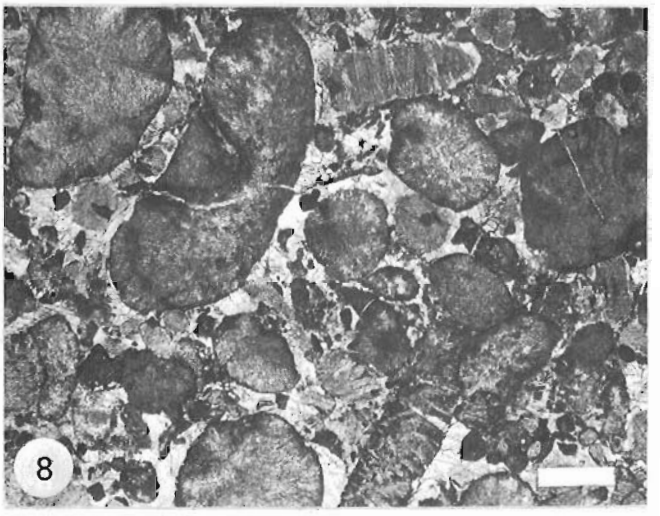
8

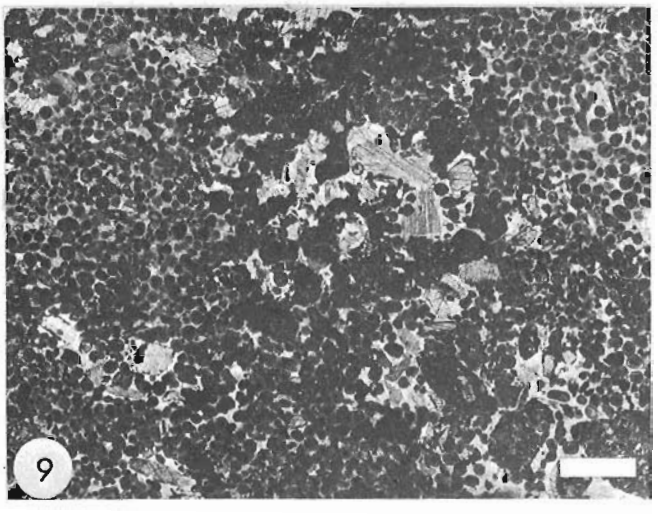
9

Table 46.1

Type and ages of fauna from GSC localities indicated on Figure 46.2

GSC Loc. No.	Fauna	Age	Identified by
53081 to 53087	graptolites	Early Devonian (Emsian)	D.E. Jackson[2]
90607, 90608	trilobites	Late Cambrian (Franconian, *Elvinia* Zone)	W.H. Fritz
90609	"	Early Ordovician (probably late Arenig)	W.T. Dean
C-26684	corals	probably late Early to early Middle Silurian (late Llandovery to early Wenlock)	B.S. Norford
C-26688	brachiopods	Late Silurian, Ludlow to Pridoli	B.S. Norford
C-26690, C-26691, C-26692	trilobites "	Late Cambrian (Dresbachian, *Cedaria-Crepicephalus* Zone	W.H. Fritz
C-26705	conodonts	probably Early Ordovician	C.R. Barnes[3]
C-26706	"	Early Ordovician (probably early Arenig)	"
C-26707	"	Early Ordovician (probably early Arenig)	"
C-26708	"	Early Ordovician (late Tremadoc or early Arenig)	"
C-26710	"	Early Ordovician (early Arenig)	"
C-26711	"	" " "	"
C-26715	"	Early Ordovician (late Tremadoc or early Arenig)	"
C-26717	"	Early Ordovician (early Arenig)	"
C-26719	"	Early Middle Ordovician (late Chazy)	"
C-26720	"	probably early Late Ordovician (?late Eden to early Maysville)	"
C-26727	corals	Late Ordovician	B.S. Norford
C-26732	corals, brachiopods	Silurian (probably late Llandovery)	"
C-26735	corals, brachiopods	" "	"
C-26744	ostracodes	Silurian, probably Niagaran (Wenlock)	M.J. Copeland
C-26745	"	Silurian, probably Niagaran (possibly late Wenlock or early Ludlow)	"
C-26747	"	" "	"
C-26748	corals	Early Devonian, likely Pragian (≈late Gedinnian - early Emsian)	A.E.H. Pedder
C-26749	"	Early Devonian, late Pragian (≈early Emsian)	"
C-26750	"	Early Devonian (Pragian) to Middle Devonian (Eifelian)	"
C-26751	corals, brachiopods	Early Devonian (mid Emsian)	A.E.H. Pedder, A.W. Norris
C-26752	brachiopods	Early Devonian (probably Emsian)	A.W. Norris
C-26753	"	Early Devonian (Emsian)	"
C-26754	"	Early Devonian	"

[1] personal communications (GSC internal reports) to R.W. Macqueen, 1973-75, by paleontologists of the Geological Survey of Canada excepting those otherwise identified.

[2] Department of Earth Sciences, The Open University, Buckinghamshire, England.

[3] Department of Earth Sciences, University of Waterloo, Waterloo, Ontario.

(D.K. Norris, pers. comm., 1975). For part of the succession to the north in White Mountains, Norford (1964) proposed the Vunta Formation to encompass an approximately 870 m (2853 ft.) thick pelletoid grain limestone unit, very similar to rocks of the unnamed carbonate succession in the Illtyd Range, and of Early Ordovician or older to Late Silurian age. The Vunta is underlain by carbonate breccia (Fritz, 1974, Fig. 2a) of presumed Cambrian age. Over 740 m (2431 ft.) carbonates overlie the Vunta in White Mountains, and at least some of this interval is of late Silurian age (Norford, 1964, p. 11). Thus, the Late Cambrian to Early Devonian carbonate sequence in White Mountains apparently contains two and possible three mappable units.

In contrast, the Late Cambrian to Early Devonian carbonate succession of the southern Rocky Mountains contains a variety of distinctive sediments, arranged in cyclic fashion in the lower part (Cambrian to Early Ordovician) and encompassing up to 12 formations over the whole interval (Aitken, 1966; Aitken *et al.*, 1972). Similarly, the Arctic Islands Late Cambrian to Early Devonian succession present in the Parry Islands Fold Belt contains 10 or more formations within the platformal carbonate sequence (Thorsteinsson, 1970), and a carbonate-shale facies change of Ordovician to Devonain age similar to that of the northern Yukon. Clearly much remains to be learned about the unnamed carbonate succession in the northern Yukon. The paucity or lack of units of formational rank within the succession reflects a real difference in epeirogenic regime and not merely a lack of knowledge.

Basinal "clastic" Succession: Road River Formation

Stratigraphy and age

Only one section of the Road River Formation, exposed along Royal Creek and earlier studied by Norford, was examined in detail (Figs. 46.1, 46.2; Norford, 1964; A.W. Norris, 1968). In Norford's measured section, unit 1 was assigned to what is here termed the unnamed carbonate succession; units 2 to 5 to the Road River Formation, suggested to be exclusively Silurian by Norford (1964, p. 41) on the basis of the presence of *Monograptus* sp., thought at that time to be pre-Devonian but now known to range through most of the Lower Devonian; and units 6 to 8 to an unnamed interval of Devonian age (unit numbers appear on section on Fig. 46.2). Units 6 to 8 of this section, 751 m (2464 ft.) in thickness, were later chosen as the type section of the Prongs Creek Formation by A.W. Norris (1968, p. 23-27). This formation is not recognized herein, because neither a mappable nor a major lithologic break exists between units 5 and 6, the proposed contact between the Road River and Prongs Creek Formation. Furthermore, X-ray diffraciton data discussed below show that there is no recognizable compositional change across this contact. The Silurian-Devonian boundary does not correspond to this contact as previously suggested, but occurs not less than 140 m (458 ft.) lower in the section, beneath GSC locality 53081 (Emsian) as discussed below, but the positioning of this boundary, of course, has no bearing on lithostratigraphic nomenclature. Accordingly, all strata above unit 1 in the Royal Creek section are assigned to the Road River Formation. This reassignment is consistent with geological mapping in the area by D.K. Norris (1975). With this reassignment of units, the Road River Formation at Royal Creek reaches an exposed thickness of 1034 m (3416 ft.).

D.E. Jackson examined faunal collections from GSC localities 53081 to 53087, collected by Norford approximately 150 to 245 m (494-803 ft.) above the base of the Road River Formation along Royal Creek (Fig. 2). Jackson (pers. comm., 1975) assigns an Emsian (late Early Devonian) age to all these graptolite collections. These new faunal data demonstrate that the Silurian-Devonian boundary must occur below GSC locality 53081. These new data also have the effect of shrinking the probable Silurian part of the Road River to only 150 m (494 ft.), and emphasizing the contrast in thickness of Silurian strata along Royal Creek with those on Royal Mountain only about 3 km (2 miles) distant, as discussed below.

The Road River Formation at Royal Creek thus ranges in age from ?Late Ordovician or younger (GSC loc. C-26720) to at least late Early Devonian (Emsian) and almost certainly younger: the uppermost 796 m (2613 ft.) of the formation above GSC locality 53087 remain undated. Strata believed by A.W. Norris to be correlative with at least part of the upper, undated 796 m interval of the Royal Creek section occur on the west flank of the Richardson Mountains and form the upper part of Norris's (1968) Prongs Creek Formation. There, these strata are of early Frasnian age (Late Devonian), based on contained conodonts (A.W. Norris, pers. comm., 1975). To the northwest in the headwaters of the Porcupine River area, the top of the Road River is at least as young as Siegenian (mid-Early Devonian) as noted by Churkin and Brabb (1968).

Composition and sedimentology

Even lamination, thin bedding, and local redeposited graded limestone-shale couplets characterize the Road River along Royal Creek and upslope along the west flank of Royal Mountain (Figs. 46.10, 46.11; Norford's section 6, 1964). These fine grained rocks are difficult to study on cut surfaces or in thin section; accordingly, semi-quantitative X-ray diffraction studies were completed on a suite of 53 samples from an interval approximately 81 to 440 m (269-1452 ft.) above the base of the formation at Royal Creek - units 2, 3, 4, 5 and most of unit 6 of Norford's section (Analyst A.G. Heinrich; operating conditions as described for X-ray diffraction data given in Appendix 5 of Norford and Macqueen, 1975). This work shows that the Road River at Royal Creek consists of quartz- and carbonate-rich "shale" with other constituents present in only minor amounts. Quartz, present in all samples, ranges from a low of about 10 per cent to over 80 per cent, and in general is more abundant about 270 m (≈ 900 ft.) above the base of the formation. Not all quartz is of

detrital origin: some occurs as chert and recrystallized ?opaline silica of biogenic origin - proportions are unknown. Calcite is present in all samples in variable amounts, but is less common above about 250 to 300 m (800-1000 ft.) above the base of the formation. Dolomite, less abundant than calcite, shows a distribution similar to calcite. Amounts of calcite and dolomite are influenced by the presence or absence of allodapic carbonate beds (e.g. Figs. 46.10, 46.11); no attempt was made to treat samples selectively in this reconnaissance X-ray diffraction work. Siderite is present in about one third of the samples in trace amounts of approximately 2 per cent, and seems to show random variation. Illite group clay minerals are present in 24 samples, up to a maximum of approximately 3 per cent semi-quantitative. Feldspars of indeterminate species are present in 40 of the samples, in trace amounts to a few per cent. Like quartz, both clay minerals and feldspars are more common in the upper part of the stratigraphic section, more than 270 m (900 ft.) above the base of the formation, although the upward increase in abundance of all three of these components is gradational. Pyrite is common in most samples, in amounts from traces to a few per cent.

X-ray fluorescence analyses were completed also on the 53 samples (analyst A. G. Heinrich; operating conditions - LiF 200 analyzing crystal with vacuum fine collimator and flow plus scintillation counter in series). This work was done primarily to determine whether these "shales" contain zinc and lead in amounts significantly above background, and involved only the range 5° - 45° 2θ. Qualitatively, the following elements are present in amounts slightly(?) above background: Fe, Sr, Cu in all samples; Zn and Ni in most samples; Pb in 34 samples. No other elements appear to be present in more than trace amounts (a few ppm?), within the 5° - 45° 2θ range. There seems to be a slight tendency for larger amounts of Ni, Zn, Pb, and Cu to occur in samples which contain clay minerals of the illite group: but this is not so for Sr. At present, standards are not available at the Institute of Sedimentary and Petroleum Geology to quantify these data.

The pattern of sedimentation that emerges from these observations is one of abrupt upward change from pure carbonates of shallow-water bank origin assigned to the unnamed carbonate succession, to impure carbonates and carbonate rich, quartzose sediments representative of deeper water environments and assigned to the Road River Formation. The carbonate likely was derived from the adjacent carbonate platform, and mainly transported to the deeper water environment of the Road River basinal facies by periodic storm action. The occurrence of relatively few redeposited limestones (Fig. 46.11) along Royal Creek suggests that carbonate turbidites or debris flows were unimportant, despite proximity of the bank margin. Because the bulk of the carbonate in the Road River sequence on Royal Creek probably was bank-derived, it follows that the upper, carbonate-poor part of the Road River (more than 200-300 m above the base of the formation) should indicate drowning of the adjacent Royal Mountain carbonate bank during Emsian or latter time. Because the upper part of the section consists mainly of "shale" and chert with only minor carbonate, accumulation apparently took place under deep-water conditions remote from platformal carbonates [uppermost 555 m (1821 ft.); unit 8 of Norford, 1964; Fig. 46.2].

Platform Carbonate: Basinal Shale Relationships

Two stratigraphic sections, Royal Mountain and Royal Creek, and observations on a sequence of strata located on the west flank of Royal Mountain above Royal Creek and thus geographically intermediate between the two sections, demonstrate, the abruptness of the Silurian-Devonian facies change in this area (Fig. 46.2). In the creek section, the youngest beds of the unnamed carbonate succession are questionably dated as early Late Ordovician: late Early Devonian (Emsian) graptolites occur only 150 m (494 ft.) higher in the section. On Royal Mountain, the highest beds of the section, tentatively dated as Middle Silurian, occur approximately 667 m (2188 ft.) above a stratigraphic level believed to be equivalent to the base of the Road River in the creek section. (It is possible that a slightly higher stratigraphic level in mountain section than that shown equates with the base of the Road River in the creek section, but lithology, fauna, and photogeologic tracing of units suggest the relationship between the two sections is as shown in Fig. 46.2.) It is very likely that the uppermost beds on Royal Mountain, inaccessible above the Royal Mountain stratigraphic section, are of Early Devonian age. This is suggested because: a) redeposited limestones present at GSC localities C-26748 to C-26753 (Fig. 46.2) on the west flank of Royal Mountain can be traced on aerial photographs into carbonate strata outcropping within the uppermost part of the Royal Mountain carbonate sequence; and b) these redeposited limestones contain corals and brachiopods of Early Devonian age (Fig. 46.2; Table 46.1). Thus, the best time line that can be drawn at present between the two sections is that connecting the stratigraphically lowest Devonian beds known in each section, as shown by the dashed line in Figure 46.2. In the creek section, whatever strata are representative of the Late Ordovician, all of the Silurian, and the pre-Emsian Early Devonian must occur within the 150 m interval between the top of the unnamed carbonate and GSC locality 53081: in the mountain section, the best estimate that can be made for this interval is in excess of 700 m, between the suggested stratigraphic equivalent the Road River Formation base and strata at GSC localities C-26748, C-26750. This implies a relief of up to 500 to 600 m between the two sections. How much of this relief is depositional is unknown: certainly some of it can be accounted for by differential compaction of the fine grained Road River sequence upon burial. Additional detailed geologic mapping and stratigraphic work in the area should refine relationships, but a major difference in the thickness of Silurian-Early Devonian strata between the two sections is an inescapable conclusion.

An implied difference in relief of this magnitude suggests that sediments of the carbonate bank on Royal Mountain were, upon accumulation, lithified by frame-building, sessile organisms (corals, stromatoporoids,

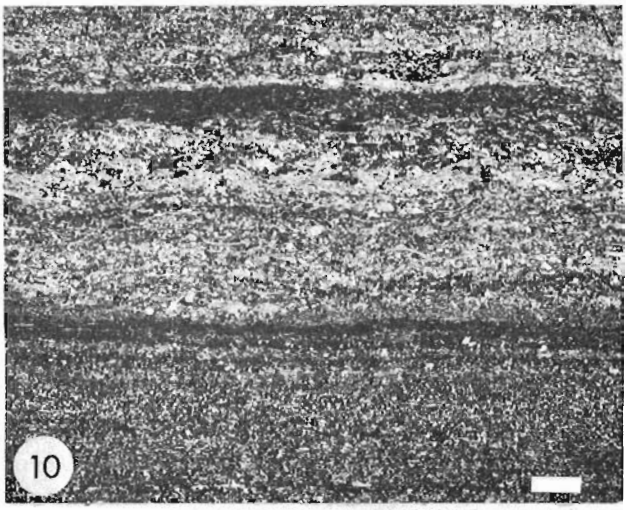

Figure 46. 10. Graded skeletal limestone containing ostracodes, brachiopods, sponge(?) spicules (light grey) to calcareous shale (dark grey). Two full graded sequences present, and base of a third. Road River Formation, west flank of Royal Mountain, estimated stratigraphic level ≈ 125 m above top of Royal Mountain section. GSC fossil locality C-26748, Early Devonian. Thin section, plane light, oriented. Bar scale = 2 mm.

Figure 46. 11. Redeposited limestone with transported, platform-derived fragments of corals, brachiopods, ostracodes, molluscs, and calcareous algae, sharply overlain by laminated calcareous shale. Road River Formation, location as in Figure 46. 10. Thin section, plane light, oriented. Bar scale = 2 mm.

calcareous algae) and by processes of submarine cementation, as described by Schroeder and Zankl (1974) and others for modern reef and bank settings. Considering the proximity of the platform and basinal facies, a puzzling feature is the paucity of carbonate debris flow material in the basinal Road River sequence along Royal Creek. Perhaps the explanation lies in the transgressive relationship between the Road River Formation and the unnamed carbonate succession. G. R. Davies (pers. comm.) has pointed out that carbonate debris flows commonly tend to be associated with regressive conditions and associated subaerial exposure of adjacent carbonate bank facies. Features indicative of subaerial exposure are not evident in the Royal Mountain carbonate bank margin facies of the unnamed carbonate succession, suggesting that subaerial exposure did not occur. This reinforces, on a local scale, the regional observation made by Norford (1964) and Lenz (1972) that the relationship between the Road River Formation and what is here termed the unnamed carbonate succession is a transgressive one. Because debris flows may be triggered by tectonic instability, remarkably stable conditions over a long interval of time are also indicated by the paucity of debris flows on Royal Creek. Does this also mean that there are no erosional breaks or gaps in the Silurian-Devonian bank margin sequence on Royal Mountain? Although this is implied in the stratigraphic and faunal data outlined above, as well as by sedimentological arguments noted here, clearly more study is required on this point.

References

Aitken, J. D.
1966: Middle Cambrian to Middle Ordovician cyclic sedimentation, southern Rocky Mountains of Alberta; Can. Petrol. Geol., Bull., v. 14, p. 405-441.

Aitken, J. D., Fritz, W. H., and Norford, B. S.
1972: Cambrian and Ordovician biostratigraphy of the southern Canadian Rocky Mountains; 24th Intern. Geol. Congr., Guidebook to Field Excursion A19.

Aitken, J. D., Macqueen, R. W., and Usher, J. L.
1973: Reconnaissance studies of Proterozoic and Cambrian stratigraphy lower Mackenzie River area (Operation Norman), District of Mackenzie; Geol. Surv. Can., Paper 73-9, 178 p.

Bathurst, R. G. C.
1971: Carbonate sediments and their diagenesis; Developments in sedimentology, v. 12, Elsevier Publ. Co., Amsterdam.

Bell, J. S.
1974: Late Paleozoic orogeny in the northern Yukon; *in* Symposium on the geology of the Canadian Arctic, eds. J. D. Aitken, D. J. Glass; Can. Soc. Pet. Geol. and Geol. Assoc. Can., p. 25-38.

Churkin, M., Jr.
1975: Basement rocks of Barrow Arch, Alaska, and circum-Arctic Paleozoic Mobile Belt; Am. Assoc. Pet. Geol., Bull., v. 59, p. 451-456.

Churkin, M. Jr. and Brabb, E. E.
1968: Devonian rocks of the Yukon-Porcupine Rivers area and their tectonic relation to other Devonian sequences in Alaska; *in* Intern. Symp. on the Devonian System, ed. D. H. Oswald; Alberta Soc. Pet. Geol., Calgary, v. 2, p. 227-258.

Dean, W. T.
1973: Ordovician trilobites from the Keele Range, northwestern Yukon Territory; Geol. Surv. Can., Bull. 223, 43 p.

Dutro, J. T., Jr.
1970: Pre-Carboniferous carbonate rocks, north-eastern Alaska; *in* Geological seminar on the north slope of Alaska, eds. W. L. Adkisan and M. M. Brosgé; Am. Assoc. Petrol. Geologists, Pacific Section, p. M_1-M_8.

Fritz, W. H.
1974: Cambrian biostratigraphy, northern Yukon Territory and adjacent areas; *in* Report of Activities, Part A, Geol. Surv. Can., Paper 74-1A, p. 309-313.

Goodell, H. G. and Garman, R. K.
1969: Carbonate geochemistry of Superior deep test well, Andros Island, Bahamas; Am. Assoc. Pet. Geol., Bull., v. 53, p. 513-536.

Green, L. H.
1972: Geology of Nash Creek, Larsen Creek, and Dawson map-areas, Yukon Territory; Geol. Surv. Can., Mem. 364, 157 p.

Jackson, D. E. and Lenz, A. C.
1962: Zonation of Ordovician and Silurian graptolites of northern Yukon, Canada; Am. Assoc. Pet. Geol., Bull., v. 46, no. 1, p. 30-45.

Kunst, H.
1973: The Peel Plateau in Future petroleum provinces of Canada ed. R. G. McCrossan; Can. Soc. Pet. Geol., Mem. 1, p. 245-273.

Lenz, A. C.
1972: Ordovician to Devonian history of northern Yukon and adjacent District of Mackenzie; Can. Pet. Geol., Bull., v. 20, p. 321-361.

Lenz, A. C. and Pedder, A. E. H.
1972: Lower and middle Paleozoic sediments and paleontology at Royal Creek and Peel River, Yukon, and Powell Creek, N. W. T.; 24th Intern. Geol. Congr., Guidebook to Field Excursion A14.

MacKenzie, W. S.
1974: Lower Paleozoic carbonates C. D. R. Tenlen Lake A-73 well, Northwest Territories; *in* Report of Activities, Part B, Geol. Surv. Can., Paper 74-1B, p. 265-270.

Macqueen, R. W.
1974: Lower and middle Paleozoic studies, northern Yukon Territory (106E, F, L); *in* Report of Activities, Part A, Geol. Surv. Can., Paper 74-1A, p. 323-326.

Norford, B. S.
1964: Reconnaissance of the Ordovician and Silurian rocks of northern Yukon Territory; Geol. Surv. Can., Paper 63-39, 139 p.

Norford, B. S. and Macqueen, R. W.
1975: Lower Paleozoic Franklin Mountain and mount Kindle Formations, District of Mackenzie: their type sections and regional development; Geol. Surv. Can., Paper 74-34, 37 p.

Norris, A. W.
1968: Reconnaissance Devonian stratigraphy of northern Yukon Territory and northwestern District of Mackenzie; Geol. Surv. Can., Paper 67-53, 282 p.

Norris, D. K.
1973: Tectonic styles of northern Yukon Territory and northwestern District of Mackenzie, Canada *in* Arctic Geology, ed. M. G. Pitcher; Am. Assoc. Pet. Geol., Mem. 19, p. 23-40.

1975: Geological maps comprising Hart River, Y. T., Wind River, Y. T. and Snake River, Y. T. and N. W. T.; Geol. Surv. Can., Open File 279.

Norris, D. K., Price, R. A., and Mountjoy, E. W.
1963: Geology, northern Yukon Territory and northwestern District of Mackenzie; Geol. Surv. Can., Map 10-1963.

Schroeder, J. H. and Zankl, H.
1974: Dynamic reef formation: a sedimentological concept based on studies of Recent Bermuda and Bahama reefs; Proc. Second Intern. Coral Reef Symp., 2, Great Barrier Reef Committee, Brisbane, p. 413-428.

Shinn, E. A.
1968: Practical significance of birdseye structure in carbonate rocks; J. Sediment. Petrol., v. 38, p. 215-223.

Thorsteinsson, R.
1970: Geology of the Arctic Archipelago; *in* Geology and economic minerals of Canada, ed. R. J. W. Douglas, Econ. Geol. Rept. no. 1, p. 552-561.

Van Eysingna, F. W. B., compiler
1975: Geological time table (3rd ed.); Elsevier Scientific Publishing Co., Amsterdam.

47. THE ROLE OF ADSORBED OR STRUCTURED WATER IN THE DIAGENESIS OF THE TERTIARY SEDIMENTS IN THE MACKENZIE DELTA: A PRELIMINARY REPORT

Project 750025

R. R. Barefoot and J. N. Van Elsberg
Institute of Sedimentary and Petroleum Geology, Calgary

Introduction

Previous experience of the junior author had suggested a relationship between a major phase of clay diagenesis resulting in the deposition of diagenetic cements and the main phase of organic maturation and migration. The presence of diagenetic quartz in much greater quantities than could be explained as resulting from clay mineral diagenesis had been observed. It was observed also that in the Tertiary sequence of the Mackenzie Delta, a major change in sonic transit time gradient, suggestive of a major diagenetic event, coincides with major petroleum occurrences and with the beginning of organic maturation. Compilation of formation water data from the area indicated a change in formation water chemistry to be associated with the break in sonic transit time gradient.

Based on this information and on published literature, the authors jointly developed their concept on the nature and behaviour of adsorbed water. This in turn led to the experiments with equilibrium water. Significant results were achieved in this study but much work remains to be done to fully document the preliminary conclusions. Because of the economic significance of the results, and the fact that much feedback is anticipated from presentation of the analytical data and preliminary conclusions, this report is published at this time.

The purpose of this study is to provide a framework in which chemical changes in both the sediment and its associated water, resulting from diagenesis, can be correlated with physical changes.

Sonic transit time plots

Sonic transit time plots were constructed for some 40 wells penetrating the Tertiary sequence of the Mackenzie Delta. Figure 47.1 illustrates diagrammatically the type of plot that results. The depth scale on this plot is reduced considerably so that changes in transit time gradient are enhanced. The transit time-depth plot is constructed by plotting average transit times at 150 m (500 ft.) intervals. The transit time at each point represents the average transit time of a 300 m (1000 ft.) interval of the shaly sand to sandy shale portion of the sediment. By plotting transit time in this manner, several segments can be recognized. In total, 4 characteristic segments were found which are interpreted to represent 4 diagenetic zones (Fig. 47.1).

Zone 1 starts below the permafrost and may extend to a depth of as much as 1200 m (4000 ft.). Its maximum transit time just below the permafrost may be as high as 220μ sec/ft: this high transit time may indicate the presence of gas trapped below the permafrost. Zone 1 is interpreted to represent that portion of the column in which the clays have taken up pore water subsequent to uplift which brought these shales to a shallower depth.

Zone 2 may extend to a depth of as much as 3120 m (10 400 ft.) or be as shallow as 600 m (2000 ft.). The transition from Zone 2 to Zone 3, or Zone 4 directly, occurs at a transit time in the 70-100μ sec/ft range. Zone 2 is considered to represent the zone of pore water loss due to shale compaction.

Zone 3 follows below Zone 2. It is present only where permeable sediments occur below Zone 2.

Where impermeable sediments underlie Zone 2, Zone 3 is missing and Zone 4 follows immediately below Zone 2. Zones 3 and 4 are thought to represent the interval in which adsorbed water removal occurs. It is suggested that Zones 1 and 2 correspond to the stage of eodiagenesis or early diagensis as defined by Foscolos *et al.* (in press) and Foscolos and Kodama (1974).

Chemistry

The transition from Zone 2 to Zone 3 and/or 4 as a result of the change in the mechanism of water release, from pore water release due to compaction to adsorbed water release, coincided with a major chemical change in the formation water and more clearly in the equilibrium water.

1. Formation water.

Five hundred commercially analyzed formation waters recovered on drill stem test were plotted statistically. The data were separated according to the 4 diagenetic zones recognized from the sonic transit time gradients. Frequency plots were constructed of all analyzed elements and of the pH and conductivity data for all 4 zones. Comparison of the frequency plots of the data in each of the 4 zones for a particular element showed that a major peak was common to all 4 zones. Because this peak was common to all 4 zones and also because it was associated with a high pH and with high ion concentration, it was assumed that this peak was owing to contamination of the formation water by drilling mud. A secondary peak also was found. It was assumed that this peak was more representative of the true formation water. All elements, as well as the pH and conductivity, showed a significant shift of the secondary peak between Zones 1 and 2 and Zones 3 and 4.

The most significant conclusion to be drawn from these data is that in Zones 3 and 4 the conductivity was considerably lower and the pH significantly higher than in Zones 1 and 2. Commercial water analyses do not incorporate the elements Si and Al, whereas K is combined with Na and this concentration is calculated

Table 47. 1

Concentrations of Si, Al, Fe and K ions in equilibrium water before and after treated with KOH

Well No. 1

Sample Depth	Si ppm		Al ppm		Fe ppm		K ppm	DIAGENETIC Zones
	equil water	KOH treated	equil water	KOH treated	equil water	KOH treated	equil water	
5495	1	10	0	0	0	0	13	
8161	0	10	0	1	0	0	10. 5	
8174	0	15	1	2	0	0	14. 4	
8182	2	11	0	0	0	0	14. 8	
8203	4	10	1	0	0	0	16. 2	
8218	4	23	1	4	0	0	14. 3	
8227	4	32	1	1	0	0	10. 6	ZONE 2
8770	39	164	6	9	1	1	10. 3	
8837	28	116	4	6	1	1	8. 5	
8845	8	46	2	2	1	0	8. 8	
10211	52	122	6	11	1	2	9. 1	
10218	11	30	2	2	1	1	9. 1	
10222	48	34	2	20	1	4	10. 3	
10226	128	65	4	32	1	12	18. 8	
10230	102	70	4	26	1	5	12. 2	
10483	94	103	11	22	3	5	14. 3	ZONE 4
10490	10	33	3	2	1	1	12. 5	
10500	104	262	9	31	1	7	16. 5	
11341	155	26	8	38	1	8	19. 5	
11357	50	44	6	17	1	4	17. 9	
11377	64	35	6	22	1	4	15. 2	

Table 47. 2

Concentrations of Si, Al, Fe and K ions in equilibrium water before and after treatment with KOH

Well No. 2

Sample Depth	Si ppm		Al ppm		Fe ppm		K ppm	DIAGENETIC Zones
	equil water	KOH treated	equil water	KOH treated	equil water	KOH treated	equil water	
1809	2	20	1	5	0	1	13. 5	
2891	42	68	11	18	1	3	12	
2896	19	31	3	10	0	2	12	ZONE 2
3928	7	35	1	8	0	1	16. 5	
3943	5	6	0	0	15	0	14	
6281	191	156	66	40	8	1	23. 5	
6291	122	69	41	18	6	4	21. 5	
6303	144	93	46	23	6	3	18. 5	
7873	64	23	20	4	3	1	14. 5	
7883	97	67	34	18	3	2	14. 5	
7904	105	54	38	13	4	2	14. 5	
7918	129	40	42	10	4	2	17. 5	ZONE 3
8840	110	38	41	10	4	1	27. 5	
8858	129	36	43	10	4	1	23	
8873	110	50	37	12	4	2	20. 5	
9475	3	11	0	2	0	0	15. 5	
9489	86	43	25	11	2	1	12. 5	
9508	124	42	40	11	3	1	25	
9518	63	34	20	7	2	1	14	
9522	81	46	27	12	2	1	13	

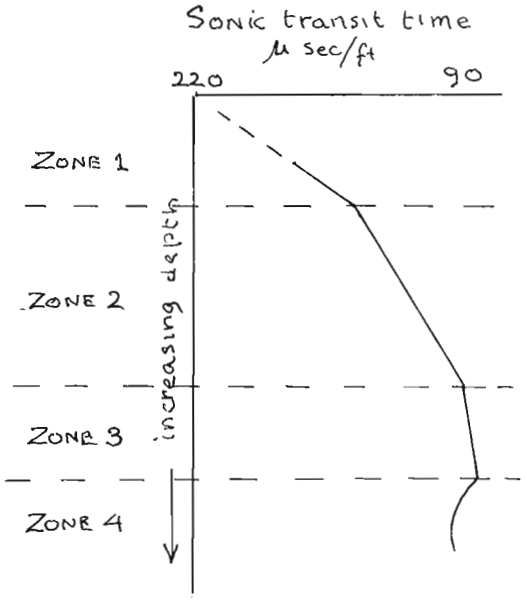

Figure 47. 1. Sonic transit time versus depth.

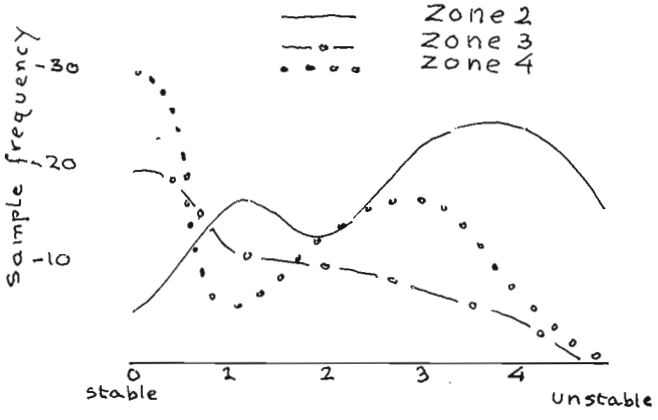

Figure 47. 2. Stability Index.

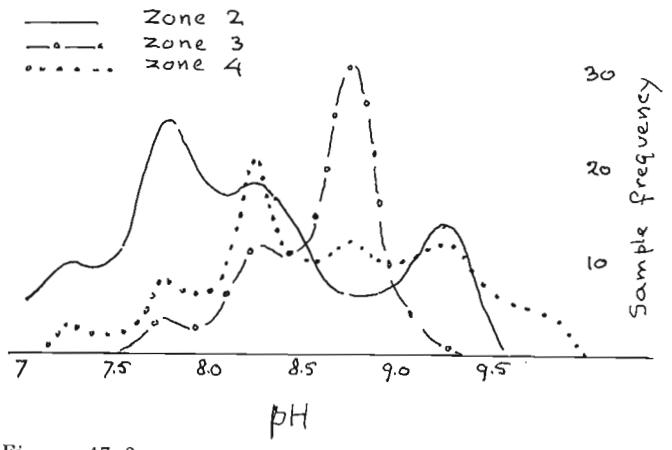

Figure 47. 3

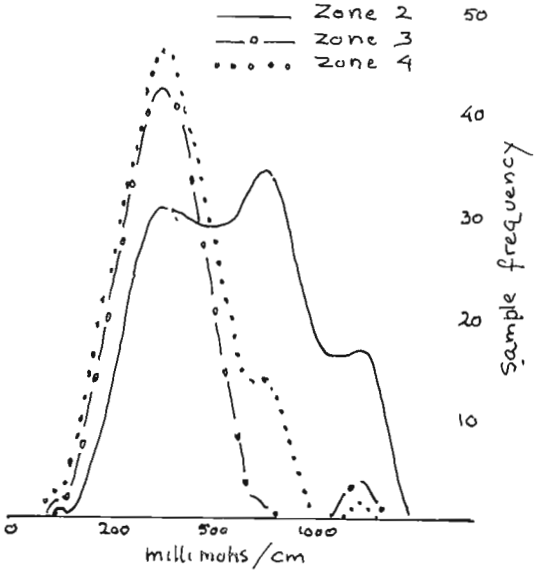

Figure 47. 4. Conductivity.

by difference. This is unfortunate because, as will be shown in this report, Si, Al, Fe and K can provide significant clues in the understanding of the diagenetic history of a sediment sequence.

2. Equilibrium water.

Equilibrium water is defined here as the water which results from immersion of a centre core sample in distilled water for a period of 2 weeks. When rock chips are used in the preparation of equilibrium water, a number of significant observations can be made. A total of 250 centre core samples of shales from 25 wells were treated in this way.

2a. Stability index.

When centre core shale samples are immersed in distilled water, some samples disintegrate rapidly, others disintegrate only partly, and some do not disintegrate at all. This property is termed stability. A stability index ranging from 0 to 5 was assigned to each sample; a stability index of 0 indicates that no disintegration had occurred after two weeks, an index of 5 indicates instant disintegration. Figure 47. 2 represents the frequency distribution of the stability index for Zones 2 to 4. A drastic change in stability index is apparent and the data indicate that, statistically, samples from Zone 2 are far less stable than those from Zone 3. The instability of certain samples in Zone 4 may result from incomplete reactions in this zone.

2b. pH.

Figure 47. 3 shows the frequency distribution of the pH in the equilibrium water of Zones 2, 3 and 4. Again, a drastic change is apparent between Zone 2 and Zones 3 and 4, with the major change occurring between Zones 2 and 3. In Zone 3, the pH peaks at a considerably higher value than in Zone 2.

2c Electrical conductivity.

Figure 47. 4 illustrated the frequency distribution of the electrical conductivities of the equilibrium waters derived from samples from Zones 2, 3 and 4. Again, a considerable change is apparent between samples from Zone 2 and those from Zones 3 and 4; Zone 2 waters peak at a much higher conductivity than those from Zones 3 and 4. Some overlap results, probably representing the migration of fluids from Zones 3 and 4 into the basal portions of Zone 2.

The stability index of rock chips and the pH and conductivity of the equilibrium water all show a significant change between Zone 3 and Zones 3 and 4. From Zone 2 to Zones 3 and 4, the stability of the rock increases, the pH of the equilibrium water increases, and the conductivity of the equilibrium water decreases. The change in pH and the conductivity of the equilibrium water is in accordance with the changes observed in the formation water recovered on drill-stem test.

3. Si, Al, Fe and K in equilibrium water and KOH extracts.

Centre core samples from 3 wells drilled in the Tertiary strata of the Mackenzie Delta were crushed, divided into 2 sets and immersed in distilled water. Both sets of samples were allowed to equilibrate for 2 weeks. KOH was added to one set of samples until the pH had increased above 9. 2 but not above 9. 9. The KOH treated samples were centrifuged, and Si, Al and Fe were analyzed in the supernatant liquids of both sets of samples. K was measured only in the untreated samples. The analytical results from 2 of the wells are presented in Tables 47. 1 and 47. 2. Also shown are the diagenetic zones recognized from the sonic transit time plots.

Table 47. 1, representing data of the first well, shows that Si, Al and Fe are present in small amounts or are absent in the untreated equilibrium waters in Zone 2, but are present in much greater amounts in Zone 4. Zone 3 is missing in this well. A partial increase is apparent in the basal portion of Zone 2. The K ion concentration of the untreated equilibrium water is relatively high near the surface, decreases markedly just above Zone 4 and increases again in Zone 4. The KOH treatment resulted in a general increase of Si, Al and Fe in Zone 2, but a decrease in Zone 4 material.

Table 47. 2 gives the analytical data from the second well: the trend is similar. In the untreated equilibrium water Si, Al and Fe concentrations are low in Zone 2 but much higher in Zone 3. The KOH treated samples again show an increase of Si, Al and Fe in the supernatant solution from Zone 2 while in Zone 3 their concentrations decreased.

4. The effect of KOH on hydrocarbon yield.

Preliminary experiments conducted by T. G. Powell of the Institute of Sedimentary and Petroleum Geology on the effect of KOH on gaseous hydrocarbons (C_1 to C_4) indicate a multifold increase in hydrocarbon yield as a result of blending the samples with a KOH solution rather than with distilled water.

5. Hydrocarbon occurrences relative to the Zone 2 to Zone 3 transition.

In the Tertiary sediments of the Mackenzie Delta, most petroleum occurrences are in close proximity to the Zone 2 to Zone 3 or 4 transition. Gas data from well cuttings (Snowdon and McCrossan, 1973) have been used to establish the ability of a sediment to yield hydrocarbons other than biogenic gas. The top of the mature zone, as indicated by an increase in the proportion of wet gas (C_2 to C_4) in the total gas (C_1 to C_4) extracted, usually occurs in close proximity to the Zone 2 to Zone 3 or 4 transition.

Conceptual framework

All clays have in common a large surface area and, with the exception of kaolinite, a very large surface activity. Because of the large surface activity, they have a large amount of adsorbed material. Two adsorbed layers are recognized; an outer poorly structured layer and an inner, more structured layer. On heating, the two layers are removed in sequence as can be established by Thermogravimetric Analysis (TGA). An example is shown in Figure 47. 5. Differential Thermal Analysis (DTA) shows that removal of the outer layer involves an endothermic reaction (Fig. 47. 5) However, removal of the inner layer frequently appears to involve an exothermic reaction. This suggests that, coincident with the inner layer removal, organic materials are oxidized. Whether these organic materials actually are imbedded within the inner adsorbed layer or not is unknown at this time, but experiments, bearing on this question are in progress.

Browning (1964), in an infrared microscopy study of adsorbed water on clays, also recognized two adsorbed layers (Fig. 47. 6). He recognized an outer layer containing mainly water and an inner layer in which he located silanol groups.

The hypothesis presented here is that the outer adsorbed layer is poorly structured and consists mainly of water, although mineral complexes, both organic and inorganic, may be present. The inner adsorbed layer is far more structured and in it the silanol groups may occur[1]. It is speculated that specific organic compounds and metals, such as Fe, Mn, Pb, Zn and other heavy metals may occur also in this inner layer. However, further experimentation is required before this aspect can be expanded.

Discussion

Present data suggest that a major diagenetic change takes place between Zone 2 and Zones 3 and 4, as recognized from sonic transit time data. This change can be attributed to a change in the system of water release. In Zone 2, pore water is released as a result of compaction. In Zones 3 and 4, the release of water

[1] Silanols are reported also to have a function in the catalytic cracking of hydrocarbons (Commereuc and Martino, 1975).

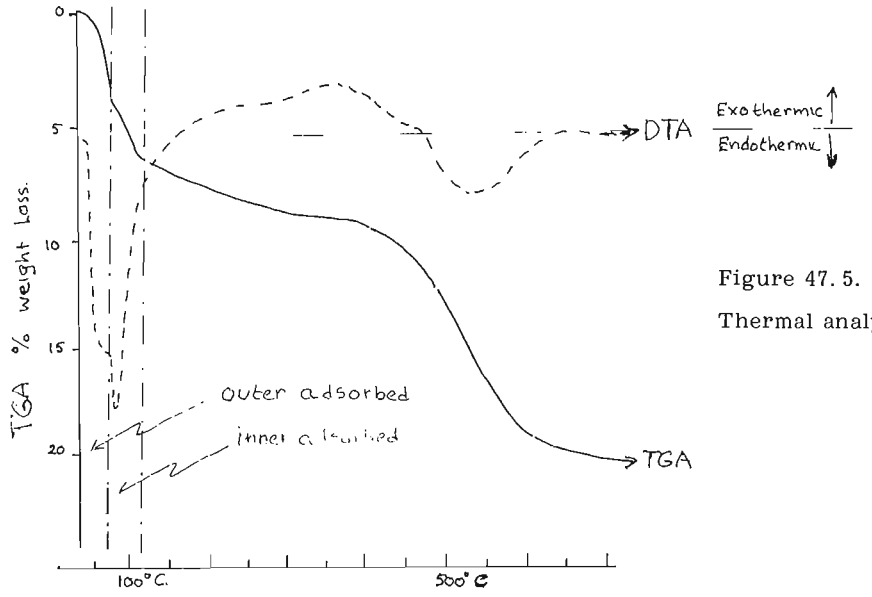

Figure 47. 5.

Thermal analysis of Na saturated shale.

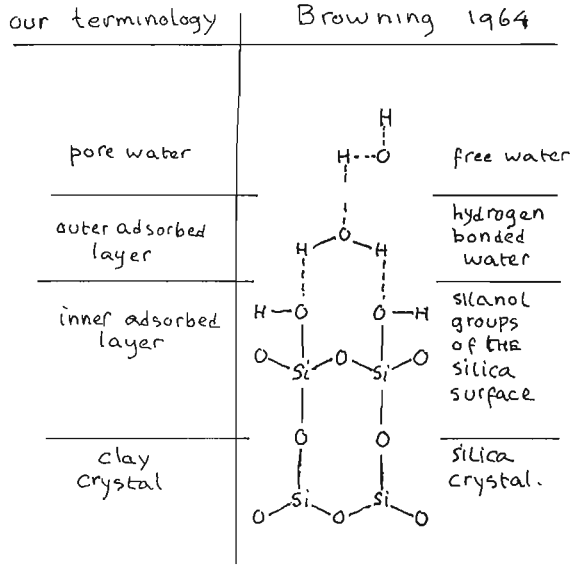

Figure 47. 6. Structure of the adsorbed layers on clays (Browning 1964).

is mainly the result of the removal of adsorbed water from the clays. Adsorbed water can be removed from the clays by increased temperature. However, the experiments indicate that it will be removed also when the clays are brought into an environment enriched in K^+ ions with a pH in excess of 9. 2, and that this process plays a significant role in the diagenesis of Tertiary sediments in the Mackenzie Delta.

In Zone 2, the adsorbed water has not yet been removed and, therefore, the equilibrium water shows low concentrations of Si, Al and Fe ions. The K^+ ion concentration is relatively high but, due to the low pH, no reaction occurs. Approaching the base of Zone 2 where, probably as a result of limited upward migration of water from Zone 3 or 4, the Si, Al and Fe ion concentration had increased, minor clay deposition may have occurred resulting in a depletion of K^+ ions in the equilibrium waters.

At the transition to Zone 3 or, where Zone 3 is missing, to Zone 4, the K ion concentration increases again and the pH rises to a critical level. These two changes may result from thermal destruction of K-feldspars in this zone.

On reaching a critical pH of 9. 2 in the presence of K^+ ions, collapse of the adsorbed layer occurs with a resulting release of Si, probably also of Fe, and possibly also of organic compounds. The clay surface from which the protective layer has been removed starts to react with its environment, supplying Al to the pore water system. Aluminum may also be coming from other silicates. The water that was originally held in both adsorbed layers in a much denser state expands on release and a large quantity of water is supplied to the pore system. The amount of water with dissolved matter released by this process may be in excess of 25 per cent of the total volume in some clays. Organic compounds released together with the water become available for migration and, where they already have reached a mature state, migration of hydrocarbons can take place.

The experiments on the effect of KOH on the yield of gaseous hydrocarbons indicate that an increased hydrocarbon yield may be expected in Zones 3 and 4. Further experiments should indicate whether the increased yield as a result of KOH treatment is due to desorption of gases from the kerogen matrix, or is the result of hydrocarbons being removed from the adsorbed layer. The effect of KOH on the analytical results indicates partial induced diagenesis in Zone 2 because of adsorbed water removal, resulting in an increase in Si and, to a lesser extent, in Al and Fe. In Zones 3 and 4, where the adsorbed layers already have been partly removed, the addition of K^+ ions results in the deposition of solid products such as clays and quartz with a resultant depletion of Si, Al and Fe in solution.

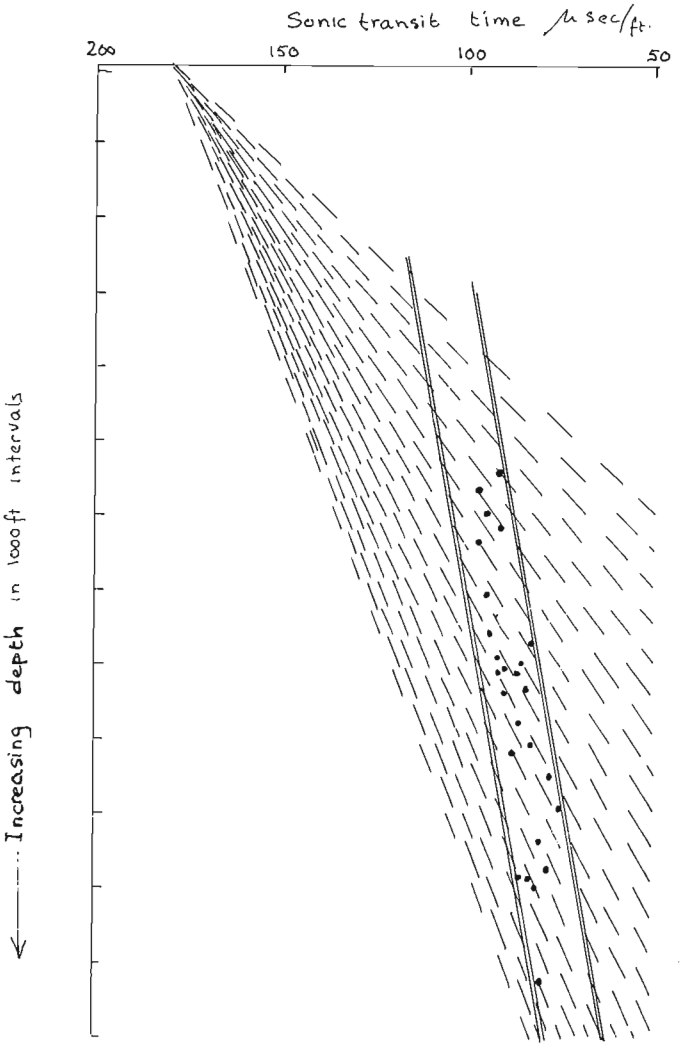

Figure 47. 7. Transit-time-depth plots of Zone 2 (dashed lines) and associated transit time at which transition to Zone 3 or 4 occurs (dots).
Transit time depth plots are made in intersect at an arbitrary transit time of 180 μ sec/ft. Double lines indicate correlation.

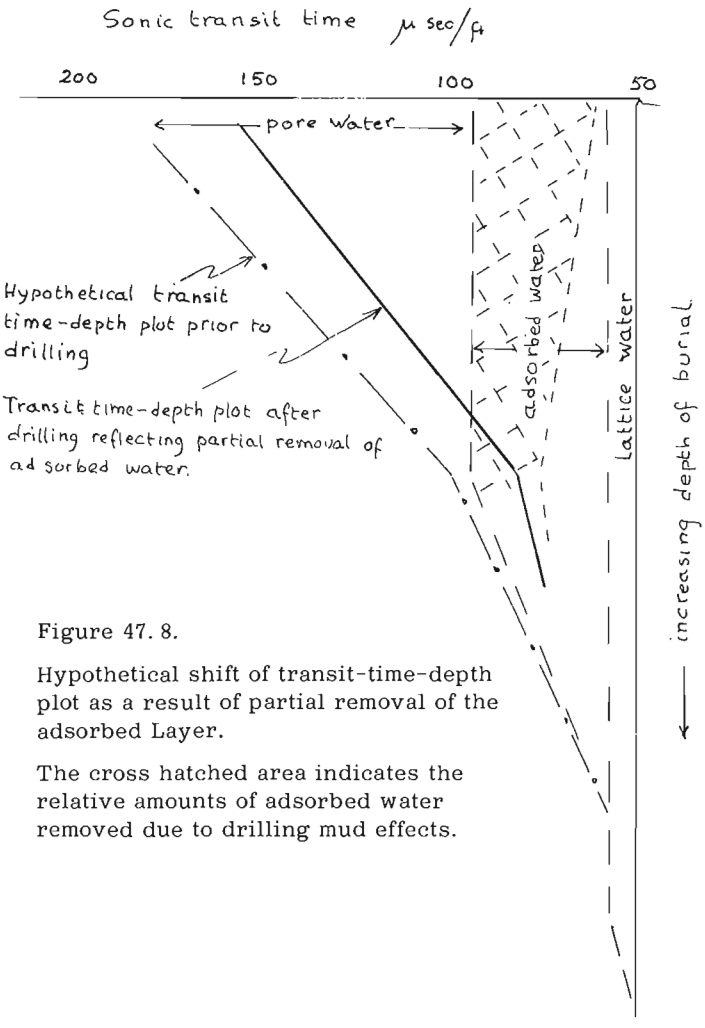

Figure 47. 8.

Hypothetical shift of transit-time-depth plot as a result of partial removal of the adsorbed Layer.

The cross hatched area indicates the relative amounts of adsorbed water removed due to drilling mud effects.

Implications of Results

1. The possible use of seismic data in locating the transition between Zone 2 and Zones 3 and 4

Good quality seismic interval velocity data can be converted readily to transit time data. From these, transit time gradients can be constructed in much the same way as it is done from sonic logs. From the transit time gradients the transition between Zone 2 and Zones 3 or 4 can be recognized. Since this transition has been shown to correspond with a major change in both organic and inorganic diagenesis, it would appear that knowledge of its depth before drilling would be of economic significance, not only in planning a well program but also in reconstructing the diagenetic history of a basin.

2. Induced diagenesis caused by drilling muds

In the Mackenzie Delta, drilling muds usually contain large quantities of K^+ ions and the pH commonly is maintained above 12. Since the laboratory experiments indicate a considerable diagenetic change at a pH of from 9. 2 to 9. 9 in the presence of K^+ ions, presumably as a result of adsorbed water removal, there is little doubt that the drilling muds presently in use cause severe induced diagenesis, bringing into solution large quantities of material that will eventually precipitate as cementing materials. This will of course reduce the permeability around the borehole[1]. In Figure 47. 7, the decrease in transit time with depth in Zone 2 (dashed lines) and the transit time at which

[1] Removal of the adsorbed water will also affect the sonic transit time. As a result of induced diagenesis, the sonic tool may read an "apparent" transit time that may not be representative of the true formation transit time.

the transition to Zones 3 or 4 (dots) occurs, are plotted for a total of 26 wells. A good correlation is apparent which does not reflect age or facies differences. It is independent also of the areal distribution of the wells. A steep apparent transit times versus depth slope corresponds to a lower transit time at which the transition to Zone 3 or 4 occurs. A less steep transit time versus depth slope corresponds to a higher transit time at which the transition occurs. Figure 47.7 may reflect the degree of induced diagenesis of the formation near the borehole as a result of exposure to the drilling mud. In Figure 47.8, it is shown diagrammatically how the transit time versus depth slope in Zone 2 as well as the transit time at which the transition to Zone 3 or 4 occurs, would change as a result of the removal of adsorbed water. The shallower portions of the hole would be exposed longer to the drilling mud than the deeper portions and, therefore, more adsorbed water would be removed at shallower depth than at greater depth. This would result in a steepening of the apparent compaction transit time versus depth slope in Zone 2. At the same time, the transit time at the transition between Zone 2 and Zone 3 or 4 would shift to a lower value as a result of adsorbed water removal. The more severe the induced diagenesis, the steeper the transit time-depth slope in Zone 2 and the lower the transit time at which the transition to Zone 3 or 4 occurs.

Thus, although stabilization of the hole is attained as a result of collapsing the clays with potassium, severe cementation may be induced either immediately during drilling or at a later date after the formation waters have returned to their natural equilibrium.

Conclusions

1. Most clays have large amounts of adsorbed material. Two adsorbed layers can be recognized, and removal of these layers results in transfer of Si, Al, Fe and large quantities of water to the pore water system. The silanol groups of the inner adsorbed layer may be the major source of Si. Adsorbed water can be removed when brought into an environment that is rich in K^+ ions and has a pH in excess of 9.2. In nature, this medium is supplied in diagenetic Zones 3 and 4. A process such as thermal breakdown of K-feldspars may play a key role in creating the right environment for adsorbed water removal with all its consequences.

2. Much information about the removal of the adsorbed layers with all its diagenetic consequences can be gained by analysis of the formation water and especially the equilibrium water. Present commercial analyses, however, do not account for the critical elements such as Si, Al, Fe and K.

3. The removal of the adsorbed layers coincides with an increased content of organic compounds in the pore water as well as an increase of the pore water itself. If the process of removal of the adsorbed material does not have a function in the maturation process of the organic material, it becomes critical that the time of maturation relative to removal of the adsorbed layer be established. If maturation were to occur much later, migration may be prohibited due to lack of a migrating medium. If it occurs at the same time, or slighly before removal of the adsorbed layer, a much more favourable environment for hydrocarbon migration and accumulation would be established.

4. In the Tertiary sediments of the Mackenzie Delta, the major diagenetic change occurring between Zone 2 and Zone 3 or 4 coincides with the occurrence of most hydrocarbon accumulations found to date. The organic maturation level, as indicated by gas logs, also corresponds in most cases with this transition. The depth at which this transition occurs can be derived not only from sonic transit time data but, also, from good quality seismic velocity information. It follows, therefore, that seismic data can be used to locate this major diagenetic event.

5. Drilling muds used at present in the Mackenzie Delta may induce severe diagenetic reactions resulting in deposition of solids such as quartz and clay as diagenetic cements near the borehole. Severe plugging of the reservoir may result.

References

Browning, W. C.
1964: The hydroxyl factor in shale control; J. Petrol. Tech., October, p. 1177-1186.

Commereuc, D. and Martino, G.
1975: Catalyse Homogène Supportée; Rev. Inst. Français de Pétrol., Jan.-Feb., p. 8-112.

Foscolos, A.E. and Kodama, H.
1974: Diagenesis of clay minerals from Lower Cretaceous shales of northeastern British Columbia; Clays Clay Miner., v. 22, no. 4, p. 319-335.

Foscolos, A.E., Powell, T.G. and Gunther, P.R.
The use of mineralogical, inorganic and organic indicators for evaluating the degree of diagenesis and oil generating potential of shales; Geochim. Cosmochim. Acta. (in press).

Snowdon, L.R. and McCrossan, R.G.
1973: Identification of petroleum source rocks using hydrocarbon gas and organic carbon content; Geol. Surv. Can., Paper 72-36.

48. GEOCHEMICAL ORIENTATION SURVEYS FOR URANIUM IN SOUTHERN BRITISH COLUMBIA

Project No. 750052: Uranium Reconnaissance Program

S. B. Ballantyne and K. Bottriell
Resource Geophysics and Geochemistry Division

As part of the Federal-Provincial Uranium Reconnaissance Program geochemical orientation surveys were carried out during July and August in south-central and southeastern British Columbia. In particular three pilot study areas were sampled, each with distinctly different modes of occurrence, physiographic, climatic and mineralogical features.

Fuki Donen Prospect Area

Situated within the Greenwood Mining Division, 11 miles northeast of Beaverdell or about 35 miles southeast of Kelowna, an area 18 by 15 km centred around the Dear Creek Fuki outcrop was sampled.

The original discovery was made in August, 1968 by geologists of Power Reactor and Nuclear Fuel Development Corporation, now operator, who were conducting a carborne scintillometer survey in the area. Since 1969, Nissho-Iwai Canada Ltd., the owners, have conducted yearly diamond drill programs on this claim group and others in the vicinity of Beaverdell.

Secondary uranium mineralization, identified as meta-autunite, in a rock specimen taken from the Dear Creek Fuki outcrop and analyzed spectrographically assayed 0.3 per cent U (Ruzicka, 1971). It is reported that "radiometric anomalies equivalent to 0.02 - 0.70 per cent U_3O_8 have been recognized" (Anon., 1973). Mineralization occurs in the basal sediments, mainly sandstone and conglomerate, of a Tertiary olivine basalt named the "Plateau Basalt Formation" (Anon., 1973). This flat-lying formation has a direct effect on the topography of the area which is a plateau with an elevation of 1300 m. Eleven small lakes are situated on the plateau with overburden and Quaternary sediments covering almost 70 per cent of the lakeshore and low lying area.

Stream sediments and lake sediments were collected at an average sample density of one sample per 5.8 km^2. Wherever possible, a heavy mineral concentrate was collected by means of a gold pan at the stream sediment sample location. Some stream and surface lake waters were also collected. The sediments were dried, sieved to minus 80-mesh and sent to Atomic Energy Canada, Ltd. (A.E.C.L.), Ottawa for uranium determination by delayed neutron activation. Preliminary results would seem to indicate that the lake sediment and stream sediment anomalies coincide with drilled buried uranium mineralization while the heavy mineral concentrates are not a reliable indicator.

Grand Forks Study Area

This study area is located north of Grand Forks, British Columbia, between Christina Lake to the east and the Granby River to the west. The Christina Range of the Monashee Mountains runs roughly north-south at elevations to 1680 m while the Granby River Valley parallels it at approximately 465 m above sea level. Steep V-shaped valleys of all major creeks in the area cross-cut this north-south trend. The area is semi-arid with the drainage systems often being intermittent or dry. South-facing slopes are sparsely treed and show more outcrop than the heavily wooded north slopes or drift-covered flat area.

The general geology of the area is a raised fault block of high grade metamorphic igneous and sedimentary rocks which Little (1957), named the Grand Forks Group. A part of the Eastern Tectonic Belt (Wheeler, 1966), they are folded about east-southeast and northerly trending axes bounded to the east and west by two major Tertiary faults, namely the Kettle River Fault and the Granby River Fault (Preto, 1970). Preto (1970) divided this part of the Shuswap Metamorphic Complex into ten map-units.

The mineralization, uraninite with secondary uranophane, occurs in quartz-feldspar-mica pegmatites interlayering with other members of the gneissic complex (Anon., 1970).

Armstrong (1974) in his discussion on "porphyry" uranium deposits quotes assays of 0.60 - 100 per cent U_3O_8 for grab samples of the granite pegmatites taken from the Boundary Explorations prospect.

An 18- by 14-km area was sampled for stream sediments giving an average sample density of one sample per 3.45 km^2. Heavy mineral concentrates and stream waters were also collected where possible; however, many of the creeks were dry.

The samples were dried, sieved and sent to A.E.C.L. for uranium determination by delayed neutron activation. Further analysis is being completed and rock specimens taken from the study area examined.

Horsethief Creek and Forster Creek Study Area

This area is located within the Golden Mining Division Horsethief Creek, Forster Creek and much of their drainage system was sampled in the middle of August. Both lie within the Purcell Mountains that have elevations greater than 3000 m; they are glacier fed and they cross-cut the main structural and stratigraphic trends. The area is accessible by logging roads which run directly west from Radium Hot Springs.

Horsethief Creek was sampled to an elevation of 1500 m and Forster Creek to 1800 m elevation.

Concentrations of mechanically transported black sand containing columbium- and uranium-bearing minerals (uraninite, pyrochlore-microlite, euxenite-polycrase) are found in Forster Creek, and are thought to be representative of the Horsethief Batholith, a

porphyritic quartz monzonite of Cretaceous age (Reesor, 1973). On the other hand, sediments from the upper reaches of Horsethief Creek reflect the presence of Proterozoic Dutch Creek Formation consisting of slate, argillite, quartzite and some carbonate rocks.

References

Anon.
1970: Geology, exploration, and mining in British Columbia, 1970; p. 432-433.

1973: Geology, exploration and mining in British Columbia, 1973; p. 49-50.

Armstrong, F. C.
1974: Uranium Resources of the Future- "porphyry" uranium deposits IAEA-SM-183/12; *in* Formation of Uranium Ore Deposits, Proceedings of a Symposium, Athens, p. 631.

Little, H. W.
1957: Kettle River, east half; Geol. Surv. Can., Map 6-1957.

Preto, V. A.
1970: Structure and petrology of the Grand Forks Group, British Columbia; Geol. Surv. Can., Paper 69-22.

Reesor, J. E.
1973: Geology of the Lardeau map-area, east-half, British Columbia; Geol. Surv. Can., Mem. 369, p. 92.

Ruzicka, V.
1971: Geological comparison between East European and Canadian Uranium Deposits; Geol. Surv. Can., Paper 70-48, p. 91-92.

Wheeler, J. O.
1966: Eastern tectonic belt of Western Cordillera in British Columbia; *in* Tectonic history and mineral deposits of the Western Cordillera; Can. Inst. Min. Met., Special Vol. no. 8, p. 27-45.

WELL WATER URANIUM RECONNAISSANCE IN EASTERN MARITIME CANADA

Project 720067: Uranium Reconnaissance Program

W. Dyck[1], E.W. Garrison[1], G.S. Wells[1], and H.O. Godoi[2]
Resource Geophysics and Geochemistry Division

Introduction

To test the feasibility of using well waters as a means of tracing U occurrences in the Carboniferous basin of the Maritimes, a survey of parts of the basin was carried out during the summer of 1975. This survey was conducted under the auspices of the newly established Federal-Provincial Uranium Reconnaissance Program with the provinces of Prince Edward Island, Nova Scotia and New Brunswick providing background information and student manpower and the Department of Energy, Mines and Resources providing funds and facilities for field and analytical work. The Geology Department of Mount Allison University provided laboratory space and services for the "field" laboratory.

Approximately 2000 wells were sampled from an area comprising all of Prince Edward Island and roughly 7000 square miles (18 000 km^2) of coastal mainland Nova Scotia and New Brunswick from Miramichi Bay to New Glasgow. An overall sample density of one sample/5 square miles (13 km^2) was aimed for but in swampy and mountainous areas this density could not be achieved. In addition to the above samples approximately 120 well water samples and 100 stream water and stream sediment samples were taken from the Triassic region of the northern Annapolis valley over an area of about 500 square miles (1300 km^2). Also in two areas within the sampled region the wells and streams were sampled in greater detail. One area of 260 square miles (665 km^2) situated between Sackville and Moncton was sampled at a density of one sample per 2.4 square miles (6.2 km^2). In the other, about 150 square miles (390 km^2) near Pugwash, N.S., one sample per 1.1 square miles (2.5 km^2) was collected.

In the field laboratory an unacidified water sample was analyzed for U, Rn, O_2 F, Eh, pH, alkalinity and conductivity. A second unacidified sample was sent to the Department of the Environment Laboratory in Moncton for NO_3, SO_4, Cl, Ca, and K analysis, and an acidified sample was sent to the Geological Survey of Canada Laboratories for He, CH_4, H_2, Cu, Zn, Pb, Fe, and Mn analysis.

Results

Well water U and Rn anomalies occur along the northern coast of Nova Scotia and New Brunswick between New Glasgow and Cape Tormentine. There are known Cu-U occurrences in this area (Brummer, 1958) but the extent and frequency of these well water anomalies suggest other possible occurrences of U. U and Rn values of up to 60 ppb and 5700 pc/l, respectively, were encountered in this region with highest values in the vicinity of the following places: Baie Verte; Pugwash, where a Cu-U occurrence near Chisholm Brook has been known for some time; near Fox Harbour; Tatamagouche; and River John. Element concentrations generally decrease from the coast inland. The high relief and granitic rocks of the Cobequid could very well have been the source of the U now being leached by the groundwaters in the coastal plains. Figures 49.1 and 49.2 show the well water U and Rn distribution patterns of the Pugwash area. The location of the Chisholm Brook Cu-U occurrence is marked with a circle. According to Brummer (1958) selected samples from this occurrence contained up to 0.025 per cent U_3O_8 and 60.1 per cent Cu. It is hard to imagine that such a weak occurrence could cause such extensive well water U and Rn anomalies. One is tempted to postulate more occurrences in this and other areas with similar U and Rn highs, but only a thorough detailed investigation will reveal the cause of these anomalies. Smaller U highs were encountered in a band between Sussex and Moncton ($\leq$ 18 ppb U and $\leq$ 3600 pc/l Rn). In the lowlands around Sackville, Amherst, and Truro U levels of up to 6 ppb and Rn levels up to 5000 pc/l were encountered. On Prince Edward Island the U-Rn levels did not exceed 7 ppb and 2700 pc/l, respectively, with the higher values occurring mainly in the northern third of the island. Regionally the U-Rn coincidence is clearly visible although individual sites did not always show positive correlation.

Commentary

As a guide to the possible significance of these results, 277 spring and well water samples in the U districts of Wyoming and South Dakota were found to contain up to 200 ppb U and a mean of 25 ppb U. (Denson, 1956); and Rn levels of up to 200 000 pc/l were encountered in Wyoming (Harshman, 1968).

The abundance of U in well waters in the sedimentary rocks of the sampled area relative to surface waters, suggests an active, oxidizing water regime which effectively leaches U from the rocks and/or the numerous weak U occurrences in the area. The relatively low Rn levels encountered suggest weak U mineralization, although the wide sample spacing could make this conclusion invalid because of the relatively short range of Rn compared to that of U. While one might expect weak U occurrences to be associated with economically significant mineralization in any area, the converse is not necessarily true.

[1]Geological Survey of Canada, Ottawa

[2]DNPM, Brazil

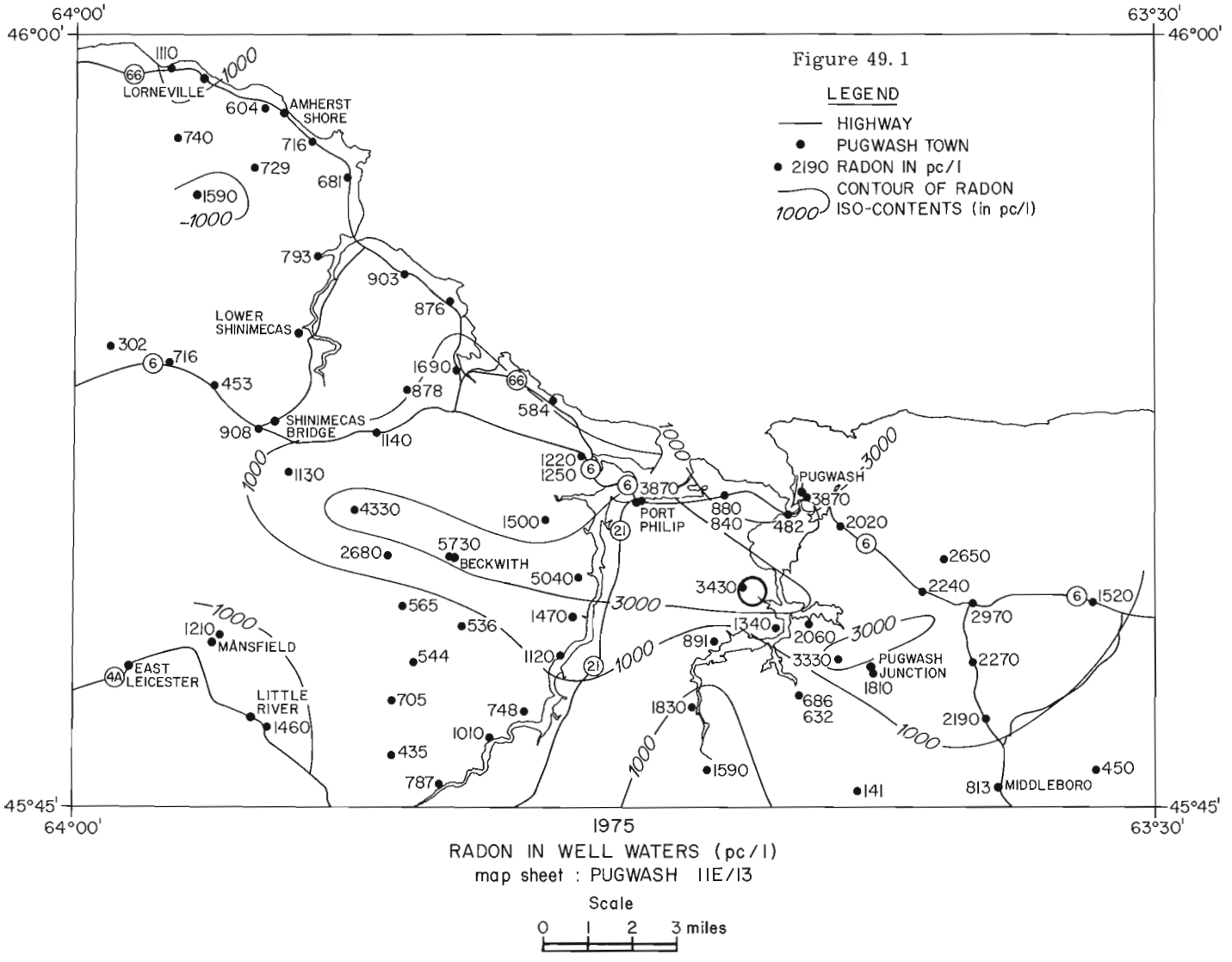

Other Gases

He, CH_4, H_2 results are available from about half the samples at this time. No significant H_2 results have been obtained to date. However, a prominent CH_4 anomaly with samples containing up to 60 standard cc of CH_4/l water was encountered between Sackville and Moncton along the east bank of the Peticodiac River and both banks of the Memramcook River. The proximity of the Stony Creek gas and oil field on the west bank of the Peticodiac River suggests itself immediately as the source of this CH_4. Perhaps it should be mentioned that the second highest He value (6800 x 10^{-5} std cc/l water) was also found in this area, but its significance is unknown. Although the great majority of samples analyzed so far contain background or equilibrium amounts of He (~11 x 10^{-5} std cc/l H_2O) isolated anomalous values of up to n x 1000 x 10^{-5} std cc/l H_2O as well as two anomalous areas have shown up so far. One, rather weak, anomalous area coincides roughly with the east-west trending faults and the Egmont Bay anticline on Prince Edward Island where the basement rocks come to within 4000 feet (1200 m) of the surface. The second area is just west of Cape Tormentine. Here up to 4400 x 10^{-5} std cc/l were encountered. It also appears to be centred on an anticline with basement rocks within 3000 feet to 5000 feet (900 m to 1500 m) from the surface. The highest He value encountered to date (10 200 x 10^{-5} std cc/l) comes from the southern edge of this anomaly on the southern shore of Baie Verte where the sediment cover has reached a thickness of 10 000 feet (3000 m). It is too early to draw conclusions on the value of He in exploration. The evidence so far suggests that it may be useful in elucidating geologic structure. There is as yet no evidence that the He is related to the U or Rn in the well waters.

Conclusion

The well water reconnaissance orientation survey has shown that U and Rn are useful tracers in outlining U mineralization in the Carboniferous basin of the Maritimes. As results for other trace elements such as Cu and Zn become available and the U and Rn results are studied in more detail other aspects of the hydrogeochemistry of the Carboniferous of the region will become evident.

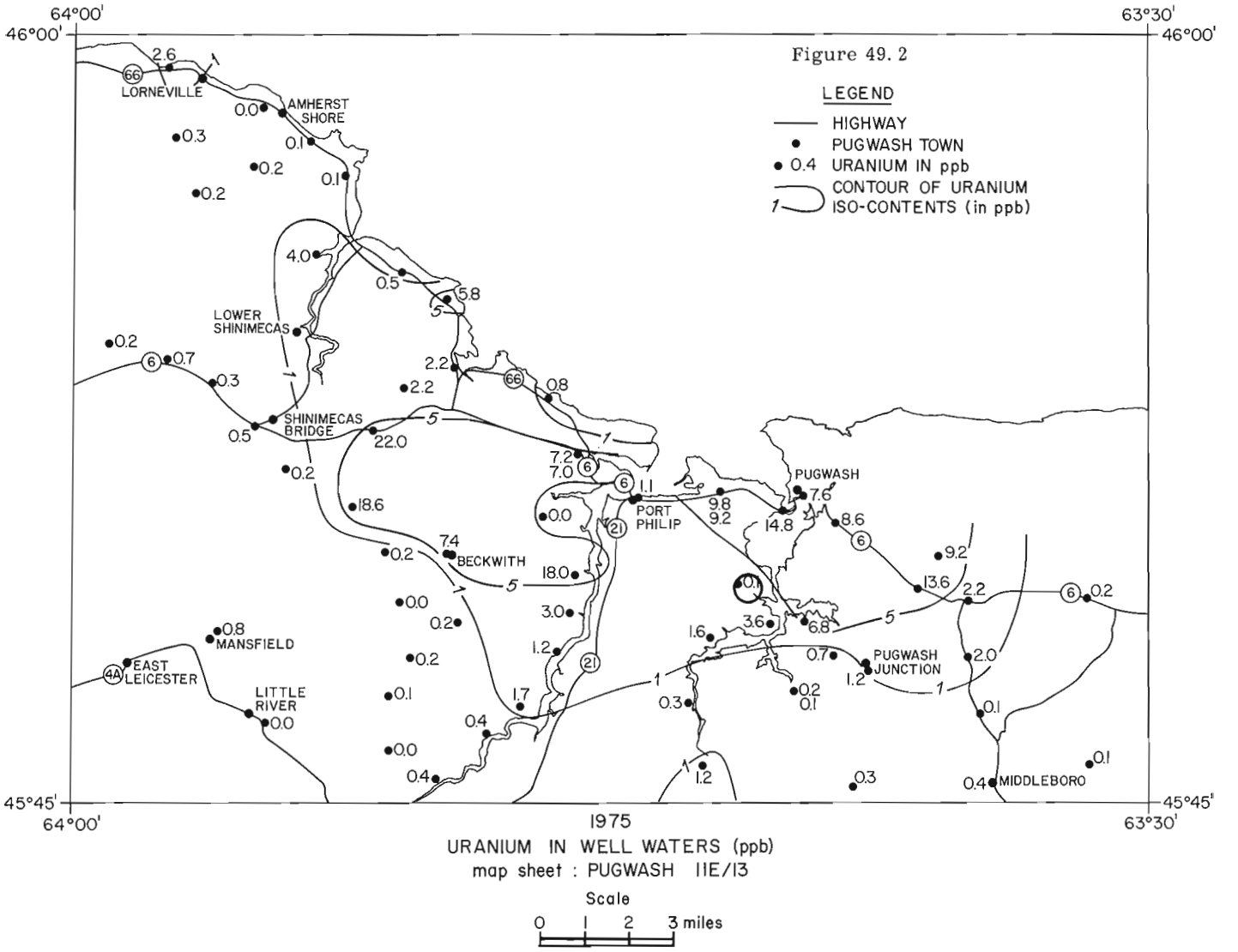

Figure 49. 2

References

Brummer, J. J.
1958: Supergene Copper-Uranium Deposits in Northern Nova Scotia; Econ. Geol., v. 53, p. 309-324.

Denson, N. M., Zeller, H. D., and Stephens, J. G.
1956: Water Sampling as a Guide in the Search for Uranium Deposits and its use in Evaluating Widespread Volcanic Units as Po' ntial Source Beds for Uranium; *in* U. S. Geol. Surv. Prof. Paper no. 300, p. 673-680.

Harshman, E. N.
1968: Uranium Deposits of the Shirley Basin, Wyoming; *in* Ore Deposits of the U. S. 1933-1967, v. 1, p. 852, ed. Ridge, J. D.; Am. Min. Met. Pet. Eng., New York.

50. URANIUM ORIENTATION SURVEYS - ONTARIO

Project 750052: Uranium Reconnaissance Program

W. B. Coker
Resource Geophysics and Geochemistry Division

An orientation survey concerned with examining the dispersion of uranium in lakes in areas of Ontario containing different types of uranium mineralization was carried out as a basis for an assessment of lake sediment composition as an indicator of uranium mineralization. The areas surveyed include Bancroft (Faraday, Cardiff and Monmouth townships), Agnew Lake (Porter, Hyman and parts of Drury, Baldwin, Shakespeare and Dunlop townships), Montreal River (Township 28 Ranges 14, 15, and 16 and Township 29 Ranges 14, 15, and 16), and Tustin-Bridges (Bridges, Docker, Tustin and MacNicol townships). The survey comprised two parts: a detailed study of selected lakes and restricted regional surveys within each area.

The five selected lakes studied in detail include Bow, Bay and Hadlington lakes in the Bancroft area and Kimber and Richard lakes in the Tustin-Bridges area. All lakes, with the exception of Bay Lake, are associated with different types and grades of uranium mineralization, in varied geological settings. At a number of sites (from 15 to 37) within each lake, surface and bottom water samples, acidified with nitric acid on the day of collection, and surface (0-5 cm depth) and subsurface (> 10 cm depth) sediment samples were collected. A Van-Dorn Bottle and Ekman-Birge Dredge were used for water and sediment collection respectively. A monitoring station was established at the deepest central part of each lake, with the exclusion of Bow Lake which is composed of three separate basins each of which had a monitoring station established in it. At each monitoring station measurement of temperature, conductivity, pH and dissolved oxygen content of the water from surface to the bottom were taken utilizing a Martek Mark V Water Quality Analyzer. Both filtered and unfiltered water samples were collected from the epilimnion, metalimnion, and the top and bottom of the hypolimnion. At each sampling depth one sample of filtered water and one of unfiltered water was left untreated, one was acidified with nitric acid, and one was acidified with hydrochloric acid. In addition, at each monitoring station core samples were taken using a Phleger Corer and a series of replicate grab samples were taken using both the Hornbrook Sampler and Ekman-Birge Dredge. To assist in interpretation of the lake water-lake sediment geochemical data, bedrock and associated overlying soil samples were also obtained from around each lake. These detailed geochemical studies should give a preliminary understanding of the distribution and dispersion characteristics of uranium, and associated elements, within the lake water-lake sediment environment and associated surficial environment of the areas of Ontario surveyed.

The regional surveys of each area involved the collection of lake-centre organic-rich sediment samples, using a Hornbrook Sampler, and surface water samples, acidified with nitric acid on the day of collection. At each sample site the temperature, conductivity, pH and dissolved oxygen content of the surficial and bottom waters were measured using the Martek Mark V Water Quality Analyzer. This work was done employing a Hughes 500 helicopter. To aid in the interpretation of the regional lake water-lake sediment geochemical data, bedrock and associated overlying soils and stream waters and stream sediments were also collected on a regional basis. The regional geochemical surveys will enable the distribution and dispersion patterns of uranium, and associated elements, in the lake waters and lake sediments on a regional scale to be examined and the potential of these media for use in reconnaissance uranium exploration assessed.

51. PINITE, PRESSURE, TEMPERATURE, AND RETROGRESSIVE METAMORPHISM, WOLLASTON LAKE, SASKATCHEWAN

Project 740015

F. W. Chandler
Regional and Economic Geology Division

A northeast trending belt of migmatites of sedimentary origin, with mainly granodioritic mobilisate lies between two areas of granitic migmatite at the northern end of Wollaston Lake (Chandler and Mukherji, 1975). The granodioritic migmatites are included (Scott, 1973) in the Daly Lake Group which makes up most of the Wollaston Lake Fold Belt. As regionally, the Daly Lake Group in the Wollaston Lake area is composed of cordierite-sillimanite-biotite (garnet) gneiss, calc-silicates, psammite and some quartzite.

In recent papers (listed by Winkler, 1974, p. 244, 245) partition of iron and magnesium between garnet and cordierite was considered to be a measure of the pressure and temperature of metamorphism. Thus to estimate the metamorphic conditions of the Daly Lake Group in the Wollaston Lake area, rocks were chemically analyzed and the results used to calculate pressure and temperature of metamorphism according to the method of Hutcheon *et al.* (1974).

The samples used in the analyses are biotite gneiss and schist with granodiorite and granodiorite pegmatite mobilisate. Minerals identified optically in all the samples include garnet, cordierite, pinite, fibrolite and plagioclase. Samples C46 and C274 (table) contained potash feldspar (porphyroblastic in C46). White mica chlorite and hematite are associated with green and yellow pinite in some samples.

Analyses were performed on an MAC electron microprobe equipped with an energy dispersive spectrometer automated to produce simultaneous multi-element analyses and data reduction. Cordierite and garnet were each analyzed for ten elements. The analyses (Table 51.1) of garnet and cordierite and the pinite of C56 are averages of six to ten closely agreeing spot analyses from the centre and edge of at least three grains of each mineral in each section. No zoning was seen in the garnet. Cordierite was pinitized to varied degrees. Other pinite analyses in the table are closely agreeing spot analyses made while searching for cordierite. C46 is the average of two analyses, C274 is one, and M321 is the average of three. In sample C56 no fresh cordierite was seen, and in the microprobe samples on M321 no garnet was found.

The calculated conditions, 3.5 kb and c. 490° are hardly suggestive of entry at moderate pressure into the medium grade of metamorphism (terminology of Winkler, 1974), that is, the amphibolite facies.

Observations at the sampled locations and from thin sections of the probed samples show the following: Migmatization, absence of hypersthene, presence of sillimanite, coexistence of garnet and cordierite and presence of white mica, probably only as a secondary mineral. Together, these imply metamorphism in the middle pressure range of high grade metamorphism (upper amphibolite facies), that is, at a pressure of four to eight kb and above 650°C (Winkler, 1974).

Thus the calculations suggest conditions somewhat milder than do the field and petrographic criteria. Two suggestions are made to explain this variance; either the calibration of the p-t meter of Hutcheon *et al.* (1974) is incorrect or iron/magnesium partition has adjusted to some stage during the waning of metamorphism. Evidence for retrogression lies in the pinitization widespread in the area, and in reports in the literature on the Wollaston Lake Fold Belt (Scott, 1973).

A third explanation was examined. Perhaps incipient pinitization, not visible under the microscope could be affecting iron/magnesium ratios. Examination of Table 51.1 shows the iron/magnesium ratio of pinites to be only slightly more iron rich than those of "fresh cordierites". This agrees with the results of Guidotti *et al.* (1974) who found that the iron/magnesium ratio of chlorite coexisting with biotite and cordierite was only very slightly higher than that of the other two minerals. This being the case it is not surprising that using pinite in the calculations instead of cordierite does not give very different estimates of pressure and temperature (table).

Tentative conclusions to be drawn from the above are:

(1) In this retrogressed area the p-t meter of Hutcheon *et al.* (1974) appears to reflect retrogressive conditions.
(2) Where fresh cordierite is not available in a retrogressed area, using pinite will give approximate pressure and temperature of retrogressive metamorphism.
(3) To calculate the conditions of the peak of metamorphism pinitized samples ought to be avoided.

Acknowledgments

The writer is grateful to E. Froese and J. Bourne for criticism and suggestions, to G. Plant who operated the electron microprobe, to I. Hutcheon who supplied a computer program, and to W. Houston who modified it.

References

Chandler, F. W. and Mukherji, K. K.
1975: Bedrock geology (the Daly Lake Group), north Wollaston Lake, Saskatchewan (64 L/6, parts of 64L/5 and 7); *in* Report of Activities, Part A, Geol. Surv. Can., Paper 75-1A, p. 307-309.

Table 51. 1

Composition of garnet, cordierite, and pinite from migmatites of the Wollaston Lake area, Saskatchewan, and estimated conditions of metamorphism. Asterisked conditions are taken from pinite analyses

	CGA 74 C46			CGA 74 C56		CGA 74 C207		CGA 74 C274			CGA 74 M198		CGA 74 M321
Minerals	Garnet	Cordier	Pinite	Garnet	Pinite	Garnet	Cordier	Garnet	Cordier	Pinite	Garnet	Cordier	Pinite
Oxides in wt. per cent													
SiO_2	36. 86	46. 87	34. 00	36. 95	42. 57	37. 14	47. 18	37. 30	46. 97	38. 34	36. 68	46. 82	43. 14
TiO_2	0. 06	0. 03	0. 06	0. 05	0. 03	0. 04	0. 05	0. 04	0. 03	0. 01	0. 08	0. 02	. 10
Al_2O_3	20. 35	32. 38	31. 17	20. 46	34. 88	20. 56	33. 46	20. 53	33. 90	31. 41	20. 34	34. 26	31. 94
Cr_2O_3	0. 06	0. 01	0. 00	0. 07	0. 02	0. 05	0. 02	0. 06	0. 03	0. 03	0. 08	0. 02	. 01
Total Fe as FeO	36. 45	10. 84	6. 54	37. 58	4. 24	36. 89	11. 33	34. 76	9. 39	5. 52	36. 94	9. 81	4. 73
MnO	1. 36	0. 10	0. 04	0. 85	0. 02	1. 87	0. 20	1. 95	0. 15	0. 11	0. 94	0. 05	. 04
MgO	3. 11	7. 27	3. 84	2. 90	2. 58	3. 08	7. 06	3. 61	7. 65	3. 79	3. 46	7. 41	2. 84
CaO	1. 00	0. 00	0. 47	0. 74	0. 08	0. 74	0. 00	1. 44	0. 00	1. 09	0. 98	0. 00	. 17
Na_2O	0. 08	0. 33	0. 35	0. 07	0. 48	0. 12	0. 32	0. 00	0. 54	0. 29	0. 02	0. 41	. 34
K_2O	0. 00	0. 00	0. 54	0. 00	3. 19	0. 00	0. 01	0. 00	0. 02	0. 41	0. 00	0. 00	3. 39
Total	99. 33	97. 83	77. 01	99. 67	88. 09	100. 49	99. 63	99. 69	98. 68	81. 00	99. 52	98. 80	86. 70
P. bars	3435	3685*		3376*		3508		3576	3912*		3506		-----
T. ^{o}C	491	556*		490*		515		491	576*		479		-----

Guidotti, C. V., Cheney, J. T., and Conatore, P. D.
1975: Coexisting cordierite + biotite + chlorite from the Rumford quadrangle, Maine; Geology, March 1975, p. 147-148.

Hutcheon, I., Froese, E., and Gordon, T. M.
1974: The assemblage quartz-sillimanite garnet-cordierite as an indicator of metamorphic conditions in the Daly Bay Complex, N. W. T.; Contrib. Mineral. Petrol., v. 44, p. 29-34.

Scott, B. P.
1973: Progress report on the geology of the Wollaston Lake Belt, p. 53-80; *in* An excursion guide to the geology of Saskatchewan, Simpson, Frank (Ed.), Sask. Geol. Soc., Pub. 1.

Winkler, H. G. F.
1974: Petrogenesis of metamorphic rocks; Third Edition, Springer (Pub.), 320 p.

Project 730019

J. J. Veillette and F. M. Nixon
Terrain Sciences Division

Introduction

A project was initiated in early spring 1975 with the purpose of developing a mast-equipped, light-weight drill adapted to an all terrain vehicle for use in Arctic regions. An arbitrary depth of 3 m (10 feet) for subsurface investigation was considered satisfactory for most surficial geology mapping programs and geo-technical reconnaissance studies in permafrost terrain, provided a reasonable borehole coverage could be obtained. The following objectives were pursued:

- reduction of helicopter use;
- provision of ground mobility of drill and necessary coring equipment within the weight limits acceptable by land use regulations for summer work in the Arctic;
- increased production of shallow boreholes when compared with conventional hand-held augers and light-weight drills;
- adaptability to Twin Otter aircrafts and Bell 206 helicopters for transportation.

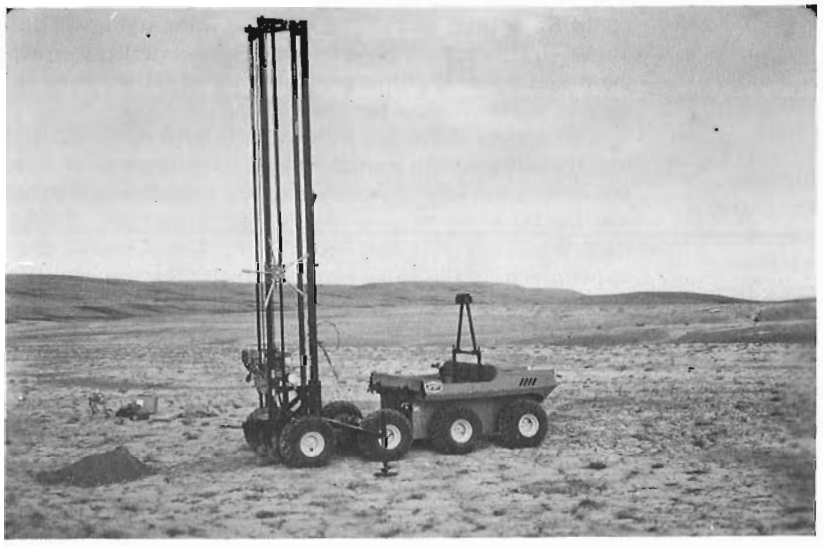

Figure 52.1. ATV-drill in coring position.

Figure 52.2. ATV-drill with retracted mast for travel.

It was proposed that actual coring time spent at a drill site could be reduced substantially through the use of a mast that would allow a minimum of 3 m travel. When using CRREL augers in frozen soils several trips down the borehole may be necessary to fill the core barrel. The use of a mast can eliminate rod breaking between successive trips down the borehole, for the necessary time to fill the barrel. It also reduces the overall handling of drill rods and permits a better control of the coring operation. The drill power source considered was a small two-stroke engine independent from the carrier power source. The vehicle had to be of a rugged design capable of supporting 300 to 500 pounds of drilling gear while being compatable with land use weight regulations.

This proposal, along with the weight and transport restrictions, was presented to J. K. Smit International, Toronto, and Ontario Drive and Gear, New Hamburg. Both firms submitted designs, Smit for the drill mast and Ontario Drive and Gear for a modified 8-wheel Argo all terrain vehicle as drill carrier. The accepted designs resulted in the products described below.

Technical Description

Drill mast

The mast consists of an extended Unipress reinforced by tying the guide rods to a rear tubular structural member with two triangular yokes at the top and bottom of the mast. The drill power unit is supported in a cradle which runs on the rear mast tube as well as the two normal guide rod bushings. A feed wheel mounted on a rail can be adjusted to the operator's height. A 2:1 sprocket reduction at the feed chains facilitates hoisting for the several trips necessary when using a coring auger (Fig. 52.1).

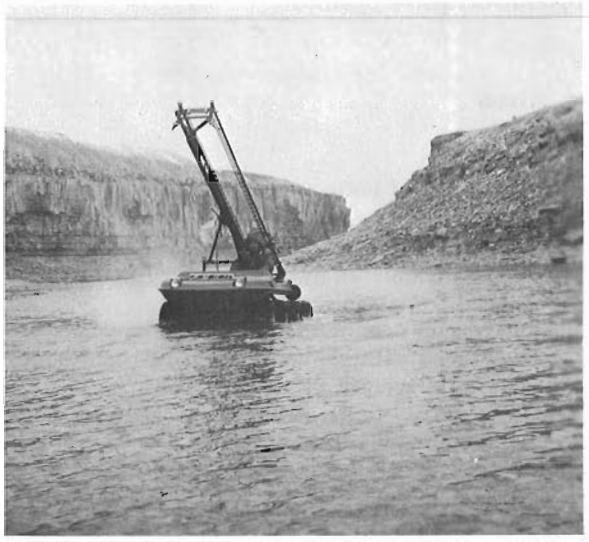

Figure 52. 3. ATV-drill crossing a shallow river.

All terrain vehicle

Modifications to the standard 8-wheel Argo model were necessary for drill mounting, additional structural strength, and transport. Power is supplied by a 28-h. p., forced air cooled, twin cylinder, two stroke engine. The 8 Terra tires are chain driven from a two-speed and reverse differential gear box. Disc brakes on the output shafts are used to steer and to stop the vehicle. A major modification was the removal of the rear half of the plastic body for drill mounting. Mounting points include a swivel pin and a lower lock pin supported by twin reinforced uprights at the rear of the vehicle and a raised cradle in front of the driver's seat to support the forward mast section during transport. The frame is strengthened with a steel plate welded between the members, and the wheel base is increased by 46 cm (18 inches) over the full length of the frame to lower the angle of the mast while in transit. A split drum electric winch is used to raise and lower the mast. Extended pads offer lateral support while in drilling position. Figures 52. 2 and 52. 3 show the vehicle in motion.

Drill power unit

A standard Winkie GW15 equipped with a 6. 5: 1 auger reduction planetary gear box was selected for the initial augering trials.

Assembly and Transportation

Twin Otter moves require disassembly of the vehicle, while the mast and drill can be loaded by three men without any dismantling. Disassembly time for the ATV is about 4 hours for a two-man crew. All other components can be handled by a two-man crew. For shipping over long distances the mast can be completely disassembled in 3 hours by one man, and the vehicle can be shipped in one piece.

Results

Field trials of the ATV-drill combination were conducted at New Hamburg, Ontario and at Resolute Bay and Somerset Island, N. W. T. during August 1975. Less than 5 minutes were necessary to auger a 3 m hole in clay using open-flight continuous augers in New Hamburg. In frozen, ice-rich silts on Somerset Island 3 m holes could be drilled and cored in 45 minutes using CRREL auger equipment. Trials using diamond drilling equipment and open-flight augers also were satisfactory in coarse material near Resolute Bay.

Overland stability of the vehicle both in the drilling and transit position was assessed. Testing was carried out over a variety of summer arctic terrains including wet lands, steep slopes, and river crossings. These field trials suggest that the ATV-drill will travel over approximately the same range of arctic terrain conditions as the Honda Tricycles, with the exception of some rugged stony river beds and felsenmeer areas.

Potential Uses

As demonstrated at the New Hamburg test site the applications of the ATV-drill are not restricted to northern terrain types. It probably could be used in a variety of shallow soil investigations in fine-textured material, as well as shallow rock drilling. Due to the mast component and ground mobility it probably could be of more economical use than heavier equipment for some applications where extensive quick coverage of an area takes priority over depth of investigation.

Acknowledgments

The valuable suggestions and design of Karel Jansen, J. K. Smit International, for the drill mast and Siegfried Kleine, Ontario Drive and Gear, for the all terrain vehicle are greatly appreciated.

Project 730021

R. B. Taylor
Terrain Sciences Division

Introduction

On May 8, 1973 a landslide occurred as a result of an embankment foundation failure of the Highway No. 5 extension north of Chelsea, Quebec (Fig. 53.1, 53.2). The overlying rockfill caused a compression of the underlying soils and an extrusion of the highly sensitive marine clays. The fluid-like mass of soil flowed down the small adjacent ravine towards Highway No. 11 and the Gatineau River. By May 11 a portion of the railroad embankment at the east end of the ravine (Fig. 53.1, 53.2) was washed out but it was not until May 15 and 16 when the largest amount of landslide debris spilled into the Gatineau River (Fig. 53.3). Some aspects of the landslides have been dealt with previously by T. Alföldi (1973), and a detailed picture of the events during the landslide presently is being compiled by N. R. Gadd of the Geological Survey of Canada.

The testing of echo sounding equipment in the Gatineau River reservoir on June 19-21, 1973 provided an opportunity to obtain depth soundings and to estimate where and how much of the landslide debris was deposited there. Horizontal control for the soundings was provided by markers set up on physiographic features, also identifiable on the aerial photographs, and by four marker buoys located in the middle of the reservoir. The buoys were positioned with a pocket sextant. The bathymetric contour map (Fig. 53.4) was interpolated using the U. G. A. I. S. (Urban Geology Automated Information System) devised by J. R. Bélanger.

Observations

The shores of the eastern part of the reservoir are generally rocky and drop sharply to depths of over 20 m, whereas in the "Narrows" (unofficial name - Fig. 53.1) the water depths are shallower than 15 m. The bed of the reservoir at the western end of the Narrows is littered with fallen trees and is composed of a grey silt-clay material which represents a substantial amount of the soil and debris carried into the Gatineau River by the landslide on May 5 (W. Gadzos, pers. comm.). Farther east the strong reflections registered on the echogram imply a rocky bottom which extends to a maximum depth of 46 m. Two submerged channels were detected (Fig. 53.4), a shallow one which flows eastward out of the Narrows and a deeper channel which flows south between the island and the western shore of the Gatineau River, then eastward towards the dam (Fig. 53.1).

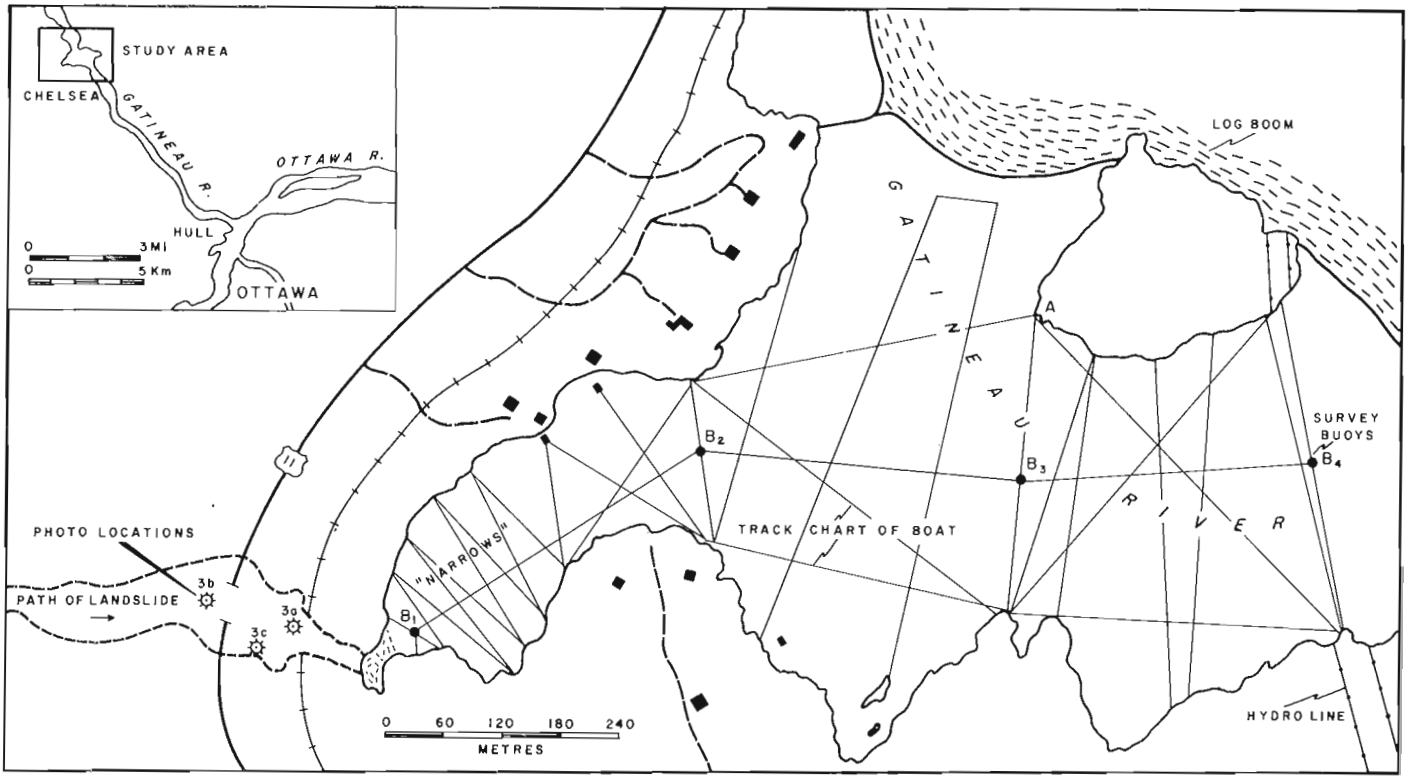

Figure 53.1. Location map of study area and boat track chart.

Figure 53. 2. Aerial photographs of study area 1973 (RSA 30660 - 31 to 33).

Figure 53. 3a.

View of C. P. R. railway embankment and Gatineau River, June 26, 1973.

Figure 53. 3b.

Landslide area as viewed from Highway No. 11 looking west June 20, 1973.

Figure 53. 3c.

Side of ravine between Highway No. 11 and the C. P. R. railway embankment.

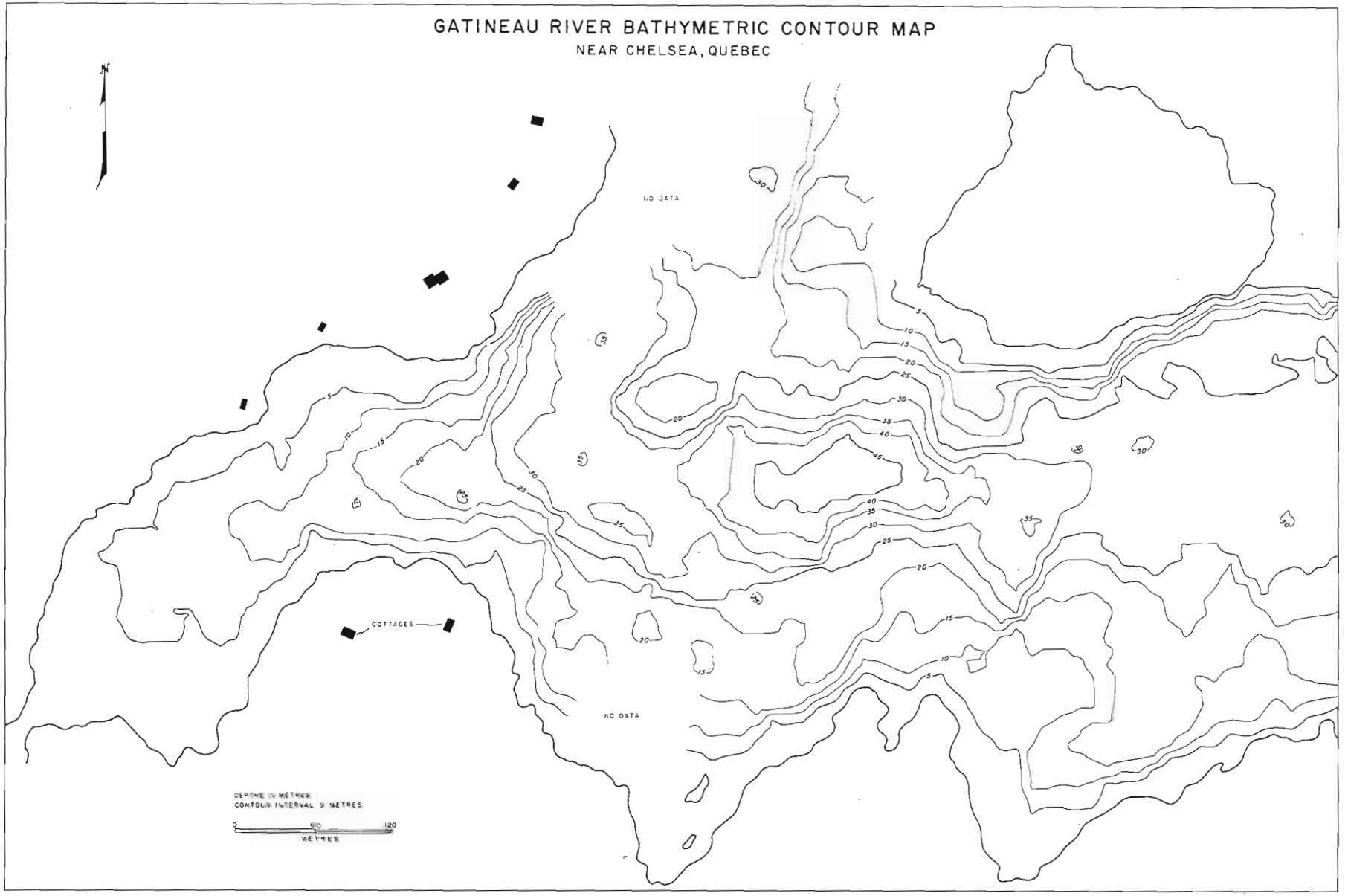

Figure 53. 4. Bathymetric contour map of study area.

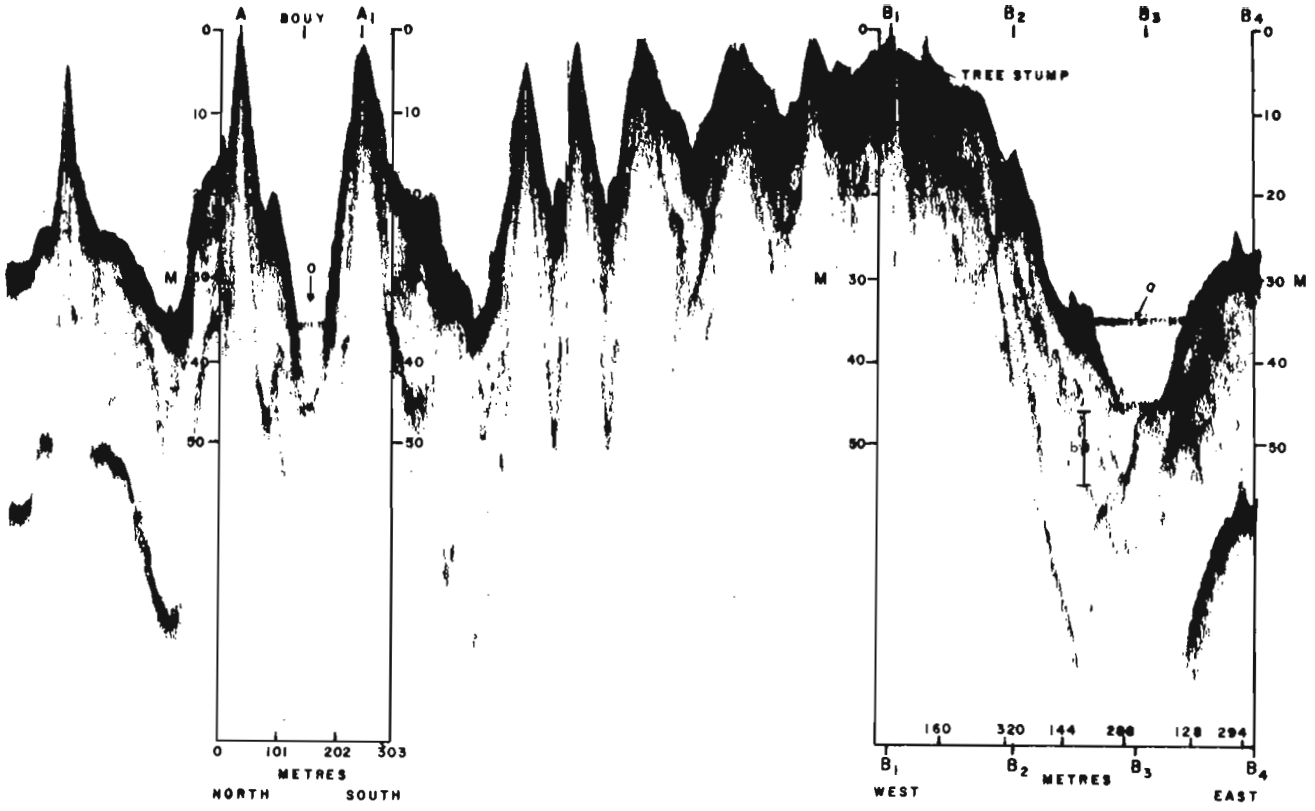

Figure 53.5. Echograms of the deepest sector of the study area illustrating a possible area of sediment infilling.

The lack of an earlier bathymetric map of the reservoir prevents a calculation of the total amount of infilling, nevertheless pockets of deposition can be detected from the echograms. For instance Figure 53.5 shows a cross-sectional view of the deep-water pocket (Fig. 53.1) and another real reflector (a of Fig. 53.5) across it at a depth of 36 m. This horizontal reflector could represent a change in water density on the surface of a new deposit of unconsolidated fine-grained sediment. Evidence supporting the latter hypothesis is: the aerial photographs of May 23, 1973 show considerable suspended sediment as well as turbulent waters approximately where the pockets exists; the water pocket is deeper than the normal reservoir bottom and near the convergence of the two submerged channels, and thus is a likely site for sediment accumulation; furthermore, the strong echo reflections observed elsewhere along the reservoir bed are less prominent beneath the zone of suspected sedimentation. In fact a close examination of the echogram (Fig. 53.5) shows an additional reflector below 46 m that may represent the actual rock bottom which has been previously infilled by normal river sedimentation (b of Fig. 53.5).

An estimate of the total area of spoiled land as a result of the landslide was 68 000 square yards and the volume of highway (No. 5) embankment moved was 195 000 cubic yards (Alföldi, 1973, p. 13). It is not known how much of this sediment reached the reservoir but in the site of suspected sedimentation, between the 36 m and 46 m depths, it is estimated that 5526.6 cubic yards of unconsolidated fine-grained sediments have accumulated. This deposit of sediment is thought to represent a portion of the finer grained sediments entrained when the debris from the landslide flowed into the western end of the reservoir.

Conclusion

The study, although only originally intended for the purpose of testing equipment, has resulted in sufficient information to produce a rough bathymetric map of the reservoir and an estimate of infilling (5526.6 cubic yards) in the deeper part of the reservoir probably as a result of the landslide. The reader should be aware that the soundings in the shallower depths may be due to the inadequacies of the deep-water echo sounder used. It is also suggested that a further study of present and past sedimentation rates in the reservoir be conducted using a gravity or piston coring device.

The author acknowledges the comments of Dr. N.R. Gadd and Dr. B.D. Bornhold of the Geological Survey, and D. Bernard, J. Arcuri and W. Gadzos for help in the field.

Reference

Alföldi, T.T.
1973: Remote sensing analysis of the Chelsea Landslide; Canada Centre for Remote Sensing, Tech. Paper 73-2, 31 p.

54. A HYDROGEOCHEMICAL SURVEY FOR URANIUM IN THE NORTHERN PART OF THE BEAR PROVINCE, NORTHWEST TERRITORIES

Project 730009; Uranium Reconnaissance Program

C. C. Durham and E. M. Cameron
Resource Geophysics and Geochemistry Divison

Introduction

The northern part of the Bear Province, where Helikian sediments overlie rocks of the Great Bear batholith, contains a number of features that attract interest to its uranium potential. Firstly, the granitic rocks of the batholith, of Hudsonian age, are known in places to contain relatively high contents of uranium (e.g., Eade and Fahrig, 1971). The rocks underlying the Helikian sediments are deeply weathered (Hoffman and Bell, 1975), which would have caused mobilization of uranium. Finally, at the base of the Helikian sediments there is a thick sequence of relatively flat-lying sandstones and conglomerates. Potential for three distinct types of uranium deposits exists: primary concentrations associated with the Hudsonian plutonism; secondary accumulations near the sub-Helikian unconformity; and possible "roll-type" mineralization in the Hornby Bay sandstones, a mineralization derived from the interaction of uranium-rich groundwater with any parts of the sandstones with reducing characteristics. The Port Radium uranium deposit is within the region and there are a number of scattered prospects.

The survey area was chosen to represent these three geological environments for uranium occurrences: the Aphebian basement, the sub-Helikian unconformity, and the Hornby Bay sandstones (Fig. 54.1). It is 6600 km^2 (2500 square miles) and was sampled at a density of one sample per 5 km^2 (1.9 square miles). During the 1975 summer when this work was done, lake waters and sediments were also sampled within the adjacent 1:250 000 map-sheets 86H and 86K. This work was carried out for the Geological Survey by a contractor at a sample density of one per 5 square miles (13 km^2). Both projects are in support of the Uranium Reconnaissance Program.

That part of the area underlain by Aphebian rocks is typical lake-dotted Shield country of modest relief. There is little glacial cover. To the northwest, the Hornby Bay sandstones and up-faulted basement rocks form rounded hills. In many places the bedrock is concealed by sandy overburden. The survey area is within the zone of continuous permafrost and the northern limit of trees passes through the area.

Sample Collection

Water sampling was carried out using a Hughes 500 helicopter equipped with newly designed water sampling and monitoring equipment. This equipment is described elsewhere (Cameron and Durham, 1975). In addition to the pilot, the crew comprised a navigator and an operator for the sampling equipment. At each site the apparatus was flushed prior to collecting the samples. pH was measured en route to the next site. A sampling rate of 25 per hour was maintained.

Lake waters were the primary objective of the survey. However, in some parts of the area, principally that underlain by Hornby Bay sandstone, it was not possible to obtain lake samples at this density. In these cases, water from streams, bogs, or potholes was collected.

Discussion

Hydrogeochemical methods are well suited to exploration for uranium in the Shield (Dyck, 1975). This is because of the abundance of water and excellent mobility of uranium in surface waters. However, previous work in the northern Shield had alerted us to the probability that the content of uranium in the waters would be very low, with even anomalous contents being less than average levels for more southerly areas of North America. For instance, in a study of an area in the eastern part of the Slave Province, previously defined as anomalous for uranium by a lake sediment survey, Dyck and Cameron (1975) found a mean content of 0.2 ppb U in lake waters. The more anomalous parts of this area were defined by the 0.3 ppb contour. In an unpublished orientation survey of lake waters around the Rabbit Lake uranium deposit, Saskatchewan, we found background to be < 0.05 ppb U and the threshold for outlining anomalous areas approximately 0.07 ppb. For the Beaverlodge region, Dyck *et al.* (1971) found the background content to be 0.4 ppb U.

The analytical method used was fluorimetric (Smith and Lynch, 1969), carried out on the residue from the evaporation of 50 ml of unacidified and unfiltered water. Initially, analyses were carried out in a temporary laboratory established at Yellowknife. This was done to allow a limited follow-up sampling to be completed during the 1975 season. However, these facilities were not adequate for the demanding requirements of sub-ppb analysis and all samples were later analyzed in Ottawa. In particular, trouble was experienced with contamination from road dust and in obtaining a stable power supply.

Preliminary results are shown in Figure 54.1, in which areas containing 0.1 ppb U or greater are outlined. Precision is relatively poor at this level and we plan to reanalyze the anomalous sample. The effects of filtering and acidification of the water samples will be examined. It should be noted that all the areas shown in Figure 54.1 to be 0.1 ppb or greater are based on a number of samples.

Because of the preliminary nature of the results, it is inappropriate to comment at this time on their nature and their relationship to the local geology. A value of 2.1 ppb was found near to a known uranium occurrence near Mountain Lake. The highest value obtained during the survey, 5 ppb U, was found to the northwest of Lac Rouviere.

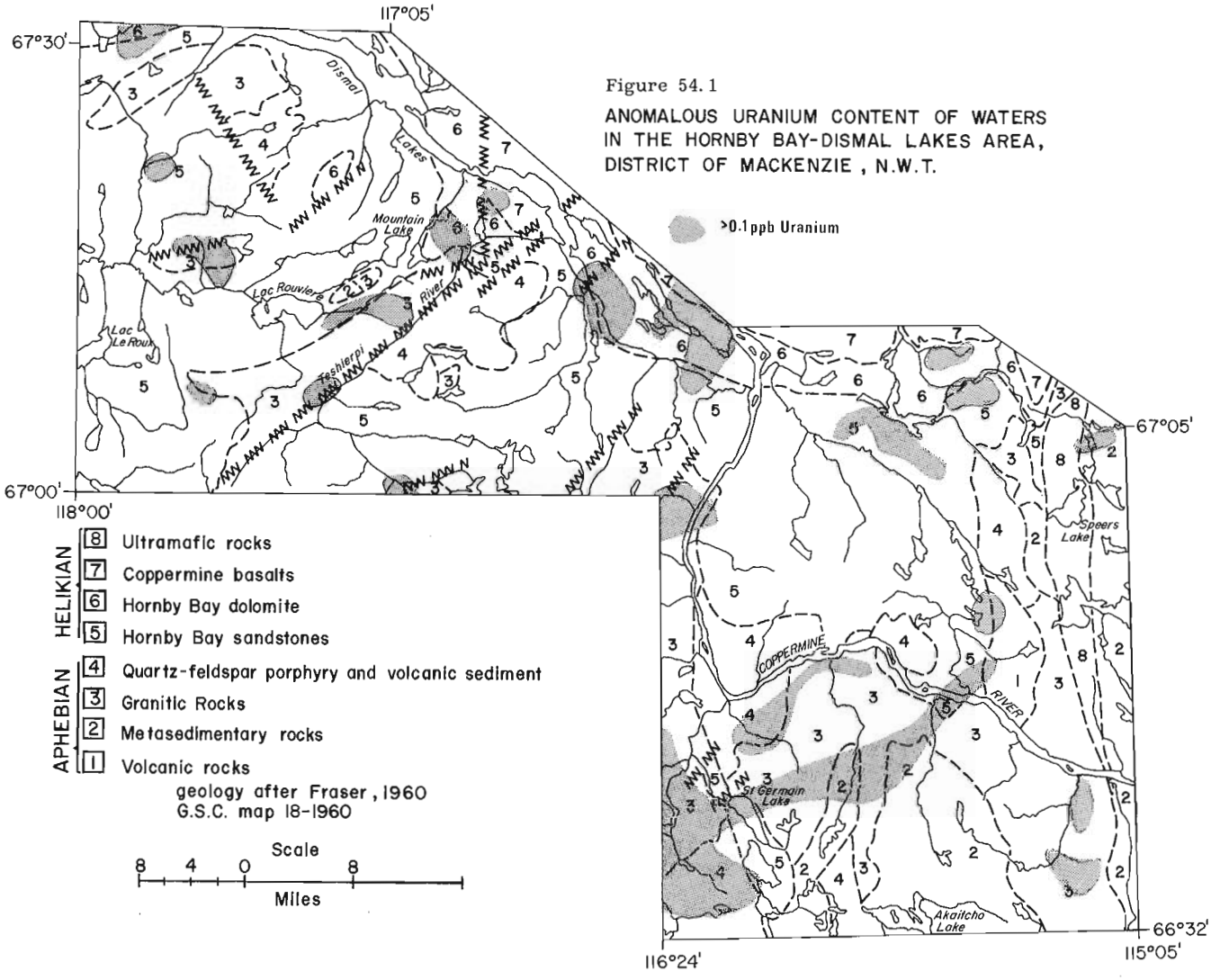

Figure 54.1

ANOMALOUS URANIUM CONTENT OF WATERS IN THE HORNBY BAY-DISMAL LAKES AREA, DISTRICT OF MACKENZIE, N.W.T.

References

Cameron, E.M. and Durham, C.C.
1975: Further studies of Hydrogeochemistry applied to mineral exploration in the northern Canadian Shield; (report 39, this publication).

Dyck, W.
1975: Geochemistry applied to uranium exploration; Geol. Surv. Can., Paper 75-26, p. 33-47.

Dyck, W. and Cameron, E.M.
1975: Surface lake water uranium-radon survey of Lineament Lake area, District of Mackenzie; *in* Report of Activities, Pt. A., Geol. Surv. Can., Paper 75-1A, p. 209-212.

Dyck, W., Dass, A.S., Durham, C.C., Hobbs, J.D., Pelchat, J.C., and Galbraith, J.M.
1971: Comparison of regional geochemical uranium exploration methods in the Beaverlodge area, Saskatchewan; Inst. Min. Metall. Spec., v. 11, p. 132-150.

Eade, K.E. and Fahrig, W.F.
1971: Geochemical evolutionary trends of continental plates — a preliminary study of the Canadian Shield; Geol. Surv. Can., Bull. 179, 51 p.

Fraser, J.A.
1960: North-central District of Mackenzie, Northwest Territories; Geol. Surv. Can., Map 18-1960.

Hoffman, P.F. and Bell, I.
1975: Volcanism and plutonism, Sloan River map-area (86K), Great Bear Lake, District of Mackenzie; *in* Report of Activities, Pt. A., Geol. Surv. Can., Paper 75-1A, p. 331-337.

Smith, A.Y. and Lynch, J.J.
1969: Field and laboratory methods used by the Geological Survey of Canada *in* Geochemical Surveys, No. 11, Uranium in soil, stream sediment, and waters; Geol. Surv. Can., Paper 69-40, 9 p.

55. GLACIAL FEATURES OF THE HERMITAGE-BURIN PENINSULA AREA, NEWFOUNDLAND

Project 740028

Douglas R. Grant
Terrain Sciences Division

Reconnaissance mapping of surficial deposits and terrain features of central and southern Newfoundland has been completed this summer that complements earlier work on the Northern Peninsula and along the coastal belt and Trans-Canada Highway from Stephenville to the Avalon Peninsula. This report is an outline of some findings on the Burin Peninsula and neighbouring areas that may be of economic value; namely, evidence of diverse and unexpected directions of glacial transport that pertain to geochemical and drift prospecting, and cases of subtill stratified sediment that could serve buried confined aquifers for local groundwater development.

These interpretations are based on 1975 observations by the author and by a field mapping team lead by C. M. Tucker that largely confirm data gathered for the author in 1974 by P. E. Miller and C. D. Brisco. A few 1973 measurements donated by D. G. Vanderveer (Nfld. Dept. Mines and Energy) are incorporated.

The most significant aspect of the Pleistocene geology of the Burin Peninsula is that late Wisconsin glaciers moved mainly north and west, that is to say onshore from a source centred in Placentia Bay or on the banks beyond, and not southward from the interior of the island as is commonly believed. Specifically, there are numerous observations (Fig. 55.1) of crossing striae and of intersecting, glacially faceted outcrops that show one bevelled striated surface, with miniature crag-and-tail features pointing south-southeast, which is iron-stained and weathered. This surface is truncated by a second, west- and north-stossed facet that is fresh and unstained. Clearly a nonglacial period of weathering intervened between the first phase of outflow across the peninsula from interior, and the maximal, presumably final glacial phase that stemmed from an offshore source. The early southerly indicators are found throughout the region with little deviation, and are paralleled by large, clearly visible drumlins and fluted till plains. The later northward flow, which may have more westward components near Dantzig Point and Terranceville, oddly enough is poorly represented on the southern or stoss coast where the till is thickest and leaves no sign of having reshaped the earlier formed drumlins. This flow may have extended across Fortune Bay at least to Mose Ambrose where northward-stossed hills are seen, and the till contains a small per cent of red rhyolite erratics derived from the Burin Peninsula.

During subsequent recession onshore from Fortune Bay there appears to have been a pause when the ice lay along the present coast because end moraines with outwash graded to higher (+27 m) water levels are found at several places. These ice-marginal deposits display wave-planed distal parts and kettled proximal areas are found at Fortune, Grand Bank, Garnish, Bay L'Argent, Hermitage, and Harbour Breton. The ensuing postglacial fall of water level cut lower terraces, some of which pass laterally to benches in bedrock. Widmer (1953) has collated numerous measurements of these and attributed them to a proglacial lake in Fortune Bay. This poses two problems — the means of containing the water body with no evidence of ice impinging from the west, and how to differentiate the young benches from those found beneath till, which are clearly of much greater, probably interglacial age, and which could have been exhumed by glacial scour or wave action. There is no direct evidence whether the water body was marine or lacustrine, nor has the distribution of the many different shorelines been examined for tilt and relationship to ice masses. In any case, the last active ice to affect the Burin Peninsula flowed radially from a remnant ice cap situated along the topographic axis. Its upslope retreat is marked by eskers, outwash plains, and meltwater channels. In the Hermitage area, a late ice mass on the Garrison Hills may have become isolated from the inland ice sheet and may have fed narrow tongues terminating in several bays.

The practical significance of the new data on ice flow is that it raises the possibility of more tills of different lithology, particularly the likelihood of two very dissimilar superposed tills — one old and weathered and produced by the early southward flow, and a fresh upper one of diametrically opposed provenance. Exposures of this kind are seen near Marystown, and others may come to light in deeper road-cuts through the drumlinized areas. As well, with north-flowing ice moving onshore, upslope, and across the main drainage routes, proglacial sediments would be ponded and overridden together with existing nonglacial sediments. As support for this hypothesis are exposures of silts and sands beneath till near Marystown, Lamaline, and Dantzig Cove, an extensive drumlinized sand plain around Freshwater Pond, and a layer of peat encountered beneath 15 m of till in a drillhole near St. Lawrence.

Reference

Widmer, K.
1953: The geology of the Hermitage Bay area, Newfoundland; unpub. Ph.D. dissert., Princeton University, 464 p.

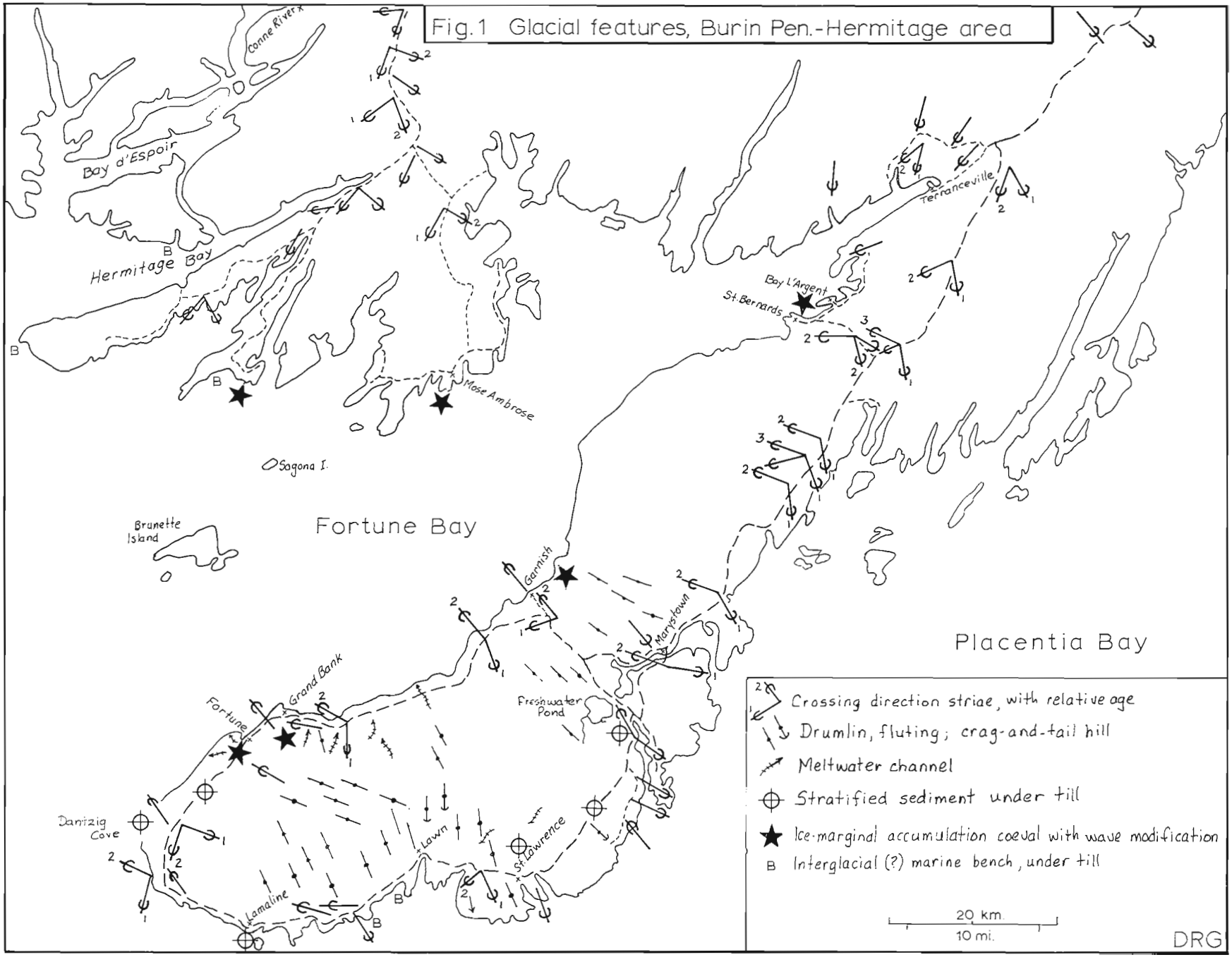
Fig.1 Glacial features, Burin Pen.-Hermitage area
Conne River
Bay d'Espoir
Hermitage Bay
Terranceville
Bay L'Argent
St. Bernards
Mose Ambrose
Sagona I.
Brunette Island
Fortune Bay
Garnish
Marystown
Placentia Bay
Grand Bank
Fortune
Freshwater Pond
Danzig Cove
Lawn
St. Lawrence
Lamaline
Crossing direction striae, with relative age
Drumlin, fluting; crag-and-tail hill
Meltwater channel
Stratified sediment under till
Ice-marginal accumulation coeval with wave modification
B Interglacial (?) marine bench, under till
20 km.
10 mi.
DRG

Projects 750037 and 670041

A. P. Annan, J. L. Davis and W. J. Scott
Resource Geophysics and Geochemistry Division

Introduction

The Electrical Methods Section of the Geological Survey of Canada has been investigating the feasibility of using VHF impulse radar to probe the structure and distribution of electrical properties in permafrost. The radar system can be deployed in two manners. For routine reconnaissance, a fixed antenna configuration is transported over the surface to obtain profiles of radar signatures versus position. In areas where the subsurface shows planar stratification (Annan *et al.*, this publication, report 57) wide angle reflection and refraction (WARR) sounding can be employed to obtain estimates of dielectric constant with depth and the depth of reflecting horizons. In a WARR sounding, the antennas are placed together in the stratified area and then moved apart continually at a constant rate. The result is a display of radar return time versus antenna separation. In this report, some of the data collected during experimental WARR soundings conducted in the vicinity

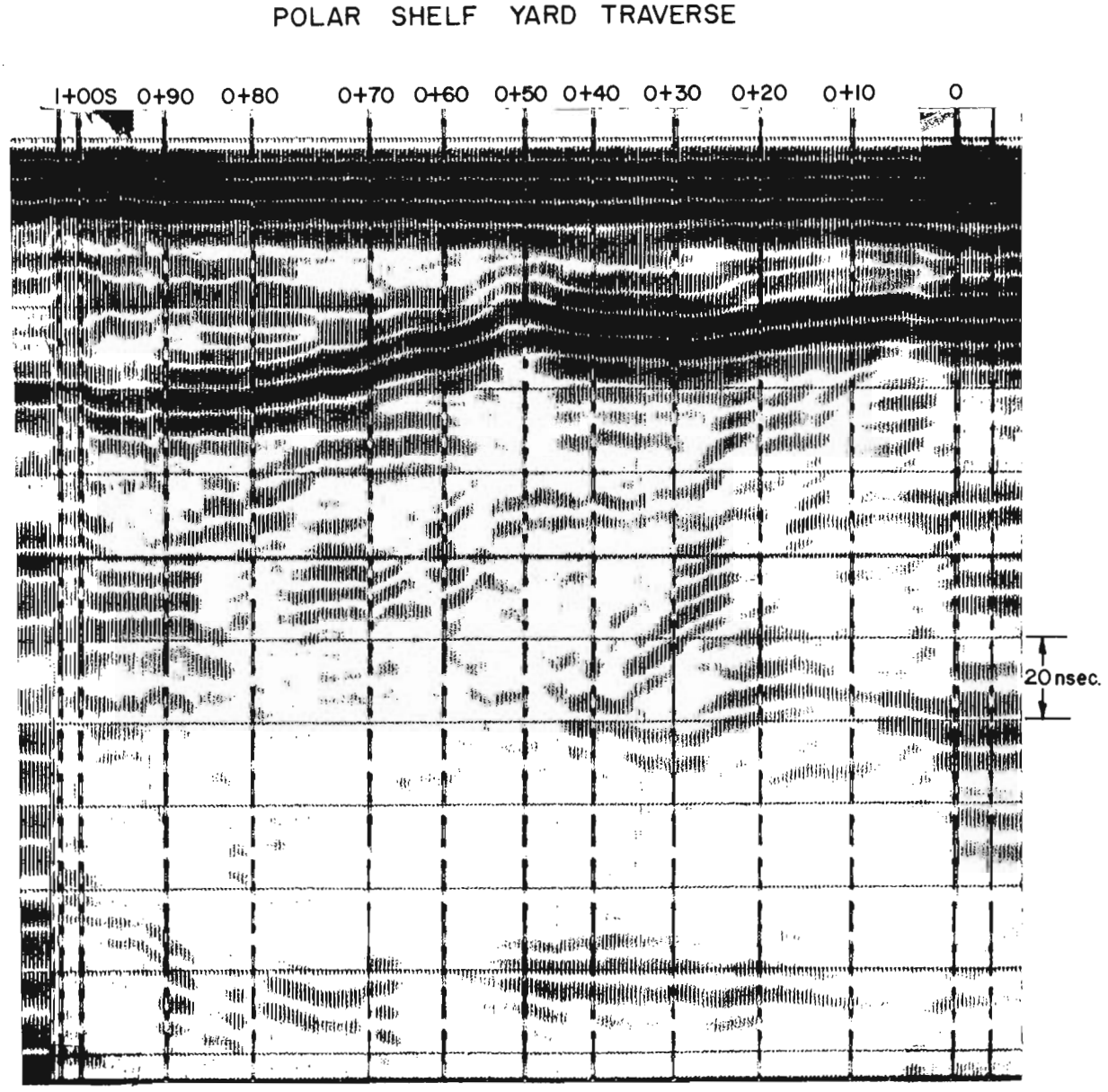

Figure 56. 1. Radar profile traverse across the Polar Continental Shelf Project yard.

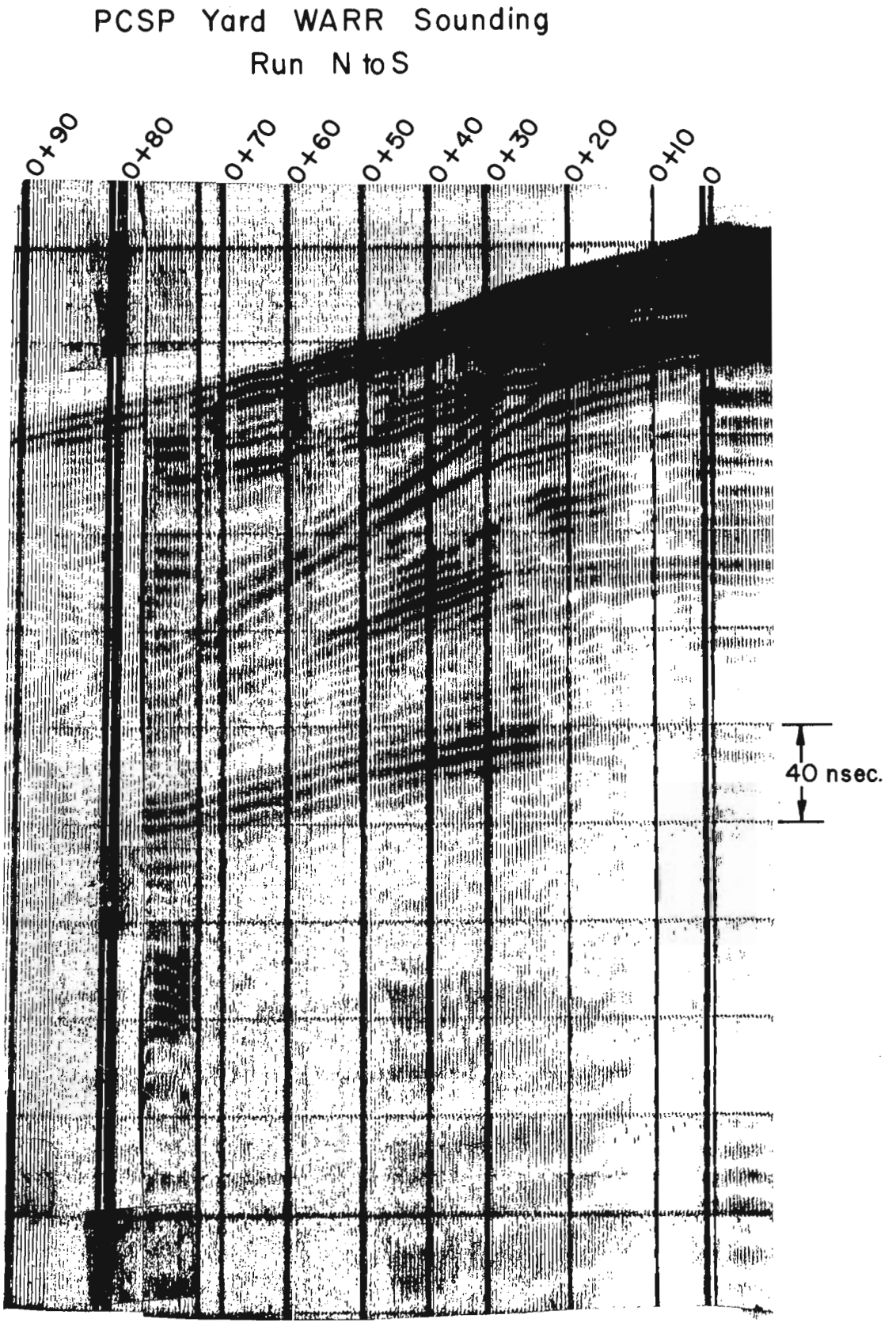

Figure 56. 2. WARR sounding in the yard with Tx at 0+00.

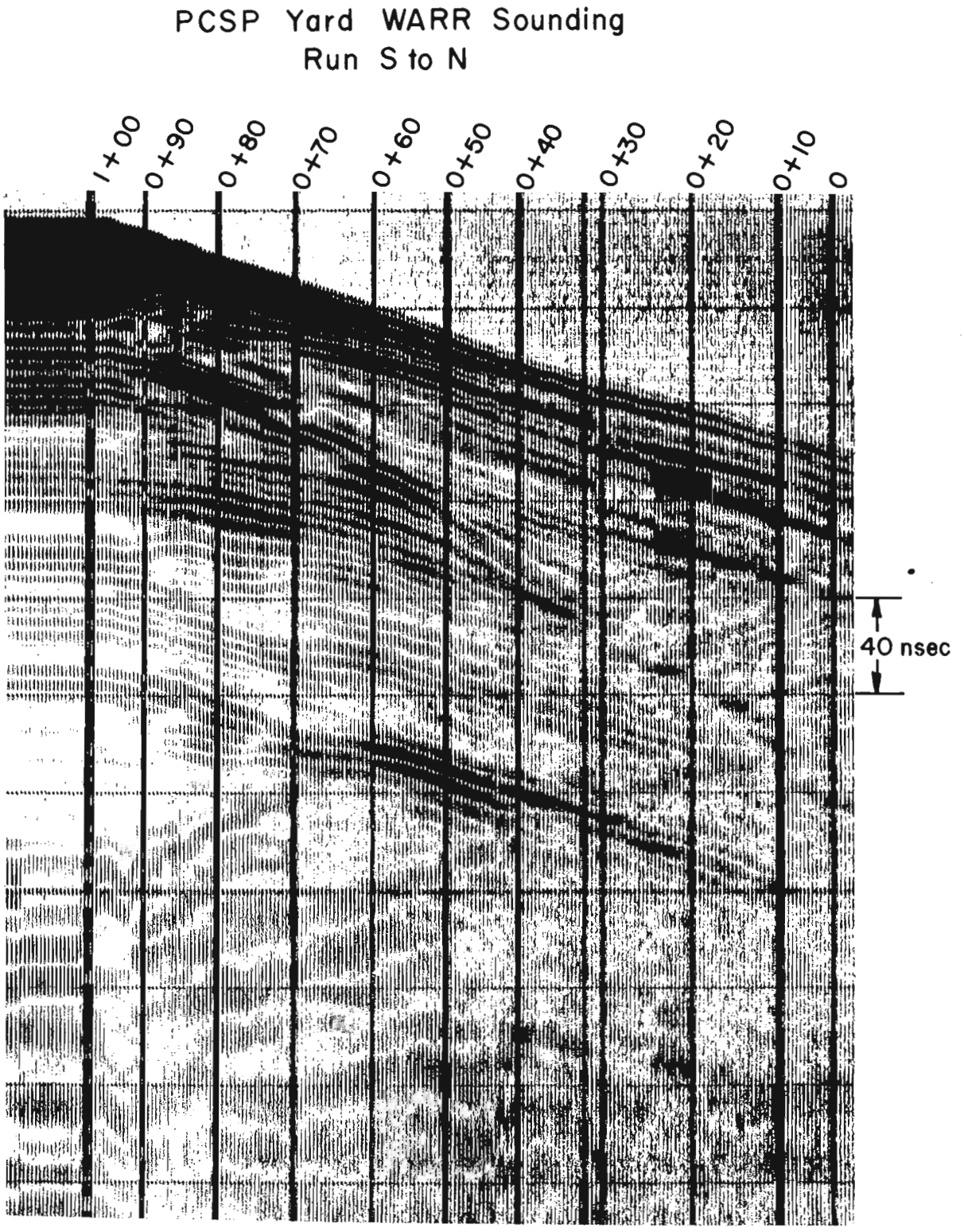

Figure 56.3. WARR sounding in the yard with Tx at 1+00.

of Tuktoyaktuk, N.W.T. in the spring of 1975 are presented. The radar equipment employed in the soundings is described by Morey (1974) and Annan *et al.* (this publication, report 57).

Field Results

The experimental results shown in Figures 56.1, 56.2, 56.3 and 56.4 were collected in the yard of Polar

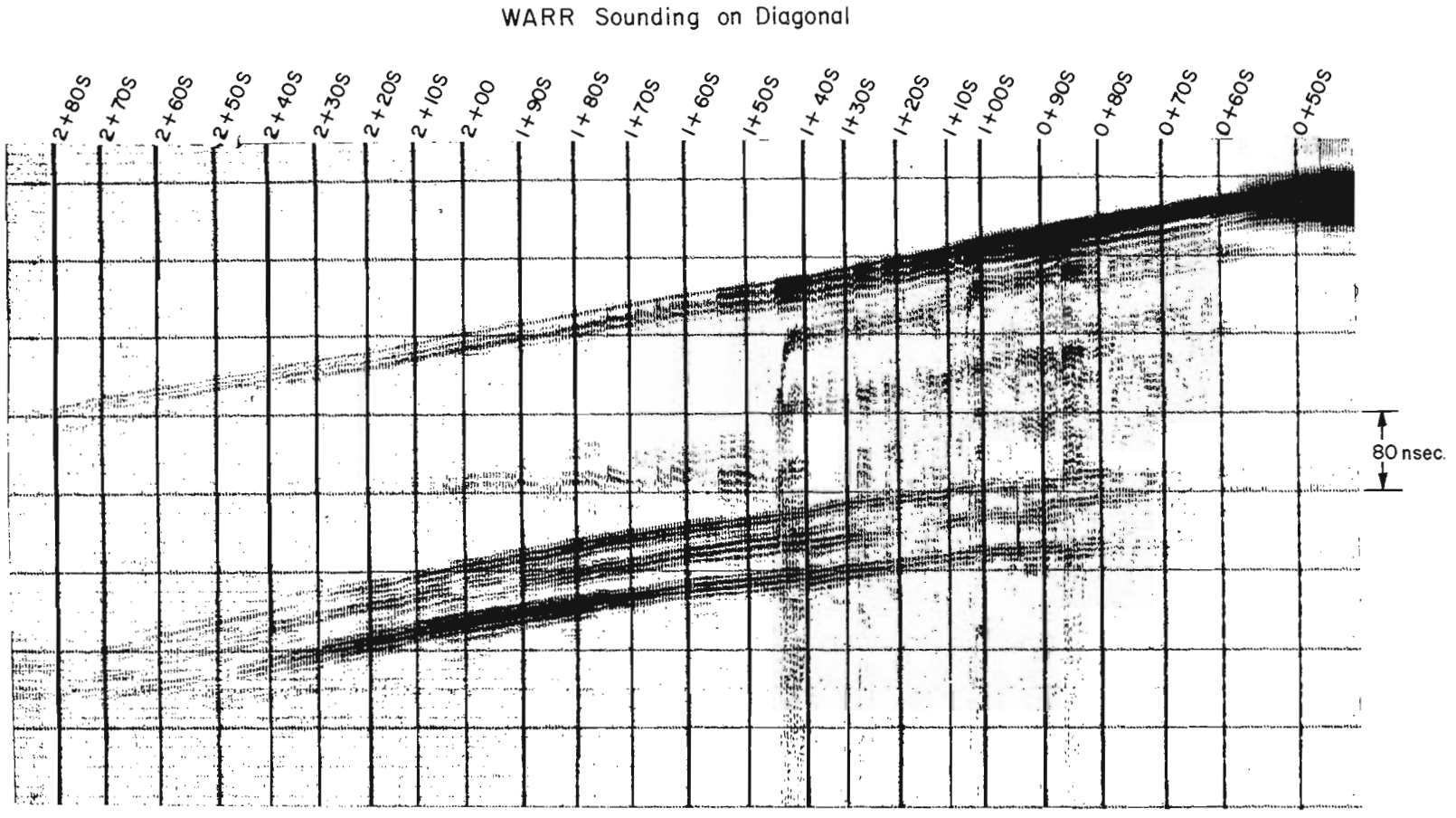

Figure 56.4. WARR sounding on the Diagonal line on the Involuted Hill with Tx at D1-0+50S.

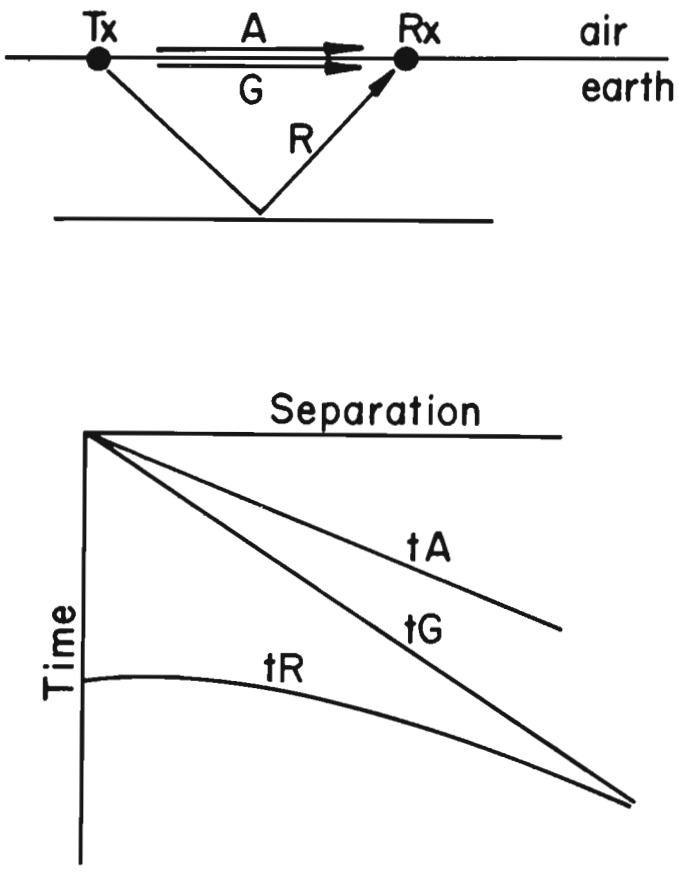

Figure 56.5. Simplistic diagram of travel time for arrivals in a WARR sounding over a single reflector.

Continental Shelf Project (PCSP) base at Tuktoyaktuk and on the Involuted Hill test site located about 16 km northeast of Tuktoyaktuk.

The Polar Continental Shelf Project base is built on a sand and gravel pad laid down over the old terrain. Extensive tests were conducted on this pad to access the radar method on coarse grained materials. Most of the Tuktoyaktuk vicinity is covered by a thin clay till layer which is quite opaque to the radar signals. This location provided an ideal area to remove the clay complications from trial surveys.

The Involuted Hill is an iced cored hill. It is typical of many hills found in the Tuktoyaktuk area (Mackay, 1963). WARR soundings were conducted on a number of sites where radar profiling indicated deep reflections could be observed over an extended area.

(i) Polar Continental Shelf Project Soundings

The Polar Continental Shelf Project data were obtained between the garage and the bunk house. Figure 56.1 shows a reconnaissance profile with fixed antenna configuration which was run across the yard. The distance between the transmitter and receiver is 3 m. The profile shows a reflector at a range of 40 to 60 ns two-way travel time. The subsurface reflection is from the pad bottom interface with the clay till which overlies most of the surrounding terrain. WARR soundings were run with the transmitting antenna up at both ends of the profile (stations 0 and 1+00) shown in Figure 56.1. These soundings are shown in Figures 56.2 and 56.3. The stations in the diagram indicate the position of the receiving antenna[1]. In Figure 56.2 the transmitting antenna is at station 0+00 while in Figure 56.3, it is located at station 1+00. The first radar event at any distance is the direct air wave. This is followed by the direct ground wave and waves reflected from the subsurface interface. The direct waves and any critically refracted waves generate linearly related travel-time versus antenna separation events. The reflected waves from the underlying interface are hyperbolic curves for travel-time versus antenna separation.

(ii) Involuted Hill Diagonal Sounding

A WARR sounding was carried out on the line called the Diagonal located on the ice cored Involuted Hill. The fixed antenna configuration profile obtained on this line is presented in an accompanying paper by Annan *et al.* (this publication, report 57). The WARR sounding shown in Figure 56.4 was run between stations 0+50S and 2+80S on leg D1 of the Diagonal. There are two main events on the sounding; the direct air wave arrival and the hyperbolic trace associated with energy reflection from the bottom of the ice slab forming the hill.

Discussion and Interpretation of the Data

The utility of WARR soundings lies in the fact that they can be used to infer both the depth of reflecting interfaces and the propagation velocity. A simplistic diagram of the basic arrivals of a WARR sounding over a single subsurface interface appears in Figure 56.5. The air wave arrives at time

$$t_A = \frac{x}{u_A} \text{ ns} \quad (1)$$

where x is the antenna separation in metres and u_A is the velocity of electromagnetic waves in air which is 0.3 m/ns. The direct ground wave arrives at time

$$t_G = \frac{x}{u_g} \text{ ns} \quad (2)$$

where u_g is the propagation velocity of ground in m/ns. Since $u_g = \frac{u_A}{\sqrt{K}}$ m/ns where K is the ground dielectric constant, an estimate of the bulk dielectric constant can be made from measurement of U_g. The reflected wave arrives in time

$$t_R = \frac{(x^2 + 4d^2)}{u_g} \text{ ns} \quad (3)$$

[1]Station numbers are the relative location given in units of feet.

Table 56.1

Summary of velocities, dielectric constants and reflector depths as inferred by WARR sounding

Site \ Parameter	U_G From t_G (m/ns)	K From t_G	U_G From t_R (m/ns)	K From t_R	d From t_R (m)
PCSP 0+0 to 0+90	.145	4.2	.145	4.3	3.7
PCSP 1+00 to 0+00	.15	4.0	.16	3.7	2.0
DIAGONAL	---	---	.19	2.5	27

where d is the depth of reflector in metres. While these three arrivals do not describe all the events observed on a WARR sounding, they do describe the strong arrivals and permit preliminary quantitative analysis.

Estimates of reflector depths and propagation velocities for the three WARR soundings (Figs. 56.2, 56.3 and 56.4) were made using the above expressions relating travel-time to antenna separation. The direct air wave arrival was used to obtain an accurate estimate of the antenna separation using equation 1 since u_A is well defined. If a direct ground wave is observed, U_g is inferred by least squares fitting of a linear relationship between observations of t_G and x (as inferred from t_A). The slope of this line yields an estimate of $1/U_g$. The reflection arrivals were used to infer both U_g and d by least squares fitting a linear relationship between observations of t_R^2 and x^2 (obtained from t_A). The slope of this line is an estimate of $1/U_g^2$ and the intercept is $4d^2/U_g^2$ which gives an estimate of d. The results of analyzing the three soundings in this manner are summarized in Table 56.1.

The Polar Continental Shelf Project soundings yield a value of about 4 for the dielectric constant of the pad which corresponds to a propagation velocity of 0.15 m/ns. These values are consistent with the known properties of frozen sands and gravels. There is about a five per cent uncertainty in the value of the dielectric constant. This is attributable to uncertainties in picking event times and the idealized interpretation model which yields the simple relations in equations 1, 2 and 3. The depth of the reflecting interface is about 3.7 m at station 1+00 and about 2.0 m at station 0 on the basis the $t_R^2 - x^2$ analysis. These estimates can be considered accurate to +0.25 m. The large uncertainty is associated with the difficulty in picking the leading edge of the reflection. More reliable estimates will become available when the signals are deconvolved using digital signal processing to compress the duration of the wavelet. Alternative estimates of the interface depth can be made from the profile in Figure 56.1 by taking the sand and gravel to have a velocity of 0.15 m/ns as inferred by the WARR soundings. At station 1+00 the depth is 3.5 m and at station 0 the depth is 1.8 m. These estimates are consistent with the WARR depth estimates.

The WARR sounding on the Diagonal yields a propagation velocity of .19 m/ns which corresponds to a dielectric constant of 2.5. There is no discernable direct ground wave on this record. Either it is below the receiver sensitivity or is attenuated by the near surface clay till. The bottom of the ice slab is interpreted to be about 27 m below the surface. Both the depth estimate and velocity obtained by WARR sounding are in agreement with the interpretation of profile data and drilling information obtained near the site. This information is in a paper by Annan *et al.* (this publication, report 57).

While the velocity and dielectric constant are somewhat contaminated by the thin layer of clay till at the surface, these values are unusually high for velocity and low for dielectric constant in the ice. The clay till would bias the observations to lower velocities and higher dielectric constants and cannot be used to account for the anomalous values. As in the discussion the profiling results on the Involuted Hill, it is necessary to postulate about a 20 per cent air content in the ice to explain the velocity and dielectric constant.

Summary and Conclusions

The results of preliminary interpretation of WARR sounding indicate reliable estimates of velocity and depth can be obtained in plane stratified regions. The sounding results are extremely valuable in that they permit an interpretation of profile data in terms of actual depth rather than travel-time. While the need for drill control is not eliminated, the amount of drilling required for ground truth can be reduced by employing WARR sounding where the lithology permits. Drill control is needed to provide a knowledge in the geologic material composing the section. Combining drill control with VHF radar WARR sounding and profiling permits measurement of bulk electrical properties of various geologic materials *in situ*.

In order to improve interpretation of the data, the WARR sounding records will require considerable signal enhancement by digital processing techniques. At the moment, the transmit pulse is long compared to the time separation of some of the arrivals on the records. As a result the leading edge of some events are very uncertain. The pulse length limits the system resolution in the top 3 to 4 m. To increase the near-surface resolution, shorter pulses (higher frequency signals) must be employed.

The WARR sounding in the Involuted Hill implies a high air content in the underlying ice. This dielectric constant of 2.5 implies a density of about 0.7 Mgm/m^3. Such a low density has important implications on the interpretation of gravity data to infer excess ice content (Rampton and Walcott, 1974).

References

Annan, A.P., Davis, J.L., and Scott, W.J.
1975: Impulse radar profiling in permafrost; *in* Report of Activities, Part C, Geol. Surv. Can., Paper 75-1C.

Rampton, V. N. and Walcott, R. I.
1974: Gravity profiles across ice-cored topography; Can. J. Earth Sci., v. 11, p. 110-122.

Robin, G. de Q., Evans, S., and Bailey, J. T.
1969: Interpretation of radio echo sounding in polar ice sheets; R. Soc. London, Philos. Trans., Ser. A, v. 265, p. 437-505.

IMPULSE RADAR PROFILING IN PERMAFROST

Projects 750037 and 670041

A. P. Annan, J. L. Davis and W. J. Scott
Resource Geophysics and Geochemistry Division

Introduction

For the past two years, the Electrical Methods Section of the Geological Survey of Canada has been investigating the feasibility of using VHF impulse radar to map the geological structure and electrical properties of permafrost *in situ*. All available information on the electrical properties of frozen soils at VHF indicates radar signals should be capable of probing to depths between 3 and 30 m. Field trials conducted in the vicinity of Tuktoyaktuk, Northwest Territories, have assessed the impulse radar method. This report presents some of the preliminary results of these trials.

Equipment, Profile Operation and Data Presentation

The equipment used for the field work was an impulse radar designed and constructed by Geophysical Survey Systems Inc. This equipment was chosen since it was commercially available and designed for subsurface probing (Morey, 1974). The radar system is depicted in the block diagram shown in Figure 57.1. The system consists of timing electronics which clock an impulse generator and a sampling head. The impulse source generates 100 volt impulses with a 150 MHz bandwidth at a repetition rate of 50 KHz. The impulse is fed to the transmitting (Tx) antenna and radiated after modification by the antenna spectral characteristics which transform the impulse into a wavelet with centre frequency about 70 MHz. The radiated power is about 50 watts and the system dynamic range is about 100 dB. Part of the radiated signal penetrates into the ground and is either reflected or scattered by changes in subsurface electrical properties or absorbed. The signal at the receiving (Rx) antenna is composed of energy radiated directly from the Tx antenna to the Rx antenna and energy re-radiated by surface or subsurface scattering structures. The received signal is fed to a sampling head which uses the repetitive nature of the signal to slow down the VHF signal to an audio frequency facsimile. The low frequency signal is then displayed on an oscilloscope and a graphic recorder. The data is also recorded on an instrumentation tape recorder for future replay and data enhancement.

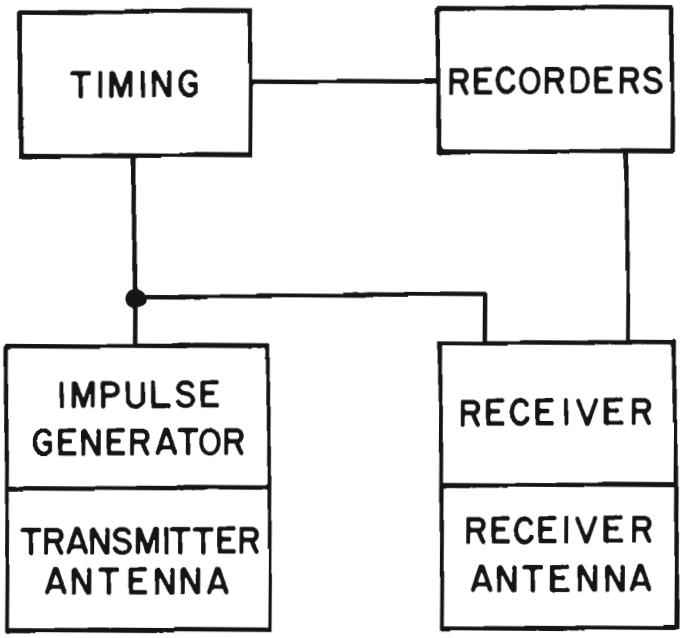

Figure 57.1. Block diagram of the impulse radar system.

Figure 57.2. Photograph of profiling operation.

For profile reconnaissance work, the Tx and Rx antennas were rigidly mounted on a sled and towed over the ground. The system in operation is shown in Figure 57.2. The antennas were housed in the two boxes on the sled. The antenna separation was 3 m from centre to centre. The electronics and recording equipment were mounted in the tracked vehicle. Several kilometres of line could be profiled in a day when all mechanical equipment was in working order.

The data presented in the rest of this report was generated on the graphic recorder. To assist the uninitiated in deciphering the diagrams, Figure 57.3 shows a typical received radar signal accompanied by its graphic recorder display. The graphic recorder yields a plot of the signal level versus two time variables. For the data presented here, the horizontal time scale represents antenna position (the black vertical lines are event markers associated with fieldgrid markers) and the vertical time scale represents the radar return delay time. The grey level of the plot is proportional to the amplitude of the signal. At times the signal level is too light or too dark during a return since the recorder intensity has only a 20 dB dynamic range.

Field Data

The following examples of profile data were collected on the Involuted Hill and the Tuktoyaktuk runway. The Involuted Hill is located about 16 km northeast of Tuktoyaktuk and has been used extensively as a geophysical test site. Figure 57.4 shows an aerial photograph (A234422-113) of the central portion of the survey grid located at the Involuted Hill site.

(i) Involuted Hill: Baseline West

Profile data collected on the baseline between 0 and 6+00 W is displayed in Figure 57.5 (the grid on the hill is laid out in feet and 6+00 w indicates 600 feet west of the origin. Similar references to stations in other diagrams are in feet from the start of the line). The dark constant band at the top of the record beginning at time zero is the arrival of direct Tx to Rx waves. These waves have a duration of about 20 ns. Events appearing on the record after this time are due to reflections or refractions from subsurface structures. For most of the record, there are no visible returns for times greater than about 60 to 70 ns. Between 2+00 w and 4+00 w, significant returns can be seen for times 70 to 130 ns and again at times of 300 to 400 ns.

A detailed survey was carried out near the baseline west profile by profiling on a grid of lines spaced at 25 feet (7.6 m) intervals parallel and perpendicular to the baseline. These grid-lines were enclosed by the boxed areas indicated on the aerial photo in Figure 57.4. The results of this detailed mapping are shown by meanings of a travel-time contour map (Fig. 57.6). The areas where reflections were observed at times greater than 250 ns are enclosed by the dotted contours while areas with reflections in the time span 50 to 250 ns are enclosed by the solid contours.

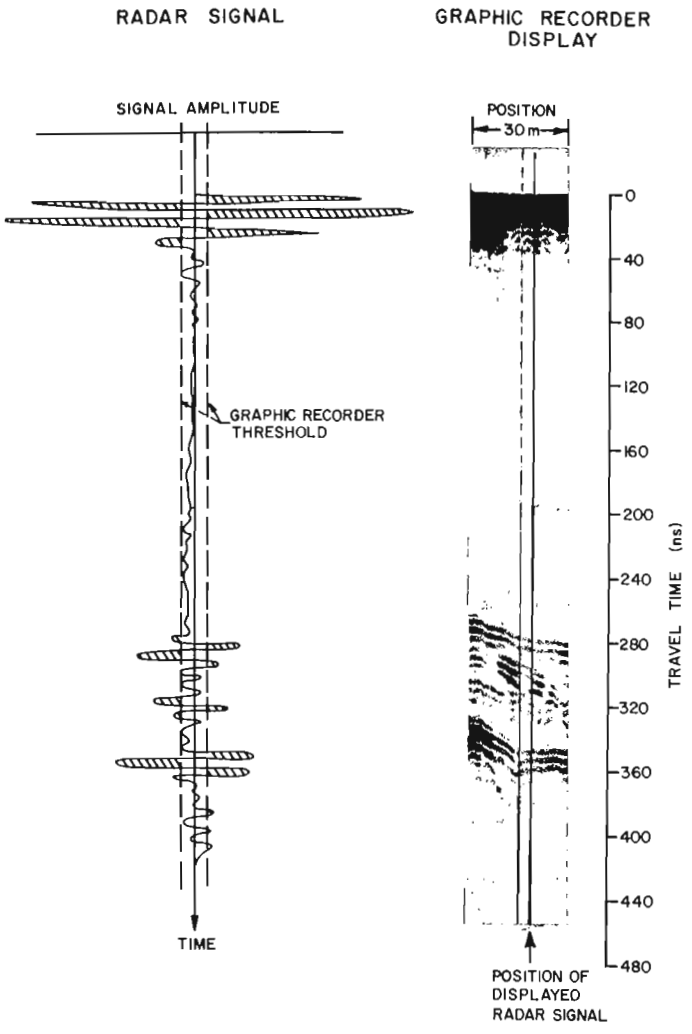

Figure 57.3. Radar signal versus time and its equivalent display on the graphic recorder.

(ii) Involuted Hill: Diagonal

Another set of profile data was collected on the Involuted Hill (Fig. 57.7). This data was collected along a line called the Diagonal which is the dog-leg line (Fig. 57.4) running from 5+00S on line 0 to 5+50E on the baseline. The Diagonal consists of two straight line segments denoted D1 and D2. The D1 segment was roughly southwest from 5+50E on the baseline and D2 segment runs roughly northeast from 5+00S on line 0. The short time returns are similar to those observed on the baseline west. The significant feature of this profile is the strong returns at times 300 to 400 ns along nearly the whole length of the traverse.

(iii) Tuktoyaktuk Runway

A number of experiments were conducted near the Polar Continental Shelf Project (PCSP) base in Tuktoyaktuk. A number of these trials were on the 1 to 3 m thick gravel pad laid down for the construction of the base and airstrip. A sample of the data is shown in

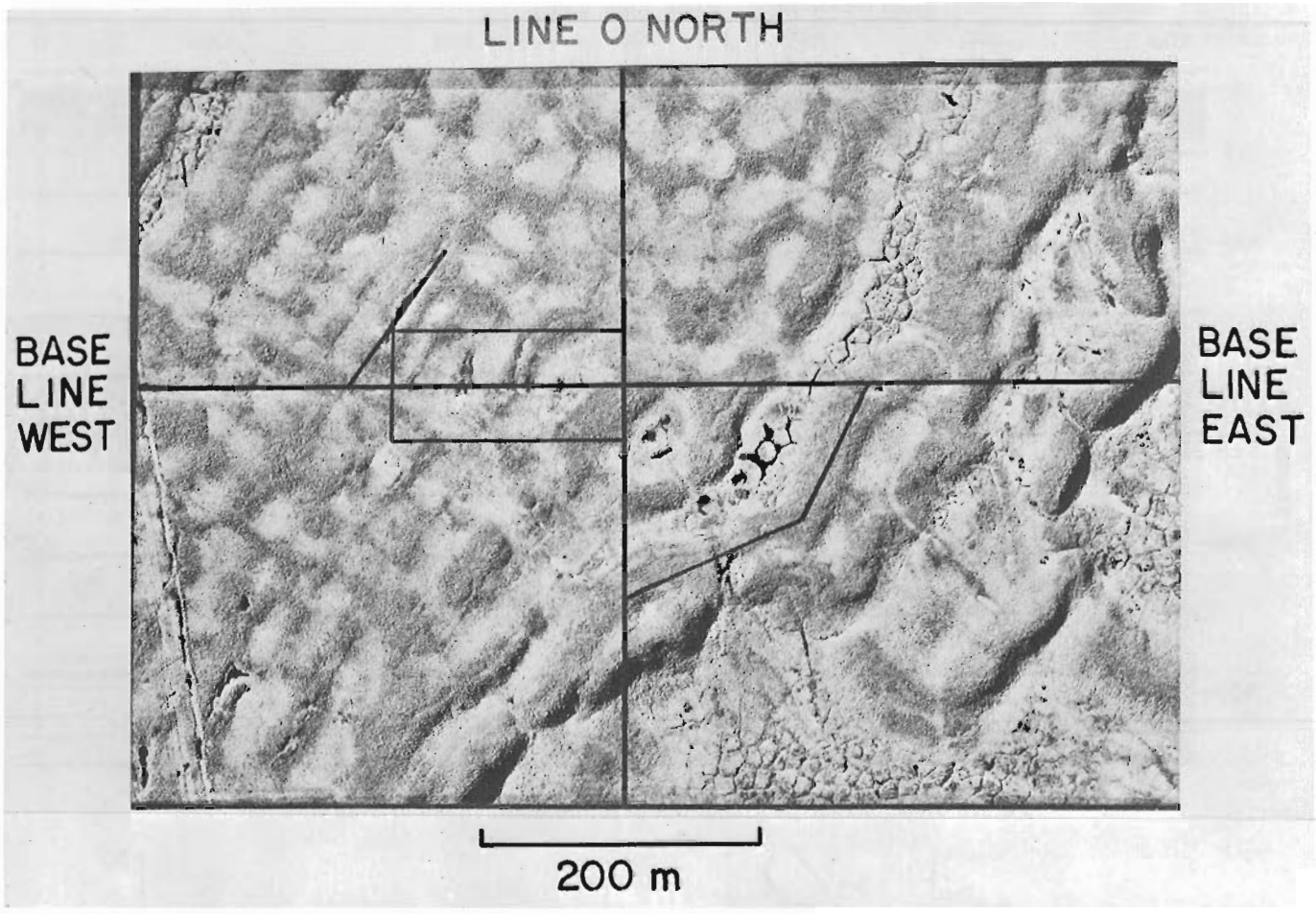

Figure 57.4. Aerial photograph of the Involuted Hill.

Figure 57.8. In this profile, a line was run perpendicular to the runway. The runway shows up clearly on an otherwise non-descript profile.

Discussion and Interpretation of Data

(i) Involuted Hill: Baseline West

The Involuted Hill is one of a large number of ice cored hills found near Tuktoyaktuk (Mackay, 1963, 1966, 1971; Rampton and Mackay, 1971). The hill consists of a 20 m thick slab of ice overlain by 5 to 10 m of icy clay till mixed with peat. The overlying material has been highly reworked by frost action and is interlaced with ice wedges. The results of a detailed drilling program along the baseline between 0 and 6+00 W are shown in Figure 57.9. In this area the tabular ice sheet is underlain by sand containing ice lenses.

A comparison of the radar profile along the baseline west (Fig. 57.5) and the drilling cross-section (Fig. 57.9) indicates a correlation between return times in the time span 300 to 400 ns and areas where there is an ice window to the ground surface. The clay till has a higher attenuation than the ice and thus behaves like an opaque screen which has holes in it. The plan view contour map (Fig. 57.6) shows that the windows are continuous over distances of 10 to 100 m. Examination of the aerial photo (Fig. 57.4) shows that the windows in this case are ice wedges. The shorter time returns in the range 70 to 130 ns are associated with the ice wedge structure and its contact with the underlying ice slab. Examination of the 300 to 400 ns returns shows that these are not single reflections but two or three closely spaced arrivals. This response is generated by the ice lensing in the sand underlying the ice slab indicated by the drilling.

The drill control permits the radar system to be used to measure the electrical properties of the hill where deep reflections are observed. At 3+50 W, the bottom of the ice slab is seen by the radar at a range of 290 ns. Time zero on the plot is 10 ns due to the finite Tx-Rx separation. After the signal is transmitted, the actual travel time is 300 ns. From the drilling, the ice bottom is about 28 m deep. The mean propagation velocity of the radar signal is

$$V_m = \frac{2 \times \text{depth}}{\text{time}} = .186 \text{ m/ns} \qquad (1)$$

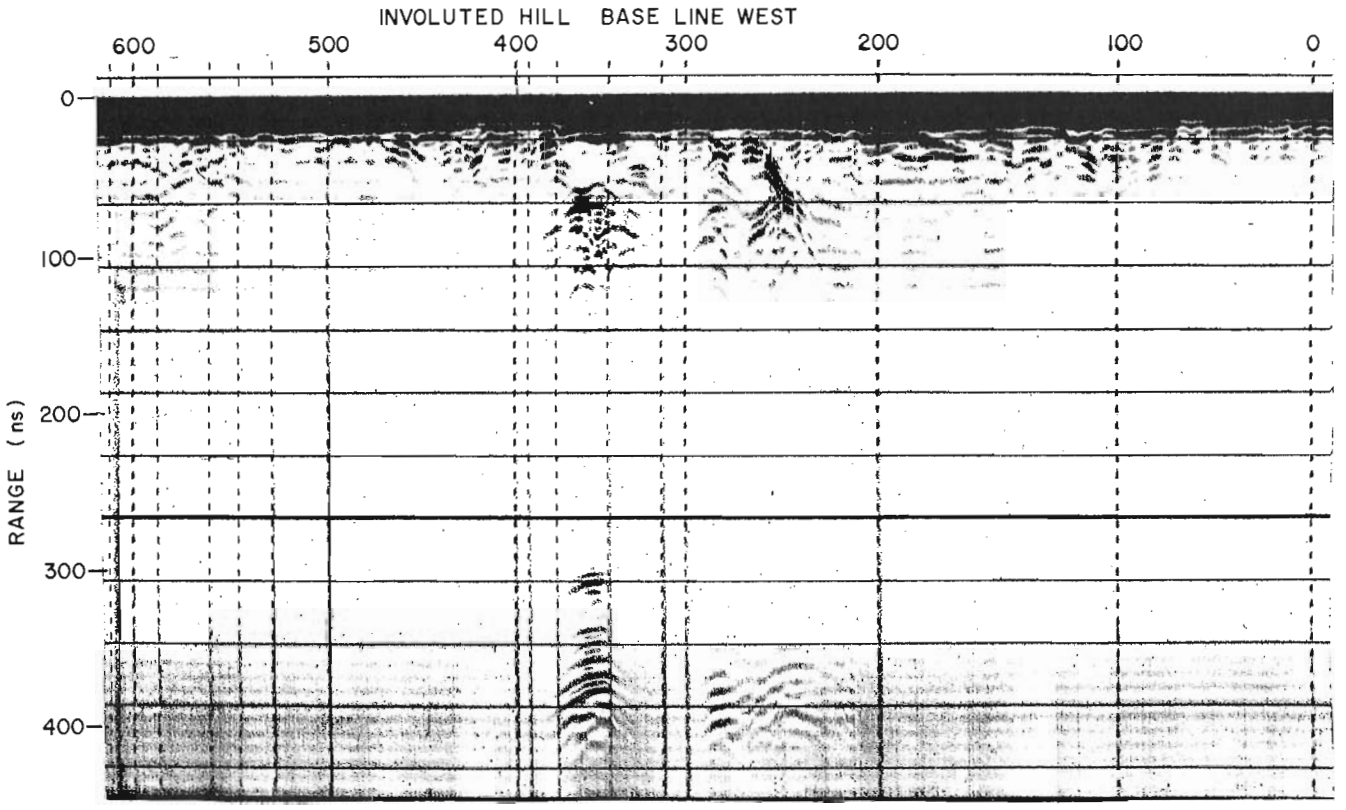

Figure 57. 5. Radar profile of the baseline between 0 and 6+00 W.

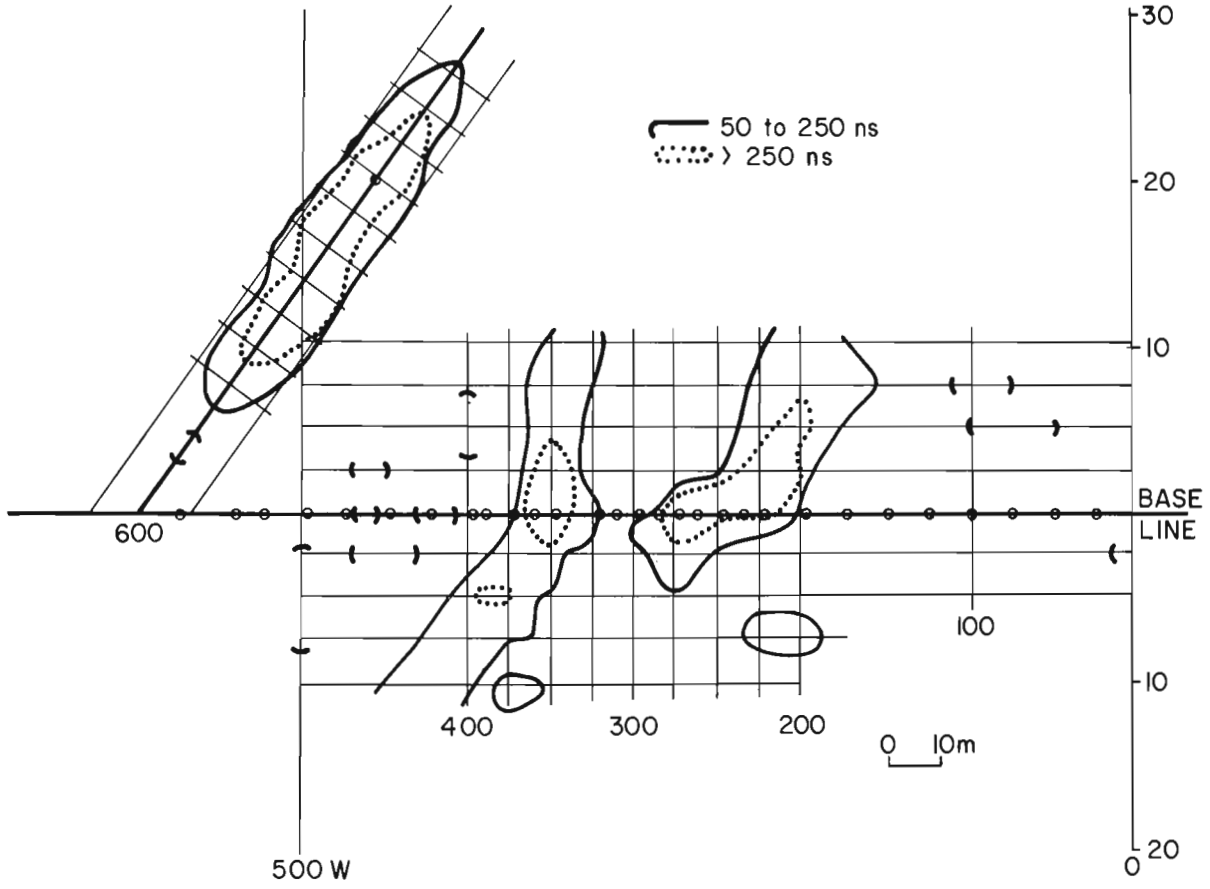

Figure 57. 6. Contour map of radar returns in the area of 0 to 6+00 W on the baseline.

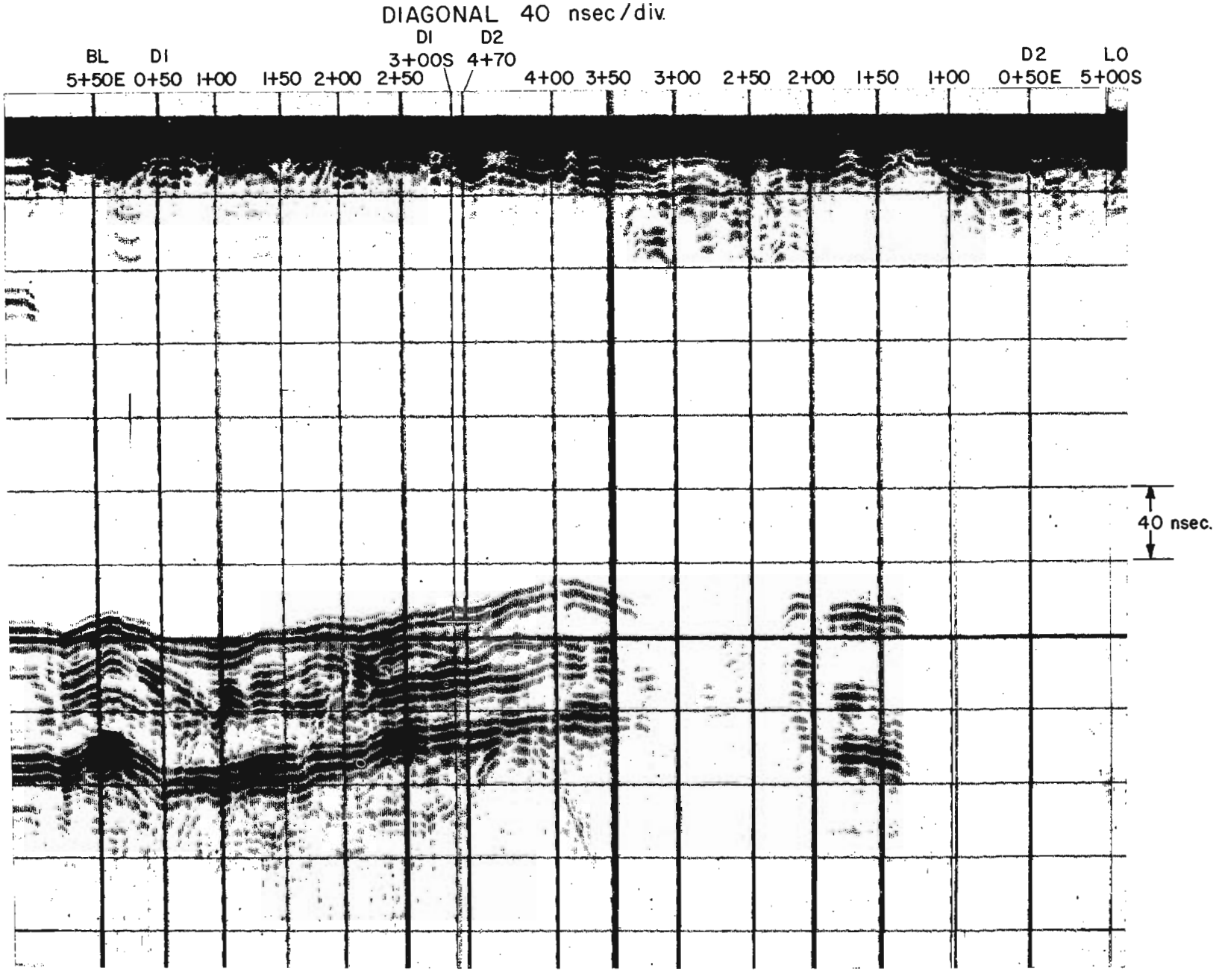

Figure 57.7. Radar profile of the diagonal line.

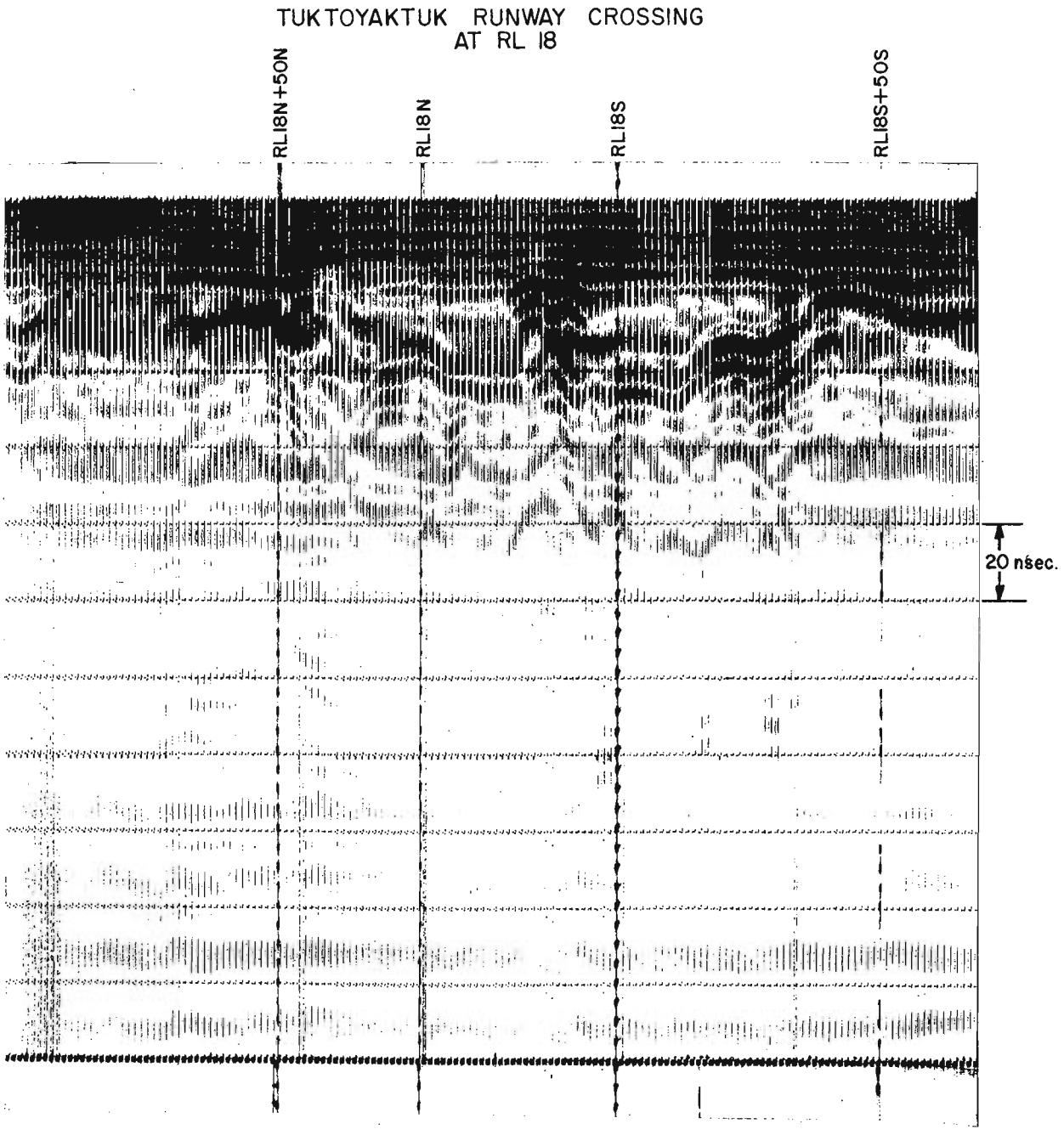

Figure 57.8. Radar profile of the Tuktoyaktuk runway.

Since the propagation velocity is directly related to the dielectric constant in low loss materials by

$$V = \frac{0.3}{\sqrt{K}} \text{ m/ns} \qquad (2)$$

an estimate of the mean dielectric constant, K_m, is 2.6. This value of dielectric constant is quite surprising in that the propagation path where deep reflections are seen is almost totally ice which has a dielectric constant of 3.2 at VHF. Since frozen soils exhibit higher dielectric constants than ice, any soil in the path should increase K_m.

In order to explain the low value of K_m, a number of alternatives are available. The observed travel-time could be in error. This is unlikely, however, since several sets of data have been recorded at this site in the springs of 1974 and 1975 and all yield the same travel-time estimates. The errors in travel-time are caused by the time resolution limitations of the graphic display and are at most 1 or 2 per cent. The next

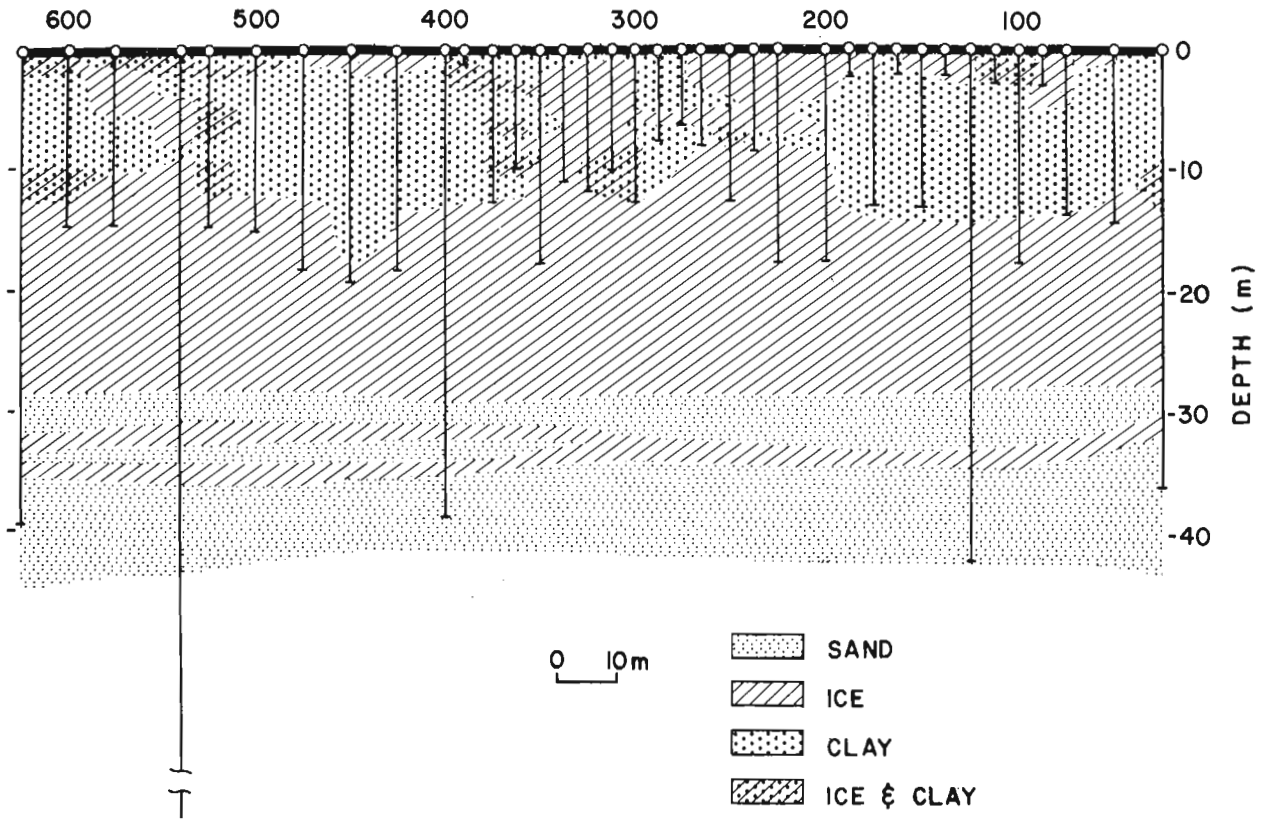

Figure 57.9. Geological cross-section of the Involuted Hill baseline west 0 to 6+00 W as inferred from drilling.

source of error is the depth to the bottom of the ice. There is not a drill hole at the exact location where the radar sees the bottom. As a result, the depth is obtained by interpolating between the depths observed at sites 4+00 W and 1+20 W. The reason that this interpolation is justified is that all drilling to the bottom of the ice both in the section 0 to 6+00 W and in other areas indicate the bottom of the ice to be remarkably flat. An error of less than +1.5 m (5%) in the depth determination is a reasonable assumption. The travel-time and depth error cannot explain the anomalously low value of K_m totally. The only other explanation is to accept the value for K_m and find a physical explanation for it.

Examination of the ice taken in drill cores showed large numbers of air bubbles in the ice. A discussion of the dielectric constant of ice and snow versus density is given Robin *et al.* (1969) which indicates that the empirical relationship

$$K = 1 + 2.36\rho \qquad (3)$$

where ρ is the density in Mg/m^3 yields reasonable estimates of K when the density is known. The density of an air rich ice is given by

$$\rho = (1-\varepsilon)\ 0.92\ Mg/m^3 \qquad (4)$$

where 0.92 is the density of solid ice and ε is the volume fraction of air trapped in the ice. The observed value of K_m corresponds to a mean density, ρ_m, of .67 Mg/m^3 and a mean volume fraction of air, ε_m, of 0.27. Table 57.1 shows the number of spherical air bubbles per 10^{-6} m^3 (1 cm^3) of ice required to give a volume fraction 0.27 of air. Visual examination of available ice cores shows that these numbers are frequently exceeded. Hence the observed K_m of 2.6 is not as unreasonable as first thought.

Table 57.1

Number of bubbles versus bubble radius required to generate 0.27 volume fraction of air in 1 cm^3 sample

Bubble Radius (mm)	No. of Bubbles
0.5	515
1.0	64
1.5	19
2.0	8
2.5	4

(ii) Involuted Hill: Diagonal

The Diagonal profile exhibits a response which was characteristic of the ridge which circumscribes most of the Involuted Hill. The clay till overlying the ice slab appears to become thinner in this area. As a result, the bottom of ice is visible to the radar along most of the length of profiles run on this ridge. The bottom reflection shows at least three distinct arrivals that indicate the ice lenses present in the sand beneath the ice have considerably horizontal continuity. The undulations in the bottom reflector are mostly due to surface elevation changes and not necessarily variations in the bottom of the ice sheet itself. The area between D2-2+00 E and D2=3+50 E where the bottom reflections fade is the location of a thaw gully which crosses the ridge. The gully is clearly visible on the photo in Figure 57.4. The fading signal is probably due to a thickening of the clay till in this region.

The mean velocity and dielectric constant for the section of the Diagonal near the baseline east are inferred to be about 0.18 m/ns and 2.7. This estimate is not as reliable as the one on the baseline west since drilling shows the depth to the ice bottom is more irregular in this area. This dielectric constant corresponds to a mean density for the ice of about 0.72 and 0.22 volume fraction of air. These estimates are somewhat contaminated by the fact there is 1 to 3 m of clay till cover on the ice slab.

(iii) Tuktoyaktuk Runway

The runway at Tuktoyaktuk consists of a pad of sand and gravel fill laid down over the old terrain. The primary reason for working on the runway was to evaluate the radar system on a controlled area where the near surface was composed of coarse grained materials. Most of the Tuktoyaktuk area is blanketed with a clay till which was quite opaque to the radar signal. The profile across the runway is almost self explanatory. The subsurface reflection is from the interface between the fill and the old terrain. The strong signal near the centre of the runway response is believed to be due to buried cables which power the runway lights. An estimate of the gravel pad thickness is given by

$$d = \left(\frac{(0.15t)}{(2)}^2 - 2.25\right)^{\frac{1}{2}} \text{ m} \qquad (5)$$

where a value of 4.0 was chosen for the dielectric constant of the till. This estimate of dielectric constant was obtained by radar sounding on the fill as described by Annan *et al.* (this publication, report 56). The central part of the runway is about 3 m thick where this profile was run.

Summary and Conclusions

While experiments in the Tuktoyaktuk area were hampered by the presence of a layer of quite opaque clay till overlying much of the region, the results to date have been very encouraging. The runway trials show that far better results would be obtained in areas not having the clay problem. The impulse radar method can be used to delineate subsurface structure. When used in conjunction with a drilling program, the radar can be used to laterally extend the drilling information and define new drill sites. The radar would reduce the number of holes required and allow holes to be placed at more strategic positions.

A byproduct of these experiments has been the surprising value of a mean dielectric constant of 2.6 to 2.7 in the massive ground ice at the Involuted Hill test site. If current laboratory measurements on ice cores confirm these values, the density of massive ground ice cannot safely be assumed to be .92 Mg/m^3. A value of 0.7 Mg/m^3 would be more reasonable. Since most exposed ice masses appear to be quite air rich (Mackay, 1971) in Tuktoyaktuk area, care must be taken in interpretation of gravity data to infer excess ground ice thickness variations based on a 0.92 Mg/m^3 density (Rampton and Walcott, 1974).

The use of radar alone to predict the ice content of soils does not appear feasible. The dielectric constant of frozen soils and ice so far measured with the radar system lie in the range of 2 to 4. While this is not a very representative sample, there are more variables than per cent ice content which affect the dielectric constant and make ice content inferences unrealistic. The percentage of trapped air in pure ice discussed here is a simple example of this problem.

References

Annan, A.P., Davis, J.L., and Scott, W.J.
1975: Impulse radar wide angle reflection and refraction sounding in permafrost; *in* Report of Activities, Part C, Geol. Surv. Can., Paper 75-1C.

Mackay, J.R.
1963: The Mackenzie Delta area, N.W.T.; Geographical Branch Memoir 8, represented as Geol. Surv. Can., Miscell. Report 23, 202 p.

1966: Segregated epigenetic ice and slumps in permafrost Mackenzie Delta area, N.W.T.; Geogr. Bull. (Canada), v. 8, p. 54-80.

1971: The origin of massive icy beds in permafrost, Western Arctic Coast, Canada; Can. J. Earth Sci., v. 8, p. 397-421.

Morey, R.M.
1974: Continuous subsurface profiling by impulse radar, Proceedings of Engineering Foundation Conference on "Subsurface exploration for underground excavation and heavy construction"; American Society of Civil Engineers.

Rampton, V.N. and Mackay, J.R.
1971: Massive ice and icy sediments throughout the Tuktoyaktuk Peninsula, Richards Island and nearby areas, District of Mackenzie; Geol. Surv. Can., Paper 71-21.

Rampton, V.N. and Walcott, R.I.
1974: Gravity profiles across ice-cored topography; Can. J. Earth Sci., v. 11, p. 110-122.

Robin, G. de Q., Evans, S., and Bailey, J.T.
1969: Interpretation of radio echo sounding in polar ice sheets; R. Soc. London, Philos. Trans., Ser. A, v. 265, p. 437-505.

Project 630049

T. J. Katsube
Resource Geophysics and Geochemistry Division

Introduction

Information on the frequency spectrum of resistivity and dielectric constant of rocks is necessary for data interpretation and as a basis for new developments in electrical methods for geophysical exploration. However, resistivity and dielectric constant vary with frequency, and this raises a question of whether users of the information have to be furnished with knowledge of the entire frequency spectrum or whether a more simple and efficient form of representation of the electrical characteristics of rocks is possible. Recent studies (Katsube, 1974, 1975b) have shown that a simplified form of expressing the electrical characteristics of rocks is possible, by using a new concept of a "Three Electrical Polarization Mechanism Model". By using this model for the analysis of the electrical rock property data, it is possible to discriminate between the effect of different types of electrical mechanisms. The electrical mechanisms are closely related to the mineralogy, sulphide mineral content, texture and other petrographical features. Thus, this new model forms a basis for a new technique for obtaining geological information from electrical measurements. This paper reviews past work, shows experimental evidence on measurements of some serpentinite samples that supports the new model, and suggests the use of a new set of parameters to represent the electrical characteristics of moist rocks.

Review of Past Work

Keller and Licastro (1959) made measurements on the frequency spectrum of resistivity and indicated that resistivity showed little dependence on frequency until the frequency rises above a certain frequency. Katsube and Collett (1972) referred to this frequency as the critical frequency. Above the critical frequency the resistivity decreases rapidly with increase in frequency. Laboratory measurements (Katsube and Collett, 1974) showed that though the frequency dependence of resistivity is small below the critical frequency, it is significant enough to have an important implication on the interpretation of field geophysical data. The dielectric constant is also frequency dependent below the critical frequency. Katsube (1975) summarized these characteristics. Thus the questions are over what frequency range should the electrical parameters be measured in the laboratory, and how should the electrical characteristics of a rock that is frequency dependent be presented.

The frequency dependence of the electrical characteristics is caused by various electrical mechanisms in the rock. The dielectric polarization (Keller and Licastro, 1959; Katsube and Collett, 1972, 1974) and electrode polarization (Marshall and Madden, 1959; Collett, 1959) mechanisms are well known as two of the causes. The membrane polarization mechanism that has been suggested by Marshall and Madden (1959), can be considered a third cause, but there is a lack of data that clearly shows the effect of this mechanism. Olhoeft (1975a) suggests that there exist many other electrical mechanisms in rocks. These mechanisms are affected by the general mineralogy, sulphide mineral content, texture and other petrographical features of the rock. Thus it is necessary to make use of the frequency dependence of the electrical characteristics to obtain petrographical information.

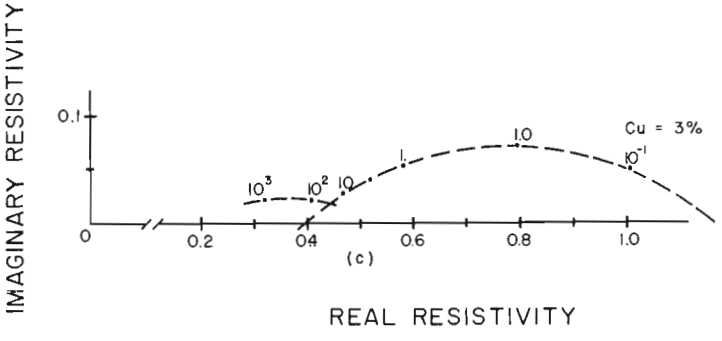

Figure 58. 1. Complex resistivity plot for a rock sample disseminated with sulphides. Resistivity is normalized at 10^{-1} Hz. The main circular arc is due to electrode polarization of the sulphide minerals (after Zonge, 1972).

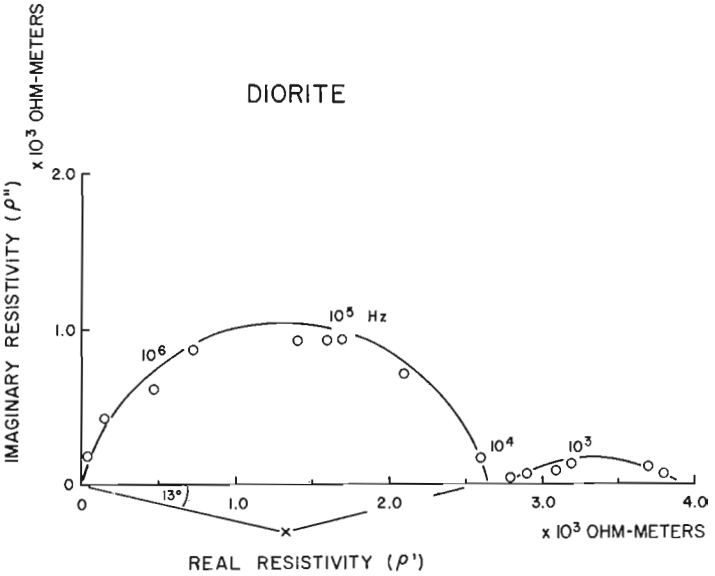

Figure 58. 2. Complex resistivity plot of a diorite sample which lacks sulphide or other conductive minerals. The large circular arc on the left is due to the dielectric polarization (after Katsube and Collett, 1974).

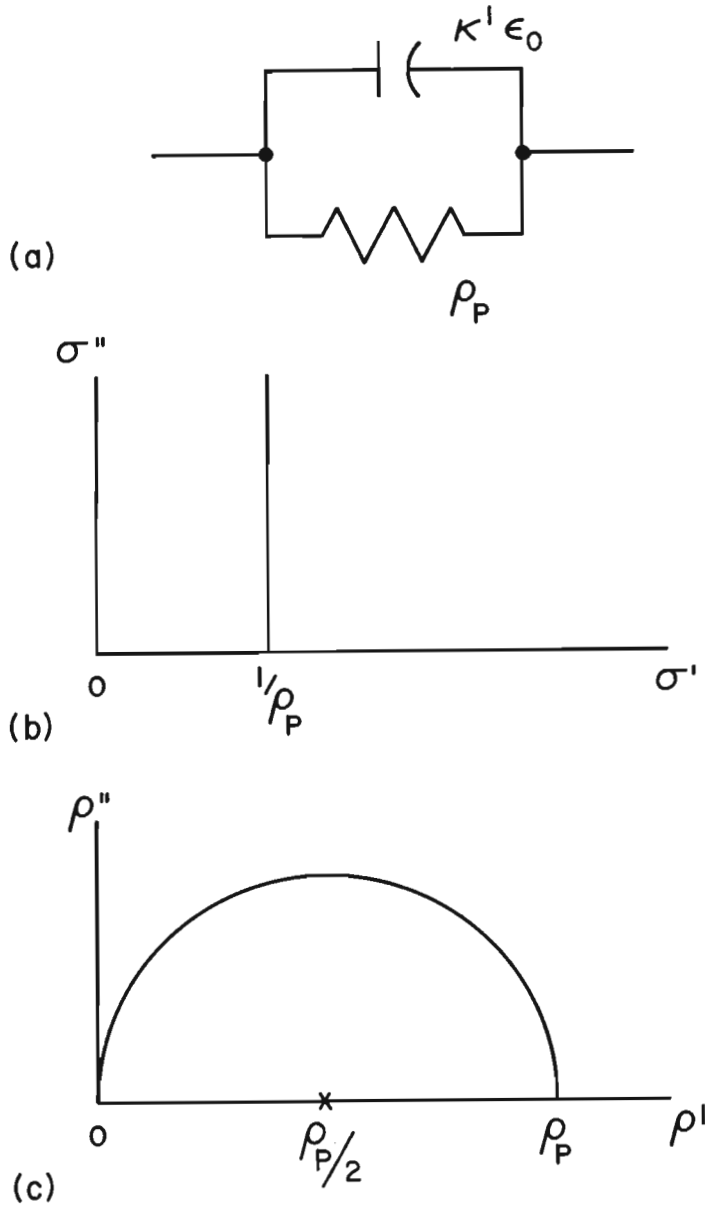

Figure 58.3. Theoretical plots of complex conductivity and complex resistivity for a parallel RC circuit, which the resistance and capacitance are ρ_p and $K'\varepsilon_o$, respectively.

Cole-Cole plots (complex permittivity, complex conductivity and complex resistivity plots) are useful for analyzing and observing various electrical phenomena in dry (Saint Amant and Strangway, 1970; Olhoeft *et al.*, 1973) and moist rocks (Zonge, 1972; Katsube and Collett, 1974). Electrical parameters, when plotted, as Cole-Cole plots, appear as a series of circular arcs, and each of these arcs are due to a particular electrical mechanism. A complex resistivity plot which shows an arc due to the electrode polarization mechanism is seen in Figure 58.1 (Zonge, 1972). Two circular arcs which are due to dielectric and perhaps membrane polarization mechanisms are presented in Figure 58.2 (Katsube and Collett, 1974). These complex resistivity plots can be used to analyze the electrical rock property data and obtain information on the electrical mechanism of rocks. It is also clear, as will be shown in the following section, that the results of the data analysis can be used to represent the electrical characteristics of rocks.

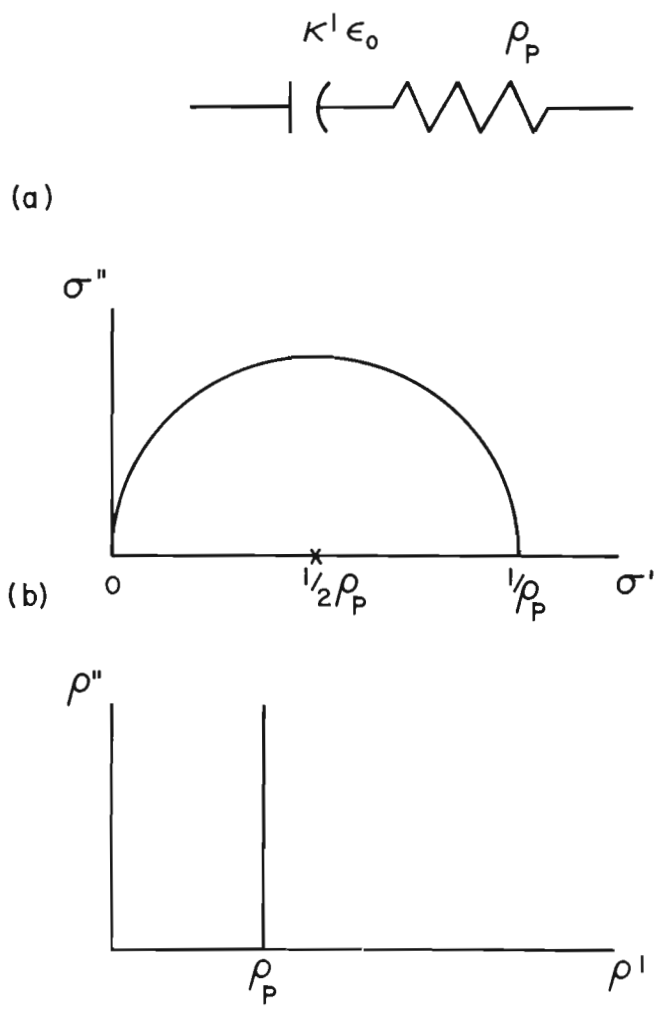

Figure 58.4. Theoretical plots of complex conductivity and complex resistivity for a series RC circuit, which the resistance and capacitance are ρ_p and $K'\varepsilon_o$, respectively.

Theory

The paper by Cole and Cole (1941) gives a good introduction to the theory behind the complex permittivity plots. Bauerle (1969) has published a useful paper as an introduction to complex conductivity plots. The theory behind these complex plots can also be applied to complex resistivity plots.

For a parallel RC circuit where the resistivity and permittivity are ρ_p and $K'\varepsilon_o$, respectively (Fig. 58.3a), the real and imaginary conductivity are:

$$\begin{cases} \sigma' = 1/\rho_p \\ \sigma'' = \omega K'\varepsilon_o \end{cases} \quad (1)$$

K' : real relative permittivity
ε_o : permittivity of air or vacuum (8.854×10^{-12} F/m)
ω : angular frequency

Thus, the complex conductivity plot of this circuit is a straight line (Fig. 58.3b). The real and imaginary resistivity (ρ', ρ'') of the same circuit are expressed by:

$$\begin{cases} \rho' = \dfrac{\rho_p}{1 + (\omega\tau)^2} \\ \rho'' = \dfrac{\omega\rho_p\tau}{+ (\omega\tau)^2} \end{cases} \qquad (2)$$

where τ is the time constant:

$$\tau = \kappa'\varepsilon_o\rho_p \qquad (3)$$

From Equation 2 the following is obtained:

$$(\rho' - \rho_p/2)^2 + \rho''^2 = (\rho_p/2)^2 \qquad (4)$$

Since $\rho'' > o$, Equation 4 describes a semi-circular arc with the diameter and centre co-ordinates being ρ_p and $(\rho_p/2, 0)$, respectively (Fig. 58.3c).

Similarly, the complex conductivity and complex resistivity plots for a series RC circuit, where the resistivity and permittivity are ρ_p and $\kappa'\varepsilon_o'$ are shown in Figure 58.4. Complex permittivity plots are discussed in many other publications, thus will not be discussed here. The advantages and disadvantages of the Cole-Cole or complex plots vary according to the plane they are plotted in. This implies that the selection of the complex plane for plotting the diagram is a crucial point in data analysis. It has been found that complex resistivity plots are usually most convenient for analysis of the electrical measurements of moist rocks.

The real and imaginary resistivity of a multiple type of parallel RC circuit (Fig. 58.5a) is,

$$\begin{cases} \rho' = \sum_{i=1}^{n} \dfrac{\rho_{pi}}{1 + (\omega\tau_i)^2} \\ \rho'' = \sum_{i=1}^{n} \dfrac{\rho_{pi}\tau_i}{1 + (\omega\tau_i)^2} \end{cases} \qquad (5)$$

where

$$\tau_i = \rho_{pi}\kappa_i'\varepsilon_o$$

In this case it is assumed that,

$$\tau_1 << \tau_2 << \tau_3 \ldots\ldots\ldots << \tau_{n-1} << \tau_n \qquad (6)$$

The complex resistivity plot for Equation 5 is shown in Figure 58.5b. It is important to note that the circular arcs appear from left to right in the same order as the

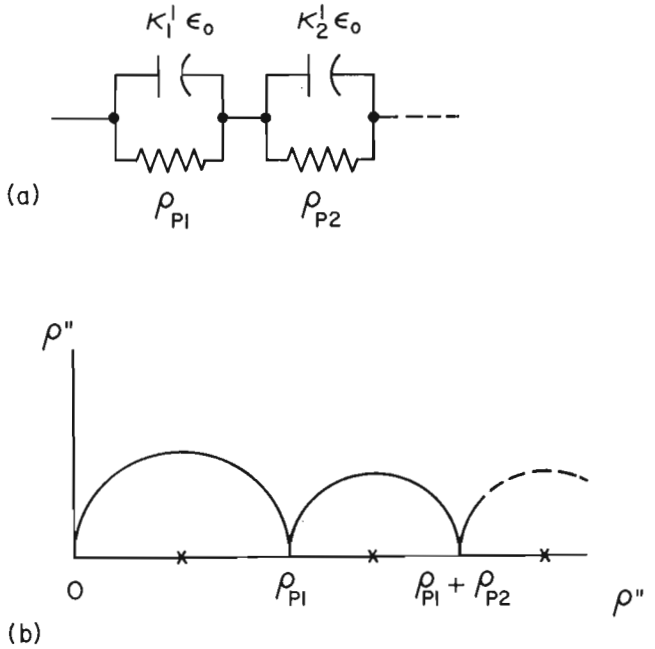

Figure 58.5. Theoretical plots of complex resistivity for a multiple type of RC parallel circuit.

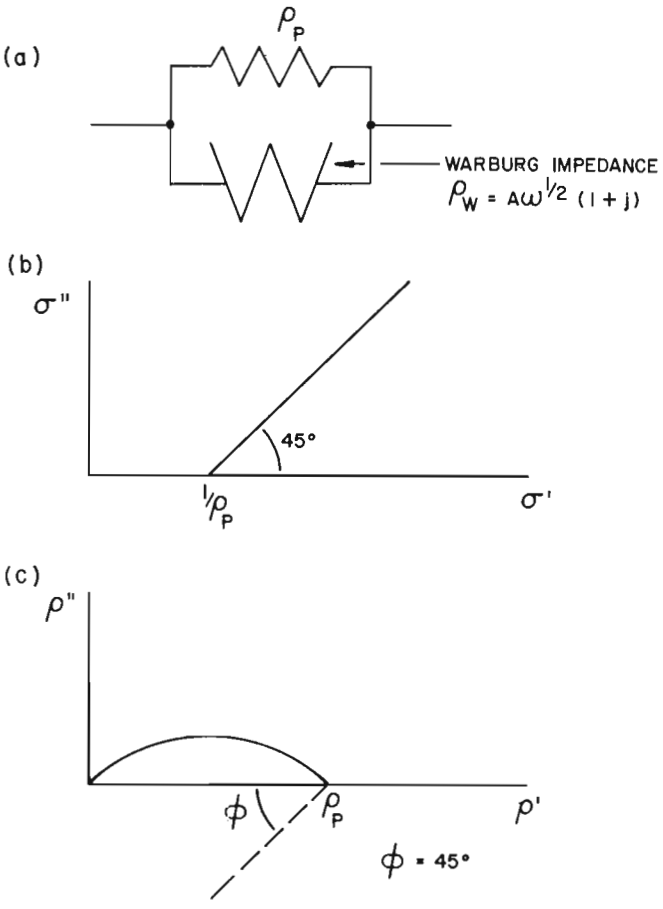

Figure 58.6. Theoretical plots of complex conductivity and complex resistivity for a circuit containing a Warburg Impedance.

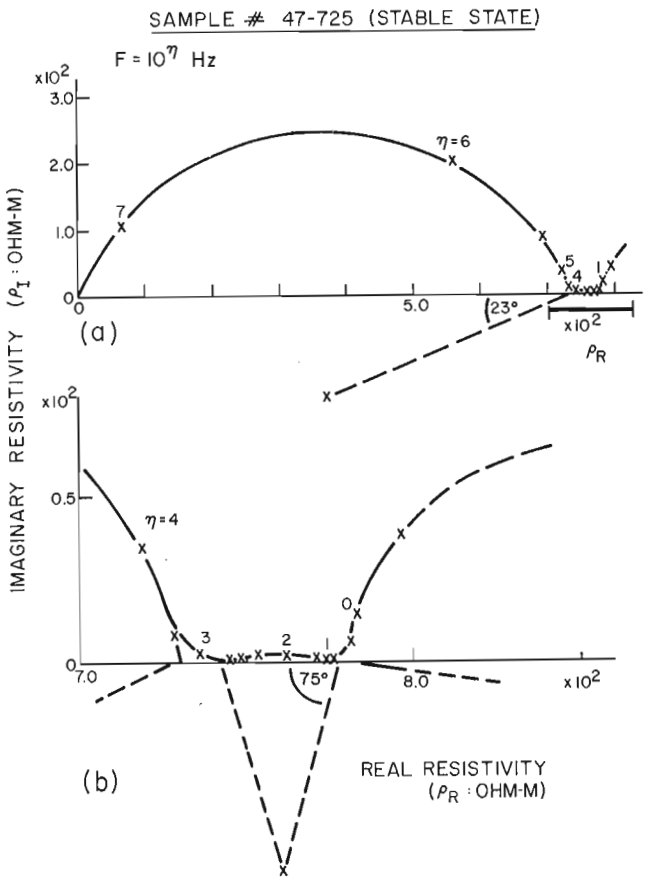

Figure 58.7. Complex resistivity plot for a serpentinite sample (No. 47-725), with electrode effects eliminated. Measurements were taken several days after the sample was vacuum saturated.

(a) plot for the resistivity range of ρ_R = 0-8.0 x 10^2 ohm-m

(b) detailed plot for ρ_R = 700-800 ohm-m range

ρ_R : real resistivity (=ρ')

ρ_I : imaginary resistivity (=ρ'')

magnitude of their time constants. This rule on the "order of circular arcs and their time constants" shall be referred to as "Rule A". In the paper by Bauerle (1969, Fig. 7), an example of a multiple arc type plot can be found, where n=3 (the capacitance C_3 is considered to be zero).

In actual measurements, it is very seldom that the centre of the circular arc in a complex diagram is located on the horizontal axis, as shown in Figures 58.3 to 58.5. Usually it appears below the horizontal axis, as shown in Figures 58.1 and 58.2. This is referred to as a "distributed type of circular arc". Many types of circuits can produce this type of arc. Some examples using Warburg Impedances are shown in the paper by Bauerle (1969). The Warburg Impedance ρ_W is expressed by:

$$1/\rho_W = A\omega^{\frac{1}{2}} + jA\omega^{\frac{1}{2}} \qquad (7)$$

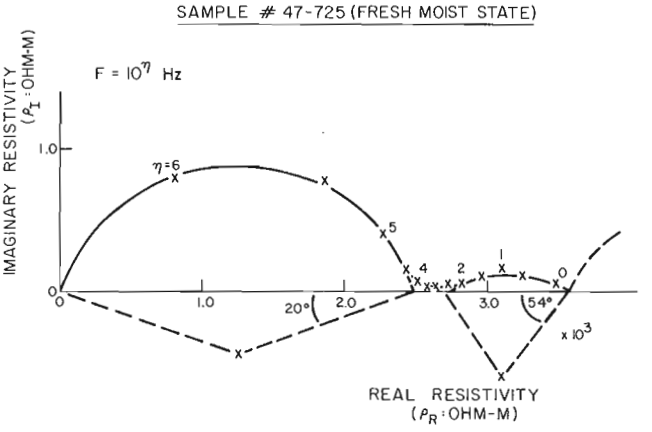

Figure 58.8. Complex resistivity plot for a serpentinite sample (No. 47-725), with electrode effects eliminated. Measurements were taken soon after the sample was vacuum saturated.

Therefore, the following expression is obtained for a circuit where a resistor and Warburg Impedance are in parallel (Fig. 58.6a):

$$(\rho' - \rho_p/2)^2 + (\rho'' + \rho_{p/2})^2 = (\rho_{p/2})^2 \qquad (8)$$

Equation 8 represents a distributed type of circular arc in the complex resistivity plane (Fig. 58.6c). The angle ϕ in this figure is the "distribution angle". Multiple type of parallel RC circuits can also produce a distributed type of circular arc, if the difference between the consecutive time constants is small. This subject will be discussed in further detail in a later paper. The expression generally used for this type of distributed circuit is the Cole-Cole frequency distribution equation which is an extended version of the Debye Single Relaxation equation (Cole and Cole, 1941):

$$\kappa^* = \kappa' - j\kappa'' = \kappa_\infty + \frac{\kappa_0 - \kappa_\infty}{1 + (j\omega\tau)^{1-\alpha}} \qquad (9)$$

F

where,

κ^* : complex relative permittivity

κ'' : imaginary relative permittivity

κ'_∞ : high frequency relative permittivity

κ_0' : low frequency relative permittivity

τ : time constant

α : distribution constant

The relation between the distribution constant (α) and distribution angle (ϕ) is:

$$\phi = \frac{\alpha\pi}{2} \qquad (10)$$

This relaxation equation expresses the state of transition from $\kappa^* = \kappa_0$ at the lower frequencies to $\kappa^* = \kappa'_\infty$

at the higher frequencies. The constant α controls the rate at which the transition takes place (Olhoeft *et al.*, 1973). This equation has a wide application, and it can be used to express a transition which takes place in the frequency spectrum of resistivity, where $\rho^* = \rho_o$ at the lower frequencies and $\rho^* = \rho_\infty$ at the higher frequencies:

$$\rho^* = \rho' - j\rho'' = \rho_\infty + \frac{\rho_o - \rho_\infty}{1 + (j\omega\tau)^{1-\alpha}} \qquad (11)$$

ρ_∞ : high frequency resistivity
ρ_o : low frequency resistivity

When a number of distributed type of circular arcs is seen on a complex plot, a multiple type of Cole-Cole frequency distribution equation is required to express them. Olhoeft (1975b) uses:

$$\kappa^* = \kappa' - j\kappa'' = \kappa'_1 + \sum_{i=1}^{n} \frac{\kappa_{i-1} - \kappa'_i}{1 + (j\omega\tau_i)^{1-\alpha}} \qquad (12)$$

for expressing arcs which appear in the complex permittivity plots. Similarly, the expression:

$$\rho^* = \rho' - j\rho'' = \rho_i + \sum_{i=1}^{n} \frac{\rho_{i-1} - \rho_i}{1 + (j\omega\tau_i)^{1-\alpha}} \qquad (13)$$

can be used for the multiple type of distributed arcs in the complex resistivity plots. The same "Rule A" will apply when determining the order in which the distributed type of arcs appear in the complex diagrams.

It is well known that rocks show both ohmic and dielectric phenomena, so that there is little doubt about the adequacy of using RC parallel equivalent circuits as an electrical model for rocks. Distributed types of circular arcs, however, usually show better fits to the measurements, compared to the circular arcs based on a single parallel RC circuit. From initial observations, it seems that this is related to the fact that rocks consist of various types of minerals. If a rock sample consists of a pure single mineral, it seems that the distribution angle is small. On the other hand, if the rock consists of various types of minerals with various dielectric constants and resistivities, it seems that the time constants are of the distributed type, and thus cause the distribution angle to be large. It is known that a Warburg Impedance can develop along the pores of the rock, and this can also be a cause of the distributed type of circular arcs. There is still much knowledge to be gained on the effect of the various types of minerals and textures on the electrical characteristics.

The reason for multiple types of circular arcs to appear in the complex plots of actual measurement can be explained. A good example of it is a moist sample clamped between two electrodes. The rock sample and the electrode surfaces are two completely different electrical mechanisms, of which each of them can be simulated by a RC parallel circuit. Since the sample and electrode surfaces are connected the equivalent circuit of the combination is two parallel RC circuits in series. The capacities and resistance of the sample and electrodes are usually in the order of 3 pico-farads and 50 ohms, and 100 micro-farads and 10^4 ohms, respectively, in which case the time constants are 150 pico seconds and 1.0 seconds, respectively. This indicates a large difference in the time constants of the sample and electrodes and thus fits the conditions for the model expressed by Equations 5 and 6. Thus, the resulting complex resistivity plot will show two consecutive arcs.

Sample Preparation, Instrumentation

Three serpentinite samples supplied by AMAX Exploration Inc. (No. 47-725, No. 38-1000, No. 8-402) have been measured and studied in detail. A description of the samples is given in Table 58.1. The samples are cut into discs of 2.54 cm in diameter and 0.5 cm thick. They are vacuum saturated with fresh water (from the Ottawa River), and left in that water for at least two days before measurement. The resistivity of the sample varies with time after being saturated, but reaches a steady state, usually after 48 hours. Both two and four electrode sample holders have been used in the measurement. Details of these sample holders are being compiled in a separate paper. The main electronic measuring system used for these measurements is the Automatic Measuring System described by Gauvreau and Katsube (1975).

Table 58.1

Description of samples

Sample Number	Type	Magnetite	Pyrite
8-402	Light green serpentinite	5%	1%
38-1000	Grey, hematite stained talc-rich serpentinite	Minor	-
47-725	Grey to green serpentinite	Minor	-

Results

Cole-Cole diagrams of measurements for two serpentinite samples are shown in Figures 58.7 to 58.11. Figure 58.7a depicts the result of a serpentinite sample (No. 47-725) with the sample holder electrode effects eliminated. After being vacuum saturated, this sample has been left in water for several days before measurement. The large circular arc on the left hand side is

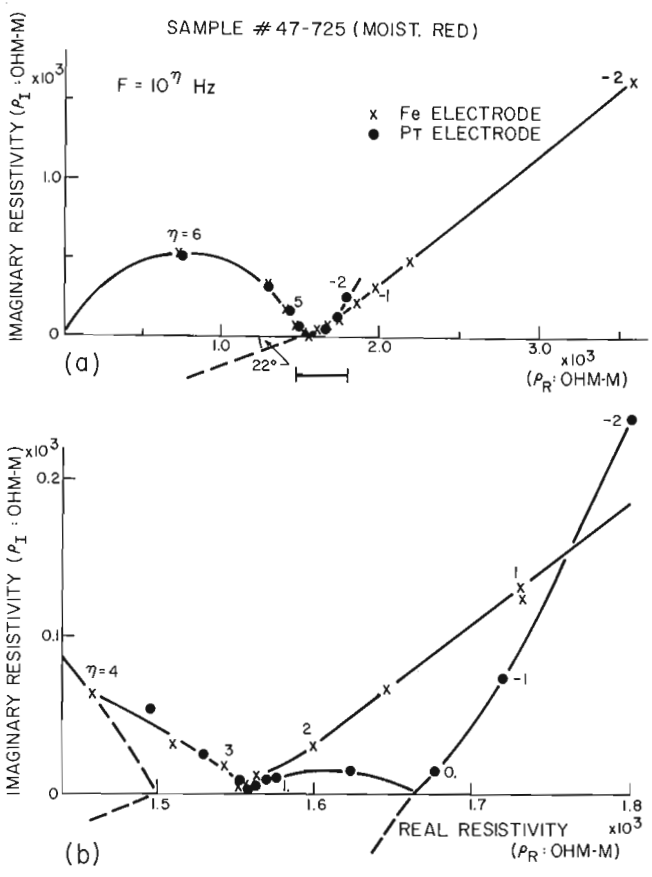

Figure 58.9. Complex resistivity plot of a serpentinite sample (No. 47-725), with stainless-steel and platinized-platinum electrode effects present. Measurements were taken several days after the sample was vacuum saturated. A certain amount of water has evaporated.

(a) measurement results for ρ_R = 0-3.5 x 10^3 ohm-m

(b) detailed measurements for ρ_R = 1.4-1.8 x 10^3 ohm-m

due to the dielectric polarization, similar to the results shown in Figure 58.2. The rise of ρ_I (same as ρ'') with increase of ρ_R (same as ρ') at the right hand side in Figure 58.7a is perhaps part of another circular arc which is due to electrode polarization of the magnetite. Note the region between ρ_R = 700-800 ohms where the curve of ρ_I is almost flat. Detailed measurements of that region are shown in Figure 58.7b on an expanded scale. Between the two large circular arcs, an intermediate circular arc which has a very large distribution angle can be seen.

Measurements of the same serpentinite sample (No. 47-725) was taken soon after it was vacuum saturated, and thus the resistivity was still changing with time (Fig. 58.8). At this stage the values of ρ_R were much higher than those shown in Figure 58.7. It can be seen that there exist two distinct circular arcs.

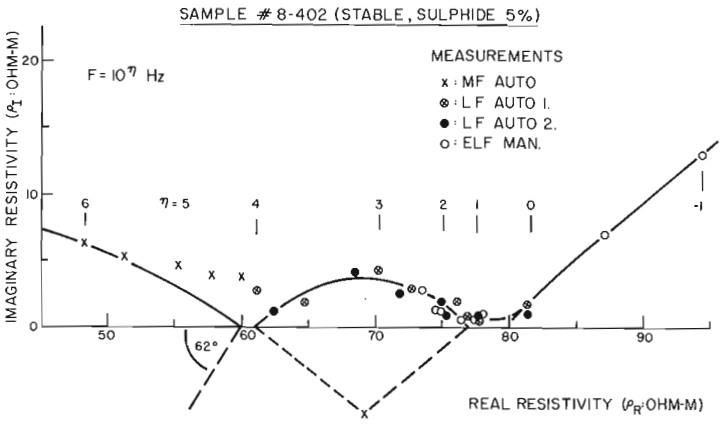

Figure 58.10. Complex resistivity plots for a serpentinite sample (No. 8-402), with electrode effects eliminated. Measurements were taken several days after the sample was vacuum saturated.

MF : Medium frequency
LF : Low frequency
ELF : Extremely low frequency
AUTO : Automatic measuring system
MAN : Manual measuring system

The arc on the left hand side is due to dielectric polarization, and the one on the right hand side is perhaps equivalent to the intermediate circular arc seen in Figure 58.7. It is interesting to note that the magnitude of this arc shrinks, and the distribution angle increases as time passes, after vacuum saturation.

Figure 58.9 depicts results of the same sample with sample holder electrode effects present. These measurements were taken after the sample had reached a steady state, but the resistivity had increased due to some loss of moisture. Note the difference between the effects of the platinized-platinum and stainless-steel electrodes. The region in Figure 58.9a where ρ_R = 1500-1800 ohms has been enlarged and shown in Figure 58.9b. It can be seen that the intermediate circular arc which was visible in Figure 58.7b is also visible in Figure 58.9b when platinized-platinum electrodes are used, but is masked when stainless-steel electrodes are used. Based on Rule A, it is suggested that the time constant of the intermediate arc is shorter than that of the platinized-platinum electrode, but is longer than that of the stainless-steel electrodes.

Figure 58.10 depicts the results (electrode effect eliminated) of another serpentinite sample (No. 8-402), which contains sulphide minerals (Table 58.1). The parts of the circular arcs on the left and right hand side are due to the dielectric polarization, and electrode polarization of sulphide minerals, respectively. The existence of the intermediate circular arc is quite evident in this case. Figure 58.11 depicts the result (electrode effect eliminated) of a serpentinite sample (No. 38-1000) which contains a minor amount of magnetite (Table 58.1). The part of the arc on the left hand

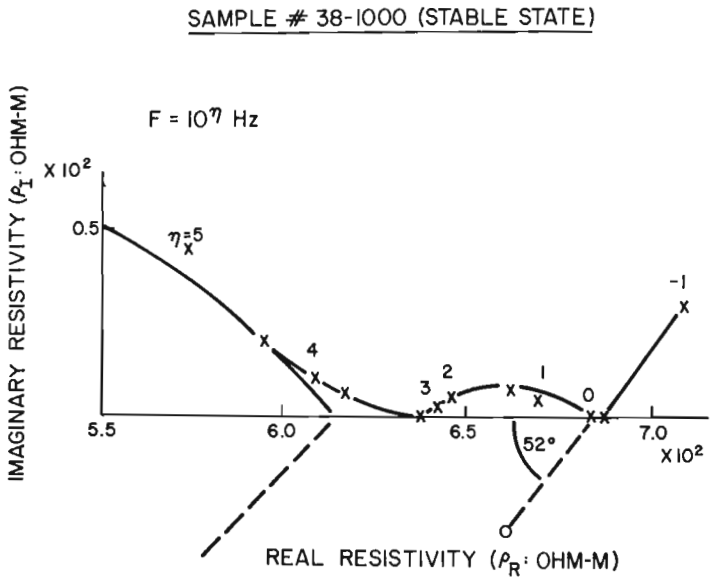

Figure 58.11. Complex resistivity plot for serpentinite sample (No. 38-1000), with electrode effects eliminated. Measurements were taken several days after the sample was vacuum saturated.

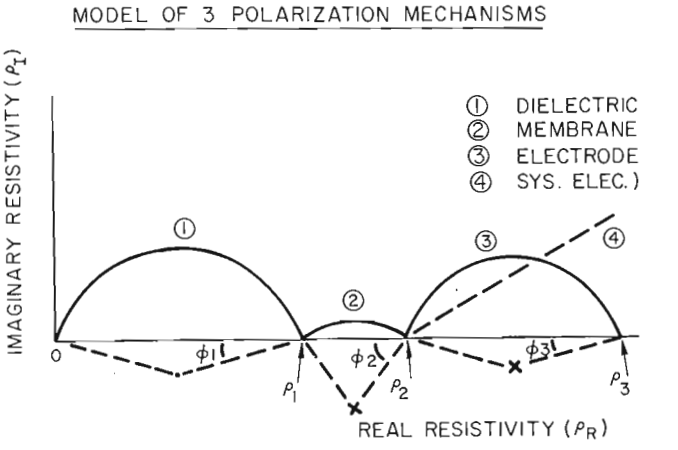

Figure 58.12. Complex resistivity plot of the "Three Electrical Polarization Mechanism Model", for moist rocks.
1) Dielectric polarization mechanism of rocks.
2) Membrane polarization mechanism of rocks.
3) Electrode polarization mechanism of conductive minerals in rocks.
4) Systems electrode polarization mechanism.

side is due to the dielectric polarization, and the rise of ρ_I with increase of ρ_R at the right hand size is part of the circular arc which is due to the electrode polarization. The existence of the immediate circular arc is quite evident.

Discussion

It is thought that sufficient evidence can be seen in the past work to prove the existence of two electrical mechanisms: dielectric and electrode polarization mechanisms. Results in this paper show evidence of the existence of an intermediate circular arc which is due to a third mechanism. It is possible that this third mechanism is the membrane polarization mechanism which Marshall and Madden (1959) suggested, but no clear evidence of it had been shown in the past.

Olhoeft (1975a) suggests that more than three electrical mechanisms are present in moist rocks. The data in this paper which shows the three circular arcs, suggests that the electrical mechanisms in moist rocks may be divided into three groups of electrical mechanisms.

Rule A, regarding the time constant and the order of the arcs in the complex plots, is very important and should be taken into consideration in the interpretation of field IP data and development of new electrical methods, especially for mineral exploration. Little is known about the cause of the distribution characteristics of the circular arcs. Much study is required on this subject.

Considering all the foregoing discussions, it is thought important to introduce a "Three Electrical Polarization Mechanism Model" (Fig. 58.12) as a basis for the analysis of electrical rocks property data. It is proposed that the resistivities, ρ_1, ρ_2 and ρ_3; the frequencies that these resistivities have determined; f_1, f_2 and f_3; and the distribution angles, ϕ_1, ϕ_2 and ϕ_3, be determined to represent the electrical characteristics of a sample.

The relationship between these resistivities and those in Figure 58.5 are:

$$\begin{cases} \rho_{p1} = \rho_1 \\ \rho_{p2} = \rho_2 - \rho_1 \\ \rho_{p3} = \rho_3 - \rho_2 \end{cases}$$

The proposed parameters are based on the "Three Electrical Polarization Mechanism Model". Thus, it is expected that the use of it to make correlations with geological features of the rock will produce more distinct results, as compared to the use of resistivity or permittivity values taken from any part of the frequency spectrum, as has been the practice in the past.

Conclusion

Based on experimental data and a number of discussions, a "Three Electrical Polarization Mechanism Model" for moist rocks is proposed. It forms a basis for the analysis of electrical rock property data. It is suggested that complex resistivity plots be used as a

technique for analysis, and that resistivity and frequency at the points that the arcs intercept the horizontal axis, and the distribution angle for each of the three arcs be determined. It is believed that dielectric, membrane and electrode polarization mechanisms form the background of the "Three Electrical Polarization Mechanism Model", but there is a lack of knowledge on the membrane polarization mechanism. The background assumptions imply that if a rock lacks one of the electrical mechanisms: for example the electrode polarization mechanism, only two circular arcs will appear in the complex resistivity plot.

Though the data used as evidence for the proposed model is still limited, it is thought that there is sufficient evidence to suggest that this study should be continued. The "Time Constant Rule" (Rule A), regarding the relation between time constants and the order in which the arcs appear in the complex resistivity plots, is significant. It forms a basis for understanding the polarization phenomena in rocks, particularly in connection with the IP phenomena.

Acknowledgments

Thanks are expressed to AMAX Exploration Inc. for supplying the serpentinite samples. Great appreciation is expressed to Mr. L. S. Collett for his general guidance and understanding of this work, and for making it possible to facilitate the laboratory with the Automatic Measuring System. Many thanks are expressed to Mr. C. Gauvreau for setting up the Automatic Measuring System. Gratitude is also expressed to Mr. J. Frechette for many of the measurements and for the maintenance of the laboratory equipment. Thanks are also expressed to Mr. R. J. Sloka for his aid in the measurements. Mrs. R.R. Morra drafted the illustrations.

References

Bauerle, J. E.
1969: Study of solid electrolyte polarization by a complex admittance method; J. Phys. Chem. Solids, v. 30, p. 2657-2670.

Cole, K. S. and Cole, R. H.
1941: Dispersion and absorption in dielectrics: I. Alternating current characteristics; J. Chem. Phys., v. 9, p. 341-351.

Collett, L. S.
1959: Laboratory investigation of overvoltage; *in* Overvoltage Research and Geophysical Applications; London, Pergamon Press, p. 50-69.

Gauvreau, C. and Katsube, T. J.
1975: Automation in electrical rock property measurements; *in* Report of Activities, Part A, Geol. Surv. Can., Paper 75-1A, p. 83-86.

Katsube, T. J.
1974: Electrical characteristics and electrical mechanism of some ultramafic rocks. Presented at the Second Workshop on Electromagnetic Induction in the Earth. Ottawa, Ont., Aug. 22-28.

Katsube, T. J. (cont'd.)
1975a: The critical frequency and its effect on EM propagation; *in* Report of Activities, Part A, Geol. Surv. Can., Paper 75-1A, p. 101-105.

1975b: Electrical properties of serpentinites. Presented at "Waterloo '75", Waterloo, Ontario, May 15-17.

Katsube, T. J. and Collett, L. S.
1972: Electrical and EM propagation characteristics of igneous rocks. Presented at the 42nd Annual International meeting of the Society of Exploration Geophysicists. Anaheim, Calif., Nov. 26-30.

1973: Electrical characteristics of rocks and their application to planetary and terrestrial EM sounding; Proc. Fourth Lunar Sci. Conference, Supplement 4, Geophysica et Cosmochemica Acta, Pergamon Press, v. 3, p. 3111-3131.

1974: Electromagnetic propagation characteristics of rocks. Presented at NATO Advanced Study Institute of Petrophysics, Newcastle upon Tyne, England, Apr. 23 (Submitted to be published in "The Physics and Chemistry of Rocks and Minerals", John Wiley and Sons Ltd.).

Keller, G. V. and Licastro, P. H.
1959: Dielectric constant and electrical resistivity of natural-state cores; U. S. Geol. Surv., Bull. 1053H, p. 257-285.

Marshall, D. J. and Madden, T. R.
1959: Induced polarization, a study of its causes; Geophysics, v. 24, p. 790-816.

Olhoeft, G. R.
1975a: The role of water in the electrical properties of rocks; Presented at "Waterloo '75", Waterloo, Ontario, May 15-17.

1975b: The electrical properties of permafrost; Ph. D. thesis, University of Toronto.

Olhoeft, G. R., Strangway, D. W., and Frisillo, A. L.
1973: Lunar sample electrical properties; Proc. Fourth Lunar Sci. Conference, v. 3, p. 3133-3149.

Saint-Amant, M. and Strangway, D. W.
1970: Dielectric properties of dry, geologic materials; Geophysics, v. 35, p. 624-645.

Zonge, K. L.
1972: *In situ* mineral discrimination using a complex resistivity method. Presented at the 42nd Annual International Meeting of the Society of Exploration Geophysicists, Anaheim, Calif., Nov. 26-30.

Project 750028

J. L. Davis
Resource Geophysics and Geochemistry Division

Introduction

A non-destructive method of measuring the near surface soil moisture content is of prime importance to agriculturalists and foresters for crop yield optimization. Hydrologists are interested in soil moisture measurements for predicting runoff. Meteorologists are interested in monitoring the soil moisture over extended areas to help obtain the relationship between mass and energy exchange at the air-soil interface. For the gamma ray spectrometer surveys, knowledge of soil moisture and its attenuating effect on radiation is important in the interpretation of the survey data. The engineering geologist is interested in soil moisture for structural and engineering projects, natural hazard prediction and trafficability of terrain.

The Electrical Methods Section of the Geological Survey of Canada is studying techniques for measuring the relative permittivity* at high radio frequencies of geologic material *in situ*. Changes of relative permittivity in the ground may be caused by changes of material, moisture, temperature, density and frequency. At frequencies between 1 and 1000 MHz at 20°C, the relative permittivity of water is 80 compared to a relative permittivity of less than 10 for most geologic materials (Von Hippel, 1954). It has been found that the variable causing the most significant changes of relative permittivity in geologic materials is the moisture content. Preliminary laboratory experiments indicate that there is a good correlation between relative permittivity and volumetric soil moisture content at frequencies between 10 and 1000 MHz. Changes of less than 10 per cent in relative permittivity were due to soil type and density at moisture contents greater than 1 kg of H_2O per m^3 of soil (10 per cent by volume). The relative permittivity increased by 15 per cent in a clay soil with a moisture content of 400 kg of H_2O per m^3 of soil as the temperature was increased from +1°C to +40°C. Further laboratory experiments with better control are required but at present it appears that the high frequency relative permittivity is a good measure of volumetric soil moisture content.

The most reliable method of measuring soil moisture at present is to physically remove samples of soil and measure the water content in the laboratory. This technique is time consuming, tedious and destructive. A contacting technique for measuring the relative permittivity of soils and thus soil moisture, is being developed by the Electrical Methods Section of the Geological Survey of Canada in co-operation with the Communication Research Centre, Department of Communications, and the Soils Research Institute, Agriculture Canada. The method uses a wide-band time-domain reflectometer (TDR) and a balanced parallel transmission line inserted vertically into the

*Relative permittivity is used in place of dielectric constant in this paper.

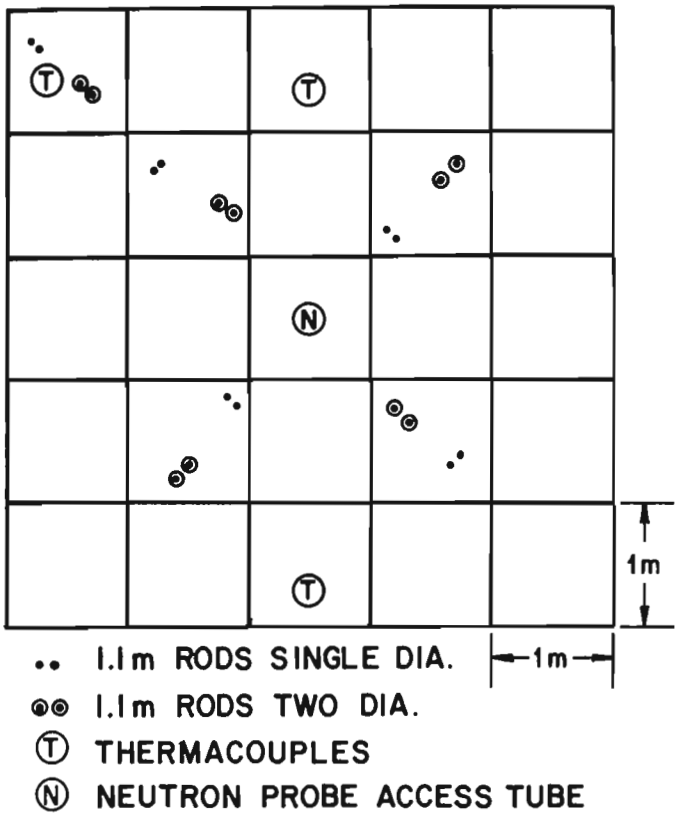

Figure 59.1. Plan of each plot.

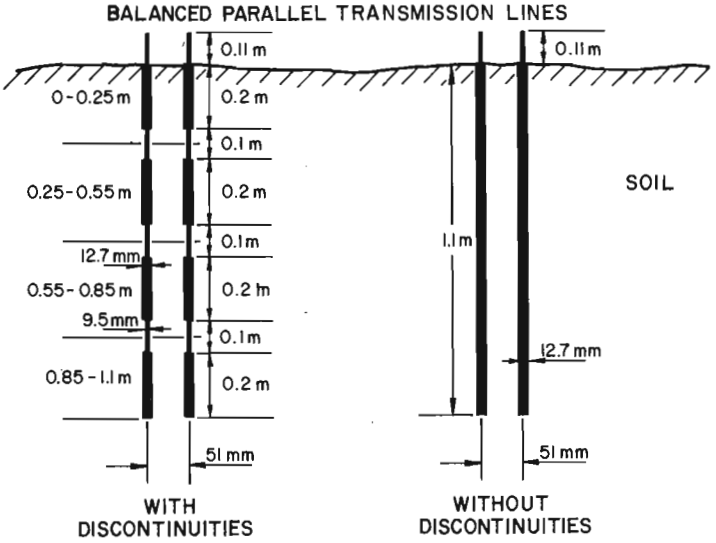

Figure 59.2. Balanced parallel transmission lines.

soil. The transmission lines are left in the soil permanently and measurements are made periodically. The techniques and principles of operation are outlined by Davis and Chudobiak (1975). This paper describes the procedure and some initial results of an experiment that has been going on during part of the winter, spring and summer months of 1974-1975.

Method

Two plots, one in a sand soil and one in a clay soil, have been chosen for the initial experiments. Both plots are located at the Caldwell site of the Central Experimental Farm, Ottawa. To obtain a better average value over a representative area at least four transmission lines are inserted in each plot. Figure 59.1 shows the plan of each plot. An area 5 by 5 m is staked off. Rods with and without discontinuities are placed in 4 of the 25 one metre squares. The dimensions of the balanced parallel transmission lines are shown in Figure 59.2.

To insert the rods of the transmission line in the soil, a pilot hole the same diameter as the rod is drilled. A slow speed drill, 375 RPM, and an auger bit on the end of either a 1 m or 2 m extension rod depending on the length of line to be inserted is used. A jig is used to align the spacing and direction of the holes. In both the sand and clay plots each transmission line was inserted in less than one half hour.

The lines with discontinuities enable measurements of the average relative permittivity to be made at various depths over the length of the line. Changes of the relative permittivity in the soil can be seen on the lines without discontinuities. These changes may be masked by the discontinuities inserted in the line. Figure 59.3 shows a record from the wide-band time-domain reflectometer on two-metre-long transmission lines with (b) and without (a) discontinuities in the sand plot. Table 59.1 shows the average relative permittivity with depth for these two transmission lines. The lower the level of the trace on the photographs the higher the relative permittivity. At this site a layer of sand about 0.85 m thick lies on clay. The sharp change in level at about 15 ns is due to the sand/clay interface. The first dip between 0 and 4 ns on both traces is due to 20 mm of rain that fell the previous night. The dip at 8 ns in Figure 59.3a is the wetting from the melting which occurred during late April. The slight change in slope at 15 ns on both photos may be due to a thin layer of sand just below the sand/clay interface. The reason the discontinuities and the open circuit of the transmission line are not large is because much of the energy is reflected at the air/sand and sand/clay interfaces.

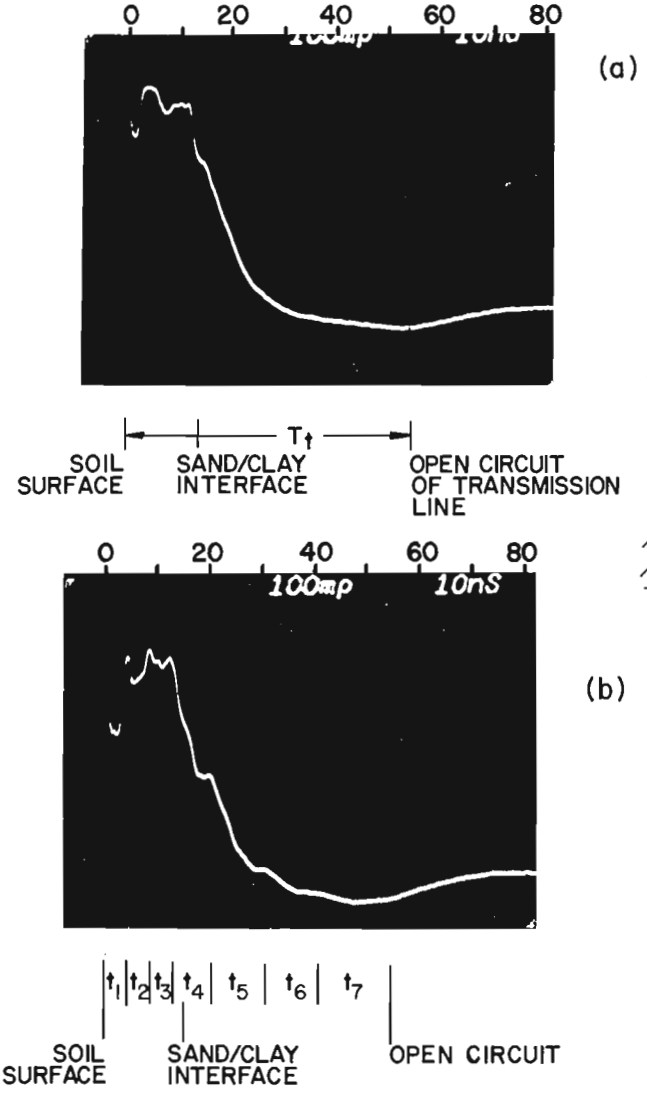

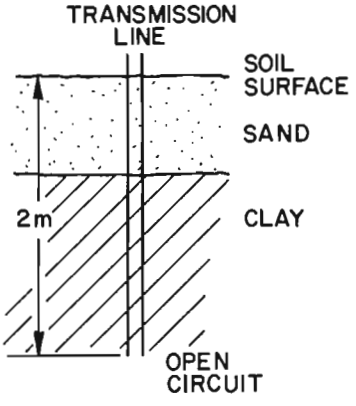

Figure 59.3. Wide-band time-domain reflectometer record along 2 m transmission line inserted in the sand plot.

a) without discontinuities
b) with discontinuities.

TABLE 59.1. Average relative permittivity with depth in sand plot

Length (m)	Depth (m)	Two way travel time t (ns)	Average relative permittivity ε_r
a) Transmission line without discontinuities			
ℓ_t = 2.0	0 – 2.0	t_1 = 57	ε_1 = 18.3
b) Transmission line with discontinuities			
ℓ_1 = 0.25	0 – 0.25	t_1 = 4.9	ε_1 = 8.6
ℓ_2 = 0.30	0.25 – 0.55	t_2 = 4.2	ε_2 = 4.4
ℓ_3 = 0.30	0.55 – 0.85	t_3 = 4.5	ε_3 = 5.1
ℓ_4 = 0.30	0.85 – 1.15	t_4 = 8.0	ε_4 = 16.0
ℓ_5 = 0.30	1.15 – 1.45	t_5 = 11.0	ε_5 = 30.0
ℓ_6 = 0.30	1.45 – 1.75	t_6 11.0	ε_6 30.0
ℓ_7 = 0.25	1.75 – 2.0	t_7 13.0	ε_7 61.0

Thermocouples were inserted at depths of 0, 0.05, 0.15, 0.4, 0.7, 0.95 and 1.5 m during May, 1975 to measure the ground temperature and to determine the effects on temperature caused by the metal rods in the soil. Below 0.15 m the difference in temperature caused by the rods is usually less than ± 1°C but at the soil surface the difference may be as much as ± 5°C. It is expected that during the winter the rods cool the ground significantly. The temperature differences due to the rods can be reduced if necessary by making the transmission line out of thin metal tubing and by keeping the top of the line below the soil surface.

Gravimetric soil moisture measurements were taken on the plots on the same days that the relative permittivity measurements were made. Initial comparison of the results show similar trends but soil density measurements at each plot are necessary before volumetric soil moisture values can be compared. The variability of the soil, though homogeneous to the eye, also complicates the comparison of values. The rate at which the moisture travels into the soil after a heavy rain varies between transmission line sites in the same soil type. Neutron probe and gamma meter measurements are also being made on the same plots. A rain gauge is located near both sites to help correlate the measurements with rainfall.

In non-magnetic materials the relative permittivity, ε_r, is determined by measuring the signal travel time, t, in a known length of transmission line, ℓ

$$\varepsilon_r = \left(\frac{ct}{\ell}^2\right)$$

where c = free space velocity, 3×10^8 m/s
t = travel time in seconds,
ℓ = length of transmission line in metres.

To determine relative permittivity from this equation the rods of the transmission line do not need to be absolutely parallel but the deviation should be small compared to the signal wavelength in the soil.

Discussion of Relative Permittivity Results

Figures 59.4a to f show the changes of relative permittivity and approximate volumetric soil moisture content with time from November, 1974 to June, 1975 and depth for the sand site and Figures 59.5a to d for the clay site. All the measured values are shown by a dot and the mean of the measured values are shown by a dot in a circle.

Figure 59.4a shows the relative permittivity measured from the surface to a 1.1 m depth in the sand plot. The decrease of relative permittivity during January is probably due to the soil freezing around the transmission lines. The sharp increase of relative permittivity in late April is due to the spring thaw and the smaller spikes on the 22nd of May and the 10th of June occur after heavy rain storms. Figure 59.5 shows the relative permittivity measured in the top 0.25 m on the sand site. The sharp and rapid changes correlate with rain storms and these effects are smoothed out with depth (Figs. 59.4c to f). The spread of measured values is due to the variability of the soil properties at each transmission line. In Figure 59.4d for a 0.55-0.85 m depth, the large increase around mid-April is probably due to the meltwater reaching the sand/clay interface, which is located between 0.80 and 1.0 m depth. Since the clay is less permeable than sand there is a buildup of water at the interface. The large spread of measured values in Figure 59.4e is due to different depths to the sand/clay interface at each of the transmission lines. Figure 59.4f shows the data from one transmission line between 1.15 and 2.0 m all in the clay.

Figure 59.5a shows the measured values of relative permittivity over the top 1.1 m on the clay plot. The snow melted on the clay plot about five days after the snow had melted on the sand plot. The changes of relative permittivity correlate well in the top 0.25 m

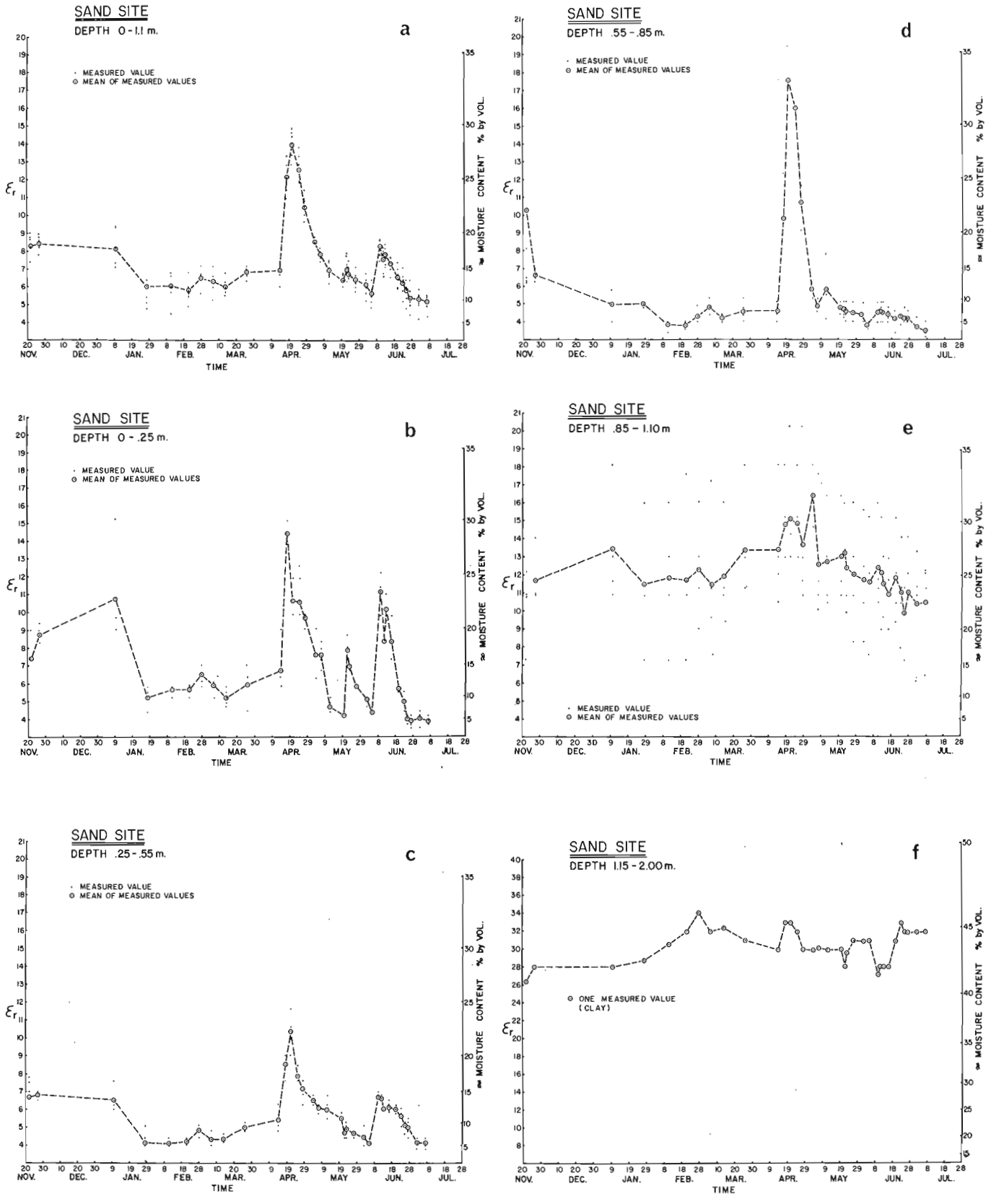

Figure 59. 4. Relative permittivity and per cent (by volume) moisture content in sand site with time.

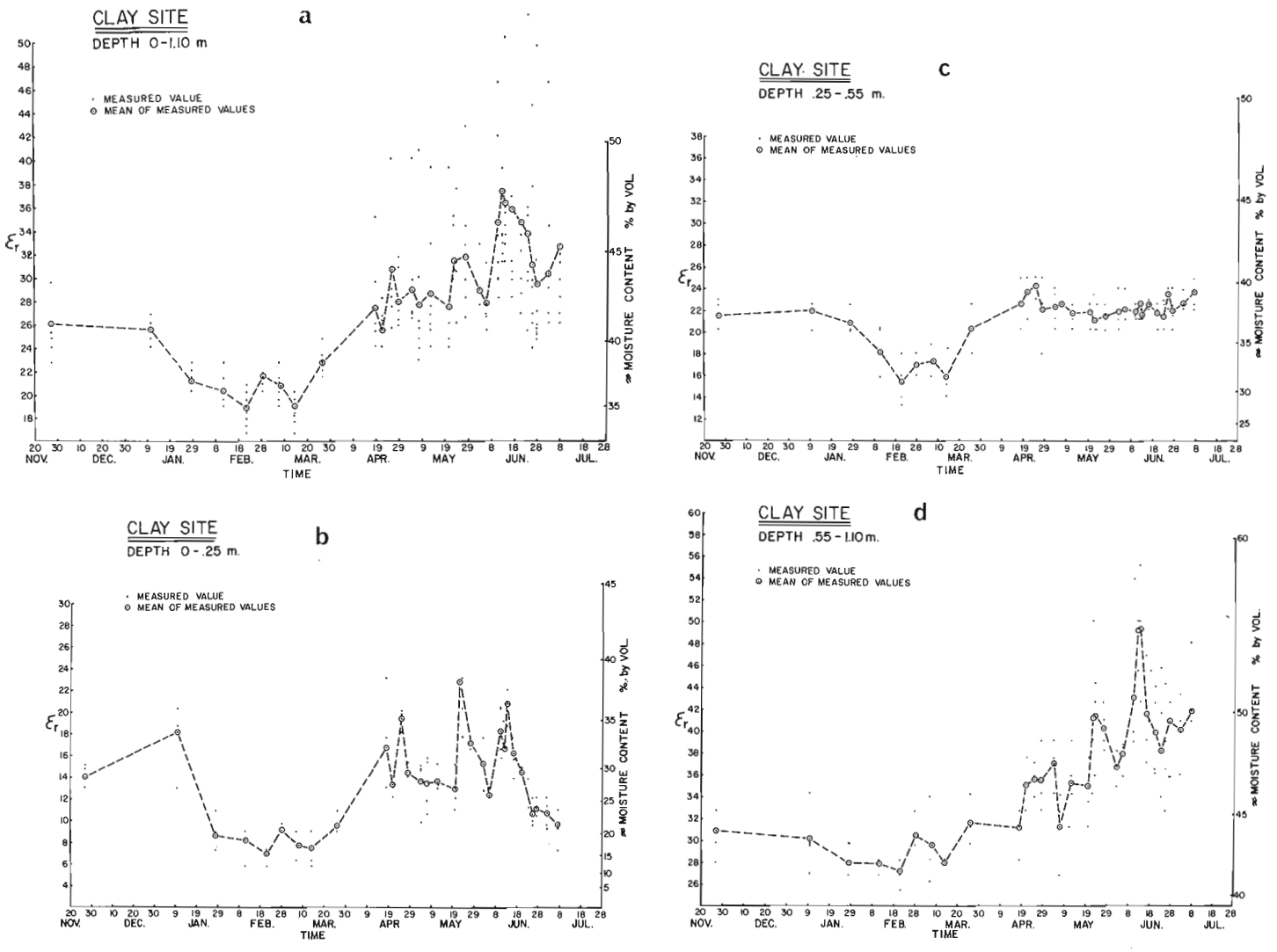

Figure 59.5. Relative permittivity and per cent (by volume) moisture content in clay site with time.

with rainfall (Fig. 59.5b). As the depth in the clay section increases (Figs. 59.5c and d), the changes or lack of changes are not clearly understood at present. It seems that at this clay location the change of moisture in the top 0.25 m is due to surface changes and that below about 0.5 m the change of moisture is due to the varying level of the water table.

Conclusions

The field results shown are an encouraging indication that balanced parallel transmission lines and wide-band time-domain reflectometer is a useful technique to measure soil moisture. It is still necessary to determine the accuracy that one can estimate volumetric soil moisture content from measurements of relative permittivity. With the basic information gained from the field measurements using this contacting technique and from the future laboratory experiments, it is hoped that the details for a non-contacting soil moisture measuring instrument can be specified.

Acknowledgments

I wish to thank Dr. G.C. Topp and W. Zebchuck of the Soil Research Institute, Agriculture Canada, for their helpful suggestions and practical assistance in setting this experiment up. I wish to thank P. Zinghnesse of Communications Research Centre, Department of Communications, for his help in inserting the rods in the ground in late November. I also wish to thank J. Frechette of the Geological Survey of Canada for making the measurements during March under some of the coldest and most miserable conditions.

References

Davis, J.L. and Chudobiak, W.J.
1975: *In situ* meter for measuring relative permittivity of soils; *in* Report of Activities, Part A, Geol. Surv. Can., Paper 75-1A, p. 75-79.

Von Hippel, A.R. (ed),
1954: Dielectric materials and applications; The M.I.T. Press, Cambridge, Massachusetts, 438 p.

60. THE GEOLOGY OF THE HACKETT-BACK RIVER GREENSTONE BELT – PRELIMINARY ACCOUNT

Project 75009

R.A. Frith and J.D. Hill
Regional and Economic Geology Division

Introduction

The area within the heavy lines of Figure 60.1 were mapped during the 1975 field season to (a) extend the known greenstone belt boundaries recently mapped at a scale of 2 inches to the mile by Padgham *et al.* (1974a, 1974b, 1974c, 1974d and 1974e) and at a larger scale by Fraser (1964), Wright (1957) and Tremblay (1971), (b) to study the deformation and metamorphic history of the area and (c) to study the granitic bodies that intrude the supracrustal rocks of the area. This report deals with the more important stratigraphic and economic aspects of the season's work and is based solely on field observations.

"Basement" Gneisses (Unit 1)

In the Hackett River map-area (Fig. 60.1) the sedimentary unit that surrounds the granitic gneiss contains a quartz pebble paraconglomerate, that in places contains large (up to 2 m), rounded blocks of granitic gneiss of dioritic composition. A probable source is the dioritic rock that forms a marginal phase of the Hackett River "diapir". The bulk of the body is aplitic or pegmatitic due to later migmatization and/or metasomatism that developed a widespread salmon pink coloration. The first deformation planar fabric within the diapir is a horizontal to gently dipping gneissosity and the fabric appears to be conformable with that of the overlying metasediments. A later, steeply dipping cleavage is only locally developed (Fig. 60.2).

Pre-volcanic Metasedimentary Rocks (Unit 2)

The metasediments that overlie the basement gneiss have axial planar structures that wrap around the Hackett River "diapir" (Unit 1). The metasediments are dominantly quartzofeldspathic gneiss with biotite schist and biotite and hornblende gneiss and a considerable amount of undeformed alaskitic- and muscovite-bearing pegmatite. The paraconglomerate that makes up part of the unit consists for the most part of quartz pebbles deformed into irregular "gobs" (Padgham *et al.*, 1974a, b) in a mica-rich matrix. Locally, large rounded to subrounded clasts of dioritic gneiss occur (Fig. 60.2). Metamorphism has reached at least sillimanite grade in places.

The pebbles are intensely stretched parallel to the dip of the contact between the body and the overlying metasediments. It is probable that the fabric was more steeply dipping prior to the "diapiric" upwelling.

Basic to Intermediate Volcanic Rocks (Unit 3)

The relationship of these rocks to those of Unit 2 is unclear. They may, however, be older than Unit 2. In the southern part of map-area 76G/5 minor gossans, quartzofeldspathic gneisses and carbonate-bearing rocks, which may correlate with those of Unit 2, occur within (as inliers?) and between Unit 3 and Unit 4 along a highly deformed surface or zone. The volcanic rocks of Unit 3 consist primarily of andesitic agglomerates with locally prominent metabasalts, or more felsic agglomerates. Unit 3 forms a doubly plunging anticlinorial structure flanked by the more felsic, apparently conformable volcanic rocks of Unit 4. The metamorphic grade of Unit 3 is high and plagioclase augen gneiss or garnetiferous gneiss, both of dioritic composition are present. Hornblende plagioclase gneiss is present, possibly developed from basalt or diabase.

Intermediate to Felsic Volcanics (Unit 4)

Unit 4a is composed of rhyolitic agglomerates with locally prominent andesitic agglomerates, rhyolite flows or porphyries, ash fall tuffs and pillowed andesites; these rocks are intruded by minor acid and basic sills. The lowermost units are commonly carbonate-bearing fragmental pyroclastics and the pile is commonly capped by stratified carbonate-bearing pyroclastic or sedimentary rocks that are near sulphide-bearing stratabound volcanic horizons, as at the Yava and Bathurst-Norsemines deposits (Fig. 60.1).

The volcanic rocks that make up this unit overlie (conformably?) the metasedimentary rocks of Unit 2, which in turn may unconformably overlie the granitic "basement" gneisses of Unit 1. However, elsewhere they appear to overlie the more basic volcanic rocks of Unit 3. Unit 4b is less deformed and appears to be of lower metamorphic grade than Unit 3 so it may overlie Unit 3 unconformably.

Metasedimentary Rocks (Unit 5)

Unit 5 conformably overlies Unit 4. The oldest part (5a) is commonly argillaceous (locally graphitic). It forms a thin sequence for the most part, but in the southern part of map-area 76F/1 it covers a large area. The argillaceous rocks are overlain by turbidite greywackes or their metamorphosed equivalents and these occupy much of the area to the northeast of the greenstone belt. In map-area 76F/1, the argillaceous rocks are overlain by either volcanic rocks of Unit 6, by

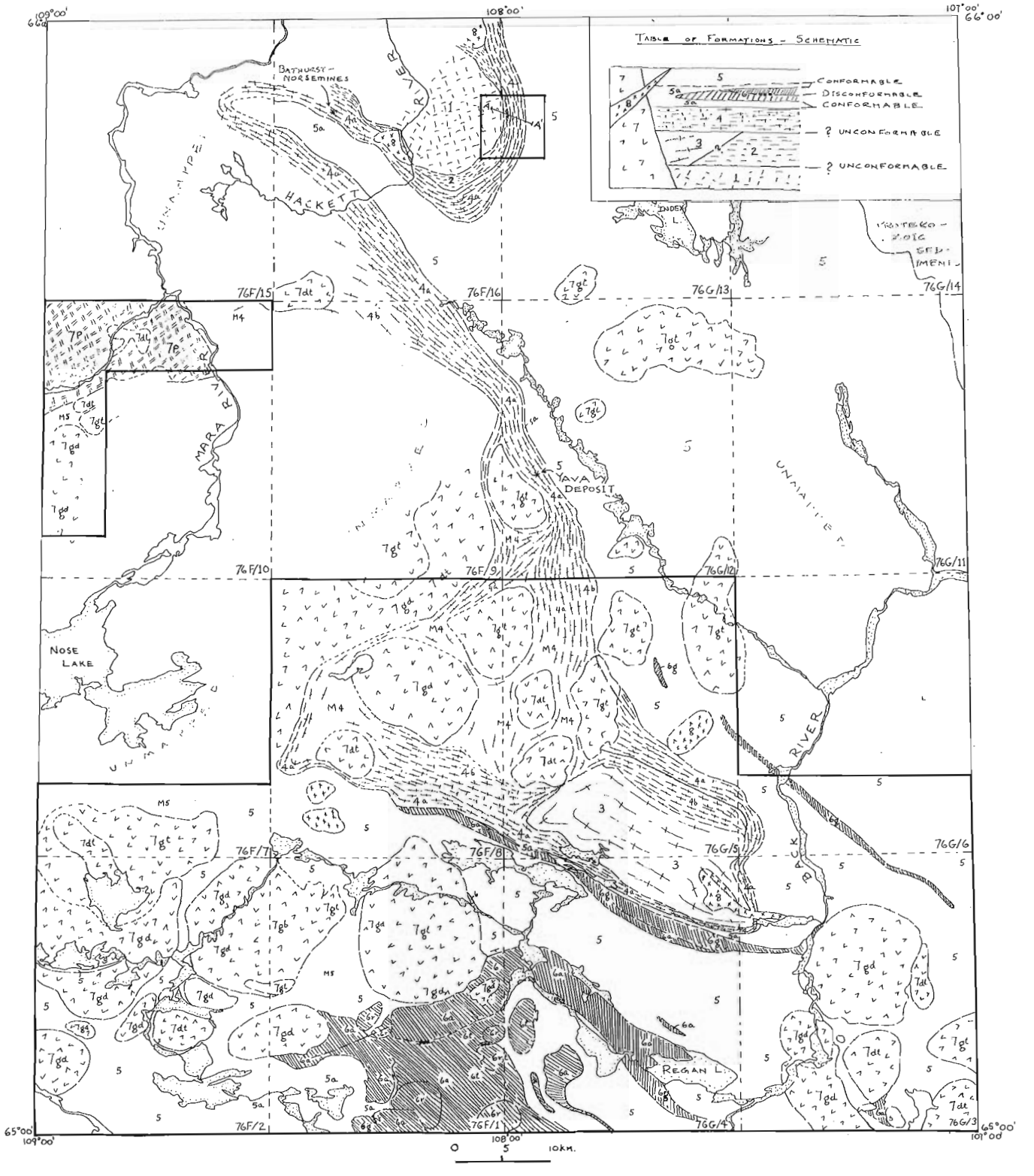

Figure 60. 1. A generalized geological map of the Hackett-Back River greenstone belts. Major units are: (1) granodioritic gneiss with granitic dioritic margins; (2) quartzofeldspathic paragneiss schist and paraconglomerate; (3) basic to intermediate volcanic flows and pyroclasts; (4a) dominantly intermediate volcanic rocks; (4b) acid pyroclastic rocks, tuff and volcanic flows; (M4) metamorphosed or migmatized equivalents of unit 4; (5) greywacke, siltstone and argillite turbidites and their metamorphosed equivalents; (6a) dominantly pillowed andesite flows; (6g) andesitic agglomerate; (6t) rhyolitic tuff; (6r) rhyolitic quartz-eye domes with brecciated margins; (7dt) dioritic; (7gd) granodioritic; (7gt) granitic or monzonitic gneiss; (7p) porphyritic or porphyroblastic granodiorite, diorite; (8) muscovite granite and pegmatite.

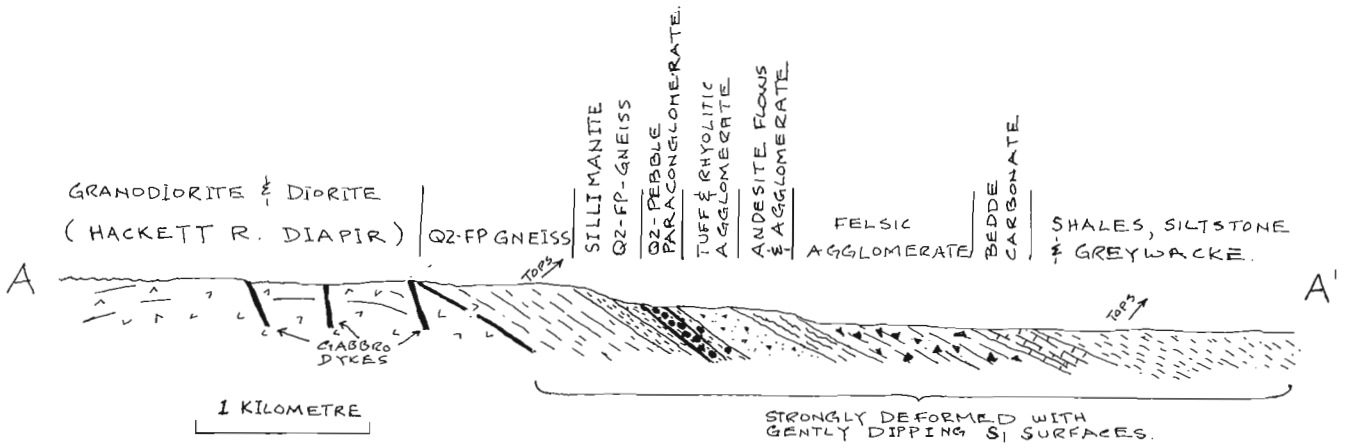

Figure 60.2. Schematic cross-section showing the relationship between the Hackett River diapir and the overlying sediments and volcanic rocks.

gritty paraconglomerate or by coarse, crossbedded greywacke units. Tops in Units 5a and 6 indicate that Unit 6 overlies Unit 5a. Felsic dykes and sills, up to 20 m wide, cut the metasediments and are presumably related to the later volcanism. The thin layer of Unit 5a in the northeast part of map-area 76G/4 consists of rusty-weathering graphitic rocks (between Units 4a and 6g); locally it is only a few metres thick.

Much of the area around Regan Lake is occupied by a turbidite greywacke – argillite sequence. Parts of this sequence are little deformed and only slightly metamorphosed and preserve primary sedimentary structures such as graded bedding, crossbedding, load-casting, de-watering structures and other primary features.

Younger Metavolcanic Rocks (Unit 6)

Most of this rock unit consists of pillowed andesites (6a). The lowermost units are carbonate-bearing volcanogenic pyroclastic and sedimentary units with a maximum thickness of a few tens of metres (westernmost map-area 76F/1). The pillowed andesites are locally agglomeritic with a carbonate-bearing matrix and locally prominent cross-cutting veins of calcium carbonate. The pillowed andesites (6a) form a horseshoe-shaped pattern that opens to the southeast (map-areas 76F/1 and 76F/4). The upper units of (6a) are characterized by rhyolitic breccia, wide carbonate-bearing volcanogenic sediments of tuff, and small-pebble conglomerates, and paraconglomerates. Overlying these horizons are rhyolitic tuffs (6t) and rhyolites and rhyolite porphyries (6r) that occur as small domes of either massive flow or shallow intrusive origin. These dome structures may be of some economic interest. The margins of the domes are usually brecciated and grade into rhyolitic tuffs and agglomerates.

Narrow northwest-trending belts of rhyolitic to andesitic breccia (6g) occur within metasediments of Unit 5 in the south part of map-area 76G/4 and along the boundary between map-areas 76G/3-76G/6. Breccia fragments appear to decrease in size toward the southeast.

Intrusive Granitic Rocks (Units 7 and 8)

The intrusive rocks range in composition from leucocratic muscovite granites to melanocratic hornblende diorites with small areas underlain by gabbros, pyroxenite and other mafic rock types. Most of Unit 7 is contemporaneous with the first major deformation and hence is of Kenoran age. Some, however, are devoid of fabric and may be Proterozoic (Unit 8).

Metamorphism and Structure

To the northeast of the main greenstone belt the metasedimentary sequence is apparently little deformed and metamorphosed, grading from greenschist facies with no porphyroblasts, to more highly metamorphosed units near the granitic plutons of Unit 7. Proximity to granitic plutons is not the prime control of the grade of metamorphism, and it is suggested that much of the metamorphism is regional rather than contact. The latter is narrowly restricted to margins of the granitic bodies.

Within the more argillaceous units, tight isoclinal folding is in marked contrast to the open folding of the coarser sequences. The earliest planar fabric is parallel to or close to the trends of the volcanic belts. The supracrustal rocks appear, in places, to be shouldered aside by the granitic bodies, suggesting that emplacement of these bodies came during or after the main period of upright folding. However, it should be noted that the granitic rocks are of several ages, and some granitic bodies appear to pierce the supracrustals. A second fabric, present in the metasediments, appears to be related to later movements of some of the granitic plutons. Planar features may radiate from the intrusive centres, for example in the large pluton in the Malley Rapids map-area (76G/3).

Economic Geology

Two base metal deposits in the area are being actively explored; the Bathurst-Norsemines and the

Yava Syndicate. Both are located near the gossan-bearing volcanic-sedimentary boundary between the rocks of Units 4a and 5. Exploration during the field season was active along the length of this interface, around the inlier of andesitic agglomerate (Unit 3) and along the gossan zone of carbonaceous argillite (5a) between Units 6a and 4a (southwest part of map-area 76G/5).

Exploration was also active along the north boundary between the volcanics of Unit 6g and the sediments of Unit 5a in the north part of map-area 76G/4 and along the Regan Lake belt in map-areas 76G/4 and 76F/1.

References

Fraser, J.A.
1964: Geological notes on the northeastern District of Mackenzie, Northwest Territories; Geol. Surv. Can., Paper 63-40.

Padgham, W.A., Jefferson, C.W., Ronayne, E.A., and Sterenberg, V.Z.
1974a: Geology of Index Lake, 76-G-13, preliminary edition; Dept. Indian Affairs and Northern Development, Ottawa.

Padgham, W.A., Bryan, M.P.D., Ronayne, E.A., and Sterenberg, V.Z.
1974b: Geology of Hackett River, 76-F-16, preliminary edition; Dept. Indian Affairs and Northern Development, Ottawa.

Padgham, W.A., Bryan, M.P.D., Ronayne, E.A., and Sterenberg, V.Z. (cont'd.)
1974c: Geology of 76-F-9, preliminary edition; Dept. Indian Affairs and Northern Development, Ottawa.

Padgham, W.A., Sterenberg, V.Z., Bryan, E.A., Ronayne, E.A., and Jefferson, C.W.
1974d: Geology of 76-G-5, preliminary edition; Dept. Indian Affairs and Northern Development, Ottawa.

Padgham, W.A., Bryan, M.D.P., Jefferson, C.W., Ronayne, E.A., and Sterenberg, V.Z.
1974e: Geology of Agricola Lake, 76-G-12, preliminary edition; Dept. Indian Affairs and Northern Development, Ottawa.

Tremblay, L.P.
1971: Geology of the Beechey Lake map-area, District of Mackenzie, Northwest Territories; Geol. Surv. Can., Mem. 365.

Wright, G.M.
1957: Geological notes on the eastern District of Mackenzie, Northwest Territories; Geol. Surv. Can., Paper 56-10.

AUTHOR INDEX